EMERGING INFECTIOUS DISEASES®

U.S. CENTERS FOR DISEASE CONTROL AND PREVENTION

Spirochetes and Other Bacteria

July 2025

Albrecht Dürer (1471–1528), *The Syphilitic*, 1496. Broadsheet: text and woodcut. 15.7 in × 11.4 in/40 cm × 29 cm. Source: Wellcome Collection, London, UK (https://wellcomecollection.org/works/pt87tf6m).

EMERGING INFECTIOUS DISEASES®

Emerging Infectious Diseases is published monthly by the Centers for Disease Control and Prevention, 1600 Clifton Rd NE, Mailstop H16-2, Atlanta, GA 30329-4018, USA. Telephone 404-639-1960; email eideditor@cdc.gov

EMERGING INFECTIOUS DISEASES®

Spirochetes and Other Bacteria **July 2025**

On the Cover

Albrecht Dürer (1471–1528), *The Syphilitic,* 1496.
Broadsheet: text and woodcut. 15.7 in × 11.4 in/
40 cm × 29 cm. Source: Wellcome Collection, London, UK
(https://wellcomecollection.org/works/pt87tf6m).

About the Cover p. 1496

Synopses

Research

Medscape EDUCATION ACTIVITY

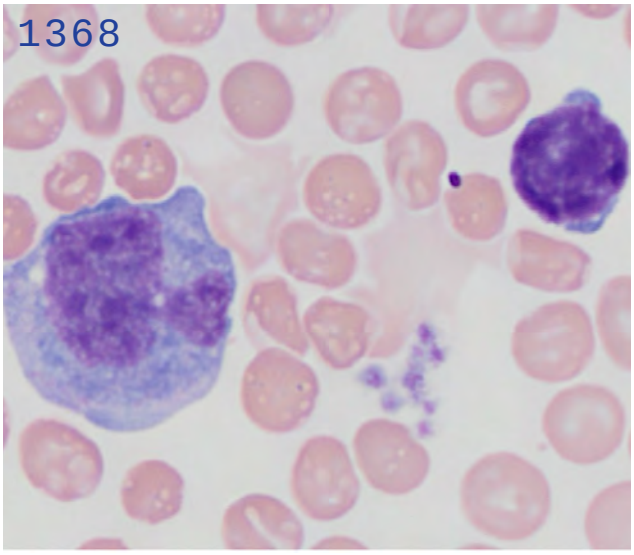

Historical Review

EMERGING INFECTIOUS DISEASES®
July 2025

Dispatches

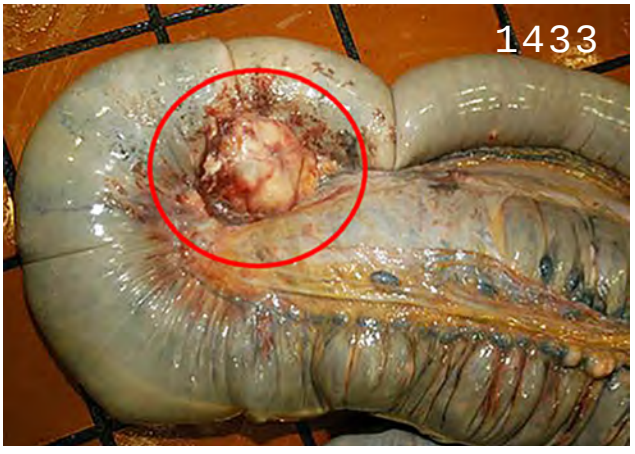

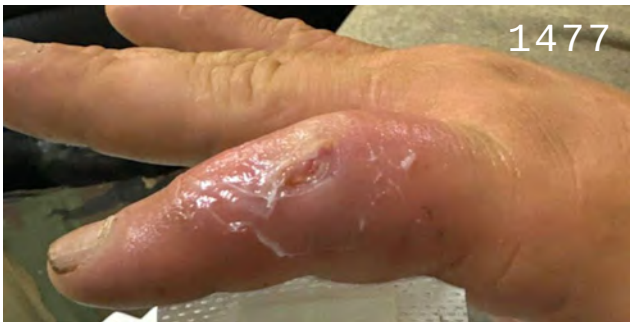

Research Letters

EMERGING INFECTIOUS DISEASES®
July 2025

EIN Letter

About the Cover

Etymologia

Corrections

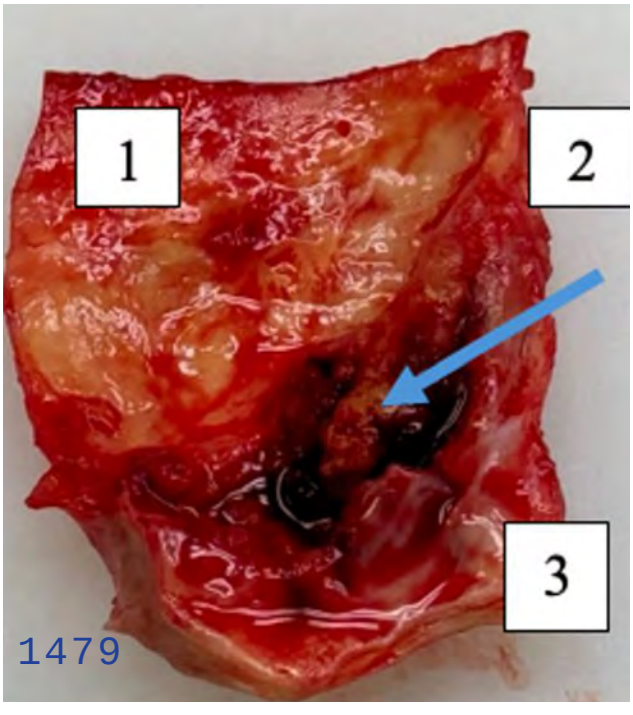

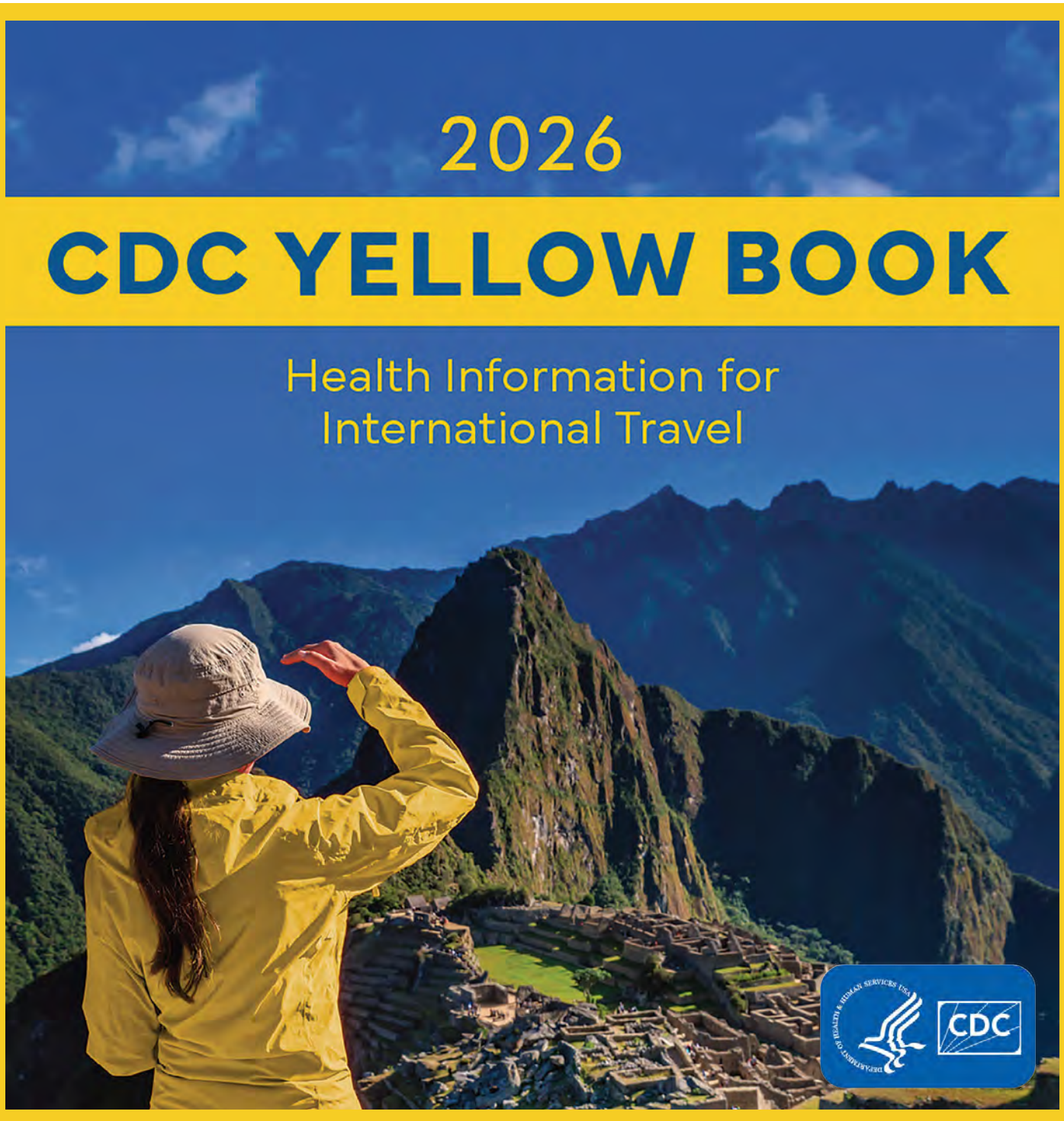

Launch of CDC Yellow Book 2026– A Trusted Travel Medicine Resource

CDC is pleased to announce the launch of the **CDC Yellow Book 2026**. The CDC Yellow Book is a resource containing the U.S. government's travel medicine recommendations and has been trusted by the travel medicine community for over 50 years. Healthcare professionals can use the print and digital versions to find the most up-to-date travel medicine information to better serve their patients' healthcare needs.

The CDC Yellow Book is available online now at www.cdc.gov/yellowbook and in print starting in June 2025 through Oxford University Press and other major online booksellers.

Human *Streptococcus suis* Infections, South America, 1995–2024

M'hensa Vincent De Paul Bakpatina-Batako, Kevin Li, Sonia Lacouture, Lucía Cipolla, Ariel Gianecini, Mónica Prieto, Marcelo Gottschalk, Nahuel Fittipaldi

Streptococcus suis, a swine pathogen that causes zoonotic infections in Europe and Asia, has increasingly been observed in South America. We reviewed all available reports from the continent and identified *S. suis* cases in Argentina, Brazil, Chile, French Guiana, and Uruguay. We also identified 8 novel infections from Argentina, bringing the total documented human cases in South America to 47. We reclassified 1 previously reported infection as *S. parasuis*. Among the 47 *S. suis* cases, 40 (85%) patients had meningitis, 2 (4%) had toxic shock–like illness, 2 (4%) had nonshock sepsis, 1 (2%) had arthritis, and 1 (2%) had endocarditis. The case-fatality rate was 4% (2/47). Infections were primarily linked to pig or pork exposure, although some occurred after consuming undercooked meat. Case distribution varied by country, and Argentina reported a disproportionately high number of cases despite a smaller swine industry. Our findings highlight the need for more consistent regional *S. suis* surveillance.

Streptococcus suis is a swine pathogen and a zoonotic agent responsible for meningitis, septicemia, streptococcal toxic shock–like syndrome (STSLS), and other diseases in humans, particularly among persons who have close contact with pigs or pork by-products or who consume dishes made with raw pork or pig blood (*1*,*2*). *S. suis* is phenotypically and genetically highly diverse, has 29 recognized serotypes on the basis of serologic reactions against its polysaccharide capsule, and has >2,900 sequence types (STs) defined by multilocus sequence typing (MLST) (*3*,*4*). Resistance to macrolide, lincosamide, and tetracycline antibiotics is common, and recent reports indicate emerging β-lactam resistance (*5*).

Most human infections are caused by *S. suis* serotype 2, although cases caused by serotypes 1, 4, 5, 7, 9, 14, 16, 21, 24, and 31 have been reported (*6*,*7*). Most human infections have been reported in East and Southeast Asia (*2*). In Europe, *S. suis* is considered an occupational disease, and human infections are less frequently reported than in Asia but still relatively common (*8*). Sporadic *S. suis* cases have also been documented in Hawaii (USA), Australia, Togo, and Madagascar (*9*–*12*), but <10 cases have been described from the continental United States and Canada (*13*), despite the large swine farming industries in those regions. Reports from South America have been less integrated into the global understanding of *S. suis* zoonotic disease, partly because many were not published in English. To address that gap, we reviewed published cases from South America, identified and report on novel human infections from Argentina, and assessed epidemiologic and clinical characteristics of *S. suis* infections on the continent.

Materials and Methods

Literature Review

To identify reported cases of human *S. suis* infections in South America, we conducted a comprehensive literature review as a critical narrative synthesis rather than a systematic review or meta-analysis. We included PubMed, ScienceDirect, SciELO (Scientific Electronic Library Online), and Google Scholar databases, as well as gray literature, by using the following key terms: *S. suis*, South America, human infection, meningitis, sepsis, zoonosis, pig, pork, and the names of all countries in South America. We conducted searches in English, Dutch, French, Portuguese, and

Author affiliations: Université de Montréal Faculté de médecine vétérinaire, St-Hyacinthe, Quebec, Canada (M.V.D.P. Bakpatina-Batako, K. Li, S. Lacouture, M. Gottschalk, N. Fittipaldi); Instituto Nacional de Enfermedades Infecciosas, ANLIS Dr. Carlos G. Malbrán, Buenos Aires, Argentina (L. Cipolla, A. Gianecini, M. Prieto)

DOI: https://doi.org/10.3201/eid3107.241835

Spanish. We also reviewed PubMLST (https://pubmlst.org) and GenBank to identify potentially unreported human cases. We selected studies and case reports on human *S. suis* from South America, excluded duplicates or reports involving isolates from outside the continent, and extracted relevant patient and causative-isolate metadata. Through the literature review, we identified 39 confirmed *S. suis* human cases in South America during 1995–2024 (*14*–*28*). We also noted a potential additional case on the basis of a human isolate submitted to PubMLST.

Data Collection and Microbiology Methods for Previously Undescribed Cases from Argentina

In addition to cases identified by reviewing the literature, we report 8 previously undescribed *S. suis* human infections diagnosed and microbiologically confirmed during 2017–2024 through national laboratory surveillance in Argentina, bringing the total *S. suis* cases in the continent to 47. For the 8 new cases, we collected clinical data including demographic details, risk factors, diagnostic methods, treatment, and outcomes from patient medical records at hospitals participating in the Argentine National Laboratory Network for Meningitis and Invasive Bacterial Diseases, which does not require ethics approvals to share anonymized patient data and isolates with the Instituto Nacional de Enfermedades Infecciosas, ANLIS Dr. Carlos G. Malbrán, where the data were centralized. The same hospitals submitted the causative agent associated with those cases (i.e., the α-hemolytic gram-positive isolates identified as *S. suis* through biochemical testing) to the reference laboratory. Species confirmation was carried out via matrix-assisted laser desorption/ionization time-of-flight mass spectrometry and by PCR targeting the species-specific *recN* gene (*29*). Serotyping was performed using the co-agglutination test (*30*), a multiplex PCR targeting genes in the *S. suis* capsular polysaccharide (*cps*) locus (*31*), or both. To differentiate between *S. suis* and *S. parasuis*, we performed an in silico PCR targeting the *recN* gene using primers from an established identification scheme (*32*).

Whole-Genome Sequencing and Analysis

We prepared genomic libraries for the 8 new and 1 previously reported *S. suis* isolates from Argentina by using Nextera XT kits (Illumina, https://www.illumina.com) and sequenced them on an Illumina MiSeq as 150-bp paired end reads. We deposited data into the National Center for Biotechnology Information Sequence Read Archive (https://www.ncbi.nlm.nih.gov/sra) (Appendix Table 1). We determined or confirmed speciation, serotyping, MLST profiles, and antimicrobial resistance (AMR) gene content by using the short-read genomic data and an *S. suis* typing pipeline (*33*), SRST2 software (*34*), and the Comprehensive Antibiotic Resistance Database version 3.0.8 (*35*).

Phylogenetic Analysis

We used Snippy (https://github.com/tseemann/snippy) to identify single-nucleotide polymorphisms in the genome of the isolates (Table 1) relative to the genome of the ST1 serotype 2 *S. suis* reference strain P1/7 (GenBank accession no. NC_012925.1). We used the Snippy-core function to define core-genome single-nucleotide polymorphisms, which we used to build a maximum-likelihood phylogenetic tree in FastTree 2.1.10 (*37*) with Shimodaira–Hasegawa–like local support values based on 1,000 resamples. We visualized and annotated trees in R (The R Project for Statistical Computing, https://www.r-project.org) by using the ggtree library (*38*).

Results

Epidemiology of Human *S. suis* Infections in South America

Including the 8 novel *S. suis* infection we report here, we found a total of 47 confirmed *S. suis* human cases in South America during 1995–2024 (*14*–*28*). We also noted a potential additional case from a human isolate submitted to PubMLST. Most (n = 38) patients were adult or older adult men; 6 cases were among female patients, including 1 infant, and sex was unreported for 3 cases (Table 1). Forty (85%) patients had meningitis, and 7 of those patients experienced permanent or temporary hearing loss. The other 7 cases involved severe sepsis and STSLS (2 each) and septic arthritis and endocarditis (1 each); 1 case had no available diagnosis (Table 1). Only 2 deaths were reported, a fatality rate of 4%. Contact with pigs or pig products was a common risk factor: 28 patients were workers or farmers with direct exposure, and 7 patients reported contact through handling, exposure to, or consuming swine or wild boar. Exposure information was unavailable for 5 cases, and 7 persons reported no known exposure (Table 1).

Previously Reported *S. suis* Human Infections in Argentina

Before our analysis, Argentina had documented a total of 21 *S. suis* infections (*14*–*18*) (Appendix Table 2). The first reported case, in 2005, involved a female patient in whom bacterial meningitis developed

Table 1. Summary of human *Streptococcus suis* infections, South America, 1995–2024*

Patient characteristics	Argentina	Brazil	Chile	French Guiana	Uruguay	South America
Total no. cases	29	5	7†	1	5	47
Sex						
M	25	5	3	1	4	38
F	4	0	2	0	0	6
Not reported	0	0	2	0	1	3
Age, y						
Mean age, y (range)‡	46.6 (38–55)	65.6 (50–82)	49.6 (44–55)	42 (NA)	55 (50–66)	48.5 (38–82)
Median age, y‡	47	68	48	NA	52	50
Not reported	20	0	2	0	1	23
Clinical manifestation						
Meningitis	26	4	5	1	4	40
STSLS	1	1	0	0	0	2
Other§	2	0	2	0	0	4
Not known	0	0	0	0	1	1
Outcomes						
Recovered	27	5	5	1	5	43
Died	2	0	0	0	0	2
Hearing loss	1	3	1	1	1	7
Not known	0	0	0	0	1	1
Contact with pigs						
Worker or farmer	18	3	2	1	4	28
Other contact¶	4	2	1	0	0	7
No contact	7	0	0	0	0	7
Not known	0	0	4	0	1	5
Isolates						
Serotyping						
Reported#	26	1	7	1	0	35
Not reported	3	4	0	0	5	12
MLST						
Reported**	25	0	0	1	0	26
Not reported	4	5	7	0	5	21

*MLST, multilocus sequence typing; ST, sequence type; STSLS, streptococcal toxic shock-like syndrome.
†Because 1 human isolate from Chile was available in PubMLST, an additional human case is possible. That isolate belonged to MLST ST1172, but it was not serotyped. Thus, whether that isolate represents an eighth human infection in Chile or if it corresponds to one of the 7 previously reported infections is not known.
‡One case occurring in a 1-y-old infant from Argentina was excluded when calculating mean, range, and median patient age.
§Includes 1 case of septic arthritis and 1 case of endocarditis in Argentina and 2 cases of sepsis in Chile.
¶Includes contact while handling pigs for consumption, consuming undercooked pork, hunting wild boars, or a combination of those factors.
#All cases where serotyping was performed revealed serotype 2 isolates except for 1 serotype 5 and 1 untypable isolate in Argentina.
**All cases where MLST was performed revealed ST1 isolates, except for an ST5 strain that was retrospectively ascribed to ST483 in a different investigation (*36*).

after occupational pig exposure (*18*). The isolate, identified as *S. suis* serotype 2 with the muramidase released protein (*mrp*), extracellular protein factor (*epf*), and suilysin (*sly*) (*mrp/epf/sly*) virulence gene profile typical of strains from Eurasia, was later typed by MLST as ST1 (*14*,*18*). A second report, from 2006, described a 49-year-old man from Santa Fe Province with meningitis who had occupational exposure at a slaughterhouse (*15*). That patient was treated with ampicillin and ceftriaxone, initially improved, but later had complete hearing loss in the left ear and partial loss in the right develop. Cerebrospinal fluid (CSF) cultures grew *S. suis*, but the isolate was not typed. Another report described a 54-year-old man from a rural area of Tucumán Province with meningitis who had occupational exposure to pigs (*16*). *S. suis* was isolated from CSF, but the strain was not typed. He was treated with ceftriaxone and dexamethasone and recovered without long-term neurologic sequelae.

Those 3 cases, along with a fourth potential human infection with *S. suis* serotype 21 (*39*), reclassified in this investigation as *S. parasuis*, prompted the retrospective investigation of 17 additional infections, including 5 involving male patients with meningitis that predated previous reports, 2 from 1995 and 3 from 2003. The other cases spanned 2009–2016 and involved 10 male and 2 female patients, mostly from rural areas (*14*). Of those 17 cases, 12 involved direct contact with pigs or pork products, typically through farming or slaughterhouse work; 1 had no reported contact, and 4 lacked exposure data. Sixteen cases had meningitis as the clinical manifestation, and 1 involved septic arthritis (*14*). The infections were all caused by *S. suis* ST1 serotype 2, except for a 2014 case involving serotype 5, which was the only fatality in this series (*14*).

In 2024, a 42-year-old man working at a pig processing plant in Argentina was hospitalized with meningitis after 10 days of weakness, headache, progressive hearing loss, and ataxia. CSF cultures grew

S. suis serotype 2. He was treated with ceftriaxone and dexamethasone and improved clinically, but mild bilateral hearing loss persisted (*17*).

New *S. suis* Human Infections in Argentina, 2017–2024

We identified 8 additional, previously unreported *S. suis* infections from Argentina that occurred during 2017–2024 (Table 2). Case 1, from 2017, involved a 42-year-old male pig farmer who had fever, fatigue, and shortness of breath. Blood cultures grew *S. suis*, but the isolate was untypable. Further investigation revealed native valve endocarditis. The patient recovered without complications.

In a case 2, from 2018, a 1-year-old girl from a rural area was admitted to the hospital with signs of meningitis. Blood cultures grew *S. suis* serotype 2. The patient survived the infection. Exposure to pigs or pork could not be determined, and no household pig-keeping or sick contacts were reported.

Case 3, from 2019, involved an adult man with meningitis, but the source of exposure could not be determined. CSF cultures grew *S. suis* serotype 2. The patient survived and did not have residual sequelae.

Case 4 occurred in 2020 and involved a 38-year-old man with meningitis who was from an urban area and used drugs but had no reported contact with pigs or pork products. Blood and CSF cultures grew *S. suis* serotype 2. The patient survived without long-term complications.

Case 5 was identified in 2021 in a 47-year-old male hunter in whom meningitis developed after contact with wild boars and consuming a suckling pig. Blood and CSF cultures grew *S. suis* serotype 2. The patient survived without notable sequelae.

Case 6, from 2022, was in a 48-year-old man who regularly hunted wild boars and had meningitis develop after consuming pork. CSF cultures grew *S. suis* serotype 2. The patient survived without notable sequelae.

Case 7 was reported in 2022 in a 45-year-old man who had meningitis after purchasing and preparing a pig from a backyard farm. CSF cultures grew *S. suis* serotype 2. The patient survived without notable sequelae.

Finally, case 8 occurred in 2024 in a 55-year-old man in whom STSLS developed after confirmed contact with pigs. Blood cultures grew *S. suis* serotype 2. Despite aggressive treatment, the patient died, the only fatality in this 8-case series.

S. suis Human Infections in Argentina and Reclassification of 1 Isolate as *S. parasuis*

An unusual infection attributed to the rare *S. suis* serotype 21 was described in 2014 in Argentina (*39*). The patient had spontaneous bacterial peritonitis (*39*), raising questions about the initial classification, especially because co-agglutination, the serologic typing method initially used, can sometimes produce false cross-reactive results (*30*). To resolve those inconsistencies, we re-examined the isolate using genomic data. An ad hoc in silico PCR with specific primers targeting the *recN* gene of various streptococcal species reclassified the isolate as *S. parasuis*, a species closely related to *S. suis* that was not formally recognized until 2015 (*29*), after the initial erroneous identification in 2014. Further analysis corroborated that reclassification (Appendix Figure). That case predates

Table 2. Characteristics of patients and isolates for the 8 new cases of human *Streptococcus suis* infection from Argentina, South America, 2017–2024*

	Patient					Isolate				
Year	Age, y/sex	Disease	Contact with swine or pork	Outcome	Notes	Isolate ID	Source	Serotype	ST	Virulence markers
2017	42/M	NVE	Yes, pig farmer	Survived	None	26-17	Blood	Untypable†	1	*mrp*, *epf*, *sly*
2018	1/F	Meningitis	Unknown, lived in rural area	Survived	None	868-18	Blood	2	1	*mrp*, *epf*, *sly*
2019	Adult/M‡	Meningitis	Unknown	Survived	None	724-19	CSF	2	1	*mrp*, *epf*, *sly*
2020	38/M	Meningitis	No, lived in urban area	Survived	Inhalation drug user	247-20	Blood, CSF§	2	1	*mrp*, *epf*, *sly*
2021	47/M	Meningitis	Yes, consumed pork	Survived	Wild boar hunter	521-21	Blood, CSF§	2	1	*mrp*, *epf*, *sly*
2022	48/M	Meningitis	Yes, consumed pork	Survived	Wild boar hunter	395-22	CSF	2	1	*mrp*, *epf*, *sly*
2022	45/M	Meningitis	Yes, handled not commercial pig	Survived	None	931-22	CSF	2	1	*mrp*, *epf*, *sly*
2024	55/M	STSLS	Yes	Died	None	649-24	Blood	2	1	*mrp*, *epf*, *sly*

*CSF, cerebrospinal fluid; *epf* extracellular protein factor; ID, identification; *mrp*, muramidase released protein; NVE, native valve endocarditis; *sly*, suilysin; ST, sequence type as defined by multilocus sequence typing; STSLS, streptococcal toxic shock–like syndrome.
†Untypable by both serologic and molecular methods.
‡Precise age not available.
§Only the isolate recovered from CSF was included in this investigation, although both were typed.

similar cases of human *S. parasuis* infection reported in China (*40*).

S. suis Human Infections in Brazil

In Brazil, 5 human *S. suis* infections have been documented, involving both occupational exposure and ingesting undercooked pork (*19*–*22*) (Appendix Table 2). The first, which occurred in 2019 but was reported in 2024, involved a 68-year-old swine farmer from Bahia who had bacterial meningitis. CSF cultures grew *S. suis*, but serotyping was not performed. The patient experienced permanent hearing loss (*21*). In 2020, two additional cases were reported in Ceará, both involving men with occupational exposure to pigs who had meningitis. Serotyping of the isolates was not performed in either of those cases (*20*).

The other 2 cases from Brazil involved patients who reported consuming pork. The first, in 2020, involved an 82-year-old man from Rio de Janeiro who contracted *S. suis* meningitis after consuming pork that probably was undercooked; the specific serotype was not reported (*19*). The second, in 2024, involved a 50-year-old man from São Paulo who had STSLS and probably meningitis after consuming raw pork. Blood cultures confirmed *S. suis* serotype 2. Although that patient recovered, he had hearing loss develop (*22*).

S. suis Human Infections in Chile

In Chile, 7 human *S. suis* infections have been reported, all linked to occupational or incidental exposure to pigs (*23*–*25*) (Appendix Table 2). The first 2 cases, reported in 2012, involved a 54-year-old woman and a 48-year-old man, both pig farmers who had bacterial meningitis. CSF cultures grew *S. suis* serotype 2. Both patients recovered without neurologic sequelae (*23*,*24*). In 2013, two more cases were reported, both involving men who had meningitis or sepsis caused by *S. suis* serotype 2 (*23*). In 2014 and 2015, two additional cases were documented in Región de los Ríos: 1 patient had severe sepsis, the other meningitis, and serotypes were not reported (*25*). A seventh case occurred in 2018, involving a 44-year-old woman in whom meningitis developed 2 days after handling raw pork and who experienced permanent bilateral hearing loss postinfection. *S. suis* serotype 2 was confirmed through CSF cultures (*25*). We suspect a potential eighth human case in Chile on the basis of a 2019 submission of a human ST1172 *S. suis* isolate to PubMLST; whether that isolate represents a new infection or a previously documented case is unclear.

S. suis Human Infections in French Guiana.

In French Guiana, a single *S. suis* human infection was reported in 2011 (*26*) (Appendix Table 2). In that case, meningitis developed in a 42-year-old man originally from Haiti who injured his thumb while slaughtering pigs. CSF cultures grew *S. suis* ST1 serotype 2. He experienced moderate bilateral hearing loss, which later progressed to severe hearing loss in the left ear (*26*).

S. suis Human Infections in Uruguay

Five human *S. suis* infections have been reported in Uruguay (*27*,*28*) (Appendix Table 2). The first 2 cases were identified in 2008 and 2009 in men who had occupational exposure to pigs and had acute meningitis (*28*), 1 of whom experienced bilateral hearing loss. A third case was reported in Paysandú in 2009; the patient had similar occupational exposure and clinical features (*28*). Fifteen years later, 2 additional cases were reported in men who worked in rural areas (*27*). Both patients had meningitis develop after handling pigs and were treated successfully, but 1 patient had mild neurologic symptoms that persisted. None of the *S. suis* isolates responsible for human infections in Uruguay were serotyped.

Characteristics of *S. suis* Isolates from Human Infections in South America

Of the 47 confirmed and 1 potential human *S. suis* infections in South America, only 35 isolates were serotyped. Serotype 2 was identified in all but 2 isolates, 1 of which was serotype 5 and the other was untypable (Table 1). The serotype 5 isolate was retrospectively assigned to ST486 (*36*). The other isolates with available serotype and MLST data were either ST1 serotype 2 (n = 25) or untypable (n = 1).

We saw notable differences in isolate investigation among countries. The French Guiana isolate was typed as ST1 serotype 2. In Argentina, serotype was available for 26 isolates, 25 of which also had MLST data. Most isolates from Chile were serotyped but not MLST typed, except for 1 that was typed as ST1172, a close derivative of ST1, but was not serotyped. None of the 10 isolates from Uruguay and Brazil were MLST typed, and only 1 isolate from Brazil was serotyped (Table 1).

Genome data for *S. suis* isolates from South America were limited to 9 previously reported isolates from human infections in Argentina (*14*) and 8 newly sequenced genomes from our study. Seeking broader representation, we contacted authors of previous reports from other countries in South America. However, we could not obtain additional isolates because of unavailability of isolates or lack of timely responses from authors.

Because all available genomes originated from Argentina, we expanded the phylogenetic analysis by incorporating ST1 isolates from other geographic regions (Appendix Table 1). Phylogenetic analysis revealed that the isolates from Argentina clustered into 2 distinct clades (Figure 1), both relatively distantly related to ST1 isolates from other regions, except for 1 isolate from Spain that clustered tightly with isolates of 1 of the Argentina subclades. All isolates from Argentina had an *mrp/epf/sly* virulence marker profile and multiple AMR genes identified, but the AMR genes were restricted to a single clade (Figure 1).

Discussion

Because of the small sample size, uneven subgroup distribution, and missing data for key variables, our dataset did not support formal statistical analysis of associations between demographic or exposure-related factors and outcomes; therefore, we focused on descriptive patterns. As expected, based on current *S. suis* knowledge (*2*,*4*,*8*), adult men whose occupations involved direct contact with pigs or pork products were the primary at-risk population in South America. Raw pork consumption, an established risk factor for *S. suis* transmission in parts of Southeast Asia, is uncommon in South America,

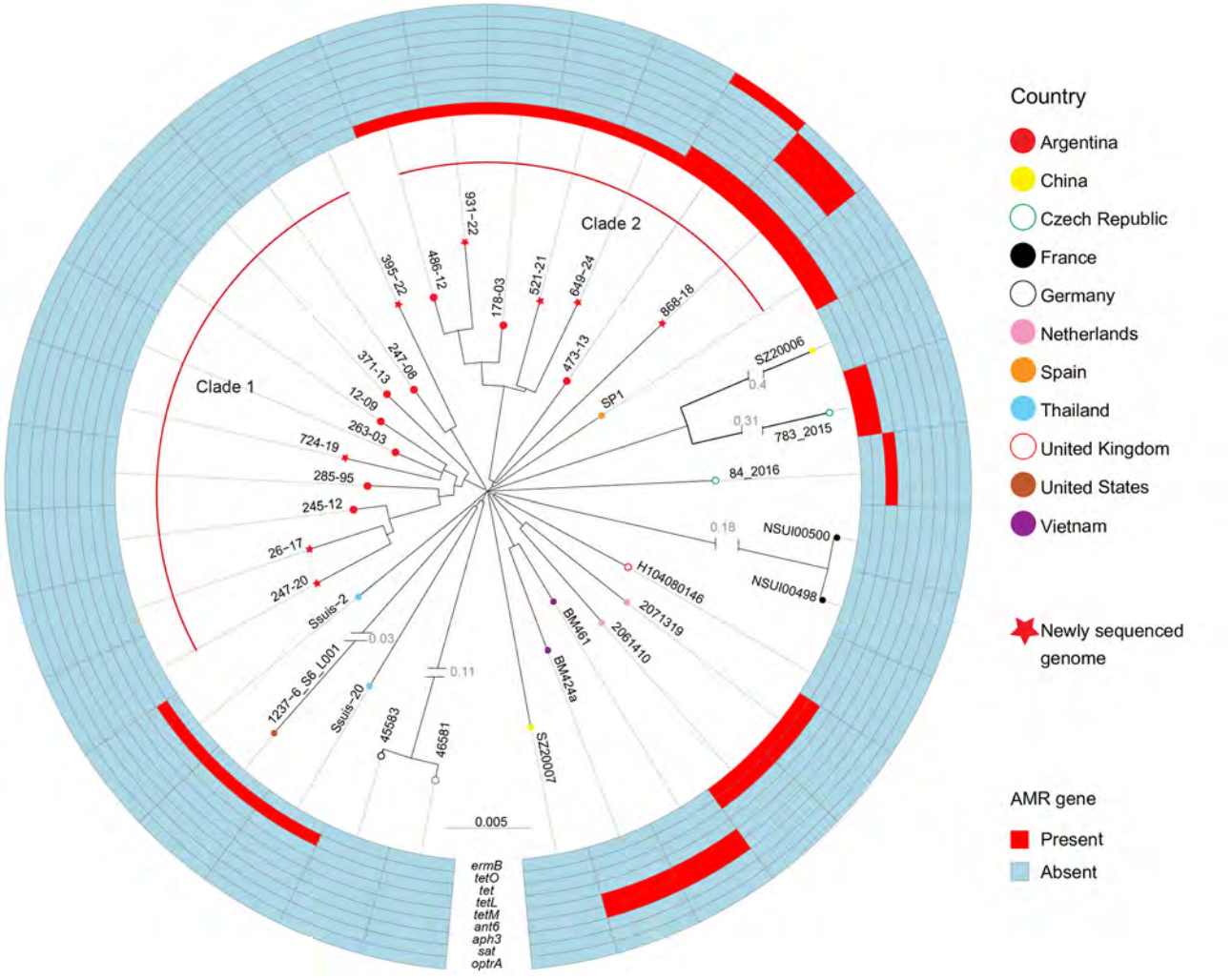

Figure 1. Phylogenetic relationships and AMR gene profiles of isolates in a study of human *Streptococcus suis* infections, South America, 1995–2024. Maximum-likelihood phylogenetic tree shows relationships among sequence type (ST) 1 serotype 2 *S. suis* isolates from human disease in Argentina and selected ST1 serotype 2 isolates from other countries. Tree was constructed by using 5,504 bp nonredundant core-genome single-nucleotide polymorphism loci identified relative to the genome sequence of ST1 serotype 2 reference strain P1/7 (not included in the depiction). The tree delineates 2 distinct clades from Argentina that differ on AMR gene content. One isolate from a human infection in Spain clusters tightly within clade 2 from Argentina, but the rest of the isolates, all from outside South America, are more distantly related genetically to either clade from Argentina. AMR genes identified in the genomes of the isolates are represented in the outer rings. AMR, antimicrobial resistance.

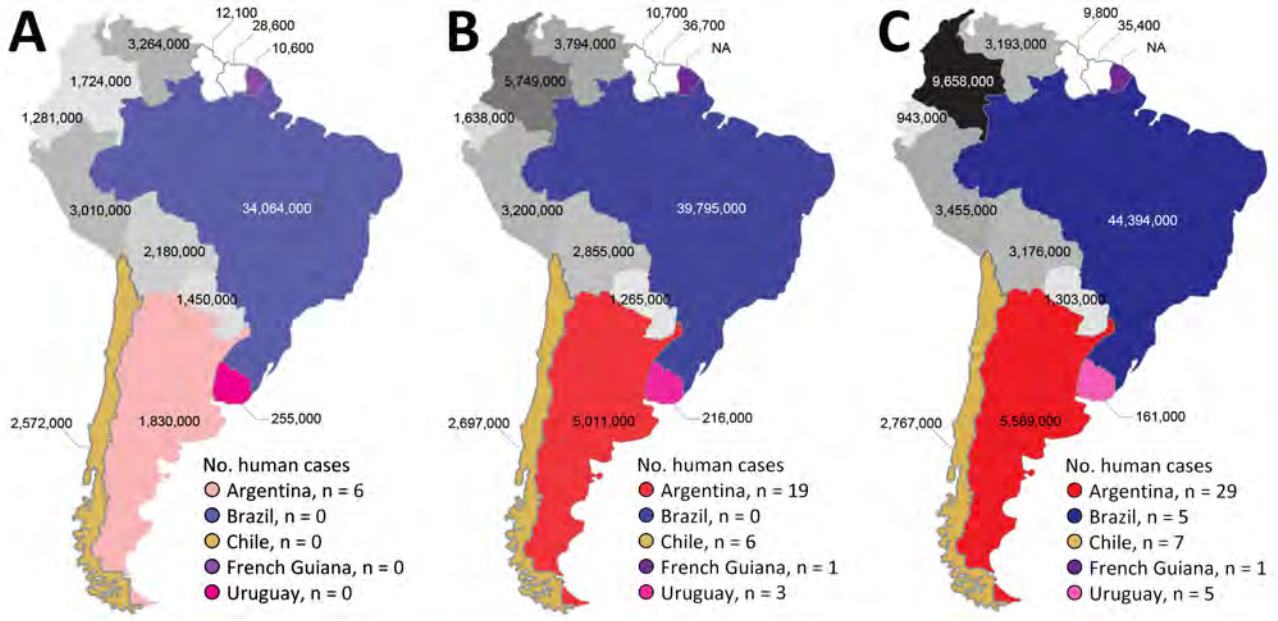

Figure 2. Estimated number of swine and cumulative reported human cases per country in a study of human *Streptococcus suis* infections, South America, 1995–2024. Shown are countries with human *S. suis* infections reported during 1995–2005 (A), 1995–2015 (B), and 1995–2024 (C). Estimated number of heads of swine is shown for each country from 2005 (A), 2015 (B), and 2022 (C). Countries with reported human *S. suis* infections are depicted in specific colors, and cumulative number of human cases during each timeframe are provided in each key. The color intensity increases proportionally to reflect changes in swine population size over time in each country. In contrast, countries without reported human *S. suis* infections are represented in grayscale, and the grayscale intensity indicates variations in swine population size, applied on a unified scale across those countries. Swine production data for French Guiana was only available until 2006. NA, not available.

where pork is typically roasted or stewed (*2*,*14*). Nonetheless, at least 3 cases in South America occurred in persons who had consumed home-prepared suckling pig or wild boar meat that might have been undercooked, highlighting foodborne transmission as the plausible route of infection.

Among the entire cohort, meningitis was the most common manifestation, and numerous cases of subsequent hearing loss were reported, likely resulting from cochlear and labyrinth damage (*2*,*41*–*44*). Early audiometric evaluation is recommended to promptly manage hearing impairment in such cases (*43*). Predominance of meningitis likely reflects its more rapid recognition in hospital settings (*43*). Similarly, severe symptoms associated with STSLS demand immediate medical attention and follow up (*45*). Conditions like arthritis and endocarditis, though, may be underdiagnosed or misattributed to other pathogens because of low awareness and outdated biochemical methods. Those factors often lead to misidentifying *S. suis* as other streptococci, such as viridans group *Streptococcus*, even in high-income countries (*2*,*13*,*46*). Training healthcare professionals to consider *S. suis* when α-hemolytic streptococci are isolated and to take detailed histories of pig or pork contact is essential. In addition, implementing referral protocols and using advanced matrix-assisted laser desorption/ionization time-of-flight mass spectrometry and molecular diagnostic testing can improve the detection and diagnosis of *S. suis* infections.

The number of reported human *S. suis* infections in South America does not correlate with the size of national swine industries (Figure 2). Brazil, a global leader in pork production with >40 million pigs, has reported only 5 human cases. In contrast, Argentina, with a much smaller swine population of 5 million, has documented 29 infections. Biosecurity, as traditionally defined in swine production, has not been shown to reduce *S. suis* disease in pigs or the associated zoonotic risk in humans; nonetheless, the structured occupational health protocols in Brazil's large-scale farms might play a role in limiting human exposure (*47*). In Argentina, the swine industry has expanded rapidly in the past 2 decades, and the number of pigs more than doubled from 2005 to 2015 (Figure 2). However, small-scale farms with limited implementation of biosafety practices remain common and may be contributing to the higher number of reported infection rates (*14*,*47*). Similarly, Uruguay has a small swine industry dominated by extensive farming (*48*) reported 5 human cases during the study period. In Chile, most reported human cases are linked to

traditional small-scale farming practices, even though the cases are geographically concentrated in the south of the country, where export-driven large-scale swine operations are located (*47*,*49*).

No human *S. suis* infections have been reported from other South America countries, including Colombia, which has a swine industry larger in scale and comparable in growth to Argentina's (*47*) (Figure 2). Thus, factors beyond the scale and type of pig farming likely influence the incidence of this zoonotic disease. We speculate that differences in the virulence of circulating *S. suis* strains likely play a role. For example, less virulent ST25 and ST28 serotype 2 strains are predominant in North America, which reports very few human infections, but highly virulent ST1 serotype 2 strains are common in Eurasia (*4*,*13*). In Argentina, highly virulent ST1 serotype 2 strains are prevalent, and ST1 or closely related ST1172 isolates have been identified in French Guiana and Chile. It may be possible that strains of lower virulence circulate among swine in Brazil, Colombia, and other countries that have few or no reported human cases. However, the paucity of molecular data on *S. suis* isolates from most countries in South America, even from pigs, hinders the ability to confirm that hypothesis. Furthermore, our retrospective reclassification of 1 misidentified isolate as *S. parasuis* highlights the value of genomic methods for accurate species identification and for advancing our understanding of *S. suis* disease epidemiology.

Another, perhaps more plausible, explanation for the higher number of reported cases in Argentina compared with other countries in South America is the well-established surveillance system for α-hemolytic bacteria associated with severe infections, particularly in rural hospitals. Suspicious isolates are systematically referred to the National Institute of Infectious Diseases for confirmation and detailed identification, enabling more accurate detection and reporting of *S. suis* infections (*14*). That systematic approach likely accounts for the relatively higher detection rates in Argentina. Enhancing surveillance systems and laboratory capacities in other countries in South America could similarly improve case identification, support more consistent and standardized reporting of demographic and clinical data, and ultimately enable more robust epidemiologic analyses across the continent.

Our findings highlight a complex interplay of factors influencing the incidence and reporting of human *S. suis* infections in South America. Reported cases tend to be more frequent in countries where small-scale or mixed farming persists, reflecting the increased risk for zoonotic transmission under those conditions. Close human–pig interactions and limited on-farm biosafety measures likely contribute to that risk. The confirmed presence of highly virulent ST1 serotype 2 strains in Argentina and the robust surveillance system in that country likely contribute to its higher detection rates and detailed epidemiologic data.

In summary, addressing *S. suis* human infections requires a coordinated approach, including improved on-farm biosafety practices, particularly among small-scale farmers, and strengthened surveillance systems. Argentina's proactive efforts could serve as a model for enhancing diagnostic capabilities across the region. International collaboration, data sharing, and partnerships with the swine industry are essential to better characterize *S. suis* strains and reduce the burden of this zoonotic disease in South America.

Acknowledgments

We thank the clinical microbiology laboratories participating in Argentina's National Laboratory Network for Meningitis and Invasive Bacterial Diseases for their contributions; their diligent efforts in case detection and isolate submission have been instrumental in strengthening Argentina's surveillance system and enhancing the ability to monitor and respond to invasive bacterial diseases in the country. We thank Kayleigh Gauvin for help with genome data submission to the Sequence Read Archive.

Genome data for the 8 isolates sequenced in this investigation have been deposited in the Sequence Read Archive and accession numbers are provided in Appendix Table 1 (https://wwwnc.cdc.gov/EID/article/31/7/24-1835-App1.pdf).

This work was supported in part by grants from the Natural Sciences and Engineering Research Council of Canada to M.G. (grant no. 2022-03730) and N.F. (grant no. 2022-04223). K.L. was supported in part by scholarships from the Groupe de recherche sur les maladies infectieuses en production animale and from the Centre de recherche en infectiologie porcine et avicole (CRIPA), a strategic research center of the Fonds de recherche du Québec (https://doi.org/10.69777/309365).

About the Author

Dr. Bakpatina-Batako is a physician training in microbial bioinformatics at Faculté de médecine vétérinaire, Université de Montréal, St-Hyacinthe, Quebec, Canada. His primary research interest is zoonotic infectious diseases.

References

1. Gottschalk M, Xu J, Calzas C, Segura M. *Streptococcus suis*: a new emerging or an old neglected zoonotic pathogen? Future Microbiol. 2010;5:371–91. https://doi.org/10.2217/fmb.10.2
2. Kerdsin A, Segura M, Fittipaldi N, Gottschalk M. Sociocultural factors influencing human *Streptococcus suis* disease in Southeast Asia. Foods. 2022;11:1190. https://doi.org/10.3390/foods11091190
3. Jolley KA, Bray JE, Maiden MCJ. Open-access bacterial population genomics: BIGSdb software, the PubMLST.org website and their applications. Wellcome Open Res. 2018;3:124. https://doi.org/10.12688/wellcomeopenres.14826.1
4. Goyette-Desjardins G, Auger JP, Xu J, Segura M, Gottschalk M. *Streptococcus suis*, an important pig pathogen and emerging zoonotic agent—an update on the worldwide distribution based on serotyping and sequence typing. Emerg Microbes Infect. 2014;3:e45. https://doi.org/10.1038/emi.2014.45
5. Yongkiettrakul S, Maneerat K, Arechanajan B, Malila Y, Srimanote P, Gottschalk M, et al. Antimicrobial susceptibility of *Streptococcus suis* isolated from diseased pigs, asymptomatic pigs, and human patients in Thailand. BMC Vet Res. 2019;15:5. https://doi.org/10.1186/s12917-018-1732-5
6. Segura M. *Streptococcus suis* research: progress and challenges. Pathogens. 2020;9:707. https://doi.org/10.3390/pathogens9090707
7. Hatrongjit R, Fittipaldi N, Jenjaroenpun P, Wongsurawat T, Visetnan S, Zheng H, et al. Genomic comparison of two *Streptococcus suis* serotype 1 strains recovered from porcine and human disease cases. Sci Rep. 2023;13:5380. https://doi.org/10.1038/s41598-023-32724-z
8. Brizuela J, Roodsant TJ, Hasnoe Q, van der Putten BCL, Kozakova J, Slotved HC, et al. Molecular epidemiology of underreported emerging zoonotic pathogen *Streptococcus suis* in Europe. Emerg Infect Dis. 2024;30:413–22. https://doi.org/10.3201/eid3003.230348
9. Fittipaldi N, Collis T, Prothero B, Gottschalk M. *Streptococcus suis* meningitis, Hawaii. Emerg Infect Dis. 2009;15:2067–9. https://doi.org/10.3201/eid1512.090825
10. Prince-David M, Salou M, Marois-Créhan C, Assogba K, Plainvert C, Balogou KA, et al. Human meningitis due to *Streptococcus suis* in Lomé, Togo: a case report. BMC Infect Dis. 2016;16:651. https://doi.org/10.1186/s12879-016-2006-0
11. Raberahona M, Rasoanandrasana S, Rahajamanana VL, Ranaivo-Rabetokotany F, Andriananja V, Rakotomalala FA, et al. Novel *Streptococcus suis* sequence type 834 among humans, Madagascar. Emerg Infect Dis. 2018;24:391–2. https://doi.org/10.3201/eid2402.171138
12. Kennedy KJ, Jadeer AA, Ong CW, Senanayake SN, Collignon PJ. Two cases of *Streptococcus suis* endocarditis in Australian piggery workers. Med J Aust. 2008;189:413. https://doi.org/10.5694/j.1326-5377.2008.tb02100.x
13. Gomez-Torres J, Nimir A, Cluett J, Aggarwal A, Elsayed S, Soares D, et al. Human case of *Streptococcus suis* disease, Ontario, Canada. Emerg Infect Dis. 2017;23:2107–9. https://doi.org/10.3201/eid2312.171005
14. Callejo R, Zheng H, Du P, Prieto M, Xu J, Zielinski G, et al. *Streptococcus suis* serotype 2 strains isolated in Argentina (South America) are different from those recovered in North America and present a higher risk for humans. JMM Case Rep. 2016;3:e005066. https://doi.org/10.1099/jmmcr.0.005066
15. Nagel A, Manias V, Busquets N, Sniadowsky S, Anzardi J, Méndez EL. *Streptococcus suis* meningitis in an immunocompetent patient [in Spanish]. Rev Argent Microbiol. 2008;40:158–60.
16. Núñez JM, Marcotullio M, Rojas A, Acuña L, Cáceres M, Mochi S. First case of meningitis by *Streptococcus suis* in the northwest area of Argentina [in Spanish]. Rev Chilena Infectol. 2013;30:554–6. https://doi.org/10.4067/S0716-10182013000500014
17. Santoya Espinosa LC, Morán Díaz DF, Díaz Aguiar P, Rodríguez Arias EA. *Streptococcus suis* meningitis [in Spanish]. Medicina (B Aires). 2024;84:329–32.
18. Lopreto C, Lopardo HA, Bardi MC, Gottschalk M. Primary *Streptococcus suis* meningitis: first case in humans described in Latin America [in Spanish]. Enferm Infecc Microbiol Clin. 2005;23:110. https://doi.org/10.1157/13071618
19. da Silva NCZ, Varaschin PA, Castanho CR, dos Santos RS, Camargos VS, Garcia RAM, et al. *Streptococcus suis* meningitis in humans: the cause of emerging bacterial infectious diseases in Brazil? Case report. SN Compr Clin Med. 2020;2:2933–4. https://doi.org/10.1007/s42399-020-00617-1
20. de Matos FBP, Farias LABG, Dias CN, Mendes LP, Bessa PPdN. Meningitis due to *Streptococcus suis* in two patients with occupational exposure from northeastern Brazil. Case Rep Infect Dis. 2021;2021:5512303. https://doi.org/0.1155/2021/5512303
21. Ramos GSS, Rego RFDS, Oliveira MFF, Rocha VFD, Oliveira EP, Reis JN. *Streptococcus suis* meningitis: an emerging zoonotic disease in Brazil. Rev Soc Bras Med Trop. 2024;57:e00805. https://doi.org/10.1590/0037-8682-0610-2023
22. Razera RJ, Santos-Oliveira JV, Boaventura-Santos M, Almeida-Pontes V, Kanegae MY, Ardengh JC. A rare cause of septicemia after pork meat ingestion. Cureus. 2024;16:e62096. https://doi.org/10.7759/cureus.62096
23. Alarcón LP, Araya RP, Aguayo C, Fernández J, Illesca V, Zaror A, et al. Laboratory confirmation of *Streptococcus suis* in Chile [in Spanish]. Rev Chilena Infectol. 2013;30:539–40. https://doi.org/10.4067/S0716-10182013000500011
24. Koch E, Fuentes G, Carvajal R, Palma R, Aguirre V, Cruz C, et al. *Streptococcus suis* meningitis in pig farmers: report of first two cases in Chile [in Spanish]. Rev Chilena Infectol. 2013;30:557–61. https://doi.org/10.4067/S0716-10182013000500015
25. Moraga J, Fica A, Navarrete B, Henríquez R, Navarrete-Asenjo C. Meningitis and hypoacusia due to swine meat handling [in Spanish]. Rev Chilena Infectol. 2018;35:731–2. https://doi.org/10.4067/S0716-10182018000600731
26. Demar M, Belzunce C, Simonnet C, Renaux A, Abboud P, Okandze A, et al. *Streptococcus suis* meningitis and bacteremia in man, French Guiana. Emerg Infect Dis. 2013;19:1545–6. https://doi.org/10.3201/eid1909.121872
27. Grasiuso L, Rodríguez F, Aguerrebere P, Bone G, Pan C, Alzugaray P. Acute meningoencephalitis due to *Streptococcus suis*. Case report [in Spanish]. Rev Med Urug (Montev). 2024;40:e701. https://doi.org/10.29193/RMU.40.3.7
28. Ventura V, Soca A, Noveri S, Seija V, Perendones M, Sartori G. Streptococcus suis meningoencephalitis: first two cases reported in Uruguay [in Spanish]. Arch Med Int (Montev). 2015;37:80–2.
29. Nomoto R, Maruyama F, Ishida S, Tohya M, Sekizaki T, Osawa R. Reappraisal of the taxonomy of *Streptococcus suis* serotypes 20, 22 and 26: *Streptococcus parasuis* sp. nov. Int J Syst Evol Microbiol. 2015;65:438–43. https://doi.org/10.1099/ijs.0.067116-0
30. Gottschalk M, Higgins R, Boudreau M. Use of polyvalent coagglutination reagents for serotyping of *Streptococcus suis*.

J Clin Microbiol. 1993;31:2192–4. https://doi.org/10.1128/jcm.31.8.2192-2194.1993
31. Okura M, Lachance C, Osaki M, Sekizaki T, Maruyama F, Nozawa T, et al. Development of a two-step multiplex PCR assay for typing of capsular polysaccharide synthesis gene clusters of *Streptococcus suis*. J Clin Microbiol. 2014;52:1714–9. https://doi.org/10.1128/JCM.03411-13
32. Yamada R, Tien LHT, Arai S, Tohya M, Ishida-Kuroki K, Nomoto R, et al. Development of PCR for identifying *Streptococcus parasuis*, a close relative of *Streptococcus suis*. J Vet Med Sci. 2018;80:1101–7. https://doi.org/10.1292/jvms.18-0083
33. Athey TB, Teatero S, Lacouture S, Takamatsu D, Gottschalk M, Fittipaldi N. Determining *Streptococcus suis* serotype from short-read whole-genome sequencing data. BMC Microbiol. 2016;16:162. https://doi.org/10.1186/s12866-016-0782-8
34. Inouye M, Dashnow H, Raven L-A, Schultz MB, Pope BJ, Tomita T, et al. SRST2: rapid genomic surveillance for public health and hospital microbiology labs. Genome Med. 2014;6:90. https://doi.org/10.1186/s13073-014-0090-6
35. Alcock BP, Raphenya AR, Lau TTY, Tsang KK, Bouchard M, Edalatmand A, et al. CARD 2020: antibiotic resistome surveillance with the comprehensive antibiotic resistance database. Nucleic Acids Res. 2020;48:D517–25.
36. Kerdsin A, Hatrongjit R, Wongsurawat T, Jenjaroenpun P, Zheng H, Chopjitt P, et al. Comparative genome analysis of *Streptococcus suis* serotype 5 strains from humans and pigs revealed pathogenic potential of virulent, antimicrobial resistance, and genetic relationship. Microbes Infect. 2025;27:105273. https://doi.org/10.1016/j.micinf.2023.105273
37. Price MN, Dehal PS, Arkin AP. FastTree 2—approximately maximum-likelihood trees for large alignments. PLoS One. 2010;5:e9490. https://doi.org/10.1371/journal.pone.0009490
38. Xu S, Li L, Luo X, Chen M, Tang W, Zhan L, et al. *Ggtree*: a serialized data object for visualization of a phylogenetic tree and annotation data. iMeta. 2022;1:e56. https://doi.org/10.1002/imt2.56
39. Callejo R, Prieto M, Salamone F, Auger JP, Goyette-Desjardins G, Gottschalk M. Atypical *Streptococcus suis* in man, Argentina, 2013. Emerg Infect Dis. 2014;20:500–2. https://doi.org/10.3201/eid2003.131148
40. Wang J, Yi X, Liang P, Tao Y, Wang Y, Jin D, et al. Investigation of the genomic and pathogenic features of the potentially zoonotic *Streptococcus parasuis*. Pathogens. 2021;10:834. https://doi.org/10.3390/pathogens10070834
41. Huong VT, Ha N, Huy NT, Horby P, Nghia HD, Thiem VD, et al. Epidemiology, clinical manifestations, and outcomes of *Streptococcus suis* infection in humans. Emerg Infect Dis. 2014;20:1105–14. https://doi.org/10.3201/eid2007.131594
42. Ma E, Chung PH, So T, Wong L, Choi KM, Cheung DT, et al.; Collaborative Study Group on Streptococcus suis infection in Hong Kong. *Streptococcus suis* infection in Hong Kong: an emerging infectious disease? Epidemiol Infect. 2008;136:1691–7. https://doi.org/10.1017/S0950268808000332
43. Hlebowicz M, Jakubowski P, Smiatacz T. *Streptococcus suis* meningitis: epidemiology, clinical presentation and treatment. Vector Borne Zoonotic Dis. 2019;19:557–62. https://doi.org/10.1089/vbz.2018.2399
44. Tan JH, Yeh BI, Seet CS. Deafness due to haemorrhagic labyrinthitis and a review of relapses in *Streptococcus suis* meningitis. Singapore Med J. 2010;51:e30–3.
45. Tang J, Wang C, Feng Y, Yang W, Song H, Chen Z, et al. Streptococcal toxic shock syndrome caused by *Streptococcus suis* serotype 2. PLoS Med. 2006;3:e151. https://doi.org/10.1371/journal.pmed.0030151
46. Gottschalk M, Segura M, Xu J. *Streptococcus suis* infections in humans: the Chinese experience and the situation in North America. Anim Health Res Rev. 2007;8:29–45. https://doi.org/10.1017/S1466252307001247
47. Roppa L, Duarte ME, Kim SW. Invited review: pig production in Latin America. Anim Biosci. 2024;37:786–93. https://doi.org/10.5713/ab.23.0453
48. Blumetto O, Calvet S, Estellés F, Villagra A. Comparison of extensive and intensive pig production systems in Uruguay in terms of ethologic, physiologic and meat quality parameters. R Bras Zootec. 2013;42:521–9. https://doi.org/10.1590/S1516-35982013000700009
49. Retamal P, Gaspar J, Benavides MB, Saenz L, Galarce N, Aravena T, et al. Virulence and antimicrobial resistance factors in *Salmonella enterica* serotypes isolated from pigs and chickens in central Chile. Front Vet Sci. 2022;9:971246. https://doi.org/10.3389/fvets.2022.971246

Address for correspondence: Nahuel Fittipaldi, Groupe de recherche sur les maladies infectieuses en production animale, Faculté de médecine vétérinaire, Université de Montréal, 3200 Sicotte St, St-Hyacinthe, QC J2S 2M2, Canada; email: n.fittipaldi@umontreal.ca

Systematic Review of Contact Investigation Costs for Tuberculosis, United States

Garrett R. Beeler Asay, Kai H. Young, Tempest D. Hill, Gibril J. Njie

Contact investigation is a fundamental component of tuberculosis (TB) programs that drives prompt diagnosis and treatment of *Mycobacterium tuberculosis* infection among those exposed. Few studies have examined contact investigation costs for TB. We conducted a systematic review of TB contact investigation costs in the United States by searching English-language articles published during January 1990–August 2024 in electronic databases, including MEDLINE, Embase, CINAHL, and Scopus. We identified 2,920 titles and abstracts; 10 studies met our inclusion criteria. We abstracted costs for labor, diagnostic tests, and chest radiographs. Labor cost per contact was estimated at $175.94 (range $79.97–$293.51); total cost, including diagnostic testing and chest radiography, was $228.93 (range $132.95–$346.49).The overall cost of contact investigation in the United States was $9.94 (range $5.77–$15.04) million in 2022; total cost during 2013–2022 was $137.35 million. Contact investigations are essential to prevent TB and avert TB-related labor and diagnostic costs.

Tuberculosis (TB) is a leading cause of infectious disease deaths globally; an estimated 1.1 million deaths occurred in 2022 (*1*). The United States is considered a low TB-incidence country by the World Health Organization, having made great strides toward reducing TB incidence since 1993 (*2*). During 1993–2020, the annual number of TB cases in the United States declined by 64%, from 25,102 to 8,920 cases (*3*). However, after the COVID-19 pandemic resulted in global health disruptions in 2020, TB cases have increased each year; an increase of 16% during 2022–2023 has been reported (*4*).

Contact investigation is a critical activity conducted by public health departments to interrupt infectious disease transmission (*5*). Contact investigation incorporates case finding and classification, case interviews to identify contacts, evaluation and testing of high-risk contacts for the presence of *Mycobacterium tuberculosis* by using either the Mantoux tuberculin skin test (TST) or an interferon-γ release assay (IGRA), and establishing a system for tracking persons exposed to *M. tuberculosis* (*6*). In addition, TB programs provide treatment to persons who have either TB infection or disease (*5*,*7*). Contact investigation prevents TB transmission and, thereby, future TB cases and costs; 1 analysis estimated that during a 10-year period, outbreak investigations could avert 5,560 TB cases and $102 million in healthcare costs (*8*).

We conducted a systematic literature review to quantify the labor cost and resources needed to conduct TB contact investigations in US settings. Moreover, to estimate national total TB contact investigation costs over a 10-year period (2013–2022), we combined labor cost estimates from the systematic review with TB contact investigation data reported to the Centers for Disease Control and Prevention (CDC) and TB testing data from a privately insured population.

Methods

Evidence Acquisition

A multidisciplinary team consisting of TB scientists (T.H. and K.H.Y.), a health economist (G.R.B.A.), and a systematic review methodologist (G.J.N.) from the CDC's Division of Tuberculosis Elimination, National Center for HIV, Viral Hepatitis, STD, and TB Prevention, convened to conduct this systematic review. We used established economic evaluation methods adapted from the Guide to Community Preventive Services (*9*,*10*). We sought to answer the following research question: what are the per contact costs of TB contact investigations from a health system perspective? We included costs for personnel, materials, or

Author affiliation: Centers for Disease Control and Prevention, Atlanta, Georgia, USA

DOI: https://doi.org/10.3201/eid3107.241827

supplies related to contact investigation; laboratory and diagnostic testing; medications; transportation; public relations; and communications in the analysis.

Search Strategy and Inclusion Criteria

We consulted a librarian to search for published studies that evaluated the cost of TB outbreak and contact investigations. We searched electronic databases, including MEDLINE, Embase, CINAHL, and Scopus, for English-language articles published during January 1990–August 2024 (Figure 1). We used the following medical subject headings: "tuberculosis" OR "latent tuberculosis"; search terms were synonyms of "outbreak investigation," "epidemiological investigation," "contact investigation," AND "cost"; and "economic," "expense," "expenditure," AND "United States." We excluded articles if the study was not conducted in the United States, did not focus on drug-susceptible TB, or did not include contact investigation time or labor cost; if the cost information within the study was repeated from an earlier study; or if the study did not provide enough information to estimate labor cost per contact.

Cost Data Abstraction

We abstracted data on study and participant characteristics, including the setting, outbreak size, contact investigation strategy, and demographic information. Using the ingredients method (*11*), in which program costs are estimated by adding each component of cost, we abstracted direct program cost components for personnel, laboratory and diagnostic procedures, labor cost associated with contact investigation, public relations and communications, and other administrative costs. We included costs of chest radiographs (but not the cost of follow-up visits), directly observed therapy, and latent TB infection treatment, because those costs were associated more with treatment rather than with contact investigation. Any disagreement on data abstraction elements between reviewers (G.R.B.A. and G.N.J.) was resolved by consensus or by a third reviewer (K.H.Y.). For each included study, we assigned a quality rating according to criteria developed for The Community Guide (*12*). We rated studies as very good, good, satisfactory, or unsatisfactory; we excluded studies rated as unsatisfactory from the analysis.

Contact Investigation Labor Cost per Contact

For studies that reported person-hours required to conduct a contact investigation, we converted the reported person-hours to a monetary value by using region-specific wage data for a registered nurse according to the US Bureau of Labor Statistics (*13*). We estimated total compensation for labor by inflating wages by 30% to account for fringe benefits (*14*). No studies reported patient costs associated with contact investigation. We converted reported cost per case to cost per contact by dividing cost per case by the number of contacts per case. Although 2 studies reported costs of contact investigation for unconfirmed cases, we only reported mean contact investigation costs for confirmed cases, because sources did not report the number of contacts for unconfirmed cases, and

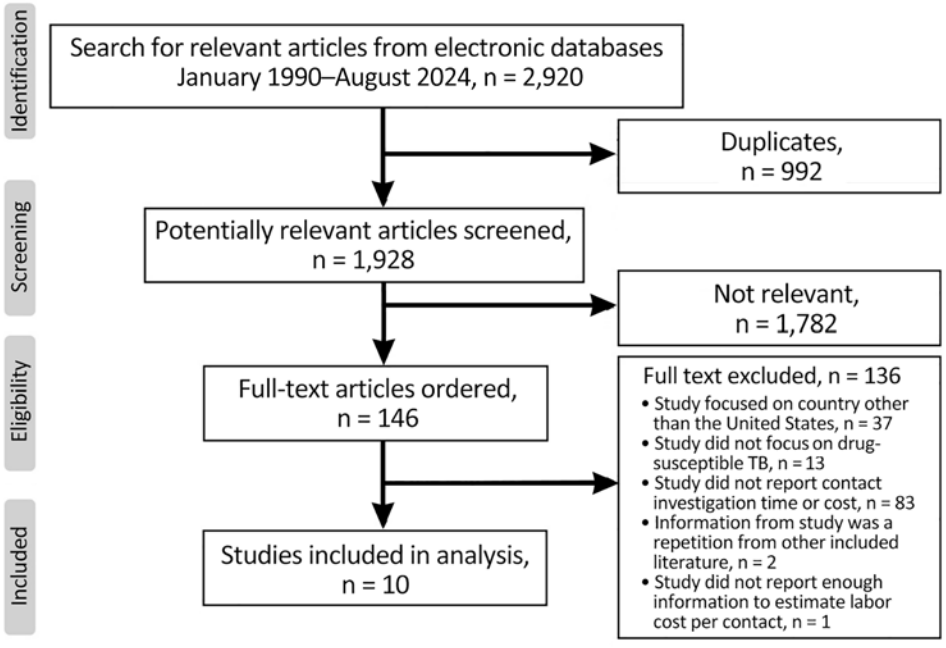

Figure 1. Flow diagram of studies identified, included, and excluded in systematic review of contact investigation costs for tuberculosis, United States. Diagram was generated from the Preferred Reporting Items for Systematic reviews and Meta-Analyses reporting guidelines template (https://www.prisma-statement.org).

some suspected cases were later identified to be non-TB cases. If a study reported labor costs that included TST costs, we used the TST cost value reported in the study. Otherwise, if the study did not report a cost for TST, we subtracted the Medicare reimbursement rate for TST costs in 2022 (*15*). We excluded reported surveillance and outbreak costs from the cost analyses because studies did not report costs in sufficient detail to determine those costs (*16*,*17*).

We updated all monetary values to 2022 US dollars by using the healthcare component of the Personal Consumption Expenditure Index from the Bureau of Economic Analysis (*18*). Because the cost data were limited in sample size and highly skewed, we used a nonparametric bootstrap to estimate the 95% CI by using the boot package in R version 4.4.1 (The R Project for Statistical Computing, https://www.r-project.org).

National Cost of Contact Investigation

To estimate the 2022 US national costs of contact investigation and the total 10-year costs of contact investigation during 2013–2022, we obtained data on contact investigation activities reported to CDC through the Aggregate Reports for Program Evaluation Contact Investigation form submitted through the CDC's National Tuberculosis Indicators Project web-based tool (*19*–*21*). In addition, we used aggregate report data on the number of contacts who tested positive for TB to estimate the percentage of contacts who might test positive and be referred for a chest radiograph (Appendix Table 1, https://wwwnc.cdc.gov/EID/article/31/7/24-1827-App1.pdf).

We used the MarketScan Truven Health commercially insured database (https://marketscan.truvenhealth.com/marketscanportal) to estimate the proportion of tests conducted during 2013–2022 according to paid claims for 3 diagnostic tests: TST, QuantiFERON-TB Gold (QFT) blood assay (QIAGEN, https://www.qiagen.com), and T-SPOT (Oxford Immunotec Ltd./Revvity, https://www.revvity.com) (*22*). Although some patients received >1 test, the analysis focused on claims for the first test (Appendix). For costs not reported by studies (e.g., cost of QFT and T-SPOT), we used published Medicare reimbursement rates (*15*,*23*). We assumed that all contacts received a test and that the tests were used at the same proportion as that in the MarketScan commercially insured population (Appendix).

Results

Our search strategy for this review identified 2,920 titles and abstracts. Of those, we determined 165 full-text articles were appropriate for review; 10 studies met the criteria for inclusion (Figure 1) (*7*,*16*,*17*,*24*–*30*). We judged all 10 studies as at least satisfactory quality, meeting the inclusion criteria (Appendix). Of the 10 included studies, we judged 6 were very good quality (*17*,*24*,*26*,*27*,*29*,*30*), 3 were good quality (*16*,*25*,*28*), and 1 was satisfactory quality (*7*).

Table 1. Studies included in systematic review of contact investigation costs for tuberculosis, United States

Characteristic	No. (%) studies, N = 10	References
Publication period		
1990s	2 (20)	(*16*,*27*)
2000s	2 (20)	(*7*,*29*)
2010s	5 (50)	(*17*,*25*–*28*)
2020s	1 (10)	(*30*)
Study location		
Northeast	1 (10)	(*26*)
Midwest	0 (0)	
South	4 (40)	(*17*,*25*,*28*,*29*)
West	3 (30)	(*7*,*24*,*30*)
Multistate	1 (10)	(*16*)
Other*	1 (10)	(*28*)
Setting		
Community	6 (60)	(*7*,*16*,*17*,*28*–*30*)
Healthcare	3 (30)	(*25*–*27*)
School	1 (10)	(*24*)

*Unknown location.

More than half (60%) of the included studies were published after January 1, 2010 (*17*,*24*–*26*,*28*,*30*); 2 studies were published in the early 2000s (*7*,*29*) and 2 in the 1990s (*16*,*27*) (Table 1). Most included studies were from the South Census region (*17*,*25*,*28*,*29*); 3 studies were from the West region (*7*,*24*,*30*), and 1 study was from the Northeast region (*26*). No studies were included from the Midwest region. Moreover, we included 1 multistate study (*16*) and 1 study with an unknown geographic location (*27*). Most studies were community-focused (*7*,*16*,*17*,*28*,*29*); other settings were hospitals (*25*–*27*) and 1 high school (*24*). Most (70%) studies comprised cost analyses; 2 studies consisted of cost-effectiveness analyses (*7*,*29*). One study provided person-hours for personnel involved in TB contact investigations without costs (*24*).

Contact Costs

We recorded outcomes for contact investigation costs and characteristics of the included studies (Table 2). Overall, the mean labor cost for contact investigation from the 10 studies was $175.94 (median $109.67) per contact in 2022 US dollars (*7*,*16*,*17*,*24*–*30*). The 95% nonparametric bootstrapped CI for the mean cost ($175.94) was $79.96–$293.51 (Figure 2). When stratified by setting, 6 studies from a community setting reported a mean labor cost of $251.98 (median $189.03) (*7*,*16*,*17*,*28*–*30*). Studies set in a hospital (n = 3) reported a lower mean labor cost of $72.95 (median $56.74) per contact (*25*–*27*), and 1 study

Table 2. Contact investigation costs for confirmed tuberculosis cases reported in systematic review, United States*

Reference	Setting	State(s)	No. cases investigated	No. contacts	Contact investigation costs, US $			
					Labor cost per contact	TST cost	Test follow-up and examination	Chest radiography
(*16*)	Community	AL, IL, NJ, TX, CA	26,283	NR	38.63	18.66	10.00	56.81
(*24*)†	School	CO	1	1,249	28.72	NR	NR	NR
(*25*)	Hospital	TX	59	880	114.18	NR	NR	NR
(*26*)†	Hospital	NY	34	1,394	56.74	NR	NR	NR
(*27*)	Hospital	NR	NR	81	47.94	14.99	88.30	NR
(*17*)	Community	TX	108	1,675	640.28	14.19	NR	NR
(*28*)	Community	NC	99	506	105.16	NR	NR	NR
(*29*)‡	Community	AL	NR	NR	349.73	NR	82.00	30.77
(*30*)	Community	CA	81	NR	235.77	NR	NR	NR
(*7*)	Community	CA	2,032	17,774	142.29	8.78	74.29	NR

*Review included 10 studies. Costs were updated to 2022 US dollars by using the healthcare component of the Personal Consumption Expenditure Price Index (*18*). NR, not reported; TST, tuberculin skin test.
†Labor time converted to labor cost by using the corresponding year's region-specific hourly wage for registered nurses from the US Bureau of Labor Statistics (*13*).
‡Included transportation cost.

conducted at a school reported a labor cost of $28.72 per contact (*24*). Among studies reporting cost per case, 3 were in a hospital setting (*25*–*27*) and 4 were in a community setting (*7*,*17*,*28*,*30*). Studies also reported costs per test for TST (n = 4; mean $15.95, median $14.59), cost of test follow-up (n = 4; mean $63.65, median $78.15), costs of chest radiographs per view (n = 2; mean and median $43.79), and surveillance and other outbreak-related costs per contact (n = 2; mean and median $33.34).

After applying the percentage of contacts who received each type of test (e.g., in 2022, 37.6% of patients received TSTs, 54.2% of patients received QFT tests, and 8.3% received T-SPOT tests) (*22*), we applied the costs of testing for TST ($15.95) and the 2022 Medicare reimbursement rates for QFT tests ($61.89) and T-SPOT tests ($100.00) to calculate a weighted average testing cost of $47.21. Finally, in 2022, 13.2% of contacts tested positive for TB and were referred for a chest radiograph (*19*) at a cost of $43.79 per patient, which yielded an average chest radiograph cost of $5.77 per contact. Therefore, adding testing and chest radiograph costs to labor costs yielded a total contact tracing cost per contact of $228.93 (range $132.95–$346.49).

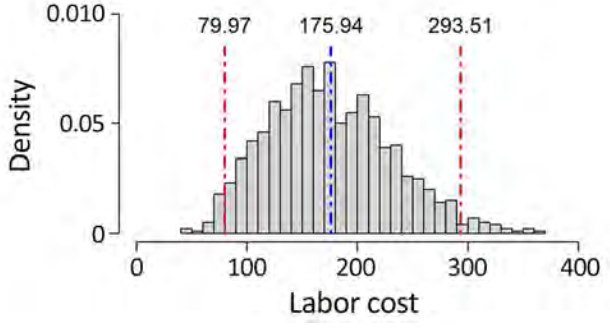

Figure 2. Density plot for labor costs of tuberculosis contact investigations in the United States. *y*-axis indicates bootstrapped probability density function (1,000 random sample draws). Costs per investigation were determined by using 2022 US dollar values. Blue dashed vertical line indicates the mean cost ($175.94); red dashed vertical lines indicate 95% CI ($79.96–$293.51).

National Cost of Contact Investigations

In 2022, jurisdictions across the United States reported conducting contact investigations for 33,576 contacts of persons with sputum smear–positive TB and 9,830 contacts of persons with sputum smear–negative, culture-positive TB (Appendix Table 1) (*19*). When extrapolating those costs to the US population, the estimated total US cost of contact investigations was $9.94 (range $5.77–$15.04) million. When totaled over the 10-year period (2013–2022), estimated contact investigation cost for health departments was $137.36 (range $75.61–$212.99) million (Appendix).

Discussion

Contact investigation is an essential part of the public health strategy for TB care and prevention and is inherently labor intensive at the local level. We identified a relatively small number of published studies compared with the large national expenses that we estimated. Therefore, more information about contact investigation costs could enable better treatment and prevention planning and elucidate how those costs vary.

Our analysis projected a substantial range ($80–$294) in labor cost per contact investigation. We generally were not able to fully account for differences in costs between studies. However, community settings had the greatest cost per contact investigation; those higher costs could be associated with greater travel and communication costs. Differences in costs could also be attributable to heterogeneity in the type of contact (e.g., household contacts vs. close contacts), which in turn could lead to differences in inherent

time spent per contact investigation. Furthermore, although this analysis accounted for costs associated with settings and labor, it is also possible that contact investigations with similar time commitments conducted by different agencies would expend greater (or less) resources simply on the basis of the locality and labor combination used. Differences in costs by locality also likely contribute to the labor cost uncertainty and, thus, the wide range in overall national costs. More information about specific costs expended by different US states or localities could help reduce the uncertainty associated with labor cost estimates.

The first limitation of our study is that some reports included costs not fully separable from overall contact investigation costs. For instance, 1 study included transportation costs; however, those transportation costs were not itemized and not separable from total costs (*29*). Similarly, not all studies delineated the type of staff conducting contact investigations, which could lead to differences in cost because of different compensation levels. Second, we did not account for surveillance costs, overhead, or other costs (e.g., telephone, computer, internet, and building costs), which could increase the estimated costs of contact investigation. Third, 4 of the 10 reports identified in this study were published before 2010, and more recent changes in TB testing and treatment could affect cost. For example, the increased use of IGRAs, which is more specific for *M. tuberculosis* infection, could reduce total contact investigation costs; fewer resources would be needed to address false-positive results that might be obtained from the less-specific TST (*6*). Nevertheless, the mean estimated cost per contact investigation for studies published after 2009 (n = 6) increased slightly from the overall mean to $196.80; however, that cost was still within the overall labor cost uncertainty interval. Recent improvements in telecommunication technologies (e.g., use of smart phones) also lowered communication costs that could affect contact investigation methods and costs. Finally, reported studies did not delineate the number of contacts used to estimate labor costs, and only 1 study provided a range ($0–$500) around the mean estimate of contact investigation costs (*29*). For this reason, we were not able to weight cost estimates by sample size or adjust for uncertainty across study estimates, which implies that users of those results should carefully consider the wide uncertainty range in addition to the mean estimate. Furthermore, our annual estimates of the proportion of patients tested by using TSTs or IGRA were derived from a sample representative of privately insured persons; estimates might differ among other types of insured populations.

Labor costs associated with contact investigation were 77% ($175.94) of the estimated total costs ($228.93) of contact investigation; contact investigations include labor costs for time spent eliciting and reaching out to contacts, as well as for diagnostic test costs and costs associated with chest radiographs. Costs associated with TB testing can sometimes be reimbursed or paid for by insurance, if the patient is insured. However, TB testing has a necessary preliminary step, which is identifying contacts who need testing by public health personnel and is often not accounted for nor reimbursable, potentially leading to underinvestment. Another key feature of contact investigation is that not all investigations are identical, and contact investigation effects and costs can vary across jurisdictions (*31*). We attempted to incorporate those differences by using nonparametric methods to estimate CIs. This method enabled skewed data to be reflected in asymmetric CIs, thereby enabling study heterogeneity to be reflected in cost ranges.

Our analyses only estimated the cost of contact investigation. A related study estimated a cost per gained quality-adjusted life year of $27,800 over a 10-year period (*8*). That cost per quality-adjusted life year estimate is lower than in other studies examining the cost-effectiveness of targeted testing and treatment of persons with latent TB infection, which typically ranged from $80,000 to $150,000 per gained quality-adjusted life year (*32*–*34*). The lower estimate implies that outbreak investigations might be one of the most cost-effective ways to prevent TB. Independent of cost-effectiveness, contact investigations are necessary to prevent the need for ongoing TB treatment and avert TB disease costs that are paid by patients, healthcare providers, and federal, state, and local health agencies.

In conclusion, we provide a national estimate of contact investigation costs for TB in the United States. Contact investigation, a core public health activity, directly identifies persons infected with TB and drives focused public health action to prevent TB-associated illness and death. Although contact investigations are essential to prevent TB, benefits only accrue when exposed contacts are identified and evaluated and when TB disease or *M. tuberculosis* infections are fully diagnosed and resolved through treatment.

Acknowledgments

We thank Joanna Taliano for her assistance in conducting the literature search and Andrew Hill, Ann Cronin, Carla Winston, Roque Miramontes, and Maureen Kolasa for guidance and support provided throughout the systematic review process.

About the Author

Dr. Beeler Asay is a senior economist in the Division of Tuberculosis Elimination, National Center for HIV, Viral Hepatitis, STD, and TB Prevention, Centers for Disease Control and Prevention. His research interests focus on public health costs associated with tuberculosis treatment, benefits of telemedicine for patients and providers, and the effects of disease on household finances.

References

1. World Health Organization. Global tuberculosis report 2023 [cited 2024 Nov 19]. https://www.who.int/publications/i/item/9789240083851
2. World Health Organization. Towards tuberculosis elimination: an action framework in low-incidence countries. 2014 [cited 2024 Nov 19]. https://www.who.int/publications/i/item/9789241507707
3. Centers for Disease Control and Prevention. Reported tuberculosis in the United States, 2023. November 2024 [cited 2025 Jun 5]. https://www.cdc.gov/tb-surveillance-report-2023/summary/national.html
4. Williams PM, Pratt RH, Walker WL, Price SF, Stewart RJ, Feng PI. Tuberculosis—United States, 2023. MMWR Morb Mortal Wkly Rep. 2024;73:265–70. https://doi.org/10.15585/mmwr.mm7312a4
5. National Tuberculosis Controllers Association; Centers for Disease Control and Prevention. Guidelines for the investigation of contacts of persons with infectious tuberculosis. Recommendations from the National Tuberculosis Controllers Association and CDC. MMWR Recomm Rep. 2005;54:1–47.
6. Mazurek GH, Jereb J, Lobue P, Iademarco MF, Metchock B, Vernon A. Guidelines for using the QuantiFERON-TB Gold Test for detecting *Mycobacterium tuberculosis* infection, United States. MMWR Recomm Rep. 2005;54:49–55.
7. Sprinson JE, Flood J, Fan CS, Shaw TA, Pascopella L, Young JA, et al. Evaluation of tuberculosis contact investigations in California. Int J Tuberc Lung Dis. 2003;7:S363–8.
8. Shrestha S, Cilloni L, Asay GRB, Kammerer JS, Raz K, Shaw T, et al. Model-based analysis of impact, costs, and cost-effectiveness of tuberculosis outbreak investigations, United States. Emerg Infect Dis. 2025;31:497–506. https://doi.org/10.3201/eid3103.240633
9. Carande-Kulis VG, Maciosek MV, Briss PA, Teutsch SM, Zaza S, Truman BI, et al.; Task Force on Community Preventive Services. Methods for systematic reviews of economic evaluations for the Guide to Community Preventive Services. Am J Prev Med. 2000;18:75–91. https://doi.org/10.1016/S0749-3797(99)00120-8
10. The Community Guide. Methods manual, part 2: economic review process [cited 2019 Jun 7]. https://www.thecommunityguide.org/pages/economic-review-methods.html
11. Levin HM, Belfield C. Guiding the development and use of cost-effectiveness analysis in education. J Res Educ Eff. 2015;8:400–18. https://doi.org/10.1080/19345747.2014.915604
12. Chattopadhyay SK, Jacob V, Hopkins DP, Lansky A, Elder R, Cuellar AE, et al.; Community Preventive Services Task Force. Community guide methods for systematic reviews of economic evidence. Am J Prev Med. 2023;64:569–78. https://doi.org/10.1016/j.amepre.2022.10.015
13. US Department of Labor, Bureau of Labor Statistics. May 2019 metropolitan and nonmetropolitan area occupational employment and wage estimates. 2019 [cited 2020 Sep 25]. https://www.bls.gov/oes/2019/may/oessrcma.htm
14. US Department of Labor, Bureau of Labor Statistics. Employer costs for employee compensation—December 2024. March 14, 2025 release [cited 2025 Jun 4]. https://www.bls.gov/news.release/pdf/ecec.pdf
15. Centers for Medicare and Medicaid Services. Physician fee schedule, 2022 [cited 2025 Jun 4]. https://www.cms.gov/medicare/physician-fee-schedule/search
16. Brown RE, Miller B, Taylor WR, Palmer C, Bosco L, Nicola RM, et al. Health-care expenditures for tuberculosis in the United States. Arch Intern Med. 1995;155:1595–600. https://doi.org/10.1001/archinte.1995.00430150057006
17. Miller TL, McNabb SJ, Hilsenrath P, Pasipanodya J, Drewyer G, Weis SE. The societal cost of tuberculosis: Tarrant County, Texas, 2002. Ann Epidemiol. 2010;20:1–7. https://doi.org/10.1016/j.annepidem.2009.09.004
18. Bureau of Economic Analysis. Personal consumption expenditures price index [cited 2023 Dec 21]. https://www.bea.gov/data/personal-consumption-expenditures-price-index
19. Centers for Disease Control and Prevention. 2022 ARPE contact investigations report [cited 2025 Jun 4]. https://www.cdc.gov/tb-data/arpe-reports/2022-contact-investigations.html
20. Centers for Disease Control and Prevention. 2020 contact investigations report (ARPE data) [cited 2025 Jun 4]. https://archive.cdc.gov/#/details?url=https://www.cdc.gov/tb/programs/evaluation/arpe-data.htm
21. Centers for Disease Control and Prevention. 2017 Contact Investigation Report (ARPE Data). Atlanta, (GA): Centers for Disease Control and Prevention; 2020.
22. Beeler Asay GR, Bohm MK. Tuberculosis diagnostic test use in the United States privately insured population, 2013–2022. Poster presented at: Joint Conference of The Union–North American Region and the National TB Coalition of America; Baltimore, MD, USA; 2024 Apr 16–19.
23. Centers for Medicare and Medicaid Services. Clinical laboratory fee schedule. 2022 [cited 2024 Nov 19]. https://www.cms.gov/medicare/payment/fee-schedules/clinical-laboratory-fee-schedule-clfs
24. Centers for Disease Control and Prevention. Transmission of *Mycobacterium tuberculosis* in a high school and school-based supervision of an isoniazid-rifapentine regimen for preventing tuberculosis—Colorado, 2011–2012. MMWR Morb Mortal Wkly Rep. 2013;62:805–9.
25. Cruz AT, Medina D, Whaley EM, Ware KM, Koy TH, Starke JR. Tuberculosis among families of children with suspected tuberculosis and employees at a children's hospital. Infect Control Hosp Epidemiol. 2011;32:188–90. https://doi.org/10.1086/657940
26. Kelly AM, D'Agostino JF, Andrada LV, Liu J, Larson E. Delayed tuberculosis diagnosis and costs of contact investigations for hospital exposure: New York City, 2010–2014. Am J Infect Control. 2017;45:483–6. https://doi.org/10.1016/j.ajic.2016.12.017
27. Kerr CM, Savage GT. Managing exposure to tuberculosis in the PACU: CDC guidelines and cost analysis. J Perianesth Nurs. 1996;11:143–6. https://doi.org/10.1016/S1089-9472(96)90003-9
28. Park PH, Holland DP, Wade A, Goswami ND, Bissette D, Stout JE. Public health costs for tuberculosis suspects in Wake County, North Carolina, United States. Int J Tuberc Lung Dis. 2013;17:759–63. https://doi.org/10.5588/ijtld.12.0739

29. Pisu M, Gerald J, Shamiyeh JE, Bailey WC, Gerald LB. Targeted tuberculosis contact investigation saves money without sacrificing health. J Public Health Manag Pract. 2009;15:319–27. https://doi.org/10.1097/PHH.0b013e31819c3ef2
30. Shiau R, Holmen J, Chitnis AS. Public health expenditures and clinical and social complexity of tuberculosis cases—Alameda County, California, July–December 2017. J Public Health Manag Pract. 2022;28:188–98. https://doi.org/10.1097/PHH.0000000000001356
31. Rainisch G, Jeon S, Pappas D, Spencer KD, Fischer LS, Adhikari BB, et al. Estimated COVID-19 cases and hospitalizations averted by case investigation and contact tracing in the US. JAMA Netw Open. 2022;5:e224042. https://doi.org/10.1001/jamanetworkopen.2022.4042
32. Beeler Asay GR, Woodruff R, Sanderson DM, Fisher CF, Marks SM, Green VD, et al. Cost-effectiveness of expanded latent TB infection testing and treatment: Lynn City, Massachusetts, USA. Int J Tuberc Lung Dis. 2024;28:21–8. https://doi.org/10.5588/ijtld.22.0654
33. Jo Y, Shrestha S, Gomes I, Marks S, Hill A, Asay G, et al. Model-based cost-effectiveness of state-level latent tuberculosis interventions in California, Florida, New York, and Texas. Clin Infect Dis. 2021;73:e3476–82. https://doi.org/10.1093/cid/ciaa857
34. Li Y, Marks SM, Beeler Asay GR, Winston CA, Pepin D, McClure S, et al. Effectiveness and cost-effectiveness of expanded targeted testing and treatment of latent tuberculosis infection among the Medicare population in 2022. Ann Intern Med. 2025;178:479–89. https://doi.org/10.7326/ANNALS-24-00870

Address for correspondence: Garrett R. Beeler Asay, Centers for Disease Control and Prevention, 1600 Clifton Rd NE, Mailstop H24-4, Atlanta, GA 30329-4018, USA; email: hrp9@cdc.gov

Assessing Readiness of International Investigations into Alleged Biological Weapons Use

Maximilian Brackmann, Anja Blasse, Júlio Gouveia Carvalho, Cindi R. Corbett, Cédric Invernizzi, Una Jakob, Stefan Kloth, Filippa Lentzos, Ines Mergler, Per Wikström

Without clarity if an outbreak is natural, accidental, or deliberate, infectious disease outbreaks of unknown or ambiguous origin can lead to speculation of a purposeful biological attack. Outbreaks in conflict settings are particularly prone to suspicions and allegations. In an increasingly confrontative global geopolitical landscape and with active information manipulation, outbreaks of ambiguous origin are likely to increase concerns of the deliberate use of biological agents. The United Nations General Assembly has agreed on and the United Nations Security Council has endorsed a mechanism to investigate allegations of deliberate use titled the United Nations Secretary-General's Mechanism for Investigation of Alleged Use of Chemical or Biological Weapons. A recent full-scale field exercise evaluated the deployment readiness of the mechanism and found it is well placed to investigate suspicious disease outbreaks, with room for continual improvement.

Unusual disease outbreaks are increasingly likely to raise suspicions about their origins, particularly during conflicts, when they might be accompanied by misinformation and active disinformation (*1*,*2*). Recent examples include the outbreak of Legionnaires' disease in Poland in a city serving as a hub for humanitarian and military aid to Ukraine (*1*,*2*) and the outbreak of Ebola virus disease in Uganda (*3*). Those outbreaks were accompanied by suspicions of deliberate release (*1*–*3*). Investigations into the source of disease outbreaks are typically conducted by local health authorities and inform measures taken to prevent further spread. In the Legionnaires' disease and Ebola virus disease outbreaks, careful and thorough investigations by local public health agencies revealed their natural origin (*3*–*7*).

If findings suggest the possibility of a deliberate origin, with indicators such as multiple geographically dispersed index cases with high sequence similarity of the infecting agent, unusually high lethality rates, atypical manifestations in humans or animals, an unusual infecting agent for the location or time of year, or suspicious circumstances linked to the outbreak, then a national law enforcement investigation might be initiated (*8*). To corroborate the investigation, especially in a conflict setting or in locations where political tensions are high, an international investigation might also be called for (*9*).

Investigating Disease Outbreaks with Unclear Origins

The use of a biological agent as a weapon or to deliberately cause harm is explicitly prohibited by the 1925 Geneva Protocol and implicitly prohibited by the 1972 Biological and Toxin Weapons Convention (BWC), which also bans development, production, acquisition, transfer, and stockpiling of biological weapons (*10*–*12*). However, those treaties do not currently provide a mandate to investigate allegations of biological weapons use. The text of the BWC only provides the option to lodge a complaint with the United Nations (UN) Security Council (UNSC) about possible breaches of the convention. There is no mechanism in place for the UNSC to act in response to such a complaint. To date, Russia is the only country

Author affiliations: Spiez Laboratory, Spiez, Switzerland (M. Brackmann, C. Invernizzi); Robert Koch Institute, Berlin, Germany (A. Blasse, S. Kloth, I. Mergler); Biological Defense Laboratory, Lisbon, Portugal (J.G. Carvalho); National Microbiology Laboratory, Winnipeg, Manitoba, Canada (C.R. Corbett); Peace Research Institute Frankfurt, Frankfurt, Germany (U. Jakob); King's College London, London, UK (F. Lentzos); Swedish Defense Research Agency FOI, Umea, Sweden (P. Wikström).

DOI: https://doi.org/10.3201/eid3107.240841

that has called for an investigation into a potential violation of the BWC through the UNSC, invoking Article VI of the convention in 2022. The UNSC did not accept the request for an investigation into the alleged violation. Independent of the UNSC, in which its composition, procedures, and political dynamics could make agreeing on an investigation difficult, an alternative investigation mechanism does exist. The UN Secretary-General's Mechanism for Investigation of Alleged Use of Chemical and Biological Weapons (UNSGM) was established by the UN General Assembly in 1987 and recognized by the UNSC in 1988 (*13*–*15*). The UNSGM was established after reports emerged of the use of chemical weapons during the 1980–1988 Iran–Iraq War.

The UN Office for Disarmament Affairs (UNODA) serves as the custodian of the UNSGM and maintains rosters of experts and laboratories the UN Secretary-General can consult and rely on when the mechanism is activated. All UN member states can nominate experts and laboratories to those rosters. The mission team would be selected, depending on the event particularities, from the roster of qualified experts. The various skills needed within the team depend on the circumstances of the mission but in most cases include interviewing and sampling skills to collect evidence. A further roster of expert consultants is available to advise the Secretary-General on many different aspects of the investigation, such as the credibility of the allegations, the composition of the mission team, or the feasibility of an on-site investigation. Expert consultants are high level specialists recognized in their fields of expertise. In addition, a network of rostered analytical laboratories is available to receive and analyze samples taken by a mission team (*13*).

Any UN member state can bring an instance of alleged use of chemical, toxin, or biological weapons to the attention of the Secretary-General and request an investigation. The Secretary-General then decides whether to launch a mission on the basis of the information submitted by the member state, and "… only in extraordinary circumstances would the Secretary-General not carry out an investigation at the site of the alleged incident…" (*16*). The countries concerned are expected to accept the investigation and cooperate with the mission team. The Secretary-General can request the advice of expert consultants on the report of alleged use of biological weapons "… and to develop continuously the measures required for the smooth conduct of the investigations" (*16*).

Once the Secretary-General deems an investigation is warranted, a team of qualified experts would conduct the investigation, likely including interviews and the collection of samples. Identical sets of samples would be sent to ≥2 rostered laboratories for analysis. Results of laboratory analyses would be reported to the mission team, which would then compile and present a final report to the Secretary-General, who communicates the results to all UN member states.

To date, the UNSGM has been activated 3 times, in each instance to investigate the alleged use of chemical weapons. The first investigation mission to Mozambique and the second to Azerbaijan were conducted in 1992. The Mozambique investigation was inconclusive, and the investigation in Azerbaijan did not find evidence of chemical weapon use (*17*). The third mission was conducted in 2013 in Syria with mission team members from several UN member states, the World Health Organization, and the Organization for the Prohibition of Chemical Weapons. The mission concluded that chemical weapons were used in 4 of the 7 instances under investigation (*17*).

The principles of the investigation mechanism are described in the guidelines and procedures of the UNSGM and their annexes (*18*). Those guidelines encourage UN member states to nominate experts to advise the Secretary-General (expert consultants) and those staffing a possible mission team (qualified experts). The guidelines also call for nominations of analytical laboratories (*16*). In all 3 categories, the western European and others group have nominated the most, followed by Asia and the Pacific region. Latin America and the Caribbean have the fewest nominations (*16*). Geographic representation on the mission team is necessary for the political credibility of investigation findings, and equitable representation of UN regions on the rosters remains a priority. In addition to nominations, the UNSGM Guidelines and Procedures asks member states to provide trainings and exercises for experts and laboratories.

Trainings and Exercises

Many countries support a range of activities to strengthen the UNSGM (*17*), such as providing quality assurance exercises for rostered laboratories (*19*). Other activities include developing training modules or guidance documents and hosting basic training or advanced skills courses for rostered experts. A structured training program for nominated qualified experts has been in place since 2017, including a basic training course laying the foundation and training the basics of the mechanism. After completing the basic training course, participants receive training on safe and secure approaches in field environments and specialized trainings on aspects of a mission. The

training courses encompass small practical modules with limited complexity to focus on specific aspects of an investigation mission. The basic training course includes a 2–3-day scenario-based exercise, in which participants can put the training into practice.

Larger-scale field exercises provide opportunities to simulate the entire investigation process of a mission, including mission planning; negotiations with local governments and relevant institutions; interviews with affected persons, medical staff, and other stakeholders; field sampling; laboratory identification and characterization of the agent; and reporting and media handling. Those large-scale field, or capstone, exercises are particularly valuable to test the alignment of different trainings with the requirements of a mission and to highlight potential areas to grow expertise.

The 2020 and 2022 Capstone Exercise

In September 2020, Germany hosted a predeployment tabletop exercise, held virtually because of COVID-19 travel restrictions. After that exercise, a 10-day full-scale field exercise in Berlin occurred 2 years later, in September 2022 (*20*). The simulated mission team consisted of 19 rostered experts from 16 countries selected by UNODA on the basis of their expertise and previous participation in basic training courses for the UNSGM. Proficiency of the qualified experts in English was necessary for the smooth conduct of the exercise and is likely also necessary for a real-world mission. Representatives from UNODA, the UN Internal Task Force, analytical laboratories, and expert consultants also participated in the exercise. This capstone exercise was the second time such an exercise was conducted for the UNSGM; the first was held in 2014.

The exercise scenario was set in a fictional UN member state with an outbreak of *Yersinia pestis* that was resistant to many antimicrobial drugs and cases of pneumonic and bubonic plague with human-to-human transmission that mainly occurred in refugees. In the scenario, German was the primary language spoken in the affected country, although many interviewees, border officials, and other country officials were proficient in English to varying degrees. The team was provided with interpreters for interviews with non–English-speaking interview partners. The affected country suspected a biological weapons attack on its refugee reception facilities by a neighboring country, with which it had a politically strained relationship. The affected country requested the UN Secretary-General to conduct a UNSGM investigation.

During the artificial deployment with the aim to conduct interviews and take samples (Figure 1), the mission team was confronted with challenging border crossings, host-country negotiations, media pressure, a delicate security situation, and high political tensions. Some of the situations were exacerbated by language barriers, which the team handled by using team members as translators. After the investigation was concluded, the mission head presented the findings in an interim report to fictional representatives of the UN.

The exercise was accompanied by an evaluation team of 10 observers, coordinated by the Swedish Defense Research Agency FOI, who summarized their observations in an evaluation report published in June 2023 (*21*). The authors of this manuscript were part of either the organizing or evaluation teams.

Key Lessons

The capstone exercise demonstrated the operational readiness of the UNSGM to be called on to investigate an allegation of biological weapons use. The exercise also demonstrated the training program for rostered experts was successful. The simulated mission team had a good understanding of the investigative process and of the UNSGM.

Field exercises are used and designed to demonstrate where there is room for continual improvement. In the capstone exercise, those key areas were identified (Figure 2). The importance of planning, both in terms of mission planning and operations planning, as well as adhering to a clear command-and-control plan and the need for familiarity with the technical equipment used, were highlighted by the exercise. The UNSGM does not list or provide a universally agreed-upon set of equipment required for

Figure 1. Environmental sampling of a mission team member during the 2020 and 2022 capstone exercises to strengthen international investigations of alleged biological weapons use. Photograph taken by Bernd Bruckmoser.

Figure 2. Design of the exercise scenario and learnings and recommendations deduced from the 2020 and 2022 capstone exercises to strengthen international investigations of alleged biological weapons use. UN, United Nations.

a UNSGM mission because of the specialized nature of the equipment required. Specific, fit-for-purpose equipment should be procured before each mission. The UN, member states, international organizations, or the private sector can provide any required equipment outside the standard UN equipment.

A large part of mission planning can be conducted before the mission starts, or even before a mission is requested, by having procedures and agreements in place for selecting the mission team members, having arrangements for equipment, and team members being aware of their roles and responsibilities. After the capstone exercise, efforts were made to address the issue of deployment timeliness with a workshop held by UNODA and VERTIC, which developed a predeployment package for qualified experts. Such preparations could shorten the time needed to prepare an investigation. A mission team is supposed to be dispatched within 48 hours after the UN Secretary-General decides to launch an investigation, and a timely investigation of a suspected biological attack increases the chances of obtaining conclusive results.

For sampling, the exercise illustrated the necessity of clarifying sampling site and sample prioritization and visual information recording. Because of the exercise, a dedicated course on sampling was developed. The exercise highlighted learnings related to sample processing, sample transfer, chain-of-custody, and analysis, which is reflected in the development of both the sampling course and a course in which qualified experts can obtain the required certification for shipment of infectious substances and toxins by the International Air Transport Association.

Any investigation of an alleged biological weapons incident will rest not only on biomedical and environmental samples but also on information gained from interviews. The capstone exercise highlighted the need to strengthen data-gathering from interviews and to train experts in the specialized interviewing skills required for such a particular investigation, which led to the establishment of a course on investigative interviewing.

Both participants and observers found that a clearer picture of the supportive and coordinative functions of the UN Internal Task Force would aid rostered experts in their roles. The importance of external communication was emphasized, and the evaluation team suggested additional training on when and how individual mission team members can practically and psychologically deal with social media pressure targeting the mission team or individual mission team members.

Conclusion

In the currently tense geopolitical climate, unusual disease outbreaks might be increasingly accompanied by information manipulation and disinformation campaigns, particularly in conflict zones. Suspicions and allegations about biological weapons are likely to become more frequent. Trends to this effect are already visible, such as in the allegations of BWC noncompliance and in disinformation campaigns on prohibited biological weapons-related activities, which formed a topic of formal consultations at the UN in Geneva, Switzerland, in 2022 (*22*–*24*). Allegations of actual use of biological weapons would have even more serious repercussions. A well-supported and well-functioning UNSGM, which can independently gather the evidence to confirm or refute allegations, is therefore in the

interest of all UN member states. Robust investigation capabilities are also in the interest of national authorities, and in particular public health authorities, whose credibility could be undermined by a bioweapons-related disinformation campaign. A concurrent advantage for member states to contribute to and participate in national activities that strengthen the UNSGM is to provide participants with relevant insights and considerations for investigating potential deliberate events. Such specialized insights and considerations are unique and can offer useful perspectives for national outbreak investigations.

Training and exercises to strengthen the UNSGM are solely funded through member states, and continued support is crucial for a well-resourced and rapidly deployable investigation team. Although the time between the first and the second capstone exercise was 8 years, future large-scale field exercises could be conducted more frequently. Field exercises combined with an augmented training schedule will support faster adaptation and evolution of training schemes and give more qualified experts the opportunity to test and refine their skills, contributing to a well-trained, regionally diverse roster of qualified experts willing and ready to offer their services to the UNSGM.

Acknowledgments

We thank Amanda R. Moodie for her support during the conduct of the exercise and for critical reading of the manuscript.

The capstone exercise was funded by the German Federal Foreign Office, the European Union, and the Weapons Threat Reduction Program of Canada. No funding was received for the preparation of this manuscript.

Author contributions: initial draft, M.B.; manuscript review and approval, all authors.

About the Author

Dr. Brackmann is a nuclear, biological, and chemical arms control expert at Spiez Laboratory, the Swiss Federal Institute for Nuclear, Biological, and Chemical Protection. His research interests include developing methods for the detection and characterization of viral and bacterial pathogens and toxins.

References

1. Boxerman A. Outbreak of legionnaires' disease in Poland kills 16. 2023 Aug 30 [cited 2024 Feb 5]. https://www.nytimes.com/2023/08/30/world/europe/poland-legionnaires-disease-rzeszow.html
2. Lentzos F, Bowsher G. Climate or conflict? Legionnaire's outbreak in Poland raises questions. 2023 [cited 2024 Feb 5]. https://thebulletin.org/2023/10/climate-or-conflict-legionnaires-outbreak-in-poland-raises-questions
3. Mwai P, Schraer R. Ebola in Uganda: the people spreading misinformation online. 2022 Nov 29 [cited 2024 Feb 5]. https://web.archive.org/web/20221129200151/https://www.bbc.com/news/63741125
4. Jain H, Sulaiman SA, Pokhrel P, Khan NU, Verma A. Unveiling the recent outbreak of *Legionella* in Poland: approaches and obstacles—an editorial. Ann Med Surg (Lond). 2023;85:5855–8. https://doi.org/10.1097/MS9.0000000000001434
5. World Health Organization. Legionellosis—Poland. 2023 Sep [cited 2024 Feb 5]. https://www.who.int/emergencies/disease-outbreak-news/item/2023-DON487
6. Reuters. Authorities investigate legionnaires' disease outbreak in Poland. 2023 Aug 25 [cited 2024 Feb 5]. https://www.reuters.com/world/europe/authorities-investigate-legionnaires-disease-outbreak-poland-2023-08-25
7. World Health Organization. Ebola outbreak 2022—Uganda. [cited 2024 Feb 5]. https://www.who.int/emergencies/situations/ebola-uganda-2022
8. Treadwell TA, Koo D, Kuker K, Khan AS. Epidemiologic clues to bioterrorism. Public Health Rep. 2003;118:92–8. https://doi.org/10.1016/S0033-3549(04)50224-8
9. Fooks AR, Holmstrom L. United Nations Secretary-General's Mechanism. Rev Sci Tech. 2017;36:629–37. https://doi.org/10.20506/rst.36.2.2680
10. United Nations Office for Disarmament Affairs. Biological weapons [cited 2024 Dec 18]. https://disarmament.unoda.org/biological-weapons
11. United Nations Office for Disarmament Affairs. 1925 Geneva protocol [cited 2024 Dec 18]. https://disarmament.unoda.org/wmd/bio/1925-geneva-protocol
12. Feakes D. The biological weapons convention. Rev Sci Tech. 2017;36:621–8. https://doi.org/10.20506/rst.36.2.2679
13. United Nations Office for Disarmament Affairs. Chemical and bacteriological (biological) weapons A/RES/42/37. 1987 [cited 2024 Feb 19]. https://docs.un.org/en/A/RES/42/37
14. United Nations Office for Disarmament Affairs. Chemical and bacteriological (biological) weapons A/RES/45/57. 1990 [cited 2024 Feb 19]. https://docs.un.org/en/A/RES/45/57
15. United Nations Security Council. Resolution 620 S/RES/620. 1988 [cited 2024 Feb 19]. https://docs.un.org/en/s/res/620(1988)
16. United Nations Office for Disarmament Affairs. Appendices to the Secretary General's Mechanism. [cited 2024 Feb 5]. https://disarmament.unoda.org/wmd/secretary-general-mechanism-old/appendices
17. United Nations Office for Disarmament Affairs. Secretary General's Mechanism for investigation of alleged use of chemical and biological weapons. [cited 2024 Feb 5] https://disarmament.unoda.org/wmd/secretary-general-mechanism
18. United Nations Office for Disarmament Affairs. UNSGM newsletter. 2024 Jun [cited 2025 Jan 8]. https://disarmament.unoda.org/wmd/unsgm-newsletter
19. Appelt S, Rohleder AM, Invernizzi C, Mikulak R, Brinkmann A, Nitsche A, et al. Strengthening the United Nations Secretary-General's Mechanism to an alleged use of bioweapons through a quality-assured laboratory response. Nat Commun. 2021;12:3078. https://doi.org/10.1038/s41467-021-23296-5
20. Robert Koch Institute. UNSGM project. [cited 2024 Feb 5]. https://www.rki.de/EN/Content/infections/biological/projects/UNSGM/UNSGM_node.html

21. Robert Koch Institute. Evaluation of the capstone exercise 2020 | 2022—executive report. 2023 Nov [cited 2024 Feb 5]. https://www.rki.de/EN/Content/infections/biological/projects/UNSGM/capstone_excercise.pdf
22. United Nations Office for Disarmament Affairs. Biological weapons convention—formal consultative meeting. 2022 [cited 2024 Feb 5]. https://meetings.unoda.org/bwc-fcm/biological-weapons-convention-formal-consultative-meeting-2022
23. United Nations Institute for Disarmament Research. The past, present and future of BWC Article V consultations. 2022 [cited 2024 Feb 12]. https://unidir.org/the-past-present-and-future-of-bwc-article-v-consultations
24. United Nations Meetings and Press Releases. United Nations unaware of any biological weapons programmes in Ukraine, top disarmament official affirms, as security council considers new claims by Russian federation. 2022 [cited 2022 May 18]. https://www.un.org/press/en/2022/sc14890.doc.htm

Address for correspondence: Maximilian Brackmann, Spiez Laboratory, Austrasse 1, 3700 Spiez, Switzerland; email: maximilian.brackmann@babs.admin.ch

Community Outbreak of OXA-48–Producing *Escherichia coli* Linked to Food Premises, New Zealand, 2018–2022

Craig N. Thornley, Matthew Kelly, Max Bloomfield, Loushy Mangalasseril, Annette Nesdale, Claire Underwood, Kristin Dyet, Juliet Elvy, Jenny Szeto, Hermes Perez, Xiaoyun Ren, Rosemary Woodhouse, Rhys T. White

In New Zealand, OXA-48–producing *Escherichia coli* is uncommon and typically associated with international travel. We investigated a cluster of 25 patients without recent travel history from Hutt Valley health district, New Zealand, who had multilocus sequence type 131 OXA-48–producing *E. coli* during August 2018–December 2022. Eighteen had been admitted to Hutt Valley Hospital but did not share a common ward or hospital service. Eighteen had visited the same community-based commercial food premises (premises A); 7 of those had not been admitted to Hutt Valley Hospital. An inspection of premises A revealed multiple hazards, primarily around staff hand hygiene. Four food handlers were colonized with OXA-48–producing *E. coli*; whole-genome sequencing confirmed genomic links between case and food handler strains, with possible introduction to New Zealand circa 2017. Community-based food premises have a role in propagating OXA-48–producing *E. coli* in high-income countries, requiring consideration in control strategies.

Carbapenemase-producing Enterobacterales (CPE) hydrolyze and inactivate carbapenems, the β-lactam antibiotic drugs with the broadest coverage spectrum, limiting treatment options for serious gram-negative infections and increasing rates of illness and death (*1*,*2*). The OXA-48 carbapenemase and variants (collectively termed OXA-48–like enzymes) demonstrate low-level hydrolysis of carbapenems. Despite that, they represent a potential source of clinical failure for β-lactams (*3*). They are also capable of spreading between strains and species because they are typically found on mobile genetic elements (*4*). Increasing global prominence of OXA-48–like carbapenemases has been attributed to horizontal spread through plasmids and vertical spread with multidrug-resistant clones (*5*), and $bla_{\text{OXA-48}}$ is one of the carbapenemase genes increasingly detected in *Escherichia coli* sequence type (ST) 131, a high-risk extraintestinal pathogenic *E. coli* lineage (*6*). In New Zealand (Aotearoa), CPE identification has increased since it was first detected in 2009 (*7*), but it remains uncommon and is typically associated with international travel or contact with travelers (*7*,*8*).

Transmission of CPE in healthcare settings has been well described (*9*,*10*), and guidance on CPE control has consequently focused on those environments (*11*). Although recognition of the importance of community acquisition of CPE is emerging (*12*,*13*), studies of transmission pathways have largely focused on within-household contact (*14*,*15*). CPE transmission might be more dynamic than current evidence suggests; research on other antibiotic-resistant Enterobacterales points to multifaceted source attribution (*16*,*17*), and similar patterns might exist for CPE. CPE have been detected in food-producing animals (*18*), in food (*19*), and among food handlers (*20*), and hospital foodborne transmission has occurred (*21*).

In August 2018, a series of patients living in Hutt Valley health district, New Zealand, without recent international travel history were found to have clinical infection with or carriage of OXA-48–producing *E. coli*, all of which were found to be multilocus ST 131. Because some of the patients had no recent hospitalizations, an investigation was undertaken to identify and control a possible common source.

Author affiliations: Health New Zealand Te Whatu Ora, Lower Hutt, New Zealand (C.N. Thornley, M. Kelly, L. Mangalasseril, A. Nesdale, C. Underwood); Awanui Labs Wellington, Wellington, New Zealand (M. Bloomfield); Institute of Environmental Science and Research, Porirua, New Zealand (K. Dyet, J. Elvy, J. Szeto, H. Perez, X. Ren, R. Woodhouse, R.T. White); Awanui Labs Dunedin, Dunedin, New Zealand (J. Elvy)

DOI: https://doi.org/10.3201/eid3107.250289

Methods

Setting

Hutt Valley health district consists of Lower Hutt and Upper Hutt local government areas and has a population of ≈150,970, which is predominantly urban and suburban. The district is served by a single main 322-bed public hospital, Hutt Valley Hospital (HVH); hospital inpatient wards consist predominantly of 4-bed rooms with a shared bathroom. Community and hospital diagnostic laboratory services for the district are provided by a single laboratory, Awanui Labs Wellington (an International Accreditation New Zealand ISO15189 accredited medical laboratory). Vitek MS is used for organism identification and Vitek II for antimicrobial susceptibility testing (both bioMérieux, https://www.biomerieux.com), using the AST N311 card and following European Committee on Antimicrobial Susceptibility Testing guidelines. All clinically significant Enterobacterales grown from clinical samples are screened for carbapenemase production according to guidelines (*22*) (Appendix, https://wwwnc.cdc.gov/EID/article/31/7/25-0289-App1.pdf).

Case Detection and Investigation

We defined cases as OXA-48–producing *E. coli* ST131 obtained from specimens collected for diagnostic purposes, routine surveillance of HVH inpatients, or hospital contact screening in Hutt Valley health district residents who had no recent international travel (Appendix). We compiled a case dataset to investigate CPE acquisition risk factors. We obtained data from hospital records for all inpatient admission episodes (defined as a hospital stay of >4 hours) during January 2015–February 2023. Data included admission dates, clinical services, and hospital locations, which we analyzed to determine whether ≥2 cases had concurrent admissions in the same ward. We interviewed case-patients using a schedule of questions on visits to ready-to-eat food premises, travel, use of health services abroad, household contacts, and other factors for a period covering the preceding 4 years (Appendix Table 1).

Enhanced Community Surveillance

To assess spread of the organism in the wider community, we conducted enhanced surveillance for CPE in routinely submitted urine and stool specimens for a fixed-term 8-month period during 2020–2021. This program applied lower laboratory thresholds for CPE screening than were used in routine processing of those samples (Appendix).

Environmental Investigation

We identified a community-based commercial food premises serving ready-to-eat food (premises A) from case interviews as a potential common exposure source. Food Act Officers undertook an environmental inspection in December 2018, with support from public health officials, that focused on hand hygiene, food storage, food preparation practices, customer bathrooms, and use of imported food. In July 2019, kitchen and bathroom surfaces, frequently touched items, and food samples were tested for *E. coli* (regardless of resistance phenotype) and CPE; testing of surfaces was repeated in January 2021 with the addition of water samples from kitchen sink drains, and further testing of surfaces occurred in June 2021 (Appendix). In May 2019 and November 2020, food handlers were invited to provide stool specimens to test for CPE; samples were processed using the same method as for the enhanced community surveillance, using an extended-spectrum β-lactamase (ESBL)/vancomycin-resistant *Enterococcus* (VRE) chromogenic agar (CHROMagar, https://www.chromagar.com) (Appendix). We interviewed those who tested positive regarding their travel history and healthcare use and collected data on their hospital attendance.

Confirmatory Testing and Whole-Genome Sequencing

We submitted all suspected CPE for confirmation and whole-genome sequencing (WGS) using the NextSeq 550 system (Illumina, https://www.illumina.com), generating 2 × 151-bp paired-end reads, at the New Zealand public health laboratory, the Institute of Environmental Science and Research, in Porirua, New Zealand. We also performed long-read sequencing (Oxford Nanopore Technologies, https://nanoporetech.com) on the index isolate to allow genome assembly and resolution of plasmid structure. We undertook nanopore read quality control, Illumina sequencing, genome assembly, multilocus sequence typing, virulence and antibiotic resistance gene genotyping, public data curation, and attempted estimation of the cluster emergence date (Appendix).

Ethics

The investigation was defined by the NZ Health and Disability Ethics Committees as a public health investigation and therefore approval was not required. CPE carriage is not a notifiable disease in New Zealand, and informed consent was obtained from all patients to access medical records and conduct case interviews.

Results

Case Investigation

During August 2018–December 2022, we identified 25 cases (Figure 1). All were detected through use of routine testing or surveillance protocols (Appendix). Of the 25 cases, 18 were first detected from urine samples; 11 were associated with uncomplicated urinary tract infections, 6 with asymptomatic bacteriuria, and 1 with pyelonephritis secondary to existing renal disease. Of the remaining 7 cases, 4 were detected on reflex testing of loose stool samples, 1 through a hospital contact screening stool sample, 1 through a blood culture associated with urosepsis, and 1 from tissue biopsy. Seven of the total cases were identified from community-collected samples (all urine); the remaining 18 cases were detected from samples collected in the hospital (11 from urine samples and 7 from non-urine samples). The median age of case-patients was 74 (range 37–94) years (Table 1). No single ward or hospital location was common to the 18 case-patients admitted to HVH. In 4 instances, 2 cases had concurrent same-ward admissions; in 3 instances, case-patients were admitted to a ward from which another case-patient had been discharged up to 7 days previously; those instances occurred in 7 different wards.

We identified a total of 44 ready-to-eat food premises in the exposure histories of the 24 case-patients interviewed (1 person died before interview). Only 2 premises had been visited by ≥3 case-patients: of those, 1 had been visited by 18 case-patients (premises A); the other had been visited by 7 case-patients, all of whom had also visited premises A. Of the 18 persons who had visited premises A, 7 had no HVH admission history. The time interval between their most recent premises A visit and collection of the clinical specimen that tested positive for OXA-48–producing *E. coli* ranged from <1 month to >48 months; 50% had visited within the previous 2-month period (Appendix Table 2).

Of the 7 case-patients without HVH admission, 4 had received no hospital-level healthcare since 2015. The remaining 3 case-patients had either been inpatients (n = 2) or outpatients (n = 1) at other hospitals in the region. Of the 7 case-patients with HVH admission but no definite premises A exposure, 2 had concurrent same-ward hospitalization with case-patients who had previous exposure to premises A. Of the 11 case-patients with both hospital admission and premises A exposure (Table 2), 2 had had concurrent admission with other case-patients before those persons' CPE diagnosis, none of whom had previous premises A exposure.

Enhanced Community Surveillance

Over the 8-month enhanced community surveillance program, we screened 217 stool samples and 2,050 urine samples from patients residing in the target suburbs. We detected no OXA-48–producing organisms in those samples.

Environmental Investigation

Premises A was registered with the local government and commenced operation in 2017 providing ready-to-eat food. Gender-specific toilets on the premises were used both by staff and customers. Multiple food safety concerns were identified during the first inspection in November 2018. The kitchen handwashing sink was not being used because of negligible water pressure and obstructed access. Food handlers used gloves, but glove changes and performance of hand hygiene measures were infrequent. Chopping

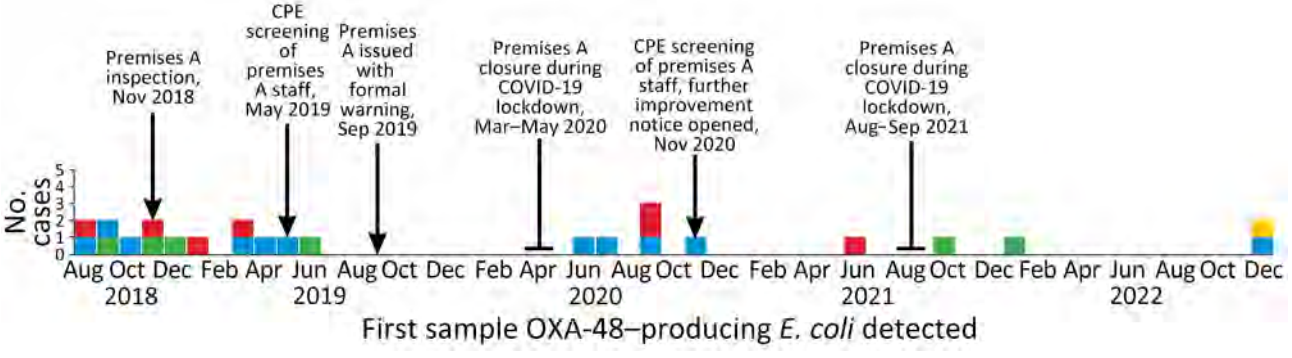

Figure 1. Epidemic curve of 25 cases of OXA-48–producing *Escherichia coli*, by month of sample collection, in study of community outbreak linked to food premises, Hutt Valley, New Zealand, August 2018–December 2022. Cases are categorized according to history of exposure to a community-based food premises (premises A) and history of inpatient admission to Hutt Valley Hospital (HVH) in the 4-year period before detection: 7 had been exposed to premises A but not HVH (red), 11 had been exposed both to premises A and to HVH (blue), 6 had been exposed to HVH but not to premises A (green), and 1 person had been exposed to HVH but premises A exposure was unknown (yellow). CPE, carbapenemase-producing Enterobacterales.

Table 1. Characteristics of 25 case-patients with OXA-48–producing *Escherichia coli* in study of community outbreak linked to a food premises, Hutt Valley, New Zealand, August 2018–December 2022

Category	No. (%) patients
Sex	
F	18 (72.0)
M	7 (28.0)
Ethnicity	
New Zealand European	20 (80.0)
Māori	4 (16.0)
Samoan	1 (4.0)
Specimen positive for OXA-48–producing *E. coli*	
Urine sample collected in community	7 (28.0)
Urine sample collected in hospital	11 (44.0)
Stool sample collected in hospital through loose stool	4 (16.0)
Blood culture	1 (4.0)
Tissue specimen	1 (4.0)
Stool sample collected in hospital through contact tracing	1 (4.0)
Infection associated with OXA-48–producing *E. coli*	
Uncomplicated urinary tract infection	11 (44.0)
Pyelonephritis/urosepsis	2 (8.0)
Osteomyelitis	1 (4.0)
No illness due to OXA-48–producing *E. coli*	11 (44.0)
Hospital exposure	
Hutt Valley Hospital admission	18 (72.0)
Wellington Regional Hospital admission	4 (16.0)
Any hospital admission in Wellington region	21 (84.0)
Healthcare use outside region or outside New Zealand	0
Other selected exposures*	
Exposure to specific community food premises (premises A)	18 (75.0)
Untreated drinking water	1 (4.2)
Recreational water exposure	5 (20.8)
Exposure to domestic animals	8 (33.3)
Exposure to farm animals	2 (8.3)

*Data on nonhealthcare exposures were available for only 24 cases, because 1 case-patient died before an interview could be undertaken.

boards were used without apparent segregation in usage between uncooked or cooked food, and equipment and food supplies were not well organized. Personal clothing items were present in the kitchen area, and the manager was laundering protective clothing at their home. Statutory measures under the Food Act 2014 were taken to address food safety concerns: improvement notices in June 2019 and November 2020 and a formal warning in September 2019. The premises closed during the New Zealand government-mandated COVID-19 lockdown periods in 2020 and 2021 (Figure 1).

No CPE was detected from surface swabs or food or water specimens in July 2019 or January 2021; however, non–OXA-48–producing *E. coli* were found in multiple sites, including frequently touched kitchen surfaces such as the microwave oven door handle and keypad, cash register, and service benchtop. All specimens collected in May 2021 tested negative for CPE and *E. coli*.

Stool specimens were obtained from 16 of 18 food handlers working in May 2019. OXA-48–producing *E. coli* was detected in 4 food handlers, 2 of whom were not residents in Hutt Valley health district; 1 had a history of travel to Thailand in 2017 but had no healthcare interaction abroad. All were asymptomatic, and none were treated with antibiotic drugs. Two had HVH admission history, neither concurrent

Table 2. Categorization of 24 case-patients with OXA-48–producing *Escherichia coli*, according to history of exposure to a community-based food premises and history of HVH admission, in study of community outbreak linked to a food premises, Hutt Valley, New Zealand, August 2018–December 2022*

Year of collection of sample from which OXA-48–producing *E. coli* was detected	No. with premises A exposure but no HVH inpatient admission	No. with premises A exposure and HVH inpatient admission	No. with HVH inpatient admission but no premises A exposure	Total no.
2018	2	3	3	8
2019	2	3	1	6
2020	2	4	–	6
2021	1	–	1	2
2022	–	1	1	2
Total	7	11	6	24

*Categorization of premises A and HVH exposure was only possible for 24 cases, because 1 case-patient died before interview could be undertaken. HVH, Hutt Valley Hospital; premises A, community-based food premises.

with case-patients; 1 person had undergone an outpatient procedure in a procedure room in which a case-patient was treated 4 days previously. After further testing in December 2020 (now of 11 staff members), 1 staff member had OXA-48–producing *E. coli*; this person was 1 of only 3 who had been working at the premises in 2019 and had returned a positive test at that time.

Microbiology

We identified a total of 48 CPE-producing organisms, 41 from the 25 case-patients and 7 from the 4 food handlers. All isolates were *E. coli* and possessed OXA-48 carbapenemase and CTX-M-174 ESBL genes. They were phenotypically resistant to ceftriaxone, aztreonam, ciprofloxacin, and sulfamethoxazole/trimethoprim and were susceptible to gentamicin, amikacin, nitrofurantoin, fosfomycin, mecillinam, colistin, and meropenem.

WGS

We sequenced and analyzed 33 isolates, with ≥1 from each case and each food handler (28 from case-patients and 5 from food handlers). The 33 draft genomes had a median total length of 5.03 Mb (interquartile range [IQR] 5.02–5.07 Mb; range 4.91–5.19 Mb), a median GC content of 50.8% (range 50.7%–50.8%), and a median N50 statistic of 138.65 kb (IQR 116.48–156.84 kb; range 69.37–183.45 kb). We characterized all 33 genomes as ST131 clade C. For context, we compared those 33 genomes against 12,185 ST131 clade C genome assemblies generated from publicly available sequence data (Appendix Figure 1, panel A). This analysis identified a cluster of 55 genomes. The genetic element $bla_{\text{OXA-48}}$ was located on a 7,872 bp Col-type plasmid (GenBank accession no. CP175693) (Appendix Table 5).

Further comparison with an already established dataset (*23*) confirmed that the 55-genome sublineage belongs to the ST131 clade C1/*H*30R sublineage (Appendix Figure 1, panel B). The 33 genomes formed a monophyletic cluster (Appendix Figure 2, panel A), with an observed median pairwise single-nucleotide variant (SNV) distance of 7 (IQR 4–12; range 0–56) SNVs. The phylogenetic analysis demonstrates that those 33 genomes share a common ancestor with the clinical strain Camb6978 (National Center for Biotechnology Institute Sequence Read Archive [https://www.ncbi.nlm.nih.gov/sra] BioProject no. ERR2538552), which was cultivated in 2016 from a patient with a bloodstream infection in Cambodia (*24*).

The outbreak isolates (n = 33) were closely related to ST131 genomes from other countries, predominantly Asia (n = 14/50, 28%) (Figure 2). Of note, genomes from Vietnam collected during 2012–2013 (*25*) appear to represent the earliest detections of this lineage. This lineage has since spread globally; representatives have been detected in Denmark (2014), France (2015 and 2018), Cambodia (2016), Ireland (2016), Thailand (2017), Australia (2018), Japan (2019), and now New Zealand (2018–2023). Screening isolates from food handlers cluster with other outbreak-associated genomes, underscoring their potential role in the dissemination of this outbreak strain (Figure 2). Furthermore, the other publicly available genomes lack the OXA-48 gene, indicating that the acquisition of this critical resistance gene likely occurred within the lineage between 2008 and 2018 (based on the 95% highest posterior density of key nodes). Evolutionary modeling estimates the cluster emerged during 2016–2018 (Appendix).

Discussion

We report a cluster of 25 patients with an OXA-48–producing ST131 *E. coli* detected from hospital and community specimens. The occurrence of a cluster of this magnitude was unprecedented in our district: during 2009–2017 in the Wellington region (of which Hutt Valley health district is part), 14 patients had been detected with CPE, only 3 of whom had OXA-48–producing Enterobacterales (K. Dyet, unpub. data). Our investigation suggests that the cluster was at least partially linked to a community-based food premises and that transmission from colonized food handlers to customers is a likely explanation.

In total, 4 food handlers found to be colonized with the outbreak strain were working at the premises; 1 was still colonized 18 months later. Concern around food as a vector for community CPE transmission has focused on food production (*26*); a complex interplay of influences includes veterinary antibiotic use and wildlife and environmental reservoirs (*27*). However, contamination from colonized food handlers is a plausible route of spread to ready-to-eat foods. In high-prevalence settings, food handlers are not uncommonly found to be CPE carriers (*28*), and highly dynamic patterns of colonization and recolonization are also not uncommon (*29*). *E. coli* transmission in food preparation environments linked to colonized food handlers has been demonstrated in community outbreaks of enteroaggregative, enterotoxigenic, and Shiga-toxigenic *E. coli* (*30*–*32*). A foodborne outbreak of ESBL-producing *Klebsiella pneumoniae* arising from hospital-prepared food detected the outbreak strain in specimens from kitchen workers, food preparation surfaces, and food items; although the role of the kitchen staff in propagating the outbreak was

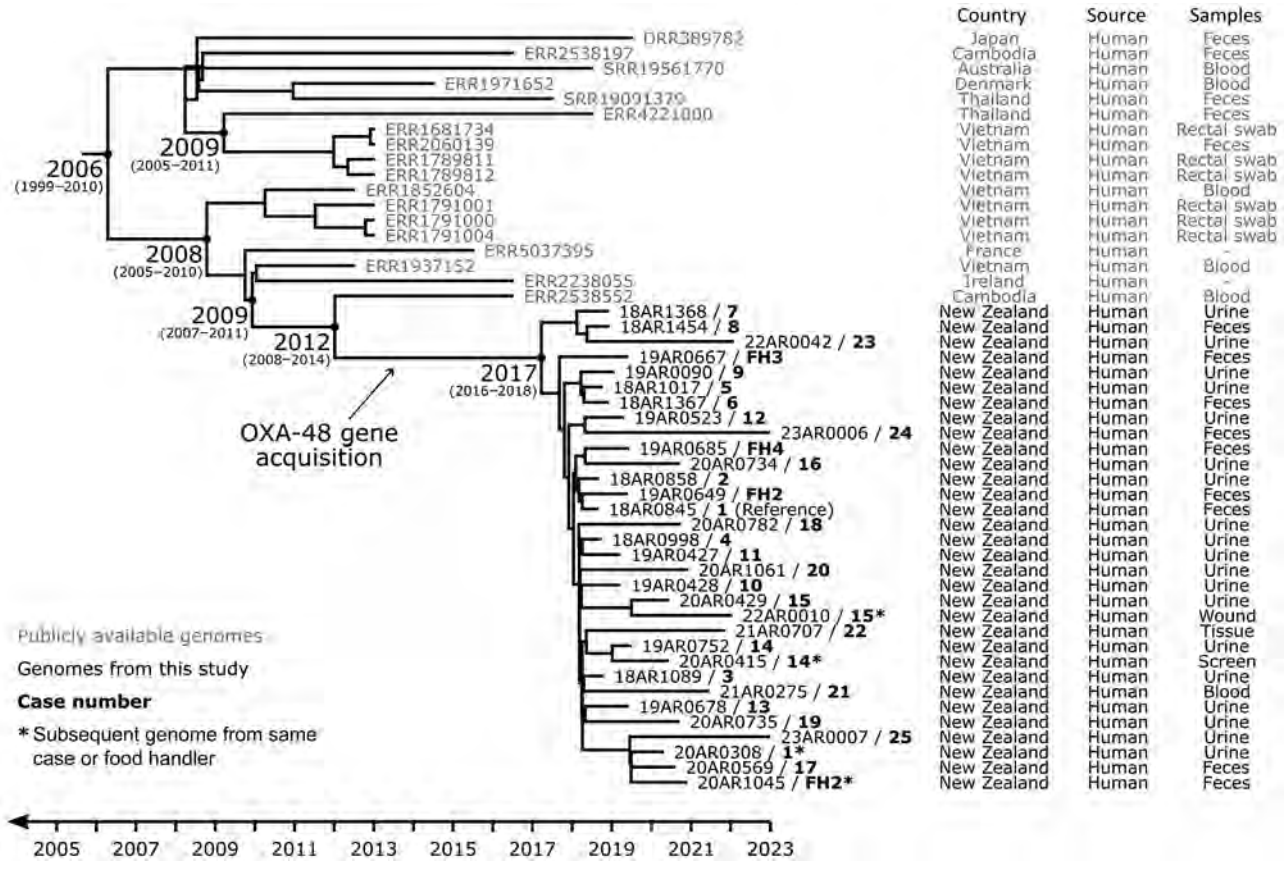

Figure 2. Evolutionary reconstruction for OXA-48–producing *Escherichia coli* sequence type (ST)131 genomes obtained from cases and food handlers compared with publicly available genomes in study of community outbreak linked to food premises, Hutt Valley, New Zealand, August 2018–December 2022. A time-calibrated maximum clade credibility tree was inferred from 323 nonrecombinant orthologous biallelic core-genome single-nucleotide variants (SNVs) from 50 ST131 genomes. SNVs were derived from a core-genome alignment of ≈4,767,900 bp and were called against the chromosome of 18AR0845 (GenBank accession no. CP175691). The x-axis represents the emergence time estimates. Case numbers (1–25), shown in bold after the genome codes, correspond to case reference numbers shown in Appendix Table 2 (https://wwwnc.cdc.gov/EID/article/31/7/25-0289-App1.pdf). Case numbers FH1–4 indicate genomes obtained from food handlers working at a community-based food premises to which 18 of the case-patients had been exposed. Asterisks indicate subsequent genomes obtained from the same case-patient or food handler.

unclear, evidence indicated that contaminated food was the vehicle for transmission (*33*). The outbreak reported in this study occurred in a population in which community CPE carriage is likely very rare (*7*). Detecting multiple cases within a relatively short period was highly unusual, which led to the subsequent investigation and source identification. This timing poses questions around how often foodborne spread of antimicrobial resistance mechanisms occurs but goes unnoticed in populations in which baseline community prevalence is higher.

Although our data suggest that the outbreak lineage likely originated abroad, possibly in Asia, the role of food handlers in importing the strain to New Zealand remains uncertain. One colonized food handler had traveled to Southeast Asia, but the sequencing data cannot definitively link that person's isolate to the introduction of the outbreak strain. Culturing and sequencing of samples from food handlers was conducted 9 months after the outbreak detection in August 2018; continuing bacteria evolution in this interval meant that the 2019 samples might not perfectly represent the strain initiating the outbreak. This factor highlights the challenge of linking transmission events retrospectively when there are delays in sampling and sequencing.

Poor hand hygiene practices are often identified in outbreaks from contaminated ready-to-eat food (*31*,*32*), and hand hygiene faults occur frequently (*34*). Among food handlers in long-term care facilities, hand cleanliness was negatively correlated with *E. coli* on food contact surfaces (*35*); pathogens on hands are less likely if gloves are worn, but hygiene advantages are lost without regular glove changes and hand

hygiene practices (*36*). In this outbreak, numerous food safety concerns were noted in the food premises, particularly hand hygiene practices and improper glove use, and *E. coli* was detected on food contact kitchen surfaces and high-touch points; although CPE was not detected, multiple possible food contamination pathways were present. Spread through other premise facilities (such as the shared toilets) was also possible, although CPE was not detected by testing. Use of toilets has been linked to CPE spread in healthcare environments independent of healthcare workers or person-to-person contact, including in a residential care home (*37*) and a hematological ward (*38*).

All case-patients without history of visiting premises A had been admitted to HVH; their CPE acquisition might have occurred through exposure to carriers in hospital or in the community. Nosocomial CPE transmission between patients with healthcare workers acting as possible intermediaries has been demonstrated previously in hospital outbreaks (*39*,*40*). Individual examples of community intrahousehold CPE transmission exist (*15*) but appear to be uncommon (*14*); in contrast, ESBL cocarriage and definite household transmission appears relatively frequent (*41*,*42*). Given the often-incidental case detection, further undetected carriers in the community might have been sources of transmission; however, the existence of a large pool of undetected community CPE carriage was not uncovered through enhanced community surveillance of routinely collected samples from residents from the area where case-patients lived.

The degree to which our findings can be generalized is limited. Case detection was often incidental; demographics and other case characteristics therefore skewed toward groups with higher frequency of hospital visits or higher likelihood of testing for urinary tract infection. Onset of case colonization or infection was unknowable; case exposure periods were therefore wide and approximate, potentially affecting accuracy of case-patients' exposure recollections. CPE was not detected in food, and so our assumption of a foodborne transmission pathway relies on circumstantial observations. We did not measure the epidemiologic association with premises A with an analytical study because of difficulties inherent in recruiting representative community controls willing to be tested for CPE colonization. Finally, the outbreak was likely larger than the number of detected cases, potentially because this organism was carbapenem-susceptible and so did not always grow reliably on standard CPE screening media (Appendix).

This outbreak raises the possible role of community food premises as a source of CPE transmission. It also demonstrates challenges with controlling community CPE spread. The justification for applying traditional individually focused public health communicable disease control measures (e.g., case restriction, identification and management of contacts) is weak in a context in which short-term health risk to ambulatory colonized persons is marginal, yet the long-term public health consequences from widespread CPE spread could be formidable. CPE colonization is not a notifiable health condition in New Zealand, limiting public health action to investigate and control spread. Those constraints are not peculiar to our context; guidelines for CPE control from other jurisdictions (*4*,*43*) are primarily oriented toward the healthcare sector, and community control focuses on antibiotic stewardship. CPE poses a daunting threat to the continued effectiveness of antibiotic treatment of gram-negative infections, and a greater understanding of the epidemiology of CPE in the community is required to develop comprehensive control strategies.

Acknowledgments

We thank Sarah Thomas, Steve Collinson, Russell Smithies, Shane Sturrock, Siobhan Murphy, Jen Randle, Nethmi Kearns, Sarah Bakker, Ernest Williams, Susan Morpeth, and Tomasz Kiedrzynski.

The study sequences are available under National Center for Biotechnology Information (NCBI) BioProject accession nos. PRJNA1102395 and PRJNA1097666. The raw Illumina sequence read data generated in this study have been deposited into the NCBI Sequence Read Archive; accession numbers are listed in Appendix Table 3 (https://wwwnc.cdc.gov/EID/article/31/7/25-0289-App1.pdf). The raw nanopore sequence read data for strain 18AR0845 has been deposited into the NCBI Sequence Read Archive (accession no. SRR31614413). The complete assembly for strain 18AR0845 has been deposited into GenBank (accession nos. CP175691–7.)

This work was supported by funding from the New Zealand Ministry of Health Manatū Hauora for surveillance of emerging resistance. This paper gives the views of the authors, and not necessarily the position of Health New Zealand Te Whatu Ora, Institute of Environmental Science and Research, or Awanui Labs.

About the Author

Dr. Thornley is a public health medicine specialist and medical officer of health at Health New Zealand Te Whatu Ora, National Public Health Service, Lower Hutt, New Zealand. His work focuses on communicable disease control, particularly tuberculosis, enteric infections, and disease outbreak investigation.

References

1. Tamma PD, Goodman KE, Harris AD, Tekle T, Roberts A, Taiwo A, et al. Comparing the outcomes of patients with carbapenemase-producing and non-carbapenemase-producing carbapenem-resistant *Enterobacteriaceae* bacteremia. Clin Infect Dis. 2017;64:257–64. https://doi.org/10.1093/cid/ciw741
2. Tischendorf J, de Avila RA, Safdar N. Risk of infection following colonization with carbapenem-resistant Enterobactericeae: a systematic review. Am J Infect Control. 2016;44:539–43. https://doi.org/10.1016/j.ajic.2015.12.005
3. Poirel L, Potron A, Nordmann P. OXA-48-like carbapenemases: the phantom menace. J Antimicrob Chemother. 2012;67:1597–606. https://doi.org/10.1093/jac/dks121
4. Australian Commission on Safety and Quality in Health Care. Recommendations for the control of carbapenemase-producing Enterobacterales (CPE). A guide for acute care health service organisations. Sydney: The Commission; 2021.
5. Peirano G, Pitout JDD. Rapidly spreading *Enterobacterales* with OXA-48-like carbapenemases. J Clin Microbiol. 2025;63:e0151524. https://doi.org/10.1128/jcm.01515-24
6. Kohlenberg A, Svartström O, Apfalter P, Hartl R, Bogaerts P, Huang T-D, et al. Emergence of *Escherichia coli* ST131 carrying carbapenemase genes, European Union/European Economic Area, August 2012 to May 2024. Euro Surveill. 2024;29:29. https://doi.org/10.2807/1560-7917.ES.2024.29.47.2400727
7. Blakiston M, Heffernan H, Roberts S, Freeman J. The clear and present danger of carbapenemase-producing Enterobacteriaceae (CPE) in New Zealand: time for a national response plan. N Z Med J. 2017;130:72–9.
8. Institute of Environmental Science and Research Limited. Carbapenemase-producing Enterobacterales (CPE) in New Zealand, 2022 [cited 2024 Aug 2]. https://www.esr.cri.nz/digital-library/2022-enterobacterales-with-acquired-carbapenemases
9. Segagni Lusignani L, Presterl E, Zatorska B, Van den Nest M, Diab-Elschahawi M. Infection control and risk factors for acquisition of carbapenemase-producing enterobacteriaceae. A 5 year (2011–2016) case-control study. Antimicrob Resist Infect Control. 2020;9:18. https://doi.org/10.1186/s13756-019-0668-2
10. Codjoe FS, Donkor ES. Carbapenem resistance: a review. Med Sci (Basel). 2017;6:1. https://doi.org/10.3390/medsci6010001
11. Tacconelli E, Cataldo MA, Dancer SJ, De Angelis G, Falcone M, Frank U, et al.; European Society of Clinical Microbiology. ESCMID guidelines for the management of the infection control measures to reduce transmission of multidrug-resistant Gram-negative bacteria in hospitalized patients. Clin Microbiol Infect. 2014;20(Suppl 1):1–55. https://doi.org/10.1111/1469-0691.12427
12. Kelly AM, Mathema B, Larson EL. Carbapenem-resistant Enterobacteriaceae in the community: a scoping review. Int J Antimicrob Agents. 2017;50:127–34. https://doi.org/10.1016/j.ijantimicag.2017.03.012
13. Temkin E, Bechor M, Lurie-Weinberger MN, Keren-Paz A, Chen D, Lugassy C, et al.; CPE Working Group. Population-based study of emergence and spread of *Escherichia coli* producing OXA-48-like carbapenemases, Israel, 2007–2023. Emerg Infect Dis. 2025;31:66–74. https://doi.org/10.3201/eid3101.240722
14. Jamal AJ, Faheem A, Farooqi L, Zhong XZ, Armstrong I, Boyd DA, et al. Household transmission of carbapenemase-producing Enterobacterales in Ontario, Canada. Clin Infect Dis. 2021;73:e4607–15. https://doi.org/10.1093/cid/ciaa1295
15. Blakiston M, Roberts SA, Freeman JT, Heffernan H. Household transmission of NDM-producing *E. coli* in New Zealand. N Z Med J. 2017;130:63–5.
16. Mughini-Gras L, Dorado-García A, van Duijkeren E, van den Bunt G, Dierikx CM, Bonten MJM, et al.; ESBL Attribution Consortium. Attributable sources of community-acquired carriage of *Escherichia coli* containing β-lactam antibiotic resistance genes: a population-based modelling study. Lancet Planet Health. 2019;3:e357–69. https://doi.org/10.1016/S2542-5196(19)30130-5
17. Allel K, Goscé L, Araos R, Toro D, Ferreccio C, Munita JM, et al. Transmission of gram-negative antibiotic-resistant bacteria following differing exposure to antibiotic-resistance reservoirs in a rural community: a modelling study for bloodstream infections. Sci Rep. 2022;12:13488. https://doi.org/10.1038/s41598-022-17598-x
18. Köck R, Daniels-Haardt I, Becker K, Mellmann A, Friedrich AW, Mevius D, et al. Carbapenem-resistant *Enterobacteriaceae* in wildlife, food-producing, and companion animals: a systematic review. Clin Microbiol Infect. 2018;24:1241–50. https://doi.org/10.1016/j.cmi.2018.04.004
19. Alelign D, Kidanewold A. Magnitude of extended-spectrum β-lactamase and carbapenemase producing *Enterobacteriaceae* among commonly vended street foods in Arba Minch town, southern Ethiopia. BMC Microbiol. 2023;23:393. https://doi.org/10.1186/s12866-023-03137-9
20. Sallem N, Hammami A, Mnif B. Trends in human intestinal carriage of ESBL- and carbapenemase-producing Enterobacterales among food handlers in Tunisia: emergence of C1-M27-ST131 subclades, bla_{OXA-48} and bla_{NDM}. J Antimicrob Chemother. 2022;77:2142–52. https://doi.org/10.1093/jac/dkac167
21. Pletz MW, Wollny A, Dobermann U-H, Rödel J, Neubauer S, Stein C, et al. A nosocomial foodborne outbreak of a VIM carbapenemase-expressing *Citrobacter freundii*. Clin Infect Dis. 2018;67:58–64. https://doi.org/10.1093/cid/ciy034
22. The European Committee on Antimicrobial Susceptibility Testing. Breakpoint tables for interpretation of MICs and zone diameters. Version 10.0, 2020 [cited 2024 Aug 21]. http://www.eucast.org/clinical_breakpoints
23. Kidsley AK, White RT, Beatson SA, Saputra S, Schembri MA, Gordon D, et al. Companion animals are spillover hosts of the multidrug-resistant human extraintestinal *Escherichia coli* pandemic clones ST131 and ST1193. Front Microbiol. 2020;11:1968. https://doi.org/10.3389/fmicb.2020.01968
24. Nadimpalli M, Vuthy Y, de Lauzanne A, Fabre L, Criscuolo A, Gouali M, et al.; BIRDY study group. Meat and fish as sources of extended-spectrum β-lactamase–producing *Escherichia coli*, Cambodia. Emerg Infect Dis. 2019;25:126–31. https://doi.org/10.3201/eid2501.180534
25. Trung NV, Matamoros S, Carrique-Mas JJ, Nghia NH, Nhung NT, Chieu TTB, et al. Zoonotic transmission of *mcr-1* colistin resistance gene from small-scale poultry farms, Vietnam. Emerg Infect Dis. 2017;23:529–32. https://doi.org/10.3201/eid2303.161553
26. Harding-Crooks R, Smith D, Fanning S, Fox EM. Dissemination of carbapenemase-producing Enterobacteriaceae and associated resistance determinants through global food systems. Compr Rev Food Sci Food Saf. 2023;22:2706–27. https://doi.org/10.1111/1541-4337.13159
27. Mairi A, Pantel A, Sotto A, Lavigne JP, Touati A. OXA-48-like carbapenemases producing *Enterobacteriaceae* in different

niches. Eur J Clin Microbiol Infect Dis. 2018;37:587–604. https://doi.org/10.1007/s10096-017-3112-7
28. Amare A, Eshetie S, Kasew D, Moges F. High prevalence of fecal carriage of extended-spectrum beta-lactamase and carbapenemase-producing Enterobacteriaceae among food handlers at the University of Gondar, Northwest Ethiopia. PLoS One. 2022;17:e0264818. https://doi.org/10.1371/journal.pone.0264818
29. Al-Mir H, Osman M, Drapeau A, Hamze M, Madec JY, Haenni M. Spread of ESC-, carbapenem- and colistin-resistant *Escherichia coli* clones and plasmids within and between food workers in Lebanon. J Antimicrob Chemother. 2021;76:3135–43. https://doi.org/10.1093/jac/dkab327
30. Shin J, Oh S-S, Oh K-H, Park J-H, Jang EJ, Chung GT, et al. An outbreak of foodborne illness caused by enteroaggregative *Escherichia coli* in a high school in South Korea. Jpn J Infect Dis. 2015;68:514–9. https://doi.org/10.7883/yoken.JJID.2014.460
31. Jain S, Chen L, Dechet A, Hertz AT, Brus DL, Hanley K, et al. An outbreak of enterotoxigenic *Escherichia coli* associated with sushi restaurants in Nevada, 2004. Clin Infect Dis. 2008;47:1–7. https://doi.org/10.1086/588666
32. Diercke M, Kirchner M, Claussen K, Mayr E, Strotmann I, Frangenberg J, et al. Transmission of shiga toxin-producing *Escherichia coli* O104:H4 at a family party possibly due to contamination by a food handler, Germany 2011. Epidemiol Infect. 2014;142:99–106. https://doi.org/10.1017/S0950268813000769
33. Calbo E, Freixas N, Xercavins M, Riera M, Nicolás C, Monistrol O, et al. Foodborne nosocomial outbreak of SHV1 and CTX-M-15-producing *Klebsiella pneumoniae*: epidemiology and control. Clin Infect Dis. 2011;52:743–9. https://doi.org/10.1093/cid/ciq238
34. Hoover ER, Masters M, Johnson J, McKelvey W, Hedeen N, Ripley D, et al. Restaurant and staff characteristics related to practices that could contribute to cross-contamination. J Food Prot. 2023;86:100182. https://doi.org/10.1016/j.jfp.2023.100182
35. Rodríguez M, Valero A, Posada-Izquierdo GD, Carrasco E, Zurera G. Evaluation of food handler practices and microbiological status of ready-to-eat foods in long-term care facilities in the Andalusia region of Spain. J Food Prot. 2011; 74:1504–12. https://doi.org/10.4315/0362-028X.JFP-10-468
36. Yap M, Chau ML, Hartantyo SHP, Oh JQ, Aung KT, Gutiérrez RA, et al. Microbial quality and safety of sushi prepared with gloved or bare hands: food handlers' impact on retail food hygiene and safety. J Food Prot. 2019;82:615–22. https://doi.org/10.4315/0362-028X.JFP-18-349
37. Bruins MJ, Koning Ter Heege AH, van den Bos-Kromhout MI, Bettenbroek R, van der Lubben M, Debast SB. VIM-carbapenemase-producing *Escherichia coli* in a residential care home in The Netherlands. J Hosp Infect. 2020;104:20–6. https://doi.org/10.1016/j.jhin.2019.08.012
38. Jolivet S, Couturier J, Vuillemin X, Gouot C, Nesa D, Adam M, et al. Outbreak of OXA-48-producing Enterobacterales in a haematological ward associated with an uncommon environmental reservoir, France, 2016 to 2019. Euro Surveill. 2021;26:2000118. https://doi.org/10.2807/1560-7917.ES.2021.26.21.2000118
39. Marmor A, Daveson K, Harley D, Coatsworth N, Kennedy K. Two carbapenemase-producing *Enterobacteriaceae* outbreaks detected retrospectively by whole-genome sequencing at an Australian tertiary hospital. Infect Dis Health. 2020;25:30–3. https://doi.org/10.1016/j.idh.2019.08.005
40. Miltgen G, Garrigos T, Cholley P, Deleume M, Allou N, Allyn J, et al. Nosocomial cluster of carbapenemase-producing *Enterobacter cloacae* in an intensive care unit dedicated COVID-19. Antimicrob Resist Infect Control. 2021;10:151. https://doi.org/10.1186/s13756-021-01022-6
41. Martischang R, Riccio ME, Abbas M, Stewardson AJ, Kluytmans JAJW, Harbarth S. Household carriage and acquisition of extended-spectrum β-lactamase-producing Enterobacteriaceae: a systematic review. Infect Control Hosp Epidemiol. 2020;41:286–94. https://doi.org/10.1017/ice.2019.336
42. Arcilla MS, van Hattem JM, Haverkate MR, Bootsma MCJ, van Genderen PJJ, Goorhuis A, et al. Import and spread of extended-spectrum β-lactamase-producing Enterobacteriaceae by international travellers (COMBAT study): a prospective, multicentre cohort study. Lancet Infect Dis. 2017;17:78–85. https://doi.org/10.1016/S1473-3099(16)30319-X
43. UK Health Security Agency. Actions to contain carbapenemase-producing Enterobacterales [cited 2024 Sep 11]. https://www.gov.uk/government/publications/actions-to-contain-carbapenemase-producing-enterobacterales-cpe

Address for correspondence: Craig N. Thornley, National Public Health Service, Level 1, Community Health Building, Hutt Valley Hospital, 638 High St, Boulcott, Lower Hutt 5010, New Zealand; email: craig.thornley@tewhatuora.govt.nz

Multicenter Case–Control Study of Behavioral, Environmental, and Geographic Risk Factors for Talaromycosis, Vietnam

Lottie Brown,[1] Brian Jonat,[1] Vo Trieu Ly, Nguyen Le Nhu Tung, Pham Si Lam, Nguyen Tat Thanh, Dang Thi Ngoc Bich, Vu Phuong Thao, Nguyen Thi Mai Thu, Ngo Thi Hoa, Thuy Le

Medscape CME Activity

In support of improving patient care, this activity has been planned and implemented by Medscape, LLC and Emerging Infectious Diseases. Medscape, LLC is jointly accredited with commendation by the Accreditation Council for Continuing Medical Education (ACCME), the Accreditation Council for Pharmacy Education (ACPE), and the American Nurses Credentialing Center (ANCC), to provide continuing education for the healthcare team.

Medscape, LLC designates this Journal-based CME activity for a maximum of 1.00 ***AMA PRA Category 1 Credit(s)™***. Physicians should claim only the credit commensurate with the extent of their participation in the activity.

Successful completion of this CME activity, which includes participation in the evaluation component, enables the participant to earn up to 1.0 MOC points in the American Board of Internal Medicine's (ABIM) Maintenance of Certification (MOC) program. Participants will earn MOC points equivalent to the amount of CME credits claimed for the activity. It is the CME activity provider's responsibility to submit participant completion information to ACCME for the purpose of granting ABIM MOC credit.

All other clinicians completing this activity will be issued a certificate of participation. To participate in this journal CME activity: (1) review the learning objectives and author disclosures; (2) study the education content; (3) take the post-test with a 75% minimum passing score and complete the evaluation at https://www.medscape.org/qna/processor/74573?showStandAlone=true&src=prt_jcme_eid_mscpedu; and (4) view/print certificate. For CME questions, see page 1500.

NOTE: It is the policy of Medscape Education to avoid the mention of brand names or specific manufacturers in accredited educational activities. However, trade and manufacturer names in this activity are provided in an effort to provide clarity. The use of brand or manufacturer names should not be viewed as an endorsement by Medscape of any specific product or manufacturer.

Release date: June 23, 2025; Expiration date: June 23, 2026

Learning Objectives

Upon completion of this activity, participants will be able to:

- Analyze the epidemiology and outcomes of talaromycosis
- Assess demographic and clinical characteristics of patients with talaromycosis
- Evaluate potential risk factors for talaromycosis
- Distinguish geographic patterns for infection with talaromycosis

CME Editor

Jill Russell, BA, Technical Writer/Editor, Emerging Infectious Diseases. *Disclosure: Jill Russell, BA, has no relevant financial relationships.*

CME Author

Charles P. Vega, MD, Health Sciences Clinical Professor of Family Medicine, University of California, Irvine School of Medicine, Irvine, California. *Disclosure: Charles P. Vega, MD, has the following relevant financial relationships: served as consultant or advisor for Boehringer Ingelheim Pharmaceuticals, Inc.; Exact Sciences Corporation.*

Authors

Lottie Brown, MD; Brian Jonat, MD; Vo Trieu Ly, MD, PhD; Nguyen Le Nhu Tung, MD; Pham Si Lam, MD; Nguyen Tat Thanh, MD; Dang Thi Ngoc Bich, MD; Vu Phuong Thao, PhD; Nguyen Thi Mai Thu, MSc; Ngo Thi Hoa, PhD; Thuy Le, MD, PhD.

Talaromycosis is a life-threatening fungal disease that primarily affects immunocompromised persons in Southeast Asia. We conducted a multicenter, case–control study recruiting participants with advanced HIV disease in Vietnam; 205 case-patients with culture-confirmed talaromycosis were matched to 405 control-patients by age, sex, and CD4 count. Occupational exposure to tropical plants (odds ratio [OR] 1.73 [95% CI 1.10–2.73]; p = 0.017) and to farmed animals (OR 2.07 [95% CI 1.20–3.55]; p = 0.009) were independent risk factors for talaromycosis. Talaromycosis risk was higher in participants from highland regions than in persons from lowland regions (p<0.05). Participants from lowland regions who had lived or traveled to highland regions had a higher risk for talaromycosis (OR 3.15 [95% CI 1.49–6.64]; p = 0.003). This study confirms the epidemiologic correlation between talaromycosis and soil exposure and demonstrates an epidemiologic link between talaromycosis and residence in or travel to highland regions of Vietnam.

Talaromycosis (formerly penicilliosis) is an invasive fungal disease caused by *Talaromyces marneffei*, a dimorphic fungus endemic to Southeast Asia. First discovered in captive wild bamboo rats (*Rhizomys sinensis*) in Vietnam in 1956, talaromycosis remained rare in humans until the onset of the HIV epidemic in the 1980s, when it rapidly emerged as a leading HIV-associated opportunistic infection and cause of HIV-associated death in Southeast Asia (*1*,*2*). The highest reported disease burden is in northern Thailand, Vietnam, and southern China, where talaromycosis accounts for 4%–20% of HIV-related hospital admissions and the mortality rate, despite antifungal treatment, is between 15% and 30% (*2*–*7*). Outside of those hyperendemic regions, talaromycosis is likely underdiagnosed, and the true burden of disease across Southeast Asia remains unknown (*7*,*8*). Although most cases (≈90%) are associated with advanced HIV disease, the incidence of talaromycosis is rising among persons with other immunocompromising conditions, such as primary immunodeficiency, malignancy, solid organ or stem cell transplant, and autoimmune or inflammatory conditions that require immunomodulating therapy (*9*–*11*). Cases are increasingly reported outside of talaromycosis-endemic regions because of increased migration and international travel (*8*).

A lack of understanding of disease reservoirs and exposure risk factors for talaromycosis has hampered disease prevention. The bamboo rat is the only known enzootic reservoir of *T. marneffei*. Surveys of rodents in talaromycosis-endemic regions have identified all 4 species of bamboo rat in Southeast Asia (*R. sinensis, R. pruinosis, R. sumatrensis,* and *Cannomys badius*) (Appendix Figure 1, https://wwwnc.cdc.gov/EID/article/31/7/25-0143-App1.pdf) as asymptomatic carriers of *T. marneffei*; reported prevalence ranges from 10% to 100% (*12*–*15*). The geographic distribution of bamboo rats follows the distribution of human talaromycosis (Appendix Figure 2), and *T. marneffei* isolates from bamboo rats have been shown to share similar genotypes to those infecting humans in the same region (*16*,*17*), suggesting the potential for bamboo rat–to–human transmission. However, epidemiologic evidence of direct bamboo rat–to–human transmission is lacking. A case–control study conducted in Chiang Mai, a rural and mountainous region of Thailand where bamboo rats are endemic, demonstrated no link between exposure or consumption of bamboo rats and human talaromycosis. Instead, agricultural work and soil exposure, particularly during the rainy season, were independent risk factors for talaromycosis (*18*). Because *T. marneffei* has been isolated more frequently in soil samples collected from bamboo rat burrows than from non–bamboo rat habitats (*16*,*19*), we hypothesize that exposure to soil associated with bamboo rats could be the primary driving factor for talaromycosis, rather than direct exposure to bamboo rats.

Aside from soil exposure, weather factors have a substantial effect on talaromycosis incidence. During the monsoon season, the incidence of talaromycosis rises 30% in Vietnam, 50% in Thailand, and 73% in southern China from that observed during the dry season and has been associated with increased temperatures and humidity, which provide favorable environmental conditions for *T. marneffei* (*4*,*6*,*20*,*21*). Talaromycosis is also known to occur in geographic hot spots in mountainous areas of Southeast Asia,

Author affiliations: City St. George's Hospital and St. George's University, London, UK (L. Brown); Boehringer Ingelheim Pharmaceuticals, Inc., Ridgefield, Connecticut, USA (B. Jonat); Tropical Medicine Research Center for Talaromycosis, Pham Ngoc Thach University of Medicine, Ho Chi Minh City, Vietnam (V.T. Ly, N.T. Hoa, T. Le); Hospital for Tropical Diseases, Ho Chi Minh City (V.T. Ly, N.L.N. Tung); Oxford University Clinical Research Unit, Ho Chi Minh City (P.S. Lam, N.T. Thanh, N.T. Hoa); National Hospital for Tropical Diseases, Hanoi, Vietnam (D.T.N. Bich); Saskatchewan Cancer Agency, Regina, Saskatchewan, Canada (V.P. Thao); Duke University Medical Center, Durham, North Carolina, USA (N.T.M. Thu, T. Le)

DOI: https://doi.org/10.3201/eid3107.250143

[1]These authors contributed equally to this article.

such as the northern provinces of Chiang Mai and Chiang Rai in Thailand, the southern provinces of Guangdong and Guangxi in China, and the northeastern states of Manipur and Assam in India (*22*). Vietnam presents a unique opportunity to study the geographic and exposure risk factors for talaromycosis because talaromycosis occurs across diverse climatic and geographic ranges, from the temperate, subtropical regions in the north to the tropical monsoon regions in the south (Figure, panel A). Three quarters of the land in Vietnam is composed of highlands (defined as hills and mountains ≥400 m above sea level), which include the Northeast and Northwest regions in the north and the Central Highland region in the south. The remaining one quarter of the land consists of lowlands, which include the Red River Delta in the north, the coastline, and the Mekong Delta in the south. Talaromycosis is seen in both rural and urban settings in Vietnam, where risk factors for infection might be very different than in the rural settings of Chiang Mai, Thailand (*18*). This study aimed to evaluate the behavioral, environmental, and geographic risk factors for talaromycosis in the diverse climatic and geographic setting of the hyperendemic country of Vietnam.

Methods

Study Design and Participants

We conducted a multicenter, matched, case–control study recruiting participants with advanced HIV disease from the inpatient and outpatient departments of the National Hospital for Tropical Diseases (Hanoi, Vietnam) and the Hospital for Tropical Diseases (Ho Chi Minh City, Vietnam), during January 2013–July 2016. Those hospitals were estimated to receive 40% of all HIV inpatient referrals in Vietnam, which has a catchment population of 72 million. We predetermined risk factors of interest (n = 13) after a comprehensive literature review and included behavioral, environmental, and geographic risk factors (Table 1).

We consecutively recruited participants from a population of adults with HIV ≥18 years of age with a CD4 cell count <100 cells/μL who had culture-proven talaromycosis (defined as a compatible clinical syndrome and isolation of *T. marneffei* in blood, skin lesion, bone marrow, lymph node, or other specimens as clinically indicated). We consecutively recruited control-patients who came from the same at-risk population but had no clinical suspicion for or microbiological evidence of talaromycosis. To reduce

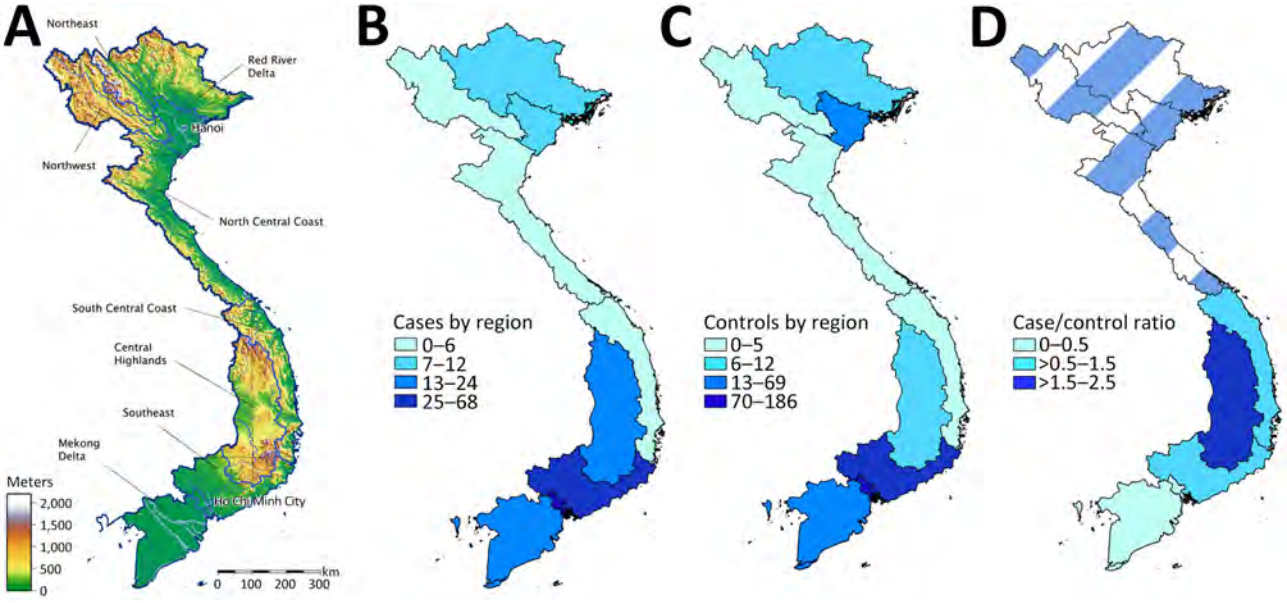

Figure. Geographic distribution of recruited cases and controls in multicenter study of behavioral, environmental, and geographic risk factors for talaromycosis, Vietnam. A) Municipal regions of Vietnam, showing topography and locations of recruitment centers in Hanoi and Ho Chi Minh City; B) number of cases by region; C) number of controls by region; D) ratio of cases to controls by region. Darker color represents a higher number of cases relative to controls for that region. A case-to-control ratio of 0.5 is expected because 2 controls were recruited for every case. A ratio ≤0.5 indicates a lower-than-expected number of cases relative to controls. A ratio >0.5 indicates a greater-than-expected number of cases relative to controls. Data for northern regions of Vietnam are excluded from panel D because study enrollment from these regions was insufficient to draw meaningful conclusions from the analysis. Both cases and controls are concentrated in Southern Vietnam, where most participants were recruited. The ratios of cases to controls are higher in the Central Highlands and the adjacent Southeast and South-Central Coast regions than in Ho Chi Minh City and the Mekong Delta; the highest ratio was seen in the Central Highlands region.

Table 1. Thirteen predefined exposure variables in multicenter case–control study of behavioral, environmental, and geographic risk factors for talaromycosis, Vietnam

Exposure variable	Definition
1. Antiretroviral therapy	Current use of antiretroviral therapy
2. Antifungal prophylaxis	Current use of antifungal prophylaxis
3. Cigarette smoking	Current cigarette smoking
4. Injection drug use	Current injection drug use
5. Outdoor occupations	Current or previous job in construction, agriculture, gardening, or long-distance truck driving
6. Soil exposure	Living within 100 meters of agricultural/industrial soil-excavation sites or direct occupational exposure to construction work, farming, soil digging, gardening, or rubbish collection
7. Natural water	Living within 100 meters of or direct occupational exposure to river, lake, pond, canal, or ditch
8. Tropical plants	Living within 100 meters of or direct occupational exposure to any type of bamboo, sugar cane, or rice
9. Highland plants	Living within 100 meters of or direct occupational exposure to rubber, cashew, coffee, or tea
10. Bamboo rats	Any direct contact or consumption with bamboo rats
11. Farming animals	Direct occupational exposure to pigs, cows, chickens, or ducks
12. Domestic animals	Frequent contact or caring of dogs, cats, birds, or fishes
13. Raw animal products	Any consumption of uncooked meats, eggs, milk, or blood

the potential confounding effect, we matched cases to controls at a 1:2 ratio according to age (±5 years), sex, and CD4 cell count ±50 cells/μL. When a CD4 count was not performed or available, we matched participants by absolute lymphocyte count (±330 cells/μL, calculated on the basis of an assumed 15% CD4-positive lymphocyte count, 50/0.15 = 330) or HIV disease at stage 3 or 4 according to World Health Organization (WHO) clinical staging. We recruited control-patients within the same week as the corresponding case-patients from the same site.

Sample Size Estimation

We calculated the sample size estimate for the matched case–control study according to Parker and Bregman (*23*). The target sample size of 200 in the case group and 400 in the control group was chosen to allow 90% power to detect an odds ratio (OR) of ≥1.9 for a risk factor, assuming a proportion of risk exposure of 0.2.

Data Collection

After participant recruitment, trained study nurses conducted face-to-face interviews using a standardized questionnaire of prespecified exposure variables (Table 1). To control for assessment bias, study nurses were blinded to the assignment of case and control and the study hypotheses. A photograph of the 4 species of bamboo rats (Appendix Figure 1) was shown to all participants to ensure that the history of exposure was correctly elicited. We assigned participants to 8 municipal regions based on current residential address. We categorized data from Ho Chi Minh City as a separate region because of the high number of participants recruited within the city limits. We performed a posthoc follow-up of participants residing in lowland regions (Ho Chi Minh City and the Mekong Delta) to investigate the risk posed by previous travel to or previous residence in highland regions that had been identified through the geographic mapping to be talaromycosis risk regions. The post hoc follow-up consisted of phone interviews conducted by research nurses who were blinded to the participant status as case or control.

Statistical Analysis

We used univariate and multivariable conditional logistic regressions to evaluate risk factors for talaromycosis using a complete case analysis. We included all 13 predefined exposure variables (Table 1) in the regression model. The Central Highlands and some provinces in the adjacent Southeast and South Central Coast regions in southern Vietnam consist of hills and mountainous terrain ≥400 meters in elevation (Figure, panel A). To investigate whether participants residing in those highland regions were at greater risk for talaromycosis than were residents of the lowland regions of Ho Chi Minh City and the Mekong Delta, we performed conditional logistic regression with the region as the only covariate. We adjusted pairwise comparisons between regions for multiple comparisons using a parametric single-step method (*24*). Participants recruited in northern Vietnam were excluded from this geographic analysis because of the later start date, which meant a substantially smaller number of patients were recruited with too diverse geographic distribution to enable robust statistical analysis in northern regions. We estimated the number of talaromycosis cases recruited per total HIV population in each region using HIV prevalence data obtained from the Vietnam Ministry of Health Administration of HIV/AIDS Control from 2007 to evaluate for any bias in referral pattern (*25*).

We visualized maps of the number of cases, controls, and case-to-control ratios in different geographic regions in southern Vietnam using the Quantum Geographic Information System version 1.5 (https://qgis.org). We performed all statistical analyses by

using R version 3.2.1 (The R Project for Statistical Computing, https://www.r-project.org).

Ethics

This case–control study was a substudy of the Itraconazole and Amphotericin B for Talaromycosis clinical trial that was approved by the Vietnam Ministry of Health (protocol 781-Vietnam MOH), by the Oxford University Tropical Research Ethics Committee (protocol OxTREC 12–09), and by the ethical and scientific committees of the 2 study sites in Vietnam. All participants provided written consent before study enrollment.

Results

Characteristics of Study Participants

During January 2013–July 2016, a total of 236 cases of talaromycosis were diagnosed across the 2 centers, of which 205 cases were recruited into the study and matched to 405 controls. Of the 31 cases screened but not recruited (5.1%), 25 died or were discharged before the talaromycosis diagnosis was confirmed (80.6%), and the remaining 6 declined to participate. Participants were mostly men (75% [456/610]), consistent with the HIV-infected population in Vietnam. Median age was 34 years (interquartile range [IQR] 31–38 years), and median CD4 count was 17 cells/μL (IQR 7–36). Case-patients and control-patients were similar in age, sex, and absolute lymphocyte counts (Table 2). CD4 count was significantly lower in case-patients than in control-patients. According to WHO HIV disease staging, all case-patients were classified as stage 4 (severe), whereas control-patients were mostly stage 3 or 4 (moderate or severe). Most participants were inpatient (100% [205/205] of case-patients and 91% [369/405] of control-patients). Other opportunistic infections, most commonly tuberculosis, pneumonia (caused by bacteria or *Pneumocystis*), oral/esophageal candidiasis, or cryptococcosis, were diagnosed in controls. Concurrent opportunistic infections were common among case-patients with talaromycosis (Table 2).

Analysis of Behavior and Environmental Risk Factors

Data were 100% complete for all 610 participants for 12 of 13 covariables (Table 1). Data were incomplete for only 1 area, fluconazole prophylaxis, in which data were missing for 14 (2%) participants (Table 3). In the univariate analysis, patients with talaromycosis were significantly more likely to work in outdoor settings, live within 100 meters of or have direct occupational contact with a tropical plant (bamboo, sugar cane, or rice), or have direct occupational contact with a highland plant (rubber, tea, coffee) and farm animals (cattle, swine, poultry). In the multivariable

Table 2. Characteristics of participants in multicenter case–control study of behavioral, environmental, and geographic risk factors for talaromycosis, Vietnam*

Characteristic	All patients, N = 610	Cases, n = 205	Controls, n = 405	p value†
Median age, y (IQR)	34 (31–38)	33 (30–38)	34 (31–39)	0.401
Sex				
M	456 (74.8)	154 (75.1)	302 (74.6)	0.882
F	154 (25.2)	51 (24.9)	103 (25.4)	
Median CD4, cells/μL (IQR)	16.5 (7.0–36.0), n = 194	9.0 (5.0–18.8), n = 66	25.5 (9.0–54.3), n = 128	0.003
Median absolute lymphocyte, cells/μL (IQR)	520 (300–750), n = 585	410 (230–600), n = 197	570 (380–810), n = 388	0.184
WHO stage	n = 606	n = 204	n = 402	
1	3 (0.5)	0	3 (0.7)‡	0.217
2	16 (2.6)	0	16 (4.0)‡	0.004
3	146 (24.1)	0	146 (36.3)‡	<0.001
4	441 (72.8)	204 (100)	237 (59.0)	<0.001
Hospitalization status				
Inpatient	573 (93.9)	205 (100)	368 (90.9)	<0.001
Outpatient	37 (6.1)	0	37 (9.1)	
Concomitant opportunistic infections				
Nontuberculosis pneumonia, including PcP	130 (21.3)	24 (11.7)	106 (26.2)	<0.001
Oral/esophageal candidiasis	90 (14.8)	14 (6.8)	76 (18.8)	<0.001
Tuberculosis	84 (13.8)	23 (11.2)	61 (15.1)	0.193
Cryptococcosis	45 (7.4)	0	45 (11.1)	<0.001
Toxoplasmosis	40 (6.6)	1 (0.5)	39 (9.6)	<0.001
Herpes simplex virus	12 (2.0)	3 (1.5)	9 (2.2)	0.524
AIDS-associated wasting syndrome	23 (3.8)	2 (1.0)	21 (5.2)	0.010
Other opportunistic infection	73 (12.0)	22 (10.7)	51 (12.6)	0.504
No opportunistic infection	66 (10.9)	0	66 (16.3)	<0.001

*Values are no. (%) except as indicated. IQR, interquartile range; PcP, *Pneumocystis* pneumonia; WHO, World Health Organization.
†χ^2 test was used for categorical variables and 2-tailed Student *t*-test was used for continuous variables.
‡These control patients had CD4 counts or absolute lymphocyte counts in the same ranges as their matched case-patients.

Table 3. Univariate and multivariable conditional logistic regression analysis of risk factors for talaromycosis in multicenter case–control study of behavioral, environmental, and geographic risk factors for talaromycosis, Vietnam*

Exposure covariate	All patients, N = 610	Cases, n = 205	Controls, n = 405	Univariate effect		Multivariate effect	
				OR (95% CI)	p value	OR (95% CI)	p value
Antiretroviral therapy	250/610 (41.0)	72/205 (35.1)	178/405 (44.0)	**0.68 (0.47–0.97)**	**0.04**	0.75 (0.50–1.13)	0.17
Fluconazole prophylaxis	61/596 (10.2)	15/198 (7.6)	46/398 (11.6)	0.59 (0.31–1.11)	0.10	0.68 (0.35–1.34)	0.27
Cigarette smoking	413/610 (67.7)	130/205 (63.4)	283/405 (69.9)	0.65 (0.42–1.01)	0.06	0.71 (0.43–1.18)	0.19
Injection drug use	232/610 (38.0)	71/205 (34.6)	161/405 (39.8)	0.79 (0.54–1.15)	0.21	0.85 (0.54–1.35)	0.50
Outdoor occupation	263/610 (43.1)	100/205 (48.8)	163/405 (40.2)	**1.47 (1.03–2.09)**	**0.04**	1.23 (0.81–1.87)	0.34
Soil exposure	409/610 (67.0)	143/205 (69.8)	266/405 (65.7)	1.22 (0.85–1.75)	0.29	1.06 (0.69–1.63)	0.80
Natural water exposure	285/610 (46.7)	90/205 (43.9)	195/405 (48.1)	0.83 (0.58–1.19)	0.31	0.76 (0.51–1.13)	0.18
Tropical plant exposure	218/610 (35.7)	90/205 (43.9)	128/405 (31.6)	**1.75 (1.22–2.56)**	**0.002**	**1.84 (1.17–2.90)**	**0.008**
Highland plant exposure	49/610 (8.0)	25/205 (12.2)	24/405 (5.9)	**2.25 (1.24–4.01)**	**0.008**	1.71 (0.86–3.41)	0.13
Bamboo rat exposure or consumption	6/610 (1.0)	3/205 (1.5)	3/405 (0.7)	2.00 (0.40–9.91)	0.40	1.71 (0.33–8.87)	0.53
Farming animal exposure	93/610 (15.2)	40/205 (19.5)	53/405 (13.1)	**1.60 (1.02–2.51)**	**0.04**	**2.03 (1.18–3.49)**	**0.010**
Domestic animal exposure	170/610 (27.9)	57/205 (27.8)	113/405 (27.9)	1.01 (0.67–1.51)	0.97	1.39 (0.87–2.22)	0.17
Raw animal product consumption	411/610 (67.4)	132/205 (64.4)	279/405 (68.9)	0.82 (0.57–1.18)	0.28	0.91 (0.60–1.37)	0.64

*Values are no. (%) except as indicated. OR is based on conditional logistic regression. Multivariate analysis is a complete case analysis excluding 7 cases and 7 controls with missing fluconazole prophylaxis data. A p value <0.05 is considered statistically significant and highlighted in bold. For definitions of exposure covariates, refer to Table 1. OR, odds ratio.

analysis, exposure to tropical plants (OR 1.73 [95% CI 1.10–2.73]; p = 0.017) and exposure to farm animals (OR 2.07 [95% CI 1.20–3.55]; p = 0.009) were the only independent risk factors for talaromycosis (Table 3).

Mapping of Cases and Controls and Geographic Risk Analysis

Geographic data were available for 204 (99.5%) of 205 case-patients and 403 (99.5%) of 405 control-patients (Figure, panels B, C). We performed mapping and geographic analysis only for southern Vietnam because recruitment in southern Vietnam began earlier and more case-patients (86% [175/205]) and control-patients (86% [348/405]) were enrolled in southern Vietnam to provide robust data for these analyses. The case-to-control ratio demonstrated regions with a higher or lower than expected number of cases relative to controls; 0.5 was the expected case-to-control ratio, given that 2 controls were recruited for each case (Figure, panel D). We found that case-to-control ratios were highest in the Central Highlands (2.18), followed by the surrounding provinces in the South-Central Coast (1.20) and the Southeast region (0.87). Case-to-control ratios were the lowest in Ho Chi Minh City (0.32) and the Mekong Delta (0.25), where the number of persons recruited was the highest (Figure, panel D). Conditional logistic regression demonstrated that participants in the highland regions in the Central Highlands, Southeast, and South-Central Coast were significantly more likely to develop talaromycosis than those residing in the lowlands of Ho Chi Minh City and Mekong Delta (multiplicity-corrected p<0.05 for all pairwise comparisons) (Table 4). The point estimate of the risk for talaromycosis was higher in the Central Highlands than in the Southeast lowland region, suggesting a risk exposure relationship for closer proximity to the highest risk Central Highland region, but this difference did not reach statistical significance (OR 3.32; p = 0.06). In the southern regions of Vietnam, the highest relative number of talaromycosis cases was in the Central Highlands (Table 5).

To investigate whether previous travel to or residence in any of the 3 identified risk regions was associated with the risk for talaromycosis, we performed a posthoc follow-up interview of participants residing in the lowlands of Ho Chi Minh City and the Mekong Delta. A total of 69 (90%) of 77 case-patients and 82 (32%) of 254 control-patients responded to the blinded posthoc follow-up phone interview. Participants who had lived or traveled to a high-risk region for ≥3 days were at significantly higher risk for talaromycosis (55/69 [81%] case-patients vs. 47/82 [57%] control-patients; OR 2.90 [95% CI 1.33–6.59]; p = 0.005).

Discussion

This large case–control study investigated the behavioral, environmental, and geographic exposure risk factors for talaromycosis in susceptible persons living in a highly endemic region, Vietnam. Participants

Table 4. Case-to-control ratio and risk for talaromycosis per region in multicenter case–control study of behavioral, environmental, and geographic risk factors for talaromycosis, Vietnam*

Region†	No. cases	No. controls	Case-to-control ratio	OR (95% CI)‡	p value
Mekong Delta	17	69	0.25	Referent	
HCMC	60	185	0.32	1.31 (0.56–3.03)	0.91
Southeast	68	78	0.87	3.42 (1.44–8.10)	0.001
South Central Coast	6	5	1.20	8.76 (1.25–61.56)	0.02
Central Highlands	24	11	2.18	11.36 (2.92–44.24)	<0.0001
Total	175	348	0.5		

*Conditional logistic regression analysis with the region as the only covariate was conducted to investigate whether participants residing in the highland regions were at greater risk for talaromycosis than were residents of the lowland regions of HCMC and the Mekong Delta. Pairwise comparisons between regions were adjusted for multiple comparisons using a parametric single-step method. HCMC, Ho Chi Minh City; OR, odds ratio.
†Participants recruited in northern Vietnam were excluded from this geographic analysis because of the later start date and, hence, a smaller number of patients in northern regions were recruited.
‡OR is based on conditional logistic regression. p values are multiplicity-adjusted for pair-wise comparisons between all regions. Comparisons to the Mekong Delta are shown above. The remaining pair-wise comparisons are comparisons to HCMC: Southeast OR 2.62 (1.41–4.85); p = 0.0003; South Central Coast OR 6.71 (1.04–43.45); p = 0.04; Central Highlands OR 8.70 (2.61–28.97); p<0.0001. Comparisons to Southeast: South Central Coast OR 2.57 (0.40–16.52); p = 0.63; Central Highlands OR 3.32 (0.98–11.26); p = 0.06. Comparison to Central Highlands: South Central Coast OR 0.77 (0.12 – 5.06); p = 1.00.

living within 100 meters of or having direct exposure to tropical plants (bamboo, sugar cane, or rice) or to farm animals (cattle, swine, or poultry) had 2-fold higher odds for talaromycosis. Our findings are consistent with the results of a previous smaller case–control study from Chiang Mai, Thailand (n = 180), which also found a 2-fold increase in the odds of talaromycosis with recent exposure to animals or plants (*18*). The strength of those associations is also similar across the 2 studies, despite the difference in study settings (urban vs. rural) and an 8-fold larger sample size in our study. Although direct exposure to soil was not identified as a risk factor in our study, soil is a known reservoir for other dimorphic fungal pathogens including *Coccidioides* spp., *Paracoccidioides* spp., *Histoplasma capsulatum*, and *Sporothrix schenckii* (*26*–*28*). Specifically, soil contaminated with animal droppings (bird or bat) is a known reservoir for *Histoplasma* spp., whereas soil mixed with decaying plant materials has been identified as a reservoir for *Sporothrix* spp. (*29*,*30*). Soil contaminated with farmed animal excreta or decaying tropical plant substrate is likely also favorable to *T. marneffei*'s growth, which supports the observed risk for talaromycosis in persons exposed to or living in proximity to animal and agricultural farming activities.

Direct contact with or consumption of bamboo rats was not associated with talaromycosis in our study, which is consistent with the previous case–control study from Thailand (*18*). Early efforts to isolate *T. marneffei* from the soil within bamboo rat burrows yielded some success (*14*,*31*,*32*). An environmental survey in Guangdong Province, China, demonstrated a higher prevalence of *T. marneffei* in soil collected from bamboo rat burrows (8.2% [15/184]) than in soil from sites not associated with bamboo rats (2.0% [1/50]) (*19*). *T. marneffei* was isolated in bamboo rat stool on the surface of the soil and around the bamboo roots found deep in the bamboo rat burrows (*19*). In Thailand, T. marneffei DNA was found in soil around a bat cave and elephant camp (*33*). However, the bamboo rat is the only known nonhuman host of *T. marneffei* (*16*,*19*). *T. marneffei* is found in the liver, spleen, and lungs of healthy-appearing bamboo rats, suggesting that bamboo rats are asymptomatic carriers of *T. marneffei* and serve as a zoonotic reservoir (*19*). Bamboo rats construct extensive burrow systems for foraging among bamboo crops by digging 1–2 meters into the ground. Although their primary food source is bamboo roots and shoots, bamboo rats are known to feed on sugar cane and cassava roots. In our study, exposure to tropical plants was an independent risk factor for talaromycosis, possibly because of their association with the bamboo rat environment. By burrowing into the soil and feeding on a variety of tropical vegetation, bamboo rats likely enhance *T. marneffei* transmission. Soil disturbance, caused by bamboo rat foraging, heavy rainfall, or agricultural activity (e.g.,

Table 5. Recruited talaromycosis cases per regional HIV population in southern Vietnam in multicenter case–control study of behavioral, environmental, and geographic risk factors for talaromycosis, Vietnam*

Region	Talaromycosis cases	Estimated HIV population, 2007	Cases/100,000 HIV population
Mekong Delta	17	103,615	16
Ho Chi Minh City	60	72,566	83
Southeast	68	52,132	130
South Central Coast	6	11,878	51
Central Highlands	24	12,123	200

*The number of talaromycosis cases recruited per total HIV population in each region was estimated using HIV prevalence data obtained from the Vietnam Ministry of Health Administration of HIV/AIDS Control from 2007 to evaluate for any bias in referral pattern.

tillage, plowing, livestock grazing), causes aerosolization of *T. marneffei* conidia, the infective form inhaled by bamboo rats and humans (*4*,*6*,*20*,*21*). The findings of our study suggest that exposure to soil associated with bamboo rats (and possibly other animals) and activities that disturb soil are the main drivers for the acquisition of talaromycosis, rather than direct zoonotic transmission.

Geographic mapping was very informative and demonstrated that the Central Highlands and the adjacent Southeast and South-Central Coast regions are high-risk regions for talaromycosis, compared with the lowlands of Ho Chi Minh City and the Mekong Delta regions in Vietnam. Assuming the referral patterns of patients with HIV were similar among regions, talaromycosis cases per 100,000 persons with HIV were 8–10 times higher in the Southeast and Central Highlands regions than in the Mekong Delta and were 2–3 times higher than in Ho Chi Minh City. Highland regions are the known natural habitat of bamboo rats, and previous studies outside of Vietnam have demonstrated that human talaromycosis follows the geographic distribution of bamboo rats (*16*,*17*). Further interrogation of participants from the lowlands of Ho Chi Minh City and Mekong Delta revealed that previous residence in or travel to highland regions increased the odds of talaromycosis 3-fold. Our study demonstrates an epidemiologic link between human talaromycosis and residence in or travel to highland regions in a highly endemic country. Further research is needed to determine whether localized geographic hotspots of talaromycosis exist within those highland regions. Our data can inform prevention strategies for talaromycosis, including patient education and the consideration of primary itraconazole prophylaxis in high-risk persons considering travel to or living in regional hotspots.

The first limitation of our study is that 31 persons with talaromycosis were screened but not enrolled in our study, largely because of discharge or death. Those participants might have exhibited different risk factors from those enrolled in the study, which is a potential source of selection bias; however, the number is very small (5.1%). Second, control-patients who had concurrent bacteremia could potentially have been misclassified because bacteria can outgrow *T. marneffei* in culture, leading to false-negative results. CD4 count was only available for 30% of participants, and therefore matching was performed on the basis of absolute lymphocyte count and WHO HIV disease staging, which are suboptimal measures of immune susceptibility. Some characteristics of case-patients and control-patients, such as median CD4 cell count, WHO HIV stage, and proportion of inpatients, differed significantly. However, our control population consisted of clinically relevant persons with advanced HIV disease (CD4 <200 cells/mL) and other opportunistic infections, which are representative of the population at risk for talaromycosis. Although interviewers were blinded to the classification of case and control, observer bias is possible, because 40%–70% of persons with talaromycosis display characteristic umbilicated skin lesions (*6*,*34*,*35*). However, that possibility was mitigated because interviewers were blinded to study hypotheses to minimize observer bias. The differential referral pattern between cases and controls in different regions might have skewed the geographic results, but that skewing was unavoidable because of limited diagnostic capacities outside of major referral centers in Vietnam. The number of cases recruited in Ho Chi Minh City and Hanoi was imbalanced because enrollment started earlier in Ho Chi Minh City, resulting in overrepresentation of residents from southern Vietnam. Finally, potential for recall bias is inherent to a case–control study design. Further studies are needed to uncover more specific geographic risk factors and risk behaviors and to establish the causal link between environmental exposure and the development of talaromycosis.

In conclusion, this study demonstrates an epidemiologic link between human talaromycosis and geospatial proximity or travel to highland regions in a hyperendemic country, thus informing disease education and prevention strategies. Results from this large case–control study validate the previous findings that disturbance of soil associated with tropical plants and farmed animals, such as through agricultural or construction activity, increases the risk for talaromycosis.

Acknowledgments

We thank Noel Weiss for his advice on the study design. We thank the patients for their participation in this study. We thank the physicians at the study sites for their assistance with study recruitment: at the Hospital for Tropical Diseases in Ho Chi Minh City, Nguyen Huu Chi, Ngo Thi Kim Cuc, Nguyen Le Nhu Tung, Nguyen Thanh Liem, Le Duc Vinh, and Ly Quoc Cong; at the National Hospital for Tropical Diseases in Hanoi, Nguyen Tien Lam, Ta Thi Dieu Ngan, and Nguyen Kim Thu. We thank nurses Phan Thi Hong Dao and Hoang Suong Nguyet Anh for their assistance with the interviews. We thank Tran Phuong Thuy for the coordination of the project and Vo Thi Hoang Anh for assistance with Appendix Figure 1 and for obtaining photographers' permission for the use of the bamboo rat photos. Finally, we thank Pierce Gardner and Marc Foca for their mentorship of Brian Jonat on the project.

This study was jointly funded by the University of Washington Center for AIDS Research (National Institutes of Health grant P30 AI027757 through a pilot international award to T.L.), by the Stony Brook Medicine International Research Fellowship (to B.J.), and by the National Institutes of Health (grants R01 AI181764-01 to T.L., R01AI177098-02, R01-AI143409-05, and U01AI169358-03 to N.T.H. and T.L.). L.B. is funded by the National Institute for Health Research and received fellowship grants from the Federation of European Microbiological Societies, Dowager Countess Eleanor Peel Trust, the British Society for Medical Mycology, and the Wingate Foundation.

T.L. conceptualized the study, acquired funding, and constructed the methodology. Data were curated by T.L., V.T.L., P.S.L., N.T.T., and D.T.N.B. Formal analysis and visualization were performed by T.L., B.J., and L.B. B.J. and L.B. were project administrators. T.L. and N.T.H. provided supervision. B.J. and L.B. wrote the original draft. V.T.L., P.S.L., N.T.T., D.N.T.B, V.P.T., N.T.M.T., N.T.H., and T.L. reviewed and edited the manuscript. All authors contributed to the revision of the paper for intellectual content and approved the final manuscript.

B.J. reports employment as a patient safety physician with Boehringer Ingelheim Pharmaceuticals Inc., which began after the completion of this study but before submission of this manuscript for publication. B.J.'s involvement in preparation of study materials occurred while a student at Stony Brook University School of Medicine or while employed by New York-Presbyterian Hospital or Columbia University. B.J. reports receiving consulting fees from the World Health Organization.

About the Author

Dr. Brown is an academic clinical fellow in infectious diseases and microbiology at City St George's University and Hospital in London, UK. Her research focuses on neglected fungal diseases such as talaromycosis.

References

1. Le T, Thanh NT, Thwaites GE. Talaromycosis (Penicilliosis). In: Ryan ET, Hill DR, Solomon T, Aronson N, Endy TP, editors. Hunter's tropical medicine and emerging infectious diseases. Philadelphia: Elsevier; 2020. p. 682–5.
2. Qin Y, Huang X, Chen H, Liu X, Li Y, Hou J, et al. Burden of *Talaromyces marneffei* infection in people living with HIV/AIDS in Asia during ART era: a systematic review and meta-analysis. BMC Infect Dis. 2020;20:551. https://doi.org/10.1186/s12879-020-05260-8
3. Jiang J, Meng S, Huang S, Ruan Y, Lu X, Li JZ, et al. Effects of *Talaromyces marneffei* infection on mortality of HIV/AIDS patients in southern China: a retrospective cohort study. Clin Microbiol Infect. 2019;25:233–41. https://doi.org/10.1016/j.cmi.2018.04.018
4. Le T, Wolbers M, Chi NH, Quang VM, Chinh NT, Lan NP, et al. Epidemiology, seasonality, and predictors of outcome of AIDS-associated *Penicillium marneffei* infection in Ho Chi Minh City, Viet Nam. Clin Infect Dis. 2011;52:945–52. https://doi.org/10.1093/cid/cir028
5. Hu Y, Zhang J, Li X, Yang Y, Zhang Y, Ma J, et al. *Penicillium marneffei* infection: an emerging disease in mainland China. Mycopathologia. 2013;175:57–67. https://doi.org/10.1007/s11046-012-9577-0
6. Ying RS, Le T, Cai WP, Li YR, Luo CB, Cao Y, et al. Clinical epidemiology and outcome of HIV-associated talaromycosis in Guangdong, China, during 2011–2017. HIV Med. 2020;21:729–38. https://doi.org/10.1111/hiv.13024
7. Dat VQ, Ly VT, Thu NM, Dieu NQ, Hao NT, Thach PN, et al. Triple screening for invasive mycoses in patients with advanced HIV disease in Vietnam. Presented at: 31st Conference on Retroviruses and Opportunistic Infections; March 3–6, 2024; Denver, Colorado, USA.
8. Ning C, Wei W, Xu B, Thanh N, Ye L, Liang H. The global distribution, drivers, and burden of talaromycosis 1964–2018. Conference of Retrovirus and Opportunistic Infections. 2020;2020:8–11.
9. Cao C, Xi L, Chaturvedi V. Talaromycosis (penicilliosis) due to *Talaromyces (Penicillium) marneffei*: insights into the clinical trends of a major fungal disease 60 years after the discovery of the pathogen. Mycopathologia. 2019;184:709–20. https://doi.org/10.1007/s11046-019-00410-2
10. He L, Mei X, Lu S, Ma J, Hu Y, Mo D, et al. *Talaromyces marneffei* infection in non–HIV-infected patients in mainland China. Mycoses. 2021;64:1170–6. https://doi.org/10.1111/myc.13295
11. Qiu Y, Feng X, Zeng W, Zhang H, Zhang J. Immunodeficiency disease spectrum in HIV-negative individuals with talaromycosis. J Clin Immunol. 2021;41:221–3. https://doi.org/10.1007/s10875-020-00869-5
12. Cao C, Liang L, Wang W, Luo H, Huang S, Liu D, et al. Common reservoirs for *Penicillium marneffei* infection in humans and rodents, China. Emerg Infect Dis. 2011;17:209–14. https://doi.org/10.3201/eid1702.100718
13. Wei X, Ling Y, Li C, Zhang F. Study of 179 bamboo rats carrying *Penicillium marneffei*. Chin J Zoonoses. 1987;3:34–5.
14. Chariyalertsak S, Vanittanakom P, Nelson KE, Sirisanthana T, Vanittanakom N. *Rhizomys sumatrensis* and *Cannomys badius*, new natural animal hosts of *Penicillium marneffei*. J Med Vet Mycol. 1996;34:105–10.
15. Ajello L, Padhye AA, Sukroongreung S, Nilakul CH, Tantimavanic S. Occurrence of *Penicillium marneffei* infections among wild bamboo rats in Thailand. Mycopathologia. 1995;131:1–8. https://doi.org/10.1007/BF01103897
16. Cao C, Liang L, Wang W, Luo H, Huang S, Liu D, et al. Common reservoirs for *Penicillium marneffei* infection in humans and rodents, China. Emerg Infect Dis. 2011;17:209–14. https://doi.org/10.3201/eid1702.100718
17. Fisher MC, Hanage WP, de Hoog S, Johnson E, Smith MD, White NJ, et al. Low effective dispersal of asexual genotypes in heterogeneous landscapes by the endemic pathogen *Penicillium marneffei*. PLoS Pathog. 2005;1:e20. https://doi.org/10.1371/journal.ppat.0010020
18. Chariyalertsak S, Sirisanthana T, Supparatpinyo K, Praparattanapan J, Nelson KE. Case-control study of risk factors for *Penicillium marneffei* infection in human immunodeficiency virus-infected patients in northern Thailand. Clin Infect Dis. 1997;24:1080–6. https://doi.org/10.1086/513649
19. Huang X, He G, Lu S, Liang Y, Xi L. Role of *Rhizomys pruinosus* as a natural animal host of *Penicillium marneffei* in Guangdong, China. Microb Biotechnol. 2015;8:659–64. https://doi.org/10.1111/1751-7915.12275

20. Bulterys PL, Le T, Quang VM, Nelson KE, Lloyd-Smith JO. Environmental predictors and incubation period of AIDS-associated *Penicillium marneffei* infection in Ho Chi Minh City, Vietnam. Clin Infect Dis. 2013;56:1273–9. https://doi.org/10.1093/cid/cit058
21. Wang Y, Deng K. Environmental risk factors for talaromycosis hospitalizations of HIV-infected patients in Guangzhou, China: case crossover study. Front Med (Lausanne). 2021;8:731188. https://doi.org/10.3389/fmed.2021.731188
22. Narayanasamy S, Dat VQ, Thanh NT, Ly VT, Chan JF-W, Yuen K-Y, et al. A global call for talaromycosis to be recognised as a neglected tropical disease. Lancet Glob Health. 2021;9:e1618–22. https://doi.org/10.1016/S2214-109X(21)00350-8
23. Parker RA, Bregman DJ. Sample size for individually matched case-control studies. Biometrics. 1986;42:919–26. https://doi.org/10.2307/2530705
24. Hothorn T, Bretz F, Westfall P. Simultaneous inference in general parametric models. Biom J. 2008;50:346–63. https://doi.org/10.1002/bimj.200810425
25. Health Mo. Vietnam Administration of HIV/AIDS Control. 2007 [cited 2025 May 22]. https://www.prb.org/wp-content/uploads/2007/04/VietnamHIVChartbook.pdf
26. Del Rocío Reyes-Montes M, Pérez-Huitrón MA, Ocaña-Monroy JL, Frías-De-León MG, Martínez-Herrera E, Arenas R, et al. The habitat of *Coccidioides* spp. and the role of animals as reservoirs and disseminators in nature. BMC Infect Dis. 2016;16:550. https://doi.org/10.1186/s12879-016-1902-7
27. Lockhart SR, Toda M, Benedict K, Caceres DH, Litvintseva AP. Endemic and other dimorphic mycoses in the Americas. J Fungi (Basel). 2021;7:151. https://doi.org/10.3390/jof7020151
28. Hrycyk MF, Garcia Garces H, Bosco SMG, de Oliveira SL, Marques SA, Bagagli E. Ecology of *Paracoccidioides brasiliensis*, *P. lutzii* and related species: infection in armadillos, soil occurrence and mycological aspects. Med Mycol. 2018;56:950–62. https://doi.org/10.1093/mmy/myx142
29. Barros MB, de Almeida Paes R, Schubach AO. *Sporothrix schenckii* and sporotrichosis. Clin Microbiol Rev. 2011;24:633–54. https://doi.org/10.1128/CMR.00007-11
30. Deepe GS Jr. Outbreaks of histoplasmosis: the spores set sail. PLoS Pathog. 2018;14:e1007213. https://doi.org/10.1371/journal.ppat.1007213
31. Gugnani HC, Paliwal-Joshi A, Rahman H, Padhye AA, Singh TS, Das TK, et al. Occurrence of pathogenic fungi in soil of burrows of rats and of other sites in bamboo plantations in India and Nepal. Mycoses. 2007;50:507–11. https://doi.org/10.1111/j.1439-0507.2007.01402.x
32. Li X, Yang Y, Zhang X, Zhou X, Lu S, Ma L, et al. Isolation of *Penicillium marneffei* from soil and wild rodents in Guangdong, SE China. Mycopathologia. 2011;172:447–51. https://doi.org/10.1007/s11046-011-9443-5
33. Pryce-Miller E, Aanensen D, Vanittanakom N, Fisher MC. Environmental detection of *Penicillium marneffei* and growth in soil microcosms in competition with *Talaromyces stipitatus*. Fungal Ecology. 2008;1:49–56.
34. Shen Q, Sheng L, Zhang J, Ye J, Zhou J. Analysis of clinical characteristics and prognosis of talaromycosis (with or without human immunodeficiency virus) from a non-endemic area: a retrospective study. Infection. 2022;50:169–78. https://doi.org/10.1007/s15010-021-01679-6
35. Yu Q, Wei M, Xiao R, Liang X, Liang S, Ma N, et al. Clinical characteristics, course, and long-term outcomes in patients with *Talaromyces marneffei* infection: a 10-year retrospective cohort study. Infect Dis Ther. 2023;12:1283–97. https://doi.org/10.1007/s40121-023-00801-5

Address for correspondence: Lottie Brown, Institute of Infection and Immunity, School of Health and Medical Sciences, City St George's Hospital and St George's University, London SW17 0RE, UK; email: lotbrown@sgul.ac.uk; Thuy Le, Division of Infectious Diseases and International Health, Duke University Medical Center, Duke Box 102359, Durham, NC 27710, USA; email thuy.le@duke.edu

Persistence of SARS-CoV-2 Alpha Variant in White-Tailed Deer, Ohio, USA

Natalie N. Tarbuck,[1] Sofya K. Garushyants,[1] Dillon S. McBride, Patricia M. Dennis, John Franks, Karlie Woodard, Austin Shamblin, Michael G. Sovic, Derek T. Collins, Kyle Van Why, Richard J. Webby, Martha I. Nelson, Andrew S. Bowman

Free-ranging white-tailed deer (WTD) are highly susceptible to the SARS-CoV-2 virus. Through an opportunistic sampling of WTD in northeast Ohio, USA, during January–March 2023, we identified 6 SARS-CoV-2 lineages from 36 sequences using the pangolin lineages tool, including the B.1.1.7 lineage (Alpha variant) and BQ.1.1, BQ.1.1.63, BQ.1.1.67, BQ.1.23, and XBB.1.5.35 lineages (Omicron variant). The Alpha variant, introduced by a single human-to-deer transmission event, was detected in 5 WTD in January 2023, more than 1 year after the most recent detection of the Alpha variant in humans in Ohio (August 2021). A genetically similar B.1.1.7 lineage virus from WTD in a nearby county in Pennsylvania was positioned with our Ohio deer transmission cluster, suggesting deer-to-deer transmission. The persistence of the Alpha variant in WTD in Ohio warrants continued surveillance to monitor if WTD can become a reservoir for displaced SARS-CoV-2 variants.

Since the beginning of the COVID-19 pandemic, SARS-CoV-2 evolution has produced multiple variants that affected public health by causing new epidemics, replacing prior variants, and evading existing immunity. SARS-CoV-2 is primarily transmitted from human to human, although human-to-animal transmission is documented in a wide variety of animal species (*1*). The role of host-switching in viral evolution of SARS-CoV-2 is not fully understood, yet some speculate that the emergence of the Omicron variant may be a result of animal-acquired mutations (*2*,*3*)

Free-ranging white-tailed deer (WTD) are susceptible to the SARS-CoV-2 virus, raising concerns that they might become a new animal reservoir for a diverse viral population or sustain older variants displaced in humans (*4*). SARS-CoV-2 infection in WTD was reported in northeast Ohio, USA, in 2021 (*5*) and the virus has since been detected in WTD across North America (*4*,*6*–*10*). SARS-CoV-2 evolves ≈3 times faster in deer than in humans, which makes evolutionary divergence possible (*11*). Of note, a highly divergent SARS-CoV-2 lineage, B.1.641, was linked to suspected deer-to-human transmission (*8*), emphasizing the risk associated with emergence of a deer-adapted virus in human populations.

There are ≈30 million WTD in the United States, and population levels pose ecologic and human safety challenges as hunting rates decline (*12*,*13*). Interactions between deer and humans create pathways for zoonotic transmission of SARS-CoV-2, yet the mechanisms driving this transmission remain unclear. If WTD become a natural reservoir for SARS-CoV-2, there is potential for deer-lineage and human-lineage viruses to diverge over time. To monitor the persistence and evolution of SARS-CoV-2 and define mutations and mutation rates in WTD, we conducted SARS-CoV-2 surveillance in northeast Ohio, an area with a historically high prevalence of SARS-CoV-2 in WTD.

Methods

Sample Collection

We collected 519 nasal swab specimens from free-ranging WTD that were culled during management

Author affiliations: The Ohio State University, Columbus, Ohio, USA (N.N. Tarbuck, D.S. McBride, P.M. Dennis, A. Shamblin, M.G. Sovic, A.S. Bowman); National Institutes of Health, Bethesda, Maryland, USA (S.K. Garushyants, M.I. Nelson); Cleveland Metroparks Zoo, Cleveland, Ohio, USA (P.M. Dennis); St. Jude Children's Research Hospital, Memphis, Tennessee, USA (J. Franks, K. Woodard, R.J. Webby); Animal and Plant Health Inspection Service, Fort Collins, Colorado, USA (D.T. Collins); Animal and Plant Health Inspection Service, Harrisburg, Pennsylvania, USA (K. Van Why).

DOI: https://doi.org/10.3201/eid3107.241922

[1]These authors contributed equally to this article.

activities in northeast Ohio during January–March 2023. The WTD were from 10 study sites covering ≈1,000 km² of landscape of varying human population density where hunting is not permitted. We collected nasal swab specimens from each fresh deer carcass by using a sterile polyester tipped swab then placed into a 3-mL vial containing viral transport medium (VTM). We chilled samples in the field and stored them at −80°C until testing. Sample collection was conducted after death and was exempt from oversight by The Ohio State University Institutional Animal Care and Use Committee.

Diagnostic Testing

We tested all collected samples for SARS-CoV-2 RNA by using quantitative real-time reverse transcription PCR (RT-PCR). We extracted viral RNA from 200 µL of VTM by using the MagMAX Viral/Pathogen II Nucleic Acid Isolation Kit (Thermo Fisher Scientific, https://www.thermofisher.com). We tested the extracted viral RNA from each sample with quantitative real-time RT-PCR by using the TaqPath COVID-19 Combo Kit with MS2 phage control (Thermo Fisher Scientific). We considered any sample with a cycle threshold (Ct) value of ≤37 on ≥2 targets (nucleocapsid gene, spike gene, open reading frame 1ab) SARS-CoV-2 positive. We sent samples with a Ct <33 for whole-genome sequencing.

Genomic Sequencing

We reverse transcribed extracted RNA into cDNA by using Lunascript RT Supermix (New England Biolabs, https://www.neb.com). After transcription, we divided the sample in half and separately enriched for SARS-CoV-2 with 35 cycles of PCR by using the ARTIC 4.1 primer sets and Q5 Hot Start (New England Biolabs). We then recombined the enriched products and conducted a 1.8× cleanup by using AmpureXP beads (Beckman Coulter, https://www.beckman.com) and resuspended in resuspension buffer (Illumina, https://www.illumina.com). We conducted tagmentation with enrichment beads according to the Illumina DNA Prep protocol (Illumina) with unique dual indexes. We pooled individual libraries in equimolar amounts and performed 2 × 150 bp sequencing on an Illumina NextSeq2000 (Illumina). We generated fastq files by using BCL Convert and ran the files through DRAGEN Covid Lineage v3.5.1 on Basespace (Illumina). We filtered the fastq files with sequencing reads by using fastp v0.23.4 (*14*) and mapped the filtered reads to the SARS-CoV-2 reference genome MN908947.3 with BWA-MEM v 0.7.17 (Li H, unpub. data, http://arxiv.org/abs/1303.3997). We used reference genome MN908947.3 when some positions problematic for variant calling were masked as recommended for ARTIC 4.1 protocol (https://github.com/joshquick/artic-ncov2019/tree/master/primer_schemes/nCoV-2019/V4.1). We used iVar v1.4.2 to trim primers and generate final fasta sequences (*15*).

Virus Isolation

We shipped the SARS-CoV-2–positive nasal swab specimens to St. Jude Children's Research Hospital (Memphis, TN, USA), where virus isolation, characterization, and in vivo experiments were performed under Biosafety Level 3 laboratory and animal Biosafety Level 3+ conditions. We received Vero E6 cells expressing both TMPRSS2 and ACE2 genes (VE-6A2T2; kindly provided by Dr. Barney Graham at the National Institute of Allergy and Infectious Diseases). We washed confluent cultures with sterile phosphate buffered saline and overlaid with 100 µL of swab suspension plus 900 µL of infection media (Dulbecco Modified Eagle Medium supplemented with 2% heat treated fetal bovine serum and 1× antimicrobial solution) for 1 hour to enable virus adsorption. We aspirated the inoculum and added fresh infection media to the cells. We checked the cells daily for cytopathic effect and harvested cultures reaching >90% cytopathic effect. We then subjected negative cultures from swab specimens previously identified as Alpha lineage SARS-CoV 2 to a second, undiluted blind passage.

We attempted virus isolation on all Alpha lineage swab specimens (n = 10) by first passing VTM through a 32-mm 0.8/0.2 µM syringe filter. We anesthetized 8–10-week male lakeview golden Syrian hamsters (Charles River Laboratories, https://www.criver.com) with 4% isoflurane and inoculated intranasally with 100 µL of filtered VTM (n = 1/swab). We monitored the hamsters daily. On 2 and 6 days postinfection, we anesthetized the animals with 100 mg/kg ketamine and washed nasal passages with 0.5 mL phosphate buffered saline. All animals were humanely euthanized after the second postinfection nasal wash, and we collected lung and nasal turbinate samples that were homogenized in 5× volume of media. We inoculated supernatants from nasal washes and tissue homogenates onto VE6A2T2 cell cultures for virus isolation. Animal studies were approved by St. Jude Children's Research Hospital's Animal Care and Use Committee (protocol no. 442).

Phylogenetic Analysis

We used the pangolin tppl (*16*) to determine the SARS-CoV-2 lineage for the 36 viruses sequenced for

this study. On the basis of those results, we divided the data into 2 datasets, 1 for the Alpha variant (SARS-CoV-2 B.1.1.7) and 1 for the Omicron variant, which included 5 PANGO SARS-CoV-2 lineages (BQ.1.1, BQ.1.1.63, BQ.1.1.67, BQ.1.23, and XBB.1.5.35). We downloaded separate background datasets from GISAID (https://www.gisaid.org) for Alpha and Omicron. The date range for the Omicron sequences was November 1, 2022–March 31, 2023. For the Alpha background dataset, we used the same dataset in our previously published study of Alpha viruses circulating in WTD in Ohio (*11*), with the addition of more recently published sequences from GISAID from humans, deer, and mink. Although the large human dataset was randomly subsampled, all sequences from deer and mink were retained. We aligned the 2 datasets (Alpha and Omicron) by using NextClade (version 3.13.3, https://clades.nextstrain.org) with the wild-type SARS-CoV-2 as a reference. We used in-house Python scripts to remove noncoding regions and mask sites that are known to be unreliable. We inferred phylogenetic trees by using maximum-likelihood methods available in IQ-TREE version 1.6.12 (*17*) with a general time reversible with unequal rates and unequal base frequency plus discrete gamma model of nucleotide substitution and 1,000 bootstrap replicates, by using the high-performance computational capabilities of the Biowulf Linux cluster at the National Institutes of Health (http://biowulf.nih.gov). We visualized the inferred tree by using FigTree v.1.4.4 (https://github.com/rambaut/figtree/releases). We defined deer transmission clusters by monophyletic groups of WTD viruses supported by high bootstrap values (>70) and confirmed or refined by using ultrafast sample placement on existing trees (*18*). None of the deer transmission clusters involved genetically identical viruses, which would be the case if the deer had acquired the virus from a common environmental source such as water.

We reconstructed mutations on the phylogenetic tree by using TreeTime v0.11.4 (*19*). We reconstructed root-to-tip regression and mutation contexts with in-house R scripts in R (The R Project for Statistical Computing, https://www.r-project.org), as described previously (*11*). We visualized the spike glycoprotein mutations with ChimeraX (*20*) and visualized mutations in B.1.1.7 deer clusters with the ete3 package in Python (*21*).

Bayesian Analysis

We examined the evolutionary relationships between humans and WTD in greater detail for the Alpha variant. The analysis included an additional 17 genome sequences from B.1.1.7 viruses collected from WTD in Pennsylvania during 2022–2023 that were provided by the US Department of Agriculture (USDA). We contacted the submitting authors of all B.1.1.7 sequences collected from humans in 2022–2023 and published on GISAID. Those communications resulted in identifying some GISAID entries as mislabeled; those entries were subsequently corrected and, in rare cases, confirmed as chronically infected patients. We retained all B.1.1.7 sequences with virus collection dates during 2022–2023 confirmed by submitting authors to have the correct date for our analysis. We performed a time-scaled Bayesian analysis by using the Markov chain Monte Carlo method available by using the latest version of the BEAST (*22*) package with graphics processing units available from the Biowulf Linux cluster. We used a host-specific local clock (*23*) to accommodate differences in the evolutionary rate between WTD and humans. Because WTD viruses were not monophyletic on the Alpha or Delta tree, owing to multiple independent human-to-deer transmission events, we identified separate WTD transmission clusters on the maximum-likelihood tree. We used a Bayesian nonparametric demographic model (*24*) with a general time reversible model of nucleotide substitution with gamma-distributed rate variation among sites. We ran the Markov chain Monte Carlo separately 3–5 times for each dataset by using the BEAGLE 3 library (*25*) to improve computational performance, until all parameters reached convergence as assessed visually by using Tracer v.1.7.2 (*26*). We removed ≥10% of the chain as burn-in and combined runs for the same dataset by using LogCombiner v1.10.4 (https://beast.community/logcombiner). We summarized a maximum clade credibility tree by using TreeAnnotator version 1.10.4 (https://beast.community/treeannotator). We conducted a phylogeographic discrete trait analysis (*27*) to quantify rates of viral gene flow, particularly in the directions of human-to-deer and long-distance deer-to-deer transmission. We specified a location state for each viral sequence. The 5 categories were B.1.1.7 viruses collected in humans; B.1.1.7 viruses collected in WTD in Ohio, including northern Ohio sequences generated for this study and sequences from southern Ohio generated for our previous study; B.1.1.7 viruses collected in WTD in Pennsylvania during 2022–2023 that were provided by USDA; all other B.1.1.7 viruses collected in WTD; and B.1.1.7 viruses collected from mink in Europe (including Poland and Lithuania). We estimated the expected number of location state transitions in the ancestral history on the basis of the data observed from the tree tips by using

Markov jump counts (*28*,*29*), which provided a quantitative measure of asymmetry in gene flow between defined populations.

Results

High Prevalence of SARS-CoV-2 in WTD in Northeast Ohio

Of nasal swab samples collected from WTD in northeast Ohio during January–March 2023, a total of 12.3% (64/519) were positive for SARS-CoV-2 by RT-PCR (Appendix Table 1, Appendix Figure 1, https://wwwnc.cdc.gov/EID/article/31/7/24-1922-App1.pdf). SARS-CoV-2 was detected in 4 of the 10 study sites, ranging in estimated prevalence of 6.5%–50.0%. We estimated the highest prevalence (50.0%, 95% CI 33.38%–66.62%) at site 9, a location adjacent to an area of high human population density (Figure 1). We attempted virus isolation on 58 of the 64 SARS-CoV-2 RT-PCR–positive samples, yielding 12 SARS-CoV-2 isolates, all belonging to the Omicron lineage (Appendix Table 2).

Alpha and Omicron Variants Identified in WTD

We generated whole-genome sequences from 36 SARS-CoV-2 RT-PCR–positive samples collected from WTD in northeast Ohio during January 25–March 13, 2023. Whole-genome SARS-CoV-2 sequences are available in GenBank (Appendix Table 3). Most viruses (86.1%, 31/36) were classified as PANGO lineages belonging to the Omicron variant (BQ.1.1, BQ.1.1.63, BQ.1.1.67, BQ.1.23, and XBB.1.5.35) (Table) that was circulating in humans at the time in Ohio and globally. However, 5 viruses collected from WTD in this study were classified as PANGO lineage B.1.1.7 (Alpha variant). B.1.1.7 viruses caused an outbreak in humans in Ohio during the spring of 2021, almost 2 years before our sampling period in deer. The last B.1.1.7 virus sampled

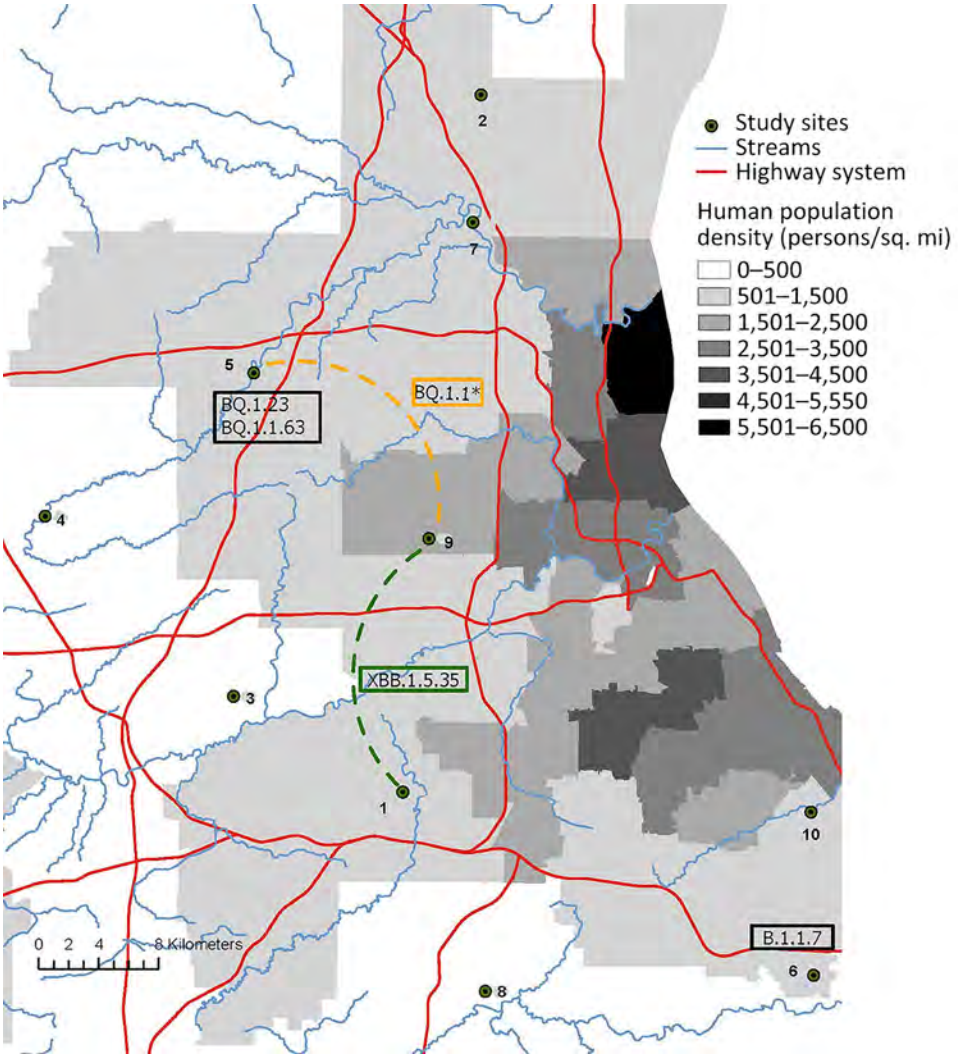

Figure 1. Locations of SARS-CoV-2 viruses in white-tailed deer in northeast Ohio, USA. The map shows the 6 pangolin lineages (*17*) identified in deer (boxes) located within 4 sampling sites during January–March 2023. The dotted lines between sampling sites represent inferred routes of transmission, as inferred from deer clusters identified on the phylogenetic tree shown in Figure 2. The SARS-CoV-2 XBB.1.5.35 lineage transmission between locations 1 and 9 is inferred from Omicron cluster 1. The SARS-CoV-2 BQ.1.1 (including BQ.1.1.67) lineage transmission between locations 5 and 9 is inferred from Omicron cluster 2. Map created by using ArcGIS Pro 3.1.0 (Esri, https://www.esri.com).

Table. SARS-CoV-2 whole genome sequences generated for a study on the persistence of SARS-CoV-2 Alpha variant in white-tailed deer, Ohio, USA

Strain name	Region	Pangolin lineage (*17*)	Date	Cluster
SC2/deer/USA/OH-OSU-COV0045057/2023	R6	B.1.1.7	2023 Jan 26	Alpha cluster
SC2/deer/USA/OH-OSU-COV0045054/2023	R6	B.1.1.7	2023 Jan 26	Alpha cluster
SC2/deer/USA/OH-OSU-COV0045056/2023	R6	B.1.1.7	2023 Jan 26	Alpha cluster
SC2/deer/USA/OH-OSU-COV0045058/2023	R6	B.1.1.7	2023 Jan 26	Alpha cluster
SC2/deer/USA/OH-OSU-COV0045967/2023	R6	B.1.1.7	2023 Jan 26	Alpha cluster
SC2/deer/USA/OH-OSU-COV0054305/2023	R1	XBB.1.5.35	2023 Feb 23	Omicron cluster 1
SC2/deer/USA/OH-OSU-COV0054309/2023	R1	XBB.1.5.35	2023 Feb 23	Omicron cluster 1
SC2/deer/USA/OH-OSU-COV0054308/2023	R1	XBB.1.5.35	2023 Feb 23	Omicron cluster 1
SC2/deer/USA/OH-OSU-COV0054313/2023	R1	XBB.1.5.35	2023 Feb 23	Omicron cluster 1
SC2/deer/USA/OH-OSU-COV0054303/2023	R1	XBB.1.5.35	2023 Feb 23	Omicron cluster 1
SC2/deer/USA/OH-OSU-COV0054306/2023	R1	XBB.1.5.35	2023 Feb 23	Omicron cluster 1
SC2/deer/USA/OH-OSU-COV0054343/2023	R9	XBB.1.5.35	2023 Feb 27	Omicron cluster 1
SC2/deer/USA/OH-OSU-COV0054342/2023	R9	XBB.1.5.35	2023 Feb 27	Omicron cluster 1
SC2/deer/USA/OH-OSU-COV0060785/2023	R1	XBB.1.5.35	2023 Mar 9	Omicron cluster 1
SC2/deer/USA/OH-OSU-COV0060778/2023	R1	XBB.1.5.35	2023 Mar 9	Omicron cluster 1
SC2/deer/USA/OH-OSU-COV0060777/2023	R1	XBB.1.5.35	2023 Mar 9	Omicron cluster 1
SC2/deer/USA/OH-OSU-COV0060782/2023	R1	XBB.1.5.35	2023 Mar 9	Omicron cluster 1
SC2/deer/USA/OH-OSU-COV0060781/2023	R1	XBB.1.5.35	2023 Mar 9	Omicron cluster 1
SC2/deer/USA/OH-OSU-COV0060793/2023	R1	XBB.1.5.35	2023 Mar 9	Omicron cluster 1
SC2/deer/USA/OH-OSU-COV0045880/2023	R9	BQ.1.1	2023 Jan 30	Omicron cluster 2
SC2/deer/USA/OH-OSU-COV0045866/2023	R9	BQ.1.1	2023 Jan 30	Omicron cluster 2
SC2/deer/USA/OH-OSU-COV0045876/2023	R9	BQ.1.1	2023 Jan 30	Omicron cluster 2
SC2/deer/USA/OH-OSU-COV0045889/2023	R9	BQ.1.1	2023 Jan 30	Omicron cluster 2
SC2/deer/USA/OH-OSU-COV0045870/2023	R9	BQ.1.1	2023 Jan 30	Omicron cluster 2
SC2/deer/USA/OH-OSU-COV0045877/2023	R9	BQ.1.1	2023 Jan 30	Omicron cluster 2
SC2/deer/USA/OH-OSU-COV0045873/2023	R9	BQ.1.1.67	2023 Jan 30	Omicron cluster 2
SC2/deer/USA/OH-OSU-COV0045874/2023	R9	BQ.1.1.67	2023 Jan 30	Omicron cluster 2
SC2/deer/USA/OH-OSU-COV0045887/2023	R9	BQ.1.1	2023 Jan 30	Omicron cluster 2
SC2/deer/USA/OH-OSU-COV0045890/2023	R9	BQ.1.1	2023 Jan 30	Omicron cluster 2
SC2/deer/USA/OH-OSU-COV0054341/2023	R9	BQ.1.1.67	2023 Feb 27	Omicron cluster 2
SC2/deer/USA/OH-OSU-COV0054302/2023	R9	BQ.1.1	2023 Feb 27	Omicron cluster 2
SC2/deer/USA/OH-OSU-COV0060771/2023	R5	BQ.1.1	2023 Mar 13	Omicron cluster 2
SC2/deer/USA/OH-OSU-COV0060768/2023	R5	BQ.1.1	2023 Mar 13	Omicron cluster 2
SC2/deer/USA/OH-OSU-COV0060769/2023	R5	BQ.1.1	2023 Mar 13	Omicron cluster 2
SC2/deer/USA/OH-OSU-COV0045465/2023	R5	BQ.1.23	2023 Jan 25	Omicron singleton 1
SC2/deer/USA/OH-OSU-COV0054384/2023	R5	BQ.1.1.63	2023 Feb 13	Omicron singleton 2

in humans in Ohio was on August 23, 2021 (GISAID accession no. EPI_ISL_3897556). All 5 B.1.1.7 viruses identified in WTD from this study were sampled at the same location (region 6) (Figure 1) on the same date (January 26, 2023). The most closely related human B.1.1.7 virus was collected >1 year earlier on November 19, 2021 (strain identification no. hCoV-19/USA/DC-DFS-PHL-03511/2021).

Deer-to-Deer Transmission between Locations

Two major deer clusters of Omicron viruses were evident on the phylogenetic tree (Table; Figure 2). Omicron cluster 1 includes 14 viruses belonging to the XBB.1.5.35 lineage sampled at the region 1 (n = 12) and region 9 (n = 2) locations (Figure 1) during February 23–March 9, 2023. Omicron cluster 2 includes 15 viruses belonging to the BQ.1.1 lineage and closely related BQ.1.1.67 lineage and was sampled in the region 5 (n = 3) and region 9 (n = 12) locations (Figure 1) during January 30–March 13, 2023. The presence of 2 clusters spanning multiple locations separated by >10 km is consistent with substantial deer-to-deer transmission of Omicron viruses. No BQ.1.1 or XBB.1.5.35 viruses were observed in any other non-human population outside this study on the basis of the sequences available in GISAID.

Persistence of the Alpha Variant in WTD

Because B.1.1.7 viruses were reported previously in WTD in Ohio, New York, Pennsylvania, and other US states, as well as in mink in Europe (Poland and Lithuania), we performed an expansive global analysis including B.1.1.7 sequences from humans, deer, and mink that were downloaded from GISAID. We also included 17 additional B.1.1.7 sequences provided by the USDA from WTD in Pennsylvania, which borders northeast Ohio. The maximum clade credibility tree inferred from this dataset (Figure 3) reveals that B.1.1.7 viruses repeatedly transmitted from humans to WTD in New York (9 introductions), Pennsylvania (6 introductions), Ohio (3 introductions), Massachusetts (1 introduction), Delaware (1 introduction), Illinois (1 introduction), and West Virginia (1 introduction). As expected, most suspected

human-to-deer B.1.1.7 transmission events occurred during spring 2021, when the Alpha variant was peaking in humans in the United States. Nearly three quarters of B.1.1.7 viruses in WTD were collected in 2021 (73.5%, n = 89/121). A small number of B.1.1.7 viruses were still found in WTD during January 1–March 31, 2022 (8.3%, n = 10/121). However, our sampling in northeast Ohio in 2023 and USDA's sampling in Pennsylvania occurred a year later, during October 2022–March 2023, and still found 3 clades of B.1.1.7 viruses circulating in WTD in Ohio and Pennsylvania (Figure 3). Our sampling occurred ≈1 year after the virus was no longer identified in WTD in other states. A small number of B.1.1.7 viruses were identified in humans in other US states during 2022–2023 that were collected from a confirmed chronically infected patient (strain identification no. hCoV-19/USA/IL-RIPHL_120858_G/2022 from July 26, 2022 [A. Kittner, Chicago Department of Public Health, pers. comm., email, 2024 Jan 1]) or a suspected chronically infected patient (strain identification no. hCoV-19/USA/VA-VCUVAS3-WCCD884559/2023). We found no other B.1.1.7 sequences in humans globally during 2022–2023, after excluding sequences on GISAID that were determined to be mislabeled, as verified by direct correspondence with the sequence

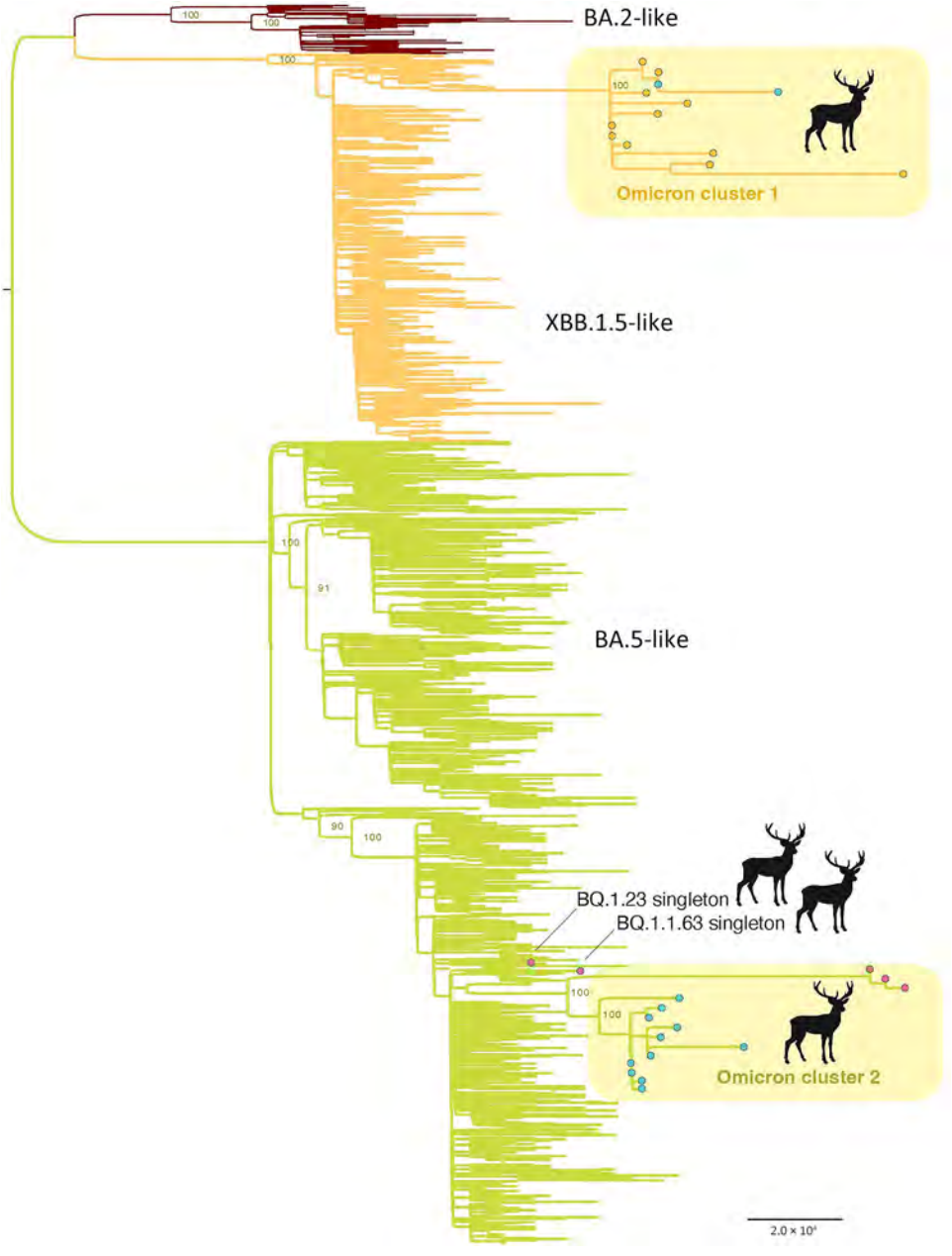

Figure 2. Maximum-likelihood tree inferred for the complete genome sequences of 31 SARS-CoV-2 viruses collected from white-tailed deer and a random subsample of 1,000 SARS-CoV-2 viruses collected from humans from northeast Ohio, November 1, 2022–March 30, 2023. Branches are shaded according to 3 categories of Omicron viruses: red, BA.2-like; orange, XBB.1.5-like; and green, BA.5-like. Circles at tips indicate the deer viruses and are shaded according to region: orange, R1; pink, R5; and blue, R9. Two deer clusters (Omicron cluster 1 and 2) are labeled, along with the 2 single deer singleton viruses. All branch lengths are drawn to scale and bootstrap values are provided for key nodes. Scale bar represents substitutions per site.

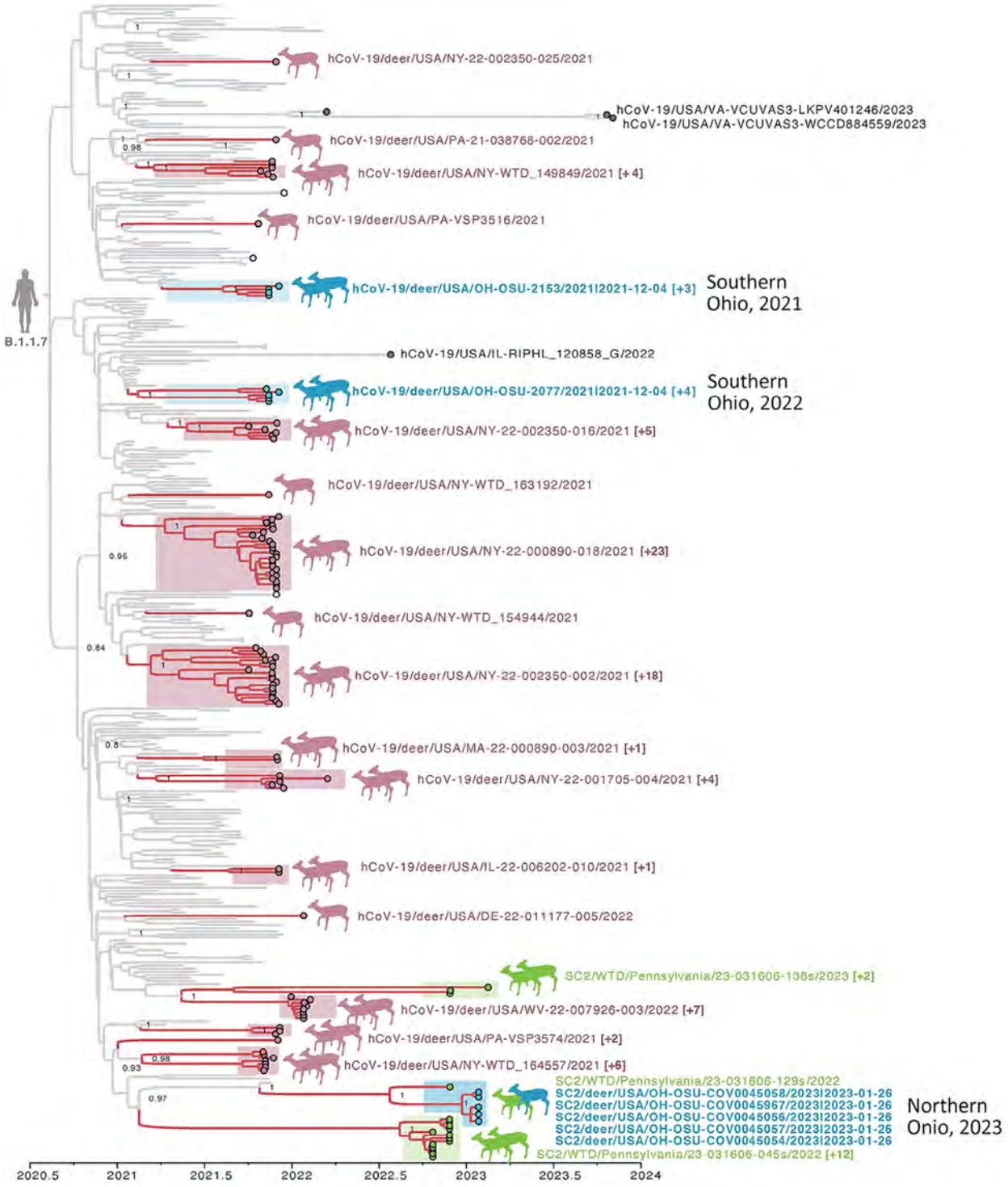

Figure 3. Time-scaled maximum clade credibility tree of the Alpha variant of SARS-CoV-2 viruses circulating in WTD in northeast Ohio, USA. The tree was inferred by using a host-specific local clock for the complete genome sequences of 362 SARS-CoV-2 clade B.1.1.7 viruses sampled December 29, 2020–November 3, 2023. Branches are shaded by host: gray, human or mink; pink, WTD. Circles at tips are shaded by location and source: blue, WTD from Ohio; green, WTD from Pennsylvania (2022–2023); pink, WTD from other states (or Pennsylvania in 2021); white, mink (Lithuania and Poland); and gray, human (2022–2023). Deer transmission clusters are shaded similarly and indicated by paired deer illustrations. Single-deer illustrations indicate singleton introductions into WTD. Singleton WTD viruses are labeled, and a representative virus is provided for each WTD transmission cluster, with the number of additional viruses in the cluster in parentheses. Posterior probabilities are provided for key nodes. WTD, white-tailed deer.

submitters. Of note, the B.1.1.7 viruses collected in deer are not closely related to the viruses sequenced from chronically infected patients (or suspected chronic infection) in Virginia or Illinois, suggesting that deer did not acquire B.1.1.7 from the chronically infected patients for which we have sequence data.

Most Pennsylvania deer B.1.1.7 viruses from 2022–2023 cluster separately from the Ohio deer B.1.1.7 viruses collected in 2023 and represent independent introductions from humans to WTD in Pennsylvania (Figure 3). However, 1 Pennsylvania virus collected from WTD on November 27, 2022 (strain identification no. SC2/WTD/Pennsylvania/23-031606-129s/2022), clusters with the 5 B.1.1.7 Ohio viruses collected in WTD 2 months later, forming a distinct clade that appears to be a deer-to-deer transmission cluster that spans Pennsylvania and Ohio. The Pennsylvania virus was collected in a county situated in the northwest region of the state, bordering northeast Ohio. The maximum clade credibility tree estimates that the human-to-deer transmission event that led to the Ohio/Pennsylvania deer transmission cluster occurred during October 26, 2021–July 23, 2022. We suspect transmission occurred closer to the 2021 end of this range, given that B.1.1.7 was more prevalent in humans in 2021 than 2022. The maximum clade credibility tree also shows that the B.1.1.7 viruses found in WTD from northeast Ohio in 2023 are not closely related to the B.1.1.7 viruses that were found in WTD from southern Ohio in 2021 from our previous study (*11*) and represent a third independent introduction of B.1.1.7 from humans into WTD in Ohio. Whether B.1.1.7 was first introduced from humans into WTD in Ohio and then spread to deer in Pennsylvania, or vice versa, is difficult to determine because of the long branch length and ≈1-year time gap between the estimated human-to-deer introduction and first detection of the cluster in deer. SARS-CoV-2 detections in WTD in Ohio were limited near the end of 2022, and no sequences were recovered from positive samples despite multiple attempts, contributing to uncertainties around transmission and persistence in deer. The most closely related human virus was sampled in the District of Columbia, but

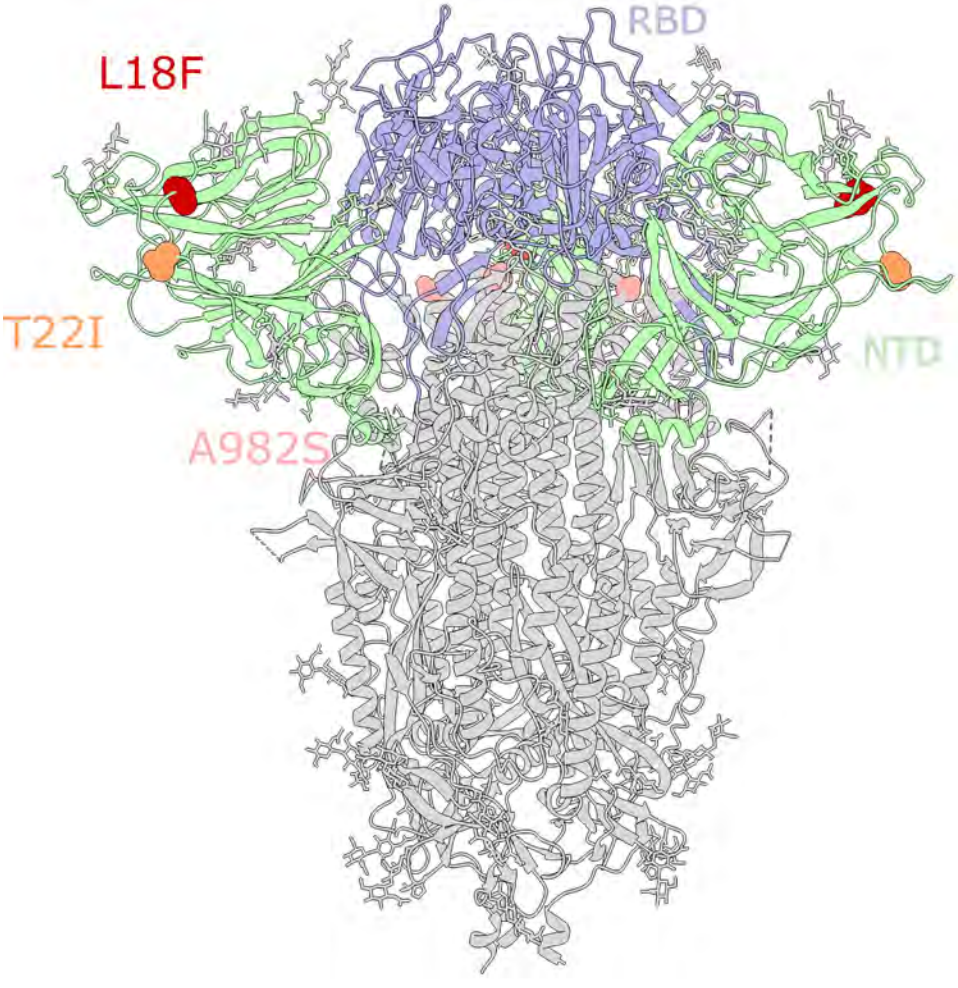

Figure 4. Mutations in the spike glycoprotein of SARS-CoV-2 viruses circulating in white-tailed deer in northeast Ohio, USA. SARS-CoV-2 spike glycoprotein structure obtained from the Protein Data Base (identification no. 7jji; https://www.rcsb.org). RBD and NTD are labeled. Circles indicate the location of mutations in the SARS-CoV-2 clade B.1.1.7 viruses collected from white-tailed deer in Ohio and other US states: red, L18F; orange, T22I; pink, A982S. Mutation S12F (located in NTD) is not shown because it is located at the flexible N terminus, for which a 3D structure is not available. NTD, N-terminal domain; RBD, receptor-binding domain.

the high mobility of humans and long lag time means this data point does not inform our inference of the location of human-to-deer transmission.

SARS-CoV-2 Mutations in Spike Protein in WTD

B.1.1.7 viruses in WTD accumulated mutations at a rate that was ≥2-fold higher than in humans (Appendix Figure 1, panel A). Consistent with our prior findings (*11*), the higher rate of evolution in WTD is not driven by a higher rate of nonsynonymous mutations, which would be evidence of strong selective pressures. Rather, both synonymous and nonsynonymous mutations are accumulated at higher rates (Appendix Figure 1, panels B, C). In particular, T>C substitutions occur more often in deer than in humans (Appendix Figure 1, panels D, E). The presence of multiple independently evolving WTD clusters of B.1.1.7 provides an opportunity to look for recurring mutations that could be adaptive to deer. We observed recurring mutations in the N-terminal domain of the spike protein (S12F, L18F, and T22I) (Figure 4) that each occur independently in 2 different deer clusters (Appendix Figures 1, 2). The L18F mutation was observed in 2021 in WTD in New York and again in 2023 in Pennsylvania. L18F is associated with escape from multiple N-terminal domain binding antibodies in humans (*30*). The 2023 B.1.1.7 viruses from Pennsylvania also contain the A982S reversion mutation in the spike protein. Although S982A was 1 of the characteristic mutations of B.1.1.7, we observed the A982S reversion in 12 samples (3 independent events).

Discussion

An apparent decrease in SARS-CoV-2 detections in North America WTD after emergence of the Omicron variant in humans in late 2021 led to speculation that the highly mutated and human-adapted Omicron variant could have reduced capacity to infect other species. Instead, we found evidence in northeast Ohio of extensive deer-to-deer transmission of ≥2 Omicron lineages (XBB.1.5.35 and BQ.1.1) that each spread between 2 sampling sites separated by interstate highways. An even more surprising finding in our study was the detection of 5 Alpha variant B.1.1.7 viruses in WTD in January 2023, more than 1 year after the last detection of B.1.1.7 in humans in Ohio. Additional B.1.1.7 deer transmission clusters were identified in Pennsylvania in late 2022, as well as a cluster in WTD in a neighboring Pennsylvania county that is positioned with our Ohio deer transmission cluster, emphasizing the importance of coordinated surveillance across state lines. Together, those data support the capacity of WTD to sustain Alpha variant transmission after the virus disappeared in humans, even longer than previously reported in WTD in New York and our previous study (*4*,*11*). The retention of SARS-CoV-2 lineages no longer circulating in humans, evolving with an increased mutation rate and accumulation of mutations evading immunity, warrants further monitoring of the persistence and evolution of SARS-CoV-2 in deer. SARS-CoV-2 evolution also provides a rare opportunity to study pathogen emergence and early adaptations in wildlife hosts, before the disease becomes widely established.

A recent report of SARS-CoV-2 spillover from humans to farmed mink to WTD underscores the virus's high capacity for host-switching (A. Crespo-Bellido, unpub. data). SARS-CoV-2 viruses were also recently detected in a wide range of species in Virginia (*31*). Given the broad host range of SARS-CoV-2, it is possible that the Alpha variant was maintained by multiple host species before detection in WTD in our study, including some that are not sampled, but no detections in other species from this region were reported (*1*). Active surveillance and serosurveys of SARS-CoV-2 in a broad range of species are warranted, along with targeted studies in WTD. Experimental studies also are needed to determine the mode of transmission (e.g., environmental, airborne) between humans and deer and from deer to deer.

More questions than answers remain surrounding the human–animal interface for SARS-CoV-2. Currently, phylogenetic analyses do not suggest the SARS-CoV-2 variants circulating in WTD in northeast Ohio have transmitted back to humans or present a major zoonotic risk, but suspected deer-to-human transmission has been documented in Ontario, Canada (*8*). If SARS-CoV-2 becomes endemic in WTD, the virus may persist with relatively few mutations over time. However, it is also possible the virus could accumulate functional mutations, leading to deer-adapted variants with unknown spillover potential to other hosts. Evidence of sustained transmission of the Alpha variant in WTD, alongside more recent introductions of Omicron lineages in WTD, highlights the need for continued surveillance to monitor the long-term dynamics of SARS-CoV-2 in WTD and the associated zoonotic risks.

Acknowledgments

We thank the Cleveland Metroparks Deer Management Team for their assistance with sample collection.

Funding was provided by the Centers of Excellence for Influenza Research and Response, National Institute of Allergy and Infectious Diseases, National Institutes of Health (contract nos. 75N93021C00014 and

75N93021C000016). This work was also supported by the Intramural Research Program of the National Library of Medicine at the National Institutes of Health.

About the Author

Ms. Tarbuck is a PhD student in the College of Veterinary Medicine Comparative Biomedical Sciences program at The Ohio State University. Her research interests include the epidemiology of zoonotic diseases at the human-animal interface.

References

1. Animal and Plant Health Inspection Service. SARS-CoV-2 in animals [cited 2024 Oct 24]. https://www.aphis.usda.gov/sars-cov-2
2. Wei C, Shan KJ, Wang W, Zhang S, Huan Q, Qian W. Evidence for a mouse origin of the SARS-CoV-2 Omicron variant. J Genet Genomics. 2021;48:1111–21. https://doi.org/10.1016/j.jgg.2021.12.003
3. Sun Y, Lin W, Dong W, Xu J. Origin and evolutionary analysis of the SARS-CoV-2 Omicron variant. J Biosaf Biosecur. 2022;4:33–7. https://doi.org/10.1016/j.jobb.2021.12.001
4. Caserta LC, Martins M, Butt SL, Hollingshead NA, Covaleda LM, Ahmed S, et al. White-tailed deer (*Odocoileus virginianus*) may serve as a wildlife reservoir for nearly extinct SARS-CoV-2 variants of concern. Proc Natl Acad Sci U S A. 2023;120:e2215067120. https://doi.org/10.1073/pnas.2215067120
5. Hale VL, Dennis PM, McBride DS, Nolting JM, Madden C, Huey D, et al. SARS-CoV-2 infection in free-ranging white-tailed deer. Nature. 2022;602:481–6. https://doi.org/10.1038/s41586-021-04353-x
6. Marques AD, Sherrill-Mix S, Everett JK, Adhikari H, Reddy S, Ellis JC, et al. Multiple introductions of SARS-CoV-2 Alpha and Delta variants into white-tailed deer in Pennsylvania. MBio. 2022;13:e0210122. https://doi.org/10.1128/mbio.02101-22
7. Kuchipudi SV, Surendran-Nair M, Ruden RM, Yon M, Nissly RH, Vandegrift KJ, et al. Multiple spillovers from humans and onward transmission of SARS-CoV-2 in white-tailed deer. Proc Natl Acad Sci U S A. 2022;119:e2121644119. https://doi.org/10.1073/pnas.2121644119
8. Pickering B, Lung O, Maguire F, Kruczkiewicz P, Kotwa JD, Buchanan T, et al. Divergent SARS-CoV-2 variant emerges in white-tailed deer with deer-to-human transmission. Nat Microbiol. 2022;7:2011–24. https://doi.org/10.1038/s41564-022-01268-9
9. Feng A, Bevins S, Chandler J, DeLiberto TJ, Ghai R, Lantz K, et al. Transmission of SARS-CoV-2 in free-ranging white-tailed deer in the United States. Nat Commun. 2023;14:4078. https://doi.org/10.1038/s41467-023-39782-x
10. Vandegrift KJ, Yon M, Surendran Nair M, Gontu A, Ramasamy S, Amirthalingam S, et al. SARS-CoV-2 Omicron (B.1.1.529) infection of wild white-tailed deer in New York City. Viruses. 2022;14:2770. https://doi.org/10.3390/v14122770
11. McBride DS, Garushyants SK, Franks J, Magee AF, Overend SH, Huey D, et al. Accelerated evolution of SARS-CoV-2 in free-ranging white-tailed deer. Nat Commun. 2023;14:5105. https://doi.org/10.1038/s41467-023-40706-y
12. Association of Fish and Wildlife Agencies. Methods for managing deer in populated areas. 2018 [cited 2024 Dec 12]. https://www.fishwildlife.org/application/files/7315/3745/9637/AFWA_Deer_Mngmt_Pop_Areas_August_31_2018_version.pdf
13. United States Fish and Wildlife Service. Fishing and hunting recruitment, retention, and reactivation in the U.S. September 2024 [cited 2024 Dec 12] https://www.fws.gov/sites/default/files/documents/2024-09/2022-fishing-and-hunting-r3-in-the-us.pdf
14. Chen S. Ultrafast one-pass FASTQ data preprocessing, quality control, and deduplication using fastp. iMeta. 2023;2:e107. https://doi.org/10.1002/imt2.107
15. Grubaugh ND, Gangavarapu K, Quick J, Matteson NL, De Jesus JG, Main BJ, et al. An amplicon-based sequencing framework for accurately measuring intrahost virus diversity using PrimalSeq and iVar. Genome Biol. 2019;20:8. https://doi.org/10.1186/s13059-018-1618-7
16. O'Toole Á, Scher E, Underwood A, Jackson B, Hill V, McCrone JT, et al. Assignment of epidemiological lineages in an emerging pandemic using the pangolin tool. Virus Evol. 2021;7:veab064. https://doi.org/10.1093/ve/veab064
17. Minh BQ, Schmidt HA, Chernomor O, Schrempf D, Woodhams MD, von Haeseler A, et al. IQ-TREE 2: new models and efficient methods for phylogenetic inference in the genomic era. Mol Biol Evol. 2020;37:1530–4. https://doi.org/10.1093/molbev/msaa015
18. Turakhia Y, Thornlow B, Hinrichs AS, De Maio N, Gozashti L, Lanfear R, et al. Ultrafast sample placement on existing trees (UShER) enables real-time phylogenetics for the SARS-CoV-2 pandemic. Nat Genet. 2021;53:809–16. https://doi.org/10.1038/s41588-021-00862-7
19. Sagulenko P, Puller V, Neher RA. TreeTime: maximum-likelihood phylodynamic analysis. Virus Evol. 2018;4:vex042. https://doi.org/10.1093/ve/vex042
20. Meng EC, Goddard TD, Pettersen EF, Couch GS, Pearson ZJ, Morris JH, et al. UCSF ChimeraX: tools for structure building and analysis. Protein Sci. 2023;32:e4792. https://doi.org/10.1002/pro.4792
21. Huerta-Cepas J, Serra F, Bork P. ETE 3: Reconstruction, analysis, and visualization of phylogenomic data. Mol Biol Evol. 2016;33:1635–8. https://doi.org/10.1093/molbev/msw046
22. Suchard MA, Lemey P, Baele G, Ayres DL, Drummond AJ, Rambaut A. Bayesian phylogenetic and phylodynamic data integration using BEAST 1.10. Virus Evol. 2018;4:vey016. https://doi.org/10.1093/ve/vey016
23. Worobey M, Han GZ, Rambaut A. A synchronized global sweep of the internal genes of modern avian influenza virus. Nature. 2014;508:254–7. https://doi.org/10.1038/nature13016
24. Gill MS, Lemey P, Faria NR, Rambaut A, Shapiro B, Suchard MA. Improving Bayesian population dynamics inference: a coalescent-based model for multiple loci. Mol Biol Evol. 2013;30:713–24. https://doi.org/10.1093/molbev/mss265
25. Ayres DL, Cummings MP, Baele G, Darling AE, Lewis PO, Swofford DL, et al. BEAGLE 3: Improved performance, scaling, and usability for a high-performance computing library for statistical phylogenetics. Syst Biol. 2019;68:1052–61. https://doi.org/10.1093/sysbio/syz020
26. Rambaut A, Drummond AJ, Xie D, Baele G, Suchard MA. Posterior summarization in Bayesian phylogenetics using tracer 1.7. Syst Biol. 2018;67:901–4. https://doi.org/10.1093/sysbio/syy032
27. Lemey P, Rambaut A, Drummond AJ, Suchard MA. Bayesian phylogeography finds its roots. PLOS Comput

Biol. 2009;5:e1000520. https://doi.org/10.1371/journal.pcbi.1000520
28. Minin VN, Suchard MA. Counting labeled transitions in continuous-time Markov models of evolution. J Math Biol. 2008;56:391–412. https://doi.org/10.1007/s00285-007-0120-8
29. Lemey P, Rambaut A, Bedford T, Faria N, Bielejec F, Baele G, et al. Unifying viral genetics and human transportation data to predict the global transmission dynamics of human influenza H3N2. PLoS Pathog. 2014; 10:e1003932. https://doi.org/10.1371/journal.ppat.1003932
30. McCallum M, De Marco A, Lempp FA, Tortorici MA, Pinto D, Walls AC, et al. N-terminal domain antigenic mapping reveals a site of vulnerability for SARS-CoV-2. Cell. 2021;184:2332–2347.e16. https://doi.org/10.1016/j.cell.2021.03.028
31. Goldberg AR, Langwig KE, Brown KL, Marano JM, Rai P, King KM, et al. Widespread exposure to SARS-CoV-2 in wildlife communities. Nat Commun. 2024;15:6210. https://doi.org/10.1038/s41467-024-49891-w

Address for correspondence: Andrew S. Bowman, The Ohio State University, 1920 Coffey Rd, Columbus, OH 43210, USA; email: bowman.214@osu.edu

Transmission Dynamics and Parameters for Pertussis during School-Based Outbreak, South Korea, 2024

U. Jin Cho,[1] Seonghui Cho,[1] Hyeokjin Lee, Seul-Ki Kang, Bryan Inho Kim, Yukyung Nam, Chiara Achangwa, Jun-Sik Lim, Dong Han Lee,[2] Sukhyun Ryu[2]

We estimated the serial interval and superspreading potential to quantify pertussis transmission dynamics in a 2024 school-based outbreak of a population in South Korea that had received a series of pertussis vaccinations. We analyzed 48 cases of pertussis and reconstructed 36 transmission pairs. We then used maximum-likelihood estimation to assess serial interval and offspring distribution from transmission pair data. We identified that the mean serial interval was 9.5 (SD 1.6) days; 15% (95% CI 8%–23%) of cases seeded 80% of all transmissions in this outbreak. Our findings suggest that pertussis was highly transmissible in vaccinated children during this outbreak. Rapid contact tracing and strict adherence to public health measures are needed to reduce community pertussis transmission.

Pertussis, also known as whooping cough, is a highly contagious respiratory infection caused by *Bordetella pertussis*, a gram-negative bacterium (*1*,*2*). *B. pertussis*, which is found only in humans, accumulates in the respiratory tract and is mainly transmitted through respiratory droplets (*1*,*3*). The distinguishing clinical characteristic of pertussis is a cough that gradually develops into a severe hacking cough, which can persist for several weeks (*1*).

After immunization programs began in the 1940s, the incidence of pertussis was reduced globally (*2*–*4*). However, since the 1980s, a resurgence in pertussis cases has been observed in countries (*2*,*4*). In 2024, the United States and Europe saw an increase in the number of reported cases (*5*,*6*). Although East Asia, including Taiwan, Singapore, and Japan, has not seen an increased number of the cases in 2024 compared to those of 2020–2023 (*7*), in South Korea, pertussis cases have risen sharply, particularly among school-age children (*7*,*8*). Pertussis vaccines are available, including the DTaP (diphtheria, tetanus, and acellular pertussis) vaccine for children and the Tdap (tetanus, diphtheria, and acellular pertussis) vaccine for adolescents and adults. Those vaccines are effective in preventing severe pertussis, but recipients may experience waning immunity acquired from the vaccination over time (*9*,*10*). In South Korea, pertussis has been managed as a notified disease since 1954; a national immunization program provides DTap vaccine at 2, 4, and 6 months of age; between 15 and 18 months of age; and between 4 and 6 years of age. Furthermore, a booster dose of Tdap is recommended for adolescents 11–12 of age in South Korea.

Identifying epidemiologic characteristics provides valuable information for public health practitioners and the public. However, pertussis's epidemiology and transmission dynamics, including its superspreading potential in a vaccinated population, remain unclear. In March 2024, a pertussis outbreak occurred in a boarding school in Busan, a city in southeastern South Korea with a population of 3.2 million (*11*). The Korea Disease Control and Prevention Agency (KDCA) implemented active case finding under the test-trace-isolate strategy to control the outbreak. In this study, we analyzed the case data associated with this pertussis outbreak and explored

Author affiliations: Gyeongnam Regional Center for Disease Control and Prevention, Busan, South Korea (U.J. Cho, H. Lee, D.H. Lee); The Catholic University of Korea, Seoul, South Korea (S. Cho, Y. Nam, C. Achangwa, S. Ryu); Korea Disease Control and Prevention Agency, Cheongju-si, South Korea (S.-K. Kang, B.I. Kim); Korea University, Seoul (S.-K. Kang, Y. Nam); National University of Singapore, Singapore (J.-S. Lim)

DOI: https://doi.org/10.3201/eid3107.241643

[1]These first authors contributed equally to this article.

[2]These authors were co–principal investigators.

the epidemiologic characteristics and transmission dynamics, including the superspreading potential of pertussis from an outbreak that occurred in the school setting. The Institutional Review Board of KDCA waived ethics approval for this study (Institutional Review Board no. KDCA-2024-09-06).

Methods

Epidemiologic Investigation

On April 17, 2024, the local education and public health authority in Busan, including the Gyeongnam Regional Center for Disease Control and Prevention, initiated an epidemiologic investigation to identify possible pertussis cases in the school, screening persons who had been in any contact with the case-patient or had any respiratory illness. The public health authority staff interviewed those persons to collect information including demographics, symptom onset date, exposure to the case-patient, and DTaP vaccination history. When vaccination history was unavailable through the interview, public health authorities obtained it from the vaccine registry database of the KDCA. We defined a case as illness in a person who had confirmed *B. pertussis* by laboratory PCR in accordance with KDCA guidelines (*12*). All specimens from all suspected carriers were collected with nasopharyngeal swabs and were tested using a KDCA-approved commercial kit that targets gene coding for an insertion element (IS481) and the pertussis toxin promoter (*12*). We defined controls as persons at the school who tested negative by PCR during the outbreak. We defined the first day of illness as the onset of coughing or cough-preceding cold symptoms. We traced subsequent transmission back to the case-patient on the basis of the epidemiologic investigation report. Then, using contact tracing data and line lists, we established a transmission network (*13*). We determined the transmission network by the timing of exposure of infector and the symptom onset of infectee. When we could not definitively determine transmission pairs based on symptoms and exposure history alone, we investigated shared environments, such as classroom and dormitory interactions, to strengthen the epidemiologic link. Furthermore, we calculated the attack rate as the proportion of persons confirmed as cases during the outbreak out of the total number of persons at risk for infection in the school.

As a response to this outbreak, case-patients were required to stay home until they completed antimicrobial drug treatment. For the person in close contact with the cases, additional pertussis vaccination and preventive drugs (e.g., macrolides) were recommended in accordance with KDCA guidelines. All persons in the school were recommended to wear face masks until June 24, 2024, when the KDCA declared the outbreak over.

Serial Interval

Serial interval is an essential epidemiologic parameter that describes the time delay between consecutive generations of infected persons. We examined cases with symptom onset dates and reconstructed the transmission pairs by identifying the infector–infectee pair from the established transmission network. We computed the serial interval as the number of days between the symptom onset of the infector and the symptom onset of infectee. Then, we fitted 3 different parametric distributions (log-normal, gamma, and Weibull), which are right-skewed continuous probability distributions, using maximum-likelihood estimation (*14*). We also opted for the best-fitted distributions for serial intervals based on the Akaike information criterion (AIC), in which lower values indicate a better-fitted model. We compared the mean serial intervals between 2 groups of infectors: those vaccinated with DTaP within the previous 5 years and those vaccinated >5 years ago. In addition, we examined the differences in the mean serial intervals between infectors who had received final vaccination doses of 4–5 doses or 6 doses total. We performed comparisons using the Student *t*-test.

Superspreading Potential

We generated the observed offspring distribution by calculating the number of secondary cases. We fitted the offspring distribution to negative binomial distributions. Then, we presented the parameters, including the effective reproduction number (R_t), which is the mean number of infected persons resulting from an infector, and overdispersion (k), which indicates the individual level of heterogeneity in transmission (*15*). We also compared the k between the 2 infectors' groups (≤5 years and >5 years from the vaccination). We examined the statistical significance of the difference using a bootstrap method, resampling with replacement from the fitted negative binomial models to construct 10,000 bootstrap samples (*16*). We then calculated 95% CIs from the 2.5th and 97.5th percentiles of the resulting distribution of differences in k values. Furthermore, we estimated the expected proportion of cases responsible for 80% of the total secondary transmission using the estimated R_t and k obtained from this study (*17*,*18*).

Waning of Tdap Effectiveness

In South Korea, after the fifth dose of DTaP in children ≤7 years of age, a booster dose of Tdap with smaller concentrations of pertussis antigens (*19*) is recommended in children 11–12 years of age (*20*,*21*). We assessed the waning of protection against pertussis after the sixth dose of the pertussis vaccine (i.e., Tdap vaccination) by comparing case-patients with controls in this outbreak. To assess the effect of time since vaccination (i.e., the number of years elapsed since the sixth dose of vaccination) on the odds of acquiring pertussis, we used logistic regression models (*9*). We first modeled time since vaccination as an ordinal categorical variable, assuming a structured trend (i.e., monotonic relationship) between the number of years postvaccination and the odds of a positive pertussis PCR test. Furthermore, to assess the validity of this assumption and explore potential nonlinear trends in waning immunity, we employed an unordered categorical model, estimating separate odds ratios for each year following vaccination. By comparing the results from these models, we assessed the appropriateness of assuming a consistent trend in waning immunity over time. Furthermore, in the model, we included covariates to adjust for sex. We performed all statistical analyses in R version 4.4.1 (The R Project for Statistical Computing, https://www.r-project.org).

Results

Characteristics of the Study Population

This outbreak started on April 2, 2024, and lasted until May 28, 2024. The overall attack rate in the study was 10.1% (48 cases/476 persons). Of the 48 case-patients, 34 (70.8%) were male and 14 (29.2%) female, and the overall median age was 15 years (range 12–18 years) (Table; Figure 1). There were 5 (10.4%), case-patients who had received the fourth dose of the pertussis vaccine, 4 (8.3%) who had received the fifth dose, and 39 (81.3%) who had received the sixth dose. There were 43 (89.6%) symptomatic infections and 5 (10.4%) asymptomatic cases (Appendix Table 1, https://wwwnc.cdc.gov/EID/article/31/7/24-1643-App1.pdf). The median delay between symptom onset and laboratory confirmation was 6 days (interquartile range 3.0–12.3 days).

Serial Interval

We identified 36 transmission pairs with a symptom onset date for both infector and infectee (Figure 2; Appendix Table 1). The Weibull distribution was the best fit for the serial interval distribution, estimated as a mean of 9.5 (95% CI 8.9–10.0) days; SD was 1.6 (95% CI 1.7–2.3) days (Figure 3; Appendix Table 2). We could not identify significant differences in the serial interval between the infector vaccinated within 5 years and those vaccinated >5 years ago, or between infectors with final vaccination doses of 4–5 (p = 0.72) and 6 (p = 0.69) (Appendix Figure).

Superspreading Potential

The overall R_t, estimated from the observed offspring distribution and negative binomial distribution, was 0.93 (95% CI 0.41–1.85), and k was 0.23 (95% CI 0.11–0.53) (Figure 4; Appendix Table 3). We identified k of 0.44 (95% CI 0.12–10.27) for persons who had the latest vaccination doses ≤5 years and 0.38 (95% CI 0.11–6.00) for those who had the latest dose >5

Table. Demographic characteristics of confirmed pertussis cases and controls in a boarding school in Busan, South Korea, 2024

Characteristic	Total	No. cases (%)	No. controls (%)	p value*
Overall	400	48 (12)	352 (88)	
Sex				0.69
M	269	34 (70.83)	235 (66.76)	
F	131	14 (29.17)	117 (33.24)	
Age group, y				0.43
12–15	134	19 (39.58)	115 (32.67)	
16–18	266	29 (60.42)	237 (67.33)	
Most recent vaccination				0.36
1st dose	5	0	5 (1.42)	
3rd dose	1	0	1 (0.28)	
4th dose	31	5 (10.42)	26 (7.39)	
5th dose	39	4 (8.33)	35 (9.94)	
6th dose	321	39 (81.25)	282 (80.11)	
Unavailable†	3	0	3 (0.85)	
Years since last vaccination				0.18
0–4	228	26 (54.17)	202 (57.39)	
5–9	138	20 (41.67)	118 (33.52)	
10–15	31	2 (4.17)	29 (8.24)	
Not available	3	0	3 (0.85)	

*Calculated by χ^2 test, Mann-Whitney U test, or Student *t*-test, where appropriate.
†Vaccine history could not be obtained either from the persons or from the vaccine registry database of the Korea Disease Control and Prevention Agency.

years previously (Appendix Table 4). The difference in *k* between the 2 groups was not statistically significant; bootstrap 95% CI for the difference was −0.11 to 0.24. We estimated that 15.4% (95% CI 8.0%–22.8%) of cases were responsible for 80% of all transmission in this outbreak.

Waning of Tdap Effectiveness

In the ordered and unordered categorical model for the time since vaccination, the odds ratio (OR) of acquiring pertussis fluctuated across the years. In the ordered model, OR was 0.39–4.72, and in the unordered model, OR was 0.36–3.98. Results for both models had wide CIs and were not statistically significant (Appendix Table 5).

Discussion

Countries in which a large portion of the population has received a series of pertussis vaccines have reported increased cases since late 2023. In our study, we identified the transmission characteristics of pertussis, including its serial interval and superspreading potential, using contact tracing data in South Korea.

The serial interval is an important factor in determining infectious disease control that is directly correlated with the infection spread rate throughout the community (*22*,*23*). We found that the gamma distribution had a similar mean serial interval with comparable AIC values to the Weibull distribution (Appendix Table 2), which indicated that our serial interval estimate is reliable and that both gamma and Weibull distributions are plausible models for our serial interval data. Previous studies in the United Kingdom, before pertussis vaccine was introduced, demonstrated that the median serial interval was 7 (range 4–56) days (*24*); another study in the Netherlands demonstrated the mean was 23 (95% CI 22–24) days (*25*). Our mean serial interval of 9.5 days is smaller than that determined in previous research (*25*), probably because of differing case definitions; the earlier study accounted for only cases with persistent coughing for >2 weeks. However, because most pertussis cases in South Korea seek care for mild respiratory illness (48%) and atypical cough (i.e., 4% had whooping cough, and 10% had night cough and paroxysmal cough) symptoms (*8*), we defined illness in any person with respiratory illness who had contact with a person with a positive PCR test result as a case. We also found that there was no significant difference in serial intervals according to the postvaccination time of infectors (i.e., 5 years before and after vaccination). Additional study is needed to determine whether the serial interval varies across settings, such as in households.

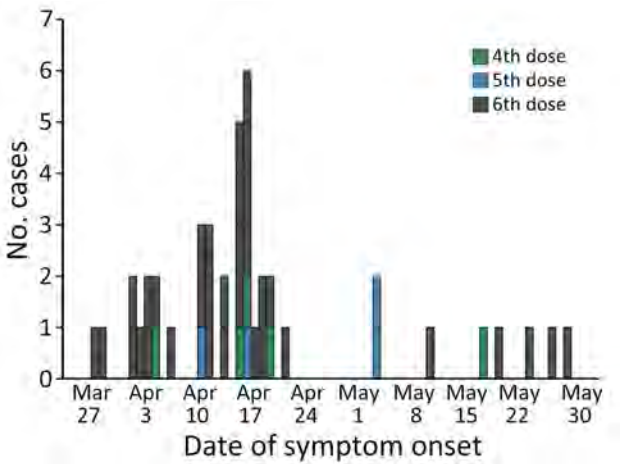

Figure 1. Epidemic curve of daily cases, by symptom onset and number of vaccine doses received, in outbreak of pertussis in a boarding school, Busan, South Korea. Asymptomatic cases (n = 5) were excluded.

Regarding superspreading potential, a previous modeling study demonstrated that irregular pertussis epidemics may arise because of stochasticity and nonlinearity in transmission (*26*). Our *k* suggests that pertussis transmission is highly overdispersed; hence, this pertussis outbreak had substantial potential for superspreading events. The *k* in our study was comparable to other outbreaks of respiratory viruses in South Korea: 0.26 for Middle East respiratory syndrome coronavirus (*27*) and 0.10 for the SARS-CoV-2 Omicron variant (*28*). Therefore, enforcing monitoring and physical distancing in high-risk settings and promptly identifying and isolating cases should be the main strategies for controlling pertussis outbreaks.

Biologic and behavioral factors are known drivers of superspreading events of infectious diseases.

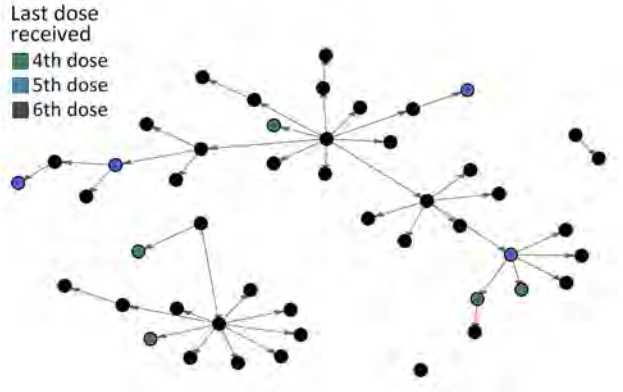

Figure 2. Transmission network of persons who received 4th, 5th, and 6th doses of the DTaP (diphtheria, tetanus, and acellular pertussis) vaccine in outbreak of pertussis in a boarding school, Busan, South Korea. The person with no epidemiologic link was the case-patient identified through laboratory confirmation who had no known contact with another case.

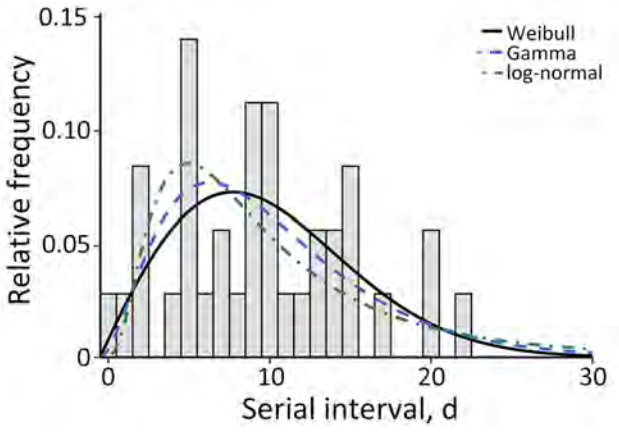

Figure 3. Estimated serial interval distribution associated with pertussis outbreak in a boarding school, Busan, South Korea. We fitted 36 infector–infectee pairs to a Weibull, gamma, and log-normal distribution. Bars indicate frequency of the serial interval; lines indicate the estimated distribution.

In other words, the superspreading potential of an infector could be associated with the infectiousness of the infector and the number of contacts made by the infector (*29*). In this study, we identified that the *k* values were not significantly different between the persons vaccinated within 5 years and those vaccinated >5 years earlier. A previous study indicated that protection against pertussis wanes 5 years after the fifth dose of DTaP (*9*). Therefore, the number of contacts made by the case-patients could play a major role in increasing the risk for infection (i.e., increasing superspreading potential in this outbreak).

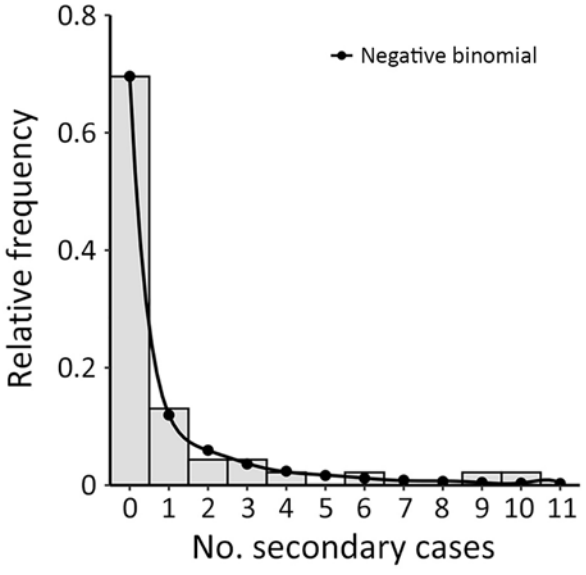

Figure 4. Estimated offspring distribution of cases associated with pertussis outbreak in a boarding school, Busan, South Korea. The offspring distribution is fitted to a negative binomial distribution using effective reproduction number = 0.93 and overdispersion $k = 0.23$.

However, because we were not able to quantify the exact number of contacts made per case, additional research with more detailed contact tracing data are warranted on how the number of contacts affects the superspreading events.

Waning immunity after acellular pertussis vaccination in children is known as a contributing factor to community pertussis transmission (*9*,*30*). Previous studies demonstrated a decline in immunity against pertussis beginning in the fourth year postvaccination (*10*); the protection against pertussis waned after the fifth dose of DTaP (*9*). However, the duration of protection after the sixth dose (i.e., Tdap vaccination), which was recommended between 11–12 years of age in South Korea, remains unclear (*2*). In this study, we could not identify a statistically significant trend of the estimated OR of acquiring pertussis infection per additional year after the sixth dose of vaccination. The likely reason for that finding is the limited sample size and variability in waning immunity and human behavior for the infection (i.e., biologic and behavioral factors) by persons over time. The age group most affected by pertussis in South Korea in 2024 was 13–14 years of age, with 25% overall incidence of pertussis, followed by 15–16 years (19% incidence), and 17–18 years (9%) (*31*); the highest vaccination coverage rate (83%) was in the 11–12 years age group. Study of the waning effectiveness of protection after the sixth dose of vaccination in a large sample size, with a detailed matrix of contact between infectors and infectees, would clarify our interpretations.

The overall attack rate in this study (10.1%) was larger than that of the previous outbreak (0.8%) in a South Korea school setting in 2017 (*32*). The increased attack rate in our study is likely a result of the different school settings (i.e., more physical activity in a sports boarding school). Furthermore, decreased immunity acquired from the reduced probability of being exposed to natural infection of pertussis in previous years (i.e., period of public health social measures implemented during the COVID-19 pandemic) is likely to affect the differences. Therefore, the recent increase in pertussis cases in many countries including South Korea may appear so because of fewer opportunities to become infected during the COVID-19 pandemic.

In 2023, South Korea immunization guidelines recommended either a Td or Tdap booster vaccination every 10 years for adults. However, this recommendation has not been fully incorporated into the National Immunization Program (*7*). Additional nationwide surveillance to support seroprevalence studies across different age groups could determine

the exact burden of pertussis in South Korea and an effective booster administration schedule (*2*). Furthermore, developing new pertussis-containing vaccines that provide long-lasting immunity would reduce the burden of pertussis (*2*,*7*,*9*).

Our study estimated the serial interval and superspreading potential among persons who received a sixth dose of the pertussis vaccine in South Korea. One limitation of our work is that, although PCR is a sensitive and widely used diagnostic method for identifying *B. pertussis* infection, it can lead to false positives from other co-circulating respiratory pathogens (*33*). False positives could overestimate our results, including the attack rate and superspreading potential. Second, we based our serial interval estimates on self-reported data, which are not free from reporting (i.e., recall) bias, which could lead to either underestimation or overestimation of serial interval depending on the accuracy of symptom onset reporting. Third, natural immunity, acquired from previous *B. pertussis* infection, could introduce bias into our results (*2*). Persons with previous infection, in combination with vaccination, may exhibit different immunity profiles and transmission potential than those who only had vaccination without prior infection (*34*). The combination could affect our result of superspreading potential estimates and the vaccine effectiveness. Fourth, some cases may have been incorrectly attributed to clusters when the true infection source was elsewhere, which could affect our serial interval estimates and offspring distribution analysis. Fifth, our mean confirmation delay (i.e., the period between symptom onset and case confirmation) was 8 days; the delay with rapid isolation of suspected cases could shorten the serial interval by truncating the infectious period. Thus, the serial interval in our result may be underestimated. Sixth, we did not account for potential confounding factors, such as underlying conditions, which could modify the viral shedding dynamics and affect our results for attack rate and superspreading potential. Last, we could not examine the household secondary attack rate because we could not obtain the information for household composition of the case-patients and their household contacts. Further study is warranted to gain a more comprehensive understanding of pertussis transmission dynamics.

In conclusion, our study reveals the superspreading potential of pertussis among vaccinated children. Strict adherence to personal preventive measures, rapid case tracing, and isolation are essential to reduce community transmission of pertussis.

The governmentwide R&D to Advance Infectious Disease Prevention and Control, South Korea (grant no. RS-2023-KH140322) and the Basic Science Research Program through the National Research Foundation of Korea, funded by the Korean Ministry of Education (grant no. NRF-2020R1I1A3066471), supported this study.

About the Author

Ms. U.J. Cho is a field epidemiologist at Gyeongnam Regional Center for Disease Control and Prevention, Busan, South Korea. Ms. S. Cho is a graduate student of public health at the Catholic University of Korea, Seoul, South Korea. Their research interests include infectious disease epidemiology with a focus on public health interventions.

References

1. Melvin JA, Scheller EV, Miller JF, Cotter PA. *Bordetella pertussis* pathogenesis: current and future challenges. Nat Rev Microbiol. 2014;12:274–88. https://doi.org/10.1038/nrmicro3235
2. Domenech de Cellès M, Rohani P. Pertussis vaccines, epidemiology and evolution. Nat Rev Microbiol. 2024;22:722–35. https://doi.org/10.1038/s41579-024-01064-8
3. Hu Y, Shi W, Meng Q, Yuan L, Gao W, Wang L, et al. Detection of *Bordetella* spp. in children with pertussis-like illness from 2018 to 2024 in China. J Infect. 2024;89:106222. https://doi.org/10.1016/j.jinf.2024.106222
4. Jog P, Memon IA, Thisyakorn U, Hozbor D, Heininger U, von König CHW, et al.; participants of the 2019 GPI Thailand Meeting. Pertussis in Asia: recent country-specific data and recommendations. Vaccine. 2022;40:1170–9. https://doi.org/10.1016/j.vaccine.2021.12.004
5. Smout E, Mellon D, Rae M. Whooping cough rises sharply in UK and Europe. BMJ. 2024;385:q736. https://doi.org/10.1136/bmj.q736
6. Centers for Disease Control and Prevention. Pertussis surveillance and trends. 2024 [cited 2024 Aug 15]. https://www.cdc.gov/pertussis/php/surveillance
7. Cho S, Kim DW, Achangwa C, Oh J, Ryu S. Pertussis in the elderly: plausible amplifiers of persistent community transmission of pertussis in South Korea. J Infect. 2024;89:106232. https://doi.org/10.1016/j.jinf.2024.106232
8. Cho UJ, Kim A-R, Park HR, An D-H, Yang S-G, Kim Y. Report on the epidemic investigation of the pertussis outbreak in Gyeongsangnam-do, 2023–2024. Public Health Weekly Report. 2024;17:1143–57.
9. Klein NP, Bartlett J, Rowhani-Rahbar A, Fireman B, Baxter R. Waning protection after fifth dose of acellular pertussis vaccine in children. N Engl J Med. 2012;367:1012–9. https://doi.org/10.1056/NEJMoa1200850
10. Schwartz KL, Kwong JC, Deeks SL, Campitelli MA, Jamieson FB, Marchand-Austin A, et al. Effectiveness of pertussis vaccination and duration of immunity. CMAJ. 2016;188:E399–406. https://doi.org/10.1503/cmaj.160193
11. Lee H, Kim K, Choi K, Hong S, Son H, Ryu S. Incubation period of the coronavirus disease 2019 (COVID-19) in Busan, South Korea. J Infect Chemother. 2020;26:1011–3. https://doi.org/10.1016/j.jiac.2020.06.018
12. Korea Disease Control and Prevention Agency. Pertussis integrated management guidelines. 2nd edition.

2015 [cited 2024 July 15]. https://www.kdca.go.kr/board/board.es?mid=a20507020000&bid=0019&act=view&list_no=138202&tag=&nPage=1
13. Hwang H, Lim JS, Song SA, Achangwa C, Sim W, Kim G, et al. Transmission dynamics of the delta variant of SARS-CoV-2 infections in South Korea. J Infect Dis. 2022;225:793–9. https://doi.org/10.1093/infdis/jiab586
14. Kim D, Ali ST, Kim S, Jo J, Lim JS, Lee S, et al. Estimation of serial interval and reproduction number to quantify the transmissibility of SARS-CoV-2 Omicron variant in South Korea. Viruses. 2022;14:533. https://doi.org/10.3390/v14030533
15. Althouse BM, Wenger EA, Miller JC, Scarpino SV, Allard A, Hébert-Dufresne L, et al. Superspreading events in the transmission dynamics of SARS-CoV-2: opportunities for interventions and control. PLoS Biol. 2020;18:e3000897. https://doi.org/10.1371/journal.pbio.3000897
16. Davison AC, Hinkley DV. Bootstrap methods and their application. Cambridge: Cambridge University Press; 1997.
17. Adam DC, Wu P, Wong JY, Lau EHY, Tsang TK, Cauchemez S, et al. Clustering and superspreading potential of SARS-CoV-2 infections in Hong Kong. Nat Med. 2020;26:1714–9. https://doi.org/10.1038/s41591-020-1092-0
18. Lim JS, Noh E, Shim E, Ryu S. Temporal changes in the risk of superspreading events of coronavirus disease 2019. Open Forum Infect Dis. 2021;8:ofab350. https://doi.org/10.1093/ofid/ofab350
19. DeDea L. The difference between Tdap and DTaP; dabigatran versus warfarin. JAAPA. 2011;24:14. https://doi.org/10.1097/01720610-201101000-00002
20. Korea Disease Control and Prevention. 2015 guideline for pertussis control. Chungju-si, South Korea: Korea Disease Control and Prevention; 2015.
21. Korea Disease Control and Prevention Agency. Information of diphtheria, tetanus, pertussis vaccination. 2024 [cited 2025 May 30]. https://nip.kdca.go.kr/irhp/infm/goVcntInfo.do?menuLv=1&menuCd=1120
22. Wallinga J, Lipsitch M. How generation intervals shape the relationship between growth rates and reproductive numbers. Proc Biol Sci. 2007;274:599–604. https://doi.org/10.1098/rspb.2006.3754
23. Ryu S, Chun JY, Lee S, Yoo D, Kim Y, Ali ST, et al. Epidemiology and transmission dynamics of infectious diseases and control measures. Viruses. 2022;14:2510. https://doi.org/10.3390/v14112510
24. Stocks P. Some epidemiological features of whooping-cough: a statistical investigation. Lancet. 1933;221:213–6. https://doi.org/10.1016/S0140-6736(00)84144-6
25. de Greeff SC, Mooi FR, Westerhof A, Verbakel JM, Peeters MF, Heuvelman CJ, et al. Pertussis disease burden in the household: how to protect young infants. Clin Infect Dis. 2010;50:1339–45. https://doi.org/10.1086/652281
26. Nguyen HT, Rohani P. Noise, nonlinearity and seasonality: the epidemics of whooping cough revisited. J R Soc Interface. 2008;5:403–13. https://doi.org/10.1098/rsif.2007.1168
27. Kucharski AJ, Althaus CL. The role of superspreading in Middle East respiratory syndrome coronavirus (MERS-CoV) transmission. Euro Surveill. 2015;20:14–8. https://doi.org/10.2807/1560-7917.ES2015.20.25.21167
28. Guo Z, Zhao S, Ryu S, Mok CKP, Hung CT, Chong KC, et al. Superspreading potential of infection seeded by the SARS-CoV-2 Omicron BA.1 variant in South Korea. J Infect. 2022;85:e77–9. https://doi.org/10.1016/j.jinf.2022.05.041
29. Pung R, Firth JA, Russell TW, Rogers T, Lee VJ, Kucharski AJ. Temporal contact patterns and the implications for predicting superspreaders and planning of targeted outbreak control. J R Soc Interface. 2024;21:20240358. https://doi.org/10.1098/rsif.2024.0358
30. Wendelboe AM, Van Rie A, Salmaso S, Englund JA. Duration of immunity against pertussis after natural infection or vaccination. Pediatr Infect Dis J. 2005;24(Suppl):S58–61. https://doi.org/10.1097/01.inf.0000160914.59160.41
31. Korea Disease Control and Prevention. Infectious disease portal [cited 2024 Jul 10]. https://ncov.kdca.go.kr
32. Ryu S, Kim JJ, Chen MY, Jin H, Lee HK, Chun BC. Outbreak investigation of pertussis in an elementary school: a case-control study among vaccinated students. Clin Exp Vaccine Res. 2018;7:70–5. https://doi.org/10.7774/cevr.2018.7.1.70
33. Loeffelholz M. Towards improved accuracy of *Bordetella pertussis* nucleic acid amplification tests. J Clin Microbiol. 2012;50:2186–90. https://doi.org/10.1128/JCM.00612-12
34. Choi HW, Achangwa C, Park J, Lee SM, Lee NY, Jeon CH, et al. Pediatric humoral immune responses and infection risk after severe acute respiratory syndrome coronavirus 2 (SARS-CoV-2) infection and two-dose vaccination during SARS-CoV-2 omicron BA.5 and BN.1 variants predominance in South Korea. Front Immunol. 2023;14:1306604. https://doi.org/10.3389/fimmu.2023.1306604

Address for correspondence: Sukhyun Ryu, Department of Preventive Medicine, College of Medicine, The Catholic University of Korea, R6117, Banpo-daero 222, Seocho-gu, Seoul, 06591 South Korea; email: gentryu@catholic.ac.kr

Estimation of Incubation Period for Oropouche Virus Disease among Travel-Associated Cases, 2024–2025

Sarah Anne J. Guagliardo, Stacey Martin, Carolyn V. Gould, Rebekah Sutter, Daniel Jacobs, Kevin O'Laughlin, Ralph Huits, Concetta Castilletti, J. Erin Staples; GeoSentinel Network Collaborators[1]

Determining the incubation period of Oropouche virus disease can inform clinical and public health practice. We analyzed data from 97 travel-associated cases identified by the Centers for Disease Control and Prevention (n = 74) or the GeoSentinel Network (n = 13) and 10 cases from published literature. Using log-normal interval-censored survival analysis, we estimated the median incubation period to be 3.2 (95% CI 2.5–3.9) days. Symptoms developed by 1.1 (95% CI 0.6–1.5) days for 5% of patients, 9.7 (95% CI 6.9–12.5) days for 95% of patients, and 15.4 (95% CI 9.6–21.3) days for 99% of patients. The estimated incubation period range of 1–10 days can be used to assess timing and potential source of exposure in patients with Oropouche symptoms. For patients with symptom onset >2 weeks after return from travel, clinicians and public health responders should consider the possibility of local vectorborne transmission or alternative modes of transmission.

Oropouche virus disease (Oropouche) is caused by infection with Oropouche virus (OROV; genus *Orthobunyavirus*, Simbu serogroup). In late 2023, a large outbreak of Oropouche originated in the Brazilian Amazon, later expanding into endemic and nonendemic regions in the Americas, and >16,000 cases were reported by the end of 2024 (*1*). Since 2023, >140 cases have been identified in travelers returning to Europe and North America, predominantly from Cuba (*2*).

Clinical manifestations of Oropouche are similar to those of other vectorborne diseases, such as dengue, Zika, and chikungunya, and are characterized by acute onset of fever, headache, myalgia, fatigue, chills, and arthralgia (*3*). Other symptoms can include diarrhea, nausea, vomiting, maculopapular rash, abdominal pain, retroorbital pain, back pain, and photophobia (*4*). Although most Oropouche cases are mild, severe disease and death have been reported (*5*). Severe manifestations of illness include hemorrhagic symptoms (e.g., gingival bleeding, melena, and menorrhagia), neurologic symptoms (e.g., meningitis, meningoencephalitis, Guillain-Barré syndrome), and adverse pregnancy outcomes (*6*–*9*).

OROV is primarily transmitted to humans through the bites of infected biting midges (*Culicoides paraensis*) and possibly certain mosquito species, such as *Culex quinquefasciatus*. Other observed transmission modes have included accidental inoculation via oral and respiratory routes in a laboratory setting (*10*). Oropouche viral RNA was recently detected in the semen of 2 travelers returning to Europe from Cuba, raising questions about the possibility of sexual transmission, although that mode of transmission has not yet been confirmed (*11*,*12*). Congenital transmission is also suspected because of reported maternal infections during pregnancy that resulted in birth defects and laboratory evidence of OROV infection in those infants (*9*).

The incubation period for Oropouche was previously estimated to range from 3 to 10 days, but that estimate was based on just 2 cases (*3*,*6*,*10*). Having a more precise estimation of the incubation period can help clinicians form a differential diagnosis on the basis of timing of potential exposures and help public health officials distinguish between travel-associated cases and local transmission. We estimated the

Author affiliations: Centers for Disease Control and Prevention, Fort Collins, Colorado, USA (S.A.J. Guagliardo, S. Martin, C.V. Gould, R. Sutter, D. Jacobs, J.E. Staples); Centers for Disease Control and Prevention, Atlanta, Georgia, USA (K. O'Laughlin); IRCCS Sacro Cuore Don Calabria Hospital, Verona, Italy (R. Huits, C. Castilletti)

DOI: https://doi.org/10.3201/eid3107.250468

[1]Members are listed at the end of this article.

Oropouche incubation period using data from infected travelers returning to nonendemic areas.

Methods

Data Sources

We used 3 data sources: the laboratory database of OROV testing conducted during 2024–2025 through the Centers for Disease Control and Prevention (CDC) Arboviral Diseases Branch (Division of Vector-borne Diseases, National Center for Emerging and Zoonotic Infectious Diseases); the GeoSentinel Network database (https://geosentinel.org) of patients identified with Oropouche during 2024; and a PubMed search of the literature through March 15, 2025, using the search terms "Oropouche" or "Oropuche" (Figure 1). At CDC, suspected cases were tested by real-time reverse transcription PCR (rRT-PCR) or 90% plaque reduction neutralization test, depending on the timing of specimen collection relative to symptom onset (*16*). The GeoSentinel Network, a collaboration between CDC and the International Society of Travel Medicine, is a global surveillance system for illnesses affecting international travelers currently comprised of ≈70 clinical sites in 30 countries. Patients identified and tested through the GeoSentinel Network were tested for evidence of OROV infection by rRT-PCR or IgG and IgM serology. For each case-patient, we extracted basic demographic data (age and sex), symptom onset date, travel dates, and whether the patient was hospitalized. Patients self-reported symptom onset date and travel dates. We ensured no overlap among patients identified through those sources by verifying that demographic data and travel dates were unique.

Case Classification and Inclusion Criteria

We included probable and confirmed cases of Oropouche. We defined a probable case as a patient with a known epidemiologic link whose blood or cerebrospinal fluid sample tested positive for OROV-specific IgM or neutralizing antibodies. We defined a confirmed case as a patient with a known epidemiologic link whose sample was OROV-positive by rRT-PCR, had a ≥4-fold change in neutralizing antibody titers in paired serum samples, or was positive for IgM in blood or cerebrospinal fluid with confirmatory virus-specific neutralizing antibodies. We only included symptomatic patients that had complete information about travel destinations, departure and return dates, and symptom onset date. We considered any of the symptoms included in the suspected case definition (e.g., fever, chills, headache, myalgia, arthralgia, retro-orbital pain, or generalized rash) to denote the onset of symptoms, as self-reported by patients.

Statistical Analysis

We conducted descriptive statistics on patient demographics (age and sex) and travel characteristics (travel duration and location). We used parametric interval-censored survival modeling to estimate the incubation period distribution (*17*,*18*). We determined the exposure period by using the dates of travel relative to the timing of illness onset. Specifically, for patients whose symptoms developed after travel, we considered the exposure period to be the duration of travel, and for patients whose symptoms developed during travel, we considered the exposure period to be from the beginning of travel through the illness onset date (Figure 2) (*17*,*18*).

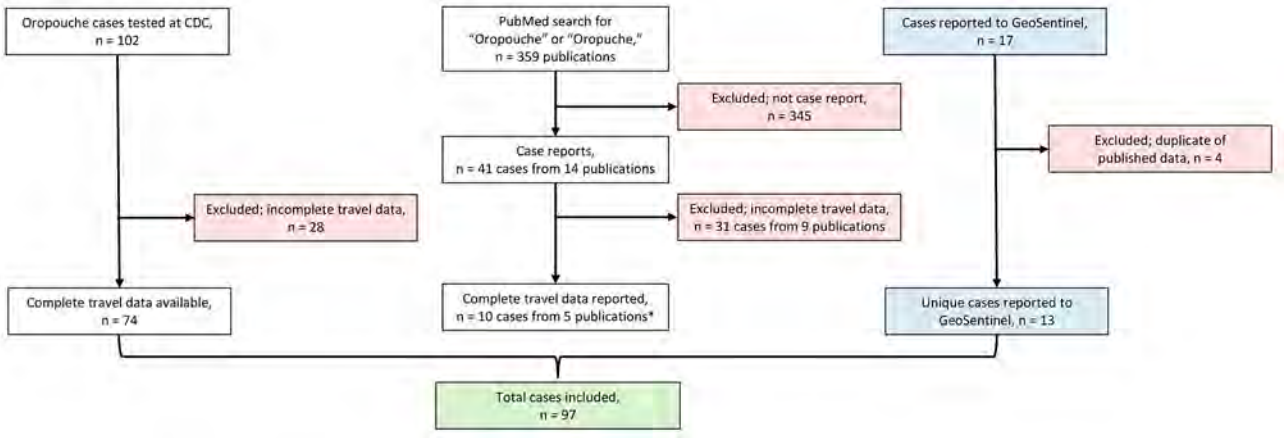

Figure 1. Flowchart of data sources and 97 cases included in an estimation of incubation period for Oropouche virus disease among travel-associated cases, 2024–2025. The study included patients who developed symptoms and had positive test results for Oropouche in the laboratory database of the CDC Arboviral Diseases Branch (Division of Vector-borne Diseases, National Center for Emerging and Zoonotic Infectious Diseases), through GeoSentinel (https://geosentinel.org), or in reports available on PubMed as of March 15, 2025. We excluded patients without complete travel data. *(*6*,*11*,*13*–*15*). CDC, Centers for Disease Control and Prevention.

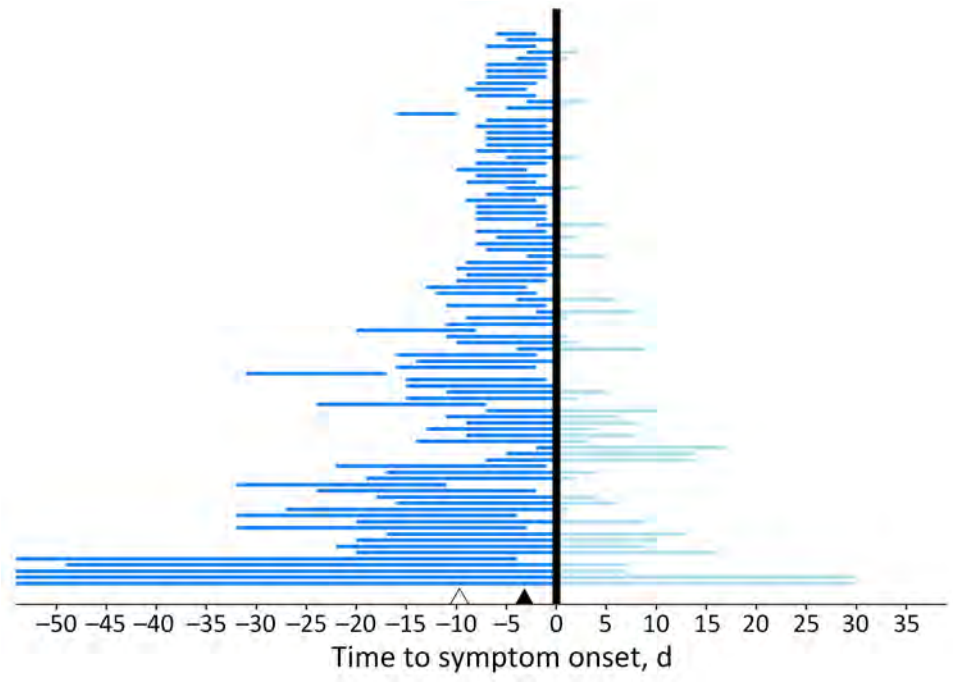

Figure 2. Time of exposure relative to symptom onset in an estimation of incubation period for Oropouche virus disease among 97 probable and confirmed travel-associated cases, 2024–2025. Each horizontal line corresponds to an individual patient's exposure time. The vertical black line represents symptom onset. The horizontal lines represent the exposure durations before (dark blue) and after (light blue) symptom onset. Observations are ordered by duration of travel, and long travel durations are truncated from the graph for ease of interpretation. The black triangle represents the median incubation period for probable and confirmed cases; the white triangle represents the 95th quantile.

We fitted probability distributions (Weibull, log-normal, and Gamma) to the data by using the dic.fit function in the coarseDataTools package in R (The R Project for Statistical Computing, https://www.r-project.org) and selected the best-fitting distribution using the Akaike information criterion (*17*,*18*). We calculated cumulative distribution functions and associated 95% CIs, along with means, medians, and 5th, 95th, and 99th quantiles. We also evaluated whether estimated incubation period varied by age, sex, and hospitalization status by fitting parametric log-normal models for each covariate using the survreg procedure in the survival package in R.

The initial analysis included all patients that met inclusion criteria. To provide a more precise estimate of incubation periods, we also performed an analysis on a subset of patients meeting the case definition for confirmed Oropouche and who had <14 days of travel. Last, we analyzed a subset of cases detected in 2024–2025 to examine if the current viral strain affected the incubation period estimates.

Ethics Considerations

This activity was reviewed by CDC, was deemed not research, and was conducted consistent with applicable federal law and CDC policy (project no. 0900f3eb824f7cc8). Applicable federal laws include 45 C.F.R. part 46.102(l) (2), 21 C.F.R. part 56; 42 U.S.C. Sect. 241(d); 5 U.S.C. Sect. 552a; 44 U.S.C. Sect. 3501 et seq. A human subjects advisor at CDC's National Center for Emerging and Zoonotic Infectious Diseases reviewed the GeoSentinel surveillance data collection protocol and classified it as public health surveillance and not human subjects research (project no. 0900f3eb81bc3a03). Additional ethics clearance was obtained by GeoSentinel sites, as required by their respective institutions.

Results

In total, 97 cases met the inclusion criteria, consisting of 74 cases identified on the basis of testing conducted at CDC, 13 reported to GeoSentinel, and 10 identified in the peer-reviewed literature (Figure 1). The symptom onset dates ranged from October 2010 to January 2025, and 98% (n = 95) of cases occurred during 2024–2025.

Most (96%, n = 93) patients were adults >19 years of age; 54 (56%) were female and 43 (44%) were male (Table 1). More than half (57%, n = 55) of patients had initial symptoms develop during travel, and the median exposure period was 7 days (interquartile range [IQR] 6.0–14.0 days; range 2–135 days) (Figure 2). The most common travel location was Cuba, as reported by 97% (n = 94) of patients. The demographic characteristics of the confirmed and probable cases compared with confirmed cases with <14 days of travel were similar (Table 1). Compared with cases identified through GeoSentinel and published literature, patients whose samples were tested at CDC were older (median age 51 years for cases tested at CDC vs. 30 years for cases identified elsewhere; p<0.0001), less likely to have been hospitalized (16% vs. 40%;

Table 1. Characteristics of probable and confirmed cases used in an estimation of incubation period for Oropouche virus disease among travel-associated cases, 2024–2025*

Characteristics	Probable and confirmed, n = 97	Confirmed, n = 40†
Age group, y		
0–19	4 (4.1)	1 (2.5)
20–39	32 (33.0)	12 (30.0)
40–59	41 (42.3)	21 (52.5)
≥60	20 (20.6)	6 (15.0)
Missing	0	0
Sex		
F	54 (55.7)	22 (55.0)
M	43 (44.3)	18 (45.0)
Missing	0	0
Hospitalized		
N	72 (78.3)	32 (80.0)
Y	20 (21.7)	8 (20.0)
Missing	5	0
Travel duration, d		
<7	21 (21.6)	11 (27.5)
7–13	38 (39.2)	25 (62.5)
14–20	17 (17.5)	4 (10.0)‡
21–27	8 (8.2)	NA
≥28	13 (13.4)	NA
Missing	0	0
Onset during travel		
N	42 (43.3)	22 (55.0)
Y	55 (56.7)	18 (45.0)
M	0	0
Exposure period, d		
Mean	13.6	7.3
Median (IQR)	7 (6.0–14.0)	7 (6–9)
Range	2–135	2–14

*Values are no. (%) except as indicated. NA, not applicable.
†Traveled <14 days.
‡Traveled for 14 days.

p = 0.041), and had shorter exposure periods (median 7 days vs. 14 days; p<0.0001) (Appendix Table 1, https://wwwnc.cdc.gov/EID/article/31/7/25-0468-App1.pdf).

The log-normal distribution was the best fit for all case sets (Appendix Table 2). For probable and confirmed cases (n = 97), the estimated median incubation period was 3.2 (95% CI 2.5–3.9) days (Table 2). We estimated symptoms developed within 1.1 (95% CI 0.6–1.5) days for 5% of patients and within 9.7 (95% CI 6.9–12.5) days for 95% of patients. We estimated that most (88%) patients' symptoms developed within 7 days (Figure 3). Our estimates show that almost all (99%) patients had symptoms develop by 15.4 (95% CI 9.6–21.3) days. The estimated median incubation period for confirmed cases only was similar at 3.1 (95% CI 2.1–4.0) days, and 95% of confirmed cases had symptoms develop within 9.3 (95% CI 5.4–13.2) days (Appendix Table 3). Estimated incubation periods did not differ substantially by age, sex, hospitalization status, or when we excluded the 2 cases that occurred before 2024 (Appendix Tables 3, 4).

Table 2. Parameters and quantiles of log-normal distribution in an estimation of incubation period for Oropouche virus disease among 97 probable and confirmed travel-associated cases, 2024–2025

Parameter and quantile	Estimate (95% CI)
Location parameter, μ	3.2 (2.6–4.0)
Dispersion parameter, σ	2.0 (1.6–2.3)
Quantile	
5th	1.1 (0.6–1.5)
50th	3.2 (2.5–3.9)
95th	9.7 (6.9–12.5)
99th	15.4 (9.6–21.3)

Discussion

In this analysis of travel-associated Oropouche cases, we estimated the median incubation period to be 3–4 days, with a range of 1 day (5% of cases) to 10 days (95% of cases). We estimated symptoms developed within 3 days of exposure for 50% of patients and within 15 days for 99% of patients.

Globally, most travel-associated Oropouche cases during the 2024 outbreak were among persons returning from Cuba to the United States, and the data used in this analysis reflect that pattern (*2*,*19*). Before 2024, OROV transmission was not suspected in Cuba, and the population likely had no immunity. By the end of 2024, Cuba had 24,259 suspected cases, of which 626 were confirmed cases (*20*), suggesting high levels of transmission and increased likelihood of repetitive exposure among visitors to Cuba. Compared with travelers to other areas, the estimated incubation period might have been shorter for US travelers to Cuba because they traveled to an area with an active outbreak and likely were exposed, potentially repeatedly, soon after arrival. Going forward, additional data from travelers to other geographic areas can be incorporated to improve the representativeness and precision of the estimate of this Oropouche incubation period.

Prior estimates for the range of the incubation period of Oropouche have included 3–8 days, 4–8 days, and 3–10 days (*3*,*21*,*22*). Our estimate of 1–10 days has a wider overall range than prior estimates, noting symptom onset can occur within 1 day of exposure for 5% of patients. The previous lower estimate of 3 days was based on the symptom onset in a laboratory worker who was exposed orally, and the previous upper estimate of 10 days was documented in a traveler from Brazil who returned to a nonendemic area after visiting the Amazon region (*6*,*10*). The incubation period of 4–8 days was based on an assessment of historical outbreaks in the Brazilian Amazon in the 1960s and 1970s but could not be determined with precision because the exact timing of exposure was unknown for cases in or near endemic areas (*10*).

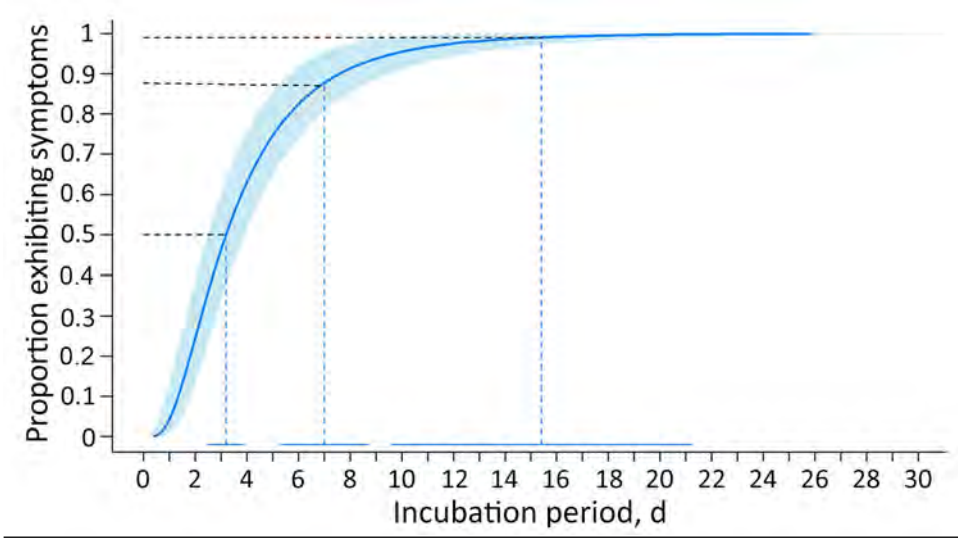

Figure 3. Estimated cumulative distribution of incubation period for Oropouche virus disease among 97 probable and confirmed travel-associated cases, 2024–2025. Solid blue line represents the estimated log-normal cumulative distribution function; shaded area represents 95% CI. Dashed lines correspond to the 50th and 99th quantiles, in addition to the proportion of patients that experienced symptoms within 1 week (88th quantile). The solid horizontal lines at bottom represent the 95% CIs for the quantiles.

However, evidence suggests that the current viral reassortant replicates faster than the prototype strain, possibly impacting incubation period for infections associated with recent outbreaks (*23*).

In clinical settings, providers should take a thorough history to determine the timing of the patient's initial symptom onset because relapse of symptoms has been described in up to 70% of Oropouche patients (*24*). Suspicion for Oropouche should be heightened when a patient has a compatible illness within 10 days of returning from an area with active virus transmission. Clinicians should also consider the patient's underlying immunocompetence, which has been shown to affect incubation period in other arboviral infections, such as West Nile virus (*25*). However, no data are available on the effect of immunosuppression on the Oropouche incubation period. For most patients with clinically compatible illness >2 weeks after return from travel, alternative diagnoses should be considered. If the patient has laboratory evidence of OROV infection, clinicians should evaluate the possibility of local vectorborne transmission or alternative transmission modes.

Although Oropouche is clinically similar to other arboviral diseases, the median incubation period estimated from this analysis (3–4 days; range 1–10 days) is shorter than those for dengue (5–7 days; range 3–10 days), chikungunya (3–7 days; range 1–12 days), and Zika (6–7 days; range 3–14 days) (*17*,*26*,*27*). However, because the estimated ranges of those incubation periods overlap, clinicians should consider potential exposures and other clinical and epidemiologic information when deciding on testing and differential diagnosis.

Knowing the Oropouche incubation period can help direct case investigations and public health response to outbreaks. For example, when OROV infection is confirmed in a traveler >2 weeks after returning to a nonendemic area, public health authorities should consider the possibility of local vectorborne transmission, provided competent vectors are present and seasonality is appropriate, or alternative modes of transmission. Although sexual transmission of OROV has not yet been documented, identification of culturable virus on a day 16 semen sample indicates sexual transmission could occur and should be investigated (*11*). Accurate incubation periods can also help develop criteria for determining the end of an outbreak. A commonly used criterion is twice the longest estimated incubation period without observing any new cases since the last transmission event (*28*). On the basis of the upper limit of the extrinsic incubation period in the vector *Cu. paraensis* midge (8 days) and the upper limit of our estimate of intrinsic incubation (95th quantile of 10 days), a period up to 5 weeks (≈18 days × 2) with no new cases in an area under adequate epidemiologic surveillance could be used to declare the end of an outbreak (*29*).

The first limitation of this study is that the clinically apparent cases included in this analysis potentially biased our results toward shorter incubation periods compared with cases of mild disease. Second, our estimates were based on data from infected travelers, who might have different underlying demographic and medical characteristics compared with nontravelers. Third, our dataset was relatively small, resulting in estimates with less certainty for the upper end of the log-normal distribution (95th and 99th quantiles). Not unexpectedly, 1 extreme observation in our dataset had an exposure window that ended >15 days (99th quantile) before symptom onset.

Unusually long lapses between the end of an exposure period and symptom onset could be explained by recall bias because travel duration and symptom onset dates were self-reported by patients. Fourth, data for this project were derived from distinct sources, so event data (e.g., symptom onset) might have been collected differently, impacting the precision of our estimates. Finally, we considered exposures to be vectorborne for cases included in the analysis, but patients with alternative exposures might also have been included in the dataset.

In conclusion, our results indicate that 50% of travelers infected with OROV will develop symptoms within 3–4 days of exposure and 99% will develop symptoms within 15 days. Clinicians and public health responders should evaluate the possibility of alternative modes of transmission (e.g., sexual transmission) or local vectorborne transmission for travelers with Oropouche who have symptoms develop >2 weeks after return from travel. Our estimate of the distribution of the Oropouche incubation period will help clinicians and public health officials develop a differential diagnosis based on the timing of travel-related exposures and inform prevention and control measures.

GeoSentinel Network Collaborators: Sami Alcedo, Hilmir Asgeirsson, Anna Barbiero, Ilsa Beig, Emmanuel Bottieau, David Brett-Major, Rosa De Miguel Buckley, Claudia Denkinger, Hedvig Glans, Frederico Gobbi, David Hamer, Michael Libman, Laura Nicolini, Francesca Norman, Jose A. Perez-Molina, Chiara Sepulcri, Theresa Sepulveda, Federica Toscanini, Els van Nood, Jesse Waggoner, and Lorenzo Zammarchi.

Acknowledgments

We thank Jennifer Lehman for management of clinical laboratory data and CDC staff members and state and local health departments that contributed to the Oropouche Virus Response.

Funding for this project was supported by CDC. GeoSentinel is supported by a cooperative agreement (no. 5U01CK000632-04) between CDC and the International Society of Travel Medicine.

About the Author

Dr. Guagliardo is an epidemiologist with the Division of Vector-Borne Diseases, National Center for Emerging and Zoonotic Infectious Diseases, CDC, Fort Collins, Colorado. Her research interests include the applied epidemiology and ecology of emerging and re-emerging vectorborne diseases.

References

1. Pan American Health Organization. Epidemiological update Oropouche in the Americas region, 11 February 2025 [cited 20025 Feb 11]. https://www.paho.org/sites/default/files/2025-02/2025-feb-10-epi-update-oropoucheeng-final_0.pdf
2. Centers for Disease Control and Prevention. Oropouche in the United States [cited 2025 Apr 29]. https://www.cdc.gov/oropouche/data-maps/current-year-data.html
3. Guagliardo SAJ, Connelly CR, Lyons S, Martin SW, Sutter R, Hughes HR, et al. Reemergence of Oropouche virus in the Americas and risk for spread in the United States and its territories, 2024. Emerg Infect Dis. 2024;30:2241–9. https://doi.org/10.3201/eid3011.241220
4. Morrison A, White JL, Hughes HR, Guagliardo SAJ, Velez JO, Fitzpatrick KA, et al. Oropouche virus disease among U.S. travelers—United States, 2024. MMWR Morb Mortal Wkly Rep. 2024;73:769–73. https://doi.org/10.15585/mmwr.mm7335e1
5. Bandeira AC, Pereira FM, Leal A, Santos SPO, Barbosa AC, Souza MSPL, et al. Fatal Oropouche virus infections in nonendemic region, Brazil, 2024. Emerg Infect Dis. 2024;30:2370–4. https://doi.org/10.3201/eid3011.241132
6. Vernal S, Martini CCR, da Fonseca BAL. Oropouche virus-associated aseptic meningoencephalitis, southeastern Brazil. Emerg Infect Dis. 2019;25:380–2. https://doi.org/10.3201/eid2502.181189
7. de Armas Fernández JR, Peña García CE, Acosta Herrera B, Betancourt Plaza I, Gutiérrez de la Cruz Y, Resik Aguirre S, et al. Report of an unusual association of Oropouche fever with Guillain-Barré syndrome in Cuba, 2024. Eur J Clin Microbiol Infect Dis. 2024;43:2233–7. https://doi.org/10.1007/s10096-024-04941-5
8. Mourão MPG, Bastos MS, Gimaque JBL, Mota BR, Souza GS, Grimmer GHN, et al. Oropouche fever outbreak, Manaus, Brazil, 2007–2008. Emerg Infect Dis. 2009;15:2063–4. https://doi.org/10.3201/eid1512.090917
9. das Neves Martins FE, Chiang JO, Nunes BTD, Ribeiro BFR, Martins LC, Casseb LMN, et al. Newborns with microcephaly in Brazil and potential vertical transmission of Oropouche virus: a case series. Lancet Infect Dis. 2025;25:155–65. https://doi.org/10.1016/S1473-3099(24)00617-0
10. Pinheiro FP, Travassos da Rosa AP, Travassos da Rosa JF, Ishak R, Freitas RB, Gomes ML, et al. Oropouche virus. I. A review of clinical, epidemiological, and ecological findings. Am J Trop Med Hyg. 1981;30:149–60. https://doi.org/10.4269/ajtmh.1981.30.149
11. Castilletti C, Huits R, Mantovani RP, Accordini S, Alladio F, Gobbi F. Replication-competent Oropouche virus in semen of traveler returning to Italy from Cuba, 2024. Emerg Infect Dis. 2024;30:2684–6. https://doi.org/10.3201/eid3012.241470
12. Iglói Z, Soochit W, Munnink BBO, Anas AA, von Eije KJ, van der Linden A, et al. Oropouche virus genome in semen and other body fluids from traveler. Emerg Infect Dis. 2025;31:205–6. https://doi.org/10.3201/eid3101.241452
13. Barbiero A, Formica G, Mantovani RP, Accordini S, Gobbi F, Spinicci M, et al. Persistent Oropouche virus viremia in two travellers returned to Italy from Cuba, July 2024. J Travel Med. 2025;32:taae148. https://doi.org/10.1093/jtm/taae148
14. Gourjault C, Pezzi L, Doudier B, Minodier P, Klitting R, Cano P, et al. Persistence of Oropouche virus in body fluids among imported cases in France, 2024. Lancet Infect Dis. 2025;25:e64–5. https://doi.org/10.1016/S1473-3099(24)00815-6
15. de Souza Luna LK, Rodrigues AH, Santos RI, Sesti-Costa R, Criado MF, Martins RB, et al. Oropouche virus is detected

in peripheral blood leukocytes from patients. J Med Virol. 2017;89:1108–11. https://doi.org/10.1002/jmv.24722
16. Naveca FG, Nascimento VAD, Souza VC, Nunes BTD, Rodrigues DSG, Vasconcelos PFDC. Multiplexed reverse transcription real-time polymerase chain reaction for simultaneous detection of Mayaro, Oropouche, and Oropouche-like viruses. Mem Inst Oswaldo Cruz. 2017;112:510–3. https://doi.org/10.1590/0074-02760160062
17. Krow-Lucal ER, Biggerstaff BJ, Staples JE. Estimated incubation period for Zika virus disease. Emerg Infect Dis. 2017;23:841–5. https://doi.org/10.3201/eid2305.161715
18. Reich NG, Lessler J, Cummings DA, Brookmeyer R. Estimating incubation period distributions with coarse data. Stat Med. 2009;28:2769–84. https://doi.org/10.1002/sim.3659
19. European Centers for Disease Control and Prevention. Threat assessment brief: Oropouche virus disease cases imported into the European Union [cited 2025 Apr 29]. https://www.ecdc.europa.eu/sites/default/files/documents/TAB-Oropouche-august-2024.pdf
20. Pan American Health Organization. Countries with cumulative reports of Oropouche cases [in Spanish] [cited 2025 Apr 29]. https://www.paho.org/es/arbo-portal/oropouche
21. Sakkas H, Bozidis P, Franks A, Papadopoulou C. Oropouche fever: a review. Viruses. 2018;10:175. https://doi.org/10.3390/v10040175
22. Pinheiro FP, Travassos da Rosa APA, Vasconcelos PF. Oropouche fever. In: Feigin RD, Demmler GJ, Cherry JD, Kaplan SL, editors. Textbook of pediatric infectious diseases, 5th ed. Philadelphia (PA): W.B. Saunders Co; 2004. p. 2418–23.
23. Scachetti GC, Forato J, Claro IM, Hua X, Salgado BB, Vieira A, et al. Re-emergence of Oropouche virus between 2023 and 2024 in Brazil: an observational epidemiological study. Lancet Infect Dis. 2025;25:166–75. https://doi.org/10.1016/S1473-3099(24)00619-4
24. Azevedo RS, Nunes MR, Chiang JO, Bensabath G, Vasconcelos HB, Pinto AY, et al. Reemergence of Oropouche fever, northern Brazil. Emerg Infect Dis. 2007;13:912–5. https://doi.org/10.3201/eid1306.061114
25. Pealer LN, Marfin AA, Petersen LR, Lanciotti RS, Page PL, Stramer SL, et al.; West Nile Virus Transmission Investigation Team. Transmission of West Nile virus through blood transfusion in the United States in 2002. N Engl J Med. 2003;349:1236–45. https://doi.org/10.1056/NEJMoa030969
26. Chan M, Johansson MA. The incubation periods of dengue viruses. PLoS One. 2012;7:e50972. https://doi.org/10.1371/journal.pone.0050972
27. Rudolph KE, Lessler J, Moloney RM, Kmush B, Cummings DA. Incubation periods of mosquito-borne viral infections: a systematic review. Am J Trop Med Hyg. 2014;90:882–91. https://doi.org/10.4269/ajtmh.13-0403
28. Djaafara BA, Imai N, Hamblion E, Impouma B, Donnelly CA, Cori A. A quantitative framework for defining the end of an infectious disease outbreak: application to Ebola virus disease. Am J Epidemiol. 2021;190:642–51. https://doi.org/10.1093/aje/kwaa212
29. Pinheiro FP, Hoch AL, Gomes ML, Roberts DR. Oropouche virus. IV. Laboratory transmission by *Culicoides paraensis*. Am J Trop Med Hyg. 1981;30:172–6. https://doi.org/10.4269/ajtmh.1981.30.172

Address for correspondence: Sarah Anne J. Guagliardo, Centers for Disease Control and Prevention, 3156 Rampart Rd, Mailstop 4-325, Fort Collins, CO 80521, USA; email: sguagliardo@cdc.gov

Spatiotemporal Distribution and Clinical Characteristics of Zoonotic Tuberculosis, Spain, 2018–2022

Álvaro Roy, Diana Gómez-Barroso, Elena Cruz-Ferro, Ana Fernández, Isabel Martínez-Pino, María del Henar Marcos, Isabel Ursúa-Díaz, Susana Miras, Nuria Echave, Evi Ounarou, Beatriz Romero, Laura Herrera-León,[1] Zaida Herrador,[1] Study Group on Zoonotic Tuberculosis[2]

Zoonotic tuberculosis (zTB) is a communicable disease that has major effects on both human and animal health. Spain reports the highest number of zTB cases in humans annually in the European Union. We describe the epidemiology of human cases of zTB caused by *Mycobacterium bovis* and *M. caprae* in Spain during 2018–2022. The incidence of *M. bovis* infection compared with *M. tuberculosis* infection was higher in patients who were native-born (adjusted odds ratio [aOR] 2.32, 95% CI 1.44–3.82), HIV-negative (aOR 3.39, 95% CI 1.24–14.0), or had extrapulmonary forms of TB (aOR 2.20, 95% CI 1.46–3.28). The spatial pattern differed by *M. tuberculosis* complex species; we identified 3 significant clusters of *M. bovis* and 1 of *M. caprae* in bovine TB–free regions. Our results show the importance of including animal and human data on circulating zoonotic pathogens under the One Health umbrella.

Tuberculosis (TB) in humans is caused by mycobacterial species of *Mycobacterium tuberculosis* complex (MTBC), mainly *M. tuberculosis*. Zoonotic TB (zTB) is a form of human TB caused by closely related species of mycobacteria, such as *M. bovis* and *M. caprae*, that are normally isolated from domestic or wild mammals, their natural hosts (*1*). *M. bovis* is the second most common cause of TB in humans and was estimated to be responsible for ≈1.4% of human TB cases worldwide (*2*). Cattle are the main reservoir of *M. bovis*, known as bovine TB, but *M. bovis* also causes TB in other animal species, including wildlife (*1*). *M. caprae* also has a notable importance in zTB incidence in Spain (*3*); it is the main causal agent of TB in goats and has also been reported in domestic and wild animals (*4*). It differs from *M. bovis* in that it is evolutionarily older and that most of the reported human cases are mainly concentrated in a few countries in central and southern Europe (*5*).

Transmission of the agents of zTB to humans is mainly indirect and usually occurs through consumption of contaminated milk and other dairy products that have not been subjected to sanitization processes. More rarely, it may result from consuming contaminated raw or undercooked meat. Cases of direct airborne transmission from animals or animal products to humans, as well as person-to-person transmission, have also been reported (*6*,*7*). Current molecular techniques suggest potential airborne transmission between animals and humans, until recently unclear and debatable (*8*); this possibility is particularly important in professions with a higher risk for exposure, such as farmers, veterinarians, hunters, or slaughterhouse workers (*9*).

The implications of zTB go beyond human health; it also causes losses to the livestock sector through reduced meat and milk production and slaughter of infected animals and movement restrictions, and losses

Author affiliations: Instituto de Salud Carlos III, Madrid, Spain (Á. Roy, D. Gómez-Barroso, N. Echave, L. Herrera-León, Z. Herrador); CIBER in Epidemiology and Public Health, Madrid (D. Gómez-Barroso, I. Martínez-Pino, L. Herrera-León, Z. Herrador); Consejería de Sanidad Xunta de Galicia, Santiago de Compostela, Spain (E. Cruz-Ferro, I. Ursúa-Díaz, S. Miras); Consejería de Salud y Servicios Sanitarios Gobierno del Principado de Asturias, Oviedo, Spain (A. Fernández); Consejería de Sanidad Junta de Castilla y León, Valladolid, Spain (I. Martínez-Pino, M.H. Marcos); Aristotle University of Thessaloniki, Thessaloniki, Greece (E. Ounarou); VISAVET Health Surveillance Centre, Madrid (B. Romero); Complutense University of Madrid Faculty of Veterinary Medicine, Madrid (B. Romero)

DOI: https://doi.org/10.3201/eid3107.250031

[1]These authors were co–principal investigators.

[2]Members of the group are listed at the end of this article.

to the state through the costs of eradication programs (*10*). Although infection in cattle herds appears to be under control in most high-income countries through bovine TB eradication programs, complete elimination of the disease is complicated by the limitations of diagnostic tests and the maintenance of infection in wild and domestic reservoirs (*11*).

Spain is the European Union (EU) country that reports the highest number of zTB cases annually in humans (0.11 confirmed cases/100,000 population in 2023) (*3*). It has a herd prevalence of tuberculosis in cattle of 1.5%, although this percentage varies widely by region (*12*). Animal TB in the Iberian Peninsula is mainly found in cattle and goats, but it also occurs in wildlife, so we should consider maintenance communities rather than specific hosts as reservoirs of infection (*13*). To estimate the real burden of disease in Spain and thus be able to design and evaluate specific and concerted actions, the zTB public health problem must be addressed with a One Health approach. In this article, we describe the reported cases of zTB in Spain during 2018–2022, making a clinical and epidemiologic comparison with TB cases caused by *M. tuberculosis* in the same study period.

Methods

Study Design, Population, and Data Sources

Our study used epidemiologic data from the National Network of Epidemiologic Surveillance (RENAVE), hosted by the National Center of Epidemiology. We conducted a retrospective descriptive study using surveillance data on human zTB and TB cases caused by *M. tuberculosis* reported to RENAVE during January 1, 2018–December 31, 2022. The regional surveillance systems of the autonomous communities (CCAA) report individual data on suspected (meeting the clinical criteria), probable (meeting both clinical criteria and laboratory criteria for a probable case), and confirmed (meeting both clinical and laboratory criteria for a confirmed case) cases of TB through the national reporting electronic platform. The notification is made following the protocol agreed by all the members of RENAVE, who are representatives of the CCAA, Carlos III Health Institute, and Ministry of Health. Case definitions in our protocol are based on the EU case definitions, as published in the Official Journal of the European Union (Commission Implementing Decision [EU] 2018/945) (*14*,*15*).

For our study, and to improve data quality, we contacted all the regions of Spain comprising 17 CCAA and 2 autonomous cities and requested they check the information provided on zTB cases from 2018–2022 at the beginning of the study. This process enabled us to recover 56 cases of zTB in RENAVE that did not have information about the causal agent. We included populations officially residing in Spain, obtained from the National Institute for Statistics, in the denominator (at national, provincial or municipal level depending on the analysis). We calculated incidence of zTB and TB cases per year and annual incidence rates per 100,000 population per year by age group and sex and by 1 million population per year by province. For the spatial cluster analysis, we calculated incidence at the municipal level.

Data Analysis

After excluding imported cases, we conducted a retrospective descriptive analysis on the main sociodemographic and clinical characteristics: age, sex, country of birth, primary location of disease, HIV status, hospitalization, and treatment outcome. For the descriptive analysis of the qualitative variables, we calculated frequencies and percentages. We explored differences in the characteristics of zTB and TB (*M. tuberculosis*) patients with bivariate analysis; we used χ^2 for multiple comparisons of qualitative variables and Mann-Whitney U tests with Bonferroni adjustment for quantitative variables. We estimated crude odds ratios (ORs) and adjusted ORs (aORs) and 95% CIs; we included those variables with $p<0.1$ in a logistic regression model. We used R version 4.4.0 (The R Project for Statistical Computing, https://www.r-project.org) for analyses.

To assess temporal and geographic patterns, we calculated zTB and TB incidence per 100,000 population by year and per 1 million population by province using population denominators obtained from the National Statistics Institute. We analyzed temporal trends using linear and joinpoint regression analysis (Joinpoint version 4.9.1.0, https://surveillance.cancer.gov/joinpoint). We used purely spatial Poisson probability model of SaTScan software version 10.2.4 (https://www.satscan.org) to analyze geographic clusters of *M. bovis* and *M. caprae* incidence at the municipal level during 2018–2022. We restricted the spatial window to a maximum radius of 25 km, representing the mean distance between municipalities in Spain. We created maps using QGIS version 3.36.0 (QGIS, https://qgis.org) and ArcGIS version 10.8.1 (ESRI, https://www.esri.com).

Ethics Considerations

We obtained data from the National Statistics Institute through open data access; thus, no ethical approval

or informed consent was required to conduct data analysis, in accordance with the Spanish Human Research Act. All data were anonymized and deidentified. The research ethics and animal welfare committee at the Health Institute Carlos III approved the overall project (CEI PI 40_2023).

Results

Characteristics of Zoonotic TB Cases

A total of 18,852 autochthonous TB cases were reported to RENAVE during 2018–2022; of those, 6,098 (32.3%) cases had information on the species of MTBC. *M. tuberculosis* was identified in 5,849 TB cases, *M. bovis* in 218 cases, and *M. caprae* in 31 cases. The male-to-female ratio in *M. caprae* cases was 4.2, more than twice the ratio for *M. bovis* (1.9) and *M. tuberculosis* (1.8) cases.

The percentage of cases born in another country was 19.4% (6/31) for *M. caprae*, 24.8% (54/2,018) for *M. bovis*, and 36.5% (2,133/5,849) for *M. tuberculosis* (Table 1). The aOR of *M. bovis* infection among confirmed TB cases was more than twice as high for those born in Spain than for those born outside (aOR 2.32; 95% CI 1.44–3.82; Table 2).

The median age of diagnosis for *M. bovis* TB was 60 years (interquartile range [IQR] 37–77 years), higher than that for *M. caprae* (55 [IQR 28–65] years) or *M. tuberculosis* (46 [IQR 32–63] years) ($p<0.001$, determined by pairwise comparisons of median age at diagnosis across the 3 *Mycobacterium* species, using the Mann-Whitney U test with Bonferroni correction for multiple comparisons.). When stratifying by country of origin, we observed significantly higher median age for case-patients infected with *M. caprae* (58 [IQR 28–65] years), *M. bovis* (68 [IQR 53–79] years), and *M. tuberculosis* (55 [IQR 40–73] years) ($p<0.001$, where p indicates statistically significant differences in median age at diagnosis between patients born in Spain and those born outside of Spain for each *Mycobacterium* species, based on Mann-Whitney U tests with Bonferroni correction for multiple comparisons). For those born elsewhere, median age for case-patients was 35 (IQR 26–44) years for those with *M. caprae*, 38 (IQR 26–62) years for those with *M. bovis*, and 36 (IQR 27–47) years for those with *M. tuberculosis*.

Table 1. Characteristics of patients with confirmed *Mycobacterium caprae*, *M. bovis*, and *M. tuberculosis* infection in study of tuberculosis, Spain, 2018–2022*

Category	*M. caprae*, no. (%), n = 31	*M. bovis*, no. (%), n = 218	*M. tuberculosis*, no. (%), n = 5,849
Age, y			
0–19	3 (9.7)	20 (9.2)	355 (6.1)
20–39	10 (32.3)	38 (17.4)	1,834 (31.4)
40–59	5 (16.1)	49 (22.5)	1,951 (33.4)
60–79	10 (32.3)	70 (32.1)	1,113 (19.0)
80–99	3 (9.7)	41 (18.8)	593 (10.1)
Unknown	0	0	3 (0.1)
Sex			
M	25 (80.7)	143 (65.6)	3,796 (64.9)
F	6 (19.4)	75 (34.4)	2,053 (35.1)
Country of birth			
Other	6 (19.4)	54 (24.8)	2,133 (36.5)
Spain	25 (80.6)	136 (62.4)	2,426 (41.5)
Unknown	0	28 (12.8)	1,290 (22.1)
Primary location			
Pulmonary	16 (51.6)	115 (52.8)	4,460 (76.3)
Extrapulmonary	15 (48.4)	98 (45.0)	1,346 (23.0)
Unknown	0	5 (2.3)	43 (0.7)
HIV laboratory result			
Positive	3 (9.7)	3 (1.4)	368 (6.3)
Negative	18 (58.1)	146 (67.0)	3,713 (63.5)
Unknown	10 (32.3)	69 (31.7)	1,738 (30.2)
Hospitalization			
No	16 (51.6)	60 (27.5)	2,016 (35.4)
Yes	14 (45.2)	145 (66.5)	3,689 (63.1)
Unknown	1 (3.2)	13 (6.0)	144 (2.5)
Treatment outcome			
Complete/cure	26 (83.9)	147 (67.4)	3,563 (60.9)
Abandon/moved/loss	0	5 (2.3)	268 (4.6)
Death	2 (6.5)	27 (12.5)	500 (8.5)
Failure/prolongation	2 (6.5)	7 (3.2)	161 (2.8)
Unknown	1 (3.2)	32 (14.7)	1,357 (23.2)

*Treatment outcome was defined as follows: complete/cure, complete treatment or cure; abandon/moved/loss, abandonment of treatment, relocation, or loss of contact; death, death during treatment; failure/prolongation, treatment failure or patient still in treatment 12 mo after initiation.

Table 2. Determinants of *Mycobacterium bovis* infection versus *M. tuberculosis* infection in study of tuberculosis in Spain, 2018–2022*

Category	Crude odds ratio (95% CI)	p value	Adjusted odds ratio (95% CI)	p value
Age, y				
0–19	Referent		Referent	
20–39	**0.37 (0.21–0.65)**	**<0.001**	0.59 (0.26–1.47)	0.28
40–59	**0.45 (0.27–0.78)**	**0.003**	0.67 (0.31–1.62)	0.34
60–79	1.12 (0.68–1.91)	0.7	1.37 (0.64–3.29)	0.45
80–99	1.23 (0.72–2.17)	0.5	1.29 (0.53–3.38)	0.58
Sex				
M	Referent			
F	0.97 (0.73–1.28)	0.8		
Country of birth				
Other	Referent		Referent	
Spain	**2.21 (1.62–3.07)**	**<0.001**	**2.32 (1.44–3.82)**	**<0.001**
Primary infection location				
Pulmonary	Referent		Referent	
Extrapulmonary	**2.82 (2.14–3.72)**	**<0.001**	**2.20 (1.46–3.28)**	**<0.001**
HIV laboratory result				
Positive	Referent		Referent	
Negative	**4.82 (1.82–19.6)**	**0.007**	**3.39 (1.24–14.0)**	**0.04**
Hospitalization				
No	Referent		Referent	
Yes	1.32 (0.98–1.80)	0.075	1.10 (0.72–1.70)	0.66
Treatment outcome†				
Complete/cure	Referent		Referent	
Abandon/moved/loss	0.45 (0.16–1.00)	0.084	0.74 (0.18–2.05)	0.61
Death	1.31 (0.84–1.96)	0.2	1.22 (0.66–2.18)	0.51
Failure/prolongation	1.05 (0.44–2.13)	0.9	0.97 (0.23–2.73)	0.96

*Bold text indicates statistical significance, defined as p<0.05 and an odds ratio with 95% CI not including 1.
†Treatment outcome was defined as follows: complete/cure, complete treatment or cure; abandon/moved/loss, abandonment of treatment, relocation, or loss of contact; death, death during treatment; failure/prolongation, treatment failure or patient still in treatment 12 mo after initiation.

The frequency of pulmonary and extrapulmonary forms was similar for both *M. bovis* and *M. caprae* TB cases; approximately half of the cases had extrapulmonary forms: 98/218 (45%) of those infected with *M. bovis* and 15/31 (48.4%) of those with *M. caprae*. *M. bovis* case-patients were 2.20 (95% CI 1.46–3.28) times more likely to have extrapulmonary TB develop than were *M. tuberculosis* case-patients (Table 2). Of note, we observed a high proportion of lymphatic forms (46/213 [21.6%]) for *M. bovis* and of genitourinary location (7/31 [22.6%]) for *M. caprae* (Appendix Table 1, https://wwwnc.cdc.gov/EID/article/31/7/25-0031-App1.pdf).

The percentage of HIV co-infection was 9.7% (3/31 [95% CI 3.3–24.9]) in *M. caprae* cases, compared with 1.4% (3/218 [95% CI 0.5–4.0]) in *M. bovis* cases. *M. bovis* case-patients were 3.39 (95% CI 1.24–14.0) times more likely to be HIV negative than were *M. tuberculosis* case-patients.

Two-thirds of *M. bovis* and *M. tuberculosis* case-patients were hospitalized: 145/218 (66.5% [95% CI 60.0%–72.4%]) of case-patients with *M. bovis* infection and 3,689/5,849 (63.1% [95% CI 61.8%–64.3%]) of those with *M. tuberculosis*. Less than half (14/31; 45.2% [95% CI 29.2%–62.2%]) of *M. caprae* TB case-patients were hospitalized. More than three-quarters (26/31; 83.9% [95% CI 67.4%–92.9%]) of *M. caprae* TB case-patients completed treatment, followed by approximately two thirds of *M. bovis* (147/218; 67.4% [95% CI 60.9%–73.3%]) and *M. tuberculosis* (3,563/5,849; 60.9% [95% CI 59.7%–62.1%]) case-patients (Table 1).

Temporal Trends

The mean incidence rate per 100,000 population in 2018–2022 was 0.092 for *M. bovis*, 0.013 for *M. caprae*, and 2.48 for *M. tuberculosis*. TB cases notified with *M. tuberculosis* as a causative agent increased in 2021 and remained stable in 2022 (Figure 1; Appendix Table 2). The statistical trend analysis by joinpoint regression revealed no significant annual percentage change of *M. bovis* and *M. caprae* incidence.

Geographic Distribution and Spatial Analysis

We observed higher rates of *M. bovis* in north and northwestern Spain. *M. caprae* cases were reported in the central and southern part of Spain and the province of Barcelona; 9 of 54 provinces reported human cases of *M. caprae* during 2018–2022 (Figure 2).

We detected 3 notable spatial clusters of *M. bovis* and 1 of *M. caprae* cases (Table 3; Figure 3). The most likely cluster of *M. bovis* was located in the eastern part of the province of León. Two other clusters with a significantly higher number of cases observed than expected were located in the coastal area of the Basque Country (relative risk [RR] 13.01; p<0.001) and the west part of Galicia (RR 14.89; p = 0.013). The only

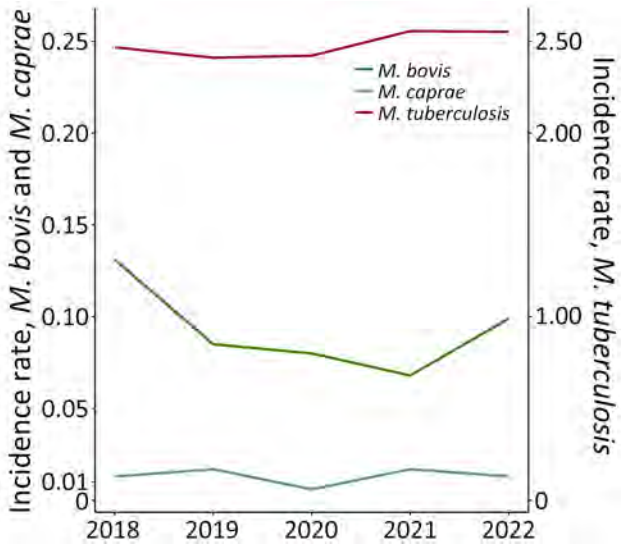

Figure 1. Incidence rates of tuberculosis cases per 100,000 population by causative agent and year of notification, Spain, 2018–2022. Scales for the y-axes differ substantially to underscore patterns but do not permit direct comparison.

significant spatial cluster of *M. caprae* TB cases was situated in the Barcelona metropolitan area (RR 9.90; p = 0.012) (Table 3; Figure 3). All case-patients from *M. bovis* clusters were native born older adults (median age 75 [IQR 66–86] years), mostly men (16/24, 63%), and all HIV-negative; 67% (16/24) had pulmonary manifestations. TB case-patients from the *M. caprae* cluster were all native born and mostly older men (median age 72 [IQR 65–74] years); 7/9 had genitourinary manifestations.

Discussion

This study describes characteristics and spatiotemporal distribution of human TB cases caused by *M. bovis* and *M. caprae* bacteria at the national level in Spain over a 5-year period. First, we aimed to describe and compare the population and clinical characteristics of the infections by different MTBC species, which may contribute to better understanding of the epidemiology of the disease. We found differences in age, country of birth, primary location of infection, and HIV status in *M. bovis*, *M. caprae*, and *M. tuberculosis* cases. Although no significant sex differences were detected, case-patients were predominantly male for all 3 MTBC species, especially for *M. caprae* infection. Higher male-to-female ratio was previously described in Spain and other countries in Europe in older adults, which has been related to different behavioral and environmental risks, lifestyle, or biological factors (*6*,*16*). Native-born case-patients were significantly older than foreign-born case-patients for all 3 MTBC species; the age difference was more pronounced for *M. bovis* cases, which could suggest reactivations rather than new infections. A similar scenario of possible reactivation of latent infections has been suggested in the United Kingdom and Italy, where *M. bovis* cases occurred predominantly in the elderly and native-born (*17*,*18*). However, recent infections associated with occupational exposure cannot be ruled out; Palacios et al. demonstrated that in a region of low incidence of bovine TB in Spain, half of patients >45 years of age shared the genotype with circulating cattle strains, suggesting a recent transmission (*19*).

M. bovis and *M. caprae* case-patients in our study were mainly native-born and had an extrapulmonary infection, in contrast to *M. tuberculosis* case-patients, corroborating previous results in Europe and the United States (*20*,*21*). Those differences could also be attributed to consuming unpasteurized dairy products as the main route of transmission of zTB. Lymph nodes and genitourinary system, followed by bones and joints, were the most common primary locations of extrapulmonary TB in *M. bovis* and *M. caprae* cases, as previously described for zTB cases (*20*,*22*). The high proportion of extrapulmonary forms observed in *M. bovis* and *M. caprae* cases may hinder the detection and diagnosis; therefore, it is essential to improve the knowledge of the clinical manifestations caused by zTB species to contribute to raising awareness and guiding clinicians' diagno-

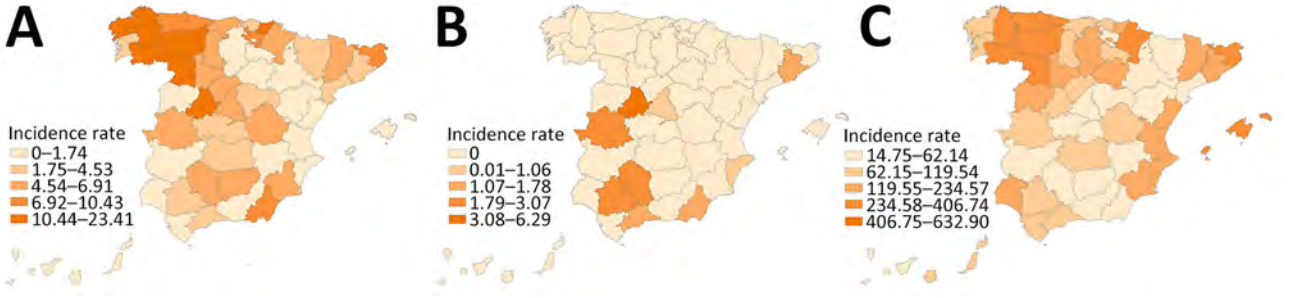

Figure 2. Incidence of tuberculosis reported by province, Spain, 2018–2022. A) *Mycobacterium bovis*; B) *M. caprae*; C) *M. tuberculosis*. Incidence rates for regions are per 1 million population.

Table 3. Spatial clusters of *Mycobacterium bovis* and *M. caprae* cases, Spain, 2018–2022

Cluster	No. municipalities	Radius, km	No. observed cases	No. expected cases	Relative risk	p value
M. bovis						
1, most likely	38	24.4	6	0.77	80.34	<0.001
2	34	18.5	11	0.89	13.01	<0.001
3	13	21.8	7	0.48	14.89	0.013
M. caprae						
1	5	6.4	9	1.26	9.90	0.012

sis and treatment.

HIV co-infection was more common in *M. tuberculosis* than *M. bovis* cases, which could be associated with younger patient age and a more urban profile of *M. tuberculosis* cases (*23*). The low number of HIV infections among *M. caprae* cases made it difficult to draw conclusions. More than two thirds of *M. bovis* and *M. tuberculosis* case-patients were hospitalized; in contrast, less than half of *M. caprae* were hospitalized. Those differences could be related to the higher age observed in *M. bovis* cases or the less severe extrapulmonary manifestations observed for *M. caprae*. Moreover, we did not observe differences in treatment outcome among MTBC species, but the limited completeness of the information collected for this variable limited its interpretation.

We did not observe a notable upward or downward temporal trend in the incidence rate during the study period for *M. bovis* or *M. caprae* cases. Similar figures were reported by EFSA and ECDC at the Europe level; Spain accounted for one third of the cases of *M. bovis and M. caprae* (*3*). We observed no decline in median age of native-born *M. bovis* and *M. caprae* cases over the study period, as previously observed in the United Kingdom during 2014–2022 (*24*). It was suggested that our findings might be related to increased consumption of unpasteurized milk; however, per capita raw milk consumption has been in steady decline since the 1990s in Spain, with the exception of the COVID-19 pandemic in 2021–2022 (*25*).

The geographic distribution indicated a pattern of higher incidence in northwest Spain for *M. bovis* and *M. tuberculosis*, whereas *M. caprae*, cases were reported in the central and southern part of Spain and the province of Barcelona. This pattern contrasted with the reported incidence of TB in bovines (*12*); northwest Spain is where most of the officially TB-free provinces, in which cattle farms are mainly for dairy animals, are concentrated. In contrast, the central-western and southern regions have the high-

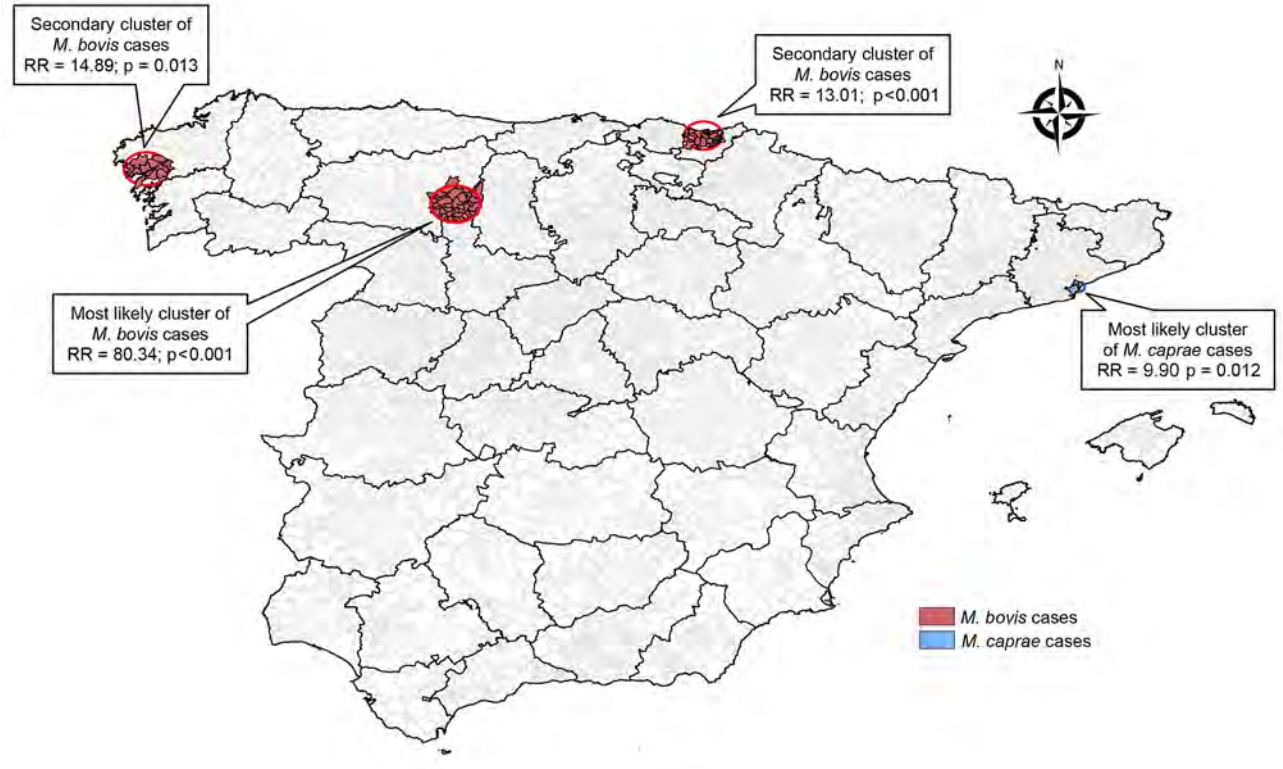

Figure 3. Spatial clusters of tuberculosis infections caused by *Mycobacterium bovis* and *M. caprae*, Spain, 2018–2022. RR, relative risk.

est incidence, where most of the beef cattle farms are located. For *M. caprae* infections, the distribution of human cases and the prevalence and population density in goats shows some overlap, as described in an integrative genomic analysis of human and goat strains in Andalusia (*26*). Three spatial clusters of *M. bovis* cases were detected in bovine TB–free regions of the northern and northwestern part of Spain, affecting mainly old native-born men with pulmonary tuberculosis. However, those clusters were located in historically milk-producing regions of northern Spain, 2 of them in a humid area with an oceanic climate (*27*), whereas higher incidence of infection has been negatively associated with sunshine exposure and vitamin D levels (*28*). The *M. caprae* cluster also affected mainly older native-born persons, but conversely to *M. bovis* clusters, it was located in a large metropolitan area and manifested as genitourinary presentation. The geographic distribution of zTB cases observed together with the characteristics of the patients could support the previously described hypothesis of reactivation of an old infection. Our study of the epidemiology of zTB in Spain is part of a larger project that will include a genomic analysis of human strains and those circulating in cattle and goats to confirm our findings and to establish epidemiologic links and zoonotic transmission.

We note that we did not have information on occupational activities and other individual risk factors or medical history for case-patients. We used place of residence, which does not have to correspond to the place of exposure, for the spatial cluster analysis. In addition, 32.3% of reported TB cases had data on MTBC species, which could have led to an underestimation of *M. bovis* and *M. caprae* cases; the low rate is likely because most TB laboratories identify mycobacteria at the level of the MTBC and do not differentiate between species or do not report the MTBC species. Zoonotic cases account for only a small proportion of TB cases; clinical management is the same, and additional molecular methods not available in all laboratories are required to distinguish species. Efforts to improve completeness of information on MTBC species have included assessment reports sent to the CCAA to retrieve information, as well as investments in the information systems interoperability; we were able to recover unreported zTB cases through collaboration with the CCAA.

The findings from our study of the clinical and demographic characteristics and spatiotemporal distribution of the different zTB cases in Spain can support future genomic epidemiology studies that include data on circulating strains in humans and animals. Understanding the epidemiology of the human cases of *M. bovis* and *M. caprae* and the underlying mechanisms of transmission can contribute to the prevention and control of zoonotic outbreaks. Our study also highlights the need for improved integrated epidemiologic and laboratory information, in particular on circulating MTBC species. We recommend the close and active collaboration of public and animal health institutions to contribute to zTB control and eradication.

Study Group on Zoonotic Tuberculosis (zTB): Juan José Palacios Gutiérrez, Servicio de Microbiología, Hospital Universitario Central de Asturias, Oviedo, Spain; Manuel Antonio Queipo Rodríguez, Servicio de Sanidad y Producción Animal del Principado de Asturias, Oviedo, Spain; Ramiro López Medrano, Complejo Asistencial Universitario de León, Spain; Ana Grau Vila, Servicio de Sanidad Animal de la Junta de Castilla y León, Valladolid, Spain; Pablo Cisneros Otero, Servicio de Sanidad Animal de la Junta de Castilla y León, Valladolid, Spain; María Luisa Pérez del Molino Bernal, Servicio de Microbiología y Parasitología, Complejo Hospitalario Universitario de Santiago Compostela, Spain; Gema Barbeito Castiñeiras, Servicio de Microbiología y Parasitología, Complejo Hospitalario Universitario de Santiago Compostela, Spain; Marta Muñoz Mendoza, Subdirección de Ganadería de la Consellería de Medio Rural de la Xunta de Galicia, Santiago de Compostela, Spain; Miren Josebe Unzaga, Servicio de Microbiología, Osakidetza, Bilbao, Spain; Iker A. Sevilla, Departamento de Sanidad Animal, NEIKER-Instituto Vasco de Investigación y Desarrollo Agrario, Basque Research and Technology Alliance (BRTA), Derio, Bizkaia, Spain; Joseba M. Garrido, Departamento de Sanidad Animal, NEIKER-Instituto Vasco de Investigación y Desarrollo Agrario, Basque Research and Technology Alliance (BRTA), Derio, Bizkaia, Spain; Estefanía Abascal Saiz, Centro Nacional de Microbiología, Instituto de Salud Carlos III, Majadahonda, Spain; Rosa Cano Portero, Centro Nacional de Epidemiología, Instituto de Salud Carlos III, Madrid, Spain; Lorena Simón Méndez, Centro Nacional de Epidemiología, Instituto de Salud Carlos III, Madrid, Spain; Víctor Lorente Leal, VISAVET Health Surveillance Centre, Universidad Complutense de Madrid, Madrid, Spain; Javier Gómez Castellá, División de Control de VIH, ITS, hepatitis virales y tuberculosis, Ministry of Health, Spain.

Acknowledgments

This work is based on data from the national surveillance system, in which a great team of people are committed. Therefore, we thank all the professionals involved in data collecting, from clinicians, coders, administrative staff, computer scientists, epidemiologists, microbiologists,

and especially to the community participating in the National Surveillance Network. Finally, we acknowledge the important work of the Spanish Working Group on Tuberculosis: Enric Durán Pla, María del Carmen Montaño Remacha, Felipe Juanas Fernández, Juan Sahagún Pareja, Ana Fernández Ibáñez, Mario Margolles Martins, Juan José Palacios, Jaume Giménez Duran, Antònia Garí Bibiloni, Antonio M. Ramírez Rosales, Ana Pilar Izquierdo Carreño, Laura García Hernández, María Isolina Campos-Herrero Navas, María Lecuona Fernández, Marta Pacheco Gorostiaga, Inmaculada Concepción Pérez del Molino, María del Henar Marcos, Isabel Martínez Pino, Ramiro López Medrano, Pilar Peces, Elena Rodríguez Zurita, Laura Gavalda Mestre, Mar López Espinilla, Pilar Ciruela, Empar Giner Ferrando, Fernando González Candelas, Juan Antonio Linares Dópido, María del Mar López-Tercero Torvisco, Cristina Muñoz Cuevas, Purificación Hernández Pérez, Susana Miras Carballal, Elena Cruz Ferro, María Luisa Pérez del Molino Bernal, Carmen Quiñones, Carla Andrea Alonso Arribas, Elena Rodríguez Baena, Jaime Esteban, Blanca Andreu, Pedro Ricardo Paredes Reyes, Jesús Castilla Catalán, José Javier García Irure, Rosa Sancho Martínez, Fernando González Carril, Pello Latasa, Diego Vicente, José María Sánchez Romero, Ana Isabel Rivas Pérez, Patricia González Donapetry, Daniel Castrillejo, and Sergio Román.

Researchers working in public and private institutions can request the databases we used by completing a questionnaire for which a signed confidentiality commitment is required.

This work was supported by a public call from the Instituto de Salud Carlos III, Ministerio de Ciencia e Innovación (AESI- PI23CIII_00053). A.R. is the recipient of a postdoctoral Sara Borrell contract funded by the Instituto de Salud Carlos III, Ministerio de Ciencia, Innovación y Universidades (no. CD23CIII/00008).

Author contributions: Z.H., L.H., and B.R. designed the study and prepared the SOPs. A.R., E.O., N.E., and Z.H. performed the statistical analysis. A.R., N.E., and Z.H. wrote the first draft of the manuscript. All the study group contributed to data interpretation, reviewed the manuscript, and approved the final version to be published. L.H. and Z.H. were involved in funding acquisition. L.H. and Z.H. directly accessed and verified the underlying data reported in the manuscript.

About the Author

Dr. Roy is currently working as a postdoctoral researcher at the National Centre for Epidemiology of the Instituto de Salud Carlos III, Spain. His current lines of research focus on the epidemiology of zoonoses and emerging and vectorborne diseases from a One Health approach.

References

1. World Health Organization, Food and Agriculture Organization of the United Nations & World Organisation for Animal Health. Roadmap for zoonotic tuberculosis. 2017 [cited 2025 Jan 3]. https://www.who.int/publications/i/item/9789241513043
2. World Health Organization. Global Tuberculosis Report 2022. 2022 [cited 2025 Jan 3]. https://iris.who.int/bitstream/handle/10665/363752/9789240061729-eng.pdf
3. European Food Safety Authority, European Centre for Disease Prevention and Control. The European Union One Health 2023 zoonoses report. EFSA J. 2024;22:e9106.
4. Rodríguez S, Bezos J, Romero B, de Juan L, Álvarez J, Castellanos E, et al.; Spanish Network on Surveillance and Monitoring of Animal Tuberculosis. *Mycobacterium caprae* infection in livestock and wildlife, Spain. Emerg Infect Dis. 2011;17:532–5. https://doi.org/10.3201/eid1703.100618
5. Prodinger WM, Indra A, Koksalan OK, Kilicaslan Z, Richter E. *Mycobacterium caprae* infection in humans. Expert Rev Anti Infect Ther. 2014;12:1501–13. https://doi.org/10.1586/14787210.2014.974560
6. Rodríguez E, Sánchez LP, Pérez S, Herrera L, Jiménez MS, Samper S, et al. Human tuberculosis due to *Mycobacterium bovis* and *M. caprae* in Spain, 2004–2007. Int J Tuberc Lung Dis. 2009;13:1536–41.
7. Müller B, Dürr S, Alonso S, Hattendorf J, Laisse CJ, Parsons SD, et al. Zoonotic *Mycobacterium bovis*–induced tuberculosis in humans. Emerg Infect Dis. 2013;19:899–908. https://doi.org/10.3201/eid1906.120543
8. de Macedo Couto R, Santana GO, Ranzani OT, Waldman EA. One Health and surveillance of zoonotic tuberculosis in selected low-income, middle-income and high-income countries: a systematic review. PLoS Negl Trop Dis. 2022; 16:e0010428. https://doi.org/10.1371/journal.pntd.0010428
9. Sunstrum J, Power LE, Fligiel HM, Lauter C, Kawam R, Dado C, et al. Human disease due to *Mycobacterium bovis* linked to free-ranging deer in Michigan. Clin Infect Dis. 2024;78:637–45. https://doi.org/10.1093/cid/ciae009
10. Kock R, Michel AL, Yeboah-Manu D, Azhar EI, Torrelles JB, Cadmus SI, et al. Zoonotic tuberculosis—the changing landscape. Int J Infect Dis. 2021;113:S68–72.
11. Bezos J, Sáez-Llorente JL, Álvarez J, Romero B, Díez-Guerrier A, Domínguez L, et al. Bovine tuberculosis in Spain, is it really the final countdown? Ir Vet J. 2023;76(Suppl 1):13. https://doi.org/10.1186/s13620-023-00241-0
12. Ministerio de Agricultura, Pesca y Alimentación. Report of the Bovine Tuberculosis Surveillance Programme and Eradication Programme in Spain [in Spanish]. 2023 [cited 2025 Jan 3]. https://www.mapa.gob.es/es/ganaderia/temas/sanidad-animal-higiene-ganadera/web_informetb2023final_2_tcm30-691027.pdf
13. Thomas J, Balseiro A, Gortázar C, Risalde MA. Diagnosis of tuberculosis in wildlife: a systematic review. Vet Res. 2021;52:31. https://doi.org/10.1186/s13567-020-00881-y
14. Commission Implementing Decision (EU) 2018/945 of 22 June 2018 on the communicable diseases and related special health issues to be covered by epidemiological surveillance as well as relevant case definitions. 2018 [cited 2025 Jan 3]. https://eur-lex.europa.eu/eli/dec_impl/2018/945/oj/eng
15. Centro Nacional de Epidemiología, Instituto de Salud Carlos III. Protocol of the National Network of Epidemiological Surveillance [in Spanish]. 2016 [cited 2025 Jan 3]. https://cne.isciii.es/documents/d/cne/protocolo-

20de-20vigilancia-20de-20tuberculosis-pdf
16. Nhamoyebonde S, Leslie A. Biological differences between the sexes and susceptibility to tuberculosis. J Infect Dis. 2014;209(Suppl 3):S100–6. https://doi.org/10.1093/infdis/jiu147
17. Mandal S, Bradshaw L, Anderson LF, Brown T, Evans JT, Drobniewski F, et al. Investigating transmission of *Mycobacterium bovis* in the United Kingdom in 2005 to 2008. J Clin Microbiol. 2011;49:1943–50. https://doi.org/10.1128/JCM.02299-10
18. Lombardi G, Botti I, Pacciarini ML, Boniotti MB, Roncarati G, Dal Monte P. Five-year surveillance of human tuberculosis caused by *Mycobacterium bovis* in Bologna, Italy: an underestimated problem. Epidemiol Infect. 2017;145:3035–9. https://doi.org/10.1017/S0950268817001996
19. Palacios JJ, Navarro Y, Romero B, Penedo A, Menéndez González Á, Pérez Hernández MD, et al. Molecular and epidemiological population-based integrative analysis of human and animal *Mycobacterium bovis* infections in a low-prevalence setting. Vet Microbiol. 2016;195:30–6. https://doi.org/10.1016/j.vetmic.2016.08.019
20. Dürr S, Müller B, Alonso S, Hattendorf J, Laisse CJM, van Helden PD, et al. Differences in primary sites of infection between zoonotic and human tuberculosis: results from a worldwide systematic review. PLoS Negl Trop Dis. 2013;7:e2399. https://doi.org/10.1371/journal.pntd.0002399
21. Scott C, Cavanaugh JS, Pratt R, Silk BJ, LoBue P, Moonan PK. Human tuberculosis caused by *Mycobacterium bovis* in the United States, 2006–2013. Clin Infect Dis. 2016;63:594–601. https://doi.org/10.1093/cid/ciw371
22. Sintchenko V, Jelfs P, Dally M, Crighton T, Gilbert GL. A case of urinary tuberculosis due to *Mycobacterium bovis* subspecies *caprae*. Pathology. 2006;38:376–8. https://doi.org/10.1080/00313020600821391
23. Pimpin L, Drumright LN, Kruijshaar ME, Abubakar I, Rice B, Delpech V, et al. Tuberculosis and HIV co-infection in European Union and European Economic Area countries. Eur Respir J. 2011;38:1382–92. https://doi.org/10.1183/09031936.00198410
24. Davidson JA, Loutet MG, O'Connor C, Kearns C, Smith RMM, Lalor MK, et al. Epidemiology of *Mycobacterium bovis* disease in humans in England, Wales, and Northern Ireland, 2002–2014. Emerg Infect Dis. 2017;23:377–86. https://doi.org/10.3201/eid2303.161408
25. Ministerio de Agricultura, Pesca y Alimentación. Household food consumption data sets [in Spanish]. 2024 [cited 2025 Jan 3]. https://www.mapa.gob.es/es/alimentacion/temas/consumo-tendencias/panel-de-consumo-alimentario/series-anuales
26. Martínez-Lirola M, Herranz M, Buenestado Serrano S, Rodríguez-Grande C, Dominguez Inarra E, Garrido-Cárdenas JA, et al. A One Health approach revealed the long-term role of *Mycobacterium caprae* as the hidden cause of human tuberculosis in a region of Spain, 2003 to 2022. Euro Surveill. 2023;28:2200852. https://doi.org/10.2807/1560-7917.ES.2023.28.12.2200852
27. Peel MC, Finlayson BL, McMahon TA. Updated world map of the Köppen-Geiger climate classification. Hydrol Earth Syst Sci. 2007;11:1633–44. https://doi.org/10.5194/hess-11-1633-2007
28. Díez Galán MDM, Redondo-Bravo L, Gómez-Barroso D, Herrera L, Amillategui R, Gómez-Castellá J, et al.; Spanish Working Group on Tuberculosis. The impact of meteorological factors on tuberculosis incidence in Spain: a spatiotemporal analysis. Epidemiol Infect. 2024;152:e58. https://doi.org/10.1017/S0950268824000499

Scotochromogenic [sko′′to-kro′mo-jən-ik]

Christoffel Opperman, Rob Warren

The scotochromogenic pigmentation pattern is named after the Greek terms σκότος (*skotos*, darkness), χρωμα (*khrôma*, color), and γενής (*genḗs*, offspring or kind). The term is used to describe bacteria that form pigmentation without exposure to light. Pigmentation in the dark has the potential evolutionary advantage to increase microbial fitness by acting as antimicrobial agents, antioxidants, or virulence factors.

In 1959, US bacteriologist Ernest Runyon (1903–1994) classified nontuberculous mycobacteria into 4 groups based on growth rates, pigmentation, and colony morphology. Group II nontuberculous mycobacteria are slow-growing scotochromogens with the unique ability to produce pigmentation without light exposure; thus, they are scotochromogenic. Common group II members include *Mycobacterium szulgai*, named after the microbiologist Teofil Szulga (Ludwik Hirszfeld institute, Wroclaw, Poland) in 1962; *M. scrofulaceum* (Greek *scrofa* [sow, female pig]) named by Prissick and Masson (McGill University, Montreal, QB, Canada) in 1956; and *M. gordonea* (Figure), documented in 1962 in honor of the US bacterial taxonomist Ruth Evelyn Gordon (1910–2003) by Bojalil, Cerbon, and Trujillo (National Autonomous University of Mexico, Mexico City, Mexico).

Professor Gordon held a doctorate in bacteriology from Cornell University. In later years, the study of streptomycetes and aerobic spore-forming bacteria became her field of expertise, which led to her employment in the United States Department of Agriculture as a soil microbiologist. After World War II, she was a curator for the American Type Culture Collection (ATCC) Society beginning in 1947. She continued her work in recording bacterial collections as an ATCC visiting investigator even after her formal retirement in 1981. During the 1950s at Rutgers University, she pioneered the classifying, naming, and reliable descriptions of rapidly growing acid-fast bacteria. Because of her international reputation, she held various prestigious positions, including honorary president of the International Symposium on the Biology of Actinomycetes in Venezuela (1974) and Germany (1979). In addition, she received numerous accolades during her life, including the Alice Evans Award from the American Society of Microbiology (1992) and the J. Roger Porter Award from the US Federation for Culture Collections (1983).

Figure. Slow-growing, scotochromogenic *Mycobacterium gordonea*, showing smooth, yellow-orange pigmented colonies. The sample was cultured aerobically on 8 mL of solid Löwenstein–Jensen media for 14 days at 37°C without exposure to light. This opportunistic nontuberculous mycobacterium was isolated repeatedly from the sputum of an immunocompromised, HIV-positive patient, who had an absolute CD4 count of 1. Sample processing and culture were performed at the National Health Laboratory Service, Green Point TB-laboratory, Cape Town, South Africa. Vial size is 28 mL. Photograph courtesy of the author.

Acknowledgments

We thank the staff at the National Health Laboratory Service, TB laboratory, Green Point, Cape Town, South Africa, for culturing the bacterium in the Figure.

Ethical approval with a waiver for informed consent was obtained from the Human Research Ethics Committee of Stellenbosch University (HREC reference no. S22/10/191). All patient identifiers were anonymized.

R.W. acknowledges funding from the South African Medical Research Council. C.O. receives funding from the NHLS Research Trust Development Grant (reference no. PR2232714) and Harry Crossley Foundation.

Author contributions: C.O. conceptualized and wrote the first draft of the manuscript. Both authors edited, critically revised, and approved the final version.

Sources

1. Runyon EH. Anonymous mycobacteria in pulmonary disease. Med Clin North Am. 1959;43:273–90. https://doi.org/10.1016/S0025-7125(16)34193-1
2. Marks J, Jenkins PA, Tsukamura M. *Mycobacterium szulgai*—a new pathogen. Tubercle. 1972;53:210–4. https://doi.org/10.1016/0041-3879(72)90018-9
3. Masson AM, Prissick FH. Cervical lymphadenitis in children caused by chromogenic *Mycobacteria*. Can Med Assoc J. 1956;75:798–803.
4. Bojalil LF, Cerbon J, Trujillo A. Adansonian classification of mycobacteria. J Gen Microbiol. 1962;28:333–46. https://doi.org/10.1099/00221287-28-2-333
5. Orlandi VT, Martegani E, Giaroni C, Baj A, Bolognese F. Bacterial pigments: A colorful palette reservoir for biotechnological applications. Biotechnol Appl Biochem. 2022;69:981–1001. https://doi.org/10.1002/bab.2170
6. Wayne TK. American women of science since 1900. Oxford (UK): ABC-CLIO; 2011.

Author affiliations: National Health Laboratory Service, Green Point TB-Laboratory, Cape Town, South Africa (C. Opperman); University of Cape Town, Cape Town (C. Opperman); SAMRC Centre for Tuberculosis Research, Stellenbosch University, Cape Town (R. Warren)

Address for correspondence: Christoffel Opperman, National Health Laboratory Service, Block D Old City Hospital Complex Green Point TB-Laboratory, 1 Portswood Rd, Green Point, Cape Town 8005, South Africa; email: christoffel.opperman@nhls.ac.za

DOI: https://doi.org/10.3201/eid3107.230974

Emergence of Flucytosine-Resistant *Candida tropicalis* Clade, the Netherlands

Fatima Zohra Delma,[1] Bram Spruijtenburg,[1] Jacques F. Meis, Auke W. de Jong, James Groot, Johanna Rhodes, Willem J.G. Melchers, Paul E. Verweij, Theun de Groot, Eelco F.J. Meijer,[2] Jochem B. Buil[2]

Candida tropicalis is the second most virulent *Candida* species after *C. albicans*. Previous studies from the Netherlands and France reported a notable reduction in susceptibility to flucytosine (5-FC) in a substantial proportion of *C. tropicalis* isolates. We investigated epidemiologic patterns of *C. tropicalis* isolates in the Netherlands and the genetic mechanisms driving widespread non–wild-type (WT) 5-FC resistance. We conducted antifungal susceptibility testing and used advanced molecular techniques, including short tandem repeat genotyping and whole-genome sequencing paired with single-nucleotide polymorphism analysis, to analyze 250 C. *tropicalis* isolates collected across the Netherlands during 2012–2022. Our findings revealed the rapid emergence of a 5-FC–resistant, non-WT *C. tropicalis* clade, accounting for >40% of all *C. tropicalis* isolates by 2022. Genomic analysis identified a homozygous nonsense mutation in the *FCY2* gene, which was exclusive to this non-WT population. Continued surveillance efforts are needed to detect and prevent the spread of drug-resistant *Candida* species.

Candida tropicalis is among the 5 most common *Candida* species found in healthcare settings (*1*–*3*). This diploid yeast is prevalent in Latin America and Asia and is occasionally reported in Africa and Europe (*3*,*4*). Since the 2000s, *C. tropicalis* has emerged as a substantial cause of candidemia, particularly in patients with neutropenia (*5*). *C. tropicalis* is considered the second most virulent *Candida* species, after *C. albicans* (*6*). Antifungal drug resistance has been increasingly reported for *C. tropicalis*, especially resistance to azoles (*7*,*8*) and, to a lesser degree, amphotericin B and echinocandins (*9*,*10*). The World Health Organization lists *C. tropicalis* as a high-risk pathogen (*11*,*12*), underscoring its considerable threat to public health and the need for research and surveillance.

Echinocandins are the first-line treatment for candidemia. Flucytosine, also known as 5-fluorocytosine (5-FC), is used to treat severe invasive candidiasis, which can cause endocarditis, endophthalmitis, or meningitis (*13*,*14*). Although 5-FC is only used in combination therapy because of the rapid emergence of isolates with high MICs (*14*), it shows potent activity against most yeasts, including *C. tropicalis* (*15*). Global rates of 5-FC–resistant, non–wild-type (WT) *C. tropicalis* are low, at ≈10% (*15*,*16*). However, we previously found a high percentage of *C. tropicalis* isolates with increased 5-FC MICs in the Netherlands (*17*), which has also been observed in France, where susceptibility to 5-FC has been documented in non-WT *C. tropicalis* since the 1980s (*18*). A 4-year survey conducted during 2002–2006 in the Paris area revealed increased 5-FC MICs in 45 (35%) of 130 *C. tropicalis* isolates recovered from blood cultures. Specific genetic mutations in the *URA3* gene were observed in all isolates with increased 5-FC MICs. In addition, the non-WT strains shared identical multilocus sequence typing (MLST) genotypes, indicating clonal spread (*18*).

To investigate the recent decrease in 5-FC susceptibility in *C. tropicalis* isolates in the Netherlands, we performed a literature review and used available epidemiologic data from the Radboud University Medical Center CWZ Center of Expertise for Mycology

Author affiliations: Radboud University Medical Center, Nijmegen, the Netherlands (F.Z. Delma, B. Spruijtenburg, J.F. Meis, J. Rhodes, W.J.G. Melchers, P.E. Verweij, T. de Groot, E.F.J. Meijer, J.B. Buil); Canisius-Wilhelmina Hospital (CWZ)/Dicoon, Nijmegen (B. Spruijtenburg, T. de Groot, E.F.J. Meijer); University of Cologne, Cologne, Germany (J.F. Meis); National Institute for Public Health and the Environment (RIVM), Bilthoven, the Netherlands (A.W. de Jong, J. Groot, P.E. Verweij)

DOI: https://doi.org/10.3201/eid3107.241918

[1]These first authors contributed equally to this article.

[2]These senior authors contributed equally to this article.

(Nijmegen, the Netherlands). We applied a newly developed, highly reproducible short tandem repeat (STR) assay and whole-genome sequencing (WGS) to genotype *C. tropicalis* isolates (*19*,*20*), describe the epidemiology of *C. tropicalis* isolates over time, and identify the genetic basis of the non-WT 5-FC–resistant phenotype. Because the data consisted solely of information about clinical strains and did not include patient details, no ethics approval was required according to local guidelines.

Materials and Methods

Literature Review

To obtain an updated overview of 5-FC resistance in *C. tropicalis*, we conducted a comprehensive literature search across electronic databases, including PubMed and Google Scholar, by using the keywords "*C. tropicalis*," "5-FC/flucytosine/fluorocytosine resistance," and "clonal resistance in *C. tropicalis*." We also reviewed citations within the retrieved studies. We identified 15 relevant studies and extracted data on geographic region, time period, number of isolates, antifungal susceptibility testing (AFST) methods, interpretation criteria, and rates of non-WT 5-FC resistance.

Clinical Isolate Collection

A total of 250 nonreplicated clinical isolates of *C. tropicalis* were collected from patients across the Netherlands during January 2012–May 2022. The sources of isolates were as follows: blood, other sterile sites, oropharynx (including sputum and bronchoalveolar lavage samples), vagina, feces, urine, and other superficial sources. We identified *Candida* spp. by using matrix-assisted laser desorption/ionization time-of-flight mass spectrometry (Bruker, https://www.bruker.com). We stored isolates at −70°C in 10% glycerol and grew them on Sabouraud dextrose agar plates at 30°C for 2–5 days before testing.

Antifungal Susceptibility Testing

We determined MICs for 5-FC and 9 other antifungal drugs (fluconazole, voriconazole, itraconazole, posaconazole, miconazole, amphotericin B, anidulafungin, caspofungin, and micafungin) according to the European Committee on Antimicrobial Susceptibility Testing (EUCAST) E.def 7.4 microdilution method (*21*). We established local epidemiologic cutoffs (ECOFFs) for 5-FC by using the eyeballing method (*17*) and classified isolates with a 5-FC MIC of >0.5 mg/L local ECOFF as non-WT. For fluconazole, we classified isolates with MICs >1 mg/L ECOFF as non-WT. We defined resistance by using EUCAST breakpoints (version 5.0) as follows: fluconazole, >4 mg/L; itraconazole, >0.125 mg/L; voriconazole, >0.25 mg/L; posaconazole, >0.06 mg/L; anidulafungin, >0.06 mg/L; micafungin, >0.06 mg/L; and amphotericin B, >1 mg/L.

DNA Extraction and STR Genotyping

We extracted DNA from the isolates after 24 hours of incubation on Sabouraud agar. We suspended single colonies in 1 mL of distilled water in a microcentrifuge tube and extracted DNA by using the High Pure PCR Template Preparation Kit (Roche Diagnostics, https://www.roche.com) according to manufacturer instructions. We genotyped the isolates by PCR amplifying and analyzing 6 STR markers, as previously described (*20*).

WGS and Single-Nucleotide Polymorphism Analysis

We selected 16 *C. tropicalis* isolates for WGS, including five 5-FC–resistant, non-WT isolates that clustered in 1 clade according to STR genotyping, 3 non-WT isolates that grouped outside the clade, and 8 phenotypically WT isolates. We extracted DNA by using InstaGene Matrix (Bio-Rad Laboratories, https://www.bio-rad.com) and sequenced by using Illumina technology (Illumina, https://www.illumina.com). Initially, we added 200 μL of InstaGene Matrix to the yeast pellets, vortexed at 500 rpm, and incubated for 30 minutes at 56°C, followed by another 30 minutes at 99°C. We then transferred samples to tubes containing glass beads with a particle size of <106 μm (Sigma Aldrich, https://www.sigmaaldrich.com) and conducted 2 rounds of bead beating at 17,000 rpm by using a MagNA Lyser (Roche Diagnostics). We assessed DNA integrity by using a TapeStation 2200 system (Agilent, https://www.agilent.com) and measured DNA concentrations by using a Qubit fluorometer (Thermo Fisher Scientific, https://www/thermofisher.com). We prepared libraries by using the Nextera DNA Flex kit (Illumina) following the manufacturer's instructions. We performed paired-end, 2 × 150-bp mode sequencing on an Illumina NextSeq 550 system (Illumina).

We compared isolate sequences to *C. tropicalis* sequences retrieved from the National Center for Biotechnology Information Sequence Read Archive (SRA) database (https://www.ncbi.nlm.nih.gov/sra) (Appendix Table 1, https://wwwnc.cdc.gov/EID/article/31/7/24-1918-App1.pdf). We performed WGS single-nucleotide polymorphism (SNP) analysis by using Illumina reads, as previously described (*19*). We aligned reads with the *C. tropicalis* reference genome MYA-3404 (SRA accession no. GCA_013177555.1)

by using BWA-MEM version 0.7.17 (https://github.com/j-levy/bwa) and subsequently filtered to remove duplicates, unpaired reads, and reads with MAPQ scores <60. We detected SNPs by using FreeBayes version 1.3.6 (https://github.com/freebayes/freebayes) and removed SNPs with a read depth of <25, quality of <100, allele frequency between 0.15 × depth and 0.45 × depth, and allele frequency between 0.55 × depth and 0.9 × depth. We performed phylogenetic analysis by using VCF2PopTree (https://github.com/sansubs/vcf2pop), MEGA11 version 11.0.10 (https://www.megasoftware.net), and iTOL version 6 (https://itol.embl.de) for visualization. We located the resistance-associated genes *FUR1* (GenBank accession no. EU327981.1), *FCY1* (accession no. EU327982.1), *FCY2* (accession no. HQ166001.1), and *URA3* (accession no. EU288195.1) within the reference genome MYA-3404 and inspected those for missense mutations by using IGV version 2.17.3 (*22*). We assessed copy number variation and large-scale deletions by using YMAP (*23*) for all *C. tropicalis* assemblies, as well as for the MYA-3404 reference strain.

URA3 Gene Sequencing

We investigated whether the mechanism underlying 5-FC resistance was related to the *URA3* gene mutation resulting in a K177E amino acid substitution (*18*). We sequenced the *URA3* gene from six 5-FC WT (susceptible) and 24 randomly selected 5-FC–resistant non-WT *C. tropicalis* isolates. We grew the isolates on yeast extract/peptone/dextrose agar plates for 24 hours at 30°C and used a standard DNA extraction protocol (*24*). We transferred cells to 1.5-mL tubes containing 600 µL glass beads (diameter 0.4–0.6 mm) and 250 µL breaking buffer (2% Triton X-100, 1% sodium dodecyl sulfate, 2 mol/L NaCl, 1 mol/L Tris-HCl pH 8, 0.5 mol/L EDTA pH 8, and Milli-Q water), shook the tubes for 30 minutes at 60°C, and centrifuged them at 1,000 × *g*. After centrifugation, we added 700 µL of phenol/chloroform/isoamyl alcohol and shook the mixture for 5 minutes at room temperature. We centrifuged the tubes at 10,000 × *g* for 5 minutes and then transferred the resulting upper layer to a new tube and stored at 20°C (room temperature) until analysis. We amplified the *URA3* gene by using the PCR primers and methods described previously (*25*). All sequence data generated in this study were deposited in the SRA database (BioProject accession nos. PRJNA1090665, PRJNA110750, PRJNA1107503).

Epidemiologic Analysis and Data Analysis

We analyzed epidemiologic data from the Radboud University Medical Center laboratory information system to assess the distribution of 5-FC non-WT isolates over time and evaluated temporal trends. We plotted the annual rates of 5-FC non-WT isolates and performed linear regression analysis by using GraphPad Prism (GraphPad, https://www.graphpad.com). We considered the trend to be significant if the slope deviated from zero ($p<0.05$). We also examined correlations between 5-FC and fluconazole resistance.

Results

Literature Review

We retrieved 15 studies describing *C. tropicalis* resistance to 5-FC and summarized those data (Table). Most (n = 12) studies were published during 2000–2012. Data on *C. tropicalis* have been reported from various regions, including global collections and countries, such as the United States, United Kingdom, Japan, South Korea, France, Italy, Spain, and Germany. The Clinical and Laboratory Standards Institute broth microdilution method (*38*) was used predominantly (8 studies) to test *C. tropicalis* isolates, followed by the EUCAST reference broth microdilution method, and then E-test gradient strips, ATB Fungus, and VITEK automated susceptibility testing (all bioMérieux, https://www.biomerieux.com).

The frequency of *C. tropicalis* isolates with elevated MICs to 5-FC ranged from 0%–10% (Italy, Spain, South Korea) to 10%–30% (including studies from Spain, United States, and United Kingdom) in global collections and was >30% in France and Germany. A genetic survey of non-WT *C. tropicalis* isolates from blood samples in Paris, collected during 2002–2006, identified a group of non-WT isolates with the same MLST profile, all having a $URA3^{K177E}$ mutation (*18*). Epidemiologic analysis indicated that the group of non-WT clones frequently caused candidemia in patients with malignancies and was associated with better outcomes; recurrent spread was noted during the study period. Genetic relatedness of 5-FC non-WT isolates from specific clades in the United Kingdom (2002–2003) and Belgium (1998) has also been suggested (*39*). The spread of the clade from Paris to other regions of France and other countries in Europe has not been investigated further.

Antifungal Drug Susceptibility Testing

To gain more insight into the susceptibility of *C. tropicalis* isolates to 5-FC in the Netherlands, we performed AFST on 250 clinical strains, for which the isolation source of 104 isolates was available, by using the EUCAST microbroth dilution (Appendix Table 2). The modal 5-FC MIC was 0.06 mg/L, and local

Table. Reported 5-FC resistance rates in different published reports in study of non–wild-type *Candida tropicalis* clade, the Netherlands*

Total no. isolates	Year collected	Body site of isolation	Methods used†	Country	MIC criteria,‡ mg/L	No. (%) isolates with elevated 5-FC MICs	Reference
70	NA	NA	NA	France	NA	NA (80)	(*26*)
60	NA	Different sites	Disc diffusion test, macrodilution with YNBG broth	United Kingdom	I, 2–8 R, >8	6 (10) 17 (28)	(*27*)
30	NA	NA	NCCLS	Italy	I, 8–16; R, ≥32	0	(*28*)
117	1998–2000	Different sites	NCCLS	Spain	I, 8–16 R, ≥32	6 (5.1) 0	(*29*)
759	1992–2001	Different sites	NCCLS	Worldwide collection§	I, 8–16 R, ≥32	60 (1) NA (7)	(*16*)
33	2000–2001	Blood	CLSI M27-A2	United States	I, 8–16 R, ≥32	0 1 (3)	(*30*)
34	NA	NA	ATB Fungus	Spain	R, ≥32	3 (8.8)	(*31*)
62	2001–2002	Blood	NCCLS M27-A2	Japan	R, ≥32	NA (8.1)	(*32*)
60	2004–2006	Different sites	CLSI M27-A2, Etest	Germany	R, ≥32	NA (58.3)	(*33*)
130	2002–2006	Blood	EUCAST	France	R, ≥8	45 (35)	(*18*)
97	2006	NA	Etest	Taiwan	I, 8–16 R, ≥32	1 (1) NA	(*34*)
303	NA	Blood	CLSI M27-A3	United States	I, 8–16 R, ≥32	5 (1.65) 4 (1.32)	(*35*)
149	2007–2008	Blood	VITEK-2	South Korea	I, 8–16; R, ≥32	0	(*36*)
126	NA	Blood	CLSI M27-A3	Worldwide collection¶	NA	NA (10.3)	(*37*)
359	2008–2024	Different sites	EUCAST	The Netherlands	>16	106 (29.5)	(*17*)

*5-FC, flucytosine; CLSI, Clinical and Laboratory Standards Institute; EUCAST, European Committee on Antimicrobial Susceptibility Testing; I, intermediate resistance; NA, not applicable; NCCLS, National Committee for Clinical Laboratory Standards; R, resistant; YNBG, yeast nitrogen base glucose.
†CLSI was formerly known as NCCLS. CLSI M27 broth dilution method for yeast (*38*). ATB Fungus test, Etest, and VITEK-2 were purchased from bioMérieux (https://www.biomerieux.com).
‡Resistance status and MICs used to interpret level of resistance to 5-FC in each study.
§North America, Latin America, Europe, and Asia-Pacific.
¶United States, Europe, Latin America, and the Asia-Pacific region.

ECOFF was 0.5 mg/L (Figure 1). *C. tropicalis* isolates displayed a bimodal distribution; we observed a clear separation of 2 subpopulations. The first subpopulation consisted of 168 (67.2%) isolates with low 5-FC MICs (≤0.5 mg/L) and were classified as WT, whereas the second subpopulation consisted of 82 (32.8%) isolates with high 5-FC MICs (>0.5 mg/L) and were classified as non-WT. AFST of 9 additional antifungal agents did not show that typical bimodal distribution (Appendix Table 3). All isolates were susceptible to amphotericin B. Resistance rates (EUCAST clinical breakpoints) were as follows: fluconazole, 11.3% (28/248); itraconazole, 7.3% (7/95); voriconazole, 8.8% (22/249); posaconazole, 7.7% (4/52); and anidulafungin, 0.8% (2/246). We did not interpret MIC data for miconazole, caspofungin, and micafungin because of the lack of EUCAST clinical breakpoints for those drugs. Overall, 25 (10%) isolates exhibited cross-resistance. We did not observe a correlation between 5-FC non-WT and azole resistance.

Phylogenetic Analysis Using STR

We performed STR genotyping for all 250 isolates. Except for 2 isolates (nos. v139–74 and v267–58), which had identical genotypes, all isolates displayed a unique genotype (Appendix Figure). Of the 82 isolates with the 5-FC non-WT phenotype, 65 (79.3%) were closely related and formed a distinct clade, whereas the remaining non-WT isolates did not cluster (Figure 2). Isolates within this clade differed by ≤4 STR markers; high variability occurred in the first and second markers of the PCR M6 panel, and little variation

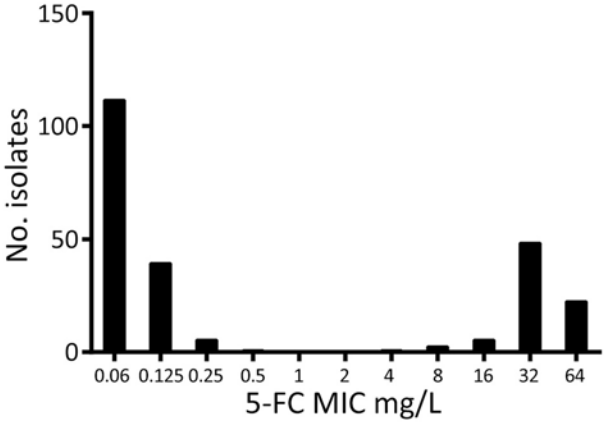

Figure 1. 5-FC MIC distribution for 250 *Candida tropicalis* isolates collected in the Netherlands in study of emerging 5-FC–resistant clade. MICs were determined according to European Committee on Antimicrobial Susceptibility Testing microdilution method (*21*). 5-FC, flucytosine.

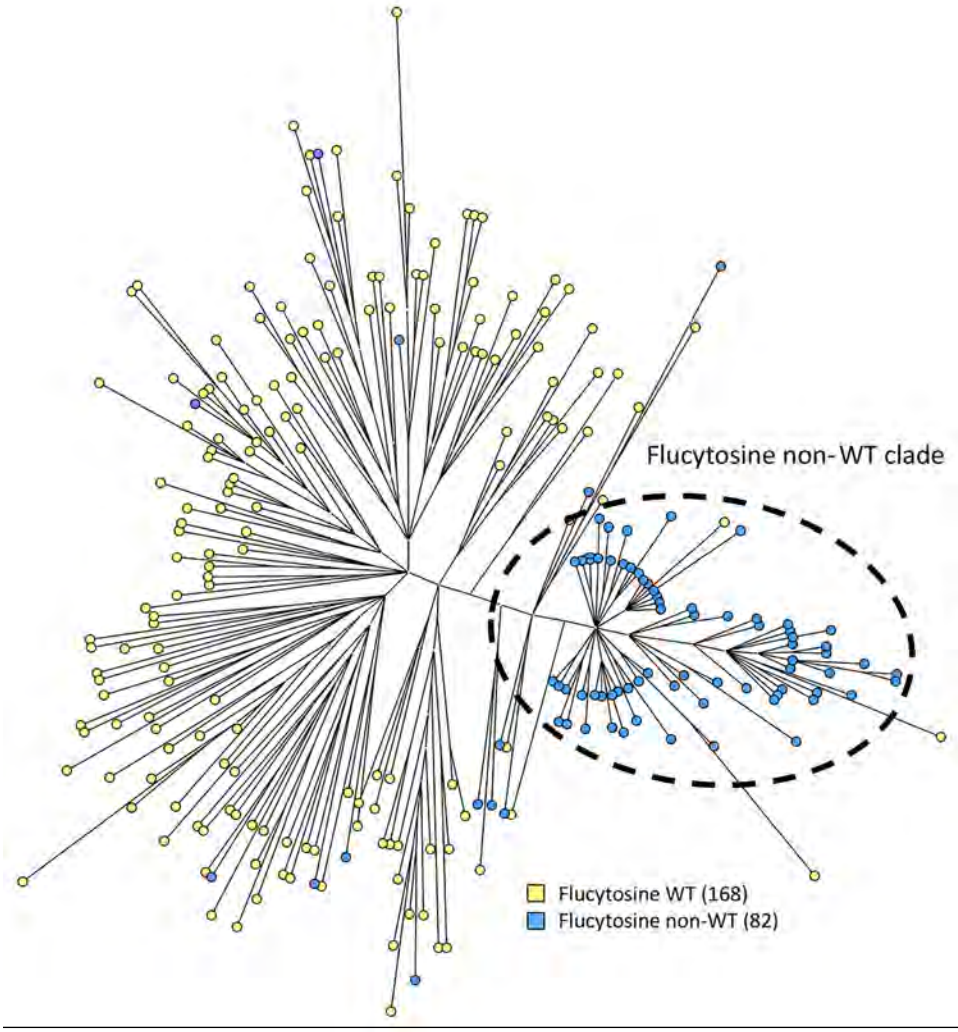

Figure 2. Phylogenetic analysis of *Candida tropicalis* isolates in study of emerging 5-FC–resistant clade, the Netherlands. Maximum parsimony tree of 250 *C. tropicalis* isolates was constructed. Colors indicate the number of isolates per flucytosine interpretive category. Isolates with a MIC of ≤0.5 mg/L were classified as WT and >0.5mg/L as non-WT. WT, wild-type.

occurred in PCR M3a and M3b panels (Appendix Figure) (*20*). In contrast, isolates outside this clade differed in ≥4 markers, usually 5 or 6, and had larger copy number differences. Non-WT strains within the distinct clade containing genotypes 84–147 were isolated during the entire study period.

WGS Analysis

To validate the inferred genetic relatedness, STR outcomes were compared with WGS SNP calling. Isolates that were part of the non-WT clade, according to the STR data (n = 5), also clustered according to WGS SNP analysis (Figure 3). Within the non-WT clade, the genetic diversity was relatively low (304/2,289 SNPs), whereas isolates outside the clade displayed >20,000 SNPs compared with the most related isolate. Isolate v186-48 was most closely related to the non-WT clade (according to 19,365 SNPs). The remaining 5-FC non-WT isolates, which were not located in this clade, did not cluster. To assess the global dispersal of the resistant clade, we compared the 5 isolates from the Netherlands belonging to the 5-FC non-WT clade, together with the other isolates from the Netherlands (from the WGS data), with 27 previously reported *C. tropicalis* MLST clades. Using WGS SNP analysis, including 1 representative isolate from each MLST clade, we found five 5-FC non-WT isolates from the Netherlands were most closely related to *C. tropicalis* MSLT 15 (Figure 4). The other isolates from the Netherlands formed a distinct branch.

Molecular Mechanisms of 5-FC Resistance

To investigate the mechanism of 5-FC resistance, we sequenced the *URA3* gene of 30 isolates (6 WT and 24 non-WT) and inspected it for substitutions. The $URA3^{K177E}$ mutation occurred in all 5-FC non-WT isolates. However, two 5-FC susceptible isolates (M.040-37 and v252-37) also exhibited this mutation (either heterozygous or homozygous mutation), which we confirmed by visual inspection of WGS reads

(Appendix Table 4). Therefore, we analyzed the resistance-associated genes *FUR1*, *FCY1*, *FCY2*, and *URA3* by using available WGS data. In *FCY2*, the mutation causing an E49X amino acid nonsense substitution was homozygous in all isolates from the non-WT clade, whereas that mutation was either absent or heterozygous in isolates outside the clade (*40*). For the other resistance-associated genes, no missense

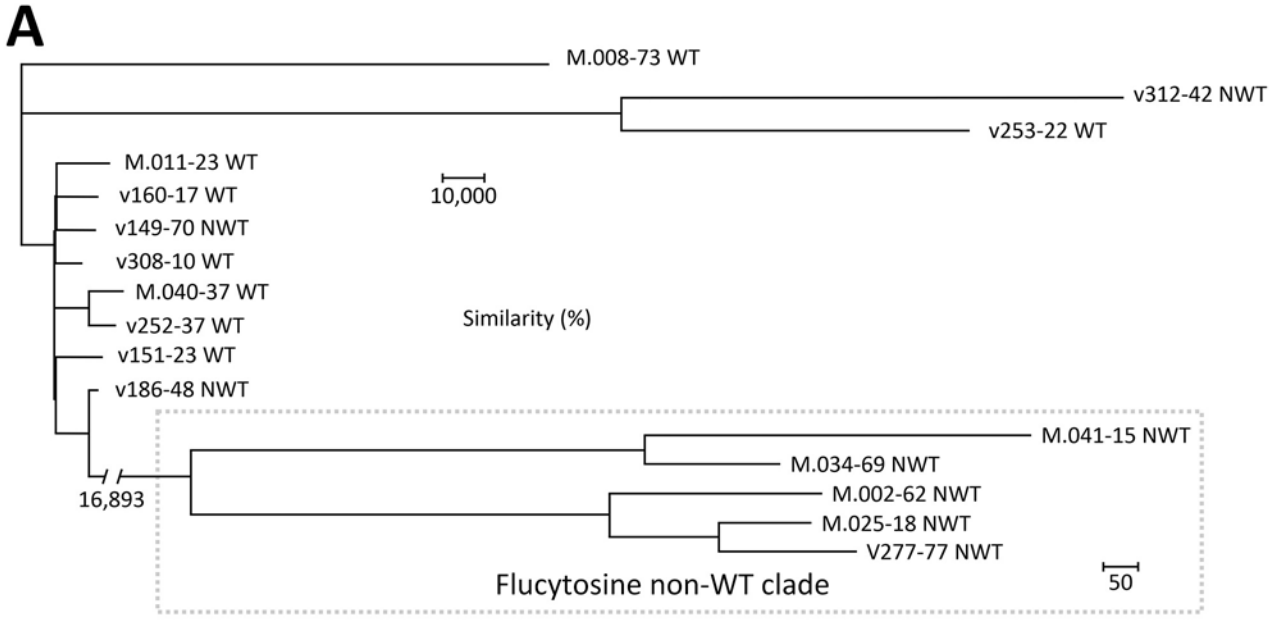

B

Similarity, %

20 40 60 80 100

M3 a	M3 b	M3 c	M6 a	M6 b	M6 c	ID
9/13	28/31	49	11	29	5	v149-70 NWT
9	28/31	49	17	26	4/9	v252-37 WT
9/13	30/33	49	3	27	5/10	M.040-37 WT
8/14	23/31	49	12/17	27	26/31	v151-23 WT
19	28	46	10/14	29	1/4	v160-17 WT
3/9	9	48	7	37	1/5	v253-22 WT
3/9	17	48	19	20/36	40/45	v308-10 WT
3/9	10/19	51	32	7	3/10	v312-42 NWT
9	27	45	3	24	3/7	M.011-23 WT
8	17	24	24	16	32	M.008-73 WT
8	17/20	51	8	16	5/19	v186-48 NWT
9	17	51	15	24	1/5	M.034-69 NWT
9	17	51	16	9	1/5	M.041-15 NWT
10	17	51	16	21	1/5	M.025-18 NWT
10	17	51	9	23	1/5	M.002-62 NWT
10	17	51	13	26	1/5	v277-77 NWT

Figure 3. Phylogenetic comparison of relatedness of 16 *Candida tropicalis* isolates in study of flucytosine-resistant *C. tropicalis* clade, the Netherlands. A) Tree was constructed by using SNPs identified by whole-genome sequencing. Number on left side below tree indicates number of SNPs for that branch. Scale bars indicate number of SNPs. B) Similarities were determined by short tandem repeat genotyping. M3 and M6 a, b, and c indicate the PCR panel used for genotyping (*20*). Numbers under each PCR panel indicate copy numbers of short tandem repeats for that specific locus. Single numbers indicate homozygous copy numbers; 2 numbers separated by slash indicate heterozygous copy numbers. Flucytosine interpretive category is indicated after the isolate identification number; a MIC of ≤0.5 mg/L was classified as WT and >0.5 mg/L as non-WT. ID, identification; NWT, non–wild-type; SNP, single-nucleotide polymorphism; WT, wild-type.

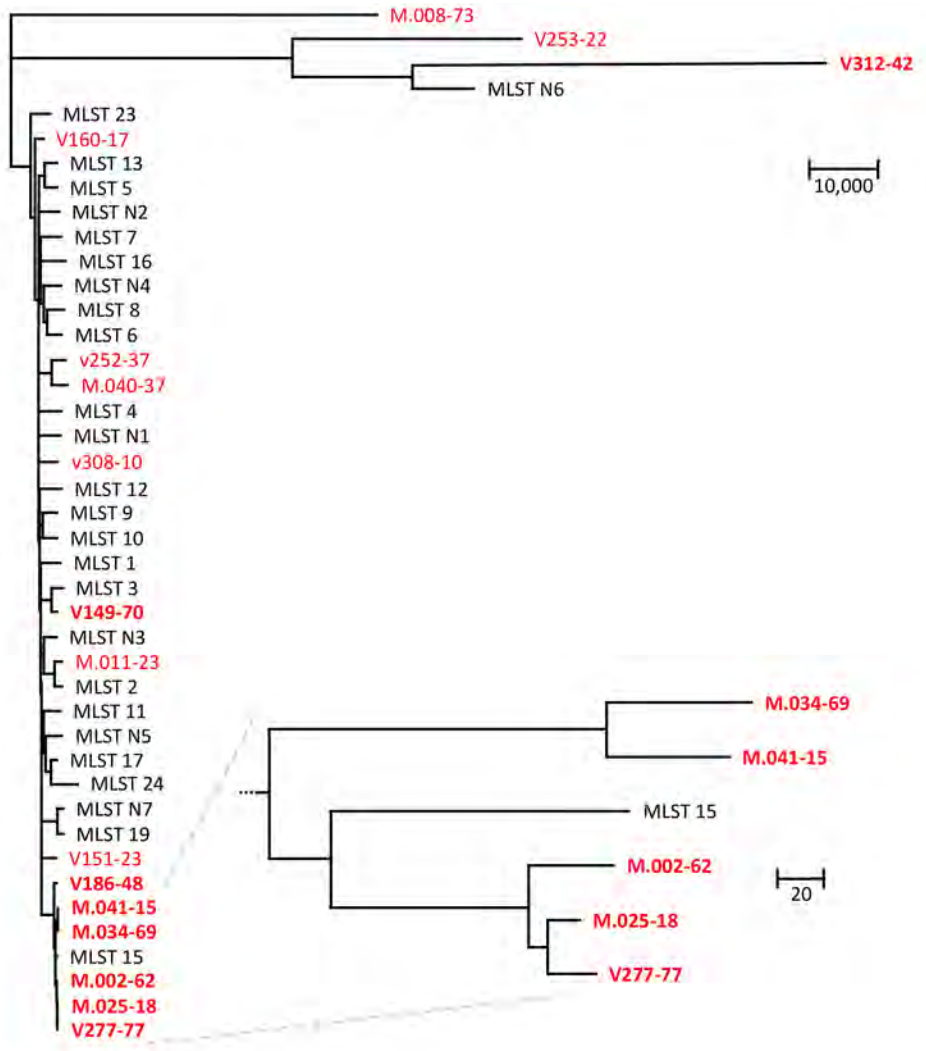

Figure 4. Phylogenetic analysis of global collection of *Candida tropicalis* isolates and 16 isolates from the Netherlands in study of flucytosine-resistant clade. Tree was constructed to compare SNPs. MLST numbers at branch tips correspond to clades. Bold font indicates isolates were flucytosine non–wild-type; red font indicates isolates originating in the Netherlands. Zoomed-in part of tree indicates the five 5-FC non-WT isolates from the Netherlands most closely related to *C. tropicalis* MSLT 15. Scale bars indicate number of SNPs. MLST, multilocus sequence typing; SNP, single-nucleotide polymorphism.

mutations were exclusively present in the non-WT isolates. Subsequently, we assessed the isolates for copy number variation by using YMAP (*23*) and compared them with the MYA-3404 reference genome. For *FUR1*, *FCY1*, *FCY2*, and *URA3*, we found no copy number variation in the non-WT clade when compared with the 5-FC–susceptible isolates.

Epidemiology of 5-FC Non-WT clade

To elucidate the emergence of 5-FC non-WT *C. tropicalis* isolates over time, we compared those isolates with fluconazole non-WT and fluconazole-resistant isolates collected during 2012–2022 (Figure 5). The percentage and clustering of 5-FC–resistant non-WT isolates both increased during this timeframe, particularly since 2018; a substantial peak indicating a higher prevalence in the non-WT population occurred in 2022. In contrast, we observed no downward or upward trend for the fluconazole non-WT or resistant isolates.

Discussion

We conducted a comprehensive analysis of 5-FC resistance in and genetic relatedness of clinical *C. tropicalis* isolates collected in the Netherlands during 2012–2022. The analyses showed a recent and substantial emergence of non-WT, 5-FC–resistant *C. tropicalis* isolates across the Netherlands since the 2010s. STR typing and WGS identified a circulating non-WT 5-FC–resistant clade; a marked increase in the percentage of isolates belonging to this clade was observed, particularly since 2018.

Approximately one third (32.4%) of the *C. tropicalis* isolates in our collection comprised non-WT strains resistant to 5-FC with a bimodal MIC distribution, indicating a heterogeneous population. Most 5-FC–resistant non-WT isolates had a MIC of 32 mg/L (Figure 1). STR genotyping demonstrated that ≈80% of non-WT isolates were genetically related and formed a distinct clade. The genetic diversity within

that clade was low (304–2,289 SNP differences) but distinct, indicating past diversification and environmental spread rather than recent clonal transmission. The increasing prevalence of this clade suggests better adaptation compared with other *C. tropicalis* strains in the Netherlands, although changes in clinical practices and referral patterns might confound this observation.

Our study raises questions regarding the relationship between the 5-FC non-WT clade identified in the Netherlands and similar clades reported in other countries of Europe. A comparison of our WGS data with those of publicly available *C. tropicalis* isolates indicated the clade from the Netherlands is closely related to *C. tropicalis* MLST clade 15 from Denmark (*41*,*42*). A previous global study of 1,571 *C. tropicalis* isolates identified 10 isolates from MLST clade 15 (*42*), which included isolates from Denmark (n = 1) (*41*), Ireland (n = 1) (*43*), United Kingdom (n = 2), Belgium (n = 2), Taiwan (n = 1), and Thailand (n = 3) (*42*). The isolates from Belgium, cultured in 1993 and 1994, had 5-FC MICs of 128 mg/L. The UK isolates, cultured in 2004, had 5-FC MICs of 32 and 64 mg/L. The 5-FC MICs of the isolate from Taiwan cultured in 2006 and those from Denmark (date unknown) and Ireland (cultured in 2018) remain unknown (*41*,*43*). Several isolates from this study clustered with isolates from Belgium and the United Kingdom that had increased 5-FC MICs, indicating spread across Europe (*39*). The MLST 15 isolates from Thailand, cultured during 2015–2017, had 5-FC MICs of ≤0.5 mg/L (*44*), suggesting intraclade variation in 5-FC susceptibility.

In this study, we analyzed *C. tropicalis* isolates collected during 2012–2022. We conducted an earlier study, which included isolates cultured before 2012 (*17*). In that study, all 18 isolates tested during 2008–2010 were phenotypically 5-FC WT. In 2011, a total of 24 isolates were tested, 6 of which were 5-FC–resistant non-WT isolates. However, genetic analysis of those isolates has not been performed. All isolates collected since 2012 have been genotyped, and the first non-WT isolate from the clade in the Netherlands was identified in 2012 (Figure 5). In parallel with our study, investigators in Denmark also showed a marked increase in 5-FC–resistant, non-WT *C. tropicalis* isolates since the 2010s (*40*). In contrast, 5-FC–resistant non-WT isolates were documented in France as early as the 1980s (*18*), suggesting a later introduction or evolution of the 5-FC–resistant, non-WT clade in the Netherlands. Previous studies using MLST in the United Kingdom, Belgium, and France have also indicated the presence of non-WT *C. tropicalis* clades

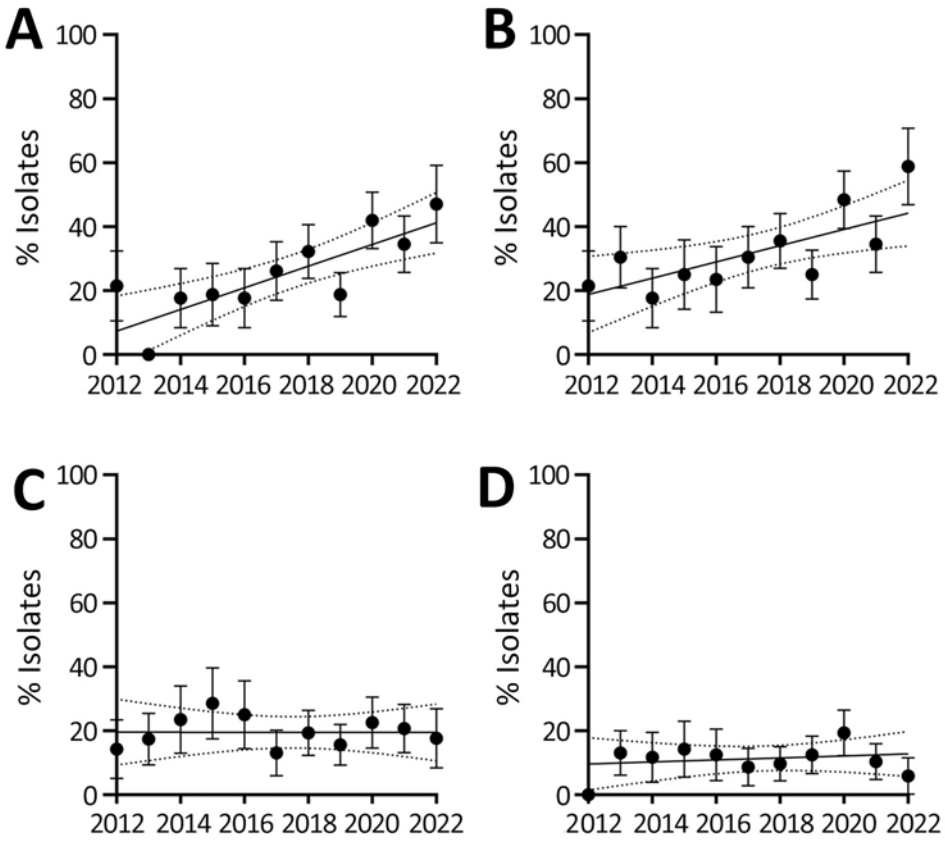

Figure 5. Trends in percentages of flucytosine-resistant and fluconazole-resistant non–wild-type (WT) *Candida tropicalis* isolates, the Netherlands, 2012–2022. A) Percentages of flucytosine (5-FC) non-WT isolates within the specific clade identified in the Netherlands. B) Percentages of all 5-FC non-WT isolates, regardless of clade affiliation. Isolates with a 5-FC MIC above the local epidemiologic cutoff of 0.5 mg/L were classified as non-WT. C) Percentage of fluconazole non-WT isolates. Isolates with a MIC above the local epidemiologic cutoff of 1 mg/L were classified as non-WT. D) Percentage of fluconazole-resistant non-WT isolates. Isolates with values above the EUCAST clinical breakpoint of 4 mg/L were classified as resistant. Solid vertical lines indicate slopes; dotted lines above and below the slope indicate 95% CIs. Error bars indicate SEM. Slopes significantly deviated from zero in panels A and B ($p<0.001$ for both) but not in panels C ($p = 0.992$) or D ($p = 0.640$).

(*18*,*39*), although the lack of full-genome sequences prevents direct comparisons with our findings.

No 5-FC–resistant, non-WT clade has been reported outside Europe. However, *C. tropicalis* has demonstrated the ability to spread globally, evidenced by the worldwide distribution of other *C. tropicalis* clades. Azole-resistant *C. tropicalis* clades have been documented worldwide (*42*). The fluconazole-resistant MLST clade 4, comprising 248 of 1,571 isolates, mainly originated from Asia, whereas fluconazole-resistant MLST clades 2 and N2 have a global distribution (*42*). Despite the confinement of 5-FC–resistant, non-WT *C tropicalis* to Europe, the widespread prevalence of MLST clades 2 and N2 suggests a potential for global dissemination, emphasizing the importance of vigilance and global surveillance.

We found that 32.4% of *C. tropicalis* isolates were 5-FC–resistant non-WT strains, which was higher than the 19% fluconazole-resistant non-WT and 11% fluconazole-resistant strains. Higher fluconazole resistance rates have been reported in lower and middle income countries, such as China (23.1%) (*42*), Algeria (31.6%) (*45*) and Egypt (37.5%) (*19*), where fluconazole is the primary treatment for invasive fungal infections. Most fluconazole-resistant isolates in our study were from the 5-FC WT population; only 2 isolates exhibited non-WT 5-FC MICs. Despite the rising rate of 5-FC–resistant non-WT isolates, a major national trend was not observed for rates of fluconazole-resistant non-WT isolates.

The factors driving the recent emergence of the 5-FC–resistant, non-WT clade in the Netherlands are unclear. Possible reasons are selective pressure from antifungal drugs or cancer treatments, such as 5-fluorouracil, and better adaptation to human hosts, leading to greater colonization and spread. Unlike azole resistance, which might be linked to extensive clinical or agricultural azole use, 5-FC is rarely used outside medical contexts and seldom prescribed for invasive candidiasis, making resistance development through drug exposure unlikely. Increased 5-FC MICs were not linked to resistance to other antifungal agents, such as fluconazole or echinocandins, and genotyping did not suggest a clonal outbreak. Therefore, the factors behind the rise of this 5-FC–resistant, non-WT *C. tropicalis* clade remain unknown, necessitating further investigation to elucidate mechanisms and prevent spread.

Although 5-FC resistance has been previously associated with the K177E amino acid substitution from a mutation in *URA3*, this association has not been confirmed through transformation studies (*18*). In our study, the K177E mutation was present in all sequenced 5-FC–resistant, non-WT clade isolates; however, it was also detected in non-WT isolates, indicating that this mutation alone cannot fully explain the non-WT resistant phenotype. In Denmark, a mutation in the *FCY2* gene resulting in the E49X amino acid substitution was found in all 5-FC non-WT isolates, possibly overlooked previously because of an error in the *FCY2* reference sequence (*40*). When checking for this mutation, we found it to be homozygous in the 5-FC clade isolates from the Netherlands, which has previously been shown to cause a 5-FC non-WT phenotype (*34*). That laboratory study exposed isolates heterozygous for this mutation to 5-FC and showed that those isolates developed a non-WT 5-FC–resistant phenotype because of loss of heterozygosity for that mutation (*34*). In addition, constructed strains homozygous for the truncated protein and for glutamic acid at amino acid position 49 indicated that the homozygous truncated protein caused a non-WT phenotype, whereas isolates with glutamic acid at position 49 were WT (*34*).

In conclusion, our study confirmed the presence of a 5-FC–resistant, non-WT clade in the Netherlands; similar trends were observed in Denmark (*40*), likely because of the same 5-FC non-WT clade. Further prospective studies are required to gain more epidemiologic insights and clarify the effect of this 5-FC non-WT clade on patient outcomes. Our findings highlight the importance of continuous surveillance, advanced genotyping techniques, and comprehensive clinical data collection to prevent the spread of drug-resistant *Candida* spp.

About the Author

Ms. Delma is a PhD candidate at the Radboudumc-CWZ Center of Expertise for Mycology in Nijmegen, the Netherlands. Her primary research interests focus on flucytosine resistance in medically important fungi.

References

1. McCarty TP, Pappas PG. Invasive candidiasis. Infect Dis Clin North Am. 2016;30:103–24. https://doi.org/10.1016/j.idc.2015.10.013
2. Lass-Flörl C, Kanj SS, Govender NP, Thompson GR 3rd, Ostrosky-Zeichner L, Govrins MA. Invasive candidiasis. Nat Rev Dis Primers. 2024;10:20. https://doi.org/10.1038/s41572-024-00503-3
3. Guinea J. Global trends in the distribution of *Candida* species causing candidemia. Clin Microbiol Infect. 2014;20:5–10. https://doi.org/10.1111/1469-0691.12539
4. Dougue AN, El-Kholy MA, Giuffrè L, Galeano G, D'Aleo F, Kountchou CL, et al. Multilocus sequence typing (MLST) analysis reveals many novel genotypes and a high level of genetic diversity in *Candida tropicalis* isolates from Italy and Africa. Mycoses. 2022;65:989–1000. https://doi.org/10.1111/myc.13483

5. Chai LY, Denning DW, Warn P. *Candida tropicalis* in human disease. Crit Rev Microbiol. 2010;36:282–98. https://doi.org/10.3109/1040841X.2010.489506
6. Zuza-Alves DL, Silva-Rocha WP, Chaves GM. An update on *Candida tropicalis* based on basic and clinical approaches. Front Microbiol. 2017;8:1927. https://doi.org/10.3389/fmicb.2017.01927
7. Spruijtenburg B, Baqueiro CCSZ, Colombo AL, Meijer EFJ, de Almeida JN Jr, Berrio I, et al.; on behalf of the Latin American Group For Investigating Candida tropicalis Resistance. Short tandem repeat genotyping and antifungal susceptibility testing of Latin American *Candida tropicalis* isolates. J Fungi (Basel). 2023;9:207. https://doi.org/10.3390/jof9020207
8. Paul S, Shaw D, Joshi H, Singh S, Chakrabarti A, Rudramurthy SM, et al. Mechanisms of azole antifungal resistance in clinical isolates of *Candida tropicalis*. PLoS One. 2022;17:e0269721. https://doi.org/10.1371/journal.pone.0269721
9. Pristov KE, Ghannoum MA. Resistance of *Candida* to azoles and echinocandins worldwide. Clin Microbiol Infect. 2019;25:792–8. https://doi.org/10.1016/j.cmi.2019.03.028
10. Khan Z, Ahmad S, Mokaddas E, Meis JF, Joseph L, Abdullah A, et al. Development of echinocandin resistance in *Candida tropicalis* following short-term exposure to caspofungin for empiric therapy. Antimicrob Agents Chemother. 2018;62:e01926-17. https://doi.org/10.1128/AAC.01926-17
11. World Health Organization. WHO fungal priority pathogens list to guide research, development and public health action. October 25, 2022 [cited 2025 May 2]. https://www.who.int/publications/i/item/9789240060241
12. Keighley C, Kim HY, Kidd S, Chen SC, Alastruey A, Dao A, et al. *Candida tropicalis*—a systematic review to inform the World Health Organization of a fungal priority pathogens list. Med Mycol. 2024;62:myae040. https://doi.org/10.1093/mmy/myae040
13. Sigera LSM, Denning DW. Flucytosine and its clinical usage. Ther Adv Infect Dis. 2023;10:20499361231161387. https://doi.org/10.1177/20499361231161387
14. Cornely OA, Sprute R, Bassetti M, Chen SC, Groll AH, Kurzai O, et al. Global guideline for the diagnosis and management of candidiasis: an initiative of the ECMM in cooperation with ISHAM and ASM. Lancet Infect Dis. 2025;25:e280–93. https://doi.org/10.1016/S1473-3099(24)00749-7
15. Delma FZ, Al-Hatmi AMS, Brüggemann RJM, Melchers WJG, de Hoog S, Verweij PE, et al. Molecular nechanisms of 5-fluorocytosine resistance in yeasts and filamentous fungi. J Fungi (Basel). 2021;7:909. https://doi.org/10.3390/jof7110909
16. Pfaller MA, Messer SA, Boyken L, Huynh H, Hollis RJ, Diekema DJ. In vitro activities of 5-fluorocytosine against 8,803 clinical isolates of *Candida* spp.: global assessment of primary resistance using National Committee for Clinical Laboratory Standards susceptibility testing methods. Antimicrob Agents Chemother. 2002;46:3518–21. https://doi.org/10.1128/AAC.46.11.3518-3521.2002
17. Delma FZ, Melchers WJG, Verweij PE, Buil JB. Wild-type MIC distributions and epidemiological cutoff values for 5-flucytosine and *Candida* species as determined by EUCAST broth microdilution. JAC Antimicrob Resist. 2024;6:dlae153. https://doi.org/10.1093/jacamr/dlae153
18. Desnos-Ollivier M, Bretagne S, Bernède C, Robert V, Raoux D, Chachaty E, et al.; Yeasts Group. Clonal population of flucytosine-resistant *Candida tropicalis* from blood cultures, Paris, France. Emerg Infect Dis. 2008;14:557–65. https://doi.org/10.3201/eid1404.071083
19. Spruijtenburg B, Meijer EFJ, Xiao M, Shawky SM, Meis JF, de Groot T, et al. Genotyping and susceptibility testing uncovers large azole-resistant *Candida tropicalis* clade in Alexandria, Egypt. J Glob Antimicrob Resist. 2023;34:99–105. https://doi.org/10.1016/j.jgar.2023.06.012
20. Spruijtenburg B, van Haren MHI, Chowdhary A, Meis JF, de Groot T. Development and application of a short tandem repeat multiplex typing assay for *Candida tropicalis*. Microbiol Spectr. 2023;11:e0461822. https://doi.org/10.1128/spectrum.04618-22
21. European Committee for Antimicrobial Susceptibility Testing. EUCAST Definitive Document E.Def 7.4. Method for the determination of broth dilution minimum inhibitory concentrations of antifungal agents for yeasts. October 2023 [cited 2024 Mar 20]. https://www.eucast.org/fileadmin/src/media/PDFs/EUCAST_files/AFST/Files/EUCAST_E.Def_7.4_Yeast_definitive_revised_2023.pdf
22. Robinson JT, Thorvaldsdóttir H, Winckler W, Guttman M, Lander ES, Getz G, et al. Integrative genomics viewer. Nat Biotechnol. 2011;29:24–6. https://doi.org/10.1038/nbt.1754
23. Abbey DA, Funt J, Lurie-Weinberger MN, Thompson DA, Regev A, Myers CL, et al. YMAP: a pipeline for visualization of copy number variation and loss of heterozygosity in eukaryotic pathogens. Genome Med. 2014;6:100. https://doi.org/10.1186/s13073-014-0100-8
24. Arentshorst M, Ram AF, Meyer V. Using non-homologous end-joining-deficient strains for functional gene analyses in filamentous fungi. Methods Mol Biol. 2012;835:133–50. https://doi.org/10.1007/978-1-61779-501-5_9
25. Dodgson AR, Dodgson KJ, Pujol C, Pfaller MA, Soll DR. Clade-specific flucytosine resistance is due to a single nucleotide change in the *FUR1* gene of *Candida albicans*. Antimicrob Agents Chemother. 2004;48:2223–7. https://doi.org/10.1128/AAC.48.6.2223-2227.2004
26. Nerson D, De Closets F, Dupouy-Camet J, Kures L, Marjollet M, Poirot J, et al. Antifungal susceptibility of yeasts (and a few filamentous fungi) by a standardized micromethod [in French]. Bulletin de la Société Francaise de Mycologie Médicale. 1987;16:395–8.
27. Law D, Moore CB, Joseph LA, Keaney MG, Denning DW. High incidence of antifungal drug resistance in *Candida tropicalis*. Int J Antimicrob Agents. 1996;7:241–5. https://doi.org/10.1016/S0924-8579(96)00328-7
28. Barchiesi F, Arzeni D, Caselli F, Scalise G. Primary resistance to flucytosine among clinical isolates of *Candida* spp. J Antimicrob Chemother. 2000;45:408–9. https://doi.org/10.1093/jac/45.3.408
29. Cuenca-Estrella M, Díaz-Guerra TM, Mellado E, Rodríguez-Tudela JL. Flucytosine primary resistance in *Candida* species and *Cryptococcus neoformans*. Eur J Clin Microbiol Infect Dis. 2001;20:276–9. https://doi.org/10.1007/PL00011265
30. Alexander BD, Byrne TC, Smith KL, Hanson KE, Anstrom KJ, Perfect JR, et al. Comparative evaluation of Etest and sensititre yeastone panels against the Clinical and Laboratory Standards Institute M27-A2 reference broth microdilution method for testing *Candida* susceptibility to seven antifungal agents. J Clin Microbiol. 2007;45:698–706. https://doi.org/10.1128/JCM.01840-06
31. Quindós G, Ruesga MT, Martín-Mazuelos E, Salesa R, Alonso-Vargas R, Carrillo-Muñoz AJ, et al. In-vitro activity of 5-fluorocytosine against 1,021 Spanish clinical isolates of *Candida* and other medically important yeasts. Rev Iberoam Micol. 2004;21:63–9.

32. Takakura S, Fujihara N, Saito T, Kudo T, Iinuma Y, Ichiyama S. National surveillance of species distribution in blood isolates of *Candida* species in Japan and their susceptibility to six antifungal agents including voriconazole and micafungin. J Antimicrob Chemother. 2004;53:283–9. https://doi.org/10.1093/jac/dkh053
33. Fleck R, Dietz A, Hof H. In vitro susceptibility of *Candida* species to five antifungal agents in a German university hospital assessed by the reference broth microdilution method and Etest. J Antimicrob Chemother. 2007;59:767–71. https://doi.org/10.1093/jac/dkl555
34. Chen YN, Lo HJ, Wu CC, Ko HC, Chang TP, Yang YL. Loss of heterozygosity of *FCY2* leading to the development of flucytosine resistance in *Candida tropicalis*. Antimicrob Agents Chemother. 2011;55:2506–14. https://doi.org/10.1128/AAC.01777-10
35. Lockhart SR, Bolden CB, Iqbal N, Kuykendall RJ. Validation of 24-hour flucytosine MIC determination by comparison with 48-hour determination by the Clinical and Laboratory Standards Institute M27-A3 broth microdilution reference method. J Clin Microbiol. 2011;49:4322–5. https://doi.org/10.1128/JCM.05479-11
36. Jung SI, Shin JH, Choi HJ, Ju MY, Kim SH, Lee WG, et al.; Korean Study Group for Candidemia. Antifungal susceptibility to amphotericin B, fluconazole, voriconazole, and flucytosine in *Candida* bloodstream isolates from 15 tertiary hospitals in Korea. Ann Lab Med. 2012;32:426–8. https://doi.org/10.3343/alm.2012.32.6.426
37. Messer SA, Jones RN, Moet GJ, Kirby JT, Castanheira M. Potency of anidulafungin compared to nine other antifungal agents tested against *Candida* spp., *Cryptococcus* spp., and *Aspergillus* spp.: results from the global SENTRY Antimicrobial Surveillance Program (2008). J Clin Microbiol. 2010;48:2984–7. https://doi.org/10.1128/JCM.00328-10
38. Clinical and Laboratory Standards Institute. Reference method for broth dilution antifungal susceptibility testing of yeasts, 4th edition (M27). Wayne (PA): The Institute; 2017.
39. Tavanti A, Davidson AD, Johnson EM, Maiden MC, Shaw DJ, Gow NA, et al. Multilocus sequence typing for differentiation of strains of *Candida tropicalis*. J Clin Microbiol. 2005;43:5593–600. https://doi.org/10.1128/JCM.43.11.5593-5600.2005
40. Abou-Chakra N, Astvad KMT, Martinussen J, Munksgaard ASE, Arendrup MC. Exponential clonal expansion of 5-fluorocytosine–resistant *C. tropicalis* and new insights into underlying molecular mechanisms. Emerg Infect Dis. 2025;31:977–85. PubMed https://doi.org/10.3201/eid3105.241910
41. Szarvas J, Rebelo AR, Bortolaia V, Leekitcharoenphon P, Schrøder Hansen D, Nielsen HL, et al. Danish whole-genome-sequenced *Candida albicans* and *Candida glabrata* samples fit into globally prevalent clades. J Fungi (Basel). 2021;7:962. https://doi.org/10.3390/jof7110962
42. Fan X, Dai RC, Zhang S, Geng YY, Kang M, Guo DW, et al. Tandem gene duplications contributed to high-level azole resistance in a rapidly expanding *Candida tropicalis* population. Nat Commun. 2023;14:8369. https://doi.org/10.1038/s41467-023-43380-2
43. O'Brien CE, Oliveira-Pacheco J, Ó Cinnéide E, Haase MAB, Hittinger CT, Rogers TR, et al. Population genomics of the pathogenic yeast *Candida tropicalis* identifies hybrid isolates in environmental samples. PLoS Pathog. 2021;17:e1009138. https://doi.org/10.1371/journal.ppat.1009138
44. Tulyaprawat O, Pharkjaksu S, Chongtrakool P, Ngamskulrungroj P. An association of an eBURST group with triazole resistance of *Candida tropicalis* blood isolates. Front Microbiol. 2020;11:934. https://doi.org/10.3389/fmicb.2020.00934
45. Megri Y, Arastehfar A, Boekhout T, Daneshnia F, Hörtnagl C, Sartori B, et al. *Candida tropicalis* is the most prevalent yeast species causing candidemia in Algeria: the urgent need for antifungal stewardship and infection control measures. Antimicrob Resist Infect Control. 2020;9:50. https://doi.org/10.1186/s13756-020-00710-z

Address for correspondence: Jochem B. Buil, Department of Medical Microbiology, Radboud University Medical Center, Geert grooteplein zuid 10, 6525 GA, Nijmegen, the Netherlands; email: jochem.buil@radboudumc.nl

Peromyscus spp. Deer Mice as Rodent Model of Acute Leptospirosis

Ellie J. Putz, Claire B. Andreasen, Paola Boggiatto, Mitchell V. Palmer, Luis G.V. Fernandes, Bienvenido W. Tibbs-Cortes, Judith A. Stasko, Camila Hamond, Steven C. Olsen, Jarlath E. Nally

Leptospirosis is a global zoonotic disease affecting humans, wildlife, companion, and domestic animals. Incidental hosts can contract the disease directly or indirectly from asymptomatic reservoir hosts, most commonly small rodents. The Golden Syrian hamster is recognized as the dominant rodent model for acute leptospirosis because the animals are susceptible to many serovars and are used to maintain laboratory strains and test bacterin vaccine efficacy. However, hamsters are primarily used in survival-based studies, and investigations into host immune response and disease pathogenesis are limited. We found that *Peromyscus leucopus* white-footed deer mice are susceptible to acute leptospirosis, and thus might be an alternative rodent model. Furthermore, similar to hamsters, deer mice produce circulating foamy macrophages in response to *Leptospira* challenge. Deer mice exhibit differences in response to different serovars, clinical disease severity, kidney and liver lesions, and an overall sex effect, with male mice demonstrating more severe clinical signs and higher bacterial burden.

Leptospirosis is a global zoonosis causing severe disease in humans, domestic animals, and wildlife (*1*). In cattle and most livestock species, leptospirosis causes abortions and reproductive losses, resulting in serious veterinary health and economic concerns for producers (*2*,*3*). Commercial vaccines are available but are not cross-protective across *Leptospira* serogroups. Because of the range in clinical sign severity and the fastidious nature of culturing the pathogen, leptospirosis diagnosis can be challenging, and the disease is consistently underrecognized by clinicians. *Leptospira* spp. bacteria colonize the kidneys and are typically shed by reservoir hosts in their urine, where they are transmitted from the environment to incidental hosts (*4*). The primary reservoir hosts are members of the rodent family. Infected mice and rats are largely asymptomatic, and cohabitation in field environments, barns, and dwellings presents ample opportunity to foster transmission to humans and domestic animals.

The small animal models used to study acute leptospirosis are hamsters, guinea pigs, and gerbils (*5*–*7*). Although vaccines exist for many domestic species, commercial bacterins require validation before release. For those purposes, Golden Syrian hamsters (*Mesocricetus auratus*) are widely considered the standard model for leptospirosis research (*8*). Unlike most wildlife rodents, hamsters demonstrate acute and typically fatal signs of infection when challenged, although severity of disease can vary among *Leptospira* serovars, species, and strains (*9*–*11*). Hamsters are used to passage laboratory strains for research purposes, such as tests or the recovery of virulence (*8*). Similarly, hamsters are used in survival studies to test commercial bacterin vaccines (as required by the US Department of Agriculture), regardless of the intended host species (*12*). Although the research community relies heavily on the hamster model, it has notable limitations. They are mostly used for survival metrics instead of disease mechanism or immunology–based studies and suffer from a lack of reagents (such as markers of immune cell types) and resources (such as genomic/proteomic databases). Further, hamsters are largely not found in the wild and thus do not accurately model naturally occurring leptospirosis transmission.

Peromyscus mice, commonly known as deer mice, are phylogenetically more similar to hamsters in the Cricetidae family than are the classic Muridae *Mus musculus* mice (*13*,*14*). Wild deer mice, including a variety of subspecies (one of the most abundant being *P. leucopus* white-footed deer mice), are found in parts of North America and are used for bacterial and viral disease research, including research into Lyme

Author affiliations: National Animal Disease Center, US Department of Agriculture Agricultural Research Service, Ames, Iowa, USA (E.J. Putz, P. Boggiatto, M.V. Palmer, L.G.V. Fernandes, B.W. Tibbs-Cortes, J.A. Stasko, S.C. Olsen, J.E. Nally); Iowa State University College of Veterinary Medicine, Ames (C.B. Andreasen); National Veterinary Services Laboratories, US Department of Agriculture Animal and Plant Health Inspection Service, Ames (C. Hamond)

DOI: https://doi.org/10.3201/eid3107.241579

disease, anaplasmosis, hantavirus (*P. maniculatus* mice), and viral encephalitis (*15*,*16*). For many of those diseases, deer mice serve as reservoir hosts and play crucial roles in tickborne disease life cycles and transmission kinetics, where they are characterized by a lack of clinical signs and reduced inflammatory immunological responses (*16*,*17*). Some aspects of the transmission and movement of strains of *Leptospira* from wildlife to livestock are unknown, and deer mice might serve as a potential environmental wildlife reservoir similar to other documented rodent hosts (*18*).

Our group strives to improve tools and metrics to assess immunological responses in rodent models that are key for leptospirosis research. Previously, we established that hamsters produce circulating foamy macrophages in response to *Leptospira* and bacillus Calmette-Guérin challenge, and the presence of those cell populations is correlated with disease severity (*11*,*19*,*20*). Foamy macrophages are best known for their characteristic appearance in the tissue of granulomas caused by *Mycobacterium tuberculosis* complex but are not typically found in circulation. Foamy macrophage vacuoles contain defined lipid droplets, but unlike the foamy macrophages that contain mycobacteria in tuberculous granulomas, those cells do not appear to contain leptospires in the challenged hamster model (*11*,*21*). In this study, we sought to assess the suitability of *Peromyscus* spp. mice as an alternative rodent model of leptospirosis.

Materials and Methods

Animals

We obtained *P. leucopus* deer mice 6–13 weeks of age from the LL stock *Peromyscus* Genetic Stock Center at the University of South Carolina (Columbia, SC, USA). All procedures and experiments were approved by the National Animal Disease Center Animal Care and Use Committee. Deer mice were monitored daily for health evaluation and had ad libitum access to food and water.

Experimental Design

This work includes data from 3 independent experiments. *Leptospira borgpetersenii* serogroup Ballum serovar Arborea strain LR131 and *L. interrogans* serogroup Canicola serovar Canicola strain LAD1 were propagated at 29°C in HAN media (*22*). Animals were challenged by intraperitoneal injection with 0.5 mL containing 1×10^7 leptospires (LR131 or LAD1) or 0.5 mL HAN media alone. Noninjection (negative) male and female control mice were used for nontreatment comparisons.

We monitored deer mice daily for clinical signs including lethargy; blood in urine; blood from nose, urogenital tract, or on paws; or lack of grooming/hygiene. We euthanized animals at the appearance of severe clinical signs such as blood from nose, paws, or urogenital tract or extreme lethargy (monitored by response to a human handler). We collected whole blood smears, kidney and liver samples for culture and quantitative PCR (qPCR) and tissues for histopathologic examination (spleen, lung, heart, kidney, liver, pancreas, and omental adipose).

Because severe clinical signs developed in male and female mice at different timepoints, we harvested control animals of the opposite sex as necessary. In a subset of female mice challenged with *L. interrogans* strain LAD1, acute signs of disease did not develop; we euthanized those mice ≈3 weeks postchallenge.

Culture and qPCR

For all challenged animals, we harvested a kidney or section of liver and macerated the specimen in 5 mL of HAN media containing 5-fluorouracil (100 μg/μL) for *Leptospira* culture. We used numerous dilutions of macerated suspensions to inoculate HAN media plus 5-fluorouracil as described previously (*22*) and incubated at 37°C in 5% CO_2 (*23*). We determined bacterial burden of liver and kidney by using genomic *lipL32* qPCR as previously reported (*19*).

Blood and Tissue Processing and Evaluation

We collected blood smear slides using the feathered edge technique, stained them with Giemsa solution, and evaluated them by microscopy. We performed a 100-cell differential count classifying the number of neutrophils, lymphocytes, monocytes, foamy macrophages, and combined eosinophils and basophils.

We took tissue samples of similar size and section for all groups from liver, kidney, spleen, lung, heart, and omental adipose tissue. We collected tissues into formalin and transferred to 70% ethanol after 24 hours. We used standard paraffin-embedding techniques to further process the fixed samples. We transferred cut paraffin-embedded tissues sections (4-μm-thick sections) to Superfrost Plus charged microscope slides (Thermo Fisher Scientific, https://www.thermofisher.com), after which we stained them with hematoxylin and eosin. We evaluated histologic sections by light microscopy using an Olympus B41 microscope and DP 23 Olympus camera and captured images with cellSens Olympus software (Evident Scientific, https://evidentscientific.com).

We performed immunohistochemistry with the Ventana Ultra Discovery on representative formalin-fixed, paraffin-embedded tissue sections 4 μm

thick. We deparaffinized sections in Discovery Wash (Roche, https://www.roche.com) and achieved antigen retrieval by incubation with cell-conditioning solution 1, a citrate-based buffer (pH 6.0). We performed a blocking step with Discovery Goat Ig Block (Roche) for 20 minutes at 35°C. We incubated sections for 32 minutes at 35°C with primary antibody against LipL32 at 1:100 dilution in Discovery antibody diluent (Roche). The signal was detected with rabbit Dako EnVision-HRP system (Agilent, https://www.agilent.com) for 32 minutes at 35°C and visualized with 3,3′-diaminobenzidine (Roche). We counterstained the sections with Harris Hematoxylin (Leica Biosystems, https://www.leicabiosystems.com).

Statistics

We evaluated stained whole-blood smear cell counts (cell numbers/100 leukocytes) using simple linear regression models in R version 4.1.0 (The R Project for Statistical Computing, https://www.r-project.org). We evaluated each cell type independently (lymphocytes, neutrophils, monocytes, foamy macrophages, and combined eosinophils and basophils). For bacterial burden data, we evaluated genomic *lipL32* qPCR independently between kidney and liver. For all, each group was fit as a fixed effect detailing male mice with acute disease, female mice with acute disease, and time-matched nonclinical control female mice (showing no signs of disease) taken when acute male mice reached endpoint. We included 2 control groups, media alone and noninjection negative controls. We evaluated specific contrasts within cell types with pairwise contrasts. We determined significance by a p value of $\leq$0.05; error bars represent SEs. We analyzed Spearman correlations in R between foamy macrophage counts and bacterial burden of liver and kidney across all deer mice.

Results

We challenged acclimated male and female *Peromyscus* spp. deer mice with *L. interrogans* serogroup Canicola serovar Canicola (strain LAD1) and *L. borgpetersenii* serogroup Ballum serovar Arborea (strain LR131) and evaluated both media alone and noninjection controls. Deer mice showed severe clinical signs of disease within the first week postchallenge, establishing them as an alternative rodent model of acute leptospirosis (Figure 1). Although both *L. borgpetersenii* and *L. interrogans* strains caused acute disease, endpoint separation between male and female mice is striking and demonstrates that male mice were more susceptible than female mice to both LR131 and LAD1 ($p \leq 0.01$ between sexes for both) (Figure 1). Because male mice were more susceptible, we also evaluated a control group of nonclinical female mice not displaying severe signs of disease but euthanized at the same time as acutely ill male mice.

Previously, our group described the unique production of circulating foamy macrophages by hamsters challenged with *Leptospira* (*11*), a feature not replicated in experimentally infected laboratory mice, guinea pigs, or rats (E. Putz et al., unpub. data). By examining Giemsa-stained slides of whole blood smears, we identified circulating foamy macrophages, consistent with those described in hamsters, in deer mice (Table; Figure 2). Intracellular lipid droplets are defining features of foamy macrophages. We confirmed the presence of those lipids with microscopy techniques including Oil Red O staining (Figure 3) and transmission electron microscopy (Figure 4). Similar to findings in the hamster model, no leptospires were detectable within foamy macrophages by transmission electron microscopy (*24*). Additional hematologic findings included neutrophilia and lymphopenia (Table).

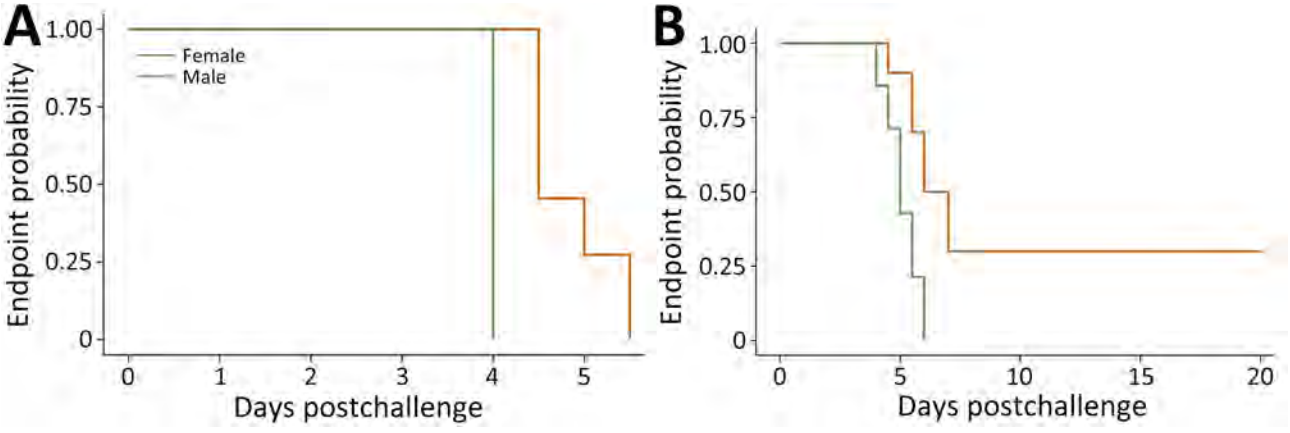

Figure 1. Endpoint and survival curves for *Peromyscus* deer mice experimentally infected with *Leptospira* in study of the species as rodent model of acute leptospirosis. Graphs indicate survival curves for severely diseased female and male deer mice infected with *Leptospira borgpetersenii* strain LR131 (A) and *L. interrogans* strain LAD1 (B). p value $\leq$0.01 between sexes for both LR131- and LAD1-infected animals.

Table. Manual differential cell counts on Giemsa-stained whole blood smears in study of *Peromyscus* species deer mice as rodent model of acute leptospirosis*

Group	Cells/100 leukocytes				
	Foamy macrophages	Monocytes	Neutrophils	Lymphocytes	Eosinophils and basophils
LR131 female	3.75 ± 1.25†	3.08 ± 0.54†	34.00 ± 3.12†	58.2 ± 3.40†	0.92 ± 0.48
LR131 male	7.63 ± 1.53†	4.13 ± 0.66†	36.62 ± 3.82†	50.4 ± 4.17†	0.88 ± 0.59
LR131 nonclinical female	0.33 ± 2.50	1.33 ± 1.07	47.33 ± 6.24†	49.7 ± 6.81†	1.33 ± 0.96
LAD1 female	1.70 ± 1.37	2.00 ± 0.59	24.00 ± 3.42	70.6 ± 3.73†	1.70 ± 0.53
LAD1 male	3.36 ± 1.16†	2.86 ± 0.50†	35.50 ± 2.89†	55.1 ± 3.15†	3.14 ± 0.45†
LAD1 nonclinical female	0.50 ± 2.17	1.75 ± 0.93	26.50 ± 5.41	68.2 ± 5.90†	2.75 ± 0.84†
HAN media	0.22 ± 0.90	1.04 ± 0.39	16.26 ± 2.26	81.6 ± 2.46	0.87 ± 0.35
Negative	0.00 ± 1.53	0.88 ± 0.66	8.38 ± 3.82	90.6 ± 4.17	0.13 ± 0.59

*Table shows the least square means of foamy macrophages, monocytes, neutrophils, lymphocytes, and combined eosinophils and basophils, with their respective SEs.
†Denotes a significant difference ($p \leq 0.05$) compared with HAN media controls.

Substantial populations of foamy macrophages were found in the blood of deer mice challenged with both *L. borgpetersenii* and *L. interrogans* (Figure 5). Control noninjected animals did not produce any foamy macrophages, but media alone controls had sparse production of an occasional foamy-filled cell, suggesting a possible immune response to HAN media. LAD1-challenged male mice produced significantly more foamy macrophages than did media alone ($p \leq 0.01$) and negative control ($p = 0.02$) animals. Male LAD1-infected deer mice also produced more foamy macrophages (3.36 ± 1.16/100 counted leukocytes) than did acute female (1.70 ± 1.37/100 counted leukocytes; $p = 0.22$) or control female counterparts (0.50 ± 2.17/100 counted leukocytes; $p = 0.12$), but differences were not significant (Figure 5, panel A). Differences among challenged groups were stronger for *L. borgpetersenii* LR131–infected animals, whereas male deer mice generated significantly greater numbers of foamy macrophages than did acute female ($p = 0.05$), nonclinical control female ($p = 0.01$), HAN media alone ($p \leq 0.01$), or negative control ($p \leq 0.01$) groups (Figure 5, panel B). Given that LR131-challenged deer mice reached endpoints more quickly than LAD1-challenged deer mice, foamy macrophage cell percentages appear to be associated with disease severity. This finding further corroborates the sex effect seen in this study; higher foamy macrophage proportions were found in male mice than in acutely diseased female mice (Figure 5).

No significant histologic findings were present in the HAN media only and negative control groups. Challenge groups for strain LR131 and strain LAD1 had variable and nonspecific changes in the spleen and lung. The spleen had variable lymphoid follicle expansion, which can result from antigenic stimulation, and extramedullary hematopoiesis. The lung had variable hemorrhage and congestion; some vessels contained neutrophils, attributed to the peripheral blood neutrophilia.

Both strains LR131 and LAD1 kidney-associated omental adipose tissue had hemorrhage and inflammatory cell infiltrates when associated with kidney inflammatory lesions. Cell infiltrates consisted of variable numbers of neutrophils, lymphocytes, macrophages, and suspected foamy macrophages (Figure 6). Some macrophages, or possible foamy macrophages, contained erythrocytes (Figure 6), also seen in the blood (Figure 2). Immunohistochemistry also confirmed the presence of leptospires within kidney adipose tissue (Appendix Figure, https://wwwnc.cdc.gov/EID/article/31/7/24-1579-App1.pdf).

Significant lesions of interest were present in the kidney and liver and varied between challenge strains; inflammatory lesions in the kidney were more severe and diffuse in a higher number of deer mice

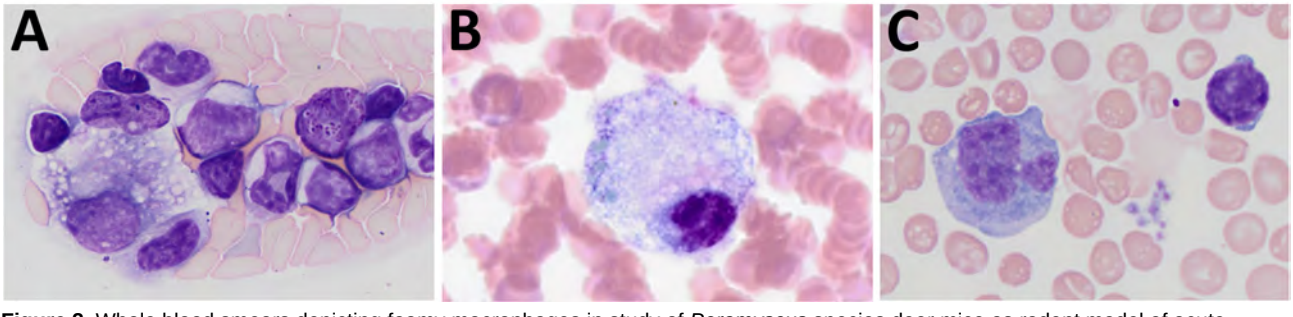

Figure 2. Whole blood smears depicting foamy macrophages in study of *Peromyscus* species deer mice as rodent model of acute leptospirosis. Representative blood smears containing foamy macrophages mice experimentally infected with *Leptospira borgpetersenii* strain LR131 (A), *L. interrogans* strain LAD1 (B), and noninfected control monocyte (C) are shown. Original magnification ×100.

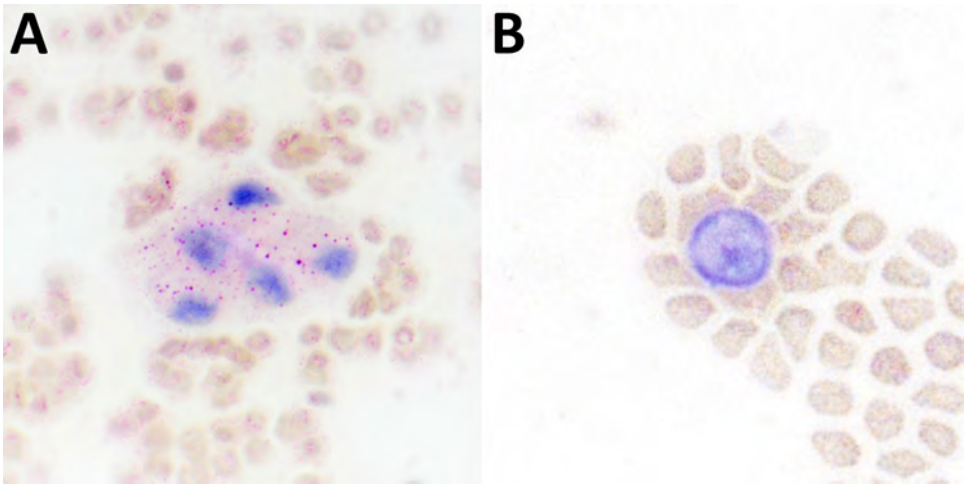

Figure 3. Microscopy presentation of lipid within foamy macrophages from infected mice in study of *Peromyscus* species deer mice as rodent model of acute leptospirosis. Representative Oil Red O-stained whole blood smears from a *Leptospira* infected animal (A) and a noninfected control (B) are shown. Original magnification ×20.

challenged with strain LR131 than those challenged with LAD1 (Figure 7). The LR131-challenged acute disease group had renal cortex intratubular neutrophils that extended into the medulla, tubular necrosis, interstitial neutrophilic nephritis, hemorrhage, and perivascular neutrophils and lymphocytes (Figure 7). The LAD1-challenged acute disease group had similar renal lesions, but they were less severe and diffuse, and hemorrhage and medullary inflammatory infiltrates were rare. Lesion severity differences were further supported by immunohistochemistry, which demonstrated a greater number of leptospires in LR131-infected mice (Figure 7).

In the histologic assessment of the liver, animals infected with strain LR131 had mild hepatic lesions consisting of intrasinusoidal neutrophils, possibly associated with peripheral neutrophils, and low numbers of occasional perivascular lymphocytes (Figure 8). This finding contrasted with the LAD1-challenged group, which had mild to severe diffuse liver lesions (Figure 8). The contrasting severity of lesions and density of leptospires differences were confirmed by immunohistochemistry (Figure 8). Milder lesions consisted of hepatocyte vacuolar change, hepatocyte swelling (cell edema), and a few areas of perivascular lymphocytic inflammation. Severe liver lesions consisted of hepatocyte dissociation and purulent hepatocyte necrosis that was multifocal to diffuse with a midzonal to centrilobular pattern, often bridging (Figure 8).

Culture was positive in liver and kidney samples from all challenged animals, and we quantified bacterial load by using genomic equivalent qPCR for *lipl32*. Bacterial loads were similar between challenges, but the highest levels of leptospires per gram were seen in the liver (Figure 9). For both *Leptospira* species–infected deer mice, bacterial load was higher in kidney and liver samples from male mice than in samples from acute female, nonclinical female, HAN media alone, and negative control groups (Figure 9, panels A, B) ($p \leq 0.01$). As seen previously in hamsters (*25*), between LAD1- and LR131-challenged female

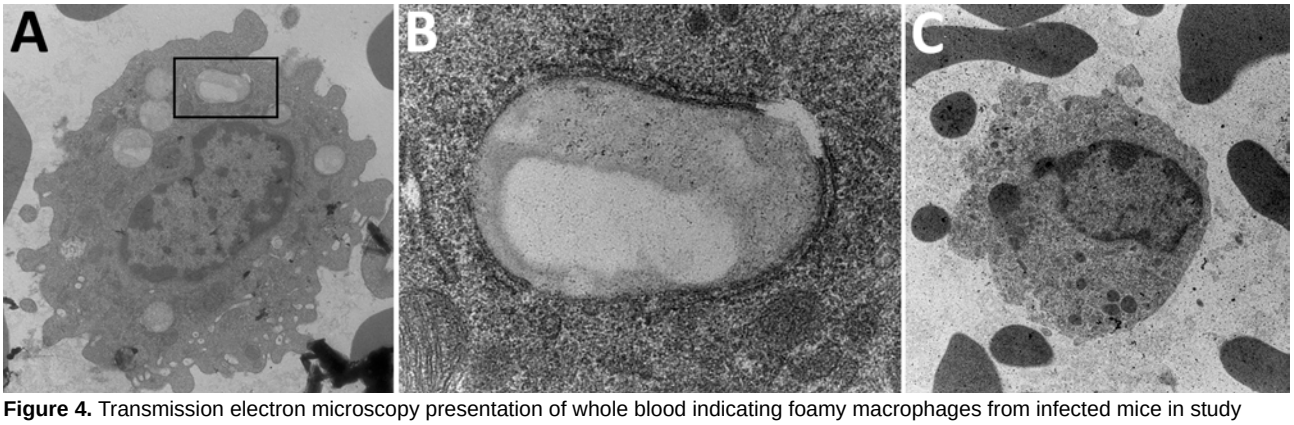

Figure 4. Transmission electron microscopy presentation of whole blood indicating foamy macrophages from infected mice in study of *Peromyscus* species deer mice as rodent model of acute leptospirosis. A) Image of foamy macrophages with membrane-bound lipid droplet in black box; original magnification ×6,800. B) Close-up of membrane-bound lipid droplet from box in panel A (original magnification ×49,000). C) Noninfected control monocyte (original magnification ×6,800).

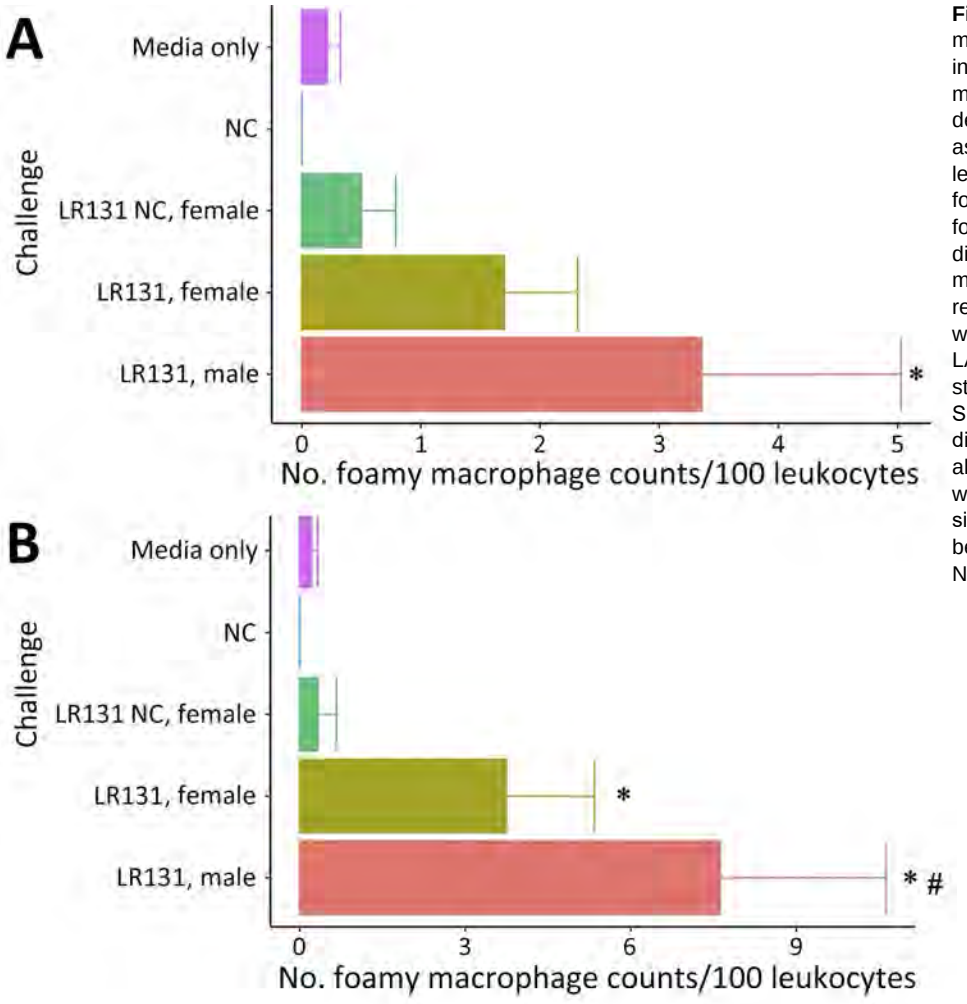

Figure 5. Concentrations of foamy macrophages per 100 leukocytes in whole blood smears from male and female *Peromyscus* deer mice in study of the species as rodent model of acute leptospirosis. Concentrations of foamy macrophages are shown for acute disease male, acute disease female, and NC female mice taken when acute male mice reached endpoint for challenge with *Leptospira interrogans* strain LAD1 (A) or *L. borgpetersenii* strain LR131 (B). Error bars depict SEs. Asterisk denotes a significant difference ($p \leq 0.05$) from media alone and negative control groups, whereas pound sign denotes a significant difference ($p \leq 0.05$) between male and female groups. NC, nonclinical.

mice, bacterial burdens were higher in both liver and kidney samples for *L. borgpetersenii* challenge than *L. interrogans* ($p \leq 0.01$). In contrast, bacterial load in male mice did not differ in kidney ($p = 0.56$) or liver ($p = 0.33$) specimens between challenge strains (Figure 9). Foamy macrophage percentages were significantly correlated with bacterial load of leptospires in liver and kidney specimens ($p \leq 0.01$), further demonstrating their association with virulence.

Discussion

Acute disease developed in *P. leucopus* deer mice in response to *Leptospira* challenge, offering an alternative acute rodent model to elucidate pathogenic mechanisms of leptospirosis. From an evolutionary standpoint, deer mice are more closely related to hamsters than to *M. musculus* mice (*13*,*14*). In addition to displaying severe clinical signs such as hematuria, blood on nose and foot pads, and lethargy, deer mice produced foamy macrophages in response to both *L. interrogans* and *L. borgpetersenii* challenge, which correlated with disease severity. Our group previously identified that hamsters produce circulating foamy macrophages in response to bacterial infection, but in our studies, those cells do not appear in mouse, guinea pig, or rat models of leptospirosis. Because circulating foamy macrophages are present in low numbers and can be unevenly distributed in blood smears, we found visual examination of the entire blood smear (versus a 100-cell count differential) was sometimes needed to detect foamy macrophages. Also, foamy macrophages can be missed if only automated analyzer evaluation is used for hematology analysis (with specific parameters flagged to require visual examination, as can occur in human medicine). This work suggests that circulating foamy macrophages might be limited to the Cricetidae family, but evaluation of additional rodent species, further investigation in *Peromyscus* subspecies, and review of blood smears from other species susceptible to leptospirosis would be necessary to confirm this unique finding.

Peromyscus spp. mice are commonly recognized as asymptomatic reservoir hosts, particularly for the Lyme disease bacteria *Borrelia burgdorferi*. Much work has been done exploring the reservoir host components and pathogen interactions between *Peromyscus* species and other rodents. Gene expression work suggests *Peromyscus* spp. mice respond differently than *M. musculus* mice to lipopolysaccharide challenge (*17*,*26*) and have altered immune cell interactions, such as largely inactive or altered immunoglobulin gamma Fc receptors (*27*). Previous work in deer mice has established that *Peromyscus* transcriptomic profiles are more aligned with M2 macrophage than M1 polarization in response to endotoxin (*26*) and are associated with alternatively activated monocytes (*17*). Specifically, deer mice showed a low inducible nitric oxide synthase 2 (Nos2), high arginase 1 (Arg1) expression ratio in response to lipopolysaccharide challenge (*28*), which is typically associated with a damage repair or antiinflammatory response. Such nonclassical activation profiles could contribute to the production of foamy macrophages, but the mechanism of circulating foamy macrophage formation and their functional capabilities are still unclear. Implications of foamy macrophages for host immune response and bacterial persistence are also of interest, because the acquisition of low-density lipoprotein cholesterol within foamy macrophage vacuoles is viewed as a nutrient source for pathogens (*29*). Of note, foamy macrophages have been tissue-associated with other infectious agents, such as *Chlamydia* spp. and *Toxoplasma* spp., so the association with foamy macrophages might not be leptospirosis-specific (*29*). However, *Leptospira* infection in hamsters, and now deer mice, is to our knowledge the only model to produce foamy macrophages in circulation. A small portion of foamy macrophages were produced in a minority of deer mice injected with HAN media absent of leptospires. Although the mechanism behind foamy macrophage formation remains unknown in the context of leptospirosis, HAN media is rich in fatty acids and nutrients (*22*), and some level of immune activation from the intraperitoneal challenge could conceivably have resulted in rare circulating foamy macrophages.

In cases of human leptospirosis, primary kidney lesions of acute tubular necrosis and acute interstitial nephritis are observed, which were also seen in deer mice histology. Both LR131- and LAD1-challenged deer mice had acute nephritis, primarily affecting the renal tubules and with more severe lesions in LR131-challenged tissues. Renal failure might have resulted in the LR131-infected animals reaching severe endpoints before their LAD1-infected counterparts. On histologic sections, suspected foamy macrophages in challenged deer mice were only associated with renal omentum. When conducting hematoxylin and eosin staining on deer mice samples in this study, identifying foamy macrophages was more complex than in hamsters because the clear round vacuoles associated with lipid content were also associated with smaller foamy diffuse vacuoles and, sometimes, erythrophagocytosis. Histologic findings of foamy macrophages, macrophages with cytoplasmic vacuoles, and the erythrophagocytosis in either macrophages or foamy macrophage tended to overlap. Collectively, this finding suggests that foamy macrophages might phagocytose erythrocytes (*30*).

Human leptospirosis patients who experience Weil's syndrome have a high mortality rate (≈10%)

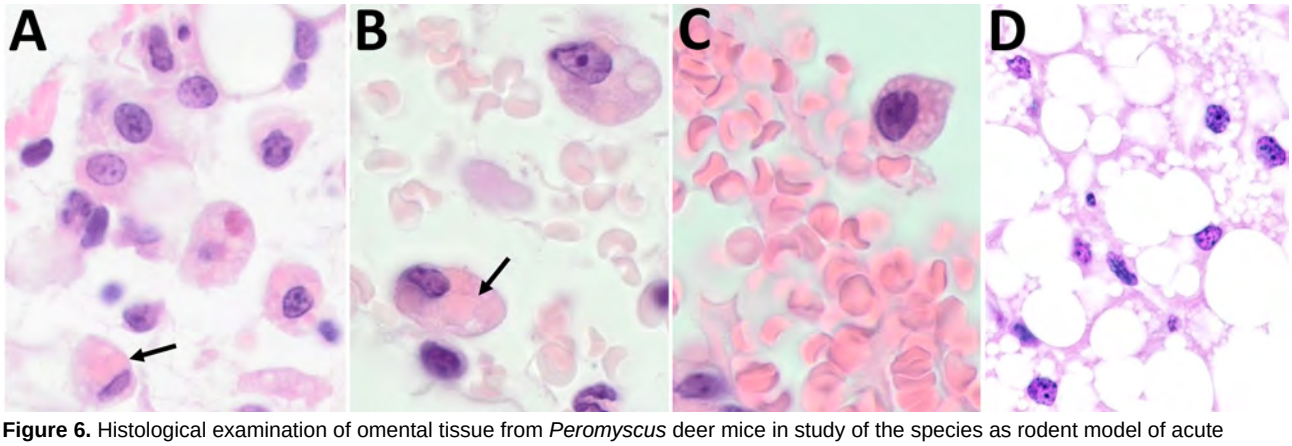

Figure 6. Histological examination of omental tissue from *Peromyscus* deer mice in study of the species as rodent model of acute leptospirosis. A) *Leptospira borgpetersenii* strain LR131–challenged deer mouse (original magnification ×40); B) foamy macrophages with intracytoplasmic erythrocytes and clear lipid vacuoles in sample taken from LR131-challenged deer mouse (original magnification ×100); C) foamy macrophage within vessel lumen and foamy macrophage, also present in peripheral blood *L. interrogans* strain LAD1–challenged deer mouse (original magnification ×100); D) omentum sample from noninfected deer mouse (original magnification ×40). Black arrows indicate possible foamy macrophages/macrophages with intracytoplasmic erythrocytes (erythrophagocytosis).

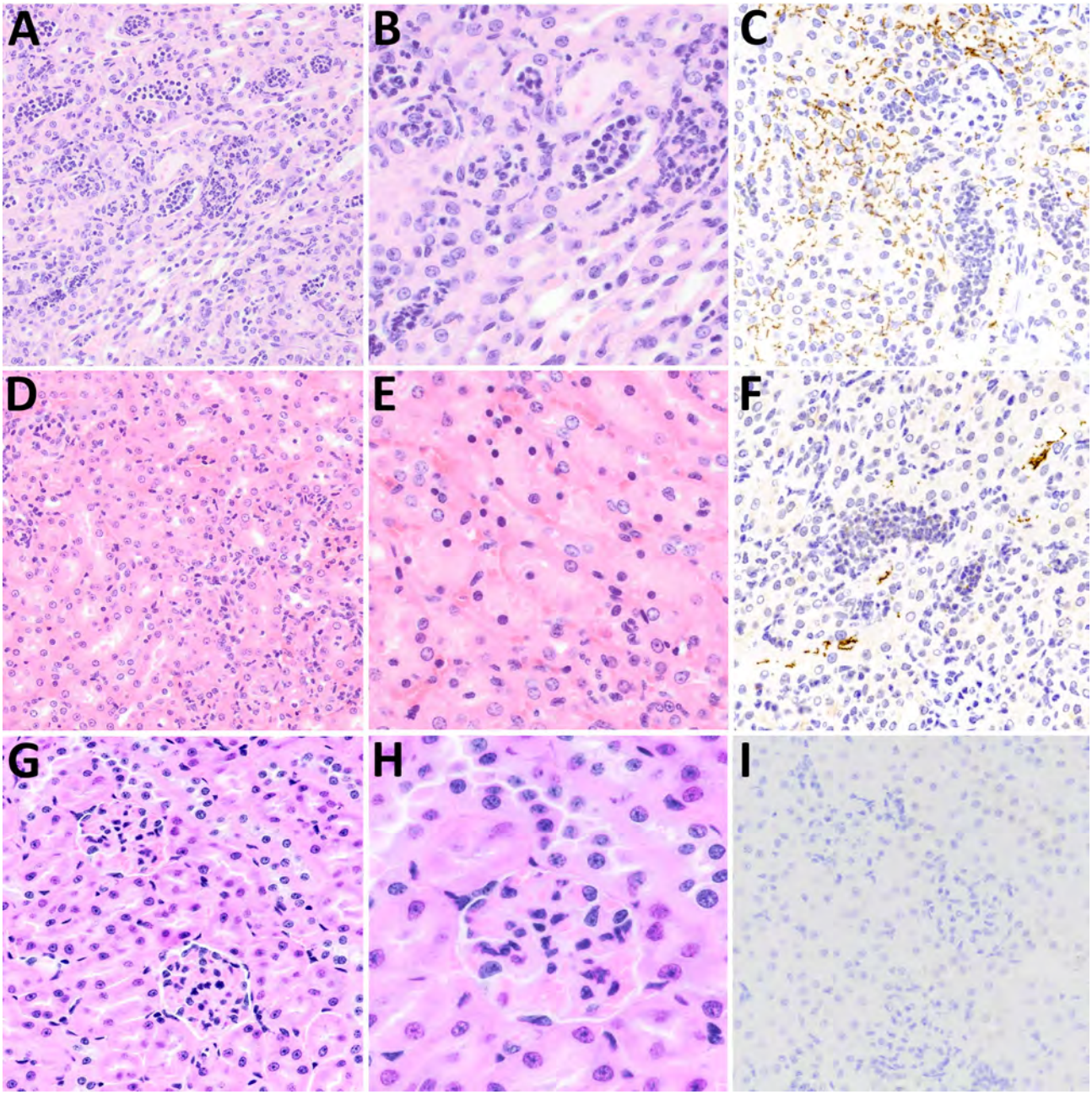

Figure 7. Microscopic and immunohistochemical examination of kidney samples taken from challenged and control deer mice in study of *Peromyscus* species deer mice as rodent model of acute leptospirosis. A–C) Samples taken from LR131-challenged deer mice showing acute diffuse purulent nephritis and nephrosis. The renal cortex and medulla appeared similar with severe diffuse intratubular neutrophilic inflammation, loss and necrosis of tubular lining cells, and resulting nephrosis. Intertubular neutrophilic infiltrates in the interstitium and some neutrophilic glomerular infiltrates (not common) were present. There were scattered areas of hemorrhage (not pictured). A, B) Hematoxylin and eosin–stained tissue (A, original magnification ×20; B, original magnification ×40); C) LipL32 immunohistochemistry-labeled kidney (original magnification ×20). D–F) Samples taken from LAD1-challenged deer mice showing most severe renal lesion associated with LAD1. Examination showed acute multifocal purulent nephritis and nephrosis with lymphocytic and slightly purulent interstitial nephritis. The renal cortex contained multifocal intratubular neutrophilic inflammation, loss and necrosis of tubular lining cells with the accumulation of eosinophilic material and resulting nephrosis. Intertubular lymphocytes and fewer neutrophils were scattered in the interstitium. D, E) Hematoxylin and eosin–stained tissue (D, original magnification ×20; E, original magnification ×40); F) LipL32 immunohistochemistry-labeled kidney (original magnification ×20). G–I) Sample of noninfected control animal kidney. G) Hematoxylin and eosin–stained tissue (G, original magnification ×20; H, original magnification ×40); I) LipL32 immunohistochemistry negative (original magnification ×20).

because of renal and hepatic failure (*31*) associated with direct damage of hepatocytes and Kupffer cells (*32*,*33*). LAD1-challenged deer mice had lesions that ranged from mild hepatocyte swelling (cell edema) with vacuolar hepatopathy, often in a centrilobular pattern, to severe necrotizing hepatitis with a

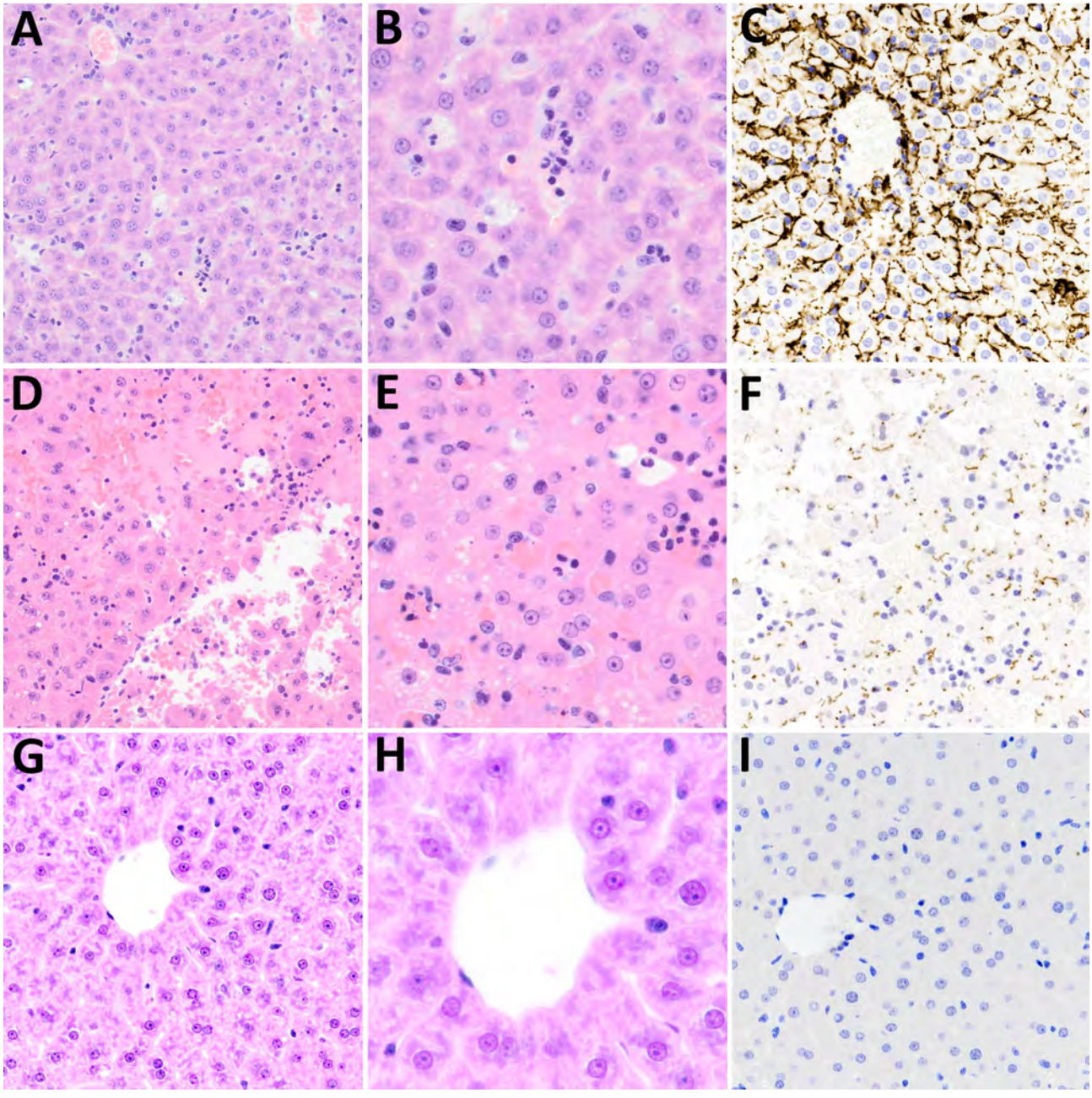

Figure 8. Microscopic and immunohistochemical examination of liver samples from challenged and control deer mice in study of *Peromyscus* species deer mice as rodent model of acute leptospirosis. A–C) Samples from LR131-challenged deer mice showing minimal change and intravascular neutrophils. The liver had intact architecture, minimal hepatocyte change, and some areas of vascular intrasinusoidal neutrophils. The presence of neutrophils may represent peripheral blood versus recruitment to the liver. A) Hematoxylin and eosin–stained tissue (A, original magnification ×20; B, original magnification ×40); (C) LipL32 immunohistochemistry-labeled liver (original magnification ×20). D–F) Samples from LAD1-challenged deer mice showing acute diffuse purulent hepatitis and necrosis. There was marked disruption of hepatic architecture with hepatocyte dissociation, diffuse neutrophilic (purulent) inflammation, and hepatocyte necrosis. Necrosis of hepatocytes resulted in confluent midzonal and centrilobular necrosis, sometimes bridging, with hemorrhage. The necrosis resulted in tissue fragility. D) Hematoxylin and eosin–stained tissue (A, original magnification ×20; B, original magnification ×40); F) LipL32 immunohistochemistry-labeled liver (original magnification ×20). G–I) Sample of noninfected control animal liver. G) Hematoxylin and eosin–stained tissue (A, original magnification ×20; B, original magnification ×40); I) LipL32 immunohistochemistry negative (original magnification ×20).

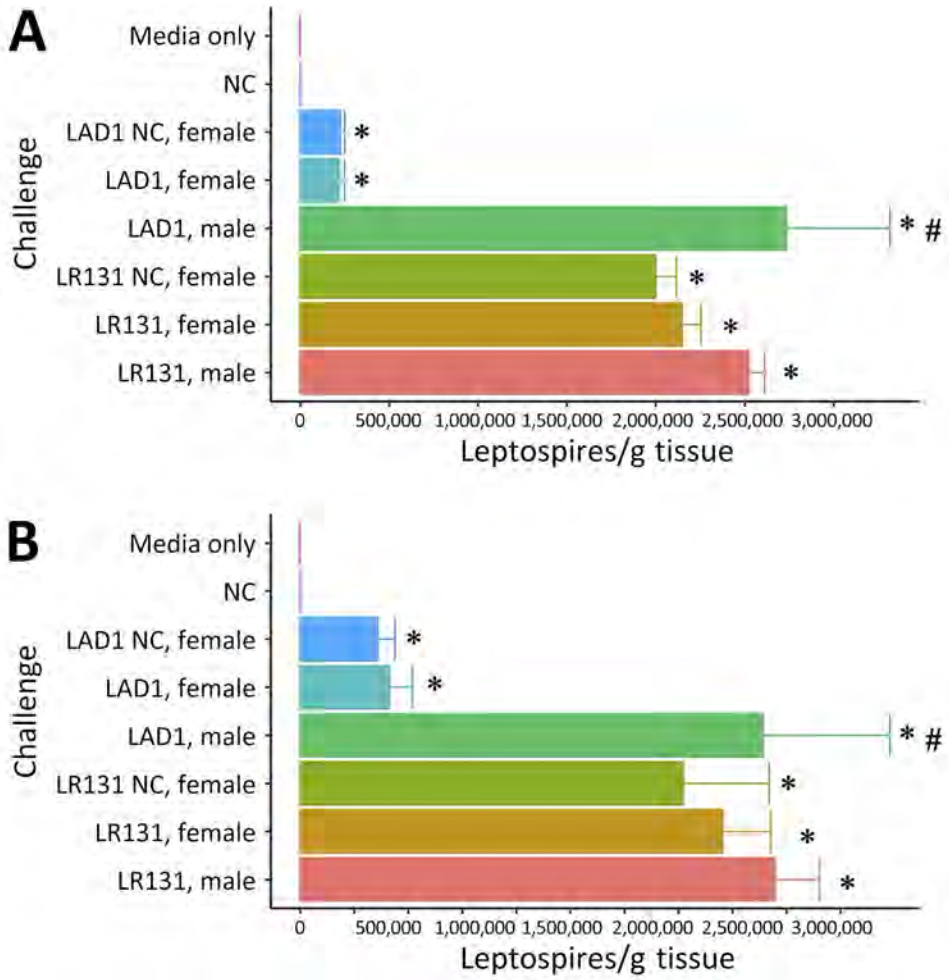

Figure 9. Genomic equivalent burden of calculated leptospires per gram of tissue between male and female *Peromyscus* deer mice in study of the species as rodent model of acute leptospirosis. Graphs show the PCR-calculated bacterial load in infected kidneys (A) and livers (B) from deer mice infected with strain LR131 *Leptospira borgpetersenii* or strain LAD1 *L. interrogans*, HAN media alone, and noninfected negative control. Groups shown consist of acute disease male mice, acute disease female mice, and NC female mice taken when acute male mice reached endpoint. Error bars depict SEs. Asterisk denotes a significant difference ($p \leq 0.05$) from media alone and negative control groups, whereas pound sign denotes a significant difference ($p \leq 0.05$) between male and female groups. NC, nonclinical.

midzonal to centrilobular pattern. The milder lesions of hepatocyte vacuolar change and cell swelling are not specific and appeared more consistent with the foamy cytoplasm of hydropic degeneration that can result from hypoxia, anorexia, or altered metabolic or nutritional states. Alternatively, those lesions might precede the more advanced necrotizing hepatitis, considering clinical signs ranged from absent to mild in the LAD1-challenged deer mice with milder hepatic lesions.

Bacterial burden data illustrate high pathogen loads in major organs of interest; the highest burden of leptospires per gram was found in liver tissue, not kidney tissue (Figure 9). That finding is consistent with pathogenesis tracking of acutely ill hamsters challenged with *L. interrogans*, where heavy dissemination to immune responsive organs is apparent (*34*). Over time in nonfatal conditions, host immune responses control leptospires in most systems, whereas persistent colonization of the kidneys enables persistent shedding. Most notable differences in burden data are reflected in the significantly reduced bacterial load in female LAD1-challenged animals and female controls (Figure 9). That finding supports the sex effect differences reported but also suggests that reduced disease severity in those animals is associated with reduced leptospire presence in liver and kidneys. Although unsurprising, the same was not true of LR131-challenged female mice and female controls, suggesting *L. interrogans* and *L. borgpetersenii* pathogenesis and interactions with host sex could be different. Although a *Leptospira* dose response was not evaluated in this study, follow-up research with the concurrent investigation of alternative routes of inoculum administration, such as conjunctival challenge, could be warranted.

Sex effects are associated with leptospirosis in humans and animals, including hamsters, and consistently favor more severe disease in male infectees (*35*–*37*). We found the same; male deer mice succumbed more quickly to severe disease endpoints (Figure 1), produced more circulating foamy macrophages (Figure 5), and harbored higher bacterial burdens in kid-

ney and liver samples (Figure 9). Of note, *Borrelia* infection studies in *P. leucopus* mice show no difference between male and female littermates (*28*), but other work illustrates older male deer mice caught in the wild were more likely to harbor tick infestation (*38*). The mechanism of the leptospirosis sex effect is still unknown, but work with hamsters in leishmaniasis showed that treating female hamsters with testosterone increased the size of lesions (*39*), suggesting androgens might play a role in pathogenesis. In other rodent models of bacterial disease with sex effects, sex differences of *Listeria monocytogenes* in mice (more resistance in males) found that more severe disease was associated with increased levels of interleukin-10 (IL-10), and IL-10 knockout mice showed no differences between sexes (*40*). Of additional relevance, M2 macrophages can secrete IL-10, illustrating another immune component that should be investigated in the deer mouse model of leptospirosis.

In conclusion, our results demonstrate that deer mice are susceptible to acute leptospirosis. Ultimately, an alternative rodent model for acute disease is valuable. Unlike hamsters, deer mice are found readily in the wild; additional field work should survey leptospirosis prevalence among those populations. The role of circulating foamy macrophages in the pathogenesis of leptospirosis is yet to be elucidated but currently appears limited to the Cricetidae family. Collectively, this work demonstrates that deer mice represent a possible real-world host that could enable further modeling of transmission kinetics and pathogenesis of leptospirosis.

Acknowledgments

We extend our immense appreciation to Denise Chapman, Jean Kaptur, and the National Animal Disease Center vivarium animal care staff for the care and handling of animals.

Mention of trade names or commercial products in this article is solely for the purpose of providing specific information and does not imply recommendations or endorsement by the US Department of Agriculture (USDA). USDA is an equal opportunity provider and employer. All opinions expressed in this paper are the authors' and do not necessarily reflect the policies and views of USDA or the Agricultural Research Service. USDA was the sole funder for this research.

About the Author

Dr. Putz is a research microbiologist specializing in zoonotic bacterial diseases within the Infectious Bacterial Research Unit at the National Animal Disease Center in Ames, Iowa. She and her team use multifaceted approaches, such as microscopy, transcriptomics, and immunological investigation, to investigate host and pathogen interactions and response to bacterial infection, principally leptospirosis, brucellosis, and tuberculosis.

References

1. Costa F, Hagan JE, Calcagno J, Kane M, Torgerson P, Martinez-Silveira MS, et al. Global morbidity and mortality of leptospirosis: a systematic review. PLoS Negl Trop Dis. 2015;9:e0003898. https://doi.org/10.1371/journal.pntd.0003898
2. Loureiro AP, Lilenbaum W. Genital bovine leptospirosis: a new look for an old disease. Theriogenology. 2020;141:41–7. https://doi.org/10.1016/j.theriogenology.2019.09.011
3. Martins G, Lilenbaum W. Control of bovine leptospirosis: aspects for consideration in a tropical environment. Res Vet Sci. 2017;112:156–60. https://doi.org/10.1016/j.rvsc.2017.03.021
4. Putz EJ, Nally JE. Investigating the immunological and biological equilibrium of reservoir hosts and pathogenic *Leptospira*: balancing the solution to an acute problem? Front Microbiol. 2020;11:2005. https://doi.org/10.3389/fmicb.2020.02005
5. Zuerner RL, Alt DP, Palmer MV. Development of chronic and acute golden Syrian hamster infection models with *Leptospira borgpetersenii* serovar Hardjo. Vet Pathol. 2012;49:403–11. https://doi.org/10.1177/0300985811409252
6. Nally JE, Chantranuwat C, Wu XY, Fishbein MC, Pereira MM, Da Silva JJ, et al. Alveolar septal deposition of immunoglobulin and complement parallels pulmonary hemorrhage in a guinea pig model of severe pulmonary leptospirosis. Am J Pathol. 2004;164:1115–27. https://doi.org/10.1016/S0002-9440(10)63198-7
7. Yukawa M, Mochizuki K, Imamura S. Susceptibility of Mongolian gerbils (*Meriones unguiculatus*) to leptospires and the protective effect of vaccination. Vet Microbiol. 1990;24:63–71. https://doi.org/10.1016/0378-1135(90)90051-V
8. Walker A, Srinivas GB. Opportunities and strategies to further reduce animal use for *Leptospira* vaccine potency testing. Biologicals. 2013;41:332–7.
9. Putz EJ, Sivasankaran SK, Fernandes LGV, Brunelle B, Lippolis JD, Alt DP, et al. Distinct transcriptional profiles of *Leptospira borgpetersenii* serovar Hardjo strains JB197 and HB203 cultured at different temperatures. PLoS Negl Trop Dis. 2021;15:e0009320. https://doi.org/10.1371/journal.pntd.0009320
10. Randall R, Cooper HK. The golden hamster (*Cricetus auratus*) as a test animal for the diagnosis of leptospirosis. Science. 1944;100:133–4. https://doi.org/10.1126/science.100.2589.133
11. Putz EJ, Andreasen CB, Stasko JA, Fernandes LGV, Palmer MV, Rauh MJ, et al. Circulating foamy macrophages in the Golden Syrian hamster (*Mesocricetus auratus*) model of leptospirosis. J Comp Pathol. 2021;189:98–109. https://doi.org/10.1016/j.jcpa.2021.10.004
12. Srinivas GB, Walker A, Rippke B. USDA regulatory guidelines and practices for veterinary *Leptospira* vaccine potency testing. Biologicals. 2013;41:298–302.
13. Steppan S, Adkins R, Anderson J. Phylogeny and divergence-date estimates of rapid radiations in Muroid rodents based on multiple nuclear genes. Syst Biol. 2004;53:533–53. https://doi.org/10.1080/10635150490468701

14. Barbour AG, Shao H, Cook VJ, Baldwin-Brown J, Tsao JI, Long AD. Genomes, expression profiles, and diversity of mitochondria of the white-footed deermouse *Peromyscus leucopus*, reservoir of Lyme disease and other zoonoses. Sci Rep. 2019;9:17618. https://doi.org/10.1038/s41598-019-54389-3
15. Yawitz TA, Barts N, Kohl KD. Comparative digestive morphology and physiology of five species of *Peromyscus* under controlled environment and diet. Comp Biochem Physiol A Mol Integr Physiol. 2022;271:111265. https://doi.org/10.1016/j.cbpa.2022.111265
16. Barbour AG. Infection resistance and tolerance in *Peromyscus* spp., natural reservoirs of microbes that are virulent for humans. Semin Cell Dev Biol. 2017;61:115–22. https://doi.org/10.1016/j.semcdb.2016.07.002
17. Milovic A, Duong JV, Barbour AG. The infection-tolerant white-footed deermouse tempers interferon responses to endotoxin in comparison to the mouse and rat. eLife. 2024;12:12. https://doi.org/10.7554/eLife.90135
18. Caraballo L, Rangel Y, Reyna-Bello A, Muñoz M, Figueroa-Espinosa R, Sanz-Rodriguez CE, et al. Outbreak of intermediate species *Leptospira venezuelensis* spread by rodents to cows and humans in *L. interrogans*–endemic region, Venezuela. Emerg Infect Dis. 2024;30:1514–22. https://doi.org/10.3201/eid3008.231562
19. Fernandes LGV, Putz EJ, Stasko J, Lippolis JD, Nascimento ALTO, Nally JE. Evaluation of LipL32 and LigA/LigB knockdown mutants in *Leptospira interrogans* serovar Copenhageni: impacts to proteome and virulence. Front Microbiol. 2022;12:799012. https://doi.org/10.3389/fmicb.2021.799012
20. Putz EJ, Andreasen CB, Stasko JA, Hamond C, Olsen SC, Nally JE, et al. Circulating foamy macrophages and other features of bacillus Calmette-Guérin challenge in Golden Syrian hamsters. Vaccine. 2025;55:127037. https://doi.org/10.1016/j.vaccine.2025.127037
21. Russell DG, Cardona PJ, Kim MJ, Allain S, Altare F. Foamy macrophages and the progression of the human tuberculosis granuloma. 2009;10:943–8. https://doi.org/10.1038/ni.1781
22. Wallinga J, Lipsitch M. How generation intervals shape the relationship between growth rates and reproductive numbers. Proc Biol Sci. 2007;274:599–604. https://doi.org/10.1098/rspb.2006.3754
23. Ryu S, Chun JY, Lee S, Yoo D, Kim Y, Ali ST, et al. Epidemiology and transmission dynamics of infectious diseases and control measures. Viruses. 2022;14:2510. https://doi.org/10.3390/v14112510
24. Putz EJ, Andreasen CB, Stasko JA, Fernandes LGV, Palmer MV, Rauh MJ, et al. Circulating foamy macrophages in the Golden Syrian hamster (*Mesocricetus auratus*) model of leptospirosis. J Comp Pathol. 2021;189:98–109. https://doi.org/10.1016/j.jcpa.2021.10.004
25. Fernandes LGV, Hamond C, Tibbs-Cortes BW, Putz EJ, Olsen SC, Palmer MV, et al. CRISPR-prime editing, a versatile genetic tool to create specific mutations with a single nucleotide resolution in *Leptospira.* MBio. 2024;15:e0151624. https://doi.org/10.1128/mbio.01516-24
26. Balderrama-Gutierrez G, Milovic A, Cook VJ, Islam MN, Zhang Y, Kiaris H, et al. An infection-tolerant mammalian reservoir for several zoonotic agents broadly counters the inflammatory effects of endotoxin. MBio. 2021;12:12. https://doi.org/10.1128/mBio.00588-21
27. Barbour AG, Duong JV, Long AD. Lyme disease agent reservoirs *Peromyscus leucopus* and *P. maniculatus* have natively inactivated genes for the high-affinity immunoglobulin gamma Fc Receptor I (CD64). Pathogens. 2023;12:12. https://doi.org/10.3390/pathogens12081056
28. Cook V, Barbour AG. Broad diversity of host responses of the white-footed mouse *Peromyscus leucopus* to *Borrelia* infection and antigens. Ticks Tick Borne Dis. 2015;6:549–58. https://doi.org/10.1016/j.ttbdis.2015.04.009
29. Guerrini V, Gennaro ML. Foam cells: one size doesn't fit all. Trends Immunol. 2019;40:1163–79. https://doi.org/10.1016/j.it.2019.10.002
30. Wang W, Liu W, Fidler T, Wang Y, Tang Y, Woods B, et al. Macrophage inflammation, erythrophagocytosis, and accelerated atherosclerosis in Jak2^{V617F} mice. Circ Res. 2018;123:e35–47. https://doi.org/10.1161/CIRCRESAHA.118.313283
31. Petakh P, Isevych V, Kamyshnyi A, Oksenych V. Weil's disease-immunopathogenesis, multiple organ failure, and potential role of gut microbiota. Biomolecules. 2022;12:12. https://doi.org/10.3390/biom12121830
32. De Brito T, Silva AMGD, Abreu PAE. Pathology and pathogenesis of human leptospirosis: a commented review. Rev Inst Med Trop São Paulo. 2018;60:e23. https://doi.org/10.1590/s1678-9946201860023
33. Miyahara S, Saito M, Kanemaru T, Villanueva SY, Gloriani NG, Yoshida S. Destruction of the hepatocyte junction by intercellular invasion of *Leptospira* causes jaundice in a hamster model of Weil's disease. Int J Exp Pathol. 2014;95:271–81. https://doi.org/10.1111/iep.12085
34. Philip N, Priya SP, Jumah Badawi AH, Mohd Izhar MH, Mohtarrudin N, Tengku Ibrahim TA, et al. Pulmonary haemorrhage as the earliest sign of severe leptospirosis in hamster model challenged with *Leptospira interrogans* strain HP358. PLoS Negl Trop Dis. 2022;16:e0010409. https://doi.org/10.1371/journal.pntd.0010409
35. Jansen A, Stark K, Schneider T, Schöneberg I. Sex differences in clinical leptospirosis in Germany: 1997–2005. Clin Infect Dis. 2007;44:e69–72. https://doi.org/10.1086/513431
36. Traxler RM, Callinan LS, Holman RC, Steiner C, Guerra MA. Leptospirosis-associated hospitalizations, United States, 1998–2009. Emerg Infect Dis. 2014;20:1273–9. https://doi.org/10.3201/eid2008.130450
37. Tomizawa R, Sugiyama H, Sato R, Ohnishi M, Koizumi N. Male-specific pulmonary hemorrhage and cytokine gene expression in golden hamster in early-phase *Leptospira interrogans* serovar Hebdomadis infection. Microb Pathog. 2017;111:33–40. https://doi.org/10.1016/j.micpath.2017.08.016
38. Poje JE, Azevedo JF, Nair N, Mahachi K, Frank LE, Sherpa P, et al. *Borrelia burgdorferi* (Spirochaetales: Spirochaetaceae) infection prevalence and host associations of ticks found on *Peromyscus* spp. in Maryland. J Med Entomol. 2022;59:752–7. https://doi.org/10.1093/jme/tjab206
39. Travi BL, Osorio Y, Melby PC, Chandrasekar B, Arteaga L, Saravia NG. Gender is a major determinant of the clinical evolution and immune response in hamsters infected with *Leishmania* spp. Infect Immun. 2002;70:2288–96. https://doi.org/10.1128/IAI.70.5.2288-2296.2002
40. Pasche B, Kalaydjiev S, Franz TJ, Kremmer E, Gailus-Durner V, Fuchs H, et al. Sex-dependent susceptibility to *Listeria monocytogenes* infection is mediated by differential interleukin-10 production. Infect Immun. 2005;73:5952–60. https://doi.org/10.1128/IAI.73.9.5952-5960.2005

Address for correspondence: Ellie J. Putz, National Animal Disease Center, USDA Agricultural Research Service, 1920 Dayton Ave, Ames, IA 50010, USA; email: ellie.putz@usda.gov

Disseminated Histoplasmosis in Persons Living with HIV, France and Overseas Territories, 1992–2021

Mathieu Nacher, Esaïe Marshall, Firouze Bani-Sadr, Sandrine Peugny, Blandine Denis, Elise Ouedraogo, Sebastien Gallien, Agnes Meybeck, Ugo Françoise, Antoine Adenis, Nicolas Vignier, Pierre Couppié, Pierre Sellier, Sophie Grabar

Disseminated histoplasmosis is a major issue among persons with advanced HIV in the Americas; it might also affect persons in sub-Saharan Africa, the Caribbean, and Asia and can be mistaken for other infections. By using 1992–2021 data from the French hospital database on HIV, we analyzed 198,798 persons with HIV follow-up in France and its overseas territories, identifying 553 (2.8/1,000 person-years) first episodes of disseminated histoplasmosis. Incidence rates varied by site of follow-up: 9.41 in French Guiana, 0.76 in Guadeloupe, 0.62 in Martinique, and 0.079 in mainland France. Incidence rates in France also varied between regions of origin or travel: 4.73 for Central or South America, 1.36 for the Caribbean, and 0.19 for sub-Saharan Africa or Asia. Differences persisted after adjusting for age, sex, CD4 count, and viral load at baseline. Overall, incidence and early death have declined, likely because of antiretroviral drug rollout in France.

Histoplasmosis is common in the Mississippi and Ohio Valleys in the United States, and the disseminated form was classified as an AIDS-defining disease in 1987 (*1*,*2*). Although much of the early work on disseminated histoplasmosis in persons with HIV (PWH) took place in the United States, Central and South America have also recognized the effects in PWH (*3*–*5*). Disseminated histoplasmosis is the leading AIDS-defining infection and cause of death in French Guiana and possibly in other South and Central America countries (*6*). In most endemic countries, the nonspecific manifestation of histoplasmosis, the low awareness of its epidemiologic importance among clinicians, and the lack of diagnostic tools leads to delays in timely diagnosis and treatment. The problem of histoplasmosis also seems to be ignored in Africa and Asia, where *Histoplasma capsulatum* is endemic (*7*–*9*). In the Caribbean, the extent of histoplasmosis is unclear (*10*). Given the movement of people between endemic zones and Europe, the number of cases in hospitals in France and its overseas territories might not be negligible.

The surge of disseminated histoplasmosis was closely linked to the HIV epidemic and the large numbers of PWH with advanced HIV disease. However, because antiretroviral drug therapy has been recommended for all PWH, the epidemiology is likely to have evolved with the gradual decrease in the proportion of severely immunocompromised patients (*11*). We have located few reports to date assessing this evolution.

Author affiliations: Centre Hospitalier Universitaire de Guyane, Cayenne, French Guiana (M. Nacher, A. Adenis, N. Vignier); Université de Guyane, Cayenne (M. Nacher, A. Adenis, P. Couppié); Santé des Populations en Amazonie, Cayenne (M. Nacher, A. Adenis, P. Couppié); Institut Pierre Louis d'Epidémiologie et de Santé Publique, Paris, France (E. Marshall, S. Grabar); Centre Hospitalier Universitaire de Reims, Reims, France (F. Bani-Sadr); Centre Hospitalier Universitaire de Guadeloupe, Les Abymes, Guadeloupe (S. Peugny); Hôpital Saint Louis, Paris, France (B. Denis); Centre Hospitalier Universitaire La Pitié Salpêtrière, Paris (E. Ouedraogo); Hôpital Henri-Mondor, Créteil, France (S. Gallien); Centre Hospitalier de Tourcoing, Tourcoing, France (A. Meybeck); Hôpital Saint Antoine, Paris, France (U. Françoise); Hôpital Avicenne, Bobigny, France (U. Françoise, N. Vignier); Université Paris Cité, Paris, France (N. Vignier); Université Sorbonne Paris Nord, Paris (N. Vignier); Centre Hospitalier Universitaire de Guyane, Cayenne, French Guiana (P. Couppié); Hôpital Lariboisière, Paris, France (P. Sellier); Hôpital St Antoine, Paris (S. Grabar)

DOI: https://doi.org/10.3201/eid3107.241931

For >30 years, the Agence Nationale de Recherche sur le SIDA et les Hépatites (ANRS) cohort 4 (CO4) French hospital database on HIV (FHDH), a large national hospital cohort, collects data from hospitals throughout France and, of note, from hospitals from overseas territories of France in South America (French Guiana), the Caribbean (Martinique and Guadeloupe), and the Indian Ocean (Reunion Island and Mayotte) (*12*). The cohort includes many PWH coming from a wide range of countries that are known as or suspected to be endemic for histoplasmosis (*7*,*8*,*13*,*14*). The different exposure to *Histoplasma* among PWH, combined with most being cared for by university hospitals with diagnostic tools capable of testing for fungal pathogens, enables assessment of the incidence of disseminated histoplasmosis according to the territory of residence or origin of PWH.

We used the ANRS CO4 FHDH to study the incidence of disseminated histoplasmosis in territories of France and the main factors associated with the disease and its prognosis in PWH during 1992–2021. We focused on the national or regional origins of PWH with disseminated histoplasmosis.

Methods

The ANRS CO4 FHDH

Starting in 1989, the ANRS CO4 FHDH was an open hospital cohort of PWH. The cohort collects clinical, biological, and treatment data from adult PWH. The cohort is populated by data from 23 regional coordination committees for the fight against sexually transmitted infections and HIV (Comité de Coordination de la lutte contre le VIH et les IST [COREVIH]), including those from overseas territories (*12*). Each COREVIH has trained clinical research technicians collecting and verifying the quality of the local data and then transferring the data to the FHDH, where additional verifications are conducted to avoid inconsistencies and duplicates. Approximately 180 hospitals in France currently collect data for this cohort that includes 64% of PWH receiving care in France.

Study Design

From data collected during January 1, 1992–December 31, 2021, we selected PWH with a confirmed HIV-1 or HIV-2 infection with ≥2 follow-up visits and 1 CD4+ T-cell measurement. Because diagnostic tools and first-line treatment for histoplasmosis are not always extensively collected in the FHDH, we contacted hospitals reporting cases of histoplasmosis over a 5-year period (2015–2020) to obtain additional information.

ANRS CO4 FHDH Variables Studied

We extracted for the patients with (as main or secondary diagnoses, irrespective of the number of associated diagnoses) the B39 series of codes from the International Classification of Diseases, 10th Revision: B39, B390, B391, B392, B393, B394, B395, and B399, all defining histoplasmosis (*15*). We extracted date of birth, country of birth, and notion of residence in another country as a composite variable accounting for the geographic origin; we also extracted date of HIV diagnosis, date of first inclusion in the cohort, date of antiretroviral treatment initiation, first CD4 count, first viral load, date of histoplasmosis, date of follow-up, location of follow-up (mainland France, overseas territory), date of last news, and date of death. We classified AIDS by using the Centers for Disease Control and Prevention definition (*16*).

Statistical Analysis

We computed incidence rates by using the Stata 16 (https://www.stata.com) suite of commands for survival analyses. We measured follow-up time from the date of inclusion in FHDH until a first diagnosis of histoplasmosis, death, last follow-up visit, or December 31, 2021. We computed crude incidence rates stratified for mainland France and different overseas territories and for different countries or regions of origin. We also computed the incidence rate of histoplasmosis by year in mainland France; in the French Antilles (Guadeloupe and Martinique); in French Guiana, Reunion Island and Mayotte; and by the following calendar periods: 1993–1996, 1997–2001, 2002–2006, 2007–2011, 2012–2016, and 2017–2021. For the initial viral load measurements, we categorized the variable as <20, 21–400, 401–1,000, 1,001–10,000, 10,001–100,000, >100,000 copies/mL, or missing. We introduced a missing category because viral load measurements only became available in 1997. For the first CD4+ T-cell count measurements, we categorized the variable as <50, 50–199, 200–349, 350–500, or >500 cells/mm^3.

We identified factors associated with the risk for histoplasmosis by using a multivariable Cox proportional hazard model adjusted for first CD4 count at inclusion in the FHDH, categorized first viral load at inclusion in the FHDH, antiretroviral treatment status before histoplasmosis diagnosis, age at inclusion, sex, origin (categorized as France, Western Europe, Eastern Europe, North Africa, sub-Saharan Africa, Middle East, Asia, Australasia, Oceania, North America, South and Central America, and the Caribbean), and residence in mainland France or in 1 of the overseas territories. For participants treated in mainland France whose origin was 1 of the overseas territories,

we classified their origin as French Guiana in South America; Martinique, Guadeloupe and Saint Martin in the Caribbean; or Reunion Island and Mayotte in the Indian Ocean. We verified the proportionality of hazards graphically. Age, a time-varying covariate, violated the assumption, and therefore we removed it from the Cox model and used it for stratification.

We computed overall mortality rates as the number of deaths divided by the total person-time since histoplasmosis diagnosis. We plotted Kaplan-Meier curves for the first 6 months after diagnosis of histoplasmosis to avoid misattributing death from another cause (*17*). For the subsample analysis, we conducted cross-tabulations between different hospitals and diagnostic methods used.

Ethical and Regulatory Aspects

All persons enrolled in the cohort provided written informed consent for the use of their data for research purposes. The French data protection authority, the Commission Nationale de l'Informatique et des Libertés, first approved the cohort on November 27, 1991 (*18*). This authorization was later updated to comply with the new regulations, including the European Union's general data protection regulation. On July 20, 2018, the ANRS CO4-FHDH cohort was also approved by the Comité d'Expertise pour les Recherches, les Études et les Évaluations dans le domaine de la Santé. On February 19, 2021, the cohort was also approved as a hospital data warehouse by the Commission Nationale Informatique et Libertés. On March 30, 2021, the ANRS CO4 FHDH cohort received the authorization to conduct research projects on the data warehouse by the Commission Nationale Informatique et Libertés (*18*). This study was approved by the scientific committee of the ANRS CO4 FHDH cohort.

Results

Description of Study Population

We analyzed 198,798 PWH (130,866 men, 66,625 women, and 1,307 other [persons whose personal identity is discordant from their birth sex]) during January 1, 1992–December 31, 2021, contributing 2,188,750 person-years of follow-up with a median follow-up of 9 (interquartile range [IQR] 2.6–7.2) years. The median age at inclusion in the FHDH was 34.4 years (IQR 28.8–41.9) years, and the median age at first episode of histoplasmosis was 41.3 (IQR 33.2–48.8) years. The median CD4 count in the cohort at last follow-up visit or on December 31, 2021, was 542 [IQR 361–753] cells/mm^3, and 8.6% had CD4 counts <200 cells/mm^3. Of live patients in the cohort, 22.5% were classified with AIDS at the last follow-up visit or on December 31, 2021.

Among the 198,798 PWH, the living area was recorded in 182,352 (91.7%) of cases. Most, 168,330 (91.9%) cases, were living in mainland France, 4,689 (2.5%) in French Guiana, 4,426 (2.4%) in Guadeloupe, 2,617 (1.4%) in Martinique, 1,863 (1%) in La Reunion Island, and 427 (0.2%) in Mayotte; information was missing for 16,446 (8.3%) cases. Patient origin was recorded in 183,650 (92.4%) cases, including 117,251 (58.9%) cases from mainland France, 49,103 (24.7%) from sub-Saharan Africa, 6,163 (3.1%) from Northern Africa, 5,765 (2.9%) from Central and South America, and 5,368 (2.7%) from the Caribbean; for 15,148 (7.6%) PWH, the information was missing.

Overall, there were 553 first incident episodes of disseminated histoplasmosis (Table 1). Apart from those first incident cases, 232 prevalent cases were reported at enrollment (171 men, 59 women, and 2 other), and in 92 cases (66 men, 25 women, 1 other), histoplasmosis occurred before enrollment in the FHDH. Those cases did not account for the incidence calculations.

For the 553 first episodes of disseminated histoplasmosis, median CD4 count was 171 (IQR 6–53) cells/mm^3, and 89.9% of PWH were not on antiretroviral treatment when disseminated histoplasmosis occurred. Nearly two thirds (61%) of PWH were followed in French Guiana, and 15% of PWH originated from sub-Saharan Africa. No cases were reported from Eastern Europe, North Africa, Australasia, or Oceania.

Diagnostic and Treatment Characteristics of 2015–2020 Samples

We identified 138 PWH to contact for additional information and received 90 responses with the requested information. Of those who responded, diagnosis was confirmed by PCR for 11 PWH (12.2%), direct examination for 29 PWH (32.2%), culture for 60 PWH (66.6%), and pathology for 35 PWH (38.8%). Antigen detection testing was not available.

Patients received induction treatment with liposomal amphotericin B in 61 (72.2%) cases (52.2% alone, 20% in combination with itraconazole) and with itraconazole alone in 25 (27.8%) cases. Information about treatment was missing in 4 cases. There was no statistical difference between hospitals (p = 0.36).

Subgroups Associated with Incidence Variations

We organized specific incidence rates for disseminated histoplasmosis according to different subgroups (Figure 1). Younger patients, persons with low CD4 counts, persons originating from Central and South America and the Caribbean, and persons living in

Table 1. Summary characteristics of first disseminated histoplasmosis cases among persons living with HIV from the French Hospital Database on HIV, France and overseas territories, 1993–2021*

Variable	Value
Median age, y (IQR)	41.3 (33.2–48.8)
Sex	
M	352 (63.7)
F	197 (35.6)
Other†	4 (0.7)
Geographic origin	
Mainland France	166 (30)
Western Europe	1 (0.2)
Sub-Saharan Africa	83 (15)
Middle East	2 (0.3)
Asia	6 (1.1)
North America	1 (0.2)
South and Central America	189 (34.2)
Caribbean	105 (19)
Residence	
Mainland France	150 (28.8)
Martinique	17 (3.3)
Guadeloupe	34 (6.5)
French Guiana	318 (61)
Reunion Island	2 (0.4)
AIDS stage before histoplasmosis	
Yes	244 (44.1)
No	309 (55.9)
On antiretroviral treatment before histoplasmosis	
Yes	56 (10.1)
No	497 (89.9)
Median CD4, cells/mm³ (IQR)	20 (6–53)
CD4/CD8 ratio >1 at time of histoplasmosis	
Yes	29 (5.7)
No	479 (94.3)
Median viral load at time of histoplasmoses, copies/mL (IQR)	16,480 (485–205,000)

*Values are no. (%) except as indicated. IQR, interquartile range
†Other indicates that personal identity is discordant from birth sex.

French Guiana or the French Antilles had higher incidences than other groups. The incidence rate was 9.41/1,000 person-years in French Guiana, 0.76/1,000 person-years in Guadeloupe, 0.62/1,000 person-years in Martinique, and 0.079/1,000 person-years in mainland France. The incidence rate was 4.73/1,000 person-years for PWH originating from Central and South America, 1.36/1,000 person-years for PWH originating from the Caribbean, and 0.19/1,000 person-years for PWH originating from sub-Saharan Africa or Asia.

After adjustments, a lower initial CD4 count, a higher initial HIV viral load, and residing in French Guiana or in the French Antilles (Guadeloupe/Martinique) were associated with higher hazard ratios of histoplasmosis. Regarding country or region of origin, PWH from Central and South America, Asia, and sub-Saharan Africa had an independently greater hazard ratio of histoplasmosis than those from mainland France (Table 2).

Incidence and Trends According to Places of Residence

The crude overall incidence of disseminated histoplasmosis was 0.25/1,000 person-years, and we observed an incidence decline of histoplasmosis in mainland France, the French Antilles, and in French Guiana (Figure 2). No cases were reported in the Antilles in 2003, 2008, 2014, or 2017. Incidence rates were considerably higher in French Guiana and in the French Antilles than in mainland France. Incidence declined over time in all 3 locations. In 2020, there seemed to be a reversal of the trend in French Guiana, the French Antilles, and mainland France.

Mortality Rates in PWH with Disseminated Histoplasmosis

Of the 553 PWH with histoplasmosis, 128 died. The incidence rate of death was 2.98 (95% CI 2.20–4.04)/100 person-years. Most deaths occurred within 6 months of the diagnosis of histoplasmosis; 17.7% deaths overall occurred by 1 month after diagnosis. Over time, there was a marked reduction of early death after histoplasmosis, from 51% during 1992–1996 to 3% during 2017–2021 ($p<0.0001$ by log-rank test) (Figure 3).

Discussion

We found the incidence of disseminated histoplasmosis in PWH was much higher (>100-fold) among persons residing in French Guiana and among persons

residing in the French Antilles (≈10-fold) than among persons residing in mainland France. Analysis of incidence by country or region of origin revealed persons originating from Central and South America and from the Caribbean were at greatest risk for disseminated histoplasmosis. Of note, the incidence of disseminated histoplasmosis was higher among PWH who had lived in sub-Saharan Africa or Asia than those originating from mainland France who had not lived elsewhere.

We demonstrated that, over the 30-year study period, with the increased proportion of virologically controlled HIV and with high CD4 count PWH, the incidence of disseminated histoplasmosis has decreased everywhere by 2–3-fold. However, the decrease of the incidence was the most critical in French Guiana and the French Antilles. Early death after a first episode of histoplasmosis was very high in the 1990s but also substantially decreased over time, as shown previously (*19*).

This study provides an overview of the risk for disseminated histoplasmosis in PWH having lived with or currently living with different levels of exposure. Because of the lack of diagnostic tools, histoplasmosis has often been overlooked in Latin America, the Caribbean, and in sub-Saharan Africa, where the reservoir of PWH with advanced HIV is the largest (*7*–*9*,*20*). In this cohort, around one quarter of PWH originated from sub-Saharan Africa. We hypothesized if the incidence of histoplasmosis is so much higher in PWH originating from Latin America and the Caribbean than from other regions, it is because histoplasmosis is endemic in the former. New studies in different parts of the world seem more frequent since the Manaus declaration and the greater availability of antigen detection tests (*5*,*21*–*32*). However, a systematic review found only 6 studies using antigen detection to determine prevalence in PWH in Latin America and 9 in sub-Saharan Africa, but even fewer

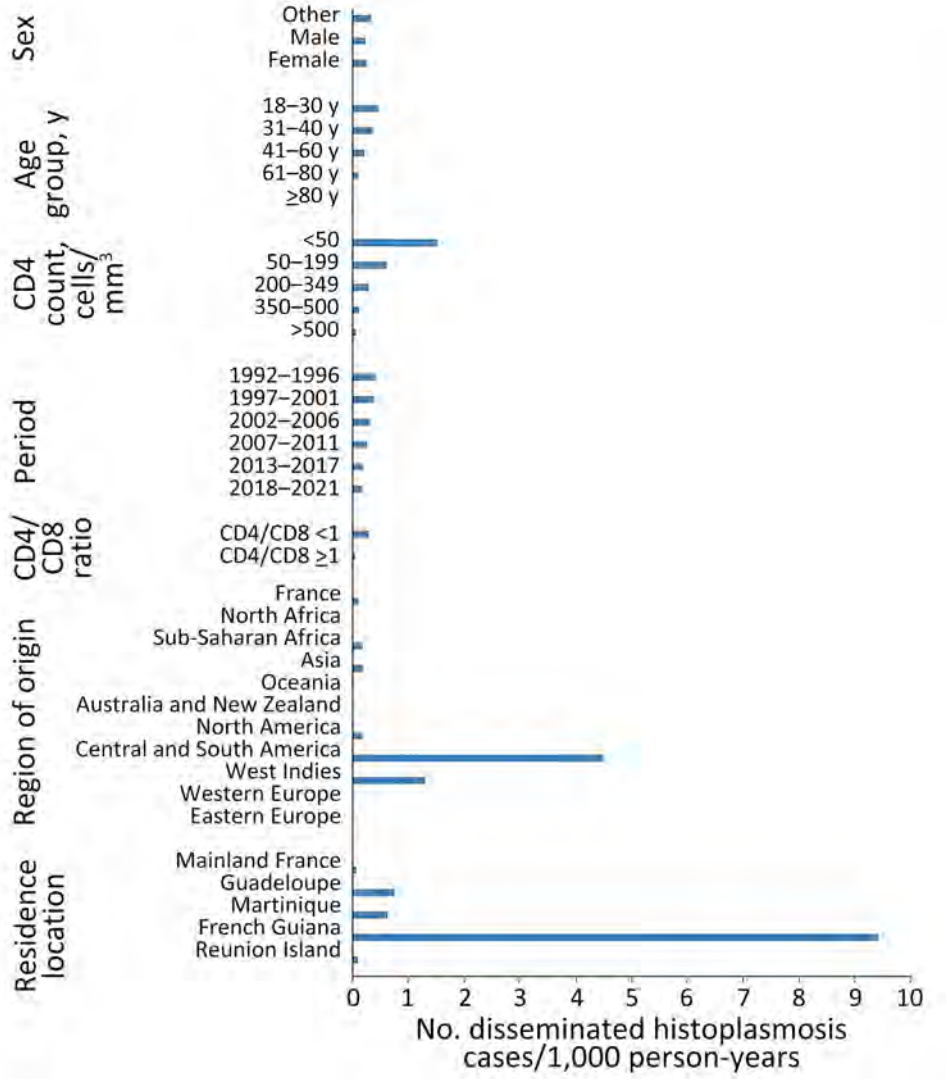

Figure 1. Incidence rate of disseminated histoplasmosis in persons living with HIV from France and overseas territories of France by different subgroups,1992–2021. Other sex refers to persons whose personal identity is discordant from their birth sex.

Table 2. Crude and adjusted hazard ratios for disseminated histoplasmosis in persons living with HIV from France and overseas territories of France,1992–2021*

Variable	Person-time, y	First events	Hazard ratio (95% CI)		p value
			Crude	Adjusted†	
Sex					<0.0001
M	1,438,462	352	Referent	Referent	
F	741,990	197	1.1 (0.92–1.30)	0.50 (0.40–0.63)	
Initial CD4 count, cells/mm^3					
<50	51,925	79	15.40 (11.10–21.38)	8.94 (6.26–12.77)	<0.0001
51–199	181,448	113	8.11 (6.00–10.96)	4.63 (3.38–6.35)	<0.0001
200–349	326,745	97	4.09 (3.00–5.58)	2.60 (1.88–3.58)	<0.0001
350–500	406,760	52	1.78 (1.24–2.56)	1.36 (0.94–1.97)	0.10
>500	948,770	68	Referent	Referent	
Initial viral load, copies/mm^3					
<20	1,069,688	94	Referent	Referent	0.24
21–400	240,498	51	2.40 (1.70–3.37)	1.27 (0.84–1.93)	0.001
401–1,000	53,468	22	4.68 (2.94–7-44)	2.42 (1.40–4.17)	0.003
1,001–10,000	135,410	35	2.93 (1.99–4.33)	1.89 (1.23–2.91)	0.005
10,001–100,000	143,257	51	4.04 (2.87–5.69)	1.78 (1.18–2.67)	<0.0001
>100,000	64,702	79	13.79 (10.22–18.61)	4.20 (2.88–6.13)	<0.0001
Missing	485,100	221	5.21 (4.08–6.66)	3.26 (2.43–4.36)	
Residence					
Mainland France	1,889,675	150	Referent	Referent	<0.0001
Guadeloupe	44,325	34	9.35 (6.44–13.57)	12.15 (7.42–19.91)	<0.0001
Martinique	27,112	17	7.69 (4.65–12.69)	11.95 (6.47–22.07)	<0.0001
French Guiana	33,767	318	102.88 (84.64–125.06)	111.43 (79.18–156.82)	0.36
Reunion Island	19,482	2	1.28 (0.31–5.16)	1.90 (0.46–7.73)	
Origin					
France	1,437,390	166	Referent	Referent	0.47
Western Europe	58,573	1	0.16 (0.02–1.15)	0.48 (0.06–3.50)	NA
North America	5,414	1	1.67 (0.23–11.94)	NA	<0.0001
Central and South America	39,905	189	31.88 (25–70–39.54)	2.57 (1.84–3.58)	0.36
Caribbean	76,849	105	13.30 (10.38–17.03)	1.17 (0.82–1.65)	<0.0001
Sub-Saharan Africa	435,761	83	2.00 (1.52–2.62)	4.52 (3.18–6.42)	NA
Middle East	9,368	2	2.14 (0.53–8.66)	NA	<0.0001
Asia	30,572	6	1.99 (0.88–4.51)	5.50 (2.21–13.69)	NA

*NA, not available.
†Model stratified on age group (age categories are time-varying and violate hazard proportionality assumption); excluded by Stata (https://www.stata.com).

from Asia, North America, Europe, and Australia (*33*). Studies using biobanked samples could enable assessment of the extent of histoplasma in countries without any data. The study also shows the dramatic decrease of incidence and early death from disseminated histoplasmosis with virological control and high CD4 count in PWH.

The first limitation of our study is that our cohort could reflect the global epidemiology of histoplasmosis, but we cannot rule out biases because of varying

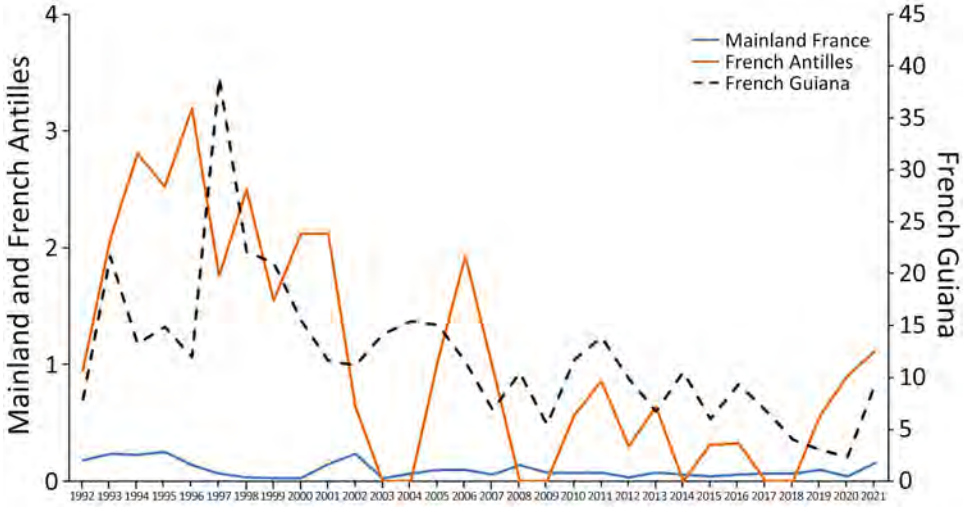

Figure 2. Evolution of the annual incidence rate of disseminated histoplasmosis per 1,000 person-years in mainland France, the French Antilles, and French Guiana, 1992–2021. Scales for the y-axes differ substantially to underscore patterns but do not permit direct comparisons.

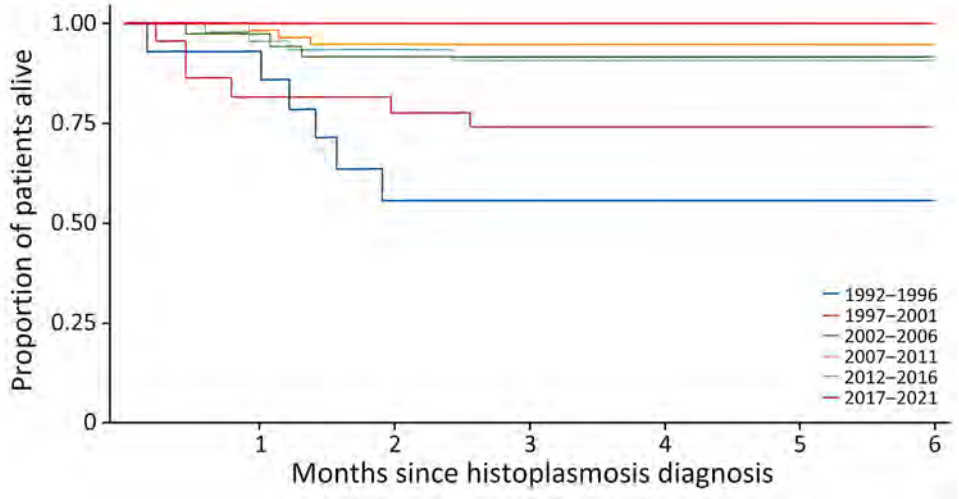

Figure 3. Kaplan-Meier survival curve representing deaths among disseminated histoplasmosis in persons living with HIV, by calendar time periods, France and overseas territories, 1992–2021.

durations and levels of exposure. Second, the case records, the types of diagnostic tools (sometimes by using the European Organization for Research and Treatment of Cancer's Mycoses Study Group criteria [*34*]), and treatment schedules were not standardized and may vary from 1 clinician to another or from 1 hospital to another. Third, in our 2015–2020 sample, none of the diagnoses were on the basis of antigen detection tests (unavailable in France), despite most PWH in our cohort being followed in university hospitals. Fourth, in our 2015–2020 sample, the first-line treatment was liposomal amphotericin B in about three quarters of cases, which, according to World Health Organization guidelines (*35*), implied most cases were severe or moderately severe. We did not observe such severity in French Guiana, which has the largest histoplasmosis cohort (*17*). Fifth, the cause of death was not always precisely defined so similar to previously published reports, so we could only assume that early deaths were because of histoplasmosis (*17*). Finally, differing from the residence enables categorizing a patient in a potential endemic zone, the country or region of origin is a more inconclusive variable: we assumed that the patient born or having spent time in a potential endemic zone (or not) influenced the probability of acquiring histoplasmosis. In 2019, a doctoral thesis based on the French National Mycology Reference Laboratory data identified 107 cases of histoplasmosis (61% in PWH); all either came from or had traveled to endemic areas, mostly the Americas, western sub-Saharan Africa, and Asia (*36*). Despite those potential limitations, the large size and longitudinal design provide precious information about a major global pathogen.

This article underscores that the Americas have the highest prevalence of histoplasmosis (*37*) and suggests there are cases elsewhere, perhaps fewer than the number of cases found in simulations (*9*). Because of the burden of HIV in sub-Saharan Africa or Asia, even modest prevalence could lead to substantial illness and death in those regions. Finally, with the antiretroviral-for-all recommendations for PWH (*11*), the effects of histoplasmosis could decline worldwide. Because the prevalence of histoplasmosis appears related to advanced HIV disease, HIV testing and proactive care are potent tools to decrease the prevalence of histoplasmosis.

In conclusion, this article reveals the incidence of disseminated histoplasmosis was highest in PWH whose follow-up was in French Guiana and the French Antilles. Among those living in mainland France, incidences were highest in PWH coming from or having stayed in Central and South America, followed by Caribbean. PWH originating from sub-Saharan Africa or Asia had higher incidences than those originating from mainland France. Because having spent time in each region can correspond to a range of durations, studies should directly estimate the incidence of histoplasmosis among PWH in each region. During the 30-year study period, the incidence and early death rates of histoplasmosis have steadily decreased, likely because of broadening use of antiretroviral drugs.

About the Author

Dr. Nacher is the director of the Institut National de la Santé et de la Recherche Médicale clinical investigation center number 1424, from the UA17 Institut National de la Santé et de la Recherche Médicale Amazonian Population Heath research unit, and president of the regional coordination for the fight against HIV of French Guiana. His research interests include the epidemiology and effects of disseminated histoplasmosis in persons living with HIV.

References

1. Hajjeh RA. Disseminated histoplasmosis in persons infected with human immunodeficiency virus. Clin Infect Dis. 1995; 21(Suppl 1):S108–10. https://doi.org/10.1093/clinids/21.Supplement_1.S108
2. Bahr NC, Antinori S, Wheat LJ, Sarosi GA. Histoplasmosis infections worldwide: thinking outside of the Ohio River valley. Curr Trop Med Rep. 2015;2:70–80. https://doi.org/10.1007/s40475-015-0044-0
3. Samayoa B, Roy M, Cleveland AA, Medina N, Lau-Bonilla D, Scheel CM, et al. High mortality and coinfection in a prospective cohort of human immunodeficiency virus/acquired immune deficiency syndrome patients with histoplasmosis in Guatemala. Am J Trop Med Hyg. 2017;97:42–8. https://doi.org/10.4269/ajtmh.16-0009
4. Daher EF, Silva GB Jr, Barros FA, Takeda CF, Mota RM, Ferreira MT, et al. Clinical and laboratory features of disseminated histoplasmosis in HIV patients from Brazil. Trop Med Int Health. 2007;12:1108–15. https://doi.org/10.1111/j.1365-3156.2007.01894.x
5. Falci DR, Monteiro AA, Braz Caurio CF, Magalhães TCO, Xavier MO, Basso RP, et al. Histoplasmosis, an underdiagnosed disease affecting people living with HIV/AIDS in Brazil: results of a multicenter prospective cohort study using both classical mycology tests and histoplasma urine antigen detection. Open Forum Infect Dis. 2019;6:ofz073. https://doi.org/10.1093/ofid/ofz073
6. Adenis AA, Valdes A, Cropet C, McCotter OZ, Derado G, Couppie P, et al. Burden of HIV-associated histoplasmosis compared with tuberculosis in Latin America: a modelling study. Lancet Infect Dis. 2018;18:1150–9. https://doi.org/10.1016/S1473-3099(18)30354-2
7. Oladele RO, Ayanlowo OO, Richardson MD, Denning DW. Histoplasmosis in Africa: an emerging or a neglected disease? PLoS Negl Trop Dis. 2018;12:e0006046. https://doi.org/10.1371/journal.pntd.0006046
8. Baker J, Setianingrum F, Wahyuningsih R, Denning DW. Mapping histoplasmosis in south east Asia—implications for diagnosis in AIDS. Emerg Microbes Infect. 2019;8:1139–45. https://doi.org/10.1080/22221751.2019.1644539
9. Nacher M, Couppié P, Epelboin L, Djossou F, Demar M, Adenis A. Disseminated histoplasmosis: fighting a neglected killer of patients with advanced HIV disease in Latin America. PLoS Pathog. 2020;16:e1008449. https://doi.org/10.1371/journal.ppat.1008449
10. Nacher MA. Proceedings of first histoplasmosis in the Americas and the Caribbean meeting, Paramaribo, Suriname, December 4–6, 2015. Emerg Inf Dis. 2016;22:160408
11. World Health Organization. Guidelines for managing advanced HIV disease and rapid initiation of antiretroviral therapy [cited 2022 Apr 30]. https://www.who.int/publications-detail-redirect/9789241550062
12. Mary-Krause M, Grabar S, Lièvre L, Abgrall S, Billaud E, Boué F, et al. Cohort profile: French hospital database on HIV (FHDH-ANRS CO4). Int J Epidemiol. 2014;43:1425–36. https://doi.org/10.1093/ije/dyu002
13. Mandengue CE, Ngandjio A, Atangana PJ. Histoplasmosis in HIV-infected persons, Yaoundé, Cameroon. Emerg Infect Dis. 2015;21:2094–6. https://doi.org/10.3201/eid2111.150278
14. Kuate MPN, Ekeng BE, Kwizera R, Mandengue C, Bongomin F. Histoplasmosis overlapping with HIV and tuberculosis in sub-Saharan Africa: challenges and research priorities. Ther Adv Infect Dis. 2021;8:20499361211008675. https://doi.org/10.1177/20499361211008675
15. World Health Organization. International Statistical Classification of Diseases and Related Health Problems, 10th Revision. 2019 [cited 2024 Apr 25]. https://icd.who.int/browse10/2019/en
16. Centers for Disease Control and Prevention. 1993 revised classification system for HIV infection and expanded surveillance case definition for AIDS among adolescents and adults [cited 2025 Mar 5]. https://www.cdc.gov/mmwr/preview/mmwrhtml/00018871.htm
17. Françoise U, Nacher M, Bourne-Watrin M, Epelboin L, Thorey C, Demar M, et al. Development of a case fatality prognostic score for HIV-associated histoplasmosis. Int J Infect Dis. 2023;132:26–33. https://doi.org/10.1016/j.ijid.2023.03.048
18. French Hospital Database on HIV. Regulatory documents [in French]. 2022 [cited 2024 Dec 9]. https://anrs-co4.fhdh.fr/documents-de-reference-2
19. Peigne V, Dromer F, Elie C, Lidove O, Lortholary O; French Mycosis Study Group. Imported acquired immunodeficiency syndrome-related histoplasmosis in metropolitan France: a comparison of pre-highly active anti-retroviral therapy and highly active anti-retroviral therapy eras. Am J Trop Med Hyg. 2011;85:934–41. https://doi.org/10.4269/ajtmh.2011.11-0224
20. Mapengo RE, Maphanga TG, Grayson W, Govender NP. Endemic mycoses in South Africa, 2010–2020: a decade-long description of laboratory-diagnosed cases and prospects for the future. PLoS Negl Trop Dis. 2022;16:e0010737. https://doi.org/10.1371/journal.pntd.0010737
21. Aguilar G, Lopez G, Sued O, Medina N, Caceres DH, Pereira J, et al. Implementation of a rapid diagnostic assay package for cryptococcosis, histoplasmosis and tuberculosis in people living with HIV in Paraguay. BMC Infect Dis. 2024;24:406. https://doi.org/10.1186/s12879-024-09257-5
22. Caceres DH, Scheel CM, Tobón AM, Ahlquist Cleveland A, Restrepo A, Brandt ME, et al. Validation of an enzyme-linked immunosorbent assay that detects *Histoplasma capsulatum* antigenuria in Colombian patients with AIDS for diagnosis and follow-up during therapy. Clin Vaccine Immunol. 2014;21:1364–8. https://doi.org/10.1128/CVI.00101-14
23. Caceres DH, Adenis A, de Souza JVB, Gomez BL, Cruz KS, Pasqualotto AC, et al. The Manaus declaration: current situation of histoplasmosis in the Americas, report of the II regional meeting of the international histoplasmosis advocacy group. Curr Fungal Infect Rep. 2019;13:244–9. https://doi.org/10.1007/s12281-019-00365-3
24. Caceres DH, Arauz AB, Flores C, Santiago E, Montoya S, Saenz C, et al. Implementation of rapid diagnostics assays for detection of histoplasmosis and cryptococcosis in Central American people living with HIV. Mycoses. 2021;64:1396–401. https://doi.org/10.1111/myc.13303
25. Messina FA, Marin E, Caceres DH, Romero M, Manrique M, Santiso GM. Evaluation of a commercial *Histoplasma* antigen detection enzyme immunoassay for the follow-up of histoplasmosis treatment in people living with HIV from Argentina. Med Mycol. 2024;63:myae121. https://doi.org/10.1093/mmy/myae121
26. Sebro A, Edwards J, Sued O, Lavia LO, Elder T, Edwards RJ, et al. Implementation of antigen-based diagnostic assays for detection of histoplasmosis and cryptococcosis among patients with advanced HIV in Trinidad and Tobago: a cross-sectional study. J Fungi (Basel). 2024;10:695. https://doi.org/10.3390/jof10100695
27. Kuate MPN, Nyasa R, Mandengue C, Tendongfor N, Bongomin F, Denning DW. Screening for acute disseminated histoplasmosis in HIV disease using urinary antigen detection enzyme immunoassay: a pilot study in Cameroon. J Microbiol Methods. 2021;185:106226. https://doi.org/10.1016/j.mimet.2021.106226

28. Blan BDS, Poester VR, Basso RP, Sanchotene KO, Caceres DH, Ramis de Souza IB, et al. Histoplasmosis screening using urinary antigen detection in people living with HIV in southern Brazil. Med Mycol. 2025;63:myaf017. https://doi.org/10.1093/mmy/myaf017
29. Toscanini MA, Laboccetta CR, Videla Garrido A, Posse GB, Capece P, Valdez RM, et al. Role of recombinant *Histoplasma capsulatum* 100-kilodalton antigen in the diagnosis of histoplasmosis among HIV/AIDS patients: antigenuria and antibodies detection. Mycoses. 2023;66:609–20. https://doi.org/10.1111/myc.13587
30. Martínez-Gamboa A, Niembro-Ortega MD, Torres-González P, Santiago-Cruz J, Velázquez-Zavala NG, Rangel-Cordero A, et al. Diagnostic accuracy of antigen detection in urine and molecular assays testing in different clinical samples for the diagnosis of progressive disseminated histoplasmosis in patients living with HIV/AIDS: a prospective multicenter study in Mexico. PLoS Negl Trop Dis. 2021;15:e0009215. https://doi.org/10.1371/journal.pntd.0009215
31. Hoyos Pulgarin JA, Alzate Piedrahita JA, Moreno Gómez GA, Sierra Palacio JF, Ordoñez KM, Arias Ramos D. Closing gaps in histoplasmosis: clinical characteristics and factors associated with probable/histoplasmosis in HIV/AIDS hospitalized patients, a retrospective cross-sectional study in two tertiary centers in Pereira, Colombia. AIDS Res Ther. 2021;18:51. https://doi.org/10.1186/s12981-021-00377-5
32. Medina N, Alastruey-Izquierdo A, Mercado D, Bonilla O, Pérez JC, Aguirre L, et al.; Fungired. Comparative performance of the laboratory assays used by a diagnostic laboratory hub for opportunistic infections in people living with HIV. AIDS. 2020;34:1625–32. https://doi.org/10.1097/QAD.0000000000002631
33. Sekar P, Hale G, Gakuru J, Meya DB, Boulware DR, Ellis J, et al. Systematic review of prevalence of *Histoplasma* antigenuria in persons with HIV in Latin America and Africa. Emerg Infect Dis. 2024;30:1523–30. https://doi.org/10.3201/eid3008.231710
34. De Pauw B, Walsh TJ, Donnelly JP, Stevens DA, Edwards JE, Calandra T, et al.; European Organization for Research and Treatment of Cancer/Invasive Fungal Infections Cooperative Group; National Institute of Allergy and Infectious Diseases Mycoses Study Group (EORTC/MSG) Consensus Group. Revised definitions of invasive fungal disease from the European Organization for Research and Treatment of Cancer/Invasive Fungal Infections Cooperative Group and the National Institute of Allergy and Infectious Diseases Mycoses Study Group (EORTC/MSG) consensus group. Clin Infect Dis. 2008;46:1813–21. https://doi.org/10.1086/588660
35. World Health Organization. Guidelines for diagnosing and managing disseminated histoplasmosis among people living with HIV [cited 2024 Dec 9]. Available from: https://www.who.int/publications/i/item/9789240006430
36. Chiaruzzi M, Adenis A, Bonifay T, Djossou F, Brittany S, Lanternier F, et al. Epidemiology of *Histoplasma capsulatum* sp. infections diagnosed in metropolitan France. Multicenter cross-sectional study 2007–2018 [in French]. Med Mal Infect. 2020;50:s5. https://doi.org/10.1016/j.medmal.2020.06.016
37. Teixeira MM, Patané JSL, Taylor ML, Gómez BL, Theodoro RC, de Hoog S, et al. Worldwide phylogenetic distributions and population dynamics of the genus *Histoplasma*. PLoS Negl Trop Dis. 2016;10:e0004732. https://doi.org/10.1371/journal.pntd.0004732

Address for correspondence: Mathieu Nacher, Centre Hospitalier Universitaire de Guyane, CIC 1424, Cayenne, French Guiana; email: mathieu.nacher66@gmail.com

Emergence of Distinct *Salmonella enterica* Serovar Enteritidis Lineage since 2020, South Korea

Eunkyung Shin,[1] Tae-Min La,[1] Jaeil Yoo, Junyoung Kim,[2] Ji-Yeon Hyeon[2]

We analyzed whole-genome sequences of *Salmonella enterica* serovar Enteritidis isolates in South Korea that had the SEGX01.049 pulsed-field gel electrophoresis pattern. That lineage has emerged and circulated in South Korea since 2020, leading to 2 fatal infection cases. We investigated the genomic characteristics and identified potential sources of that lineage. Isolates from outbreaks during 2020–2023 clustered in the Global IIa clade, along with other *Salmonella* Enteritidis strains from chicken farms in South Korea and human isolates from the United Kingdom. Bayesian molecular clock analysis estimated the time to the most recent common ancestor of our isolates in the Global IIa clade was 2017.57. Moreover, phylogeographic analysis supported substantial statistical evidence (Bayes factor 111.415; posterior probability 0.97) for the introduction of this lineage into South Korea from the United Kingdom. Continued genomic surveillance will be needed to monitor the spread of foodborne pathogens such as *Salmonella* Enteritidis and improve prevention strategies.

Salmonella enterica serovar Enteritidis is a major pathogen responsible for human salmonellosis worldwide; substantial public health implications exist because of its rapid transmission and frequent association with foodborne outbreaks (*1*). In South Korea, *Salmonella* Enteritidis has emerged as a leading cause of foodborne illness and one of the most prevalent bacterial pathogens (*2*,*3*). Poultry products, especially eggs, have been consistently identified as primary sources of transmission; recent severe outbreaks have led to fatal salmonellosis cases (*4*). That trend highlights the critical need for comprehensive surveillance systems and effective outbreak response strategies to control *Salmonella* Enteritidis infections.

In South Korea, surveillance of *Salmonella* Enteritidis has substantially transitioned within the PulseNet Korea network, part of a global network designed to detect and investigate foodborne infections. PulseNet Korea has evolved from reliance on pulsed-field gel electrophoresis (PFGE) to the use of whole-genome sequencing (WGS) to track genomic patterns and trace infection sources. Since the nationwide implementation of WGS in 2020, more detailed analyses of genetic diversity and phylogenetic relationships among strains exhibiting identical PFGE patterns has become possible. High-resolution typing methods, such as whole-genome single-nucleotide polymorphism (SNP) analysis and core-genome multilocus sequence typing (cgMLST), have become standard for pathogen surveillance, including for *S. enterica* (*5*–*7*). Furthermore, cgMLST data are commonly analyzed by using the HierCC hierarchical clustering package, a threshold-based method grouping isolates by allelic differences, implemented in the EnteroBase web-based platform (*7*,*8*). Although previous studies in South Korea have applied WGS to *Salmonella* Enteritidis strains isolated from poultry and food sources (*9*,*10*), research focusing on human *Salmonella* Enteritidis isolates remains limited.

We analyzed whole-genome sequences of *Salmonella* Enteritidis isolates with the SEGX01.049 PFGE pattern submitted to the Korea Disease Control and Prevention Agency (KDCA); isolates with that pattern have emerged and circulated in South Korea since 2020 and have caused 2 fatal salmonellosis cases. Two foodborne outbreaks associated with that PFGE pattern were reported in Gyeongnam Province, South Korea, in 2021 (*11*). Despite repeated detection

Author affiliations: Korea Centers for Diseases Control and Prevention Agency, Cheongju, South Korea (E. Shin, J. Yoo, J. Kim); Konkuk University College of Veterinary Medicine, Seoul, South Korea (T.-M. La, J.-Y. Hyeon)

DOI: https://doi.org/10.3201/eid3107.250043

[1]These first authors contributed equally to this article.

[2]These senior authors contributed equally to this article.

in outbreak investigations, limited genomic data have been available to contextualize that *Salmonella* subtype within a global framework. Therefore, we investigated the genomic characteristics and phylogenetic relationships of those isolates and compared them with *Salmonella* Enteritidis strains from other global regions to identify potential food sources and trace the origins of this subtype in South Korea. No ethics approvals were required for this study.

Materials and Methods

Bacterial Isolates

Member laboratories of national gastrointestinal infection disease surveillance networks (EnterNet and PulseNet Korea) collected and anonymously submitted *Salmonella* spp. isolates to KDCA. We identified the bacteria by using a VITEK-II automated system (bioMérieux, https://www.biomerieux.com). We performed *Salmonella* serotyping according to the Kauffmann-White scheme using specific antiserum (BD Biosciences, https://www.bdbiosciences.com). We analyzed isolates by using PFGE after DNA restriction enzyme digestion with *Xba*I in accordance with the PulseNet International protocol (https://www.pulsenetinternational.org). We determined genetic similarities between PFGE patterns by using BioNumerics version 7.5 (bioMérieux). For WGS, we selected 38 SEGX01.049 *Salmonella* Enteritidis isolates collected from patients, workers, the environment, and food associated with 3 sporadic infection cases in 2013 and 2014 and 8 outbreaks during 2020–2023 (Appendix 1 Table 1, https://wwwnc.cdc.gov/EID/article/31/7/25-0043-App1.pdf).

Whole-Genome Sequence Analysis

We isolated genomic DNA by using a DNA Blood and Tissue Kit (QIAGEN, https://www.qiagen.com). We performed WGS on the MiSeq platform by using the v2 kit (500 cycles, 2 × 250-nt reads) (Illumina Inc., https://www.illumina.com). We adaptor-trimmed raw reads by using Bbduk (https://sourceforge.net/projects/bbmap) and used a quality threshold of Q>20 and a minimum length of 50 bp. We de novo assembled trimmed reads by using SPAdes 3.15.5 (*12*) with default settings in Geneious Prime 10 (https://www.geneious.com). We determined the presence of acquired antimicrobial resistance genes by using ABRicate version 1.0.1 (https://github.com/tseemann/abricate) and the ResFinder database (*13*) and determined virulence genes by using default settings in the virulence factor database (*14*). We identified prophages by using PHASTEST (*15*). We deposited paired-end reads of *Salmonella* Enteritidis isolates from this study into the National Center for Biotechnology Information (NCBI; https://www.ncbi.nlm.nih.gov) Bioproject database (accession no. PRJNA1150652).

Phylogenetic Analysis

We constructed 2 whole-genome SNP (wgSNP) phylogenetic trees: 1 tree to compare the 38 isolates from this study with 223 *Salmonella* Enteritidis isolates from South Korea and 1 tree to compare the 38 isolates with 1,230 *Salmonella* Enteritidis isolates, which included the 223 genomic sequences from South Korea, 93 selected sequences from the HC5_2301 cluster (*7*), and 914 sequences reported previously (*16*). We compiled genomic sequences of *Salmonella* Enteritidis isolates from South Korea (n = 223) from multiple sources (Appendix 1 Table 2). We retrieved 118 genome sequences from GenBank and EnteroBase (https://enterobase.warwick.ac.uk) public databases by using the search terms "*Salmonella* Enteritidis" and "South Korea" for GenBank and "Enteritidis" (serovar) and "South Korea" (country) for Enterobase (both databases accessed January 2024). We identified and excluded duplicate or redundant entries across the 2 databases. We obtained an additional 24 genomes from our previous study (*9*); those were not indexed under the "*Salmonella* Enteritidis" in GenBank and, thus, could not be retrieved by using standard search terms. Furthermore, 81 genomes were provided by KDCA and Konkuk University, Seoul, South Korea. We identified wgSNPs for the downloaded sequences and 38 *Salmonella* Enteritidis isolates from this study by using Snippy version 4.6.0 (https://github.com/tseemann/snippy); we used *Salmonella* Enteritidis strain P125109 (GenBank accession no. NC011294) as the reference genome. We identified prophages in the reference genome by using PHASTEST (*15*). We identified repetitive regions by aligning the reference genome to itself by using the NUCmer commands in the MUMmer package version 3.23 (*17*) along with the --maxmatch and --nosimplify options. We predicted recombination regions by using Gubbins version 3.3.1 (*18*) and defined repetitive regions by using the default threshold of $\geq$20 bp; the shortest masked region in this study was 68 bp. We excluded prophage, repetitive, and recombinant regions, and the final alignment had 4,326 SNP sites for the dataset from Korea and 4,591 SNP sites for the global dataset. We constructed a maximum-likelihood phylogenetic tree from the clean alignment by using a transversion model plus empirical base frequencies, selected by ModelFinder in IQ-TREE (*19*), with 1,000 bootstrap

replicates. We analyzed the population structure of *Salmonella* Enteritidis isolates by using default parameters in FastBAPS (*20*).

For global phylogenetic analysis, we retrieved 914 whole-genome sequences of *Salmonella* Enteritidis used in a previous study (*16*) from the NCBI SRA database (https://www.ncbi.nlm.nih.gov/sra) according to their accession numbers by using fasterq-dump from the SRA Toolkit (https://github.com/ncbi/sra-tools); those sequences represented epidemiologic, geographic, and phylogenetic diversity. In addition, we downloaded 3,609 genomic sequences in the cgMLST HC5_2301 cluster from EnteroBase (*8*), because the isolates from this study clustered with *Salmonella* Enteritidis strain MFDS1018147 (GenBank accession no. CP110220.1) within that cluster. We constructed a neighbor-joining tree by using Mashtree version 1.4.6 (*21*) according to Mash distance; the tree included the 3,609 cgMLST HC5_2301 genomes and 261 isolates from South Korea (including the 38 isolates from this study). From this tree, we selected 93 of the 3,609 sequences showing close Mash distance proximity to the isolates in this study for wgSNP analysis. (Appendix 1 Table 2, Figure). For wgSNP analysis, we used a total of 1,268 sequences, comprising the isolates from this study (n = 38), those from the cgMLST HC5_2301 cluster (n = 93), sequences used in a previous study (n = 914) (*16*), and other *Salmonella* Enteritidis isolates from South Korea (n = 223), and we determined the population structure by using FastBAPS (*20*).

Bayesian Phylogenetic Analysis

To reconstruct the evolutionary history, we aligned wgSNPs sequences (n = 180) within the FastBAPS Global II clade from the phylogenetic tree of 1,268 sequences (Figure 1, panel A). Among 185 sequences in the FastBAPS Global II clade, we excluded 1 wild animal sample from Germany, 1 from the United Kingdom, and 1 isolate labeled as ND from the United Kingdom within the cgMLST HC5_2301 cluster because of ambiguous host or source metadata, including undefined host or sampling origin. In addition, we excluded sequences from Vietnam and Australia (n = 1 each) reported in the previous study (*16*) because of their limited representation.

We explored the temporal signal (R^2>0.686) for molecular clock analysis of the phylogenetic tree by using TempEst version 1.5.3 (*22*). We performed Bayesian phylogenetic analysis by using BEAST version 1.10.4 (*23*). We selected the transversion nucleotide substitution model with empirical base frequencies by using ModelTest-NG (*24*). To identify the best-fit model for the data, we compared the marginal likelihood of 2 clock models (strict and lognormal relaxed) in combination with 3 tree priors (constant population size, exponential growth, and Bayesian skyline) by using path sampling and stepping-stone sampling (*25*). The lognormal relaxed clock model with a constant population size prior consistently yielded the highest Bayes factor, indicating the best fit for our dataset.

For Bayesian discrete trait phylogeographic analysis, we reconstructed ancestral locations and estimated asymmetric exchanges between regions by using a nonreversible, continuous-time Markov chain model. To minimize potential sample size bias, we grouped sequences from regions with low representation into broader categories according to geographic relevance. The Africa group had 11 sequences from Mauritius (n = 3), Côte d'Ivoire (n = 1), Uganda (n = 2), and South Africa (n = 5). The Other Europe group comprised 25 sequences from Austria (n = 3), Belgium (n = 2), Denmark (n = 3), Finland (n = 1), Germany (n = 3), Italy (n = 5), Poland (n = 7), and Sweden (n = 1). The United Kingdom group was the largest group with 97 sequences, followed by South Korea with 38 sequences and the United States with 10 sequences.

We applied a Bayesian stochastic search variable selection procedure to identify well-supported transitions between discrete states by using the Bayes factors test in SPREAD3 software version 0.9.6 (*26*). We considered transitions to be significant when the posterior probability was >0.5 and the Bayes factor was >3 (*26*). We ran 3 independent chains of 100 million generations in parallel, sampling every 10,000 generations. We evaluated the results in TRACER version 1.7.1 (http://beast.community/tracer) to ensure that the effective sample sizes were >200 and to ensure convergence between all 3 runs. We combined the log and tree files of 3 independent runs by using LogCombiner version 1.8.3 (https://beast.community/logcombiner) and 10% burn-in. We generated a maximum clade credibility tree by using TreeAnnotator version 1.8.2 (https://beast.community/treeannotator) and 10% burn-in and common ancestor node heights. We used Interactive Tree of Life version 6 (https://itol.embl.de) to annotate the tree.

To evaluate the potential effect of sampling bias, we constructed a generalized linear model as an extension of phylogeographic inference by using BEAST. That analysis assessed the influence of source and sink sample sizes as predictors on migration rates within the Bayesian framework. Coefficients quantified the

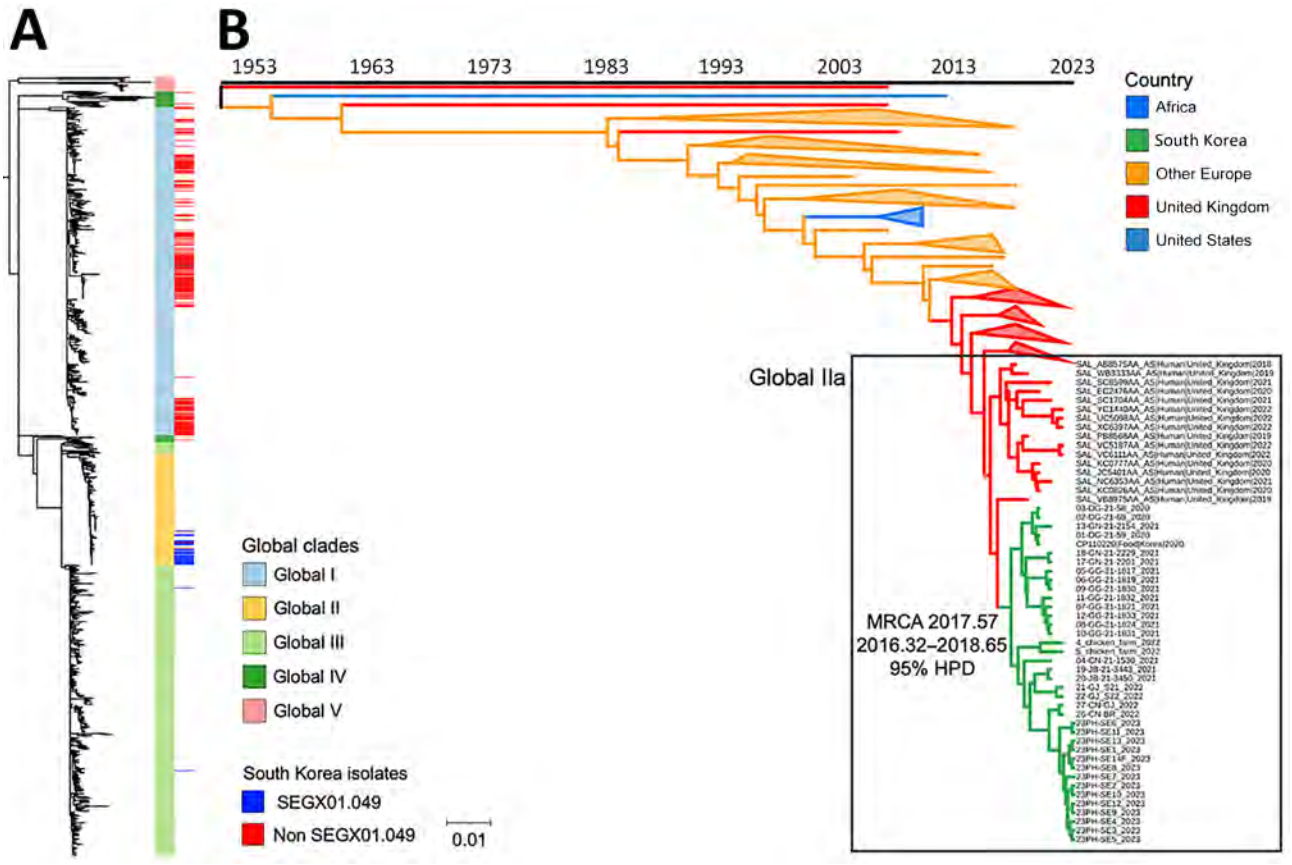

Figure 1. Phylogenetic analysis of *Salmonella enterica* serovar Enteritidis global lineages and those from South Korea. A) Maximum-likelihood phylogenetic tree of whole-genome single-nucleotide polymorphisms of 1,268 global *Salmonella* Enteritidis isolates. Global clades separated by using FastBAPS (*20*) and isolates from South Korea are indicated. Scale bar indicates number of single-nucleotide polymorphisms per site. B) Time-scaled maximum clade credibility tree of the Global II clade of *Salmonella* Enteritidis. Box shows Global IIa clade sequences from South Korea and the United Kingdom; inferred median MRCA and 95% HPD interval are indicated for isolates from South Korea. HPD, highest posterior density; MRCA, most recent common ancestor.

effect size, whereas indicators determined predictor inclusion, which we analyzed by using TRACER. We used sample sizes for each discrete state as predictors to inform transition rate estimates.

Results

Prevalence of SEGX01.049 PFGE Patterns

We determined the 10 most prevalent PFGE patterns of *Salmonella* Enteritidis isolates from sporadic cases and outbreaks submitted to the KDCA during 2013–2024 (Appendix 1 Table 3). The frequency of SEGX01.049 isolates markedly increased from 3.2% in 2018 to 96.5% by August 2024; in addition, the percentage of SEGX01.049-related outbreaks rose from 33.3% in 2020 to 91.7% in 2024 (Appendix 1 Table 3). Among the 23 reported SEGX01.049 outbreaks during 2020–2024, 13 (56%) outbreaks were caused by egg-associated foods, 9 from an unknown source, and 1 from another food type (Appendix 1 Table 4).

Phylogenetic Analysis of *Salmonella* Enteritidis Isolates

We constructed 2 wgSNP phylogenetic trees to compare the isolates from this study with 223 other *Salmonella* Enteritidis genome sequences from South Korea or 1,230 global *Salmonella* Enteritidis genome sequences. The genomes from South Korea grouped into 5 clades (Korea I–V) (Figure 2). All 38 isolates in this study grouped within the distinct Korea III clade, except for isolate 25-DJ-24–5950, which was obtained from a sporadic case in 2014 and grouped within the Korea V clade (Figure 2; Appendix 1 Table 1). Among the 223 *Salmonella* Enteritidis genome sequences from South Korea, 3 sequences from poultry sources (4_chicken farm, 5_chicken farm, and KR40) and 1 sequence (CP11020.1) from food associated with an outbreak (braised burdock) grouped within the Korea III clade (Figure 2). Other genome sequences from poultry sources clustered in Korea I, II, IV, and V clades, indicating a divergence from the isolates in the Korea III clade.

In the phylogenetic tree comprising 1,268 global *Salmonella* Enteritidis sequences (Figure 1, panel A), the sequences grouped into 5 clades (Global I–V); isolates from South Korea grouped into Global I–IV clades. All outbreak-associated isolates collected during 2020–2023 in this study (n = 35) grouped in the Global II clade, along with 3 *Salmonella* Enteritidis genome sequences (CP11020.1, 4_chicken farm, and 5_chicken farm) from South Korea, all isolates selected from the HC5_2301 cluster, and isolates from the Atlantic lineages described previously (*16*) (Appendix 1 Table 1). Three isolates from sporadic cases in 2013 and 2014 in this study belonged to Global I and Global III clades (Appendix 1 Table 1).

Phylogeographic Analysis of Isolates from Other Countries

We performed Bayesian phylogenetic analysis to reconstruct the temporal history of the Global II clade (Figure 1, panel A). The time to most recent common

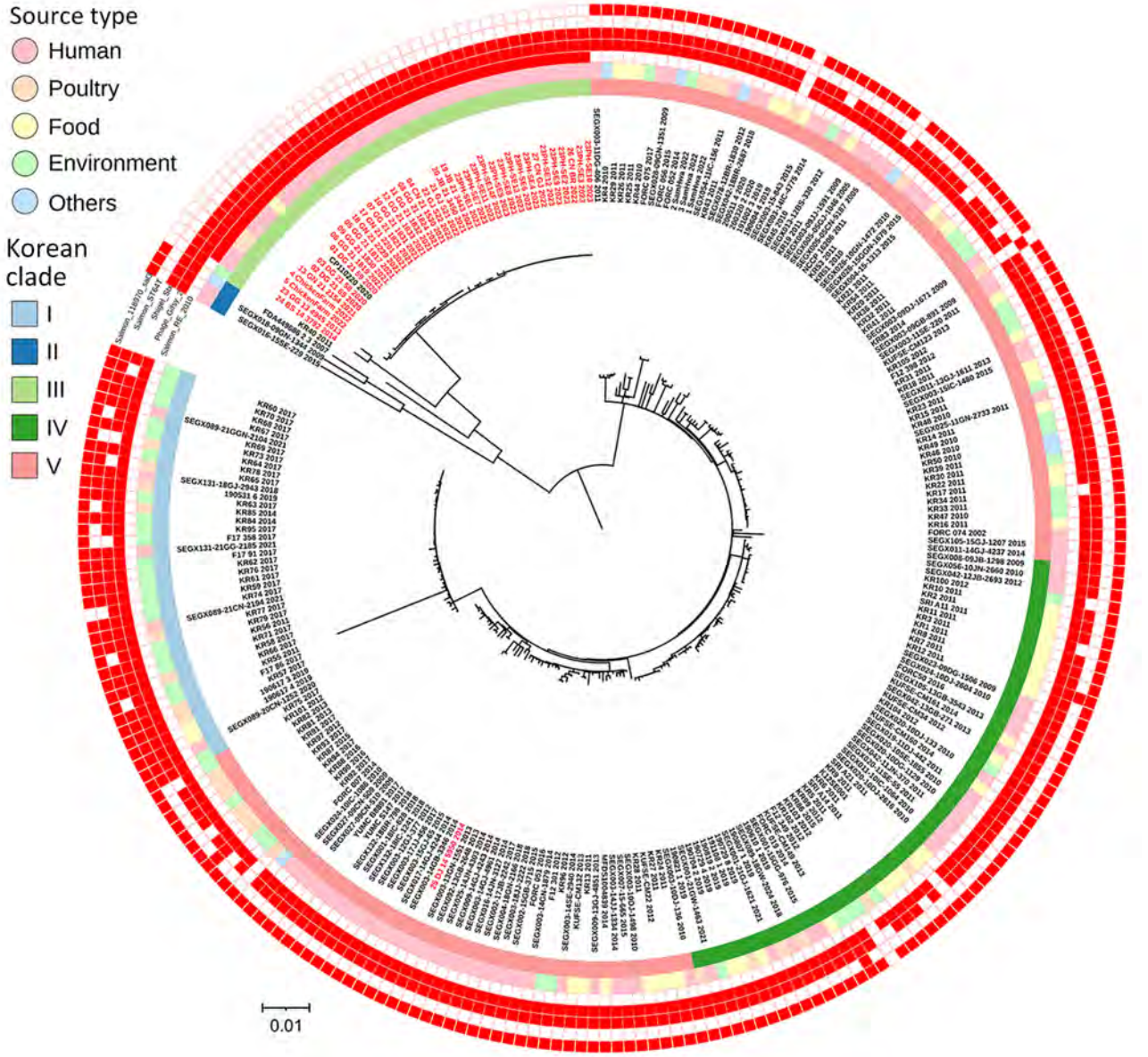

Figure 2. Phylogenetic analysis of distinct *Salmonella enterica* serovar Enteritidis lineage since 2020, South Korea. Maximum-likelihood phylogenetic tree was constructed for whole-genome single-nucleotide polymorphisms of *Salmonella* Enteritidis from South Korea (n = 223) and isolates sequenced in this study (n = 38). Red text indicates isolates from this study. Innermost ring indicates clades separated by using FastBAPS (*20*), followed by sources of isolates. Five outer rings indicate the presence of different prophages; red boxes indicate the presence of prophages with a total count of >30. Isolation year is indicated at the end of each isolate number. Scale bar indicates number of single-nucleotide polymorphisms per site.

ancestor of isolates from South Korea, including the isolates from outbreaks during 2020–2023 (4_chicken farm, 5_chicken farm, and CP110220.1), was estimated as 2017.57 (95% credible interval 2016.32–2018.65) (Figure 1, panel B). The isolates from South Korea within the Global II clade shared recent common ancestors with human isolates (n = 16; Global IIa clade) from the United Kingdom (Figure 1, panel B).

Bayesian phylogeographic analysis of the Global II clade strongly supported the most likely introduction of *Salmonella* Enteritidis into South Korea from the United Kingdom (Bayes factor 111.414; posterior probability 0.97), suggesting the most probable source of this distinct lineage (Appendix 1 Table 5). Other transmission routes were also possible (Appendix 1 Table 5). The generalized linear model analysis indicated sample size had minimal influence on introducing potential bias toward the origin or destination state in the analysis (source indicator, 1.555×10^{-3}; source coefficient, 4.346×10^{-3}; sink indicator, 8.88×10^{-4}; and sink coefficient, 2.48×10^{-2}).

Prophage Patterns, Antimicrobial Drug Resistance, and Virulence Gene Profiles

We summarized the prophage pattern, antimicrobial drug resistance, and virulence gene profiles of the isolates in this study, along with the isolates from the United Kingdom that shared recent common ancestors with our isolates in the Global IIa clade (Appendix 1 Table 6; Appendix 2 Tables 1, 2, https://wwwnc.cdc.gov/EID/article/31/7/24-0043-App2.xlsx). We identified 21 prophages in the isolates from South Korea and those in the Global IIa clade (Figure 2; Appendix 1 Table 6). All isolates within the Global IIa clade exhibited a distinct prophage pattern, harboring Shigel Stx, Phage_Gifsy_2, and Salmon_RE_2010; the Salmon_RE_2010 prophage pattern was absent in other isolates from Korea (Figure 2; Appendix 1 Table 6). All isolates from South Korea carried the *aac(6')-Iaa* aminoglycoside resistance gene. All isolates in the Global II clade, except for 1 isolate (4_chicken farm), exhibited an identical antimicrobial drug resistance profile; the *aac(6')-Iaa* gene was their sole antimicrobial drug resistance determinant (Appendix 2 Table 1). We identified 115 virulence genes in the isolates (Appendix 2 Table 2). The isolates from this study, along with those from the United Kingdom within the Global IIa clade, exhibited similar virulence gene profiles. All isolates carried the complete set of 115 virulence genes, except for *gogB* and *ssek2*, and were divided into 2 distinct profiles according to the presence or absence of the *shdA* gene.

Discussion

Nontyphoidal *Salmonella* serovars generally cause self-limiting gastroenteritis in humans. However, in industrialized countries, ≤5% of cases can progress to invasive extraintestinal disease, leading to bacteremia and focal systemic infections (*27*). Despite the 2 fatal cases associated with the SEGX01.049 type *Salmonella* Enteritidis strains in the Korea III clade, the antimicrobial drug resistance and virulence gene profiles of the fatality-linked isolates from this study were not substantially different from those of other *Salmonella* Enteritidis isolates in South Korea. According to clinical data submitted to KDCA, both fatal cases occurred in patients without documented underlying health conditions. Although host-related factors are known to considerably affect disease outcomes, those clinical findings raise the possibility that pathogen-specific factors, potentially located in noncoding or regulatory regions of the bacterial genome, might also contribute to clinical outcomes. Furthermore, the HC5_2301 cluster has been associated with fatal cases and elevated hospitalization rates in a multicountry outbreak in Europe (*5*).

Phylogenetic analyses suggested that SEGX01.049 *Salmonella* Enteritidis isolates from outbreaks during 2020–2024 formed a distinct group, separate from other isolates from South Korea, and shared a recent common ancestor with human Global IIa clade isolates from the United Kingdom. Moreover, the human isolates within the Global IIa clade exhibited similar prophage patterns, antimicrobial drug resistance profiles, and virulence gene profiles, further supporting the hypothesis of potential introduction of those strains into South Korea. The estimated time to most recent common ancestor of isolates from South Korea within the Global IIa clade was 2017.57, suggesting that introduction into South Korea occurred ≈5 months before the first detection of the SEGX01.049 PFGE pattern in October 2018.

Global dissemination of *Salmonella* Enteritidis has been driven by centralized poultry breeding and international trade (*16*). On the basis of genome sequences and their metadata used in our analysis, it was not possible to determine whether the SEGX01.049 strain was introduced into South Korea via poultry products, trade, or infected travelers. Data from the Food and Agriculture Organization of the United Nations indicated that an average of ≈177,000 live chickens per year were imported into South Korea from the United Kingdom during 2015–2020; the average annual declared value was ≈$3.26 million US (*28*). Although the specific breed and production purpose of live chickens imported from

the United Kingdom are not disclosed in those data, such shipments typically involve breeding stock. Given the central role of imported breeding stock in South Korea's poultry industry, this trade route represents a plausible pathway for the introduction of the SEGX01.049 type *Salmonella* Enteritidis lineage. After the introduction, poultry products played a substantial role in dissemination of that strain, leading to foodborne outbreaks. We showed that 12 of 23 SEGX01.049 outbreaks during 2020–2024 were caused by contaminated eggs (Appendix 1 Table 4), and outbreak-related isolates sequenced in this study, which included samples from human, food, and environmental sources, phylogenetically clustered with *Salmonella* Enteritidis strains from chicken farms in South Korea (Figure 1); those data support the association between SEGX01.049 outbreaks in Korea and domestically produced poultry products. Consistent with that finding, *Salmonella* Enteritidis isolates within the HC5_2301 cluster have been linked to multiple foodborne illness outbreaks associated with the consumption of chicken meat or eggs across Europe since 2014 (*5*,*6*,*29*).

The first limitation of our study is that the analyses relied on retrospective data, which might not capture all instances of SEGX01.049 strains. Second, the genomic analysis was constrained by the availability of reference genomes. Future research should focus on expanding genomic studies to include more diverse isolates and regions. Investigating the role of specific genetic elements in pathogenicity and exploring environmental factors influencing the prevalence of SEGX01.049 would provide valuable insights. Moreover, studies on the potential effects of preventive measures and interventions in controlling outbreaks would be beneficial.

In conclusion, we provide insights into the phylogenetic relationships and potential introduction routes of *Salmonella* Enteritidis into South Korea. Enhanced biosecurity is required to prevent the introduction and dissemination of *Salmonella* Enteritidis across the poultry industry; the role that human activity can play in spread should not be underestimated. Continued genomic surveillance remains invaluable to monitor the spread of foodborne pathogens; such efforts could further the design of improved prevention strategies.

This work was supported by the Konkuk University Research Professor Program and a grant from the Korea Disease Control and Prevention Agency (grant no. 6331-301-210).

About the Author

Dr. Shin is a staff scientist at the Division of Bacterial Diseases, Korea Disease Control and Prevention Agency, and manager of the Kore PulseNet Korea System. Her research interests focus on molecular epidemiology and foodborne bacterial pathogens.

References

1. Ferrari RG, Rosario DKA, Cunha-Neto A, Mano SB, Figueiredo EES, Conte-Junior CA. Worldwide epidemiology of *Salmonella* serovars in animal-based foods: a meta-analysis. Appl Environ Microbiol. 2019;85:e00591–19. https://doi.org/10.1128/AEM.00591-19
2. Jeong HJ, Shin E, Park J, Han J, Kim J, Yoo J. Trends in serotype distribution of *Salmonella enterica* isolated from diarrheal patients in Korea, 2019 to 2021. Public Health Wkly Rep. 2022;15:2615–31. https://doi.org/10.56786/PHWR.2022.15.38.2615
3. Hwang MJ, Park SY, Kim H, Yang SJ, Yang S, Yang JS. Waterborne and foodborne disease outbreaks in the Republic of Korea, 2023. Public Health Wkly Rep. 2025;18:17–32. https://doi.org/10.56786/PHWR.2025.18.1.2
4. Eun JS, Han J, Lim JH, Shin E, Kim J, Ko DJ, et al. Salmonellosis outbreaks linked to eggs at 2 gimbap restaurants in Korea. Epidemiol Health. 2024;46:e2024036. https://doi.org/10.4178/epih.e2024036
5. European Centre for Disease Prevention and Control, European Food Safety Authority. Multi-country outbreak of *Salmonella* Enteritidis sequence type (ST)11 infections linked to eggs and egg products—8 February 2022. EFSA Support Publ. 2022;19:7180E. https://doi.org/10.2903/sp.efsa.2022.EN-7180
6. Benson HE, Reeve L, Findlater L, Vusirikala A, Pietzsch M, Olufon O, et al.; Incident Management Team. Local *Salmonella* Enteritidis restaurant outbreak investigation in England provides further evidence for eggs as source in widespread international cluster, March to April 2023. Euro Surveill. 2023;28:2300309. https://doi.org/10.2807/1560-7917.ES.2023.28.27.2300309
7. Zhou Z, Alikhan NF, Mohamed K, Fan Y, Achtman M, Agama Study Group. The EnteroBase user's guide, with case studies on *Salmonella* transmissions, *Yersinia pestis* phylogeny, and *Escherichia* core genomic diversity. Genome Res. 2020;30:138–52. PubMed https://doi.org/10.1101/gr.251678.119
8. Zhou Z, Charlesworth J, Achtman M. HierCC: a multi-level clustering scheme for population assignments based on core genome MLST. Bioinformatics. 2021;37:3645–6. https://doi.org/10.1093/bioinformatics/btab234
9. La TM, Kim T, Lee HJ, Lee JB, Park SY, Choi IS, et al. Whole-genome analysis of multidrug-resistant *Salmonella* Enteritidis strains isolated from poultry sources in Korea. Pathogens. 2021;10:1615. https://doi.org/10.3390/pathogens10121615
10. Hyeon JY, Li S, Mann DA, Zhang S, Kim KJ, Lee DH, et al. Whole-genome sequencing analysis of *Salmonella enterica* serotype Enteritidis isolated from poultry sources in South Korea, 2010–2017. Pathogens. 2021;10:45. https://doi.org/10.3390/pathogens10010045
11. Jang HJ, Ha YK, Yu SN, Kim SY, Um J, Ha GJ, et al. Molecular epidemiological analysis of food poisoning caused by *Salmonella enterica* serotype Enteritidis in Gyeongnam Province of Korea. J Life Sci. 2023;33:56–63. https://doi.org/10.5352/JLS.2023.33.1.56

12. Bankevich A, Nurk S, Antipov D, Gurevich AA, Dvorkin M, Kulikov AS, et al. SPAdes: a new genome assembly algorithm and its applications to single-cell sequencing. J Comput Biol. 2012;19:455–77. https://doi.org/10.1089/cmb.2012.0021
13. Zankari E, Hasman H, Cosentino S, Vestergaard M, Rasmussen S, Lund O, et al. Identification of acquired antimicrobial resistance genes. J Antimicrob Chemother. 2012;67:2640–4. https://doi.org/10.1093/jac/dks261
14. Liu B, Zheng D, Zhou S, Chen L, Yang J. VFDB 2022: a general classification scheme for bacterial virulence factors. Nucleic Acids Res. 2022;50:D912–7. https://doi.org/10.1093/nar/gkab1107
15. Wishart DS, Han S, Saha S, Oler E, Peters H, Grant JR, et al. PHASTEST: faster than PHASTER, better than PHAST. Nucleic Acids Res. 2023;51:W443–50. https://doi.org/10.1093/nar/gkad382
16. Li S, He Y, Mann DA, Deng X. Global spread of *Salmonella* Enteritidis via centralized sourcing and international trade of poultry breeding stocks. Nat Commun. 2021;12:5109. https://doi.org/10.1038/s41467-021-25319-7
17. Marçais G, Delcher AL, Phillippy AM, Coston R, Salzberg SL, Zimin A. MUMmer4: a fast and versatile genome alignment system. PLOS Comput Biol. 2018;14:e1005944. https://doi.org/10.1371/journal.pcbi.1005944
18. Croucher NJ, Page AJ, Connor TR, Delaney AJ, Keane JA, Bentley SD, et al. Rapid phylogenetic analysis of large samples of recombinant bacterial whole genome sequences using Gubbins. Nucleic Acids Res. 2015;43:e15. https://doi.org/10.1093/nar/gku1196
19. Nguyen LT, Schmidt HA, von Haeseler A, Minh BQ. IQ-TREE: a fast and effective stochastic algorithm for estimating maximum-likelihood phylogenies. Mol Biol Evol. 2015;32:268–74. https://doi.org/10.1093/molbev/msu300
20. Tonkin-Hill G, Lees JA, Bentley SD, Frost SDW, Corander J. Fast hierarchical Bayesian analysis of population structure. Nucleic Acids Res. 2019;47:5539–49. https://doi.org/10.1093/nar/gkz361
21. Katz LS, Griswold T, Morrison SS, Caravas JA, Zhang S, den Bakker HC, et al. Mashtree: a rapid comparison of whole genome sequence files. J Open Source Softw. 2019;4:1762. PubMed https://doi.org/10.21105/joss.01762
22. Rambaut A, Lam TT, Max Carvalho L, Pybus OG. Exploring the temporal structure of heterochronous sequences using TempEst (formerly Path-O-Gen). Virus Evol. 2016;2:vew007. https://doi.org/10.1093/ve/vew007
23. Suchard MA, Lemey P, Baele G, Ayres DL, Drummond AJ, Rambaut A. Bayesian phylogenetic and phylodynamic data integration using BEAST 1.10. Virus Evol. 2018;4:vey016. https://doi.org/10.1093/ve/vey016
24. Darriba D, Posada D, Kozlov AM, Stamatakis A, Morel B, Flouri T. ModelTest-NG: a new and scalable tool for the selection of DNA and protein evolutionary models. Mol Biol Evol. 2020;37:291–4. https://doi.org/10.1093/molbev/msz189
25. Xie W, Lewis PO, Fan Y, Kuo L, Chen MH. Improving marginal likelihood estimation for Bayesian phylogenetic model selection. Syst Biol. 2011;60:150–60. https://doi.org/10.1093/sysbio/syq085
26. Bielejec F, Baele G, Vrancken B, Suchard MA, Rambaut A, Lemey P. SpreaD3: interactive visualization of spatiotemporal history and trait evolutionary processes. Mol Biol Evol. 2016;33:2167–9. https://doi.org/10.1093/molbev/msw082
27. Hajra D, Nair AV, Chakravortty D. Decoding the invasive nature of a tropical pathogen of concern: the invasive non-typhoidal *Salmonella* strains causing host-restricted extraintestinal infections worldwide. Microbiol Res. 2023;277:127488. https://doi.org/10.1016/j.micres.2023.127488
28. Food and Agriculture Organization of the United Nations. Food and agriculture data, 2025 [cited 2025 May 5]. http://www.fao.org/faostat
29. European Centre for Disease Prevention and Control. European Food Safety Authority. Multi-country outbreak of *Salmonella* Enteritidis sequence type (ST)11 infections linked to poultry products in the EU/EEA and the United Kingdom. EFSA Support Publ. 2021;18:6486E. https://doi.org/10.2903/sp.efsa.2021.EN-6486

Address for correspondence: Junyoung Kim, Division of Bacterial Diseases, Department of Disease Diagnosis and Analysis, Korea Disease Control and Prevention Agency, 187, Osongsaengmyeong 2-ro, Osong-eup, Heungdeok-gu, Cheongju-si. Chungcheongbuk-do 28159, South Korea; email: jun49@hanmail.net; and Ji-Yeon Hyeon, 120, Neungdong-ro, College of Veterinary Medicine, Konkuk University, Seoul 05029, South Korea; email: sh702@konkuk.ac.kr

Epidemiologic and Genomic Investigation of Sexually Transmitted *Shigella sonnei*, England

Hannah Charles, David R. Greig, Craig Swift, Israel Olonade, Ian Simms, Katy Sinka, Kate S. Baker, Gauri Godbole, Claire Jenkins

Shigellosis is a bacterial infection that causes enteric illness and can be sexually transmitted, particularly among gay, bisexual, and other men who have sex with men. Multiple extensively drug-resistant *Shigella* strains have been detected through genomic surveillance and are associated with plasmids carrying the gene variant $bla_{\text{CTX-M-27}}$ in the United Kingdom. We report an increase in possible sexually transmitted cases of *Shigella* bacteria carrying the $bla_{\text{CTX-M-15}}$ gene variant, which was previously associated with travel. In 2023, there were 117 cases belonging to the 10 single-nucleotide polymorphism linkage cluster t10.1814. Although this cluster has been documented in England since August 2019, genetic analyses revealed that the $bla_{\text{CTX-M-15}}$ gene variant entered the lineage on a novel resistance plasmid coinciding with the first outbreak case. Our analysis highlights the shifting antimicrobial resistance landscape of sexually transmitted *Shigella* bacteria. Parallel emergence of resistance determinants against third-generation cephalosporins in sexual transmission networks suggests high levels of antimicrobial selection pressure.

Shigellosis is a gastrointestinal infection caused by 1 of 4 bacterial species, *Shigella sonnei*, *S. flexneri*, *S. boydii*, or *S. dysenteriae*. Common symptoms include bloody diarrhea, abdominal pain, cramps, fever, nausea, and vomiting (*1*). *Shigella* spp. are anthroponotic and transmitted by fecal–oral contact (*1*), from hands or objects that were in contact with human feces, including through sexual contact (*2*). Infection can also occur through contaminated food and water (*3*,*4*) or travel to endemic countries (*5*). Community outbreaks are associated with childcare settings, schools, residential institutions, and restaurants (*6*–*8*). Persons at highest risk for infection include those attending childcare settings, travelers to endemic countries, and gay, bisexual, and other men who have sex with men (GBMSM).

The implementation of whole-genome sequencing (WGS) for public health surveillance of bacterial pathogens has enabled global monitoring of the emergence and transmission of epidemic strains of *Shigella* spp. and antimicrobial resistance. Antimicrobial-resistant *S. sonnei* were first described >60 years ago (*9*–*11*), and multidrug-resistant (MDR) strains resistant to aminoglycosides, sulphonamides, trimethoprim, or chloramphenicol are endemic in the human population on every continent (*12*). Resistance to fluroquinolones has recently emerged, including from regions where antimicrobial use is unregulated (*13*–*15*). The increasing incidence of MDR and extensively drug-resistant (XDR) shigellosis in high-prevalence regions where surveillance is limited can be monitored by sequencing strains of *S. flexneri* and *S. sonnei* isolated from returning travelers and analyzing the genome derived antimicrobial resistance profiles.

Since 2010, surveillance systems maintained by the United Kingdom Health Security Agency (UKHSA) have identified a series of epidemics of MDR *S. flexneri* serotypes 3a, 2a, and 1b and *S. sonnei* among GBMSM; the strains are circulating nationally and internationally (*12*,*16*–*18*). Previous studies have demonstrated the acquisition of a plasmid encoding resistance to macrolides corresponded with the emergence of epidemics of *S. flexneri* 3a and 2a and *S. sonnei* during 2010–2015 (*17*,*19*). The subsequent global increase in notification of *S. sonnei* among GBMSM was enabled by strains belonging to global lineage

Author affiliations: United Kingdom Health Security Agency, London, UK (H. Charles, D.R. Greig, C. Swift, I. Olonade, I. Simms, K. Sinka, G. Godbole, C. Jenkins); University of Liverpool, Liverpool, UK (D.R. Greig, K.S. Baker, C. Jenkins); University of Cambridge, Cambridge, UK (K.S. Baker)

DOI: https://doi.org/10.3201/eid3107.241584

3.6.1.1.2 (clonal complex [CC] 152), exhibiting resistance to both macrolides and fluroquinolones (*16*). During the COVID-19 pandemic, a rapid decrease in notifications of *S. sonnei* was observed in the United Kingdom. However, after the relaxation of social distancing and travel restrictions, notifications quickly returned to prepandemic levels (*20*). We observed an increase in XDR *S. sonnei* with the $bla_{\text{CTX-M-27}}$ gene variant conferring resistance to third-generation cephalosporins (*21*). Localized and short-lived outbreaks of XDR *S. sonnei* and *S. flexneri* containing the $bla_{\text{CTX-M-27}}$ gene variant, primarily circulating within GBMSM sexual networks, were described previously (*18*,*22*). In contrast, an epidemic of sexually transmitted XDR *S. sonnei* was recorded in September 2021 (designated t10.377 by using the UKHSA single-linkage hierarchical clustering methodology, contained within global lineage 3.6.1.1.2 and CC152), continued into 2022 and was reported internationally (*21*).

After the publication of a study from France reporting an increase in the proportion of *Shigella* spp. isolates simultaneously resistant to ciprofloxacin, third-generation cephalosporins, and azithromycin (*23*), we reviewed genome-derived antimicrobial resistance profiles of the *S. sonnei* in the UKHSA archive isolated during 2016–2023. We identified an increasing trend of XDR strains of *S. sonnei* and found XDR *S. sonnei* isolated from MSM almost exclusively had the $bla_{\text{CTX-M-27}}$ gene variant, whereas XDR *S. sonnei* isolated from travelers returning from high-risk regions almost exclusively had the $bla_{\text{CTX-M-15}}$ gene variant (*24*). In 2023, we detected an increase of XDR *S. sonnei* in England that contained the $bla_{\text{CTX-M-15}}$ gene variant. The aim of this study was to use a combination of epidemiologic data with short-read and long-read genomic sequencing data for outbreak investigation to determine emergence and transmission patterns of the *S. sonnei* outbreak strain and acquisition of the $bla_{\text{CTX-M-15}}$ gene variant.

Methods

Routine Laboratory and Epidemiologic Surveillance

Shigella spp. isolates from hospital and community cases with gastrointestinal symptoms are referred to the gastrointestinal bacterial reference unit at the UKHSA for confirmation and typing. Since September 2015, we have conducted WGS for all *Shigella* isolates submitted to the gastrointestinal bacterial reference unit as previously described (*25*) and derived the serotype and antimicrobial resistance profile in silico from the genome. *S. sonnei* isolates submitted to the gastrointestinal bacterial reference unit during January 2016–December 2023 were included in this study. Because of the lack of sexual orientation information available in this dataset, we used a proxy indicator of cases that might be attributed to sexual transmission among GBMSM, defined as cases among male adults (≥16 years) without a history of travel or where travel history was unknown (presumptive men who have sex with men [MSM]) (*26*).

We analyzed the sequencing data for genomic markers of resistance to azithromycin (defined as the presence of *ermB* or *mphA*), ciprofloxacin (defined as the presence of mutations in *gyrA*, *parC*, or *qnr*), and third-generation cephalosporins (defined by the presence of $bla_{\text{CTX-M}}$ genes). We defined XDR isolates as those containing genomic markers of resistance to azithromycin, ciprofloxacin, and third-generation cephalosporins.

We conducted single-nucleotide polymorphism (SNP) typing on *S. sonnei* isolates. We applied single-linkage hierarchical clustering at 7 descending thresholds of SNP distances (Δ250, Δ100, Δ50, Δ25, Δ10, Δ5, Δ0) as previously described (*26*). That clustering resulted in a discrete 7-digit code in which each number represents the cluster membership at each descending SNP distance threshold. For *Shigella* spp. surveillance, we designated isolates that cluster at the 10 SNP threshold t10.X. We duplicated sequencing data in line with routine genomic surveillance of *Shigella* spp. at UKHSA. We tested the differences in proportions by using 2-proportion Z-tests and defined $p \leq 0.05$ as significant.

Phylogenetic Tree Construction

We used the WGS data from routine laboratory surveillance to create a phylogenetic tree of *S. sonnei* isolates with $bla_{\text{CTX-M}}$ gene variants. We produced 1,325 samples from a soft-core genome alignment of CC152 within nucleotide cluster t25:1, in which a given variant position belonged to ≤80% of strains in the alignment, by using SnapperDB v0.2.8 (*27*). We previously masked recombinant sequences from a whole genome alignment derived from SnapperDB v0.2.8 (*27*) on the same dataset by using Gubbins v3.2 (*28*). We used the alignment (2,142,354 bp) as the input for IQ-TREE v2.0.4 (*29*) to generate a phylogenetic tree. We then repeated the methodology to produce subtrees of each cluster containing genomes with $bla_{\text{CTX-M}}$ variants. For each phylogeny, the tree was rooted by the most closely related strain outside the cluster range in question.

Nanopore Sequencing and De Novo Assembly

We used Illumina (Illumina, https://www.illumina.com) for routine sequencing and Oxford Nanopore

(Oxford Nanopore Technologies, https://nanoporetech.com) for long-read sequencing to generate complete assemblies of selected bla_{CTX-M} variant samples to understand the genetic context for antimicrobial resistance determinants. We extracted and sequenced genomic DNA by using the MinION (Oxford Nanopore Technologies) and processed data, trimmed reads, and assembled as described previously (*30*).

We conducted de novo assembly by using Flye v2.9.2 (*31*). We corrected the assemblies by using Medaka version 1.0.3 (https://github.com/nanoporetech/medaka) with a *Shigella*-specific medaka-trained model, and then by using Polypolish v0.5.0 (*32*) with the equivalent Illumina FASTQs (Illumina) for each assembly. Because all the contigs were circular and closed, we reoriented them to start at the *dnaA* gene (GenBank accession no. NC_000913) from *E. coli* K12, by using the fix start parameter in Circlator version 1.5.5 (*33*).

Antimicrobial Resistance Gene Detection and Plasmid Typing

We detected the plasmid replicon for each nonchromosomal contig within the final assembly of each sample by using PlasmidFinder version 2.1 (*34*) with the Enterobacteriaceae database and these parameters: minimum identity = 90% and minimum coverage = 90%. We annotated the mobile genetic elements with antimicrobial resistance determinants by using the Prokaryotic Genome Annotation Pipeline build 2022-12-13 (*35*). We generated gene-level alignments by using Clinker version 0.0.27 (*36*).

Data Deposition

We submitted the FASTQ files and gene assemblies to the National Center for Biotechnology Information (BioProject no. PRJNA315192). Accession numbers have been provided (Appendix Table 1, https://wwwnc.cdc.gov/EID/article/31/7/24-1584-App1.xlsx).

Ethics Statement

This study was undertaken for health protection purposes. Permission was granted to UKHSA to collect and process confidential patient data under Regulation 3 of The Health Service (Control of Patient Information) Regulations 2020 and Section 251 of the National Health Service Act 2006.

Results

Descriptive Epidemiology

S. sonnei diagnoses increased during 2016–2018, then declined slightly in 2019 and declined markedly in 2020 and 2021, likely because of reduced access to healthcare services and testing, social distancing, and travel restrictions during the COVID-19 pandemic (Figure 1). In 2022 and 2023, there was a substantial increase in *S. sonnei* diagnosis notifications, and the 2023 notifications exceeded prepandemic levels. The trends of *S. sonnei* among presumptive MSM mirror those among all persons. However, the rate of increase was larger among presumptive MSM, leading to an increase in the proportion of all *S. sonnei* diagnoses seen among presumptive MSM, from 26% in 2016 to 46% in 2023. The increase between 2022 and 2023 was also higher among presumptive MSM (82% increase) compared with all persons (50% increase).

Including the increase in *S. sonnei* among presumptive MSM in 2023, there was a corresponding increase in the number and proportion of *S. sonnei* isolates with the $bla_{CTX-M-15}$ gene variant in the population.

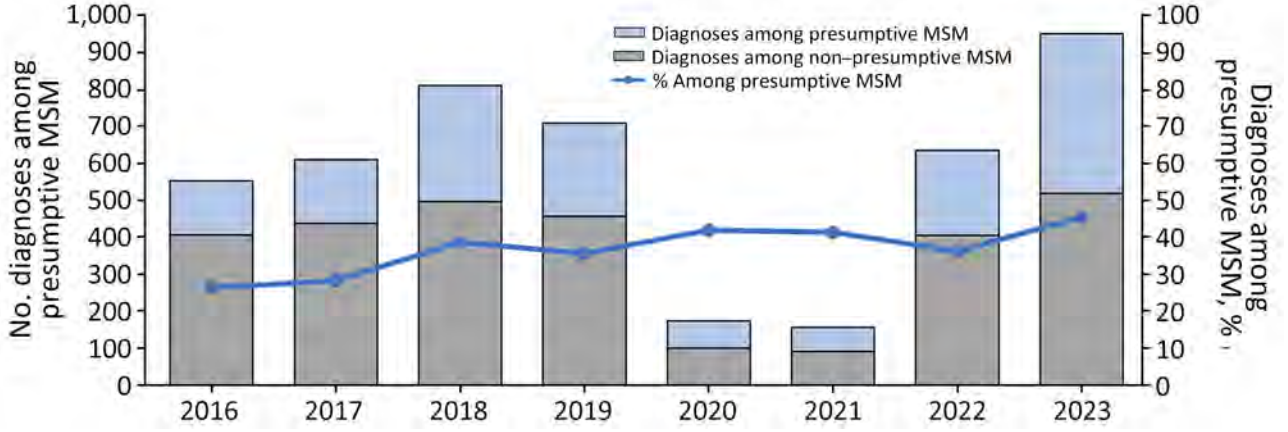

Figure 1. Epidemiologic and genomic investigation of sexually transmitted *Shigella sonnei* diagnoses in presumptive MSM classification, England, 2016–2023. Presumptive MSM category was defined as cases among male adults (≥16 years of age) without a history of travel or where travel history was unknown. MSM, men who have sex with men.

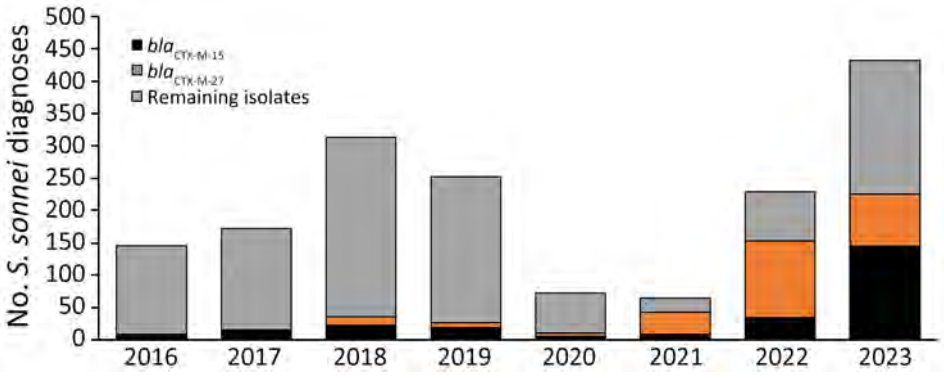

Figure 2. Sexually transmitted *Shigella sonnei* isolates among presumptive men who have sex with men by the presence of the $bla_{\text{CTX-M-15}}$ or $bla_{\text{CTX-M-27}}$ gene variant from an epidemiologic and genomic investigation, England, 2016–2023. Presumptive men who have sex with men category was defined as cases among male adults (≥16 years of age) without a history of travel or where travel history was unknown.

During 2016–2022, an average of 10% of *S. sonnei* isolates contained the $bla_{\text{CTX-M-15}}$ gene variant, increasing to 33% in 2023. That increase in the proportion of *S. sonnei* isolates with the $bla_{\text{CTX-M-15}}$ gene variant in 2023 corresponded with a decrease in *S. sonnei* isolates with the $bla_{\text{CTX-M-27}}$ gene variant in this population group (Figure 2).

Before 2023, *S. sonnei* isolates with the $bla_{\text{CTX-M-15}}$ gene variant were identified at a much lower frequency among presumptive MSM compared with non–presumptive MSM (i.e., women, children, and men reporting recent travel). During 2016–2022, the proportion of *S. sonnei* with the $bla_{\text{CTX-M-15}}$ gene variant among presumptive MSM remained stable at an average of 17%, increasing to 38% in 2023 (Figure 3).

Phylogenetic Analysis of *S. sonnei* with the $bla_{\text{CTX-M-15}}$ Gene Variant

Of the 262 *S. sonnei* isolates with the $bla_{\text{CTX-M-15}}$ gene variant collected during 2016–2023 from presumptive MSM, 84 (32%) fell within a 10-SNP single linkage cluster (SCL) designated t10.1814 (full SNP address 1.1.1.1.1814) and belonging to global lineage 3.6.1.1 (*37*) (Figure 4). In addition, 2 other 10-SNP SCLs contained isolates with the $bla_{\text{CTX-M-15}}$ gene variant were identified, t10.1148 (full SNP address 1.1.29.49.1148) and t10.2187 (full SNP address 1.1.29.49.2187). Those 2 clusters fall within the same 25-SNP SCL (t25:49), a lineage that is associated with travel to Pakistan (82% of case-patients reporting travel to Pakistan) and Tunisia (94% of case-patients reporting travel to Tunisia), but distinct from the 25-SNP SCL containing t25:1. The remaining *S. sonnei* isolates with the $bla_{\text{CTX-M-15}}$ gene variant from presumptive MSM were phylogenetically sporadic and did not form large clusters (Figure 5). Therefore, our phylogenetic analysis focuses on the t10.1814 cluster to explore the increase in *S. sonnei* containing the $bla_{\text{CTX-M-15}}$ gene variant among presumptive MSM (Figure 4).

At the end of 2023, the t10.1814 cluster contained 124 isolates in total. The first 3 cases within the cluster were diagnosed in August and October 2019. None of those isolates contained $bla_{\text{CTX-M-15}}$; however, 2 of the 3 isolates contained the $bla_{\text{CTX-M-27}}$ gene variant (Figures 4, 5, and 6). There was no reported activity within the t10.1814 cluster until March 2022, but 4 cases were reported during March–December 2022. There was a substantial increase in cases in 2023, and most isolates (94%, 117/124) in the cluster had specimen dates in 2023. Of the 2023 isolates, 92% (108/117) contained the $bla_{\text{CTX-M-15}}$ gene variant (Figure 6). Of the 124 cases in the cluster, 75% (n = 93) were adult men with no or unknown travel, 16% (n = 20) were adult men with travel outside the UK (mostly to countries in Europe), and 9% (n = 11) were women or children with no or unknown travel (Table 1).

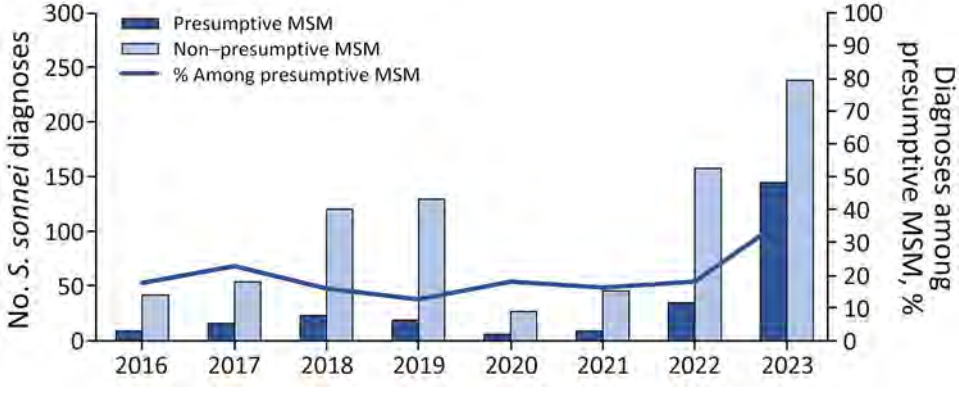

Figure 3. *Shigella sonnei* isolates with the $bla_{\text{CTX-M-15}}$ gene variant among presumptive men who have sex with men compared with nonpresumptive men who have sex with men from an epidemiologic and genomic investigation, England, 2016–2023. Presumptive MSM was defined as cases among male adults (≥16 years of age) without a history of travel or where travel history was unknown.MSM, men who have sex with men.

Figure 4. Maximum-likelihood phylogenetic tree of the *Shigella sonnei* clonal complex 152 within the 10 single-nucleotide polymorphism linkage cluster t10.1814 (n = 125) found during an epidemiologic and genomic investigation of sexually transmitted *S. sonnei* from presumptive men who have sex with men, England, 2016–2023. A total of 125 isolates included in tree. Sequence read run accession is sample identification, additional information provided is gender, presence of $bla_{\text{CTX-M}}$ gene variants, and association with travel. Presumptive men who have sex with men was defined as cases among male adults (≥16 years of age) without a history of travel or where travel history was unknown.

The increase in t10.1814 occurred in parallel to a decline in cases within the 1.1.1.1.377.% cluster (designated t10.377; the % indicates that t3 and t0 positions of the SNP address can take any value). The cluster was dominant since 2017, declined substantially during the first few months of the COVID-19 pandemic, but reemerged in September 2021 with third-generation cephalosporin resistance caused by the $bla_{\text{CTX-M-27}}$ gene variant (*21*) (Figure 7). Despite the different trends in those clusters, t10.1814 and t10.377 share similarities in demographic characteristics of cases; the t10.377 cluster was also associated with presumptive MSM (Appendix Table 2).

Of the 124 isolates in the t10.1814 cluster, 112 (90%) harbored the $bla_{\text{CTX-M-15}}$ gene variant, whereas only 2 isolates had the $bla_{\text{CTX-M-27}}$ gene variant; no isolates expressed both the $bla_{\text{CTX-M-15}}$ and $bla_{\text{CTX-M-27}}$ gene variants. Resistance to ciprofloxacin and azithromycin was very high; 94% of isolates (116/124) exhibited mutations in either *gyrA*, *parC*, or the plasmid

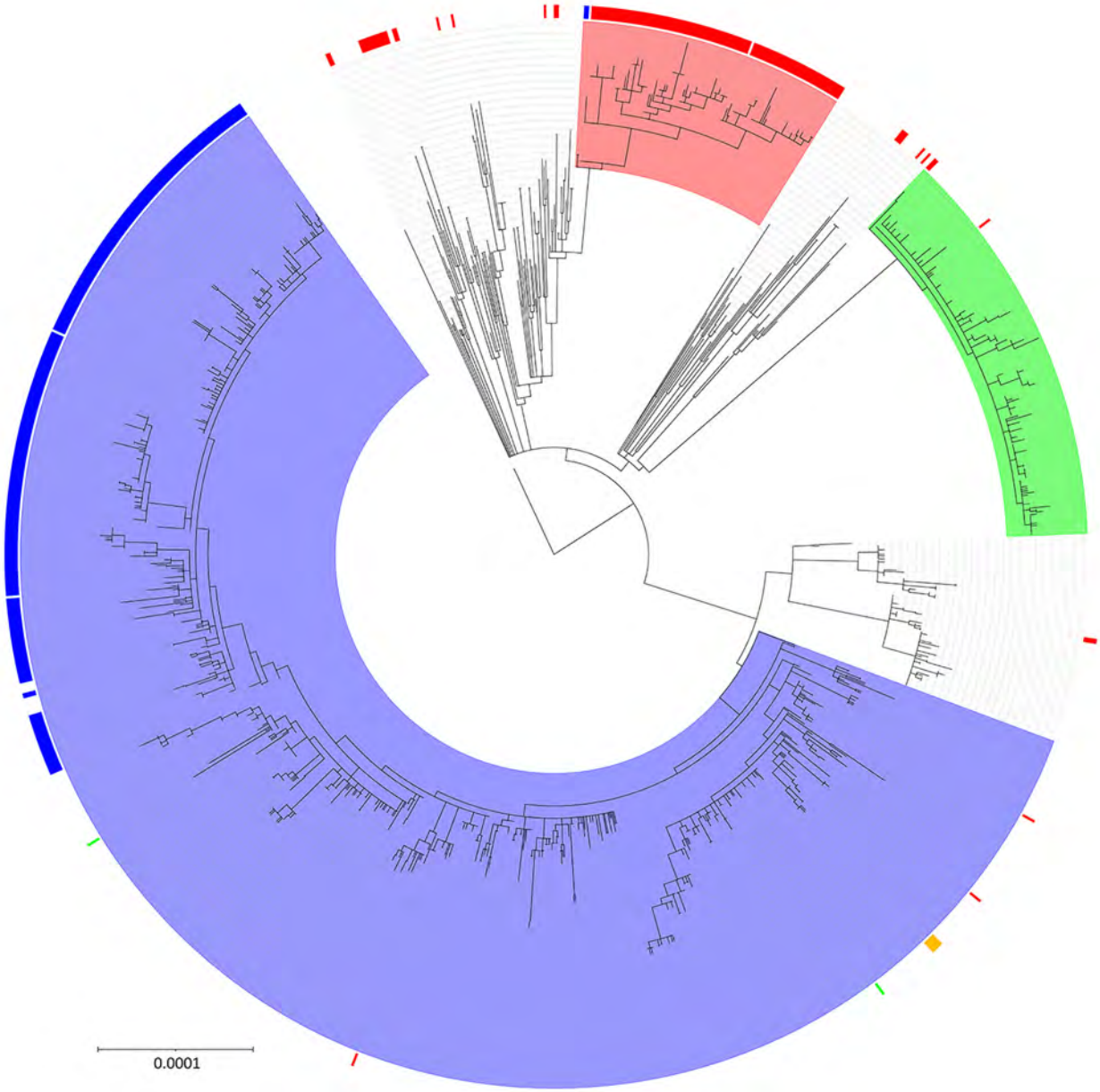

Figure 5. Maximum-likelihood phylogenetic tree of clonal complex 152 within nucleotide cluster t25:1 found during an epidemiologic and genomic investigation of sexually transmitted *Shigella sonnei* from presumptive men who have sex with men, England, 2016–2023. Included in the tree were 1,325 isolates. Blue, t10.377 cluster; green, t10.2218 cluster; red, t10.1814. The outer ring indicates presence of $bla_{\text{CTX-M}}$; red, $bla_{\text{CTX-M-15}}$; blue, $bla_{\text{CTX-M-27}}$; orange, $bla_{\text{CTX-M-134}}$; green, $bla_{\text{CTX-M-55}}$. Presumptive men who have sex with men was defined as cases among male adults (≥16 years of age) without a history of travel or where travel history was unknown.

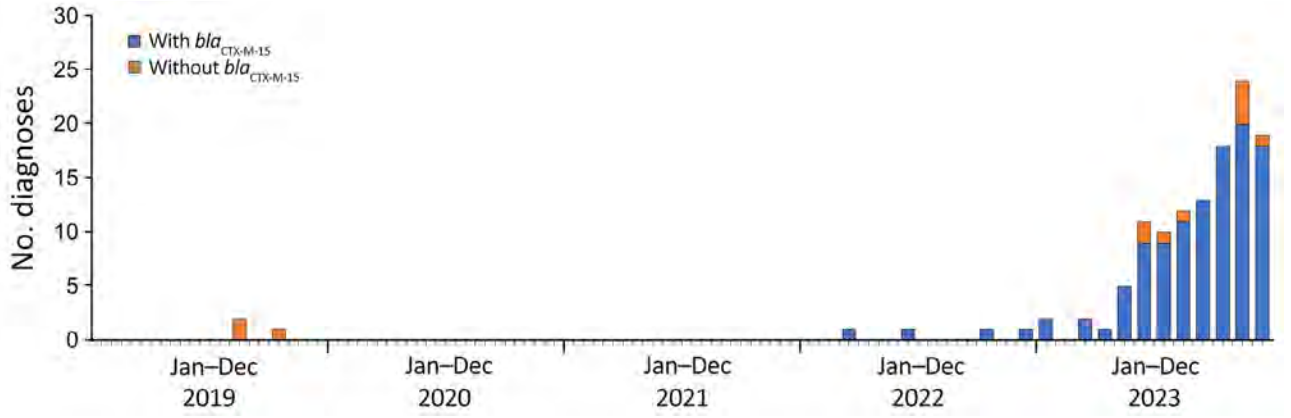

Figure 6. Diagnoses of *Shigella sonnei* in cluster t10.1814 by the $bla_{CTX-M-15}$ gene variant status from an epidemiologic and genomic investigation, England, 2016–2023.

mediated *qnr* gene variant, and 88% of isolates (109/124) had genomic markers for azithromycin resistance (*ermB* or *mphA*). Most (86%) isolates had both the $bla_{CTX-M-15}$ gene variant and markers of azithromycin resistance. Overall, 109 (88%) isolates in the t10.1814 cluster were XDR (Table 2).

Phylogenetic analysis revealed that t10.1814 fell within the wider t25:1 cluster that also includes t10.377. Although located within the same t25 SLC, the t10.1814 cluster with $bla_{CTX-M-15}$ was located on a separate branch and did not evolve from the t10.377 cluster with the $bla_{CTX-M-27}$ gene variant (Figure 5). The progenitor strains of t10.1814 clustered with the $bla_{CTX-M-15}$ gene variant also contained the $bla_{CTX-M-27}$ gene variant.

Table 1. Characteristics of sexually transmitted *Shigella sonnei* from an epidemiologic and genomic investigation of the t10.1814 cluster, England, 2016–2023*

Characteristics	Cases, N = 124
Sex	
M	113 (91)
F	11 (9)
Age, y	
Median [IQR]	35 [30–43]
Adult, ≥16	123 (99)
Child, <16	1 (1)
Travel	
Yes	20 (16)
No/Unknown	104 (84)
Travel destination of those reporting travel	
Belgium	1 (5)
Brazil	1 (5)
Europe, country unknown	1 (5)
Germany	1 (5)
India	1 (5)
Netherlands	1 (5)
North America	1 (5)
Spain	8 (40)
Thailand	1 (5)
United states	1 (5)
Unknown	3 (15)
Presumptive MSM	
Yes	93 (75)
No	31 (25)

*Values are no. (%) except as indicated. Presumptive MSM category was defined as cases among male adults (≥16 years of age) without a history of travel or where travel history was unknown. MSM, men who have sex with men.

Analysis of t10.1814 IncFII Plasmids and Comparison to t10.377 IncFII Plasmids

Plasmids within t10.1814 with the $bla_{CTX-M-15}$ gene variant were all determined to be of the IncFII replicon type and ranged from 77.6 to 149.0 kbp in size (Figure 8). Plasmids from progenitor strains within t10.1814 with the $bla_{CTX-M-27}$ gene variant were larger on average (148 kbp) than plasmids with the $bla_{CTX-M-15}$ gene variant (78.4 kbp). Despite the difference in size, almost all the gene content of the ≈74 kbp plasmids were also found within the larger ≈148 kbp plasmids. Of note, when comparing t10.1814 plasmids to IncFII plasmids from t10.377, the plasmid structure is the same except for small alterations to the variable region, including the $bla_{CTX-M-15}$ and $bla_{CTX-M-27}$ integrons (Figure 8).

After the analysis of the long-read sequencing data, we identified 1 isolate of *S. sonnei* with the $bla_{CTX-M-15}$ gene variant in the same clade as t10.1814 but in a different t10 SLC (t10.2404). In that cluster, the $bla_{CTX-M-15}$ gene variant was located on a 7.6-kbp cassette or an element integrated on the chromosome. The integration site appears to be a prophage remnant near a tRNA-Phe gene (Figure 9). The IncFII plasmid was lost in this sample.

Discussion

Overall, except for 2020 and 2021 when notifications were affected by the COVID-19 pandemic, we observed a steady increase of *S. sonnei* diagnoses in England during 2016–2023. During the past decade, diagnostic methods for the detection of gastrointestinal

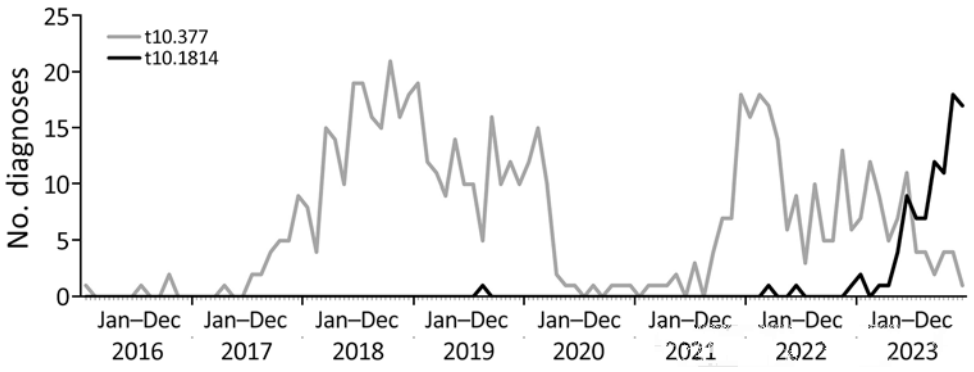

Figure 7. Diagnoses of *Shigella sonnei* in the t10.377 cluster compared with the t10.1814 cluster among presumptive men who have sex with men from an epidemiologic and genomic investigation, England, 2016–2023. Presumptive MSM was defined as cases among male adults (≥16 years of age) without a history of travel or where travel history was unknown.

pathogens have improved with widespread implementation of commercial PCRs. PCR is more sensitive than culture for detecting *Shigella* spp. (*38*,*39*), and this move toward molecular methods after culture will increase case confirmation. Furthermore, the increase might be associated with increased travel to high-risk regions outside the United Kingdom, although confirming that theory is difficult because travel history is poorly captured by the current surveillance system. We also observed a steady increase in notifications of *S. sonnei* among presumptive MSM. Although our observation may reflect a true increase in sexual transmission, it might also be influenced by increased implementation of PCR testing and travel. The increase in reported diagnoses might be because of the publication of briefing notes and other outbreak-related communications by UKHSA during the study period.

Numerous factors enable the emergence, transmission, and persistence of epidemic strains circulating within GBMSM sexual networks, involving pathogen characteristics, host behaviors, and environmental pressures. We have previously hypothesized that the sequential waves of shigellosis among GBMSM in the United Kingdom have been enabled by acquisition of antimicrobial resistance to an increasing number of classes of antimicrobial drugs (*40*). The epidemic strains of *S. sonnei* were initially resistant to macrolides, then to both azithromycin and ciprofloxacin, and most recently to macrolides, fluroquinolones, and third-generation cephalosporins (*16*,*21*). However, the acquisition of antimicrobial resistance alone does not explain the emergence and persistence of all shigellosis epidemics among GBMSM. In this study, we showed the previous epidemic *S. sonnei* strain (t10.377) was replaced by another strain of *S. sonnei* (t10.1814) with the same genotypic antimicrobial resistance profile, and the reemergent strain of *S. flexneri* 3a in 2019 was more susceptible to antimicrobials than the strain that caused the original *S. flexneri* 3a epidemic (*41*). Asymptomatic transmission of *Shigella* spp. among GBMSM might be a factor driving antimicrobial pressure in this group (*42*). Other strains during previous epidemics are examples of the emergence and persistence of strains exhibiting the same antimicrobial resistance profiles. Other factors could be at play, such as transient host immunity to circulating serotypes providing emergent serotypes with a competitive advantage. Host immunity seems an unlikely explanation for the strain replacement event because both strains were *S. sonnei*.

Overall, the case characteristics in the t10.1814 cluster were similar to those in the t10.377 cluster in terms of the proportion of male cases and age distribution. Some regional variation exists; cases in the t10.1814 cluster were more dispersed across regions of England, and the t10.377 cluster was more concentrated in London (Appendix Table 2). The difference in travel history between cases in the clusters could be because of missing data on recent travel history.

Phylogenetic analyses showed clustering of $bla_{\text{CTX-M}}$ variants within the *Shigella* spp. population structure, consistent with horizontal acquisition and vertical transmission. Non-GBMSM clades associated with the $bla_{\text{CTX-M-15}}$ gene variant comprised cases reporting travel to high-risk regions outside the United Kingdom, highlighting the possibility that this resistance determinant was brought in through travel, similar to *Shigella* in other regions (*43*,*44*). One

Table 2. Antimicrobial resistance profile of sexually transmitted cases of *Shigella sonnei* from an epidemiological and genomic investigation of cases within the t10.1814 cluster, England, 2016–2023*

Antimicrobial and resistance determinant	Cases, N = 124
Third-generation cephalosporin	
$bla_{\text{CTX-M-15}}$ gene variant	112 (90)
$bla_{\text{CTX-M-27}}$ gene variant	2 (2)
Ciprofloxacin: *gyrA*, *parC*, or *qnr*	116† (94)
Azithromycin: *ermB* or *mphA*	109 (88)
Extensively drug resistant	109 (88)

*Values are no. (%).
†All isolates had 2 point mutations in *gyrA* and 1 point mutation in *parC*.

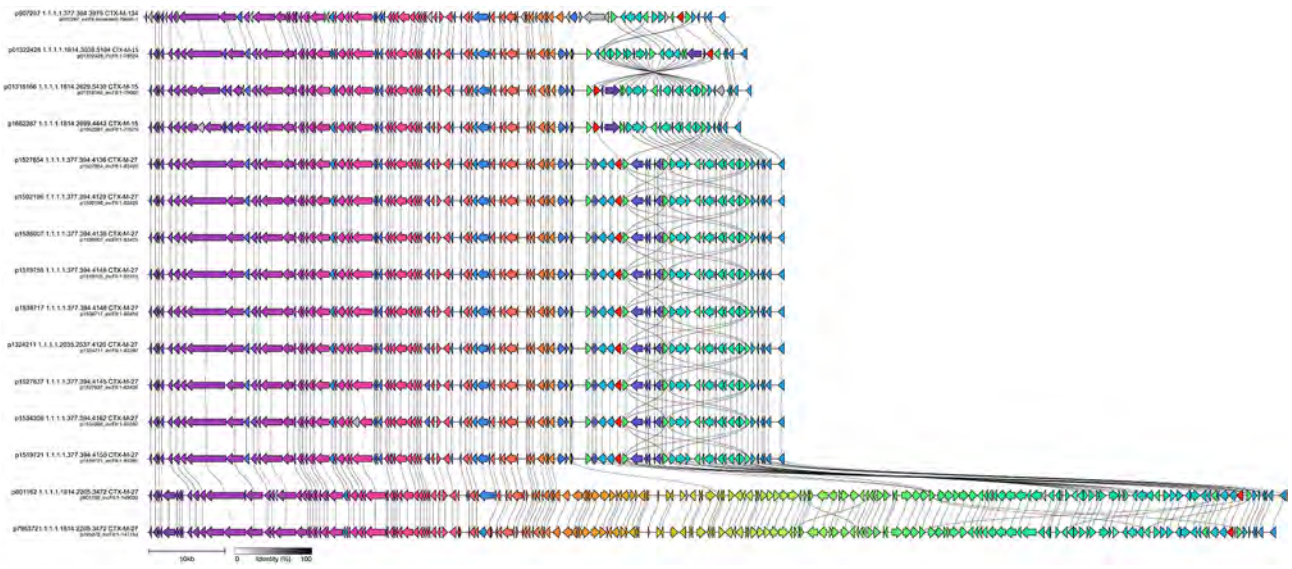

Figure 8. Alignment of IncFII plasmids in samples selected for Nanopore sequencing during an epidemiologic and genomic investigation of sexually transmitted *Shigella sonnei* from presumptive men who have sex with men, England, 2016–2023. Red gene is the *bla*$_{\text{CTX-M}}$ variant. Presumptive men who have sex with men was defined as cases among male adults (≥16 years of age) without a history of travel or where travel history was unknown

GBMSM *bla*$_{\text{CTX-M-15}}$ gene variant isolate fell within the same 10 SNP SLC, and although the *bla*$_{\text{CTX-M-27}}$ gene variant decrease coincided with the *bla*$_{\text{CTX-M-15}}$ gene variant increase, there was no evidence the *bla*$_{\text{CTX-M-15}}$ gene variant emerged from the clade with the *bla*$_{\text{CTX-M-27}}$ gene variant. The acquisition of the *bla*$_{\text{CTX-M-15}}$ gene variant appears to be an independent evolutionary event on a different branch of the phylogeny.

Long-read sequencing analysis revealed that, like the *bla*$_{\text{CTX-M-27}}$ gene variant in the t10.377 cluster, the *bla*$_{\text{CTX-M-15}}$ gene variant in the current epidemic t10.1814 cluster was located on an IncFII plasmid. Despite encoding different *bla*$_{\text{CTX-M}}$ variants, the plasmid encoding the *bla*$_{\text{CTX-M-15}}$ gene variant exhibited high levels of similarity to the plasmid encoding the *bla*$_{\text{CTX-M-27}}$ gene variant. Those data reveal similar IncFII plasmids persist and remain stable in the strains of *S. sonnei* circulating among GBMSM, despite acquisition of different antimicrobial resistance determinants. Because of the apparent plasmid stability in this population, our demonstration of the acquisition of the *bla*$_{\text{CTX-M-27}}$ and *bla*$_{\text{CTX-M-15}}$ gene variants and subsequent clonal expansion, the potential other antimicrobial resistance determinants could be acquired onto this plasmid and worsen the already concerning antimicrobial resistance picture of *S. sonnei* remains. In addition, we report an isolate in a separate clade (t10.2404) in which the *bla*$_{\text{CTX-M-15}}$ gene variant was located on the chromosome and the associated plasmid was lost.

Social distancing and travel restrictions in 2020 and 2021 related to the COVID-19 pandemic had a greater effect on reducing notifications of *S. sonnei* than *S. flexneri* (*25*). Previously, we considered that globalization and increased travel might have a role in seeding sexually transmissible shigellosis. The acquisition of the *bla*$_{\text{CTX-M-15}}$ gene variant previously associated with travel-related cases of *S. sonnei*, on the GBMSM-associated IncFII pKSR-100-like plasmid, may provide further evidence for this hypothesis. The reporting of *S. sonnei* with the *bla*$_{\text{CTX-M-15}}$ gene variant among GBMSM in other countries in Europe

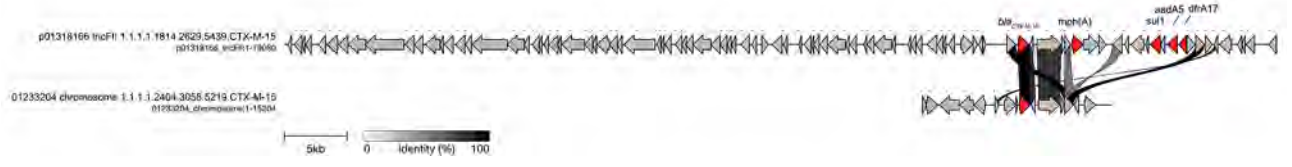

Figure 9. Alignment of exemplar IncFII plasmid from a *Shigella sonnei* strain during an epidemiologic and genomic investigation of sexually transmitted *Shigella sonnei* from presumptive men who have sex with men, England, 2016–2023. The strain fell within the 10 single-nucleotide polymorphism linkage cluster t10.1814 and strain 01233204 (GenBank accession no. SRR29176725), showing the cassette containing *bla*$_{\text{CTX-M-15}}$ (highlighted in red) has moved to the chromosome. Presumptive men who have sex with men was defined as cases among male adults (≥16 years of age) without a history of travel or where travel history was unknown.

suggests the potential international distribution of this lineage (*45*,*46*).

With a lack of information about sexual orientation and incomplete travel histories, it is possible that adult male case-patients who traveled were categorized as presumptive MSM within this cluster if the travel histories were not known. Identifying as GBMSM and reporting recent travel are also not mutually exclusive; therefore, there are limitations with the use of the presumptive MSM proxy definition. It is also not mandatory for primary diagnostic laboratories to send *S. sonnei* isolates to the gastrointestinal bacterial reference unit, so the data available for this analysis represents about two thirds of the total number of reported infections.

Despite those limitations, the introduction of WGS for typing gastrointestinal pathogens greatly improved surveillance of *S. sonnei* at UKHSA. Previously, we relied on phenotypic methods that were highly specialized, labor intensive, and difficult to standardize, such as phage typing and antimicrobial susceptibility testing. During the past decade, sequencing data has been used to construct the population structure of *S. sonnei* from UK residents and mapped clades associated with travel and associated with sexual transmission among GBMSM. We have tracked the rise and fall of different clades circulating within GBMSM sexual networks and showed that acquisition of antimicrobial resistance and genetic factors contribute to emergence, transmission, and persistence. However, notifications continue to rise, and the circulating strains are increasingly resistant to first- and second-line antimicrobial drugs.

The results in this article highlight the continued utility of genomic surveillance in detecting outbreaks of sexually transmissible shigellosis and the ever-growing importance of antimicrobial stewardship for shigellosis (*47*). Furthermore, through detailed analyses of the data, we can clarify the complex origins and transmission pathways for antimicrobial resistance in increasingly antimicrobial-resistant strains. We recurrently see conjugative plasmids carrying resistance against key antimicrobial classes mobilizing among *Shigella* spp. strains circulating in different transmission networks. This plasmid mobilization underlines the need to address *Shigella* spp. as an urgent antimicrobial threat, in line with the World Health Organization priority pathogen list of 2024 (*48*), and highlights the need to create innovative solutions to slow sexual transmission in networks in which heavy antimicrobial use drives the emergence of XDR strains.

About the Author

Hannah Charles is a principal epidemiologist at the United Kingdom Health Security Agency. Her research interests include the real-time and enhanced surveillance of sexually transmissible infections, including outbreaks and incidents of *Shigella*.

References

1. Kotloff KL, Riddle MS, Platts-Mills JA, Pavlinac P, Zaidi AKM. Shigellosis. Lancet. 2018;391:801–12. https://doi.org/10.1016/S0140-6736(17)33296-8
2. Williamson DA, Chen MY. Emerging and reemerging sexually transmitted infections. N Engl J Med. 2020;382:2023–32. https://doi.org/10.1056/NEJMra1907194
3. Warren BR, Parish ME, Schneider KR. *Shigella* as a foodborne pathogen and current methods for detection in food. Crit Rev Food Sci Nutr. 2006;46:551–67. https://doi.org/10.1080/10408390500295458
4. Qiu S, Liu K, Yang C, Xiang Y, Min K, Zhu K, et al. A *Shigella sonnei* clone with extensive drug resistance associated with waterborne outbreaks in China. Nat Commun. 2022;13:7365. https://doi.org/10.1038/s41467-022-35136-1
5. López-Vélez R, Lebens M, Bundy L, Barriga J, Steffen R. Bacterial travellers' diarrhoea: a narrative review of literature published over the past 10 years. Travel Med Infect Dis. 2022;47:102293. https://doi.org/10.1016/j.tmaid.2022.102293
6. McLarty K, Paranthaman K, Jenkins C, Sedgwick J, Crawley-Boevey E. Lessons learned from the investigation and management of an outbreak of *Shigella flexneri* associated with a restaurant in London, 2019–2020. Public Health. 2022;205:130–2. https://doi.org/10.1016/j.puhe.2022.01.036
7. Mattison CP, Calderwood LE, Marsh ZA, Wikswo ME, Balachandran N, Kambhampati AK, et al. Childcare and school acute gastroenteritis outbreaks: 2009–2020. Pediatrics. 2022;150:e2021056002. https://doi.org/10.1542/peds.2021-056002
8. Ryan MJ, Wall PG, Adak GK, Evans HS, Cowden JM. Outbreaks of infectious intestinal disease in residential institutions in England and Wales 1992–1994. J Infect. 1997;34:49–54. https://doi.org/10.1016/S0163-4453(97)80009-6
9. Farrar WE Jr, Eidson M. Antibiotic resistance in *Shigella* mediated by R factors. J Infect Dis. 1971;123:477–84. https://doi.org/10.1093/infdis/123.5.477
10. Davies JR, Farrant WN, Tomlinson AJ. Further studies on the antibiotic resistance of *Shigella sonnei*. II. The acquisition of transferable antibiotic resistance in vivo. J Hyg (Lond). 1968;66:479–87. https://doi.org/10.1017/S0022172400041346
11. Dritz SK, Ainsworth TE, Back A, Boucher LA, Garrard WF, Palmer RD, et al. Patterns of sexually transmitted enteric diseases in a city. Lancet. 1977;2:3–4. https://doi.org/10.1016/S0140-6736(77)90002-2
12. Baker KS, Dallman TJ, Ashton PM, Day M, Hughes G, Crook PD, et al. Intercontinental dissemination of azithromycin-resistant shigellosis through sexual transmission: a cross-sectional study. Lancet Infect Dis. 2015;15:913–21. https://doi.org/10.1016/S1473-3099(15)00002-X
13. Chung The H, Rabaa MA, Pham Thanh D, De Lappe N, Cormican M, Valcanis M, et al. South Asia as a reservoir for the global spread of ciprofloxacin-resistant *Shigella sonnei:* a cross-sectional study. PLoS Med. 2016;13:e1002055. https://doi.org/10.1371/journal.pmed.1002055

14. Chung The H, Boinett C, Pham Thanh D, Jenkins C, Weill FX, Howden BP, et al. Dissecting the molecular evolution of fluoroquinolone-resistant *Shigella sonnei*. Nat Commun. 2019;10:4828. https://doi.org/10.1038/s41467-019-12823-0
15. Baker KS, Dallman TJ, Field N, Childs T, Mitchell H, Day M, et al. Genomic epidemiology of *Shigella* in the United Kingdom shows transmission of pathogen sublineages and determinants of antimicrobial resistance. Sci Rep. 2018;8:7389. https://doi.org/10.1038/s41598-018-25764-3
16. Bardsley M, Jenkins C, Mitchell HD, Mikhail AFW, Baker KS, Foster K, et al. Persistent transmission of shigellosis in England is associated with a recently emerged multidrug-resistant strain of *Shigella sonnei*. J Clin Microbiol. 2020;58:e01692–19. https://doi.org/10.1128/JCM.01692-19
17. Simms I, Field N, Jenkins C, Childs T, Gilbart VL, Dallman TJ, et al. Intensified shigellosis epidemic associated with sexual transmission in men who have sex with men—*Shigella flexneri* and *S. sonnei* in England, 2004 to end of February 2015. Euro Surveill. 2015;20:21097. https://doi.org/10.2807/1560-7917.ES2015.20.15.21097
18. Mook P, McCormick J, Bains M, Cowley LA, Chattaway MA, Jenkins C, et al. ESBL-producing and macrolide-resistant *Shigella sonnei* infections among men who have sex with men, England, 2015. Emerg Infect Dis. 2016;22:1948–52. https://doi.org/10.3201/eid2211.160653
19. Borg ML, Modi A, Tostmann A, Gobin M, Cartwright J, Quigley C, et al. Ongoing outbreak of *Shigella flexneri* serotype 3a in men who have sex with men in England and Wales, data from 2009–2011. Euro Surveill. 2012;17:20137. https://doi.org/10.2807/ese.17.13.20137-en
20. Ian Simms HC. Gauri Godbole, Claire Jenkins, Katy Sinka. Sexually transmitted *Shigella* spp. in England: 2016 to 2023. UK Health Security Agency. 2024 May 16 [cited 2024 Oct 10]. https://www.gov.uk/government/publications/non-travel-associated-shigella-infections/sexually-transmitted-shigella-spp-in-england-2016-to-2023
21. Charles H, Prochazka M, Thorley K, Crewdson A, Greig DR, Jenkins C, et al.; Outbreak Control Team. Outbreak of sexually transmitted, extensively drug-resistant *Shigella sonnei* in the UK, 2021–22: a descriptive epidemiological study. Lancet Infect Dis. 2022;22:1503–10. https://doi.org/10.1016/S1473-3099(22)00370-X
22. Thorley K, Charles H, Greig DR, Prochazka M, Mason LCE, Baker KS, et al. Emergence of extensively drug-resistant and multidrug-resistant *Shigella flexneri* serotype 2a associated with sexual transmission among gay, bisexual, and other men who have sex with men, in England: a descriptive epidemiological study. Lancet Infect Dis. 2023;23:732–9. https://doi.org/10.1016/S1473-3099(22)00807-6
23. Lefèvre S, Njamkepo E, Feldman S, Ruckly C, Carle I, Lejay-Collin M, et al. Rapid emergence of extensively drug-resistant *Shigella sonnei* in France. Nat Commun. 2023;14:462. https://doi.org/10.1038/s41467-023-36222-8
24. Charles H, Sinka K, Simms I, Baker KS, Godbole G, Jenkins C. Trends in shigellosis notifications in England, January 2016 to March 2023. Epidemiol Infect. 2024;152:e115. https://doi.org/10.1017/S0950268824001006
25. Dallman TJ, Charles H, Prochazka M, Sinka K, Hughes G, Godbole G, et al. Emergence of novel strains of *Shigella flexneri* associated with sexual transmission in adult men in England, 2019–2020. J Med Microbiol. 2021;70:001437. https://doi.org/10.1099/jmm.0.001437
26. Mitchell HD, Mikhail AFW, Painset A, Dallman TJ, Jenkins C, Thomson NR, et al. Use of whole-genome sequencing to identify clusters of *Shigella flexneri* associated with sexual transmission in men who have sex with men in England: a validation study using linked behavioural data. Microb Genom. 2019;5:e000311. https://doi.org/10.1099/mgen.0.000311
27. Dallman T, Ashton P, Schafer U, Jironkin A, Painset A, Shaaban S, et al. SnapperDB: a database solution for routine sequencing analysis of bacterial isolates. Bioinformatics. 2018;34:3028–9. https://doi.org/10.1093/bioinformatics/bty212
28. Croucher NJ, Page AJ, Connor TR, Delaney AJ, Keane JA, Bentley SD, et al. Rapid phylogenetic analysis of large samples of recombinant bacterial whole genome sequences using Gubbins. Nucleic Acids Res. 2015;43:e15. https://doi.org/10.1093/nar/gku1196
29. Minh BQ, Schmidt HA, Chernomor O, Schrempf D, Woodhams MD, von Haeseler A, et al. IQ-TREE 2: new models and efficient methods for phylogenetic inference in the genomic era. Mol Biol Evol. 2020;37:1530–4. https://doi.org/10.1093/molbev/msaa015
30. Yara DA, Greig DR, Gally DL, Dallman TJ, Jenkins C. Comparison of Shiga toxin-encoding bacteriophages in highly pathogenic strains of Shiga toxin-producing *Escherichia coli* O157:H7 in the UK. Microb Genom. 2020;6:e000334. https://doi.org/10.1099/mgen.0.000334
31. Kolmogorov M, Yuan J, Lin Y, Pevzner PA. Assembly of long, error-prone reads using repeat graphs. Nat Biotechnol. 2019;37:540–6. https://doi.org/10.1038/s41587-019-0072-8
32. Wick RR, Holt KE. Polypolish: short-read polishing of long-read bacterial genome assemblies. PLOS Comput Biol. 2022;18:e1009802. https://doi.org/10.1371/journal.pcbi.1009802
33. Hunt M, Silva ND, Otto TD, Parkhill J, Keane JA, Harris SR. Circlator: automated circularization of genome assemblies using long sequencing reads. Genome Biol. 2015;16:294. https://doi.org/10.1186/s13059-015-0849-0
34. Carattoli A, Zankari E, García-Fernández A, Voldby Larsen M, Lund O, Villa L, et al. In silico detection and typing of plasmids using PlasmidFinder and plasmid multilocus sequence typing. Antimicrob Agents Chemother. 2014;58:3895–903. https://doi.org/10.1128/AAC.02412-14
35. Tatusova T, DiCuccio M, Badretdin A, Chetvernin V, Nawrocki EP, Zaslavsky L, et al. NCBI prokaryotic genome annotation pipeline. Nucleic Acids Res. 2016;44:6614–24. https://doi.org/10.1093/nar/gkw569
36. Gilchrist CLM, Chooi YH. Clinker & clustermap.js: automatic generation of gene cluster comparison figures. Bioinformatics. 2021;37:2473–5. https://doi.org/10.1093/bioinformatics/btab007
37. Hawkey J, Paranagama K, Baker KS, Bengtsson RJ, Weill FX, Thomson NR, et al. Global population structure and genotyping framework for genomic surveillance of the major dysentery pathogen, *Shigella sonnei*. Nat Commun. 2021;12:2684. https://doi.org/10.1038/s41467-021-22700-4
38. Chowdhury G, Ghosh D, Zhou Y, Deb AK, Mukhopadhyay AK, Dutta S, et al. Field evaluation of a simple and rapid diagnostic test, RLDT to detect *Shigella* and enterotoxigenic *E. coli* in Indian children. Sci Rep. 2024;14:8816. https://doi.org/10.1038/s41598-024-59181-6
39. Lindsay B, Ochieng JB, Ikumapayi UN, Toure A, Ahmed D, Li S, et al. Quantitative PCR for detection of *Shigella* improves ascertainment of *Shigella* burden in children with moderate-to-severe diarrhea in low-income countries. J Clin Microbiol. 2013;51:1740–6. https://doi.org/10.1128/JCM.02713-12

40. Bardsley M, Jenkins C, Mitchell HD, Mikhail AFW, Baker KS, Foster K, et al. Persistent transmission of shigellosis in England is associated with a recently emerged multidrug-resistant strain of *Shigella sonnei*. J Clin Microbiol. 2020;58:e01692–19. https://doi.org/10.1128/JCM.01692-19
41. Mason LCE, Charles H, Thorley K, Chong CE, De Silva PM, Jenkins C, et al. The re-emergence of sexually transmissible multidrug resistant *Shigella flexneri* 3a, England, United Kingdom. NPJ Antimicrob Resist. 2024;2:20. https://doi.org/10.1038/s44259-024-00038-3
42. Richardson D, Savary-Trathen A, Fitzpatrick C, Williams D. Estimated prevalence and associations of sexually transmissible bacterial enteric pathogens in asymptomatic men who have sex with men: a systematic review and meta-analysis. Sex Transm Infect. 2024;100:532–7. https://doi.org/10.1136/sextrans-2024-056183
43. Kim S, Park AK, Kim JS, Park J, Shin E, Jung HJ, et al. The role of international travellers in the spread of CTX-M-15-producing *Shigella sonnei* in the Republic of Korea. J Glob Antimicrob Resist. 2019;18:298–303. https://doi.org/10.1016/j.jgar.2019.07.024
44. Campos-Madueno EI, Bernasconi OJ, Moser AI, Keller PM, Luzzaro F, Maffioli C, et al. Rapid increase of CTX-M-producing *Shigella sonnei* isolates in Switzerland due to spread of common plasmids and international clones. Antimicrob Agents Chemother. 2020;64:e01057-20. https://doi.org/10.1128/AAC.01057-20
45. Vecilla DF, Urrutikoetxea Gutiérrez MJ, Nieto Toboso MC, Inchaurza KZ, Zárraga EU, Estévez BR, et al. First report of *Shigella sonnei* carrying a $bla_{CTX-M-15}$ sexually transmitted among men who have sex with men. Infection. 2025;53:443–8. https://doi.org/10.1007/s15010-024-02341-7
46. European Centre for Disease Prevention and Control. Communicable disease threats report: week 51, 17–23 December 2023 [cited 2024 Oct 10]. https://www.ecdc.europa.eu/sites/default/files/documents/communicable-disease-threats-report-week-51-2023.pdf
47. Richardson D, Pakianathan M, Ewens M, Mitchell H, Mohammed H, Wiseman E, et al. British Association of Sexual Health and HIV (BASHH) United Kingdom national guideline for the management of sexually transmitted enteric infections 2023. Int J STD AIDS. 2023; 34:588–602. https://doi.org/10.1177/09564624231168217
48. World Health Organization. WHO bacterial priority pathogens list, 2024: Bacterial pathogens of public health importance to guide research, development and strategies to prevent and control antimicrobial resistance. 2024 [cited 2024 Oct 10]. https://www.who.int/publications/i/item/9789240093461

Address for correspondence: Hannah Charles, United Kingdom Health Security Agency, 61 Colindale Ave, London NW9 5EQ, UK; email: hannah.charles@ukhssa.gov.uk

etymologia revisited

Petri Dish

[pe'tre 'dish]

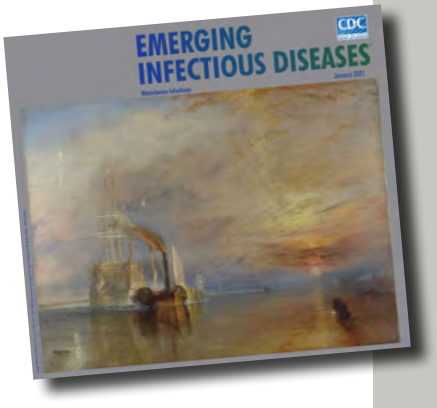

The Petri dish is named after the German inventor and bacteriologist Julius Richard Petri (1852–1921). In 1887, as an assistant to fellow German physician and pioneering microbiologist Robert Koch (1843–1910), Petri published a paper titled "A minor modification of the plating technique of Koch." This seemingly modest improvement (a slightly larger glass lid), Petri explained, reduced contamination from airborne germs in comparison with Koch's bell jar.

References:

1 Central Sheet for Bacteriology and Parasite Science [in German]. Biodiversity Heritage Library. Volume 1, 1887 [cited 2020 Aug 25]. https://www.biodiversitylibrary.org/item/210666#page/313/mode/1up
2. Petri JR. A minor modification of the plating technique of Koch [in German]. Cent für Bacteriol und Parasitenkd. 1887;1:279–80.
3. Shama G. The "Petri" dish: a case of simultaneous invention in bacteriology. Endeavour. 2019;43:11–6. DOIExternal
4. The big story: the Petri dish. The Biomedical Scientist. Institute of Biomedical Science [cited 2020 Aug 25]. https://thebiomedicalscientist.net/science/big-story-petri-dish

Originally published in January 2021

https//wwwnc.cdc.gov/eid/article/27/1/et-2701_article

Role of Nonpharmaceutical Interventions during 1918–1920 Influenza Pandemic, Alaska, USA

Uddhav Khakurel, Lisa Sattenspiel, Svenn-Erik Mamelund

Previous studies investigating the 1918–1920 influenza pandemic have provided a comprehensive overview of the spread of the pandemic and possible explanations for high mortality rates in Alaska, USA. Our understanding of the role of nonpharmaceutical interventions (NPIs) is limited, however. To gain an overview of various agencies' efforts to protect communities during the pandemic, we conducted a mixed-method assessment of a large pool of digitized historical newspapers and archival materials covering Alaska's local and territorial responses to the pandemic. The study encompassed 14 local units of Alaska that implemented NPIs during October 1918–January 1919. Analyses indicated that 8 local units avoided the outbreak by implementing NPIs and that the other 6 units controlled the spread of influenza by implementing NPIs after the virus was introduced. In addition, some Indigenous communities escaped the pandemic by implementing mandatory and voluntary restrictions. Information on the effects of NPI could guide future influenza pandemic preparedness and response.

During the 1918–1920 influenza pandemic, although scientists were aware of the existence of infectious agents smaller than bacteria (*1*), they thought that the *Hemophilus influenzae* bacterium was responsible for causing the disease. Influenza was not identified as a virus in swine until 1931 and in humans in 1933 (*2*,*3*). In 1918, however, public health officials and healthcare workers were aware that influenza spread through the air (*4*). The national and local authorities of Canada, Australia, and the United States attempted to implement different nonpharmaceutical interventions (NPIs), including travel restrictions and quarantine, to prevent the spread of the influenza pandemic (*5*). The primary focus in those countries was to avoid the worst impacts of the pandemic by directing efforts toward implementing protective measures, such as establishing quarantine stations and stopping travel between influenza-infected and uninfected communities (*6*).

However, quarantines did not prevent introduction of influenza in all communities (*7*). Once the disease was introduced, large cities across the United States implemented a wide range of NPIs to limit community-level influenza transmission. Community-level interventions included isolation, school closures, public gathering bans, and surface cleaning (*8*–*10*). Local efforts to contain the spread of the infectious agent were derived from cities' experience in managing outbreaks of tuberculosis, cholera, and smallpox in the 18th and 19th Centuries (*1*).

During the 1918–1920 influenza pandemic, Alaska was a US territory. The territorial government of Alaska was forewarned about the risk for an influenza outbreak and implemented quarantine regulations to prevent the introduction of the disease (*11*). The territorial governor ordered all communities to establish quarantines and to create cordon sanitaire (protective buffer zones), by limiting travel at trailheads and along rivers (*12*–*15*). A previous report showed that communities and residents adopted different community-level NPIs to control the spread of influenza (*8*). Those interventions included travel restrictions, quarantine of travelers, isolation, prohibition of public gatherings and native festivals, fumigation of public places, and school closures. However, implementing NPIs did not prevent introduction of influenza into Alaska (*8*). The 1918–1920 influenza pandemic killed at least 50 million persons worldwide, including 675,000 persons in the United States (*12*). In Alaska, the average influenza mortality rate ranged from 1% to 38% at the regional level, and some local communities reported mortality rates of >90% (*8*,*16*).

Researchers have previously investigated the role of NPIs in 1918–1920 influenza mortality rates in

Author affiliations: Centre for Research on Pandemics & Society, Oslo Metropolitan University, Oslo, Norway (U. Khakurel, S.-E. Mamelund); University of Missouri, Columbia, Missouri, USA (L. Sattenspiel)

DOI: https://doi.org/10.3201/eid3107.241048

urban settings (*9*). Those studies focused on the larger US cities and concluded that, although implementation of NPIs did not stop the spread of the pandemic, it helped delay its spread, known contemporarily and colloquially as flattening the curve (*17*). Peak mortality rates in cities under NPI use was lower than in cities with no reported NPIs (*9*).

Little previous research has considered the effects of NPIs on local-level variation in influenza spread and mortality rates in geographically isolated areas like Alaska. One study discussed several factors that influenced patterns of influenza deaths in Alaska and Labrador (*11*), an isolated region in Canada with a similar culture and latitude to Alaska. That study highlighted the cocirculation of other pathogens, environmental influences, and access to healthcare but did not consider the effects of NPIs implemented by the local board of health and territorial government on the variation in mortality rates across the 2 regions.

We investigated the role of NPIs in reducing the spread of the influenza during the 1918–1920 pandemic and on pneumonia and influenza (P&I) mortality rates in Alaska. We focused on the first wave of influenza in Alaska, during September 1918–January 1919 because evidence for the implementation of NPIs in later waves is lacking. We investigated the type and duration of interventions implemented at local levels, patterns of influenza spread, daily mortality rates in Alaska, and types and effects of NPIs implemented by Alaska Native populations.

Methods

Study Context

In 1910, Alaska was inhabited by 64,356 persons in an area of 1.72 million km^2 and had a predominantly male (71.25%) population. During the 1918–1920 influenza pandemic, the territory was divided into 4 judicial districts (First, Second, Third, and Fourth) and 42 local units. The territorial headquarters was located in Juneau in the First Judicial District. From 1910 to 1920, the population of Alaska dropped by 14.5% to 55,036 (*19*). The Alaska Native population numbers were similar, at ≈27,000, in both 1910 and 1920 (*16*).

Influenza in Alaska came in 3 distinct waves (*8*,*16*). The first wave started in October 1918 and corresponded with the second worldwide influenza wave. In some communities, the first wave continued until January 1919 (*12*). Influenza was introduced into Alaska by persons entering and leaving trading and fishing vessels or coastal steamers (*8*). A similar observation was made in the second influenza wave in Alaska (the third worldwide wave), which started in May 1919. A small third wave occurred in Alaska in 1920 (*16*).

We examined the role of NPIs in 14 local units and 4 Alaska Native villages during the first influenza wave, October 1918–January 1919, for which we have information on the pandemic and NPIs (Figure 1). We focused on the first wave of influenza because evidence for the implementation of NPIs in later waves is lacking. The limited information available for subsequent waves might be attributed to pandemic fatigue, a phenomenon observed during the COVID-19 pandemic (*18*). However, definitive evidence on pandemic fatigue in Alaska during the 1918–1920 influenza pandemic has not been identified.

Data Sources

We collected historical data on the influenza pandemic and NPIs implemented in Alaska during 1918–1920 from the digital archive of the Library of Congress (https://www.loc.gov) and the National Archives Catalog (https://catalog.archives.gov). Photographs and newspaper articles, a primary source of information in this study, are available in the digital archive of the Library of Congress. Government letters, announcements, reports, and regulations are available in the National Archives Catalog. We collected additional materials from the Alaska State Archives (https://archives.alaska.gov). We used all local newspapers from the first influenza wave in Alaska that were available in the digital archive (Table 1). We screened a total of 15 newspapers to identify the types of interventions implemented at the local level. Those records contained information on the influenza pandemic in Alaska and NPIs implemented by the territorial and local governments and health boards. Further, we extracted information on quarantine expenses and reimbursement, hiring of quarantine officers, arrival of steamships, and NPIs adopted by Indigenous communities from the Alaska newspaper articles and additional archival resources.

We obtained death certificates from Health Analytics and Vital Records, Division of Public Health, State of Alaska Department of Health. A total of 2,390 death certificates were recorded during October 1918–January 1919, of which 1,024 were P&I deaths and were included in the study. Death certificates include information on the place of death, sex, race, birth date, and cause of death and cover all parts of the Alaska territory. We excluded 51 death certificates from the study because the cause of death was

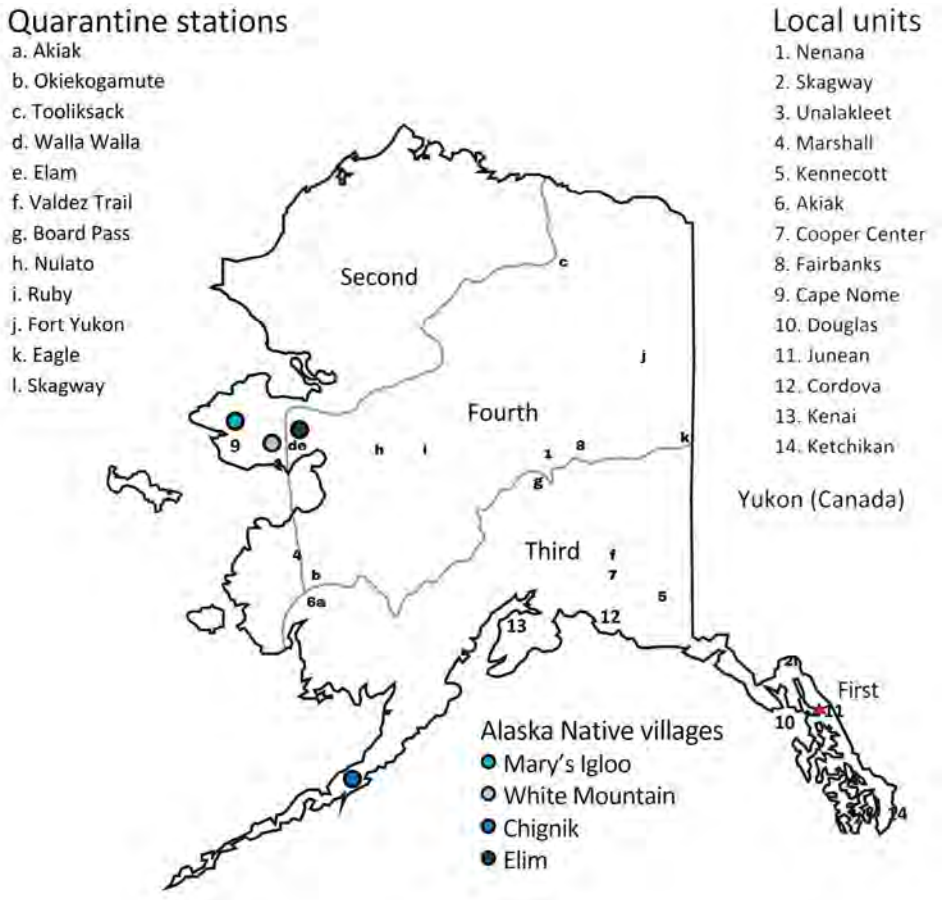

Figure 1. Locations of Judicial Districts, quarantine stations, native villages, and local units included in study of the role of nonpharmaceutical interventions during 1918–1920 influenza pandemic, Alaska, USA. Quarantine stations were located along the Iditarod, Valdez, Yukon, Innoko River, and Fairbanks Trails at Elam, Akiak, Okiekogamute, Tooliksack, Walla Walla, Piledriver, Board Pass, Nulato, Ruby, Fort Yukon, Eagle, and Skagway. This study includes data from Cape Nome, Douglas, Juneau (territorial headquarters; denoted by red star), Cordova, Kenai, Ketchikan, Nenana, Skagway, Unalakleet, Marshall, Kennecott, Akiak, Copper Center, and Fairbanks.

missing. The full analysis of the death certificates was done in a previous study (*16*).

Data Analysis

We used a mixed-method approach to analyze the role of NPIs in the spread of the influenza pandemic and the effects of NPIs on P&I mortality rates. We categorized NPIs implemented by authorities into preventive and spread control (Table 2). Preventive interventions were implemented to prevent the introduction of influenza in the community, also known as protective sequestration (*6*). We defined spread control NPIs as the interventions implemented after the introduction of influenza in the community (*9*). We further categorized spread control NPIs into 4 groups on the basis of the categorization used for the 1918 influenza pandemic (Table 2), which reflect the understanding of the authorities from 1918 (*9*,*20*,*21*). By comparison, the COVID-19 pandemic categorized NPIs into >13 categories using more granular information (*22*–*24*).

We measured NPI duration from the day the intervention began to the day it was lifted (Table 3). To study the role of NPIs in P&I deaths in Alaska, we examined the P&I deaths in the local units. We compared the mortality rate among local units that implemented NPIs with Alaska's overall average regional mortality rate. We investigated the interventions the local units applied and the spread of the pandemic. We calculated the reproduction number (R) for all of Alaska and the local units that implemented NPIs after the first reported P&I death. Finally, we examined the use of NPIs among Alaska Natives.

Table 1. List of newspapers used to investigate the role of nonpharmaceutical interventions during 1918–20 influenza pandemic, Alaska, USA

Local newspapers	City or town
Nome Tri-Weekly Nugget	Nome
Daily Progressive Miner	Ketchikan
Cordova Daily Times	Cordova
Alaska Daily Empire	Juneau
The News Letter	Kodiak
Alaska Juneau Douglas Island News	Juneau
Seward Gateway Daily Edition	Seward
The Alaska Weekly Post	Seward
Seward Gateway	Seward
Douglas Island News	Douglas City
Nenana Daily News	Nenana
Weekly Alaska Citizen	Fairbanks
Wrangell Sentinel	Wrangell
McCarthy Weekly News	McCarthy
Weekly Nome Industrial	Nome

Table 2. Nonpharmaceutical interventions used during 1918–20 influenza pandemic, Alaska, USA

Preventive NPIs	Spread control interventions
Travel restriction to the community	Quarantine and isolation: orders to separate ill persons and persons suspected of having contact with ill persons School closures: closure of all schools under the jurisdiction of local authorities
Quarantine, ≥5 days	Public gathering bans: closure of saloons, restaurants, indoor gatherings, sports halls, public libraries, and local festivals Personal and ancillary actions: mask ordinance, fumigation of mail, and cleaning of surfaces

Estimating R

We estimated R from the early growth phase of the epidemic trajectories by using the GrowthPredict toolbox (*25*) and mortality data from Alaska. GrowthPredict is a user-friendly tool designed for analysis of outbreak trajectories that accommodates subexponential growth patterns often observed in real-world situations. To calculate R, we extracted the mortality data for the first 20 days after the first reported P&I death in the local units. For that analysis, we excluded Cape Nome because the community did not introduce NPIs until after P&I deaths were reported among its population. For the calculation, we used 3 as an estimation of the serial interval for influenza on the basis of previous literature (*26*).

GrowthPredict toolbox uses the generalized growth model and characterizes the growth rate (r) and growth parameter (p). The growth parameter modulates the growth from purely exponential (p = 1) to subexponential (0<p>1). In our study, we used maximum-likelihood estimation to determine the best fit of the observed data.

We calculated R with the relationship defined in the renewal equation (*26*). The renewal equation incorporated the generation time distribution of influenza, which represents the time interval between successive infections in a transmission chain (*26*). We determined the generation time by using data from existing epidemiologic literature (*26*), which we input into the toolbox as a fixed parameter. The GrowthPredict toolbox provides CIs for R by performing parametric bootstrapping, generating multiple resampled datasets, and re-estimating R for each resample to account for statistical uncertainty (*25*).

Results

Data available from archival resources indicated that the territorial government acted promptly to attempt to prevent the onset of influenza in the whole of Alaska. Once influenza was introduced, local governments and health boards implemented NPIs to protect persons living within their jurisdiction.

Introduction of NPIs in Alaska

The territorial government of Alaska was warned about influenza spreading across the United States

Table 3. Local units with spread control NPIs in a study of the role of nonpharmaceutical interventions during 1918–1920 influenza pandemic, Alaska, United States

Location	1910 population	No. deaths	Period of NPI (start–end)	Types of NPIs
Cape Nome	3,924			
Phase 1		0	4 d (1918 Nov 20–23)	Quarantine
Phase 2		334	63 d (1918 Nov 4–1919 Jan 6)	School closure, public gathering ban, quarantine, and isolation
Douglas	1,722			
Phase 1		0	41 d (1019 Oct 30–Dec 9)	School closure, public gathering ban, quarantine, and isolation
Phase 2		6	16 d (1918 Dec 19–1919 Jan 3)	School closure, public gathering ban, quarantine, isolation, and mandatory mask ordinance
Juneau	2,910			
Phase 1		19	33 d (1918 Oct 29–Dec 1)	School closure, public gathering ban, quarantine, and isolation
Phase 2		8	13 d (1918 Dec 18–30)	School closure, public gathering ban, quarantine, isolation, and mandatory mask ordinance
Cordova	1,779			
Phase 1		6	25 d (1918 Dec 27–1919 Jan 20)	School closure, public gathering ban, quarantine, and isolation
Kenai	1,692			
Phase 1		24	28 d (1918 Nov 8–Dec 5)	School closure, public gathering ban, quarantine, and isolation
Ketchikan	3,520			
Phase 1		21	30 d (1918 Oct 23–Nov 22)	School closure, public gathering ban, quarantine, and isolation

in late September 1918. In mid-October 1918, the US Public Health Department sent an official health bulletin to Governor Riggs with details on the incubation period, mode of transmission, and preventive measures (*27*). In response to the bulletin, in early October, the territorial government introduced quarantine regulations at port towns, including Juneau, Cordova, Seward, Valdez, and Cape Nome, to prevent the introduction of influenza into Alaska from incoming steamships:

> Quarantine is established by the Governor against all incoming steamers and other marine craft on October 15th. All vessels are met at arrival at any port by designated physicians and should cases of influenza be found immediate action is taken [The Alaska Daily Empire (Juneau), October 24, 1918] (*28*).

A special request was made to steamship companies to examine all passengers for influenza. Those examinations were focused on close inspection of the nose and throat, with an emphasis on evidence of inflammation, and the gathering of information about exposure to infection.

Spread Control NPIs

On the first appearance of influenza at the local level, the territorial government requested that local units implement interventions to prevent the spread of the disease. Cape Nome, Douglas, Juneau, Cordova, Kenai, and Ketchikan implemented school closures, public gathering bans, and quarantine and travel restrictions (Table 3). Those local units further tried to restrict the transmission of influenza to neighboring communities by restricting outgoing travel, commonly known as cordon sanitaire (*29*). Mask use was recommended through an official health notice. The Red Cross made and distributed cloth masks to populations in Alaska (Figure 2), but their reach was limited.

Cape Nome introduced a short quarantine when the last steamship of the season, *Victoria*, arrived on October 20, 1918. The containment measure was lifted on October 23, 1918, because the local health officer did not record any symptoms of influenza among the incoming passengers (*30*). The early lifting of quarantine resulted in several P&I deaths in Cape Nome. After November 3, 1918, several deaths with P&I listed as a primary cause were recorded. The local board of health again implemented NPIs on November 4, 1918, a measure that lasted for 63 days and was lifted on January 6, 1919.

Douglas, a community located in the First Judicial District, isolated itself from late October to early December with quarantine regulations, school closures, and public gathering bans. After lifting the restrictions, Douglas reported P&I deaths on December 9, 1918, after which NPIs were again introduced along with mandatory mask ordinances (ancillary measures), which they strictly enforced:

Figure 2. Archival photo of Juneau Chapter of the Red Cross from study of nonpharmaceutical interventions during 1918–1920 influenza pandemic, Alaska, USA. During the pandemic, the Red Cross made cloth mask and distributed to populations in Alaska. However, their reach was limited. Source: Library of Congress (https://www.loc.gov/resource/anrc.06015).

> Several arrests were made in Douglas yesterday on account of not wearing face masks. After one or two citizens had been fined, everyone began to see that officials meant business and after the second trip of the ferry everyone on the streets were wearing the 'bug catchers' [The Alaska Daily Empire (Juneau), November 13, 1918] (*31*).

The local units of Alaska maintained NPIs until local health officers reported no new influenza cases within the community and neighboring communities, at which point they lifted restrictions (*32*). A total of 1,024 P&I deaths during the first influenza wave were reported from the parts of the First, Second, and Third Judicial Districts, an aggregate population of 27,667 persons. Besides Cape Nome, which reported high (8.5%) mortality rates, the other local units with known NPIs reported low (1%–2%) P&I mortality rates compared with the territorial average of 3.7%, including local units with reported P&I deaths. Similarly, R for local units implementing NPIs, apart from Cape Nome, was lower (R = 0.31 [95% CI 0.26–0.89]) than the overall R for the whole territory (R = 0.92 [95% CI 0.87–0.97]).

Preventive NPIs

Eight local units escaped the pandemic during Alaska's first influenza wave (Table 4). Although those

Table 4. Communities with preventive NPIs in a study of the role of nonpharmaceutical interventions during 1918–1920 influenza pandemic, Alaska, United States*

Place	1910 population†	No. days NPI implemented (start–end dates)	Types of NPIs
Nenana	190	53 (1918 Nov 8–Dec 31)	Travel restriction and quarantine
Skagway	872	110 (1919 Nov 2–1919 Feb 20)	Travel restriction
Unalakleet	247	96 (1918 Nov 6–1919 Feb 10)	Quarantine
Marshall	NA	14 (1919 Jan 24–Feb 7)	Travel restriction
Kennecott	NA	42 (1918 Dec 21–1919 Feb 1)	Travel restriction and quarantine
Akiak	NA	35 (1919 Jan 8–Feb 12)	Travel restriction
Copper Center	553	75 (1918 Dec 18–March 1919)‡	Quarantine
Fairbanks	3,511	80 (1918 Nov 11–1919 Jan 27)	Travel restriction and quarantine

*NA, not available; NPIs, nonpharmaceutical interventions.
†Marshall, Kennecott, and Akiak were not reported in the 1910 population census.
‡Minimum estimate.

units were well connected with the communities experiencing influenza outbreaks via sled roads, pack trails, and railroads (*33*), they did not report P&I deaths during September 1918–February 1919. Those local units implemented protective sequestration measures by imposing travel restrictions, establishing quarantine stations along the trails leading to their communities (Figure 1), placing armed guards at the quarantine stations, and not allowing anyone to enter their communities beginning in early November 1918 (*34*).

Nenana adopted a unique approach by requiring residents to wear a red ribbon in their headgear to indicate that they were free from influenza:

> The quarantine regulations at Nenana require the dwellers of that town to wear a red, green, blue yellow or other badge displayed upon their headgear. … The red badge is the indication that the wearer is free from such disease… dire penalties – fine and imprisonment – are threatened all who do not wear them prominently displayed on their headpieces [The Cordova Daily Times. December 23, 1918] (*35*).

Fairbanks used a similar strategy, in which health authorities examined residents periodically for influenza and gave an "OK Fairbanks Health Department" band to wear to indicate that the person was free from influenza.

NPIs among Alaska Natives

Alaska Natives experienced high mortality rates during the first influenza wave in the territory. Local newspapers repeatedly reported that Alaska Natives were at higher risk for the disease (*36*,*37*). The territorial government implemented stringent measures against public gatherings among Alaska Natives. The directive forwarded by the territorial government urged Alaska Natives not to visit neighbors, to keep houses well aired, to wear influenza masks, and to avoid gatherings; it also banned potlatch, a native festival mostly celebrated in southeastern Alaska (Figure 3).

In addition to those regulations, Alaska Natives implemented voluntary quarantine measures to safeguard themselves from influenza. The introduction of voluntary quarantine protected the Alaska Native villages of White Mountain, Elim, and Chignik (Figure 1). At Mary's Igloo, Alaska Natives coming from Teller spread influenza among residents of the lower part of the settlement:

> Chena Indians are enforcing quarantine regulations against natives from farther down the Tanana River [that river crosses through Judicial Districts 3 and 4 and passes close to Fairbanks and Nenana] [The Nome Tri-Weekly Nugget. April 18, 1919] (*38*).

Local teachers immediately enforced a quarantine measure to prevent the spread of influenza to the upper part of the settlement.

Discussion

Despite being geographically isolated, the government of Alaska became aware of the imminent threat of an influenza outbreak in early October 1918, which enabled authorities to implement protective measures. Contrary to reports from other geographically isolated areas like American Samoa, New Caledonia, and Rotuma, where the forewarned governments were able to protect their inhabitants during the 1918–1920 influenza pandemic, influenza began spreading quickly in Alaska in late October (*10*,*39*–*41*). The first P & I death occured in Cape Nome after the early lifting of quarantine because the health officer observed no symptoms among passengers quarantined from a steamship. Similar observations were made in Fiji and Tahiti in French Polynesia in 1918, where authorities released asymptomatic steamship passengers without quarantine and saw an influenza outbreak in the community (*10*).

Researchers have mentioned that infected persons can transmit diseases like influenza 24–48 hours before showing symptoms (*42*). A similar spread might have contributed to the introduction and subsequent large influenza outbreak in Cape Nome. NPIs were reintroduced only after a reported influenza death in the community. Similar observations were made in Douglas where the local authorities prevented an outbreak until early December 1918. The lifting of the quarantine resulted in a few cases in the middle of December, but Douglas reported only a few P&I deaths. In addition, except for Cape Nome, local units with NPIs had low R compared with the whole of Alaska. The increased awareness among residents during that period might have contributed to their adoption of precautionary measures against the subsequent outbreak. Despite repeated reporting by local newspapers on precautionary measures, available information is not sufficient to draw definitive conclusions.

Douglas, Juneau, Cordova, Kenai, and Ketchikan implemented influenza-informed NPIs during the pandemic (Table 3). Communities implemented NPIs on the basis of the risk for new cases as assessed by the health officer and local authorities. Researchers have concluded that low mortality rates were achieved in large cities that had long and sustained NPI implementation (*9*,*21*). In Alaska, we found that local units that implemented NPIs had lower mortality rates and reproduction numbers compared with the average mortality rate at the territorial level, which included all areas with reported influenza deaths. Although this study does not allow for a direct comparison of mortality rates between local units with varying levels of NPI use, the findings offer valuable insights into the role of NPIs in P&I mortality rates. Furthermore, the lower mortality rate in the First Judicial District might be related to greater access to healthcare (*8*,*11*). In addition, the role of NPIs in flattening the morbidity curve has been well understood from the 1918 influenza pandemic and the COVID-19 pandemic (*9*,*17*,*43*,*44*) and might have contributed to the low mortality rate in the First Judicial District.

Eight Alaska communities implemented quarantine regulations and travel restrictions that protected them from the influenza outbreak and helped stop spread of the virus into the interior of Alaska. Similar observations were made in 6 US communities where the local authorities implemented protective measures and took advantage of geographic isolation (*6*). As explained in earlier studies on the pandemic in Alaska, the mobility of the population during the fall of 1918 was limited because of rugged geography and lack of snow during the fall of that year (*8*,*11*). That limited mobility likely contributed to the effectiveness of quarantine regulations (*45*). In addition, Fairbanks and Nenana introduced an identification mechanism to separate infected and uninfected persons, comparable to COVID-19 vaccine certificates issued in many countries during that pandemic (*46*).

Indigenous communities worldwide faced high mortality rates during the 1918–1920 influenza pandemic (*8*,*47*–*49*). The local governments at the time were aware of the elevated influenza risk and implemented stringent measures to protect Indigenous communities. Our findings argue that implementing strict measures prevented influenza from reaching all Indigenous communities, which complements the results from previous research in South Pacific islands (*10*). Indigenous

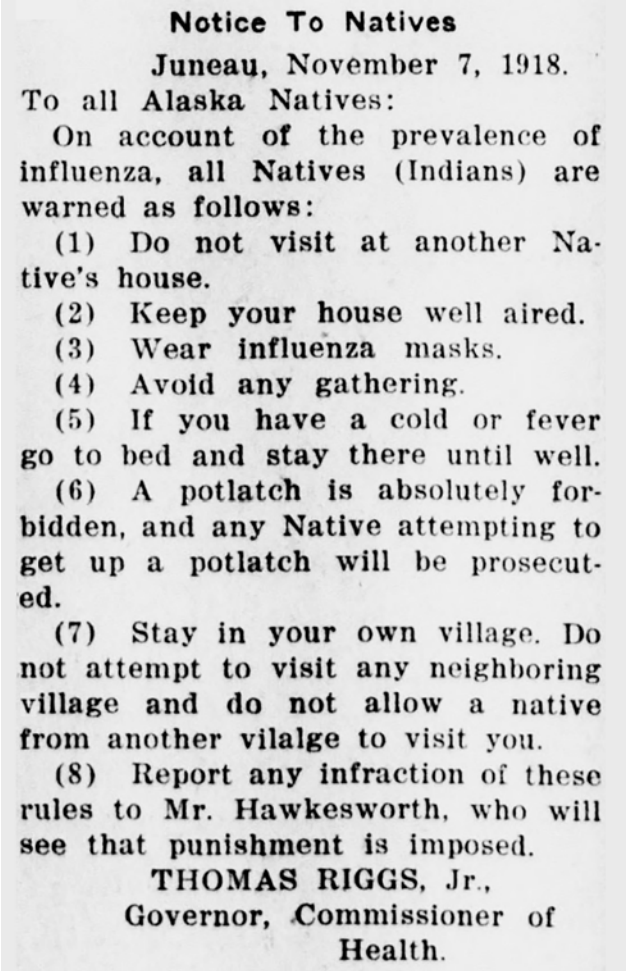

Notice To Natives

Juneau, November 7, 1918.

To all **Alaska** Natives:

On account of the prevalence of influenza, all Natives (Indians) are warned as follows:

(1) Do not visit at another Native's house.

(2) Keep your house well aired.

(3) Wear influenza masks.

(4) Avoid any gathering.

(5) If you have a cold or fever go to bed and stay there until well.

(6) A potlatch is absolutely forbidden, and any Native attempting to get up a potlatch will be prosecuted.

(7) Stay in your own village. Do not attempt to visit any neighboring village and do not allow a native from another vilalge to visit you.

(8) Report any infraction of these rules to Mr. Hawkesworth, who will see that punishment is imposed.

THOMAS RIGGS, Jr.,
Governor, Commissioner of Health.

Figure 3. News clipping used in study of the role of nonpharmaceutical interventions during 1918–1920 influenza pandemic, Alaska, USA. This clipping from The Alaska Daily Empire, Juneau, dated November 7, 1918, is an example of nonpharmaceutical interventions imposed by the territorial government against Alaska Natives. A potlatch is an Alaska Native festival mostly celebrated in southeastern Alaska. Source: Library of Congress.

communities living in Alaska also implemented protective measures through voluntary initiatives. Although this finding is specific to the 1918–1920 influenza pandemic, researchers noted similar observations from around the globe during the COVID-19 pandemic (*50*).

The first limitation of this study is that we could only include 14 local units in Alaska because of a lack of data. Second, the level of travel to Alaska's interior during the winter months is yet to be explored in full detail. Because transmission relies on human contact, we could only include the parts of Alaska with complete information on NPIs and travel. Finally, we were not able to include public opinion and opposition or adherence to the NPIs and the possible effects of those actions on P&I mortality rates. Future explorations of the 1918–1920 influenza pandemic in Alaska will be directed toward those issues.

Although several previous studies have focused on the city-to-city variation in mortality rates in the continental United States, this study provides insight into the role of NPIs in geographically isolated areas in Alaska and the role of NPIs in limiting the spread of influenza. Results from the study suggest that the territorial government made efforts to prevent the spread of the pandemic in Alaska. The eventual spread of the pandemic in October 1918, however, led the local governments to implement NPIs. School closures, public gathering bans, and quarantine and isolation were the main NPIs used in Alaska. The lower R for the areas with NPIs further provides quantitative evidence that NPIs helped to protect the communities. This study supports previous studies concluding that protective sequestration measures protect isolated communities. Further, through this study, we found additional evidence of Alaska Natives adopting voluntary NPIs.

To capture the overall picture of entire territory of Alaska, further work will examine other written sources from the time, such as diaries and letters, to investigate whether more information can be sourced. The oral traditions of the Indigenous communities need to be studied by historians to determine the ability of written documents to represent the situation.

In summary, we examined the use of NPIs and their effects on the 1918–1920 influenza pandemic in Alaska. These insights provide valuable information to inform pandemic preparedness and management in geographically isolated areas like Alaska.

Acknowledgments

We thank the Centre for Advanced Study at the Norweigan Academy of Science and Letters, Oslo, Norway, for research support and the University of Missouri for funding to procure copies of the Alaska death certificates.

About the Author

Mr. Khakurel is a research assistant at the Centre for Research on Pandemics & Society, Oslo Metropolitan University, Norway. His primary research interests include the societal impacts of pandemics, policy evaluation, mortality inequality, and related aspects of public health and social stratification.

References

1. Tomes N. "Destroyer and teacher": managing the masses during the 1918–1919 influenza pandemic. Public Health Rep. 2010;125:48–62. https://doi.org/10.1177/00333549101250S308
2. Smith W, Andrewes CH, Laidlaw PP. A virus obtained from influenza patients. Lancet. 1933;222:66–8. https://doi.org/10.1016/S0140-6736(00)78541-2
3. Tognotti E. Scientific triumphalism and learning from facts: bacteriology and the "Spanish flu" challenge of 1918. Soc Hist Med. 2003;16:97–110. https://doi.org/10.1093/shm/16.1.97
4. Simple precautions to prevent influenza. The Seward Gateway. 1918 Oct 24:2
5. Bell D, Nicoll A, Fukuda K, Horby P, Monto A, Hayden F, et al.; World Health Organization Writing Group. Nonpharmaceutical interventions for pandemic influenza, national and community measures. Emerg Infect Dis. 2006;12:88–94. https://doi.org/10.3201/eid1201.051371
6. Markel H, Stern AM, Navarro JA, Michalsen JR, Monto AS, DiGiovanni C. Nonpharmaceutical influenza mitigation strategies, US communities, 1918–1920 pandemic. Emerg Infect Dis. 2006;12:1961–4. https://doi.org/10.3201/eid1212.060506
7. Whitelaw TH. The practical aspects of quarantine for influenza. Can Med Assoc J. 1919;9:1070–4.
8. Mamelund SE, Sattenspiel L, Dimka J. Influenza-associated mortality during the 1918–1919 influenza pandemic in Alaska and Labrador: a comparison. Soc Sci Hist. 2013;37:177–229. https://doi.org/10.1017/S0145553200010634
9. Markel H, Lipman HB, Navarro JA, Sloan A, Michalsen JR, Stern AM, et al. Nonpharmaceutical interventions implemented by US cities during the 1918–1919 influenza pandemic. JAMA. 2007;298:644–54. https://doi.org/10.1001/jama.298.6.644
10. McLeod MA, Baker M, Wilson N, Kelly H, Kiedrzynski T, Kool JL. Protective effect of maritime quarantine in South Pacific jurisdictions, 1918–19 influenza pandemic. Emerg Infect Dis. 2008;14:468–70. https://doi.org/10.3201/eid1403.07-0927
11. Sattenspiel L, Mamelund SE. Cocirculating epidemics, chronic health problems, and social conditions in early 20th century Labrador and Alaska. Ann Anthropol Pract. 2012;36:402–21. https://doi.org/10.1111/napa.12011
12. Crosby AW. America's forgotten pandemic: the influenza of 1918. Cambridge (MA): Cambridge University Press; 1989.
13. Lautaret RL. Alaska's greatest disaster: the 1918 Spanish influenza epidemic. Alaska J. 1986;16:238–43.
14. Ganley ML. The dispersal of the 1918 influenza virus on the Seward Peninsula, Alaska: an ethnohistoric reconstruction. Int J Circumpolar Health. 1998;57:247–51.
15. Philip RN, Lackman DB. Observations on the present distribution of influenza A/swine antibodies among Alaskan natives relative to the occurrence of influenza in

1918–1919. Am J Hyg. 1962;75:322–34. https://doi.org/10.1093/oxfordjournals.aje.a120253
16. Sattenspiel L, Mamelund SE, Dahal S, Wissler A, Chowell G, Tinker-Fortel E. Death on the permafrost: revisiting the 1918–1920 influenza pandemic in Alaska using death certificates. Am J Epidemiol. 2025;194:152–61. https://doi.org/10.1093/aje/kwae173
17. Kenyon C. Flattening-the-curve associated with reduced COVID-19 case fatality rates—an ecological analysis of 65 countries. J Infect. 2020;81:e98–9. https://doi.org/10.1016/j.jinf.2020.04.007
18. Alaska Department of Labor and Workforce Development. A history of Alaska population settlement. Juneau: the Department; 2013.
19. Wiedicke A, Stehr P, Rossmann C. Issue fatigue over the course of the COVID-19 pandemic: a multi-method approach. Eur J Health Commun. 2023;4:114–37. https://doi.org/10.47368/ejhc.2023.307
20. Bootsma MCJ, Ferguson NM. The effect of public health measures on the 1918 influenza pandemic in U.S. cities. Proc Natl Acad Sci U S A. 2007;104:7588–93. https://doi.org/10.1073/pnas.0611071104
21. Correia S, Luck S, Verner E. Pandemics depress the economy, public health interventions do not: evidence from the 1918 flu. J Econ Hist. 2022;82:917–57. https://doi.org/10.1017/S0022050722000407
22. Bozorgmehr K, Rohleder S, Duwendag S, Mohsenpour A, Saint V, Gold AW, et al. Covid-19 pandemic policy monitor (COV-PPM)—European level tracking data of non-pharmaceutical interventions. Data Brief. 2021;39:107579. https://doi.org/10.1016/j.dib.2021.107579
23. Hale T, Angrist N, Goldszmidt R, Kira B, Petherick A, Phillips T, et al. A global panel database of pandemic policies (Oxford COVID-19 Government Response Tracker). Nat Hum Behav. 2021;5:529–38. https://doi.org/10.1038/s41562-021-01079-8
24. Haug N, Geyrhofer L, Londei A, Dervic E, Desvars-Larrive A, Loreto V, et al. Ranking the effectiveness of worldwide COVID-19 government interventions. Nat Hum Behav. 2020;4:1303–12. https://doi.org/10.1038/s41562-020-01009-0
25. Chowell G, Bleichrodt A, Dahal S, Tariq A, Roosa K, Hyman JM, et al. GrowthPredict: A toolbox and tutorial-based primer for fitting and forecasting growth trajectories using phenomenological growth models. Sci Rep. 2024;14:1630. https://doi.org/10.1038/s41598-024-51852-8
26. Nishiura H, Chowell G. The effective reproduction number as a prelude to statistical estimation of time-dependent epidemic trends. In: Chowell G, Hyman JM, Bettencourt LM, Castillo-Chavez C, editors. Mathematical and statistical estimation approaches in epidemiology. New York: Springer; 2009. p. 103–121.
27. Heath bulletin on influenza pandemic. The Alaska Daily Empire (Juneau). 1918 Oct 15:7.
28. Statement by the governor on influenza. The Alaska Daily Empire (Juneau). 1918 Oct 24:8.
29. Neuman DS. Quarantine notice. The Nome Tri-Weekly Nugget. 1918 Dec 25:1.
30. News notes. The Nome Tri-Weekly Nugget. 1918 Dec 25:4.
31. Several arrests made. The Alaska Daily Empire (Juneau). 1918 Nov 13:7.
32. Influenza ban is raised by city officers. The Alaska Daily Empire (Juneau). 1918 Dec 30:2.
33. Alaskan Engineering Commission. Alaska railroad record. Anchorage (AK): The Commission; 1920.
34. Railroad work is hampered by the influenza. The Nenana Daily News. 1918 Dec 18:2.
35. Must wear badge on hat at Nenana. The Cordova Daily Times. 1918 Dec 23:3.
36. Teller in death grip. The Nome Tri-Weekly Nugget. 1918 Dec 2:1.
37. Natives die like flies. The Alaska Daily Empire (Juneau). 1918 Nov 26:8.
38. Natives establish voluntary quarantine. The Nome Tri-Weekly Nugget. 1919 April 18:3.
39. Brown P, Gajdusek DC, Morris JA. Virus of the 1918 influenza pandemic era: new evidence about its antigenic character. Science. 1969;166:117–9. https://doi.org/10.1126/science.166.3901.117
40. Cumpston JHL. Influenza and maritime quarantine in Australia. Commonwealth of Australia; 1919.
41. Shanks GD, Brundage JF. Pacific islands which escaped the 1918–1919 influenza pandemic and their subsequent mortality experiences. Epidemiol Infect. 2013;141:353–6. https://doi.org/10.1017/S0950268812000866
42. World Health Organization Writing Group. Non-pharmaceutical interventions for pandemic influenza, international measures. Emerg Infect Dis. 2006;12:81–7. https://doi.org/10.3201/eid1201.051370
43. Zhang Z, Yao W, Wang Y, Long C, Fu X. Wuhan and Hubei COVID-19 mortality analysis reveals the critical role of timely supply of medical resources. J Infect. 2020;81:147–78. https://doi.org/10.1016/j.jinf.2020.03.018
44. Zhang R, Wang Y, Lv Z, Pei S. Evaluating the impact of stay-at-home and quarantine measures on COVID-19 spread. BMC Infect Dis. 2022;22:648. https://doi.org/10.1186/s12879-022-07636-4
45. Mamelund SE. Geography may explain adult mortality from the 1918–20 influenza pandemic. Epidemics. 2011;3:46–60. https://doi.org/10.1016/j.epidem.2011.02.001
46. Mithani SS, Bota AB, Zhu DT, Wilson K. A scoping review of global vaccine certificate solutions for COVID-19. Hum Vaccin Immunother. 2022;18:1–12. https://doi.org/10.1080/21645515.2021.1969849
47. Brady BR, Bahr HM. The Influenza Epidemic of 1918–1920 among the Navajos: marginality, mortality, and the implications of some neglected eyewitness accounts. Am Indian Q. 2014;38:459–91. https://doi.org/10.1353/aiq.2014.a564175
48. Mamelund SE. Spanish influenza mortality of ethnic minorities in Norway 1918–1919. Eur J Popul. 2003;19:83–102. https://doi.org/10.1023/A:1022179025843
49. Nygaard IH, Dahal S, Chowell G, Sattenspiel L, Sommerseth HL, Mamelund SE. Age-specific mortality and the role of living remotely: the 1918–20 influenza pandemic in Kautokeino and Karasjok, Norway. Int J Circumpolar Health. 2023;82:2179452. https://doi.org/10.1080/22423982.2023.2179452
50. Goha A, Mezue K, Edwards P, Madu K, Baugh D, Tulloch-Reid EE, et al. Indigenous people and the COVID-19 pandemic: the tip of an iceberg of social and economic inequities. J Epidemiol Community Health. 2021;75:207–8. https://doi.org/10.1136/jech-2020-214755

Address for correspondence: Uddhav Khakurel or Svenn-Erik Mamelund, Centre for Research on Pandemics & Society (PANSOC), Oslo Metropolitan University, PO Box 4, St. Olavs plass, NO-0130 Oslo, Norway; email: uddhavmailbox@gmail.com or masv@oslomet.no

Borrelia Lineages Adjacent to Zoonotic Clades in Black Flying Foxes (*Pteropus alecto*), Australia, 2018–2020

Taylor B. Verrett, Caylee A. Falvo, Evelyn Benson, Devin N. Jones-Slobodian, Daniel E. Crowley, Adrienne S. Dale, Tamika J. Lunn, Manuel Ruiz-Aravena, Agnieszka Rynda-Apple, Clifton D. McKee, Kerry L. Clark, Alexander W. Gofton, Bat One Health, Alison J. Peel, Raina K. Plowright, Daniel J. Becker

We explored the role of black flying foxes (*Pteropus alecto*) in Australia as reservoirs of *Borrelia* bacteria. We found bats infected with 2 *Borrelia* haplotypes phylogenetically distinct from Lyme or relapsing fever clades. Efforts to sample black flying foxes and their ectoparasites are needed to evaluate zoonotic potential of those *Borrelia* lineages.

Bacteria in the genus *Borrelia* are causative agents of 2 diseases of substantial public health concern, Lyme borreliosis and relapsing fever. Lyme borreliosis is the most frequently reported vectorborne infection in the Northern Hemisphere; its vector is Ixodidae family ticks (*1*). By contrast, relapsing fever is globally distributed; its vector is predominantly Argasidae family ticks, and thousands of cases of febrile illness in humans are attributed to it annually (*2*).

Two of the 3 well-recognized monophyletic *Borrelia* clades are the *B. burgdorferi* sensu lato complex that causes Lyme borreliosis and the relapsing fever group that causes relapsing fever; the third clade is a group hosted by reptiles and echidnas (*3*). *Borrelia* from the *B. burgdorferi* s.l. and relapsing fever clades are harbored by a broad range of vertebrate hosts, including birds, reptiles, and mammals. Identifying reservoir hosts and clarifying their role in propagating *Borrelia* are critical for monitoring and mitigating spillover risk. For example, migratory birds can contribute to the long-distance dispersal of *B. burgdorferi* s.l. by transporting millions of ticks within and across continents (*4*).

Bats might play an underrecognized role in the dispersal and enzootic maintenance of *Borrelia* bacteria. Bats are volant mammals that have been known for more than a century to harbor borrelial spirochaetes (*5*), and surveys within the last 5 years indicate bats can host *Borrelia* spp. from the relapsing fever group and from a clade adjacent to *B. burgdorferi* s.l. (*6*,*7*). Evidence has shown that bat-associated *Borrelia* infections can be zoonotic because *Borrelia* lineages recovered from bats and bat ticks have been implicated in febrile illness in humans (*8*). Therefore, the expansion of *Borrelia* research in chiropteran hosts could provide more information about the current and future welfare of both bat and human populations.

Pteropodidae family flying foxes (*Pteropus* spp. bats) represent a group that is highly prominent at the human–wildlife interface in Australia and therefore a target for *Borrelia* bacteria surveillance.

Author affiliations: School of Biological Sciences, University of Oklahoma, Norman, Oklahoma, USA (T.B. Verrett, D.J. Becker); Montana State University, Bozeman, Montana, USA (C.A. Falvo, E. Benson, D.N. Jones-Slobodian, D.E. Crowley, A. Rynda-Apple); College of Veterinary Medicine, Cornell University, Ithaca, New York, USA (C.A. Falvo, D.E. Crowley, M. Ruiz-Aravena, R.K. Plowright); Texas Tech University, Lubbock, Texas, USA (A.S. Dale); Odum School of Ecology, University of Georgia, Athens, Georgia, USA (T.J. Lunn); Centre for Planetary Health and Food Security, Griffith University, Nathan, Queensland, Australia (T.J. Lunn, A.J. Peel); Mississippi State University, Starkville, Mississippi, USA (M. Ruiz-Aravena); Johns Hopkins Bloomberg School of Public Health, Baltimore, Maryland, USA (C.D. McKee); University of North Florida, Jacksonville, Florida, USA (K.L. Clark); CSIRO, Health and Biosecurity, Brisbane, Queensland, Australia (A.W. Gofton); Sydney School of Veterinary Science, University of Sydney, Sydney, New South Wales, Australia (A.J. Peel)

DOI: https://doi.org/10.3201/eid3107.241864

The increasing propensity for flying foxes to roost in or near human settlements could increase the overlap of humans and bat ectoparasites and create a potential *Borrelia* bacteria spillover pathway (*9*,*10*). Although black flying foxes (*P. alecto*) have been the subject of extensive research as reservoir hosts of Hendra virus, relatively little study has been devoted to their bacterial communities, including those that could be pathogenic (*11*). We assessed the presence, diversity, and phylogenetic placement of *Borrelia* spp. associated with black flying foxes in Australia.

The Study

As part of ongoing research on the ecology of Hendra virus, we collected blood samples from 840 black flying foxes across 6 sites in southern Queensland and northern New South Wales, Australia, during May 2018–September 2020 (Figure 1). We captured bats with mist nets, anesthetized them with isoflurane, and took blood samples and preserved on Whatman FTA cards (QIAGEN, https://www.qiagen.com) until further processing (*12*). The Montana State University Institutional Animal Care and Use Committee (approval no. 201750, https://www.montana.edu/ric/iacuc/iacuc-committee.html) and Griffith University Animal Ethics Committee (approval nos. ENV/10/16/AEC and ENV/07/20/AEC, https://www.griffith.edu.au/research/research-services/research-ethics-integrity/animal/animal-ethics-committee) approved the field protocols.

We used QIAamp DNA Investigator Kits (QIAGEN) to extract genomic DNA from blood (four to five 2-mm punches per sample), according to the manufacturer's instructions. To determine *Borrelia* spp. infection, we used PCR targeting of the 16S rRNA gene, flagellin (*flaB*) gene, and 16S–23S rRNA intergenic spacer (IGS) (Appendix Table 1, https://wwwnc.cdc.gov/EID/article/31/7/24-1864-App1.pdf).

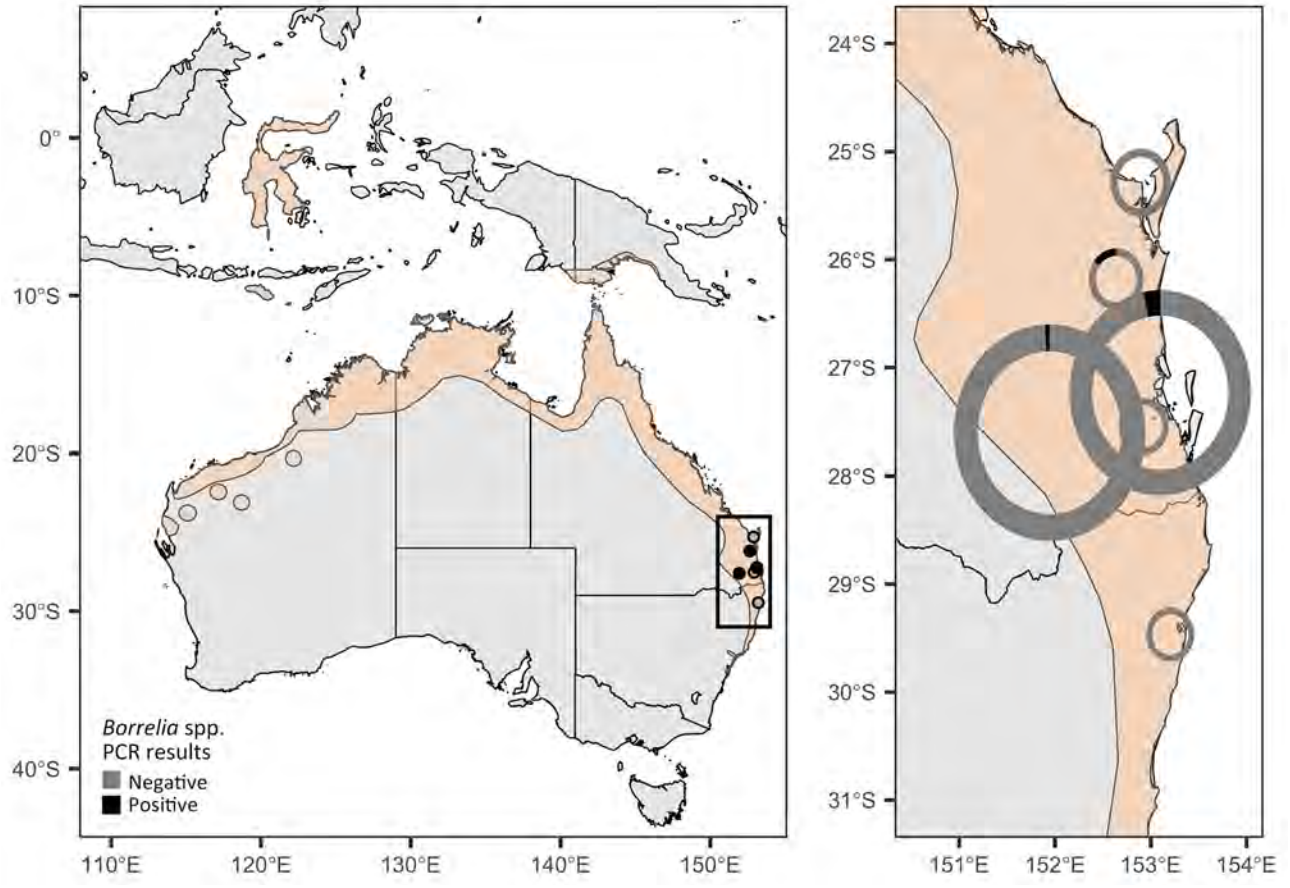

Figure 1. Sampling sites in eastern Australia (Queensland and New South Wales) of *Borrelia* lineages adjacent to zoonotic clades in black flying foxes (*Pteropus alecto*), Australia, 2018–2020. *P. alecto* geographic distribution (beige shading) is shown as defined by the International Union for Conservation of Nature. Circles are colored by the presence or absence of *Borrelia* spp. infections detected in blood samples from bats at each site. Black box at left indicates area enlarged at right, showing donut plots with the fraction of PCR-positive samples in black; circles are scaled by sample size.

We purified PCR products within the expected size range for positive results with the Wizard SV Gel and PCR Clean-Up System (Promega, https://www.promega.com) and had the products Sanger sequenced in both directions at Eurofins Genomics (https://ww.eurofinsgenomics.com). We report prevalence data for IGS, but that gene was not included in phylogenetic analyses because of insufficient reference sequences in GenBank. We manually edited and trimmed the *Borrelia* spp. sequences from black flying foxes and aligned those sequences with reference sequences in GenBank by using the MUSCLE algorithm in Geneious version 2024.0.5 (https://www.geneious.com).

We constructed single-marker phylogenies by using both Bayesian and maximum-likelihood methods because too few bat-associated reference sequences of either *flaB* or 16S were available in GenBank to provide an informative concatenated analysis. For Bayesian analyses, we used MrBayes version 3.2 (https://nbisweden.github.io/MrBayes/download.html) with 10 million Markov chain Monte Carlo generations and a default burn-in of 25%. For maximum-likelihood analyses, we used RAxML version 8.0 (https://github.com/amkozlov/raxml-ng) and a starting tree obtained by searching for the best-scoring maximum-likelihood tree in a single run and calculating branch support with 1,000 rapid bootstrap replicates. For all trees, we used a general time reversible with a proportion of invariable sites and gamma distribution nucleotide substitution model (*13*).

Across our ≈2-year study period and 6 roosts, 17 (2% [95% CI 1.3%–3.2%]) of 840 black flying foxes tested positive for *Borrelia* spp. by using PCR (Table). Roost-specific infection prevalence ranged from 0 of 20 samples (no infection found in 3 of the 6 roosts) to 3 (15% [95% CI 5.2%–36.0%]) of 20 samples in Gympie, Queensland, Australia. The roosts with greatest sampling volume were in Toowoomba (402 bats sampled, 3 [0.7%] infected) and Redcliffe (374 bats sampled, 11 [2.9%] infected) in Queensland, Australia (Appendix Table 2). Most (13/17) infected bats yielded usable sequence data from either 16S rRNA or *flaB* gene targets, which represented 2 haplotypes (p-distances = 8.2% for *flaB* and 1.3% for 16S rRNA). Topologies were similar across tree-building methods (Appendix Figures 1, 2) but were somewhat discordant between gene targets. The *flaB* phylogeny grouped black flying fox *Borrelia* spp. with lineages from Macaregua Cave in Colombia in a clade sister to *B. burgdorferi* s.l. (Figure 2), but 16S rRNA sequence data are not available from Macaregua Cave as of 2025, and no other sequences from bats in Australia are available. The 16S rRNA phylogeny (Figure 3) was also less effective at resolving relationships across the relapsing fever and *B. burgdorferi* s.l. groups supported in previous analyses using multiple markers (*3*). All sequences included here are available at GenBank (accession nos. PQ488732–41 [16S rRNA], PQ492350–60 [*flaB*], and PQ490736–46 [16S–23S IGS]).

Conclusions

This study corroborated that bats can host *Borrelia* infections evolutionarily distinct from recognized clades. However, the clades are more closely related to *B. burgdorferi* s.l. than the relapsing fever group.

Table. Metadata on bats PCR positive for *Borrelia* spp. in lineages adjacent to zoonotic clades in black flying foxes (*Pteropus alecto*), Australia, 2018–2020

Bat no.	Site	Date collected	Sex	Life stage	*Borrelia* sequence GenBank accession nos.
ACGMP001-1	Gympie	2019 Jan	F	Adult	PQ492350,* PQ490736†
ACGMP001-4	Gympie	2019 Jan	F	Adult	PQ492351,* PQ490737†
ACGMP001-5	Gympie	2019 Jan	F	Adult	PQ488732,‡ PQ490738†
ACRED001-15	Redcliffe	2018 May	M	Adult	PQ488733,‡ PQ492352,* PQ490739†
ACRED003-23	Redcliffe	2018 Sep	M	Subadult	PQ488734,‡ PQ492353,* PQ490740†
ACRED004-31	Redcliffe	2018 Dec	F	Adult	PQ488735‡
ACRED006-54	Redcliffe	2019 May	F	Adult	PQ488736,‡ PQ492354,* PQ490741†
ACRED007-51	Redcliffe	2019 Jul	F	Adult	PQ488737,‡ PQ492355,* PQ490742†
ACRED008-54	Redcliffe	2019 Sep	F	Adult	PQ492356,* PQ490743†
ACRED009-72	Redcliffe	2019 Dec	M	Subadult	PQ488738,‡ PQ492357*
ACRED010-32	Redcliffe	2020 Mar	M	Adult	PQ488739,‡ PQ492358*
ACRED010-42	Redcliffe	2020 Mar	F	Adult	PQ488740,‡ PQ490744†
ACRED011-45	Redcliffe	2020 May	F	Adult	PQ492359,* PQ490745†
ACRED011-60	Redcliffe	2020 May	M	Adult	PQ488741,‡ PQ492360,* PQ490746†
ACTOW001-15	Toowoomba	2018 Jun	F	Adult	No sequences
ACTOW002-30	Toowoomba	2018 Jul	F	Subadult	No sequences
ACTOW006-21	Toowoomba	2019 Mar	F	Subadult	No sequences

*Flagellin gene.
†16S–23S rRNA intergenic spacer.
‡16S rRNA.

We recovered sequences from 11 of 17 infected bats in 2 *Borrelia* spp. lineages (Figure 2). Haplotype 1 was represented by a single host that shared a roost in Gympie with a bat infected with haplotype 2, suggesting that variation is unlikely to be structured by geographic isolation. Phylogenetic reconstruction of *flaB* and 16S rRNA suggested *Borrelia* infections from black flying foxes belong to a clade adjacent to existing *B. burgdorferi* s.l. and that relapsing fever groups and are most closely related to *Borrelia* spp. hosted by phyllostomid bats (Chiroptera order) in Colombia (*7*).

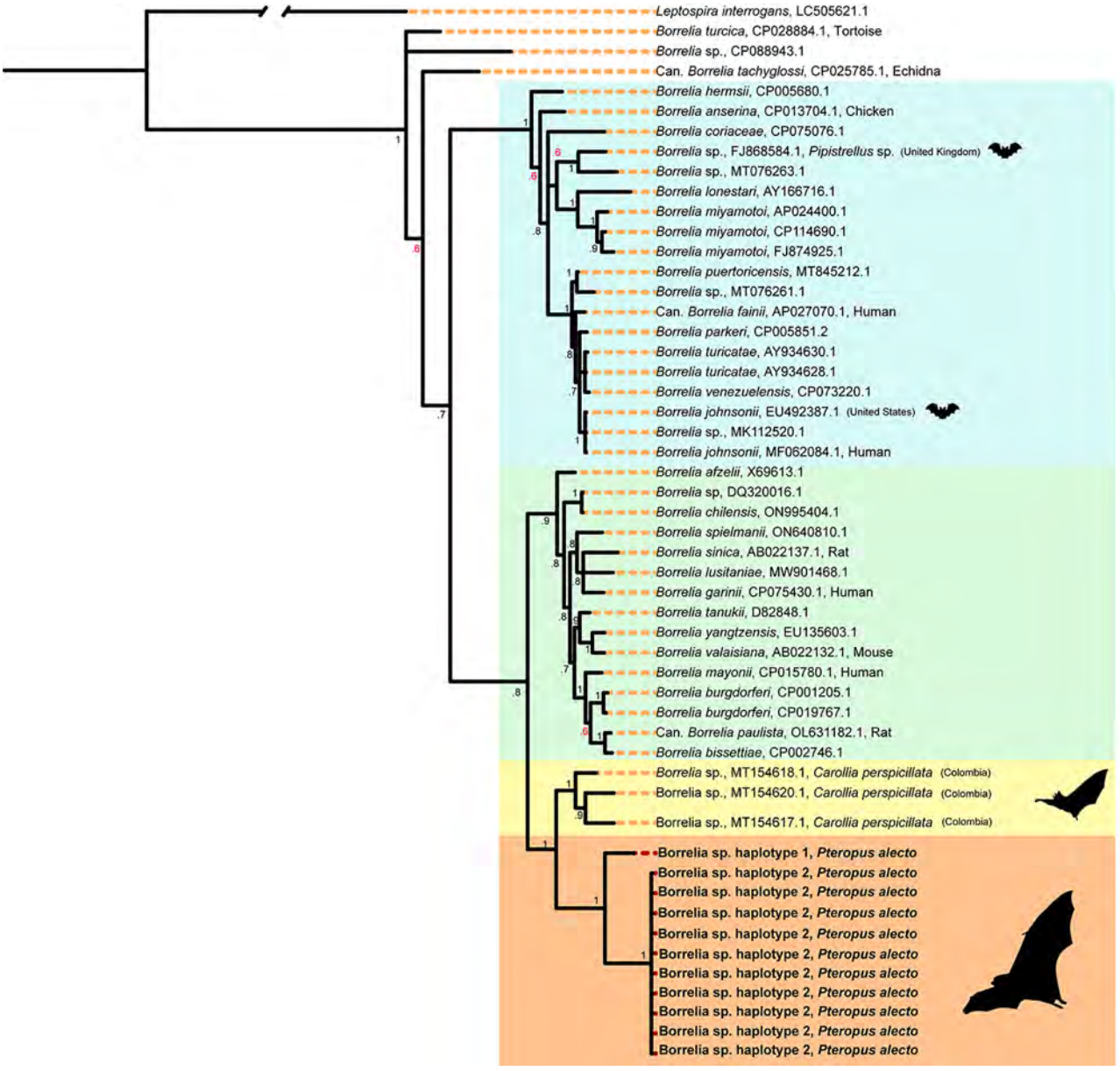

Figure 2. Bayesian phylogenetic tree of *flaB* gene in a study of *Borrelia* lineages adjacent to zoonotic clades in black flying foxes (*Pteropus alecto*), Australia, 2018–2020. The tree displays evolutionary relationships between *Borrelia* spp. and *Borrelia* lineages from black flying foxes. The tree was constructed by using a general time reversible with a proportion of invariable sites and gamma distribution substitution model and 10 million Markov chain Monte Carlo generations. Colors represent major *Borrelia* groups and clades of interest: blue, relapsing fever group; green, *Borrelia burgdorferi* sensu lato complex; yellow, *Borrelia* spp. from Macaregua Cave, Colombia; light orange, new *Borrelia* haplotypes from black flying foxes in Australia. Red node text represents posterior probabilities <0.70. Host associations are noted when GenBank lineages were isolated from vertebrates, barring experimental infections. GenBank accession numbers are provided. Lineages associated with bats or bat ticks are marked with a bat graphic (sourced from Noun Project, https://thenounproject.com).

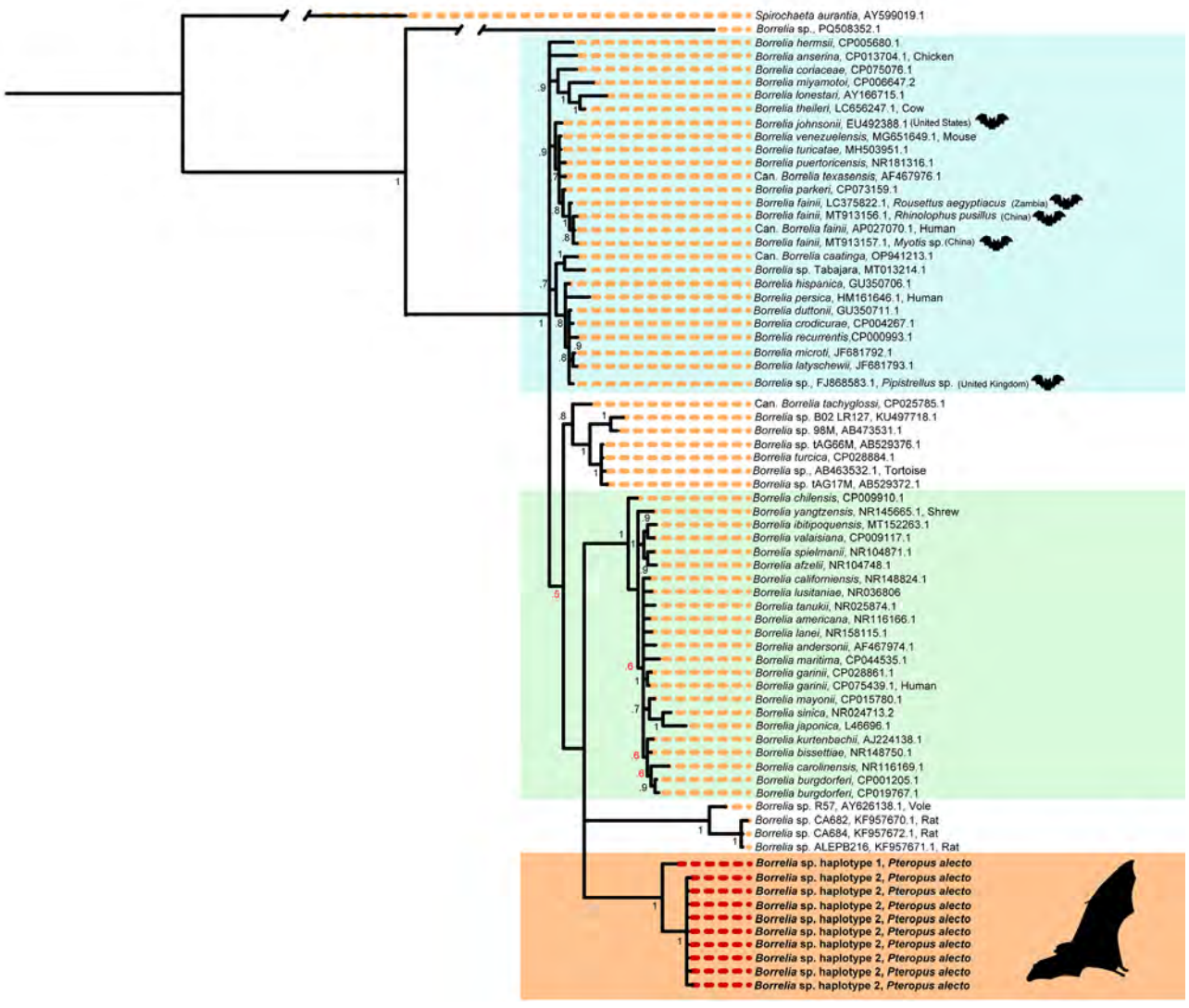

Figure 3. Bayesian phylogenetic tree 16S rRNA gene in a study of *Borrelia* lineages adjacent to zoonotic clades in black flying foxes (*Pteropus alecto*), Australia, 2018–2020. The tree displays evolutionary relationships between *Borrelia* spp. and *Borrelia* lineages from black flying foxes. The tree was constructed by using a general time reversible with a proportion of invariable sites and gamma distribution substitution model and 10 million Markov chain Monte Carlo generations. Colors represent major *Borrelia* groups and clades of interest: blue, relapsing fever group; green, *Borrelia burgdorferi* sensu lato complex; light orange, new *Borrelia* haplotypes from black flying foxes in Australia. Red node text represents posterior probabilities <0.70. Host associations are noted when GenBank lineages were isolated from vertebrates, barring experimental infections. GenBank accession numbers are provided. Lineages associated with bats or bat ticks are marked with a bat graphic (sourced from Noun Project, https://thenounproject.com).

Our results are a base for establishing the presence and phylogenetic placement of *Borrelia* infections in flying foxes but underscore research gaps in characterizing their zoonotic potential. Virulence of those lineages in flying foxes is unknown. Although bats are tolerant of multiple viruses, lethal *Borrelia* infections in bats are documented (*14*). The arthropod vector of lineages described in this study also remains unidentified, but host specificity and geographic range of that vector should strongly influence zoonotic risk. For example, certain ixodid bat ticks have generalist feeding habits that could position them as an epidemiologic link between bats, domestic animals, and humans (*15*). Targeted efforts to sample black flying foxes and their ectoparasites across their range are needed to clarify information regarding the zoonotic potential of the novel *Borrelia* lineages described in this study.

This article was preprinted at https://www.biorxiv.org/content/10.1101/2024.12.20.629695v1.

Acknowledgments

We thank the Butchulla, Gumbainggir, Kabi Kabi, Turrbal, and Yuggera Ugarapul people, who are the Traditional Custodians of the land upon which this work was conducted. We also thank government and private landholders for granting permission for fieldwork and broader team members and volunteers for their contributions, including Peggy Eby, Maureen Kessler, Liam Chirio, Mandy Allonby, Rachael Smethurst, Remy Brooks, Liam McGuire, Kirk Silas, Ticha Padgett-Stewart, Denise Karkkainen, Justine Scaccia, Ariana Ananda, Emma Glennon, Hannah Eiseman, Sara LaTrielle, Isaac Knights, Dian Riseley, and Stella Maris Januario da Silva.

Research was conducted with a Scientific Purposes Permits from the Queensland Department of Environment and Heritage Protection (permit nos. WISP17455716 and WA0012532), a permit to Take, Use, Keep or Interfere with Cultural or Natural Resources (Scientific Purpose) from the Department of National Parks, Sport and Racing (permit no. WITK18590417), a Scientific License from the New South Wales Parks and Wildlife Service (permit no. SL101800), and a general and products liability protection permit (permit no. GRI 18 GPL) and with permission to undertake research on council and private land. Sample import to Montana State University was authorized by import permit no. 20200728-2504A.

This work was funded by the Defense Advanced Research Projects Agency (DARPA) Preventing Emerging Pathogenic Threats (PREEMPT) program (cooperative agreement no. D18AC00031) and the US National Science Foundation (grant nos. DEB-1716698, EF-2133763, and EF-2231624). The content of the information does not necessarily reflect the position or the policy of the US government, and no official endorsement should be inferred. Molecular analyses were also partially supported by the Early Career Grants Programme of the Royal Society of Tropical Medicine and Hygiene.

About the Author

Ms. Verrett is a doctoral candidate at the University of Oklahoma School of Biological Sciences. Her primary research interests are in how host–parasite interactions are influenced by seasonal movement and anthropogenic change, particularly in migratory bird systems.

References

1. Khatchikian CE, Prusinski MA, Stone M, Backenson PB, Wang I-N, Foley E, et al. Recent and rapid population growth and range expansion of the Lyme disease tick vector, *Ixodes scapularis*, in North America. Evolution. 2015;69:1678–89. https://doi.org/10.1111/evo.12690
2. Jakab Á, Kahlig P, Kuenzli E, Neumayr A. Tick borne relapsing fever–a systematic review and analysis of the literature. PLoS Negl Trop Dis. 2022;16:e0010212. https://doi.org/10.1371/journal.pntd.0010212
3. Loh S-M, Gillett A, Ryan U, Irwin P, Oskam C. Molecular characterization of '*Candidatus Borrelia tachyglossi*' (family Spirochaetaceae) in echidna ticks, *Bothriocroton concolor*. Int J Syst Evol Microbiol. 2017;67:1075–80. https://doi.org/10.1099/ijsem.0.001929
4. Ogden NH, Lindsay LR, Hanincová K, Barker IK, Bigras-Poulin M, Charron DF, et al. Role of migratory birds in introduction and range expansion of *Ixodes scapularis* ticks and of *Borrelia burgdorferi* and *Anaplasma phagocytophilum* in Canada. Appl Environ Microbiol. 2008;74:1780–90. https://doi.org/10.1128/AEM.01982-07
5. Nicolle C, Comte C. On a spirillosis of a cheiroptera (Vespertilio kuhli) [in French]. Ann. de l'Inst. Pasteur 1906;20:311–20.
6. Colunga-Salas P, Sánchez-Montes S, León-Paniagua L, Becker I. *Borrelia* in neotropical bats: detection of two new phylogenetic lineages. Ticks Tick Borne Dis. 2021;12:101642. https://doi.org/10.1016/j.ttbdis.2020.101642
7. Muñoz-Leal S, Faccini-Martínez ÁA, Pérez-Torres J, Chala-Quintero SM, Herrera-Sepúlveda MT, Cuervo C, et al. Novel *Borrelia* genotypes in bats from the Macaregua Cave, Colombia. Zoonoses Public Health. 2021;68:12–8. https://doi.org/10.1111/zph.12789
8. Qiu Y, Nakao R, Hang'ombe BM, Sato K, Kajihara M, Kanchela S, et al. Human borreliosis caused by a New World relapsing fever *Borrelia*-like organism in the old world. Clin Infect Dis. 2019;69:107–12. https://doi.org/10.1093/cid/ciy850
9. Eby P, Peel AJ, Hoegh A, Madden W, Giles JR, Hudson PJ, et al. Pathogen spillover driven by rapid changes in bat ecology. Nature. 2023;613:340–4. https://doi.org/10.1038/s41586-022-05506-2
10. Szentiványi T, Takács N, Sándor AD, Péter Á, Boldogh SA, Kováts D, et al. Bat-associated ticks as a potential link for vector-borne pathogen transmission between bats and other animals. PLoS Negl Trop Dis. 2024;18:e0012584. https://doi.org/10.1371/journal.pntd.0012584
11. Szentivanyi T, McKee C, Jones G, Foster JT. Trends in bacterial pathogens of bats: global distribution and knowledge gaps. Transbound Emerg Dis. 2023;2023:1–17. https://doi.org/10.1155/2023/9285855
12. Hansen D, Hunt BE, Falvo CA, Ruiz-Aravena M, Kessler MK, Hall J, et al.; Bat One Health. Morphological and quantitative analysis of leukocytes in free-living Australian black flying foxes (*Pteropus alecto*). PLoS One. 2022;17:e0268549. https://doi.org/10.1371/journal.pone.0268549
13. Abadi S, Azouri D, Pupko T, Mayrose I. Model selection may not be a mandatory step for phylogeny reconstruction. Nat Commun. 2019;10:934. https://doi.org/10.1038/s41467-019-08822-w
14. Irving AT, Ahn M, Goh G, Anderson DE, Wang L-F. Lessons from the host defences of bats, a unique viral reservoir. Nature. 2021;589:363–70. https://doi.org/10.1038/s41586-020-03128-0
15. Evans NJ, Bown K, Timofte D, Simpson VR, Birtles RJ. Fatal borreliosis in bat caused by relapsing fever spirochete, United Kingdom. Emerg Infect Dis. 2009;15:1331–3. https://doi.org/10.3201/eid1508.090475

Address for correspondence: Taylor B. Verrett, University of Oklahoma School of Biological Sciences, 730 Van Vleet Oval, Norman, OK 73019, USA; email: tbverrett@gmail.com

Lyme Disease Testing Practices, Wisconsin, USA, 2016–2019

Kiersten J. Kugeler, Erica Scotty, Austin Earley, Alison F. Hinckley, Sarah A. Hook, Courtney C. Nawrocki, Alexandra M. Linz, Jennifer Meece, Anna M. Schotthoefer

Positive laboratory results are increasingly used for Lyme disease surveillance in the United States. We found 6%–15% of persons with a positive test each year tested positive in a prior year; repeat testing frequency increased with patient age. Repeat testing of persons with previous seropositivity could affect surveillance data interpretation.

Lyme disease, a tickborne illness caused by *Borrelia burgdorferi* spirochetes, is the most commonly reported vectorborne disease in the United States (*1*–*3*). Most cases are reported from high-incidence states in the Northeast, mid-Atlantic, and upper Midwest: Connecticut, Delaware, Maine, Maryland, Massachusetts, Minnesota, New Hampshire, New Jersey, New York, Pennsylvania, Rhode Island, West Virginia, Wisconsin, Vermont, and Virginia and the District of Columbia. Laboratory diagnostic tests primarily rely on serology. For decades, the standard approach to serologic testing for Lyme disease has been a standard 2-tier (STTT) reflex algorithm, in which specimens with positive or equivocal results on a first-tier screening assay, usually an enzyme immunoassay, are then tested by immunoblots for IgM and IgG detection to confirm specific antibody reactivity (*4*,*5*). Detectable antibodies typically persist for months to years; therefore, repeat testing is not generally expected to provide clinically relevant information about the resolution of infection or evidence of possible reinfection (*4*,*6*).

Since 2022, a positive laboratory result has been considered sufficient to report Lyme disease cases through public health surveillance in high-incidence states (*7*,*8*). However, relatively little is known about test ordering and repeat testing practices that drive the large volume of positive serologic tests in the United States. That knowledge is integral to accurately interpret Lyme disease surveillance data. We summarized Lyme disease serologic test ordering frequency, positivity rates, patient characteristics, and repeat testing patterns in a health system in Wisconsin, USA, during 2016–2019.

Author affiliations: Centers for Disease Control and Prevention, Fort Collins, Colorado, USA (K.J. Kugeler, A. Earley, A.F. Hinckley, S.A. Hook, C.C. Nawrocki); Marshfield Clinic Research Institute, Marshfield Clinic Health System, Marshfield, Wisconsin, USA (E. Scotty, A.M. Linz, J. Meece, A.M. Schotthoefer)

DOI: https://doi.org/10.3201/eid3107.250009

The Study

The Marshfield Clinic Health System serves north-central Wisconsin, which is a state that has a high incidence of Lyme disease (*3*). For this study, we used laboratory data collated from a larger effort to identify and describe Lyme disease cases in electronic health records in the Marshfield Clinic Health System (*9*).

For analytic purposes, we grouped all Lyme disease tests occurring per person per calendar month into 1 testing episode. We described the frequency of testing episodes and positive results, including repeat testing per person, and calculated 95% Wilson CIs around percentages and χ^2 tests where appropriate. We used SAS version 9.4 (SAS Institute, https://www.sas.com) for all analyses. The Marshfield Clinic and Centers for Disease Control and Prevention determined that this study was exempt from human subjects research regulations.

During 2016–2019, a total of 42,077 STTT testing episodes occurred among 36,984 unique patients. Test episodes were more common among female (51.5%) than male (48.5%) patients, among persons 50–69 years of age (29.8%), and during May–August (52.6%). We found that 2,911 (6.9%) persons had positive STTT results, and the results varied by age and sex. Positive results were highest among children, male patients, and specimens submitted in the summer months (Table 1; Figure).

Most (88.4%, 32,684) persons had only 1 testing episode during the 4-year period; of those persons,

Table 1. Patient characteristics and positivity rates of Lyme disease serologic testing, Wisconsin, USA, 2016–2019*

Characteristic	No. (%) test episodes	% Positive (95% CI)
Patient sex†		
F	21,656 (51.5)	5.8 (5.5–6.1)
M	20,420 (48.5)	8.1 (7.7–8.5)
Patient race/ethnicity		
American Indian/Alaska Native	303 (0.7)	6.9 (4.6–10.4)
Asian	302 (0.7)	8.6 (6.0–12.3)
Black or African American	130 (0.3)	5.4 (2.6–10.7)
Native Hawaiian/other Pacific Islander	28 (0.1)	7.1 (2.0–22.7)
White	37,457 (86.6)	7.1 (6.8–7.3)
>1 race	199 (0.5)	5.5 (3.1–9.6)
Hispanic	623 (1.5)	5.6 (4.1–7.7)
Unknown or not reported	4,035 (9.6)	5.9 (5.2–6.6)
Testing month		
January	1,835 (4.4)	4.6 (3.8–5.7)
February	1,563 (3.7)	4.0 (3.1–5.1)
March	1,746 (4.2)	4.8 (3.9–5.9)
April	2,243 (5.3)	5.1 (4.3–6.1)
May	4,215 (10.0)	5.0 (4.3–5.7)
June	6,229 (14.8)	6.7 (6.1–7.3)
July	6,399 (15.2)	9.6 (8.9–10.4)
August	5,306 (12.6)	9.4 (8.6–10.2)
September	3,696 (8.8)	7.3 (6.5–8.2)
October	3,648 (8.7)	7.2 (6.4–8.1)
November	3,022 (7.2)	5.8 (5.0–6.7)
December	2,175 (5.2)	5.4 (4.5–6.4)

*Results reflect 42,077 test episodes.
†One patient missing data on sex.

6.1% had a positive result. Among 34,585 persons with an initial negative serologic test, we noted that 3,892 (11.3%) were tested again during the study period, and 3,711 (95.3%) of those had negative results on all subsequent testing. The frequency of repeat testing after an initial negative test did not differ by patient sex but increased with patient age (p<0.001). Among the 2,084 persons tested again within 12 months of an initial negative serologic testing episode, 110 (5.3%) had subsequent positive STTT results.

The 2,911 positive STTT episodes occurred among 2,580 persons; 450 (17.4%) persons with a positive testing episode were tested again ≥1 time, at a mean of 12 (median 11, range 1–39) months later. Among those 450 persons, 275 were tested again within 12 months, and 64.4% of that subset remained seropositive. Another 111 persons were tested after 12 months but ≤24 months after the first positive test, and 55.0% of results from those subsequent testing episodes were positive.

The percentage of positive testing episodes per year that occurred among persons who had tested positive in a prior year ranged from 5.8% in 2017, when only 2016 testing was available, to 15.3% in 2018, when we considered data from 2016 and 2017 (Table 2). The percentage of persons who tested positive in a prior year increased with patient age (p = 0.01); 5.8% of persons with a prior positive result were <15 years of age, 17.4% were 15–44 years of age, 33.3% were 45–64 years of age, and 43.5% were ≥65 years of age.

Patterns of positive laboratory tests mirrored the demographics and seasonality of Lyme disease as demonstrated through decades of public health surveillance, having more positive results among male persons, among children, and during the summer months (*2*,*3*). However, testing more commonly occurred among older adults and female persons, and the largest discrepancy we observed between test ordering frequency and positive results occurred among middle-aged women, as documented elsewhere (*10*,*11*). Excess negative tests among this group might indicate greater frequency of healthcare visits for signs and symptoms that overlap with or have the potential to be misdiagnosed as Lyme disease or possible differences in the serologic response to *B. burgdorferi* by age and sex (*12*,*13*). Additional studies are

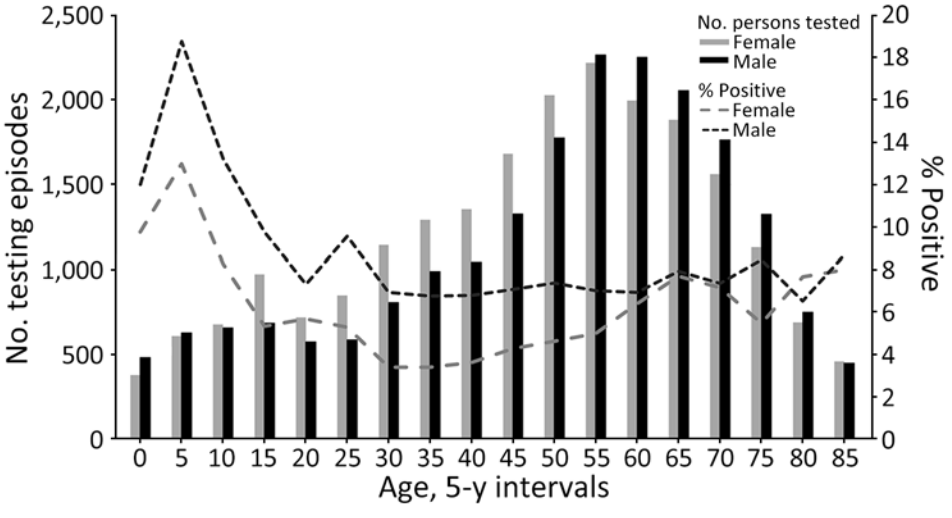

Figure. Lyme disease serologic testing episodes and percentage positivity by patient age and sex, Wisconsin, USA, 2016–2019.

Table 2. Lyme disease serologic resting episodes and repeat positive results per year, Wisconsin, USA, 2016–2019*

Year	No. serologic testing episodes (% positive)	No. positive in a prior year/no. positive (%)	No. (%) persons		
			Prior positive in 2016	Prior positive in 2017	Prior positive in 2018
2016	11,878 (6.7)	NA	NA	NA	NA
2017	12,150 (7.9)	54/928 (5.8)	54 (5.8)	NA	NA
2018	9,444 (6.2)	86/563 (15.3)	33 (5.9)	56 (10.0)	NA
2019	8,605 (6.6)	81/545 (14.9)	26 (4.8)	33 (6.1)	37 (6.8)

*Some tested positive in >1 prior year. Thus, year-specific columns sum to more than the total number of persons in that year who had previously tested positive.

needed to understand the drivers of increased testing frequency and lower positivity rate in this group.

In 2022, the Council of State and Territorial Epidemiologists implemented a revised Lyme disease surveillance case definition in high-incidence states on the basis of positive laboratory results alone. The revision in the subset of the most highly affected states was intended to reduce human resource burden on health departments in high-incidence states and improve standardization of data captured across states (*14*). However, by eliminating the requirement for a concurrent clinically relevant illness, persons might now be captured as Lyme disease cases when their positive test does not reflect incident Lyme disease. The first year of data ascertained under the new case definition showed that reliance on only positive laboratory results in high-incidence states resulted in a disproportionate increase in reported cases among persons ≥65 years of age (*8*).

The first modified 2-tier testing assays were cleared by the US Food and Drug Administration in 2019, and commercial uptake gradually occurred thereafter (*15*). The patterns associated with standard 2-tier testing positivity we report might not be generalizable to characteristics associated with testing on modified 2-tier assays, all of which have different performance characteristics from each other and standard 2-tier assays.

Conclusions

Although serologic testing on persons who previously tested positive for Lyme disease is often not clinically relevant because antibodies to *B. burgdorferi* may persist years after infection, we found up to 15% of persons with positive serologic tests per year also tested positive in a previous calendar year. The frequency of such repeat positives increased with patient age.

Our findings provide evidence that a percentage of reported Lyme disease cases each year may not reflect incident Lyme disease and that percentage increases with patient age and thus might explain the substantial increase in reported Lyme disease cases among older adults beginning in 2022. Knowledge of the frequency and characteristics of repeat testing among persons who have previously tested positive improves our ability to interpret national Lyme disease surveillance data in a more appropriate context.

Acknowledgments

We thank Veronica Burkel, Kate Cooley, and Paul Mead for scientific, analytic, and programmatic support.

This work was supported by the Centers for Disease Control and Prevention (CDC). Marshfield Clinic authors were supported in part by the CDC (contract nos. 75D30120P09851 and 75D30122C14640).

About the Author

Dr. Kugeler is an epidemiologist with the Division of Vector-borne Diseases, National Center for Emerging and Zoonotic Infectious Diseases, Centers for Disease Control and Prevention. Her interests include development of diverse approaches to improve application and interpretation of public health surveillance for bacterial vectorborne diseases.

References

1. Steere A. Lyme disease (Lyme borreliosis) due to *Borrelia burgdorferi*. In: Bennett JE, Dolin R, Blaser M, editors. Mandell, Douglas, and Bennett's principles and practice of infectious diseases. Philadelphia: Elsevier; 2020. p. 2911–22.
2. Mead P. Epidemiology of Lyme disease. Infect Dis Clin North Am. 2022;36:495–521. https://doi.org/10.1016/j.idc.2022.03.004
3. Centers for Disease Control and Prevention. Lyme disease surveillance data [cited 2024 Jul 25]. https://www.cdc.gov/lyme/data-research/facts-stats/surveillance-data-1.html
4. Branda JA, Steere AC. Laboratory diagnosis of Lyme borreliosis. Clin Microbiol Rev. 2021;34:e00018–9. https://doi.org/10.1128/CMR.00018-19
5. Centers for Disease Control and Prevention. Recommendations for test performance and interpretation from the Second National Conference on Serologic Diagnosis of Lyme Disease. MMWR Morb Mortal Wkly Rep. 1995;44:590–1.
6. Kalish RA, McHugh G, Granquist J, Shea B, Ruthazer R, Steere AC. Persistence of immunoglobulin M or immunoglobulin G antibody responses to *Borrelia burgdorferi* 10–20 years after active Lyme disease. Clin Infect Dis. 2001;33:780–5. https://doi.org/10.1086/322669
7. Council of State and Territorial Epidemiologists. Modification of Lyme disease case definition [cited 2021

Oct 18]. https://cdn.ymaws.com/www.cste.org/resource/resmgr/ps/ps2021/21-ID-05_Lyme_Disease.pdf
8. Kugeler KJ, Earley A, Mead PS, Hinckley AF. Surveillance for Lyme disease after implementation of a revised case definition–United States, 2022. MMWR Morb Mortal Wkly Rep. 2024;73:118–23. https://doi.org/10.15585/mmwr.mm7306a1
9. Kugeler KJ, Scotty E, Hinckley AF, Hook SA, Nawrocki CC, Nikolai AM, et al. Epidemiology of Lyme disease as identified through electronic health records in a large midwestern health system, 2016–2019. Open Forum Infect Dis. 2025;12:ofae758. https://doi.org/10.1093/ofid/ofae758
10. Conant JL, Powers J, Sharp G, Mead PS, Nelson CA. Lyme disease testing in a high-incidence state: clinician knowledge and patterns. Am J Clin Pathol. 2018;149:234–40. https://doi.org/10.1093/ajcp/aqx153
11. Li Y, Matsushita F, Chen Z, Jones RS, Bare LA, Petersen JM, et al. Sex- and age-specific Lyme disease testing patterns in the United States, 2019 and 2022. Public Health Rep. 2025; 333549251314419. https://doi.org/10.1177/00333549251314419
12. Rebman AW, Crowder LA, Kirkpatrick A, Aucott JN. Characteristics of seroconversion and implications for diagnosis of post-treatment Lyme disease syndrome: acute and convalescent serology among a prospective cohort of early Lyme disease patients. Clin Rheumatol. 2015;34:585–9. https://doi.org/10.1007/s10067-014-2706-z
13. Jarefors S, Bennet L, You E, Forsberg P, Ekerfelt C, Berglund J, et al. Lyme borreliosis reinfection: might it be explained by a gender difference in immune response? Immunology. 2006;118:224–32. https://doi.org/10.1111/j.1365-2567.2006.02360.x
14. Kugeler KJ, Cervantes K, Brown CM, Horiuchi K, Schiffman E, Lind L, et al. Potential quantitative effect of a laboratory-based approach to Lyme disease surveillance in high-incidence states. Zoonoses Public Health. 2022;69:451–7. https://doi.org/10.1111/zph.12933
15. Association of Public Health Laboratories. Suggested reporting language, interpretation and guidance for Lyme disease serologic test results [cited 2024 Jul 29]. https://www.aphl.org/aboutAPHL/publications/Documents/ID-2024-Lyme-Disease-Serologic-Testing-Reporting.pdf

Address for correspondence: Kiersten J. Kugeler, Centers for Disease Control and Prevention, 3156 Rampart Rd, Fort Collins, CO 80521, USA; email: kkugeler@cdc.gov

Evidence of Viremia in Dairy Cows Naturally Infected with Influenza A Virus, California, USA

Jason Lombard, Chloe Stenkamp-Strahm, Brian McCluskey,[1] Blaine Melody

We confirmed influenza A virus (IAV) by PCR in serum from 18 cows on 3 affected dairy farms in California, USA. Our findings indicate the presence of viremia and might help explain IAV transmission dynamics and shedding patterns in cows. An understanding of those dynamics could enable development of IAV mitigation strategies.

In March 2024, the US Department of Agriculture's National Veterinary Services Laboratories (NVSL) confirmed avian influenza virus (IAV) A(H5N1) clade 2.3.4.4b in dairy cows in Texas, USA (*1*,*2*). That subtype was further characterized as genotype B3.13. Since that detection, >1,070 herds in 17 states have been affected; most of those herds are in California (*3*). Clinical signs observed have been variable, but fever, nasal discharge, loss of milk production, and mastitis are common (*4*).

Experimental and field investigations into the transmission dynamics, pathogenesis, and epidemiology of H5N1 virus in cows are ongoing. Researchers have inoculated cows via the intramammary route in 3 studies, and resulting clinical signs were similar to those from field reports of affected cows, including severe disease requiring euthanasia. Viral RNA was found in milk samples in all studies (*5*–*7*) but in blood samples in only 1 study (*7*). Early in the ongoing outbreak, nasal swab, whole blood, serum, and milk samples were collected from affected dairies in Texas, New Mexico, Kansas, and Ohio. Viral RNA was detected in nasal swab (10/47 cows), whole blood (3/25 cows), serum (1/15 cows), and milk (129/192 cows) samples (*4*).

We sampled cows using a serial sampling design early in the outbreak on affected dairy farms in California. We report detection of IAV RNA in serum samples from lactating dairy cows.

Author affiliations: Colorado State University, Fort Collins, Colorado, USA (J. Lombard, C. Stenkamp-Strahm, B. McCluskey); Lander Veterinary Clinic, Turlock, California, USA (B. Melody)

DOI: https://doi.org/10.3201/eid3107.250134

The Study

In collaboration with a private veterinary practice, daily bulk tank milk (BTM) surveillance for IAV was established in 19 initially unaffected dairies in California; the dairies were in a geographic area that had not experienced IAV infection. BTM samples were collected and transported to the veterinary practice's in-house laboratory for testing for IAV by real-time reverse transcription PCR (RT-PCR). When positive results were detected, a National Animal Health Laboratory Network (NAHLN) laboratory performed confirmation testing, and NVSL confirmed the viral subtype, clade and genotype (H5N1, 2.3.4.4b, B3.13) of virus circulating in each herd. One dairy farm was dropped from surveillance because of inconsistent sampling.

During October 24–November 28, 2024, all 18 herds had IAV detected. For 5 of those herds, we initiated individual cow sampling soon after BTM detection. Individual cow samples were tested at the NAHLN laboratory using the same methods. We considered cycle threshold (Ct) values of <40 to have detectable viral RNA. For Ct values of 38–40 that were initially considered suspect, we retested and considered them positive if Ct values remained <40. The objective was to collect a battery of samples and cow-level information to investigate viral transmission dynamics, viral shedding, and other factors that might lead to development of disease mitigation strategies on affected dairies.

For the 5 dairies where we conducted individual cow sampling, the sampling plan called for collection of nasal swab, serum, urine, and milk (when applicable) samples from preweaning heifers, nonlactating cows, cows that had recently calved, and sick and healthy lactating cows. Determination of sick versus healthy cows varied by farm; we used results of pen milk sampling, dairy management using clinical signs, and

[1]Current affiliation: Lonestar Epidemiology Consulting, Livermore, Colorado, USA.

Table. Summary of influenza A virus testing where viremia was detected by PCR in cows from 3 affected dairy herds in California, USA*

Herd	Breed	No. lactating cows sampled	No. sampling periods	No. (%) lactating cows with RT-PCR–positive serum samples	Interval for each sampling period, d		No. serum samples collected
					Onset of clinical signs to positive serum samples	First bulk tank milk detection to positive serum samples	
A	Jersey	40	2	11 (27.5)	3, 10	14, 21	80
B	Holstein	74	3	5 (6.8)	3, 9, 13	5, 11, 15	107
C	Holstein	30	1	4 (13.3)	5	14	30
Total		144		20 (13.9)			217

*RT-PCR, reverse transcription PCR.

biometric data, when available. For the purposes of this study, we focused on testing serum from lactating cows to establish the presence of viremia. Overall, 3 of 5 farms had cows with detectable viral RNA in serum; samples were taken from 144 cows (Table). Although individual cows were sampled at multiple time points, IAV was detected in serum at a single sampling period.

For the 3 herds with serum RT-PCR IAV detection, we collected samples during 1 to 3 sampling periods within 21 days of BTM detection and within the first 13 days from onset of clinical signs (Figure). Of the 20 cows with serum detection, all cows had virus detected in milk at the same sampling or within 24 hours, whereas 4 (20%) also had concurrent detection in urine. We did not detect virus concurrently in any nasal swab samples. Ct values from serum ranged from 32.3 to 39.2, from milk ranged from 14.4 to 28., and from urine ranged from 28.5 to 38.7. The prevalence of viremia as a percentage of cows sampled per herd ranged from 6.8% to 27.5%; the Jersey herd (herd A) had the highest prevalence.

Conclusions

Our results suggest that a percentage of lactating cows on dairies affected by H5N1 virus experience viremia before or during the peak of clinical cases in the herd. We detected viral RNA in serum of each PCR-positive cow at a single sample date. Viremia therefore appears to be transient, but the duration is unknown because cows were not sampled daily. Although the finding of viremia does not specify how IAV made it to the bloodstream, virus present in circulation suggests that multiple exposure pathways might be possible, including oral and respiratory routes. Intramammary inoculation studies have shown viral RNA to be in multiple tissues at necropsy (*6*,*7*), although viremia had not been consistently detected.

Viremia enables virus to reach many tissues in the body, including the kidneys, which is evident in this

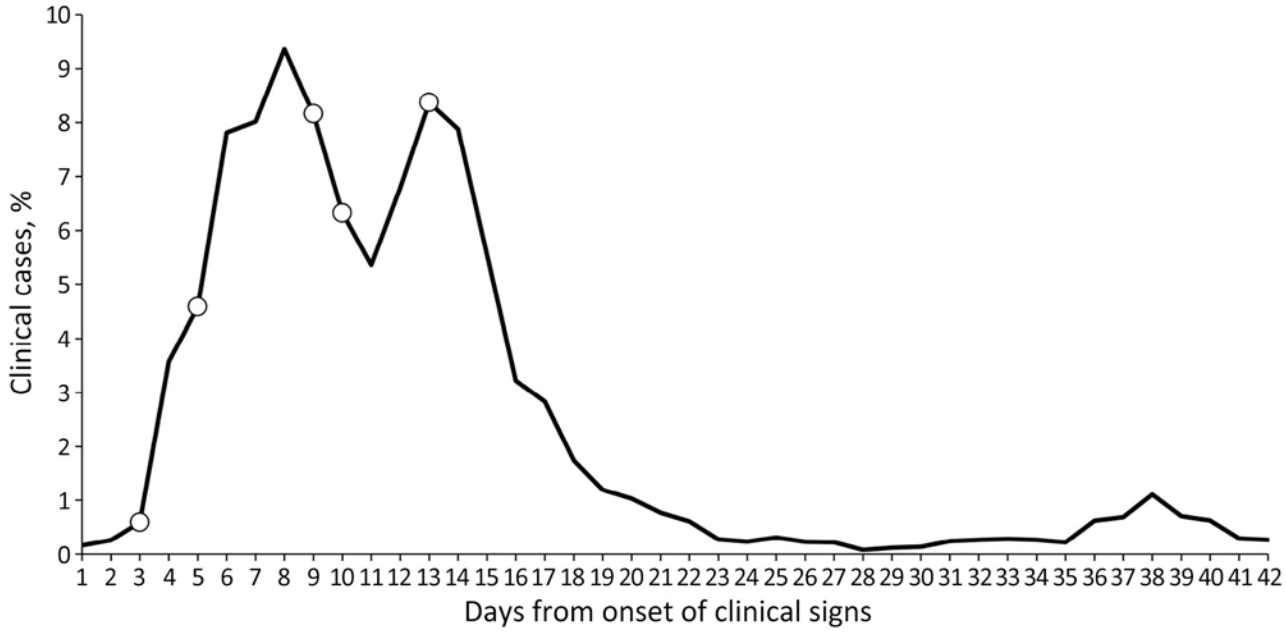

Figure. Epidemic curve for clinical cases of influenza A virus in 3 affected dairy herds in California, USA. We averaged the percentage of daily cases over the 3 farms and then calculated a rolling 3-day average. Open white circles on the curve represent days that virus was detected in serum.

study given detectable RNA in urine samples. That process raises concern for food safety and whether viremia could lead to the presence of H5N1 virus in meat from culled dairy cows. A study that evaluated condemned carcasses found viral RNA in 1 of 109 total samples (*8*). Further, an aborted fetus from farm B, not from a known viremic cow, was positive for H5N1 virus in lung and brain tissue by PCR and immunohistochemical staining. H5N1 virus can move into the reproductive tract and is associated with abortion, which also has implications for the use of fetal serum products. All cows in this study had IAV detection in serum and milk, so it is unclear whether intramammary infection led to viremia or viremia led to intramammary infection. Three cows classified as healthy had viral RNA detected in serum, and 1 of the 3 had viral RNA detected in serum and urine. The relationship between viremia and clinical signs is therefore unclear, although we might have sampled those cows before the onset of clinical disease.

Determining whether the viremia we detected is a rare event is crucial. Viremia has only been detected in 1 previous H5N1 intramammary experimental infection study and 1 field study. To clarify the frequency of viremia, more studies that evaluate IAV RNA in the serum of cattle should be completed. The prevalence of viremia detected in the Jersey breed herd compared with the 2 Holstein breed herds suggests breed differences in susceptibility to viremia from IAV infection might be involved, but differences in cow selection by farm might have affected prevalence. We also recommend a genetic comparison of viral strains collected between studies and between states. Viremia in California dairy cows could be the result of viral evolution, because viremia was not well documented previously, and experimental studies used a strain of H5N1 virus from the early stages of this outbreak. Further in-depth studies that include viral sequencing are necessary to strengthen the evidence supporting our conclusion.

In summary, findings of IAV in serum of cows on farms in California indicates the presence of viremia and could help explain viral transmission dynamics and shedding patterns in cows. Understanding such dynamics could help in development of mitigation strategies to prevent transmission and spread of IAVs, including H5N1 virus.

Acknowledgments

We thank the producers for allowing access to their cows for sampling and Iowa State University Veterinary Diagnostic Laboratory for testing of bulk tank milk and individual cow samples.

Data used in or part of this publication/presentation was made possible, in part, by an agreement from the US Department of Agriculture Animal and Plant Health Inspection Service Veterinary Services (APHIS VS). This publication may not necessarily express the views of APHIS VS. Support was also provided by the California Department of Food and Agriculture (CDFA). Any opinions, findings, conclusions, or recommendations expressed in this publication are those of the author(s) and do not necessarily reflect the views of the CDFA.

About the Author

Dr. Lombard is a veterinary epidemiologist at Colorado State University, Fort Collins, CO, USA. His research interests are infectious diseases of cattle.

References:

1. United States Department of Agriculture Animal and Plant Health Inspection Service. USDA, FDA and CDC share update on HPAI detections in dairy cattle [cited 2025 Jan 5]. https://www.aphis.usda.gov/news/agency-announcements/usda-fda-cdc-share-update-hpai-detections-dairy-cattle
2. Nguyen T-Q, Hutter CR, Markin A, Thomas M, Lantz K, Killian ML, et al. Emergence and interstate spread of highly pathogenic avian influenza A(H5N1) in dairy cattle in the United States. Science. 2025;388:eadq0900. https://doi.org/10.1126/science.adq0900
3. United States Department of Agriculture Animal and Plant Health Inspection Service. HPAI confirmed cases in livestock [cited 2025 Apr 20]. https://www.aphis.usda.gov/livestock-poultry-disease/avian/avian-influenza/hpai-detections/hpai-confirmed-cases-livestock
4. Caserta LC, Frye EA, Butt SL, Laverack M, Nooruzzaman M, Covaleda LM, et al. Spillover of highly pathogenic avian influenza H5N1 virus to dairy cattle. Nature. 2024;634:669–76. https://doi.org/10.1038/s41586-024-07849-4
5. Baker AL, Arruda B, Palmer MV, Boggiatto P, Sarlo Davila K, Buckley A, et al. Dairy cows inoculated with highly pathogenic avian influenza virus H5N1. Nature. 2025;637:913–20. https://doi.org/10.1038/s41586-024-08166-6
6. Halwe NJ, Cool K, Breithaupt A, Schön J, Trujillo JD, Nooruzzaman M, et al. H5N1 clade 2.3.4.4b dynamics in experimentally infected calves and cows. Nature. 2025;637:903–12. https://doi.org/10.1038/s41586-024-08063-y
7. Facciuolo A, Aubrey L, Barron-Castillo U, Berube N, Norleen C, McCreary S, et al. Dairy cows develop protective immunity against reinfection with bovine H5N1 influenza virus. Nat Microbiol. 2025 Apr 25. https://doi.org/10.1038/s41564-025-01998-6
8. United States Department of Agriculture Animal and Plant Health Inspection Service. H5N1 and safety of U.S. meat supply [cited 2024 Dec 4]. https://www.aphis.usda.gov/livestock-poultry-disease/avian/avian-influenza/hpai-detections/livestock/testing-and-science/meat-safety

Address for correspondence: Jason Lombard, Colorado State University, 300 West Drake Rd, Fort Collins, CO 80523-1678, USA; email: jason.lombard@colostate.edu

Emergence and Prevalence of *Vibrio cholerae* O1 Sequence Type 75 Clonal Complex, Fujian Province, China, 2009–2023

Zili Ke, Bo Pang, Jinsong Yang, Yadong Gao, Xiaoxuan Zhang, Haibin Xu, Chaochen Luo, Biao Kan

We investigated the molecular epidemiology of *Vibrio cholerae* O1 in Fujian Province, China, during 2009–2023. Sequence type (ST) 75 clonal complex has emerged continuously since 2020, and ST1480 and ST182 have dominated. ST1480 strains appear to have widespread transmission. To monitor *V. cholerae* evolution, continued global genomic surveillance is needed.

Cholera, an acute and severe diarrheal disease, remains a major public health problem in developing countries. The *Vibrio cholerae* O1 El Tor strain is responsible for the ongoing seventh pandemic of cholera (7PC) (*1*). Most 7PC clinical isolates have belonged to sequence type (ST) 69 (*2*–*4*). However, in the 2010s, ST75 instead of ST69 has emerged and become the dominant clonal group in China and South Africa, and it has several derived populations, including ST169, ST170, and ST182 (*5*,*6*).

Although Fujian, China, experienced many 7PC outbreaks in the past 100 years, cholera cases caused by ST69 strains decreased dramatically after 2006. However, diarrheal diseases caused by *V. cholerae* ST75 and its derivatives have been reported continuously during 2018–2023. To determine the molecular epidemiology of *V. cholerae* in Fujian Province, especially among ST75 and its derivatives, we performed a whole-genome sequence–based study of *V. cholerae* O1 isolated from clinical and environment samples during 2009–2023. The Medical Ethics Committee of Fujian Center for Disease Control and Prevention provided ethical approval for this study.

Author affiliations: Fujian Center for Disease Control and Prevention, Fuzhou, China (Z. Ke, J. Yang, Y. Gao, H. Xu, C. Luo); National Institute for Communicable Disease Control and Prevention, Chinese Center for Disease Control and Prevention, Beijing, China (B. Pang, B. Kan); Fujian Provincial Key Laboratory of Zoonosis Research, Fuzhou (J. Yang); School of Public Health, Fujian Medical University, Fuzhou (J. Yang, X. Zhang)

DOI: https://doi.org/10.3201/eid3107.241838

The Study

During 2009–2023, a total of 20 cases of diarrhea caused by *V. cholerae* O1 were reported in Fujian Province. We selected 1 *V. cholerae* isolate from each patient for this study and removed duplicate patient isolates (Table). All 20 isolates were serotype Ogawa, except 2 serotyped as Inaba. The epidemiologic data showed that all the patients were from China and had never traveled abroad. Twelve patients were male and 8 female, a ratio of 1.5:1. One (5.0%) patient was <14 years of age, and the other 19 (95.0%) were 15–65 years of age. During 2009–2019, only 6 sporadic cases were reported, but 1 outbreak (n = 2 cases) occurred in 2021 and 2 outbreaks (n = 3 cases per outbreak) occurred in 2023.

The results of retrospective survey showed that 75% (15/20) of the patients had eaten seafood within 3 days before illness onset, and the 3 most suspicious foods were shellfish, marine fish, and softshell turtle. All the patients recovered after treatment, and no secondary transmission was observed.

We studied the 20 isolates by obtaining whole-genomic sequences. We submitted short-read sequence data to the National Center for Biotechnology Information (BioProject accession no. PRJNA1191620). We also provide GenBank accession numbers for global sequences used in this study (Appendix 1, https://wwwnc.cdc.gov/EID/article/31/7/24-1838-App1.xlsx).

Of the 20 isolates, we identified 7 STs by multilocus sequence typing (MLST), including ST75 (n = 3), ST1480 (n = 6), ST182 (n = 4), ST170 (n = 3), ST169 (n = 1), ST176 (n = 1), and ST167 (n = 2) (Table). In

Table. Distribution of sequence types from clinical isolates in a study of emergence and prevalence of *Vibrio cholerae* O1 ST75 clonal complex, Fujian Province, China, 2009–2023*

Category	ST	2009	2011	2012	2019	2020	2021	2022	2023	Total
ST75 and derivatives	75	0	0	2	0	0	0	1	0	3
	1480	0	0	0	0	1	2	0	3	6
	182	0	0	0	0	0	4	0	0	4
	170	0	0	0	0	0	0	0	3	3
	169	0	1	0	0	0	0	0	0	1
Others	176	1	0	0	0	0	0	0	0	1
	167	0	0	0	2	0	0	0	0	2

*ST, sequence type.

the 2 Inaba isolates, we found a previously reported transposase insertion in the *rfbT* gene (*7*), which caused the serotype conversion.

For population structural analysis, we constructed a minimum spanning tree on the basis of MLST data (Appendix 2 Figure 1, https://wwwnc.cdc.gov/EID/article/31/7/24-1838-App2.pdf). According to the rules of eBURST (*8*), ST75, ST1480, ST182, ST170, and ST169 could be defined as a clonal complex (CC) of ST75. Using 2,443 core genes ubiquitous in *V. cholerae*, we obtained a minimum spanning tree of the 20 isolates from Fujian by using a core-genome MLST scheme (*9*) (Appendix 2 Figure 2). We found that during 2009–2019, ST75 derivatives were relatively dormant, and we only identified ST169 during that timeframe. However, after the appearance of ST1480 in 2020, ST75 derivatives were distinctly active, and ST1480, ST182, and ST170 emerged within 4 years. Compared with other ST75 derivatives, such as ST169 and ST170, the genetic relationships between ST75, ST1480, and ST182 were closer. The core-genome MLST of ST1480 indicated only 1–43 alleles differences between the isolates collected in 2020, 2021, and 2023.

Most ST75 CC isolates were nontoxigenic, except for 2 ST1480 isolates (strain nos. FJ2021001 and FJ2021002) in 2021 and 1 ST75 isolate (strain nos. FJ2022003) in 2022, which were toxigenic and contained CTX phages of the *ctxB3* genotype. All isolates carried *tcpA*, *rtxA*, *hlyA*, *toxR*, and *Vibrio* pathogenicity islands 1 and 2. However, we did not find *Vibrio* seventh pandemic island I or II in those isolates.

Antimicrobial susceptibility testing by broth dilution method showed that all the ST75 CC isolates were susceptible to ampicillin, cephalosporin, chloramphenicol, tetracycline, ciprofloxacin, and azithromycin. The *qnrVC4* gene was the only antimicrobial-resistance determinant found in those isolates. That gene was in the super integron and is associated with fluoroquinolone resistance (*10*). Although we found the *qnrVC4* gene in the 3 ST75 and 3 ST170 isolates, those isolates did not show fluoroquinolone resistance. Whether the *qnrVC4* gene can mediate resistance to fluoroquinolones in ST75 needs long-term monitoring data.

To investigate the potential origin and phylogenetic relationship of clinical ST75 isolates and their derivatives, we further compared those isolates with 5 environmental strains (2 ST169, 2 ST75, and 1 ST1480) collected from Fujian Province during 2009–2023, and to a global collection of 103 ST75 or closely related ST169, ST170, ST182, ST1480, and ST725–728 genomes (Appendix 1). We constructed a maximum-likelihood phylogenetic tree on the whole-genome single-nucleotide polymorphism (SNP) profiles, which revealed 5 distinct lineages: L3 (Gulf Coast), L3b.1, L3b.2, L3b.3, and L3b.4 (Figure). ST1480 and ST182 clustered in L3b.1, and had a maximum pairwise distance of 0–6 SNPs. We found that 3 ST1480 isolates (strain nos. FJ2021001 and FJ2021002 isolated from patients, and strain no. FJ2014078 isolated from turtle farming water) and 1 ST182 isolate from Fujian (strain no. FJ2021008) were genetically close to 2 ST182 isolates from Zhejiang (strain nos. 11–2_S78 and 11–1_S22 isolated in 2011), and to 2 ST75 isolates from Taiwan (strain R16.3429 isolated in 2010 and strain R16.3447 isolated in 2013). Fujian, Zhejiang, and Taiwan are geographically adjacent in the southeastern region of China. Given the geographic proximity and frequent exchanges among those regions, and because *V. cholerae* O1 ST75 has dominated in Zhejiang and Taiwan since 2009 (*5*,*6*), we speculate that the ST75 derivatives in Fujian shared a common ancestor with the isolates from those areas. ST75 seemed to be a valuable marker for those *V. cholerae* lineages, which differed from the 7PC strains. In addition, the persistence of *V. cholerae* O1 ST75 CC, such as ST1480, in the environment and in patients, especially the emergence of toxigenic isolates, suggest that *V. cholerae* ST75 CC should be monitored more closely.

Conclusions

V. cholerae O1 ST75 CC has gradually expanded in Fujian Province, China. The continuous emergence of ST1480, ST182, ST170, and ST169 indicate the dynamic evolution of this CC. Although no cholera epidemic

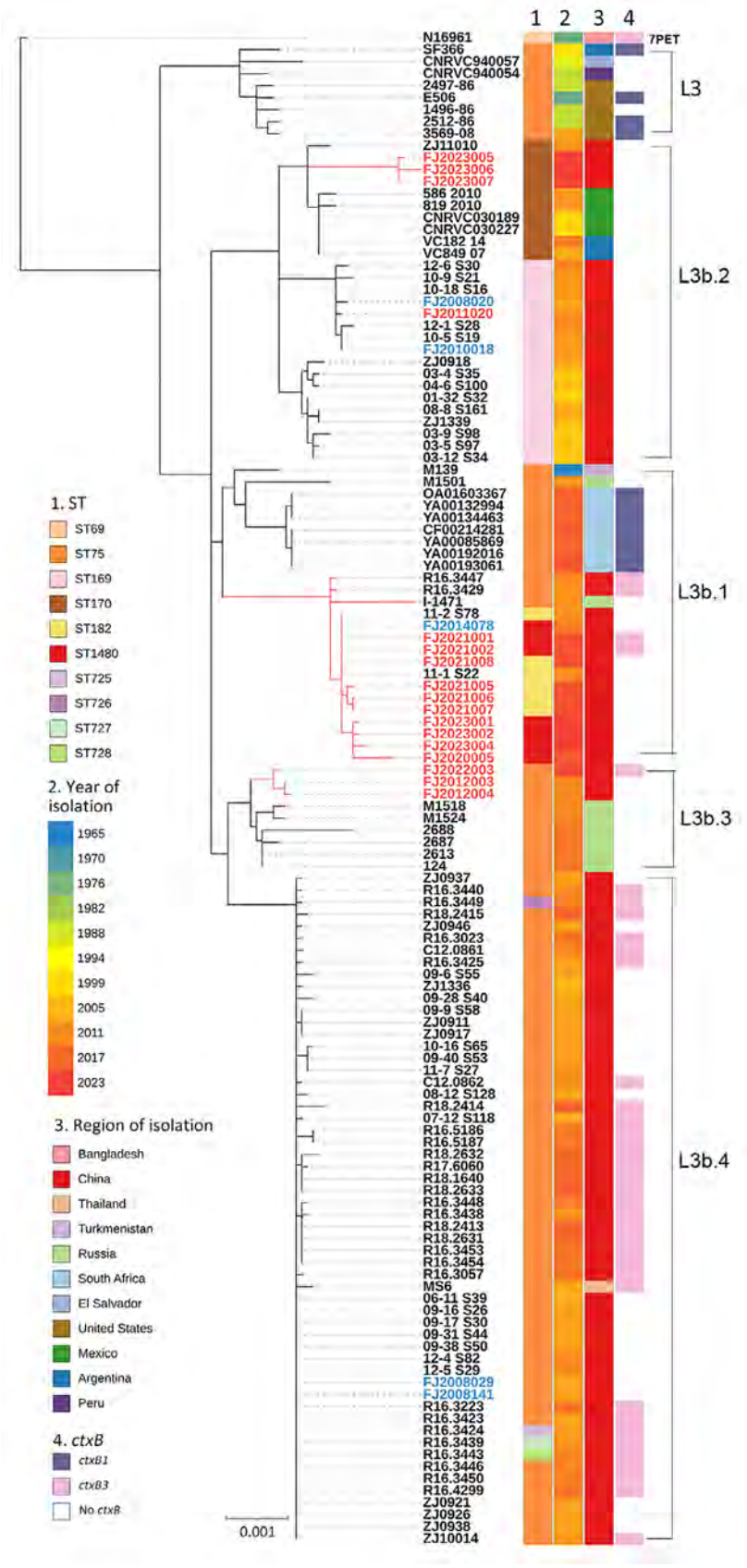

Figure. Maximum-likelihood phylogeny of genomic sequences from a study of emergence and prevalence of *Vibrio cholerae* O1 ST75 clonal complex, Fujian Province, China, 2009–2023. The tree revealed 5 distinct lineages: L3 (Gulf Coast), L3b.1, L3b.2, L3b.3, and L3b.4. ST1480 and ST182 clustered in L3b.1 and had a maximum pairwise distance of 0–6 SNPs. The 7PET genome N16961 (ST69) was included as an outgroup. Isolates from Fujian Province are show as red branch lines and labels for clinical isolates (n = 17) and blue text for environmental isolates (n = 5); and the other 102 isolates (black text) are of global origin. Sequence type, year and region of isolation, and types of *ctxB* are shown at the tips of the tree; lineages are marked on the right side of the tree. The scale bar indicates substitutions per variable site. 7PET, 7th pandemic *V. cholerae* O1 El Tor; *ctxB*, cholera toxin B subunit gene; ST, sequence type.

caused by this CC was reported in Fujian before 2021, the frequency of *ctxAB* genes and the toxin coregulated pilus gene cluster in these strains deserves an enhanced whole-genome sequence–based global surveillance to closely monitor their evolution.

This study was funded by the Natural Science Foundation of Fujian Province, China (grant no. 2022J01399), and Fujian provincial health technology project (grant no. 2021CXA024).

About the Author

Miss Ke is a research assistant with Fujian Center for Disease Control and Prevention, Fujian, China. Her research interests include evolution and genomic epidemiology of bacterial pathogens.

References

1. Kanungo S, Azman AS, Ramamurthy T, Deen J, Dutta S. Cholera. Lancet. 2022;399:1429–40. https://doi.org/10.1016/S0140-6736(22)00330-0
2. Narendrakumar L, Jaikumar VS, Chandrika SK, Thomas S. Epidemiological and pathogenic characteristics of Haitian variant *V. cholerae* circulating in India over a decade (2000–2018). Microb Pathog. 2020;149:104538. https://doi.org/10.1016/j.micpath.2020.104538
3. Greig DR, Schaefer U, Octavia S, Hunter E, Chattaway MA, Dallman TJ, et al. Evaluation of whole-genome sequencing for identification and typing of *Vibrio cholerae*. J Clin Microbiol. 2018;56:e00831-18. https://doi.org/10.1128/JCM.00831-18
4. Siriphap A, Leekitcharoenphon P, Kaas RS, Theethakaew C, Aarestrup FM, Sutheinkul O, et al. Characterization and genetic variation of *Vibrio cholerae* isolated from clinical and environmental sources in Thailand. PLoS One. 2017;12:e0169324. https://doi.org/10.1371/journal.pone.0169324
5. Smith AM, Weill FX, Njamkepo E, Ngomane HM, Ramalwa N, Sekwadi P, et al. Emergence of *Vibrio cholerae* O1 sequence type 75, South Africa, 2018–2020. Emerg Infect Dis. 2021;27:2927–31. https://doi.org/10.3201/eid2711.211144
6. Luo Y, Octavia S, Jin D, Ye J, Miao Z, Jiang T, et al. US Gulf-like toxigenic O1 *Vibrio cholerae* causing sporadic cholera outbreaks in China. J Infect. 2016;72:564–72. https://doi.org/10.1016/j.jinf.2016.02.005
7. Liang W, Wang L, Liang P, Zheng X, Zhou H, Zhang J, et al. Sequence polymorphisms of *rfbT* among the *Vibrio cholerae* O1 strains in the Ogawa and Inaba serotype shifts. BMC Microbiol. 2013;13:173. https://doi.org/10.1186/1471-2180-13-173
8. Spratt BG, Hanage WP, Li B, Aanensen DM, Feil EJ. Displaying the relatedness among isolates of bacterial species—the eBURST approach. FEMS Microbiol Lett. 2004;241:129–34. https://doi.org/10.1016/j.femsle.2004.11.015
9. Liang KYH, Orata FD, Islam MT, Nasreen T, Alam M, Tarr CL, et al. A *Vibrio cholerae* core genome multilocus sequence typing scheme to facilitate the epidemiological study of cholera. J Bacteriol. 2020;202:e00086–20. https://doi.org/10.1128/JB.00086-20
10. Fonseca EL, Vicente ACP. Epidemiology of *qnrVC* alleles and emergence out of the Vibrionaceae family. J Med Microbiol. 2013;62:1628–30. https://doi.org/10.1099/jmm.0.062661-0

Address for correspondence: Bo Pang, National Institute for Communicable Disease Control and Prevention, Chinese Center for Disease Control and Prevention, No. 155, Changbai Road, Beijing 102206, China; email: pangbo@icdc.cn; Jinsong Yang, Department for Prevention and Control of Infectious Diseases, Fujian Center for Disease Control and Prevention, No. 386 Chong'an Rd, Fuzhou 350012, China; email: 15258223@qq.com

Multisystemic Disease and Septicemia Caused by Presumptive *Burkholderia pseudomallei* in American Quarter Horse, Florida, USA

Jason J. Thornton, John F. Roberts, David P. AuCoin, Apichai Tuanyok

We report a presumptive case of melioidosis caused by an atypical *Burkholderia pseudomallei* serotype in an American quarter horse in north-central Florida, USA, through archived formalin-fixed paraffin-embedded specimens dating back to 2006. This case underscores the potential pathologic impact of emergent *B. pseudomallei* in the Gulf region of the United States.

Burkholderia pseudomallei is a gram-negative bacterium and the causative agent of the deadly disease melioidosis (*1*). This pathogen is a saprophytic bacillus distributed in the soil and water of tropical and subtropical environments. Regions where melioidosis is endemic include most of Southeast Asia, South America, the Caribbean, and northern Australia (*2*). Recently, *B. pseudomallei* was isolated from 3 unrelated patients from Mississippi, USA, who had no travel history to a melioidosis-endemic country (*3*–*5*). Those patients demonstrated symptoms consistent with melioidosis. Genetically similar organisms were isolated from the local soil and water, suggesting environmental transmission (*3*).

In addition to humans, many animal species, including horses, have been identified as susceptible to melioidosis (*6*,*7*). Clinical signs associated with melioidosis in animals mimic those of other virulent bacterial diseases and include lethargy, purulent nasal discharge, multiorgan abscesses, septicemia, and death by acute or chronic disease (*8*). Glanders, caused by the closely related *B. mallei*, can also cause similar clinical signs. *B. mallei* does not survive in the soil but can infect many species through animal–animal or zoonotic infection (*8*). Glanders has long been eradicated in the United States (*8*); however, this pathogen remains endemic in some regions of the Middle East, Asia, Africa, and Central and South America (*8*). Diagnosing either entity within the United States is critical because of the zoonotic potential of both organisms and the possible implications for public health. In addition, horses and livestock can be sentinel species for the environmental presence of *B. pseudomallei*, suggesting environmental contamination and posing risks to animals and humans. Predictive modeling studies indicate that *B. pseudomallei* might be ubiquitous throughout tropical and subtropical areas worldwide, including the southern United States (*4*,*5*).

The primary routes of *B. pseudomallei* infection are ingestion, inhalation, and percutaneous inoculation (*1*,*9*). The incidence of melioidosis increases dramatically after heavy rainfall (*9*). In addition, *B. pseudomallei* is classified as a category B bioterrorism bacterium and a Tier 1 (top tier) agent by the Centers for Disease Control and Prevention and Tier 1 by the US Department of Agriculture (*1*). Moreover, *B. pseudomallei* is highly resistant to antimicrobial drugs commonly used to treat sepsis in humans and animals, and an effective vaccine has not been approved (*1*). Furthermore, in apparently successfully treated humans and animals, relapses are common and precede development of chronic melioidosis (*9*). This article discusses a presumptive case of *B. pseudomallei* causing melioidosis-like diseases in an American quarter horse (*Equus caballus*) in Florida, USA.

Author affiliations: University of Florida College of Veterinary Medicine, Gainesville, Florida, USA (J.J. Thornton, J.F. Roberts, A. Tuanyok); University of Nevada School of Medicine, Reno, Nevada, USA (D.P. AuCoin)

DOI: https://doi.org/10.3201/eid3107.241009

The Study

In 2006, an 8-year-old quarter horse gelding with a left retropharyngeal abscess was seen at the University of Florida Veterinary Medical Center (Gainesville, Florida, USA). Clinical examination and radiographs revealed a well-circumscribed 20 × 10 × 18-cm round soft tissue mass caudal to the ramus of the mandible with displacement of the left guttural pouch. Other examination findings included diffuse interstitial pneumonia, multiple cutaneous ulcers on the dorsal midline, anterior uveitis in the right eye, enlarged mesenteric lymph nodes, and an aneurysm of the right renal artery. Because of the animal's declining clinical condition, it was humanely euthanized. At necropsy examination, gross findings included a large, soft, round abscess in the retropharyngeal space, compressing the guttural pouch with a draining tract into the epidermis (Figure 1, panel A). The mesenteric lymph nodes were diffusely enlarged, ranging from 2.0 to 6.0 cm in diameter, with purulent material and hemorrhage (Figure 1, panel B). Other gross findings included diffuse interstitial pneumonia with multifocal 2.0 × 2.0 × 2.0-cm peribronchiolar abscesses (Figure 1 panel C). Small 1.0 × 1.0 × 1.0-cm randomly scattered areas of necrosis were multifocally scattered in the liver (Figure 1, panel D); anterior uveitis was present in the right eye.

Tissue specimens were fixed in 10% neutral buffered formalin, processed routinely, and embedded in paraffin. Paraffin-embedded sections were cut 4 μm thick and examined after staining with hematoxylin and eosin. We performed histochemical Gram stain to screen for bacteria. Histologic sections from the affected submandibular lymph node (Figure 2, panel A), lung (Figure 2, panel B), and mesentery revealed multifocal to coalescing abscesses and pyogranulomas containing necrotic cellular debris and degenerative neutrophils mixed with hemosiderophages (Figure 2, panels C–E). Numerous macrophages and neutrophils contained intracytoplasmic 1–2 μm gram-negative bacilli (Figure 2, panel F).

Postmortem aerobic culture of the retropharyngeal and mesenteric lymph nodes revealed pure *B. cepacia* complex growth. A fatty acid analysis using gas chromatography of the bacterial isolate supported this finding. *B. cepacia* complex is a heterogeneous group of bacteria from the *Burkholderia* genus that typically causes opportunistic infections in immunocompromised hosts. Disease outbreaks often occur in the hospital setting through contaminated medical devices or in patients with chronic respiratory diseases, such as cystic fibrosis (*10*).

The clinical manifestations of this case were unusual for *B. cepacia* complex and more consistent with the clinical course of acute, highly pathogenic *Burkholderia* species. We suspect that the organism was misidentified. The precise methodology of the original diagnosis was not reported in the case documents and is unknown to the authors of this report. Current biochemical systems in historically nonendemic areas often mistakenly identify *B. pseudomallei* strains as members of *B. cepacia* complex (*11*). Our

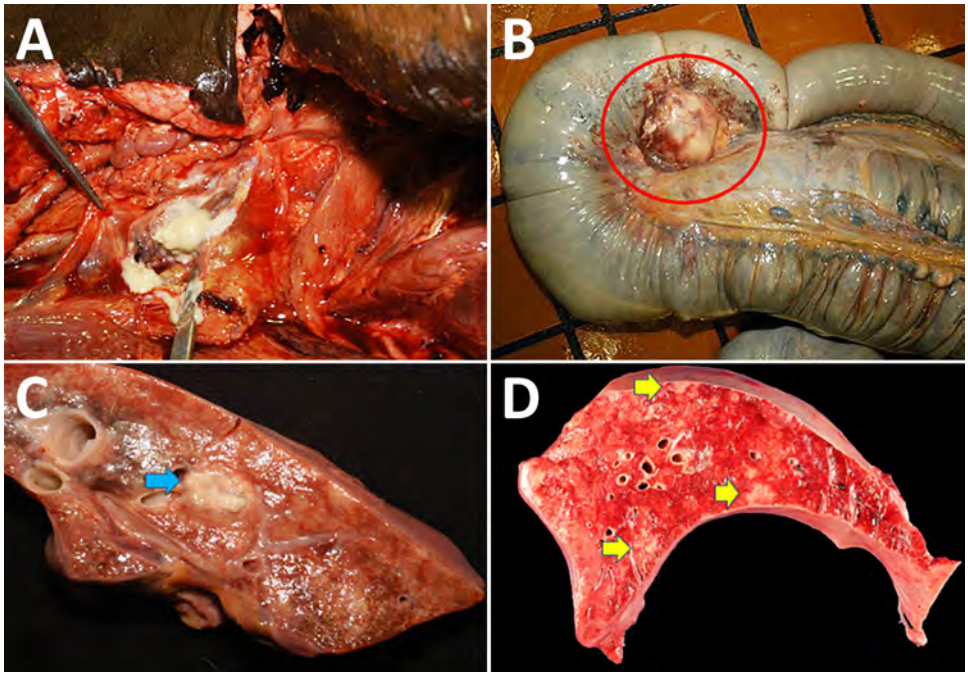

Figure 1. Postmortem photographs of an American quarter horse in study of multisystemic disease and septicemia caused by presumptive *Burkholderia pseudomallei*, Florida, USA. A) The submandibular lymph node was enlarged up to 20 cm in diameter and almost completely effaced by purulent material that extended into the retropharyngeal space and drains near the mandibular ramus. B) Cecal lymph nodes were diffusely enlarged up to 6 cm in diameter and filled with purulent material (red circle). C) The lung was diffusely firm with rib impressions and multifocal 5 × 5-mm to 1 × 2-cm abscesses (blue arrow). D) The liver contained multifocal random 1 × 1-cm pale tan foci scattered throughout the hepatic parenchyma (yellow arrows).

team concluded that further investigation was necessary. Unfortunately, because of DNA fragmentation during routine tissue processing for histopathology, attempts at isolating bacterial DNA from the formalin-fixed paraffin-embedded tissue samples were unsuccessful. A limitation of this study is the inability to extract bacterial DNA from the tissue block, preventing definitive identification of *B. pseudomallei*.

B. pseudomallei employs a network of polysaccharides, including capsular polysaccharides (CPS) and lipopolysaccharides (LPS), to enhance virulence and immune evasion (*12*,*13*). A panel of monoclonal antibodies targeting *B. pseudomallei* and *B. mallei* CPS (4C4), typical LPS O-Ag serotype A (4C7), atypical LPS O-Ag serotype B and its variant B2 (3A2, 5B4), and *B. mallei* LPS O-Ag (3D11) were used (*13*). The secondary antibody was biotinylated goat anti-mouse IgG (1:200 dilution). Intrahistiocytic bacilli were immunopositive for 4C4, 3A2, and 5B4 and immunonegative for 4C7 and 3D11 (Figure 3). We tested 19 different strains of *B. cepacia* complex and demonstrated no cross-reactivity to 4C4, 4C7, 3A2, and 5B4 on Western blot analysis (Table). Previous studies have shown *B. pseudomallei* cross-reactivity by some *B. cepacia* complex strains to *B. pseudomallei*–like CPS-specific antibodies (4C4) (*14*) and *B. mallei* to monoclonal antibodies to typical type A LPS (4C7); however, cross-reactivity of either species to *B. pseudomallei* atypical type B LPS (3A2 and 5B4) has not been reported, and cross-reactivity was not noted in our experiments (*15*). The immunohistochemistry and Western blot results suggest infection with *B. pseudomallei* with atypical O-Ag type B or B2.

Conclusions

This case report describes the histomorphology and immunohistochemical identification of an atypical

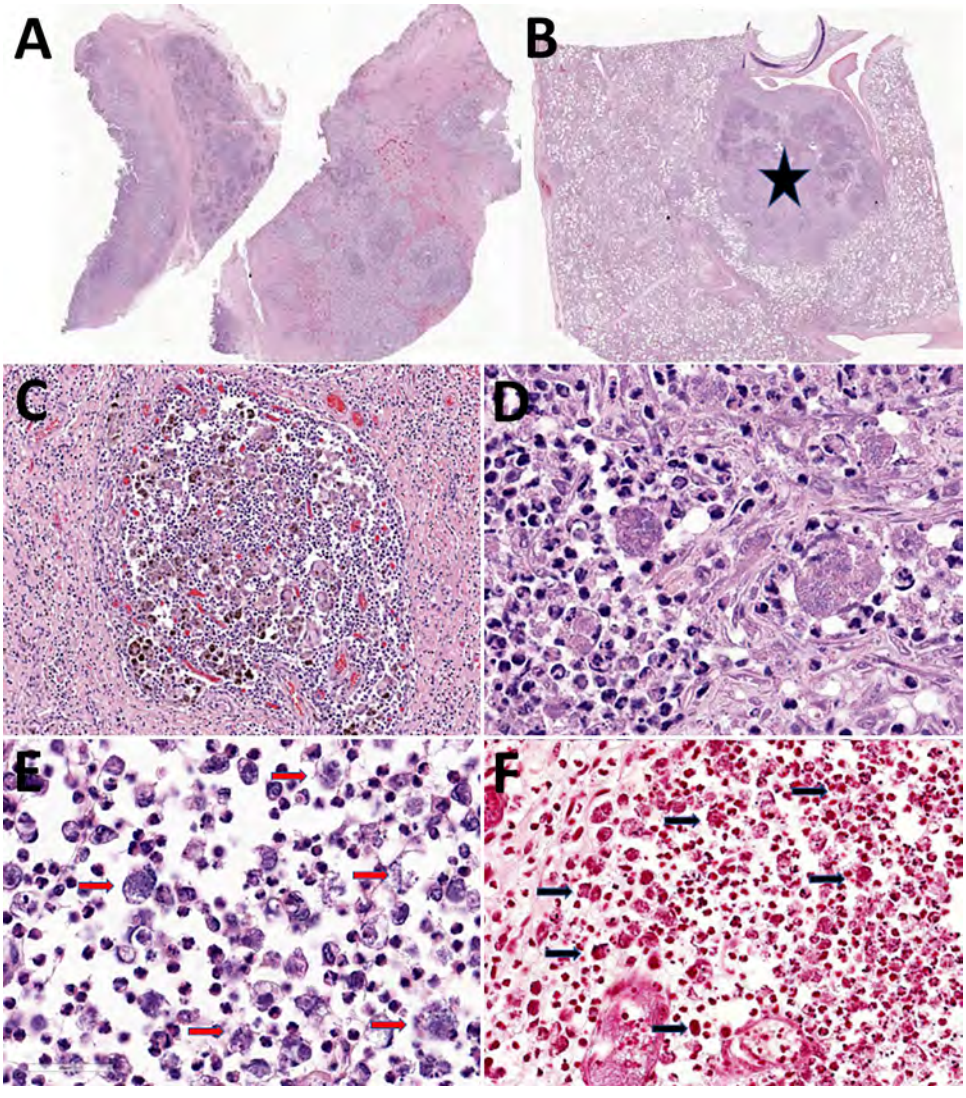

Figure 2. Photomicrography of tissues from study of multisystemic disease and septicemia caused by presumptive *Burkholderia pseudomallei* in American quarter horse, Florida, USA. Photomicrographs show hematoxylin and eosin staining of submandibular lymph node (LN) (A, C, E) and lung (B, D) and Gram stain of the submandibular LN (F). A) Submandibular LN shows multifocal to coalescing pyogranulomas. Original magnification ×2. B) The lung contains a parabronchial abscess (star). Original magnification ×2. C) The submandibular LN pyogranuloma contains necrotic debris, suppurative inflammation, and numerous hemosiderin laden macrophages, multinucleated giant cells surrounded by fibrosis. Original magnification ×20. D) Macrophages and neutrophils in the pulmonary abscess contain a mixed population of 1–2 μm coccobacilli. Original magnification ×40. E) The submandibular node neutrophils and macrophages contain numerous intracellular 1–2 μm bacilli (red arrows). Original magnification ×40. F) The bacilli in the submandibular lymph node are diffusely gram-negative (black arrows). Original magnification ×30.

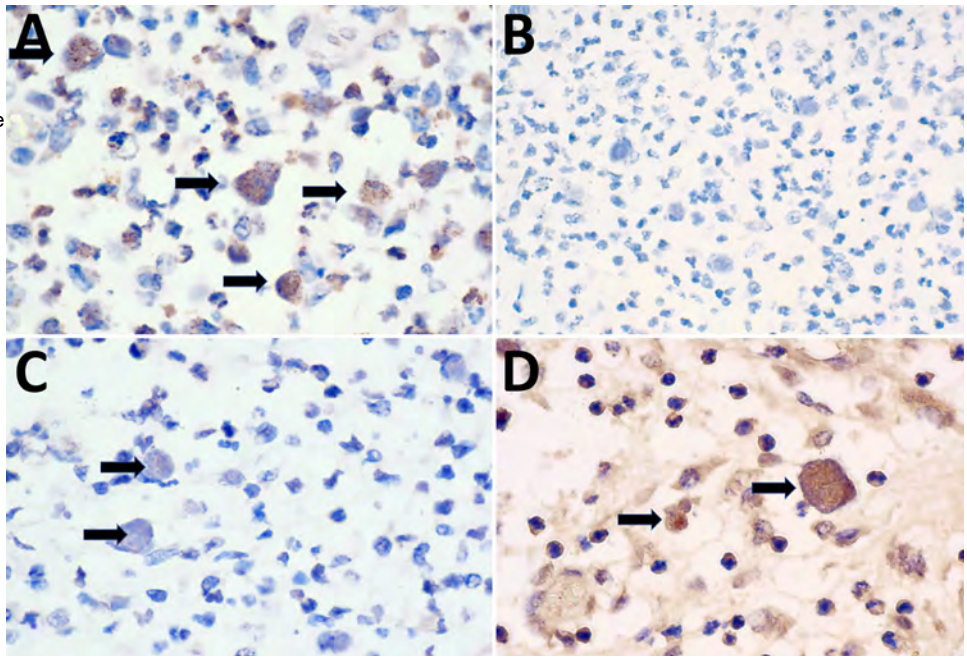

Figure 3. Immunohistochemical examination of tissues from American quarter horse with multisystemic disease and septicemia caused by presumptive *Burkholderia pseudomallei*, Florida, USA. Photomicrographs show immunohistochemistry for monoclonal antibodies 3A2 (A), 4C7 (B), 4C4 (C), and 5B4 (D) of the submandibular lymph node. A) Intra-phagocytic bacilli demonstrated strong immunoreactivity to 3A2 monoclonal antibody to *B. pseudomallei* lipopolysaccharides (LPS) O-Ag B/B2 (black arrows). Original magnification ×100. B) Intra-phagocytic bacilli were diffusely immunonegative for 4C7 monoclonal antibody to *B. pseudomallei* LPS O-ag serotype A. Original magnification ×40. C) Intra-phagocytic bacilli demonstrated weak multifocal immunoreactivity to 4C4 monoclonal antibody to *B. pseudomallei* capsular polysaccharides (black arrows). Original magnification ×100. D) Intra-phagocytic bacilli demonstrated strong immunoreactivity to 5B4 monoclonal antibody to *B. pseudomallei* LPS O-Ag B/B2 (black arrows). Original magnification ×100. Bacilli were immunonegative to 3D11 (not shown) monoclonal antibody to *Bm* LPS O-Ag.

Table. Monoclonal antibody labeling through immunohistochemistry or Western blot analysis of various strains of *Burkholderia* species in study of multisystemic disease and septicemia caused by presumptive *Burkholderia pseudomallei* in American quarter horse, Florida, USA

Monoclonal antibody	Florida case *B. pseudomallei*	*B. pseudomallei* MSHR840, serotype B2	*B. pseudomallei* Bp82, serotype A	*B. pseudomallei* 576mn, serotype B	*B. cepacia* complex (*12*), n = 19	*B. mallei* ATCC 23344, serotype A variant
4C4, Bp CPS	+	+	+	+	–	–
4C7, Bp O-Ag serotype A	–	–	+	–	–	–
3A2, Bp O-Ag serotype B	+	+	–	+	–	–
5B4, Bp O-Ag serotype B2	+	+	–	+	–	–
3D11, Bm O-Ag serotype A variant	–	–	–	–	–	+

serotype of *B. pseudomallei* in a horse with clinical signs consistent with melioidosis. Although type A is the most common LPS O-Ag type of *B. pseudomallei*, accounting for most infections, types B and B2 are found more frequently in Australia (*13*). The route of exposure and travel history of this horse is unknown. On the basis of the immunohistochemistry results in this case, we conclude that the initial culture and biochemical analysis misidentified *B. cepacia* complex. Western blot assay analysis of purified LPS from numerous bacteria in the *B. cepacia* complex failed to highlight any of the mentioned monoclonal antibodies. This case underscores the potential pathological effects of *B. pseudomallei* in horses and other animals in the United States, emphasizing the need for increased awareness and understanding of its emergence as a potential pathogen in diverse species.

Acknowledgments

We sincerely appreciate Puttawat Suphaprueksapong, Sintara Pumin, and Pacharapong Khrongsee for their invaluable assistance and contributions to this case study. We would also like to acknowledge and thank the technical and support staff at the University of Florida College of Veterinary Medicine Histopathology Laboratory, particularly Ana Herrera and Lindsay Vail, for their assistance in providing outstanding histology, histochemistry, and immunohistochemistry staining services.

This study was conducted in strict accordance with ethical principles and guidelines to ensure the highest standards of integrity, accountability, and respect for the animal subject. Because this study was a retrospective analysis of formalin-fixed paraffin-embedded tissue blocks and no live animals were used, this work is exempt from review by the University of Florida Institutional Animal Care and Use Committee.

J.J.T. is funded by a Department of Defense Long-Term Health and Education Training Program scholarship program. The views expressed in this article are those of the author and do not reflect the official policy of the Department of Army/Navy/Air Force, Department of Defense, or US Government.

About the Author

Dr. Thornton is a US Army Veterinary Corps Officer and a diplomate of the American College of Veterinary Pathologists. He is currently a PhD student at the University of Florida College of Veterinary Medicine in the Department of Infectious Diseases and Immunology, studying *Burkholderia pseudomallei* and *B. mallei* and their potential impact on the biosecurity in the United States.

References

1. Wiersinga W, Virk H, Torres AG, Currie BJ, Peacock SJ, Dance DAB, et al. Melioidosis. Nat Rev Dis Primers. 2018;4:17108. https://doi.org/10.1038/nrdp.2017.107
2. Limmathurotsakul D, Golding N, Dance DA, Messina JP, Pigott DM, Moyes CL, et al. Predicted global distribution of *Burkholderia pseudomallei* and burden of melioidosis. Nat Microbiol. 2016;1:15008. https://doi.org/10.1038/nmicrobiol.2015.8
3. Centers for Disease Control and Prevention. Melioidosis locally endemic in areas of the Mississippi Gulf Coast after *Burkholderia pseudomallei* isolated in soil and water and linked to two cases—Mississippi, 2020 and 2022 [cited 2024 Jun 15]. https://emergency.cdc.gov/han/2022/han00470.asp
4. Petras JK, Elrod MG, Ty MC, Dawson P, O'Laughlin K, Gee JE, et al. Locally acquired melioidosis linked to environment—Mississippi, 2020–2023. N Engl J Med. 2023;389:2355–62. https://doi.org/10.1056/NEJMoa2306448
5. Torres AG. The public health significance of finding autochthonous melioidosis cases in the continental United States. PLoS Negl Trop Dis. 2023;17:e0011550. https://doi.org/10.1371/journal.pntd.0011550
6. Ladds PW, Thomas AD, Pott B. Melioidosis with acute meningoencephalomyelitis in a horse. Aust Vet J. 1981;57:36–8. https://doi.org/10.1111/j.1751-0813.1981.tb07082.x
7. Choy JL, Mayo M, Janmaat A, Currie BJ. Animal melioidosis in Australia. Acta Trop. 2000;74:153–8. https://doi.org/10.1016/S0001-706X(99)00065-0
8. Khan I, Wieler LH, Melzer F, Elschner MC, Muhammad G, Ali S, et al. Glanders in animals: a review on epidemiology, clinical presentation, diagnosis and countermeasures. Transbound Emerg Dis. 2013;60:204–21. https://doi.org/10.1111/j.1865-1682.2012.01342.x
9. Chomkatekaew C, Boonklang P, Sangphukieo A, Chewapreecha C. An evolutionary arms race between *Burkholderia pseudomallei* and host immune system: what do we know? Front Microbiol. 2021;11:612568. https://doi.org/10.3389/fmicb.2020.612568
10. Łagowski D, Nowicka B, Nowakiewicz A, Polkowska I, Gnat S. Unusual penile prolapse with an infectious background caused by the *Burkholderia cepacia* complex in a stallion. J Equine Vet Sci. 2021;97:103353. https://doi.org/10.1016/j.jevs.2020.103353
11. Zakharova IB, Lopasteyskaya YA, Toporkov AV, Viktorov DV. Influence of biochemical features of *Burkholderia pseudomallei* strains on identification reliability by Vitek 2 system. J Glob Infect Dis. 2018;10:7–10. https://doi.org/10.4103/jgid.jgid_39_17
12. Nualnoi T, Norris MH, Tuanyok A, Brett PJ, Burtnick MN, Keim PS, et al. Development of immunoassays for *Burkholderia pseudomallei* typical and atypical lipopolysaccharide strain typing. Am J Trop Med Hyg. 2017;96:358–67. https://doi.org/10.4269/ajtmh.16-0308
13. Tuanyok A, Stone JK, Mayo M, Kaestli M, Gruendike J, Georgia S, et al. The genetic and molecular basis of O-antigenic diversity in *Burkholderia pseudomallei* lipopolysaccharide. PLoS Negl Trop Dis. 2012;6:e1453. https://doi.org/10.1371/journal.pntd.0001453
14. Burtnick MN, Dance DAB, Vongsouvath M, Newton PN, Dittrich S, Sendouangphachanh A, et al. Identification of *Burkholderia cepacia* strains that express a *Burkholderia pseudomallei*-like capsular polysaccharide. Microbiol Spectr. 2024;12:e0332123. https://doi.org/10.1128/spectrum.03321-23
15. Songsri J, Kinoshita Y, Kwanhian W, Wisessombat S, Tangpong J, Rahman-Khan MS, et al. Cross-reactivity of latex agglutination assay complicates the identification of *Burkholderia pseudomallei* from soil. FEMS Microbiol Lett. 2018;365. https://doi.org/10.1093/femsle/fny256

Address for correspondence: Jason Thornton, University of Florida College of Veterinary Medicine, 1945 SW 16th Ave, PO Box 11880, Gainesville, FL 32608, USA; email: jason.thornton@ufl.edu

Environmental Exposures Relative to Locally Acquired Hansen Disease, United States

Danielle Chaney, Jennifer Breiman, Jessica K. Fairley

Nine-banded armadillos (*Dasypus novemcinctus*) are suspected transmission sources of Hansen disease in North America. We conducted a telephone survey and chart review of patients with Hansen disease seen at a Georgia, USA, clinic during 1997–2022. Findings suggest frequent outdoor activities and armadillo contact were likely sources of exposure.

Hansen disease (HD), commonly known as leprosy, is caused by Mycobacterium leprae (*1*). HD is diagnosed in approximately 150–200 persons in the United States annually, with a recent high of 225 cases in 2023 (https://www.hrsa.gov/hansens-disease); the disease is diagnosed in 200,000 persons globally (https://www.who.int/news-room/fact-sheets/detail/leprosy). HD leads to nerve damage if left untreated, highlighting the need for early diagnosis (*1*).

Recent literature shows increasing incidence of HD in Florida (*2*), and case reports name Florida as a site of travel or residence in persons receiving an HD diagnosis elsewhere in the United States (*3*,*4*). In addition, a study in Georgia showed a recent increase in cases relating to US-born patients (*5*). The 9-banded armadillo (*Dasypus novemcinctus*), the only known animal reservoir of *M. leprae* in North America, is the suspected source of locally acquired cases (through molecular epidemiology) in the southeast and Gulf states of the United States (*6*–*8*). *M. leprae* can persist in free-living amoebae in soil, serving as another potential reservoir for human infection, which might explain the connection between human infections and the armadillo reservoir (*9*).

Author affiliations: Emory University Rollins School of Public Health, Atlanta, Georgia, USA (D. Chaney); Emory Healthcare, Atlanta (J. Breiman); Emory University School of Medicine, Atlanta (J.K. Fairley)

DOI: http://doi.org/10.3201/eid3107.240986

Recognizing a need to increase epidemiologic understanding of HD in the United States, we describe environmental exposures among patients from the southern portion of the country with suspected locally acquired HD infections. We also highlight clinical and demographic differences between cases involving US-born and immigrant persons.

The Study

A telephone survey assessed exposures in 7 local cases involving patients who were seen at the Emory TravelWell Center (Atlanta, GA, USA). Local cases were defined as HD in patients living in the United States for at least the past 20 years without extensive travel or residence in regions with moderate to high HD endemicity. This study received approval from the Emory Institutional Review Board, and participants provided verbal consent. To provide context for the survey, we conducted a retrospective chart review of local and immigrant cases (seen at TravelWell Center during 1997–2022) (Table 1).

Seven patients participated in the telephone survey (Table 2; Appendix Table, https://wwwnc.cdc.gov/EID/article/31/7/24-0986-App1.pdf). The median age of participants was 69 years. Survey participants lived in Georgia (3 [43%]), Florida (3 [43%]), and Mississippi (1 [14%]) (Figure 1, panel A). Two Georgia participants previously resided in Florida and regularly visited the state. Five participants lived in areas with armadillos, and 5 participants had known physical contact with an armadillo or its bodily fluids. Five participants were in occupations that required them to work outdoors. One of the 2 participants who denied direct physical contact with armadillos or armadillo droppings reported gardening.

We included 55 patients in the chart review (13 presumed local, including the 7 survey participants, and 42 immigrant), noting the year of diagnosis for each (Figure 2). Most immigrant cases originated

Table 1. Clinical characteristics from chart review of local and immigrant cases in study of environmental exposures in suspected locally acquired Hansen disease, United States*

Variable	Local cases, n = 13	Immigrant cases, n = 42	p value†	Odds ratio (95% CI)
Mean age at time of diagnosis, y (SD)	62 (±11)	36 (±13)	<0.005	NA
Sex			0.88	1.71 (0.36–11.24)
F	3 (23)	14 (33)	NA	NA
M	10 (77)	27 (64)	NA	NA
Unknown/not available	0 (0)	1 (2)	NA	NA
Type of disease			1.00	1.11 (0.21–5.01)
Paucibacillary	4 (31)	12 (29)	NA	NA
Multibacillary	9 (69)	30 (71)	NA	NA
Had leprosy reaction			0.032	4.23 (1.13–17.14)
Y	5 (39)	30 (71)	NA	NA
N	8 (62)	11 (26)	NA	NA
Unknown	0 (0)	1 (2)	NA	NA

*Values are no. (%) except as indicated. NA, not applicable.
†2-sided p value was calculated by either *t*-test, χ^2 test, or mid-P exact test (for an expected value <5) as appropriate, comparing immigrant cases to local cases as the reference.

Table 2. Survey responses for participants in survey from study of environmental exposures in suspected locally acquired Hansen disease, United States*

Variable	Survey participants, n = 7
Median age, y (range)	69 (49–79)
Primary state of residence	
Georgia	3 (43)
Florida	3 (43)
Mississippi	1 (14)
Lived internationally	
Y†	3 (43)
N	4 (57)
International travel in the past 10 y	
Y‡	4 (57)
N	3 (43)
Live in areas with armadillos	
Y	5 (71)
N	2 (29)
Physical contact with armadillos	
Y	3 (43)
N	4 (57)
Contact with armadillo bodily fluids or droppings	
Y	3 (43)
N	4 (57)
Time spent outdoors per week, h	
0–2	0 (0)
3–5	4 (57)
6–8	0
≥9	3 (43)
Occupation requires working outside	
Y	5 (71)
N	2 (29)
Takes part in at least one outdoor activity	
Y	6 (86)
N	1 (14)
Outdoor activities reported	
Gardening	4 (57)
Hiking	2 (29)
Hunting	2 (29)
Camping	3 (43)
Outdoor swimming	1 (14)
Other activity§	5 (71)

*Values are no. (%) except as indicated.
†Participants reported living in Germany, Morocco, and Canada.
‡Participants reported travel to The Bahamas, Australia, Spain, France, Germany, Belgium, England, Scotland, Estonia, Denmark, Finland, Norway, Russia, Japan, Mexico, and Canada.
§Other outdoor activities reported included kayaking, golfing, archery, and fishing.

from Brazil (11 [26%]), Mexico (6 [14%]), or India (6 [14%]) (Figure 1, panel B). The mean age at time of diagnosis was 62 (SD ±11) years for local cases and 36 (SD ±13) years for immigrant cases (p<0.005). Patients with leprosy reactions were more likely to be from outside the United States (Table 1). None of the local cases had a known contact with HD.

On the basis of the survey responses, living in an environment with armadillos and spending time outdoors were very frequently reported, lending possible exposure routes to *M. leprae* (*6*–*8*). Most interviewees reported direct physical contact with an armadillo or its bodily fluids in their lifetime, and >70% lived in an area where they see armadillos. We posited that persons who did not report physical contact acquired the bacterium through indirect means, considering that multiple studies have confirmed potentially viable *M. leprae* in environmental sources (*10*–*12*). In fact, most interviewees regularly took part in outdoor activities, such as golfing and gardening, where they might have come in contact with soil or grass contaminated with armadillo urine or feces, which might have served as the route of transmission. In addition, >70% of interviewees worked in outdoor occupations, a much higher percentage than the 2020 national average of 4.3% (*13*). Given the high level of reported outdoor activity of survey participants, we considered also that transmission of HD might have occurred via other zoonotic reservoirs, such as ticks, which have demonstrated the ability to harbor *M. leprae* (*14*).

Conclusions

The participants in this survey lacked typical risk factors for acquiring HD; none lived in or spent significant time in countries with high endemic HD or lived with or knew anyone with HD. We speculated that transmission, thus, must have occurred within

Figure 1. States of residence for patients in study of environmental exposures of suspected locally acquired Hansen disease, United States. Primary states of residence are shown for 13 local case-patients (7 surveyed as part of study, 6 from chart review).

the United States. With studies linking the 9-banded armadillo to locally acquired cases in the southern United States (*6*,*7*), combined with the similar exposure profiles of our survey participants to both armadillos and soil where armadillos live, we believe data support armadillos as a possible route of transmission. Literature is scarce regarding risk factors for HD in the United States, and anecdotal evidence from HD experts across the United States suggests that cases in US-born persons are rare outside of southern states. A recent study of presumed locally acquired HD cases in California identified 6 patients lacking traditional risk factors, such as geographic location or contact with an infected person. Although only 1 patient in that cohort reported armadillo exposure, occurring >50 years prior to diagnosis, all of the patients reported travel to either an endemic country or the US Gulf Coast (*4*).

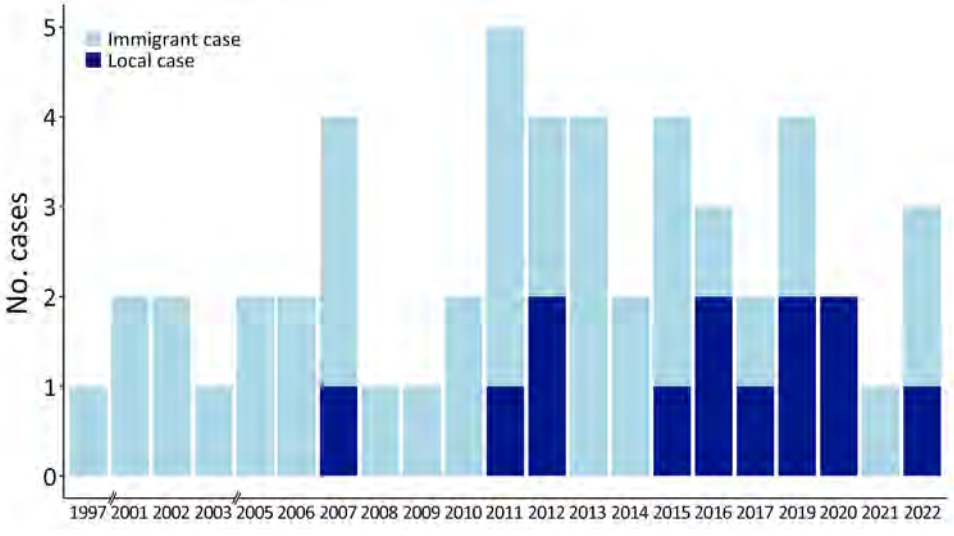

Figure 2. Number of Hansen disease cases from chart review in study of environmental exposures of suspected locally acquired Hansen disease, by year of diagnosis, United States. A total of 55 cases were included in the review.

We did find a statistically significant difference in age of diagnosis between local and immigrant cases; local case-patients were older. In addition, persons with leprosy reactions had higher odds of being from another country. We considered the possibility that US-born patients have different exposure risks to HD compared with patients born outside the United States. For instance, persons from countries with a higher HD prevalence might have a higher likelihood of encountering the bacteria and becoming infected at an earlier age. For person-to-person transmission to occur, research suggests that prolonged close contact with an untreated person is needed (*15*). If zoonotic transmission—as opposed to person-to-person transmission—is the primary source of infection in the United States, and given that *M. leprae* infection was not detected in southeastern US armadillo populations before 2009 (*6*), exposure opportunities for US-born persons compared with persons from endemic countries would be notably different. A counterpoint to this theory is that *M. leprae* is slow-growing, and disease manifestation can take years (*15*). In addition, children and young adults in the United States typically are heavily exposed to dirt and the outdoors, and thus hypothetically exposed to HD, making it highly possible that local case-patients are actually becoming infected earlier than data indicates, but clinical manifestations are occurring at a later age.

The primary limitation of this study was the small sample size, limiting the generalizability of the findings. For our results to be more widely applicable, a demographically and geographically diverse patient population would need to be sampled, an undertaking that would be difficult with this rare disease. Another limitation is the lack of routine molecular genotyping of *M. leprae* isolates from US patients. Comparing patient strains to those associated with armadillos or other reservoirs could clarify sources of infection and inform public health and clinical messaging.

Our study demonstrates the importance of studying HD in a low-endemic setting because further research into the transmission and host-pathogen interactions in the United States could shed light on the larger-scale questions plaguing HD researchers worldwide, namely, how the bacteria is transmitted and who is most at risk for disease. Early diagnosis and treatment of cases of HD in the United States depends greatly on a clear understanding of the risk factors for transmission.

Acknowledgments

We thank the participants who agreed to participate in the study in order to further our understanding of Hansen disease.

About the Author

Ms. Chaney is an epidemiologist at the Massachusetts Department of Public Health in Boston, Massachusetts, USA, where she focuses on healthcare-associated infections and antimicrobial resistance. She is interested in pathogen evolution and the molecular epidemiology of infectious diseases.

References

1. Centers for Disease Control and Prevention. Hansen's disease (leprosy): what is Hansen's disease? 2017 [cited 2022 Dec 13] https://www.cdc.gov/leprosy/about/index.html
2. Domozych R, Kim E, Hart S, Greenwald J. Increasing incidence of leprosy and transmission from armadillos in Central Florida: a case series. JAAD Case Rep. 2016;2:189–92. https://doi.org/10.1016/j.jdcr.2016.03.004
3. Bhukhan A, Dunn C, Nathoo R. Case report of leprosy in central Florida, USA, 2022. Emerg Infect Dis. 2023;29:1698–700. https://doi.org/10.3201/eid2908.220367
4. Belzer A, Ochoa MT, Adler BL. Autochthonous leprosy in the United States. N Engl J Med. 2023;388:2485–7. https://doi.org/10.1056/NEJMc2302317
5. McCormick CD, Lea J, Stryjewska BM, Thompson A, Fairley JK. Trends of leprosy and multibacillary infection in the state of Georgia since the early 1900s. PLoS Negl Trop Dis. 2019; 13:e0007713. https://doi.org/10.1371/journal.pntd.0007713
6. Sharma R, Singh P, Loughry WJ, Lockhart JM, Inman WB, Duthie MS, et al. Zoonotic leprosy in the southeastern United States. Emerg Infect Dis. 2015;21:2127–34. https://doi.org/10.3201/eid2112.150501
7. Truman RW, Singh P, Sharma R, Busso P, Rougemont J, Paniz-Mondolfi A, et al. Probable zoonotic leprosy in the southern United States. N Engl J Med. 2011;364:1626–33. https://doi.org/10.1056/NEJMoa1010536
8. Dai C, Ansari A, Shih S, Marks V, Sharma R, Greenwald J. Molecular epidemiology of locally acquired Hansen's disease in Central Florida. J Am Acad Dermatol. 2019;80:1789–91. https://doi.org/10.1016/j.jaad.2019.01.010
9. Wheat WH, Casali AL, Thomas V, Spencer JS, Lahiri R, Williams DL, et al. Long-term survival and virulence of *Mycobacterium leprae* in amoebal cysts. PLoS Negl Trop Dis. 2014;8:e3405. https://doi.org/10.1371/journal.pntd.0003405
10. Arraes MLBM, Holanda MV, Lima LNGC, Sabadia JAB, Duarte CR, Almeida RLF, et al. Natural environmental water sources in endemic regions of northeastern Brazil are potential reservoirs of viable *Mycobacterium leprae*. Mem Inst Oswaldo Cruz. 2017;112:805–11. https://doi.org/10.1590/0074-02760170117
11. Turankar RP, Lavania M, Singh M, Sengupta U, Siva Sai K, Jadhav RS. Presence of viable *Mycobacterium leprae* in environmental specimens around houses of leprosy patients. Indian J Med Microbiol. 2016;34:315–21. https://doi.org/10.4103/0255-0857.188322
12. Mohanty PS, Naaz F, Katara D, Misba L, Kumar D, Dwivedi DK, et al. Viability of *Mycobacterium leprae* in the environment and its role in leprosy dissemination. Indian J Dermatol Venereol Leprol. 2016;82:23–7. https://doi.org/10.4103/0378-6323.168935
13. US Bureau of Labor Statistics. Occupational requirements in the United States news release. 2020 [cited 2023 Jul 14]. https://www.bls.gov/news.release/archives/ors_12222020.htm

14. Tongluan N, Shelton LT, Collins JH, Ingraffia P, McCormick G, Pena M, et al. *Mycobacterium leprae* infection in ticks and tick-derived cells. Front Microbiol. 2021;12:761420. https://doi.org/10.3389/fmicb.2021.761420
15. Centers for Disease Control and Prevention. Hansen's disease (leprosy): transmission. 2017 [cited 2023 Feb 9] https://www.cdc.gov/leprosy/transmission/index.html

Address for correspondence: Danielle Chaney, Emory Division of Infectious Diseases, 1462 Clifton Rd NE, Rm 530, Atlanta, GA 30322, USA; email: daniellechaney95@gmail.com

Community Infections Linked with Parvovirus B19 Genomic DNA in Wastewater, Texas, USA, 2023–2024

Alessandro Zulli, Rebecca Y. Linfield, Dorothea Duong, Bridgette Hughes, Alexandria B. Boehm

We assessed concentrations of parvovirus B19 DNA from 2 wastewater treatment plants in a Texas, USA, county with a known outbreak in 2024. Wastewater viral concentrations correlated significantly with clinical cases, demonstrating wastewater's potential for tracking parvovirus B19 infections. Peaks in wastewater concentrations were aligned with the peak in hydrops fetalis diagnoses.

Parvovirus B19 is a single-stranded DNA virus transmitted through respiratory droplets. In 2024, infections increased substantially across the United States; seroprevalences in children rose from <3% in 2020–2022 to 24.9% in 2024 (*1*). Parvovirus B19 typically causes a mild slapped cheek rash in children but can lead to serious complications in pregnant women, including hydrops fetalis and fetal death (*2*–*4*). Persons infected with the virus, particularly those who are immunocompromised, are at risk for developing aplastic anemia (*3*,*5*).

Parvovirus B19 is highly infectious, with an estimated basic reproduction number (R_0) of 8, and studies have shown that 20%–50% of susceptible persons are infected during outbreaks in schools (*6*,*7*). No vaccine is available for the virus and treatment options are limited, meaning prevention and early detection are crucial (*1*,*4*,*8*). Nonetheless, parvovirus B19 infection is not a notifiable condition to public health authorities in the United States (*6*). This lack of surveillance led to a Health Alert Network notice from the Centers for Disease Control and Prevention in August 2024, months after the initial rise in cases had occurred (*6*).

Author affiliations: Stanford University, Stanford, California, USA (A. Zulli, R.Y. Linfield, A.B. Boehm); Verily Life Sciences LLC, South San Francisco, California, USA (D. Duong, B. Hughes)

DOI: http://doi.org/10.3201/eid3107.241981

Wastewater-based epidemiology has been shown to be an effective, real-time, and low-cost method of generating epidemiologic data for a variety of human pathogens, suggesting potential utility for parvovirus B19 (*9*,*10*). Our study aimed to evaluate whether wastewater surveillance can track parvovirus B19 infections by analyzing samples from 2 wastewater treatment plants (WWTPs) during a known outbreak in Montgomery, Texas, USA, and comparing results with clinical information from electronic health records systems. Our study was reviewed by the Stanford University Committee for the Protection of Human Subjects and determined to be exempt from oversight.

The Study

We collected 24-hour composite raw wastewater influent samples 3 times/week during December 18, 2023–August 30, 2024, from 2 treatment plants serving 65,000 (WWTP186) and 70,000 (WWTP187) persons (Appendix Figure 1, https://wwwnc.cdc.gov/EID/article/31/7/24-1981-App1.pdf). We collected a total of 220 samples. From each sample, we collected wastewater solids using settling and centrifugation.

We used a previously validated hydrolysis-probe PCR targeting the nonstructural protein 1 gene of parvovirus B19. We confirmed assay specificity and sensitivity through in silico analysis against reference genomes and in vitro testing against common respiratory viruses and bacteria (Appendix, Table 1). We extracted DNA from wastewater solids using the chemagic Viral DNA/RNA 300 kit (Revvity, https://www.revvity.com), followed by column-based PCR inhibitor removal. We quantified viral concentrations of parvovirus B19 (fluorescent molecule FAM) and SARS-CoV-2 (fluorescent molecule HEX) as a duplex assay in 6 replicate wells using digital droplet

reverse transcription PCR (Appendix Table 2). We included negative and positive extraction and PCR controls. The lowest detectable concentration was ≈1,000 copies/g of dry weight. Complete methods, including primers and thermocycling conditions and further details of various controls, are provided (Appendix). Measured concentrations in the samples are available through the Stanford Digital Repository (https://doi.org/10.25740/zn011jk5743).

We gathered clinical case and syndromic data from Epic Cosmos (Epic Systems Corporation, https://cosmos.epic.com). First, we filtered all encounters

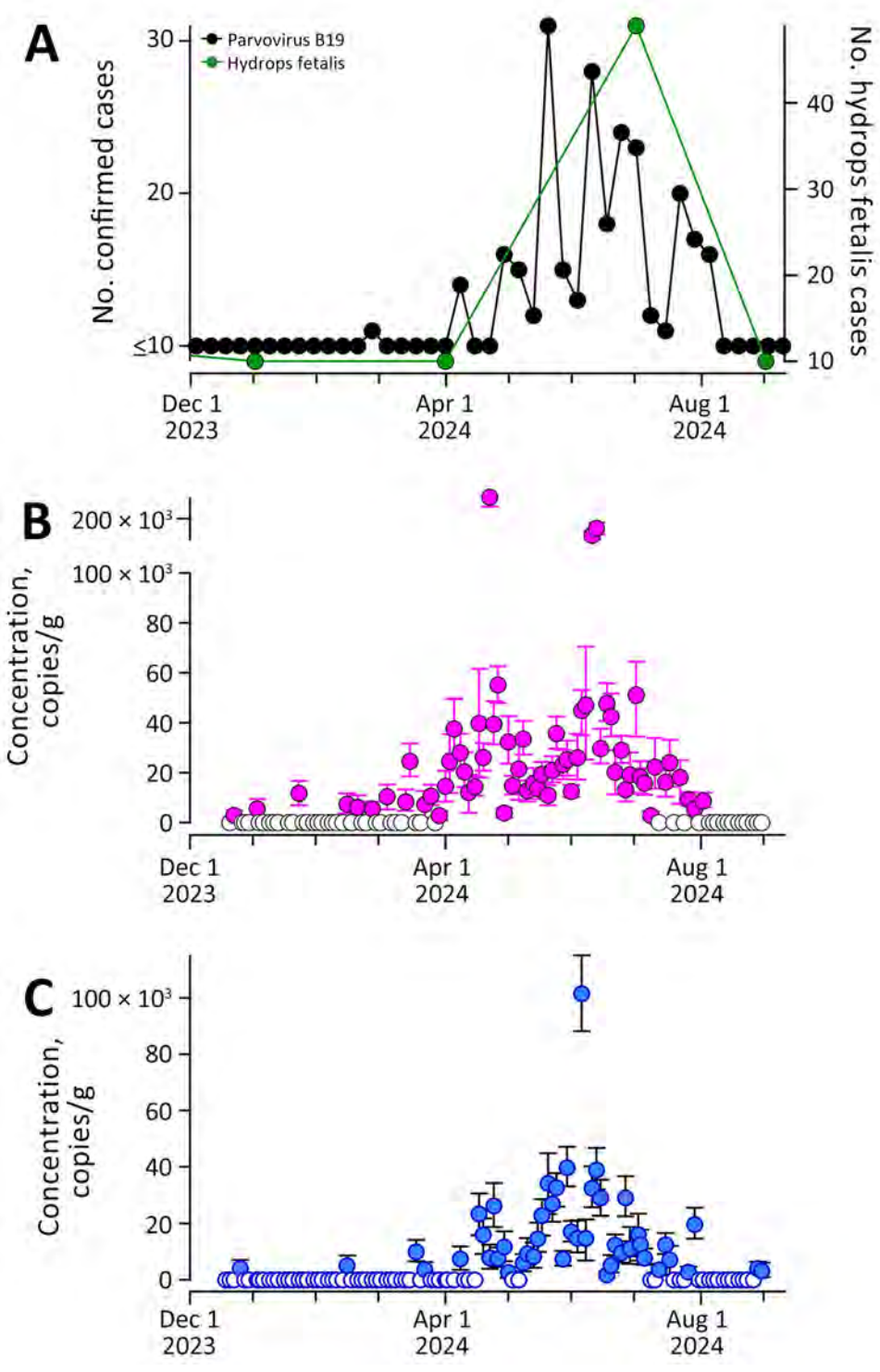

Figure. Comparison of case reports and wastewater surveillance reports from study of community infections linked with parvovirus B19 genomic DNA in wastewater, Montgomery County, Texas, USA, 2023–2024. A) Numbers of confirmed parvovirus infections and hydrops fetalis logged into Epic Cosmos (https://cosmos.epic.com) for the county. Data on fetal hydrops were provided quarterly; parvovirus infection data were provided weekly. Scales for the y-axes differ substantially to underscore patterns but do not permit direct comparisons. B, C) Concentrations of parvovirus B19 DNA in wastewater solids (in units of copies/gram of dry weight) at WWTP186 (B) and WWTP187 (C). Solid circles indicate parvovirus B19 was detected, open circles that it was not detected; error bars indicate SDs. Note the broken y-axis in panel B. For the case and syndromic data, numbers ≤10 are redacted and reported as 10. Kendall tau between weekly cases and wastewater concentrations for WWTP186 was 0.56 and between weekly cases and wastewater concentrations for WWTP187 was 0.52 ($p<0.0001$). WWTP, wastewater treatment plant.

in the dataset geographically and temporally to encounters within Montgomery County, Texas, during October 16, 2023–October 16, 2024. Montgomery County had a total population of 620,443 as of the 2020 census. From this subset, we identified parvovirus cases and hydrops fetalis diagnoses using grouped codes from the International Classification of Diseases, 10th Revision (ICD-10) (*11*). We identified parvovirus cases using ICD-10 codes B08.3, B34.3, and B97.6, and hydrops fetalis using ICD-10 codes P56.*, O36.2*, and Z36.81. We aggregated data weekly for parvovirus cases and quarterly for hydrops fetalis diagnoses; we redacted values <10 and replaced with 10 (Appendix).

Our statistical analyses used Kruskal-Wallis tests to compare viral concentrations between plants and χ^2 tests for detection frequencies. We assessed associations between wastewater concentrations and clinical cases using Kendall tau correlation. Because we made multiple comparisons (n = 11), we used p = 0.005 as the significance threshold.

Our analyses detected parvovirus B19 DNA in 45 (40%) of 111 samples from WWTP186 and in 62 (57%) of 109 samples from WWTP187; detection frequencies were not significantly different (χ^2= 5.24; p = 0.02). Concentrations were mostly nondetectable before April, peaked in June, and returned to nondetectable levels by August. Median (interquartile range [IQR]) concentrations were 0 (IQR 0–8,071 copies/g) at WWTP186 and 6,121 (IQR 0–20,998 copies/g) at WWTP187, showing significant differences between plants (effect size = 6,121 copies /g; p = 0.001) even when normalized by pepper mild mottle virus (effect size = 2.7×10^{-5}, p = 0.003).

Clinical parvovirus cases in Montgomery County showed similar seasonality: ≤10 cases until April, a peak in June, and a decline by August. Weekly viral concentrations correlated significantly with case counts at both plants (Kendall tau = 0.56 at WWTP186 and 0.52 at WWTP187; both p<0.0001). During the quarter of increasing wastewater concentrations, parvovirus cases rose from <10 to 223, coinciding with hydrops fetalis cases increasing to 49 (Figure).

Conclusions

Our study demonstrates that parvovirus B19 DNA can be quantified in wastewater and directly correlated with clinical indicators of infection. Our results validate the potential for wastewater to provide sentinel surveillance during key early periods of an outbreak, especially in the absence of mandated public health reporting. Previous studies have shown that parvovirus B19 infects the intestinal mucosa and is present in the sputum of infected patients, indicating it could be shed into wastewater (*12*). Investigators have shown related viruses, such as human bocaviruses, to be shed in stool samples (*13*). Recent studies have identified parvovirus B19 (often referred to as erythroparvovirus) in wastewater samples through shotgun sequencing and metagenomic analysis (*14*,*15*).

Parvovirus B19 DNA concentrations in wastewater at both treatment plants were significantly correlated with clinical cases of parvovirus B19 in the county. Most (>90%) of those diagnosed cases were in children and adolescents <16 years of age, likely because of the unique symptomatic presentation in children as a slapped cheek rash and clinical diagnosis without further molecular diagnostics. We also showed that B19 DNA concentrations in wastewater at both treatment plants corresponded to an increase in maternal care for hydrops fetalis, one of the known complications of parvovirus B19 in pregnant women. This finding suggests that parvovirus B19 DNA in wastewater is an indicator of not only infections in children, but infections in the adult population, for which clinical data are highly limited.

In summary, wastewater represents a rapid and cost-effective method of providing real-time information on parvovirus B19 outbreaks in populations. This early detection is especially important because children are no longer viremic by the time the characteristic rash appears. Proactive surveillance of wastewater to detect viremia could aid in mitigation strategies, such as warning or screening pregnant women and those who are immunocompromised.

This article was originally published as a preprint at https://medrxiv.org/cgi/content/short/2024.12.21.24319493v1.

Acknowledgments

We thank the participating wastewater treatment plants for their samples for the project.

Data used in this study came from Epic Cosmos, a dataset created in collaboration with a community of Epic health systems representing >284 million patient records from >1,500 hospitals and 36,000 clinics from all 50 states, DC, Lebanon, and Saudi Arabia.

This work was supported by a gift to A.B.B. from the Sergey Brin Family Foundation. R.Y.L. was supported by National Institutes of Health Institutional National Research Service Award T32 AI007502.

B.H. and D.D. are employees of Verily Life Sciences, LLC.

About the Author

Dr. Zulli is a postdoctoral scholar at Stanford University in the Division of Infectious Diseases and Geographic Medicine. His areas of interest include epidemiology of the built environment, the development of novel pathogen detection technologies, and the application of mitigation methods for the interruption of pathogen transmission.

References

1. Alfego D, Hernandez-Romieu AC, Briggs-Hagen M, Dietz S, Gillim L, Dale SE, et al. Detection of increased activity of human parvovirus B19 using commercial laboratory testing of clinical samples and source plasma donor pools—United States, 2024. MMWR Morb Mortal Wkly Rep. 2024;73:1076–81. https://doi.org/10.15585/mmwr.mm7347a2
2. Heegaard ED, Brown KE. Human parvovirus B19. Clin Microbiol Rev. 2002;15:485–505. https://doi.org/10.1128/CMR.15.3.485-505.2002
3. Qiu J, Söderlund-Venermo M, Young NS. Human parvoviruses. Clin Microbiol Rev. 2017;30:43–113. https://doi.org/10.1128/CMR.00040-16
4. Nordholm AC, Trier Møller F, Fischer Ravn S, Flink Sørensen L, Moltke-Prehn A, Elskær Mollerup J, et al. Epidemic of parvovirus B19 and disease severity in pregnant people, Denmark, January to March 2024. Euro Surveill. 2024;29:2400299. https://doi.org/10.2807/1560-7917.ES.2024.29.24.2400299
5. Young NS, Brown KE. Parvovirus B19. N Engl J Med. 2004;350:586–97. https://doi.org/10.1056/NEJMra030840
6. Health Alert Network (HAN)—00514 | Increase in human parvovirus B19 activity in the United States [cited 2024 Nov 29] https://emergency.cdc.gov/han/2024/han00514.asp.
7. Gonçalves G, Dias M. Parvovirus outbreak in a kindergarten in a municipality in the north of Portugal, April–June 2008. Euro Surveill. 2008;13:19053. https://doi.org/10.2807/ese.13.48.19053-en
8. Dittmer FP, Guimarães CM, Peixoto AB, Pontes KFM, Bonasoni MP, Tonni G, et al. Parvovirus B19 infection and pregnancy: review of the current knowledge. J Pers Med. 2024;14:139. https://doi.org/10.3390/jpm14020139
9. Boehm AB, Wolfe MK, Bidwell AL, Zulli A, Chan-Herur V, White BJ, et al. Human pathogen nucleic acids in wastewater solids from 191 wastewater treatment plants in the United States. Sci Data. 2024;11:1141. https://doi.org/10.1038/s41597-024-03969-8
10. Kaplan EH, Zulli A, Sanchez M, Peccia J. Scaling SARS-CoV-2 wastewater concentrations to population estimates of infection. Sci Rep. 2022;12:3487. https://doi.org/10.1038/s41598-022-07523-7
11. World Health Organization. ICD-10: international statistical classification of diseases and related health problems. 10th revision, 2nd ed. 2004 [cited 2025 Jun 6]. https://iris.who.int/handle/10665/42980
12. Pironi L, Bonvicini F, Gionchetti P, D'Errico A, Rizzello F, Corsini C, et al. Parvovirus B19 infection localized in the intestinal mucosa and associated with severe inflammatory bowel disease. J Clin Microbiol. 2009;47:1591–5. https://doi.org/10.1128/JCM.00706-08
13. Blinkova O, Rosario K, Li L, Kapoor A, Slikas B, Bernardin F, et al. Frequent detection of highly diverse variants of cardiovirus, cosavirus, bocavirus, and circovirus in sewage samples collected in the United States. J Clin Microbiol. 2009;47:3507–13. https://doi.org/10.1128/JCM.01062-09
14. McCall C, Wu H, Miyani B, Xagoraraki I. Identification of multiple potential viral diseases in a large urban center using wastewater surveillance. Water Res. 2020;184:116160. https://doi.org/10.1016/j.watres.2020.116160
15. Li Y, Miyani B, Faust RA, David RE, Xagoraraki I. A broad wastewater screening and clinical data surveillance for virus-related diseases in the metropolitan Detroit area in Michigan. Hum Genomics. 2024;18:14. https://doi.org/10.1186/s40246-024-00581-0

Address for correspondence: Alexandria B. Boehm, Department of Civil and Environmental Engineering, Stanford University, 473 Via Ortega, Stanford, CA 94305, USA; email: aboehm@stanford.edu

Extensively Drug-Resistant *Neisseria gonorrhoeae* Strain, Canada

Brigitte Lefebvre, Irene Martin, Robyn Thorington, Julian Gitelman, Andrew Bui-Nguyen, Claude Fortin, Judith Fafard

We identified a case of extensively drug-resistant (ceftriaxone- and cefixime-resistant and high-level azithromycin-resistant) *Neisseria gonorrhoeae* in Canada. The strain harbors the *penA* 60.001 allele, which includes the A311V and 23S rRNA A2059G single-nucleotide polymorphisms associated with high-level azithromycin resistance. The infection was likely acquired during travel in Cambodia.

Neisseria gonorrhoeae is the second most common sexually transmitted infection reported in Canada; the 92.34 cases/100,000 population reported 2022 represents an increase of 146.2% since 2010 (*1*). *N. gonorrhoeae* with third-generation cephalosporin resistance is in the high-priority category on the Bacterial Priority Pathogens List published by the World Health Organization in 2024 (https://iris.who.int/bitstream/handle/10665/376776/9789240093461-eng.pdf). Ceftriaxone is 1 of the last remaining empiric treatments options available for gonorrhea infection and is currently the recommended therapy in Canada. In 2017, we described a ceftriaxone-resistant *N. gonorrhoeae* isolate identified in North America (*2*). In 2018, we reported on the international dissemination of ceftriaxone-resistant *N. gonorrhoeae* isolates (*3*), identified in Japan as FC428. More than 10 extensively drug-resistant (XDR) *N. gonorrhoeae* isolates have been reported worldwide, most since 2022 (*4*). Those XDR isolates were found to harbor the *penA*-60.001 allele associated with ceftriaxone resistance and the 23S rRNA A2059G single-nucleotide polymorphism associated with high-level azithromycin resistance. We report an XDR *N. gonorrhoeae* isolate (no. 69155) identified in Canada that was cefixime and ceftriaxone resistant and has a high level of azithromycin resistance.

Author affiliations: Laboratoire de santé publique du Québec, Sainte-Anne-de-Bellevue, Canada (B. Lefebvre, J. Fafard); National Microbiology Laboratory, Winnipeg, Manitoba, Canada (I. Martin, R. Thorington); Direction régionale de santé publique, CIUSSS du Centre-Sud-de-l'île-de-Montréal, Montreal, Quebec, Canada (J. Gitelman); Clinique Quorum, Montreal (A. Bui-Nguyen); Centre Hospitalier de l'Université de Montréal, Montreal (C. Fortin); Faculté de médecine de l'Université de Montréal, Montreal (C. Fortin, J. Fafard)

DOI: https://doi.org/10.3201/eid3107.250023

The Study

In May 2024, a man in his 40s experiencing urethritis sought care in an outpatient STI clinic in Montreal, Quebec, Canada. A strain of XDR *N. gonorrhoeae* from a urethral specimen was isolated at Centre Hospitalier de l'Université de Montréal. The patient reported that he had traveled to Cambodia and had sex with female sex workers there. He reported sexual contact with women only. He denied sexual contacts in Canada in the 60 days before the onset of his symptoms and had no sexual contacts upon his return. He was treated with 1 dose of oral azithromycin (2 g) combined with cefixime (800 mg) in accordance with treatment guidelines for sexually transmitted infections published in 2020 by Institut national d'excellence en santé et en services sociaux (INESSS) (https://www.bibliotheque.assnat.qc.ca/DepotNumerique_v2/AffichageNotice.aspx?idn=101746) but was still symptomatic at the time of the test of cure (TOC) by nucleic acid amplification tests (NAAT) 2 weeks later. We prescribed a second round of treatment with 1 intramuscular dose of ceftriaxone (250 mg) and oral doxycycline (100 mg 2×/d for 7 days); 2 weeks after the completion of the second treatment, the TOC by NAAT still remained positive. Because the patient was still symptomatic, providers used a syndromic approach; he was treated for clinical urethritis in accordance with the INESSS guidelines. The

doxycycline was used to treat a possible *C. trachomatis* infection and not the *N. gonorrhoeae* infection. A third treatment of intramuscular ceftriaxone (500 mg) was successful; urethral culture and urine NAAT were negative at the third TOC.

We confirmed the bacterial isolate 69155 to be *N. gonorrhoeae* by matrix-assisted laser desorption/ionization time-of-flight mass spectrometry (bioMérieux, https://www.biomerieux.com) and by whole-genome sequencing. We confirmed antimicrobial susceptibilities by agar dilution in accordance with Clinical and Laboratory Standards Institute (CLSI) guidance (*5*). The ceftriaxone MIC for this *N. gonorrhoeae* isolate was 0.25 mg/L, which is susceptible by CLSI guidelines and resistant by EUCAST guidelines (*6*). The cefixime MIC was 2 mg/L, which is nonsusceptible by CLSI guidelines and resistant by EUCAST guidelines. CLSI does not have a resistant breakpoint for cefixime or ceftriaxone; however, it defines MIC ≤0.25 mg/L as susceptible. EUCAST defines cefixime and ceftriaxone resistance as MIC >0.125 mg/L, whereas World Health Organization defines decreased susceptibility to cefixime as MIC ≥0.25 mg/L and to ceftriaxone as MIC ≥0.125 mg/L (*7*). Although there is no consistent resistance breakpoint, MICs of 0.25 mg/L for ceftriaxone and 2 mg/L for cefixime were previously reported in possible treatment failure cases (*8*,*9*). The isolate was also resistant to azithromycin (MIC ≥256 mg/L), ciprofloxacin (MIC 4 mg/L), tetracycline (MIC 32 mg/L), and penicillin (MIC ≥256 mg/L) but susceptible to spectinomycin (MIC 8 mg/L). We also determined MICs for gentamicin (MIC 4 mg/L) and ertapenem (MIC 0.5 mg/L).

We performed molecular typing in silico from whole-genome sequence data and submitted to the National Center for Biotechnology Information Sequence Read Archive (BioProject PRJNA415047, Sequence Read Archive no. SRR33123384). We sequenced the strain using Illumina NextSeq platform (Illumina, https://www.illumina.com) and used genomic quality, assembly, and annotation pipelines as previously described (*10*). We identified sequence type (ST) 16406 by multilocus sequence typing (MLST), ST-22862 by *N. gonorrhoeae* multiantigen sequence typing (NG-MAST; https://pubmlst.org/organisms/neisseria-spp), and ST-5793 by *N. gonorrhoeae* Sequence Typing for Antimicrobial Resistance (NG-STAR; https://ngstar.canada.ca). The isolate had the mosaic *penA*-60.001 allele associated with

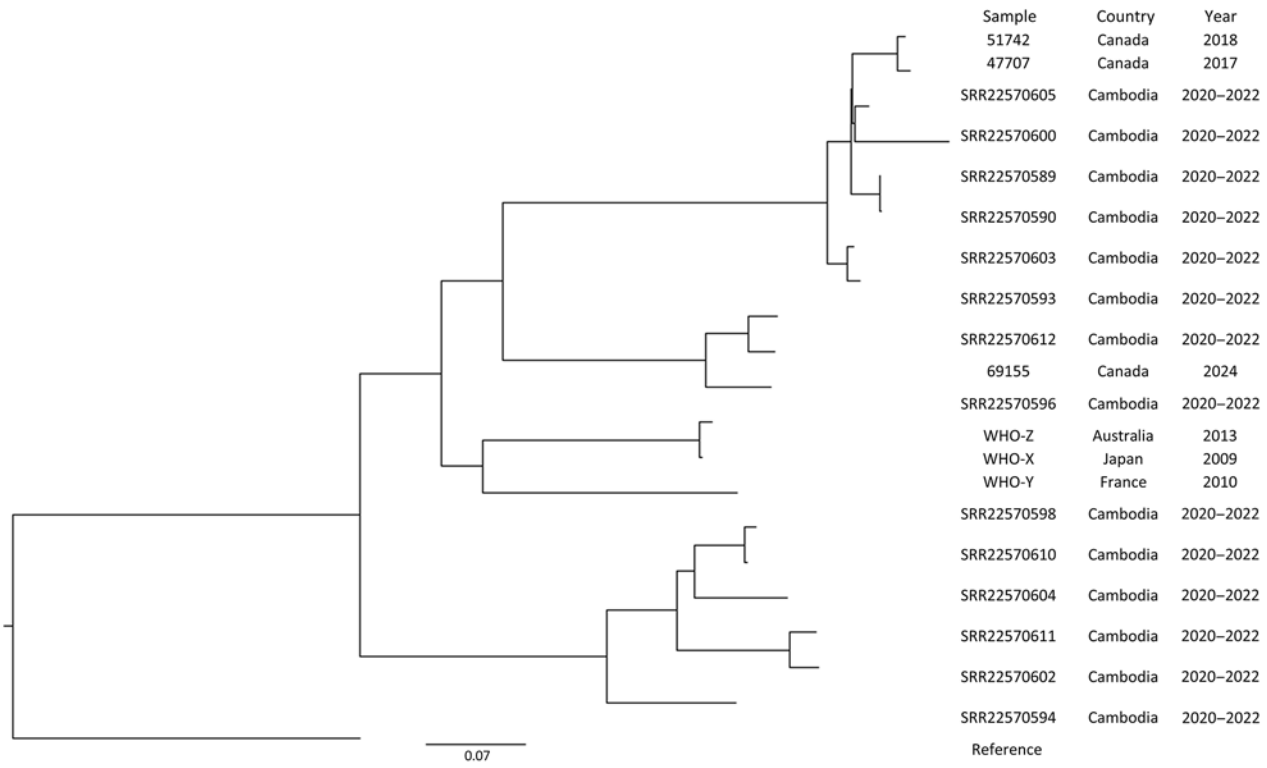

Figure. Phylogenetic analysis of *Neisseria gonorrhoeae* isolates in study of extensively drug-resistant *N. gonorrhoeae* infection, Canada. Isolate 69155 was identified from the patient in this investigation. Tree was generated using 3,691 sites. Scale bar indicates number of substitutions per site.

ceftriaxone resistance and the A2059G single-nucleotide polymorphism in 23S rRNA associated with high-level azithromycin resistance. The *penA*-60.001 allele contains the A311V amino acid substitution, which is highly associated with ceftriaxone resistance (*11*). The MLST-determined ST16406 and *penA*-60.001 allele of the study isolate in Canada was identical to that of XDR *N. gonorrhoeae* strains isolated in Cambodia, Austria, United Kingdom, and France in 2022–2023 (*4*). Because only 1 strain from initial sampling was available, we did not perform genetic comparisons with other strains from this patient.

To compare the XDR *N. gonorrhoeae* strain we isolated with other ceftriaxone-resistant isolates, we performed phylogenetic analysis to determine single-nucleotide variants (SNV) using the custom Galaxy SNVPhyl20 pipeline (SNVPhyl version 1.0.1b Paired-End, https://github.com/phac-nml/snvphyl-galaxy) and included publicly available, internationally reported ceftriaxone-resistant and XDR gonorrhea genomes (BioProject PRJNA909328) (*12*) (Figure). The phylogenetic tree demonstrates the similarity of the Canada XDR–*N. gonorrhoeae* 69155 isolate to gonorrhea genomes reported in Southeast Asia; the study isolate differs from isolate SRR22570596 by 320 SNVs and SRR22570612 (BioProject PRJNA909328) by 140 SNVs.

Conclusions

We identified the bacterial isolate 69155 from a patient in Canada as a ceftriaxone-resistant and high-level azithromycin–resistant *N. gonorrhoeae* strain. The strain is of ST-16406 (MLST) and contains the *penA-60.001* allele identical to cases previously reported in France, United Kingdom, Austria, and Cambodia. The patient's infection was not cured by cefixime (800 mg) but by a higher dose of ceftriaxone (500 mg). Consistent with US Centers for Disease Control and Prevention recommendations (*13*), Quebec has recommended use of ceftriaxone (500 mg) as first-line treatment since September 2024 (*14*).

In 2020, guidelines in Europe recommended the use of ceftriaxone (1 g) as probabilistic treatment for uncomplicated genital infections (*15*). The European Centre for Disease Prevention and Control noted an increase of antimicrobial resistance in 2022 for *N. gonorrhoeae* (*4*). Moreover, ≥6 cases of XDR *N. gonorrhoeae* infection have been reported in Europe since 2022.

The surveillance of antimicrobial resistance in *N. gonorrhoeae* is crucial in the context of treatment failure and the dissemination of XDR strains worldwide. Our isolate was susceptible to ceftriaxone according to CLSI guidelines but resistant according to EUCAST guidelines; we therefore recommend using caution when interpreting borderline MICs. In Quebec, we published a directive asking frontline laboratories to promptly submit all third-generation cephalosporin borderline MIC isolates to the provincial laboratory for testing.

Author contributions: B.L. and J.F. conceived and coordinated the study, performed experiments, analyzed data, and drafted the manuscript. I.M. and R.T. performed experiments and drafted the manuscript. A.B.-N., C.F., and J.G. coordinated the sample collection and/or provided clinical information about the case. All authors reviewed the final manuscript.

About the Author

Dr. Lefebvre is the head of bacterial STIs at Laboratoire de santé publique du Québec. Her research centers on pathogens of major public health concern, including sexually transmitted infections such as *Chlamydia trachomatis*, *Neisseria gonorrhoeae*, *Mycoplasma genitalium,* and *Haemophilus ducreyi*. She also studies vaccine-preventable pathogens including *N. meningitidis*, *Streptococcus pneumoniae*, *H. influenzae,* and *Bordetella pertussis* and other antibiotic-resistant pathogens, such as carbapenemase-producing Enterobacteriaceae, vancomycin-resistant enterococci, and methicillin-resistant *Staphylococcus aureus*.

References

1. Public Health Agency of Canada. Reported cases from 1924 to 2022 in Canada—notifiable diseases on-line. 2022 [cited 2025 Jan 6]. https://diseases.canada.ca/notifiable/charts?c=pl
2. Lefebvre B, Martin I, Demczuk W, Deshaies L, Michaud S, Labbé AC, et al. Ceftriaxone-resistant *Neisseria gonorrhoeae*, Canada, 2017. Emerg Infect Dis. 2018;24:381–3. https://doi.org/10.3201/eid2402.171756
3. Lahra MM, Martin I, Demczuk W, Jennison AV, Lee K-I, Nakayama S-I, et al. Cooperative recognition of internationally disseminated ceftriaxone-resistant *Neisseria gonorrhoeae* strain. Emerg Infect Dis. 2018;24:735–40. https://doi.org/10.3201/eid2404.171873
4. Caméléna F, Mérimèche M, Brousseau J, Mainardis M, Verger P, Le Risbé C, et al. Emergence of extensively drug-resistant *Neisseria gonorrhoeae*, France, 2023. Emerg Infect Dis. 2024;30:1903–6. https://doi.org/10.3201/eid3009.240557
5. Clinical and Laboratory Standards Institute. Performance standards for antimicrobial susceptibility testing. 34th edition. CLSI supplement M100. Wayne (PA): The Institute; 2024.
6. European Committee on Antimicrobial Susceptibility Testing (EUCAST). Clinical breakpoints for bacteria. Version 14.0, 2024–01–01. 2024 [cited 2025 Jan 6]. https://www.eucast.org/fileadmin/src/media/PDFs/EUCAST_files/Breakpoint_tables/v_14.0_Breakpoint_Tables.pdf
7. World Health Organization. Global action plan to control the spread and impact of antimicrobial resistance in

Neisseria gonorrhoeae. Geneva: The Organization; 2012 [cited 2025 Jan 6]. https://www.who.int/publications/i/item/9789241503501
8. Pleininger S, Indra A, Golparian D, Heger F, Schindler S, Jacobsson S, et al. Extensively drug-resistant (XDR) *Neisseria gonorrhoeae* causing possible gonorrhoea treatment failure with ceftriaxone plus azithromycin in Austria, April 2022. Euro Surveill. 2022;27:2200455. https://doi.org/10.2807/1560-7917.ES.2022.27.24.2200455
9. Maubaret C, Caméléna F, Mrimèche M, Braille A, Liberge M, Mainardis M, et al. Two cases of extensively drug-resistant (XDR) *Neisseria gonorrhoeae* infection combining ceftriaxone-resistance and high-level azithromycin resistance, France, November 2022 and May 2023. Euro Surveill. 2023;28:2300456. https://doi.org/10.2807/1560-7917.ES.2023.28.37.2300456
10. Demczuk W, Lynch T, Martin I, Van Domselaar G, Graham M, Bharat A, et al. Whole-genome phylogenomic heterogeneity of *Neisseria gonorrhoeae* isolates with decreased cephalosporin susceptibility collected in Canada between 1989 and 2013. J Clin Microbiol. 2015;53:191–200. https://doi.org/10.1128/JCM.02589-14
11 Zhang L, Hu L, Li Y, Xiu L, Wang D, Huang J, et al. Identification of high-level ceftriaxone-resistant *Neisseria gonorrhoeae* isolates with diverse *penA* alleles in Zhejiang, China. J Glob Antimicrob Resist. 2023;35:51–5. https://doi.org/10.1016/j.jgar.2023.08.007
12. Ouk V, Say HL, Virak M, Deng S, Frankson R, McDonald R, et al.; EGASP Cambodia working group. World Health Organization Enhanced Gonococcal Antimicrobial Surveillance Programme, Cambodia, 2023. Emerg Infect Dis. 2024;30:1493–5. https://doi.org/10.3201/eid3007.240354
13. Center for Diseases Control and Prevention. Sexually transmitted infections treatment guidelines: gonococcal infections among adolescents and adults. 2021 [cited 2025 Jan 6]. https://www.cdc.gov/std/treatment-guidelines/gonorrhea-adults.htm
14. Institut national d'excellence en santé et en services sociaux. Pharmacological treatment guide on STIs—*Chlamydia trachomatis* infection and *Neisseria gonorrhoeae* infection [in French]. 2024 [cited 2025 Jan 6]. https://www.inesss.qc.ca/fileadmin/doc/INESSS/Outils/Guides_ITSS/Guide_ITSS-Chlamydia_gonorrhoeae.pdf
15. Unemo M, Ross J, Serwin AB, Gomberg M, Cusini M, Jensen JS. 2020 European guideline for the diagnosis and treatment of gonorrhoea in adults. Int J STD AIDS. 2020; 956462420949126. https://doi.org/10.1177/0956462420949126

Address for correspondence: Brigitte Lefebvre, Laboratoire de santé publique du Québec, 20045 Chemin Ste-Marie, Ste-Anne-de-Bellevue, QB H9X 3R5, Canada; email: brigitte.lefebvre@inspq.qc.ca

etymologia revisited

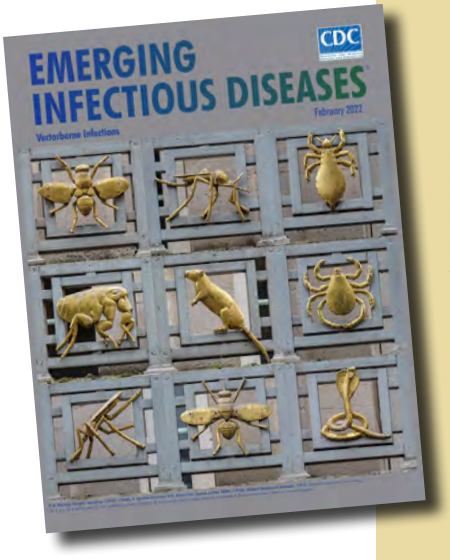

Originally published in February 2022

The Color Puce

For those with synesthesia, in whom stimulating 1 sensory pathway gives rise to a subjective sensation of a different character, the word plague may chromatically resonate with puce. In pre-revolutionary France, an era of "evocative color nomenclature," Marie Antoinette's reign was precipitating intense criticism. Her countrymen were experiencing severe socioeconomic stress, thus her sartorial self-indulgence was much resented.

After discovering the Queen wearing a new gown, her husband, Louis XVI, the King of France, chided her, describing the dress's unflattering purple–brown hue as "*couleur de puce*" (color of fleas). This admonishment had the unintended consequence of promoting puce as the exclusive color worn by the French court. Puce, the French word for flea, descends from *pulex* (Latin). Flea droppings leave puce colored "bloodstains" on bedsheets. The role of fleas, however, as a vector for bubonic plague was not proven until about 1895.

References:

1. Stedman's Medical Dictionary. 23rd ed. Baltimore: The Williams & Wilkins Company; 1976. p. 1392.
2. St. Clair K. The secret lives of color. New York: Penguin Books; 2017. p. 122–3.
3. Zietz BP, Dunkelberg H. The history of the plague and the research on the causative agent *Yersinia pestis*. Int J Hyg Environ Health. 2004;207:165–78. https://doi.org/10.1078/1438-4639-00259
4. Plague bacteria found in Arizona fleas, by Rachael Rettner, August 14, 2017 [cited 2021 Nov 4]. https://www.livescience.com/60130-plague-fleas-arizona.html.)

https//wwwnc.cdc.gov/eid/article/28/2/et-2802_article

Human Infections by Novel Zoonotic Species *Corynebacterium silvaticum*, Germany

Anja Berger,[1] Alexandra Dangel,[1] Vyacheslav G. Melnikov,[2] Katja Bengs, Thomas Rupp, Hanns-Joerg Mappes, Christian Schneider, Andreas Sing

We report 2 human *Corynebacterium silvaticum* infections in Germany with axillary lymphadenitis and abscess formation; in 1 case the infection likely originated from a slaughtered wild boar. This recently described member of the diphtheria toxin gene–bearing *C. diphtheriae* species complex might be a new zoonotic pathogen.

Diphtheria is caused by toxigenic *Corynebacterium* spp. producing the major pathogenicity factor diphtheria toxin (DT). DT is encoded on the *tox* gene and causes local respiratory or cutaneous symptoms, as well as systemic neurologic and cardiologic symptoms. The 3 potentially DT-producing species are the mainly human pathogen *C. diphtheriae* and the 2 zoonotic pathogens *C. ulcerans* and *C. pseudotuberculosis*. In recent years, the *C. diphtheriae* species complex (CdSC) was expanded, mostly on the basis of genomic data, in some instances supported by biochemical properties (*1*). Two closely related species were separated from *C. diphtheriae* (i.e., *C. belfantii* [*2*] and *C. rouxii* [*3*]), and 2 were separated from *C. ulcerans* (i.e., *C. silvaticum* [*4*] and *C. ramonii* [*5*], previously known as lineage 2 of *C. ulcerans*).

C. silvaticum (formerly *C. ulcerans* wildlife cluster), was recently described as a novel zoonotic species causing caseous lymphadenitis in 33 wild boars and a roe deer in Germany (*4*,*6*). Subsequently, *C. silvaticum* was identified in a wild boar from Germany (*7*) and in a domestic pig from Portugal (*8*). So far, all animal isolates from Germany were nontoxigenic *tox*-bearing (NTTB) (*4*,*8*,*9*), whereas isolates from Portugal and Austria were found to be either NTTB or *tox*-positive, resulting in 2 recently postulated clades depending on molecular characteristics of the *tox* gene (*10*). Although *C. silvaticum* is considered a zoonotic pathogen with the potential to infect humans, no human infections had been described. In this study, we report 2 cases of human *C. silvaticum* infection.

The Study

In case 1, a 37-year-old male butcher sought care for an indolent tumor in the lateral thorax and the right axilla that had been present for 3 weeks. A bacterial swab specimen taken during surgical extirpation grew *Corynebacterium* sp. after 48 hours in pure culture; the pathogen was *C. ulcerans* by matrix-assisted laser desorption/ionization time-of-flight mass spectrometry (Bruker, https://www.bruker.com). The strain was sent to the German Consiliary Laboratory for Diphtheria (Oberschleißheim, Germany) for further analysis. The strain (KL1848) showed an atypical colony morphology (small waxy white, discrete β-hemolytic colonies after 48 hours' incubation) and biochemical reactions: fermentation of glucose, ribose, and maltose (like *C. ulcerans*), but no use of D-xylose, mannitol, lactose, sucrose, or glycogen (like *C. pseudotuberculosis*). It was sensitive to clindamycin,

Author affiliations: Bavarian Health and Food Safety Authority, Oberschleißheim, Germany (A. Berger, A. Dangel, K. Bengs, A. Sing); German National Consiliary Laboratory for Diphtheria, Oberschleißheim (A. Berger, V.C. Melnikov, A. Sing); European Union Public Health Reference Laboratory for Diphtheria and Pertussis, Oberschleißheim (A. Berger, A. Sing); World Health Organization Collaborating Centre for Diphtheria, Oberschleißheim (A. Berger, A. Sing); Klinikum Aschaffenburg-Alzenau, Chirurgische Klinik, Aschaffenburg, Germany (T. Rupp, H.-J. Mappes); Klinikum Aschaffenburg-Alzenau, Zentrallabor, Germany (C. Schneider)

DOI: https://doi.org/10.3201/eid3107.250086

[1]These authors contributed equally to this article.

[2]Current affiliation: University of Cambridge, Cambridge, UK.

according to the European Committee on Antimicrobial Susceptibility Testing guidelines for *C. diphtheriae* and *C. ulcerans* (https://www.eucast.org/clinical_breakpoints). The isolate was identified as a NTTB *C. silvaticum* strain using previously described methods (*11*) (i.e., *tox*-PCR, an optimized Elek test, a lateral flow immunoassay and whole-genome sequencing [WGS] analyses) (Appendix 1, https://wwwnc.cdc.gov/EID/article/31/7/25-0086-App1.pdf). The patient was successfully treated with surgery and cefuroxime for 14 days. The patient reported to have recently field-dressed a hunted wild boar that showed suspicious mesenterial lymph nodes. The patient's immunization status was unknown. No secondary human cases occurred.

In case 2, a 21-year-old man sought care for an indolent axillary tumor that had been present for 4 weeks. Lymphoma was suspected on the basis of computed tomography results. The affected lymph node was removed, revealing a fibrosed soft tissue with florid purulent abscess formation and chronic granulating histiocyte-rich granulomatous inflammation. After a few days of incubation, the tissue sample grew a pure culture of *Corynebacterium* sp., identified as *C. ulcerans* by matrix-assisted laser desorption/ionization time-of-flight mass spectrometry (Bruker). The strain (KL1281) was sent to the German Consiliary Laboratory for Diphtheria. The atypical colony morphology, biochemical reactions, and antimicrobial susceptibility were identical to those of strain KL1848. We identified the isolate as NTTB *C. silvaticum* using the same methods as in case 1. The case 2 patient had a dog and lived in a rural area of northern Germany. He reported no contact with wild animals. Vaccination against diphtheria was completed. No secondary human case was observed.

Average nucleotide identity analysis of WGS assemblies compared with public type-strain genomes of the CdSC classified both isolates with highest concordance as *C. silvaticum* with identity values >99.9%. Identity values for the other species were nearly identical for both strains and clearly below the species

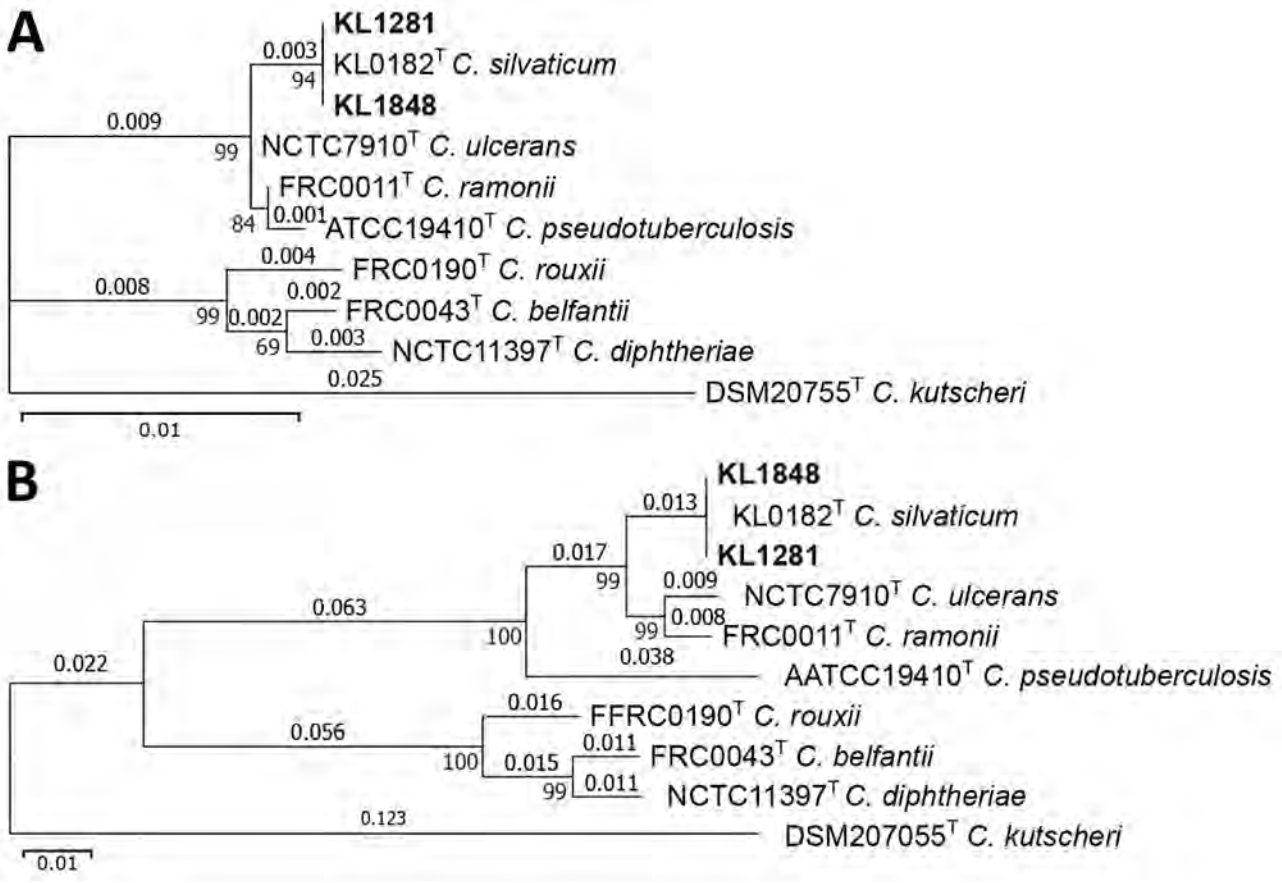

Figure 1. Gene phylogenies of isolates from 2 cases of infection by the novel zoonotic species *Corynebacterium silvaticum*, Germany (isolates KL1281 and KL1848), compared with reference sequences from publicly available type strain sequences of *C. diphtheriae* complex species and a close relative outgroup (*C. kutscheri*). A) 16S; B) rpoB. Substitutions per aligned site are indicated above branches and local supporting values at intersections of branches. Scale bars indicate number of substitutions per site.

threshold of 94%–96% (*12*); values were 90.6% for *C. ramonii* FRC0011^T, 90.5% for *C. ulcerans* NCTC7910^T, 85.0% for *C. pseudotuberculosis* ATCC19410^T, 74.3% for *C. diphtheriae* NCTC11397^T, 74.1% for *C. rouxii* FRC190^T, and 74.0% for *C. belfantii* FRC0043^T.

We constructed gene phylogenies of 16S and *rpoB* from the WGS data and compared them with the respective genes of the CdSC-type strains and *C. kutscheri* as an outgroup. The phylogenetic trees (Figure 1) show a clear assignment to *C. silvaticum*, because both isolates share the branch of the *C. silvaticum*–type strain with clear separation from the other species. Multilocus sequence typing (MLST) analysis with the *C. diphtheriae* scheme showed sequence type (ST) 578, exclusive to *C. silvaticum* and typically also found in isolates from wild boar and roe deer in Germany (Appendix 2, https://wwwnc.cdc.gov/EID/article/31/7/25-0086-App2.xlsx). Evaluation of the *tox* gene and an alignment with *tox* sequences from Germany, published sequences from Portugal (*10*) and a *C. diphtheriae tox* sequence as reference revealed the presence of the insertion of 2 guanine residues after position 44 (Appendix 1 Figure), as found in the other Germany isolates from wild boar and roe deer, enabling assignment to *C. silvaticum* clade 2 (*10*).

To investigate the clade classification with a more detailed core genome MLST analysis, we constructed an ad hoc core genome MLST scheme on the basis of publicly available *C. silvaticum* genomes from both clades (Appendix 1). We generated a minimum-spanning tree from 45 genomes, consisting of KL1281, KL1848, an additional 35 isolates from animals from Germany, and the 8 clade 1 genomes from Portugal (*10*). The tree layout (Figure 2) and the allelic distances (Appendix 2xxxxx) clearly affiliate the patient cases with the cases from clade 2 from Germany, whereas the genomes from clade 1 from Portugal sit on another branch and show >500 allelic differences to clade 2. Thus, the classification by the *tox* gene is also supported by a whole-genome context.

Conclusions

C. silvaticum (*4*) has been suspected to be a possible zoonotic member of the newly expanded CdSC. Originally isolated from forest-associated animals such as wild boars and roe deer, it has also been identified in a domestic pig. In this study, we report 2 cases of human infection linked to close animal contact (wild boar and dog). In case 1, the most probable route of infection was direct contact with infectious tissue and possible microtrauma lesions during a slaughtering or animal field-dressing procedure. In case 2, no close contact to wild animals was reported, although the patient lived in a rural area and owned a dog.

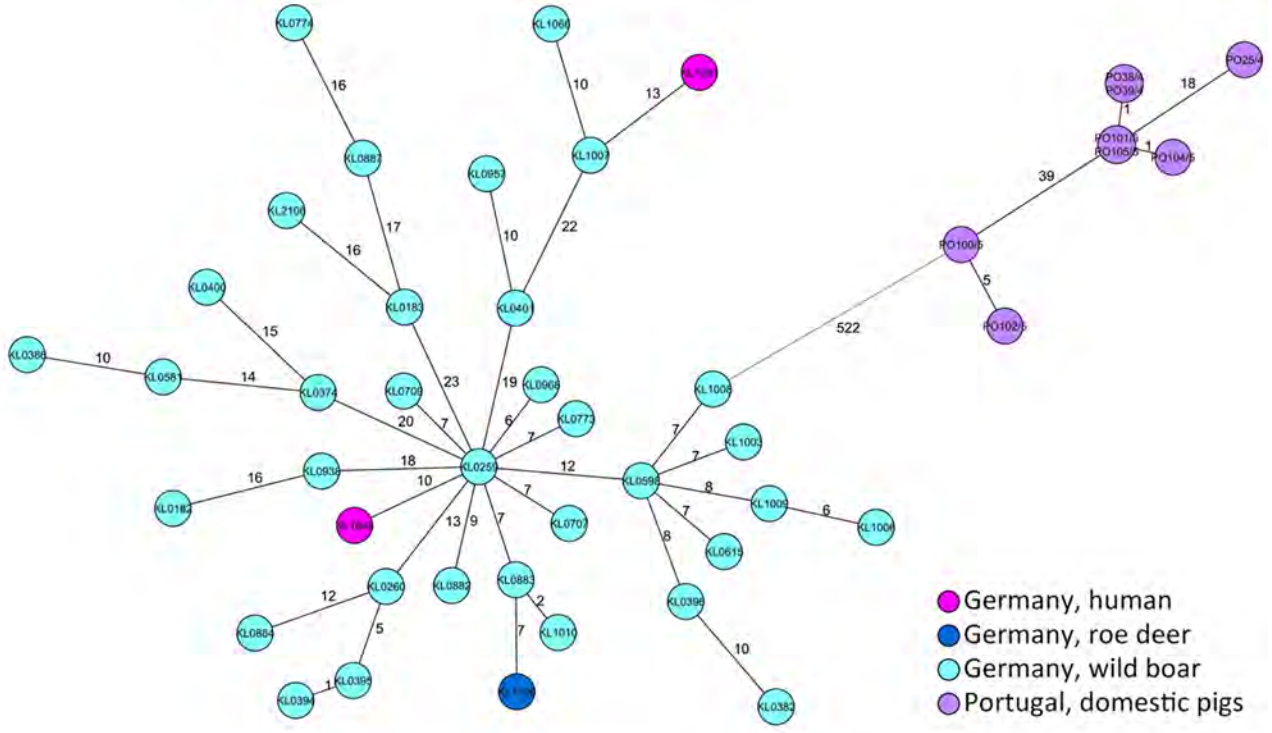

Figure 2. Minimum-spanning tree of an ad hoc *Corynebacterium silvaticum* core-genome multilocus sequence typing scheme of 2012 target loci displaying isolates from 2 cases in Germany (KL1281 and KL1848), and reference sequences. Shown are relationships with 35 animal-derived isolates from Germany and 8 isolates from clade 1 from pigs in Portugal. Allelic distances are indicated at connection lines.

However, *C. silvaticum* has so far been only identified in wild forest-dwelling animals and a pig. All cases in Germany, including the 2 human cases described in this study, were found to be NTTB and summarized in a corresponding NTTB clade with a 2-bp insertion in the *tox* gene sequence, named clade 2 (*10*). In contrast, in Portugal and Austria, another monophyletic clade of DT-producing *C. silvaticum* was reported and named clade 1 (*10*).

In conclusion, *C. silvaticum* should be considered a zoonotic pathogen with possible animal-to-human transmission. Therefore, animal sources, especially wild boar and domestic pigs, should be included when tracing sources of potentially toxigenic *Corynebacterium* spp. of the broader *C. diphtheriae* and the narrower *C. ulcerans* complex. *C. ulcerans* has also been transmitted from pigs to humans (*13*,*14*). With respect to the known clindamycin resistance in *C. ulcerans* (*15*), antimicrobial susceptibility testing should support antibiotic therapy. Suitable precaution measures should be taken when handling wild boars and pigs to avoid zoonotic risk for *C. ulcerans* or *C. silvaticum* infection.

Acknowledgments

We thank Wolfgang Schmidt, Cengiz-Turgut Dedeoglu, Juliane Breitenberger, Juliana Webersberger, Andrea Seifarth, Helga Kocak, Sabine Lohrer, Jasmin Scholz, Anne Könitzer, and Marion Lindermayer for excellent technical assistance. We thank all diagnostic laboratories submitting samples and strains to the GNCLD.

Ethical approval was not necessary for this study because it was performed as part of routine surveillance activities, outbreak investigation, and diphtheria diagnostics in Germany. Whole-genome sequencing data are available in the National Center for Biotechnology Information Short Read Archive (http://www.ncbi.nlm.nih.gov/sra; Bioproject PRJNA490531). Detailed accession numbers are given in Appendix 2.

The study was partly supported by the Bavarian State Ministry of Health, Care and Prevention, as well as by the German Federal Ministry of Health via the Robert Koch-Institute and its National Reference Laboratories Network (09-47, FKZ 1369-359, and FKZ 415).

A.B., K.B., A.S., C.S., V.G.M. were involved in laboratory work-up; A.D. performed whole-genome sequencing. T.R. and H.J.M. were involved in clinical care. All authors interpreted the results. A.B. was involved in epidemiological work-up. A.B., A.D., and A.S. wrote the paper. All authors reviewed and approved the final version of the manuscript.

About the Author

Dr. Berger is a board-certified clinical microbiologist with special interest in public health microbiology, antimicrobial resistance, and bacteriology. She is deputy head of the German National Consiliary Laboratory on Diphtheria, the German part of the EU Public Health Reference Laboratory for Diphtheria and Pertussis, and the World Health Organization Collaborating Centre for Diphtheria.

References

1. Prygiel M, Polak M, Mosiej E, Wdowiak K, Formińska K, Zasada AA. New *Corynebacterium* species with the potential to produce diphtheria toxin. Pathogens. 2022;11:1264. https://doi.org/10.3390/pathogens11111264
2. Dazas M, Badell E, Carmi-Leroy A, Criscuolo A, Brisse S. Taxonomic status of *Corynebacterium diphtheriae* biovar Belfanti and proposal of *Corynebacterium belfantii* sp. nov. Int J Syst Evol Microbiol. 2018;68:3826–31. https://doi.org/10.1099/ijsem.0.003069
3. Badell E, Hennart M, Rodrigues C, Passet V, Dazas M, Panunzi L, et al. *Corynebacterium rouxii* sp. nov., a novel member of the diphtheriae species complex. Res Microbiol. 2020;171:122–7. https://doi.org/10.1016/j.resmic.2020.02.003
4. Dangel A, Berger A, Rau J, Eisenberg T, Kämpfer P, Margos G, et al. *Corynebacterium silvaticum* sp. nov., a unique group of NTTB corynebacteria in wild boar and roe deer. Int J Syst Evol Microbiol. 2020;70:3614–24. https://doi.org/10.1099/ijsem.0.004195
5. Crestani C, Arcari G, Landier A, Passet V, Garnier D, Brémont S, et al. *Corynebacterium ramonii* sp. nov., a novel toxigenic member of the *Corynebacterium diphtheriae* species complex. Res Microbiol. 2023;174:104113. https://doi.org/10.1016/j.resmic.2023.104113
6. Eisenberg T, Kutzer P, Peters M, Sing A, Contzen M, Rau J. Nontoxigenic tox-bearing *Corynebacterium ulcerans* infection among game animals, Germany. Emerg Infect Dis. 2014;20:448–52. https://doi.org/10.3201/eid2003.130423
7. Busch A, Möller J, Burkovski A, Hotzel H. Genome sequence of a pathogenic *Corynebacterium ulcerans* strain isolated from a wild boar with necrotizing lymphadenitis. BMC Res Notes. 2019;12:692. https://doi.org/10.1186/s13104-019-4704-3
8. Viana MVC, Profeta R, da Silva AL, Hurtado R, Cerqueira JC, Ribeiro BFS, et al. Taxonomic classification of strain PO100/5 shows a broader geographic distribution and genetic markers of the recently described *Corynebacterium silvaticum.* PLoS One. 2020;15:e0244210. https://doi.org/10.1371/journal.pone.0244210
9. Möller J, Busch A, Berens C, Hotzel H, Burkovski A. Newly isolated animal pathogen *Corynebacterium silvaticum* is cytotoxic to human epithelial cells. Int J Mol Sci. 2021;22:3549. https://doi.org/10.3390/ijms22073549
10. Viana MVC, Galdino JH, Profeta R, Oliveira M, Tavares L, de Castro Soares S, et al. Analysis of *Corynebacterium silvaticum* genomes from Portugal reveals a single cluster and a clade suggested to produce diphtheria toxin. PeerJ. 2023;11:e14895. https://doi.org/10.7717/peerj.14895
11. Berger A, Zasada AA, Dangel A, Piekarska K, Paradowska-Stankiewicz I, Bengs K, et al. A case of fatal respiratory diphtheria imported from Poland to Germany: possible link to an undetected imported diphtheria cluster in

Poland? Infection. 2025; Epub ahead of print. https://doi.org/10.1007/s15010-025-02522-y
12. Richter M, Rosselló-Móra R. Shifting the genomic gold standard for the prokaryotic species definition. Proc Natl Acad Sci U S A. 2009;106:19126–31. https://doi.org/10.1073/pnas.0906412106
13. Schuhegger R, Schoerner C, Dlugaiczyk J, Lichtenfeld I, Trouillier A, Zeller-Peronnet V, et al. Pigs as source for toxigenic *Corynebacterium ulcerans*. Emerg Infect Dis. 2009;15:1314–5. https://doi.org/10.3201/eid1508.081568
14. Berger A, Boschert V, Konrad R, Schmidt-Wieland T, Hörmansdorfer S, Eddicks M, et al. Two cases of cutaneous diphtheria associated with occupational pig contact in Germany. Zoonoses Public Health. 2013;60:539–42. https://doi.org/10.1111/zph.12031
15. Berger A, Badell E, Åhman J, Matuschek E, Zidane N, Kahlmeter G, et al. *Corynebacterium diphtheriae* and *Corynebacterium ulcerans*: development of EUCAST methods and generation of data on which to determine breakpoints. J Antimicrob Chemother. 2024;79:968–76. https://doi.org/10.1093/jac/dkae056

Address for correspondence: Anja Berger, National Consiliary Laboratory for Diphtheria, WHO Collaborating for Diphtheria, Bavarian Health and Food Safety Authority, Veterinärstraße 2, 85764 Oberschleißheim, Germany; email: anja.berger@lgl.bayern.de

Detection of Novel Orthobunyavirus Reassortants in Fatal Neurologic Case in Horse and Culicoides Biting Midges, South Africa

Matshepo Elizabeth Rakaki, Miné van der Walt, June Williams, Marietjie Venter

We detected Shuni virus in horses and ovine fetuses and Shamonda virus in a caprine fetus in South Africa. We identified a Shuni/Shamonda virus reassortant in a horse and Shuni/Caimito, Shamonda/Caimito, and Shamonda/Sango virus reassortants in *Culicoides* midges. Continued genomic surveillance will be needed to detect orthobunyavirus infections in Africa.

The *Orthobunyavirus* genus, in the family Peribunyaviridae, has 18 serogroups; several of those represent emerging or reemerging viruses of importance to human and animal health transmitted by mosquitoes and *Culicoides* biting midges (*1*). Orthobunyavirus genomes have 3 negative single-stranded RNA segments, small (S), medium (M), and large (L) (*2*). Those segments can reassort in nature (*3*,*4*), leading to genetically diverse viruses with altered host ranges and pathogenicity (*3*). We characterized the genomes of orthobunyaviruses detected in animals with neurologic signs and birth defects and in *Culicoides* biting midges isolated in South Africa.

The Study

During January 2020–February 2023, samples from 280 equids, 35 ruminants, 53 wildlife species, 6 avians species, and 7 cats or dogs displaying unexplained febrile and neurologic signs or sudden unexplained death were submitted from across South Africa to the zoonotic arbovirus surveillance program at the University of Pretoria (Pretoria, South Africa). We extracted RNA from blood, serum, plasma, cerebrospinal fluid, or tissue samples in a Biosafety Level 3 laboratory by using the QIAamp Viral RNA Mini Kit or RNeasy Mini Kit (QIAGEN, https://www.qiagen.com). We screened animal samples by using in-house S segment–specific TaqMan real-time reverse transcription PCR (RT-PCR) for *Orthobunyavirus* Simbo serogroup, as previously described (*5*). We characterized the M and L segments of positive samples by using conventional nested PCR. Primers for the M segment specifically targeted orthobunyaviruses (*6*), whereas L segment primers targeted the Peribunyaviridae family (*7*) (Appendix 1 Table 1, https://wwwnc.cdc.gov/EID/article/31/7/24-1800-App1.pdf).

A total of 6/381 (1.6%) animals tested positive for orthobunyaviruses by PCR of the S segment (Table; Appendix 1 Table 2) (*5*,*8*). Sanger sequencing identified 5/6 (83.3%) viruses as Shuni virus (SHUV); 4/5 (80.0%) infections were fatal. We found SHUV in samples from 2 aborted ovine fetuses from Mpumalanga and Northwest Provinces and 3 horses from Gauteng and the Northern Cape Provinces. An orthobunyavirus detected in an aborted goat fetus from the Western Cape Province was identified as Shamonda virus (SHAV) through Sanger sequencing, as previously described (*6*). We attempted next-generation sequencing but were unable to obtain full genomes.

We determined pairwise distances between orthobunyavirus sequences and constructed maximum-likelihood phylogenetic trees by using MEGA X version 10.2.6 (https://www.megasoftware.net) (Appendix 2 Tables 1–4, https://wwwnc.cdc.gov/EID/article/31/7/24-1800-App2.xlsx). We performed conventional RT-PCR to obtain a larger S segment fragment (291 bp) and successfully amplified 4 (66.7%) of 6 sequences (Figure 1). The ZRU099/22 (ovine fetus) S segment grouped with SHUV strains from Israel (97.0%–98.0% identity) (Figure 1). Two

Author affiliations: University of Pretoria, Pretoria, South Africa (M.E. Rakaki, J. Williams, M. Venter); University of the Witwatersrand, Johannesburg, South Africa (M. van der Walt, M. Venter)

DOI: https://doi.org/10.3201/eid3107.241800

Table. Orthobunyaviruses identified by PCR and sequencing of S, M, and L segments in samples from mammals and *Culicoides* biting midges, South Africa*

	Orthobunyavirus RT-PCR	Conventional nested PCR		
Sample no.	S segment	S segment	M segment	L segment
Mammals				
ZRU053/20	Shuni virus	IS	IS	IS
ZRU012/21	Shuni virus	Shuni virus	Shamonda virus	Shamonda virus
ZRU027/21	Shuni virus	AF	AF	AF
ZRU093/21	Shamonda virus	Shamonda virus	Shamonda virus	Shamonda virus
ZRU019/22	Shuni virus	Shuni virus	AF	AF
ZRU099/22	Shuni virus	Shuni virus	AF	Shuni virus
Culicoides biting midges				
MAR538_16	Schmallenberg virus	Schmallenberg virus	Schmallenberg virus	Schmallenberg virus
MAR085_13	Sabo virus	AF	Sabo virus	AF
MAR032_12	Sango virus	AF	Shamonda virus	AF
KYA229_16	Shuni virus	Shuni virus	AF	Shuni virus
GAU272_17	Shamonda virus	AF	AF	Caimito virus
GAU110_14	Shamonda virus	AF	AF	Caimito virus
MAR057_13	Shuni virus	AF	AF	Caimito virus

*AF, amplification failed; IS, insufficient sample; RT-PCR, reverse transcription PCR.

horse samples (ZRU12/22 and ZRU19/22) grouped with SHUV strains from South Africa (97.0%–100.0% identity). The S segment of the aborted goat sample (ZRU93/21) clustered with SHAV (*6*). We amplified M segments for 2 (33.3%) of 6 animal samples. Both M segments of ZRU093/21 (*6*) and ZRU012/21 (detected in horse brain) clustered with SHAV (Figure 2); the S segment of ZRU012/21 also clustered with

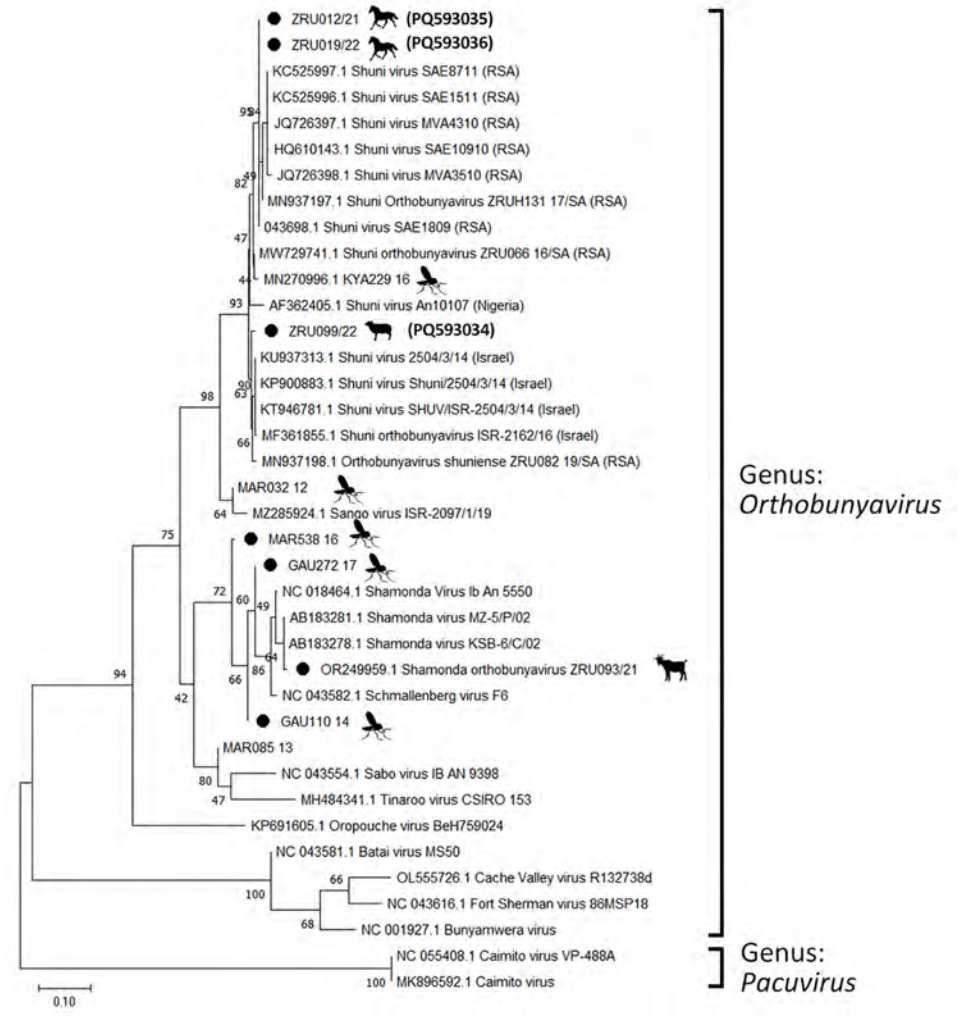

Figure 1. Phylogenetic analysis of *Orthobunyavirus* S segments in study of reassortants in fatal neurologic case in horse and *Culicoides* biting midges, South Africa. Tree shows phylogenetic analysis of positive animal cases and *Culicoides* pools for the S segment of sequences from South Africa (black dots) relative to orthobunyavirus reference strains available in GenBank within the Simbu serogroup. Tree was constructed in MEGA X (https://www.megasoftware.net) by using the Tamura 3-parameter model. Bootstrap values from 1,000 replicates are shown at each node. *Pacuvirus* genus was included as an outgroup to root the tree. Bolded accession numbers in parentheses indicate sequences from this study that were submitted to GenBank. Scale bar indicates nucleotide substitutions per site.

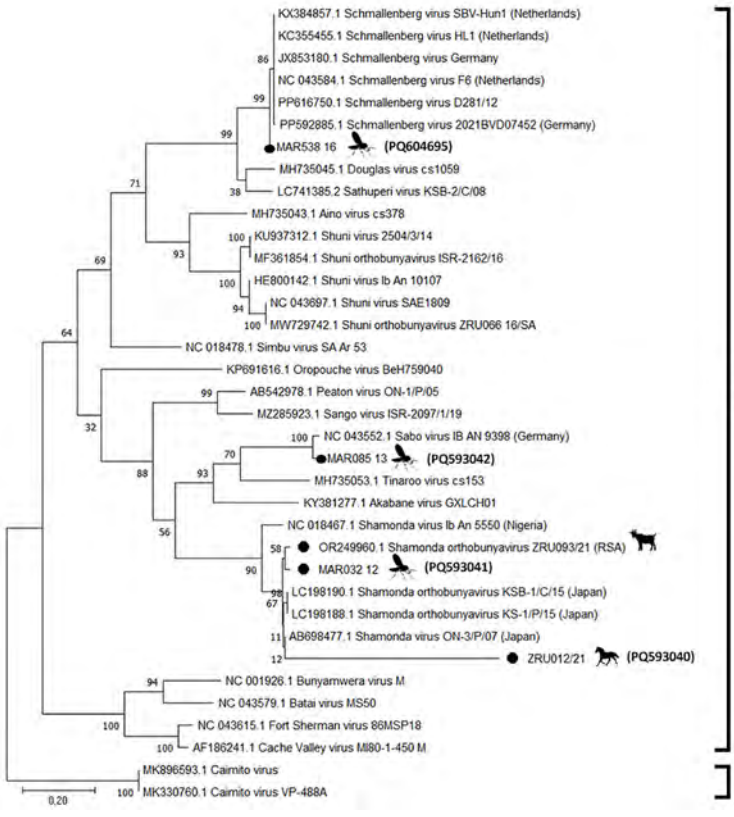

Figure 2. Phylogenetic analysis of *Orthobunyavirus* M segments in study of reassortants in fatal neurologic case in horse and *Culicoides* biting midges, South Africa. Tree shows phylogenetic analysis of the positive animal cases and *Culicoides* pools for the M segment of sequences from South Africa (black dots) relative to orthobunyavirus reference strains available in GenBank within the Simbu serogroup. Tree was constructed in MEGA X (https://www.megasoftware.net) by using the Hasegawa-Kishino-Yano model. Bootstrap values from 1,000 replicates are shown at each node. *Pacuvirus* genus was included as an outgroup to root the tree. Bolded accession numbers in parentheses indicate sequences from this study that were submitted to GenBank. Scale bar indicates nucleotide substitutions per site.

SHUV. The M segment of ZRU012/21 had 63.0%–65.0% identity with SHAV. We amplified L segments of 3/6 (50.0%) animal samples. Of those, 2 samples grouped with SHAV, including the aborted goat fetus (ZRU093/21) (*6*) and horse sample (ZRU012/21) (Figure 3), suggesting ZRU012/21 is a reassortment of the SHUV S segment and SHAV M and L segments; the L segment had 96.0%–99.0% identity with SHAV. The third sample (ZRU099/22) from the ovine fetus clustered with SHUV and had 96% identity with strains from Israel and 92% identity with strains from South Africa.

To determine if reassortants could be identified in *Culicoides* midges previously identified as orthobunyavirus positive, we screened pools of midges collected from 6 surveillance sites in Mpumalanga, Limpopo, and Gauteng Provinces during 2013–2017 (*9*). We performed M and L segment–specific RT-PCR on RNA from 7 orthobunyavirus S segment–positive *Culicoides* pools previously characterized by Sanger sequencing (Table; Figure 1). We successfully amplified the M segment from 3 pooled samples, all from Marakele National Park in Limpopo Province. MAR538_16 grouped with the Schmallenberg virus (SBV) M segment (97.0%–98.0% identity) (Figure 2), as well as the SBV S segment (*9*) (Table). MAR085_13, previously positive for the Sabo virus (SABOV) S segment, also grouped with the SABOV M segment (95.0% identity). MAR032_12 grouped with the SHAV M segment (97.0% identity) but also grouped with the Sango virus (SANV) S segment, suggesting reassortment. We amplified L segments for 5 pooled *Culicoides* midge samples: 2 from Marakele National Park in Limpopo Province, 2 from Boschkop in Pretoria Province, and 1 from Kyalami in Midrand, Gauteng Province. KYA299_16 grouped with L segments of SHUV strains from South Africa (97.0% identity) (Figure 3) and SHUV S segments. MAR538_16 grouped with SBV L segments (97.0%–98.0% identity) and both S and M segments. GAU272_17 and GAU110_14 grouped with the Caimito virus (CAIV) L segment (61.0% identity); however, both grouped with SHAV S segments, suggesting a possible reassortment. MAR057_13 also grouped with the CAIV L segment (59.0% identity) (Figure 3) but grouped with SHUV S segments, suggesting another possible reassortment. We summarized the orthobunyavirus-positive cases tested in this study (Table). We deposited sequences in GenBank (accession numbers in Figures 1–3).

SHUV has been circulating in South Africa in both *Culicoides* midge and mosquito vectors and has been detected in wildlife, ruminants, horses, birds,

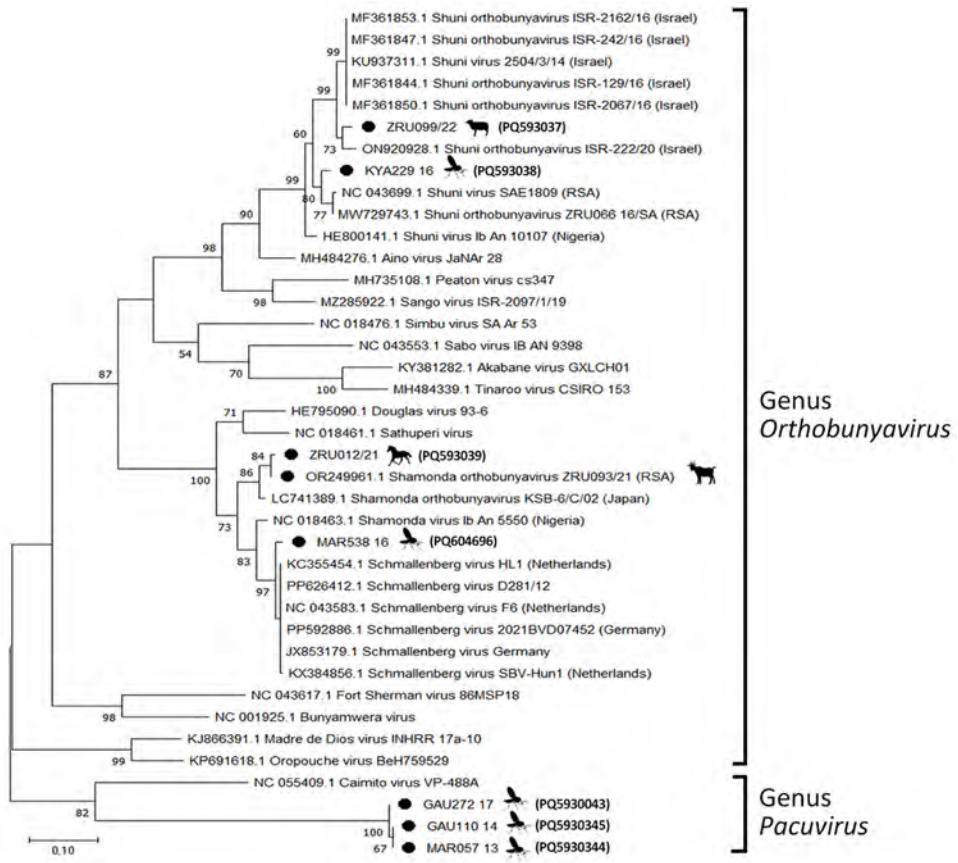

Figure 3. Phylogenetic analysis of *Orthobunyavirus* L segments in study of reassortants in fatal neurologic case in horse and *Culicoides* biting midges, South Africa. Tree shows phylogenetic analysis of the positive animal cases and *Culicoides* pools for the L segment of sequences from South Africa (black dots) relative to orthobunyavirus reference strains available in GenBank within the Simbu serogroup. Tree was constructed in MEGA X (https://www.megasoftware.net) by using the Tamura-Nei model. Bootstrap values from 1,000 replicates are shown at each node. *Pacuvirus* genus was included as an outgroup to root the tree. Bolded accession numbers in parentheses indicate sequences from this study that were submitted to GenBank. Scale bar indicates nucleotide substitutions per site.

and, more recently, in humans (*5*,*8*–*12*). SHAV was first detected in *Culicoides* biting midges in Gauteng Province of South Africa in 2017 and in an aborted goat fetus from the Western Cape in 2021 (*6*,*9*). SHUV was detected in 3 horses with neurologic signs, 2 from Gauteng and 2 from the Western Cape during 2020–2022. One of the 2 fatal cases was caused by a novel SHUV/SHAV reassortment. SHUV was also detected in 2 aborted ovine fetuses. Abortions associated with SHUV have been described in ruminants in Israel. We previously reported SHUV in cerebrospinal fluid from a 13-day-old, hospitalized infant with hydrops fetalis in Gauteng Province (*12*), suggesting SHUV might be a risk factor for birth defects in humans. SHUV, SHAV, and SBV, as well as reassortants, were detected in animals and *Culicoides* midges in this study. Therefore, orthobunyavirus infections should be considered a possible causes of birth defects in humans and animals in Africa.

Reassortments might alter pathogenesis, which has been observed for Ngari virus (*13*,*14*). Reassortants were detected in *Culicoides* midges collected in Gauteng and Limpopo Provinces; 2 were SHAV/CAIV, 1 SHUV/CAIV, and 1 SANV/SHAV reassortants. SANV was previously detected in a springbok that displayed neurologic signs in Mpumalanga Province in South Africa (*5*). Little is known about CAIV, which belongs to the genus *Pacuvirus* isolated in Brazil from rodents and sandflies (*15*). The M segment of orthobunyaviruses detected in South Africa had only 61% identity to CAIV viruses from South America, suggesting different virus species within that genus.

The first limitation of our study is that full genome sequencing was not successful for mammal and *Culicoides* samples, likely because of low RNA levels. We were also unable to reamplify all samples, suggesting RNA degradation in older samples.

Conclusions

Co-circulation of several orthobunyaviruses in Africa might give rise to novel reassortants with altered host range, tissue tropism, and pathogenesis. Reassortants might be missed without characterization of all 3 virus segments. A SHUV/SHAV reassortant described in this study was associated with severe neurologic infection and death in a horse, and SHUV and SHAV were both associated with abortions in ruminants. Several orthobunyaviruses were detected in Culicoides midges, including variants clustering with SBV and reassortants involving SHUV, SHAV, SANV, and

a CAIV-like virus. Continued One Health genomic surveillance will be needed to detect those and other orthobunyaviruses to determine risks for infections in animals and humans in Africa and elsewhere.

Acknowledgments

We thank the veterinarians across South Africa who participated in submitting samples to the surveillance programme CEARV at the Centre for Viral Zoonoses, Department of Medical Virology, University of Pretoria, Pretoria, South Africa, and all staff and students who participated in the surveillance program for their assistance.

The study was approved by the University of Pretoria animal ethics committee (155/19), and Section 20 approval was obtained from the Department of Agriculture of South Africa (reference no. 12/11/1/1 [1552SS]).

About the Author

Ms. Rakaki is a PhD candidate at the Centre for Emerging Arbo and Respiratory Virus Research, Department of Medical Virology, Faculty of Health Sciences, University of Pretoria, Pretoria, South Africa. Her primary research focuses on the molecular and serologic investigation of Shuni virus in South Africa.

References

1. Briese T, Calisher CH, Higgs S. Viruses of the family Bunyaviridae: are all available isolates reassortants? Virology. 2013;446:207–16. https://doi.org/10.1016/j.virol.2013.07.030
2. Elliott RM. Orthobunyaviruses: recent genetic and structural insights. Nat Rev Microbiol. 2014;12:673–85. https://doi.org/10.1038/nrmicro3332
3. Heitmann A, Gusmag F, Rathjens MG, Maurer M, Frankze K, Schicht S, et al. Mammals preferred: reassortment of *Batai* and *Bunyamwera orthobunyavirus* occurs in mammalian but not insect cells. Viruses. 2021;13:1702. https://doi.org/10.3390/v13091702
4. Yanase T, Aizawa M, Kato T, Yamakawa M, Shirafuji H, Tsuda T. Genetic characterization of Aino and Peaton virus field isolates reveals a genetic reassortment between these viruses in nature. Virus Res. 2010;153:1–7. https://doi.org/10.1016/j.virusres.2010.06.020
5. Steyn J, Motlou P, van Eeden C, Pretorius M, Stivaktas VI, Williams J, et al. Shuni virus in wildlife and nonequine domestic animals, South Africa. Emerg Infect Dis. 2020;26:1521–5. https://doi.org/10.3201/eid2607.190770
6. Van der Walt M, Rakaki ME, MacIntyre C, Mendes A, Junglen S, Theron C, et al. Identification and molecular characterization of Shamonda virus in an aborted goat fetus in South Africa. Pathogens. 2023;12:1100. https://doi.org/10.3390/pathogens12091100
7. Kopp A, Hübner A, Zirkel F, Hobelsberger D, Estrada A, Jordan I, et al. Detection of two highly diverse peribunyaviruses in mosquitoes from Palenque, Mexico. Viruses. 2019;11:832. https://doi.org/10.3390/v11090832
8. Motlou TP, Williams J, Venter M. Epidemiology of Shuni virus in horses in South Africa. Viruses. 2021;13:937. https://doi.org/10.3390/v13050937
9. Snyman J, Venter GJ, Venter M. An investigation of *Culicoides* (Diptera: Ceratopogonidae) as potential vectors of medically and veterinary important arboviruses in South Africa. Viruses. 2021;13:1978. https://doi.org/10.3390/v13101978
10. van Eeden C, Williams JH, Gerdes TG, van Wilpe E, Viljoen A, Swanepoel R, et al. Shuni virus as cause of neurologic disease in horses. Emerg Infect Dis. 2012;18:318–21. https://doi.org/10.3201/eid1802.111403
11. Guarido MM, Motlou T, Riddin MA, MacIntyre C, Manyana SC, Johnson T, et al. Potential mosquito vectors for Shuni virus, South Africa, 2014–2018. Emerg Infect Dis. 2021;27:3142–6. https://doi.org/10.3201/eid2712.203426
12. Motlou TP, Venter M. Shuni virus in cases of neurologic disease in humans, South Africa. Emerg Infect Dis. 2021;27:565–9. https://doi.org/10.3201/eid2702.191551
13. Gerrard SR, Li L, Barrett AD, Nichol ST. Ngari virus is a Bunyamwera virus reassortant that can be associated with large outbreaks of hemorrhagic fever in Africa. J Virol. 2004;78:8922–6. https://doi.org/10.1128/JVI.78.16.8922-8926.2004
14. Briese T, Bird B, Kapoor V, Nichol ST, Lipkin WI. Batai and Ngari viruses: M segment reassortment and association with severe febrile disease outbreaks in East Africa. J Virol. 2006;80:5627–30. https://doi.org/10.1128/JVI.02448-05
15. Rodrigues DSG, Medeiros DB, Rodrigues SG, Martins LC, de Lima CP, de Oliveira LF, et al. Pacui virus, Rio Preto da Eva virus, and Tapirape virus, three distinct viruses within the family Bunyaviridae. Genome Announc. 2014;2:1e00923-14. https://doi.org/10.1128/genomeA.00923-14

Address for correspondence: Marietjie Venter, University of the Witwatersrand Johannesburg, Infectious Disease and Oncology Research Institute, School of Medicine, Rm 3B18, Health Sciences Building, 7 York Rd, Johannesburg 2000, South Africa; email: marietjie.venter1@wits.ac.za

Outbreak of Ceftriaxone-Resistant *Salmonella enterica* Serovar Typhi, Bangladesh, 2024

Yogesh Hooda, Arif Mohammad Tanmoy, Sudipta Deb Nath, Anannya Barman Jui, Al Amin, Hafizur Rahman, Neoyman Nasir Shorkar, Naito Kanon, Md Asadur Rahman, Denise O. Garrett, Mohammad Shahidul Islam, ASM Nawshad Uddin Ahmed, Samir K. Saha, Senjuti Saha

We report an outbreak of ceftriaxone-resistant *Salmonella enterica* serovar Typhi in Bangladesh; 47 cases were identified during April–September 2024. Isolates belonged to genotype 4.3.1.2 and harbored the $bla_{CTX\text{-}M\text{-}15}$ gene on the pCROB1 plasmid. This genotype-plasmid lineage represents a recent introduction, calling for strengthened surveillance, antimicrobial stewardship, and vaccination strategies.

Salmonella enterica serovar Typhi, which causes typhoid fever, remains a major public health concern, particularly in South Asia, which accounts for ≈70% of global cases (*1*). Reports of drug-resistant *Salmonella* Typhi have increased in recent decades. Of particular concern are strains resistant to ceftriaxone, azithromycin, or both (*2*). In 2016, researchers identified an outbreak of extensively drug-resistant *Salmonella* Typhi in Pakistan (*3*), in which strains showed resistance to chloramphenicol, ampicillin, trimethoprim/sulfamethoxazole, fluoroquinolones, and third-generation cephalosporins (*3*). Additional reports noted sporadic cases of independently acquired ceftriaxone-resistant *Salmonella* Typhi from Bangladesh (*4*), India (*5*), and the United Kingdom (*6*). Routine use of ceftriaxone as empirical therapy in South Asia creates selective pressure, heightening the need for public health vigilance to prevent the spread of resistant *Salmonella* Typhi (*2*).

Author affiliations: Child Health Research Foundation, Dhaka, Bangladesh (Y. Hooda, A.M. Tanmoy, S.D. Nath, A.B. Jui, A. Amin, H. Rahman, N.N. Shorkar, N. Kanon, M.S. Islam, A.N.U. Ahmed, S.K. Saha, S. Saha); Popular Diagnostic Centre Limited, Dhaka (M.A. Rahman); Sabin Vaccine Institute, Washington, DC, USA (D.O. Garrett); Bangladesh Shishu Hospital and Institute, Dhaka (S.K. Saha)

DOI: http://doi.org/10.3201/eid3107.241987

In Bangladesh, *Salmonella* Typhi is the most common cause of bloodstream infections in children >2 months of age; Dhaka, the capital city, is the primary focus of surveillance initiatives (*7*). To broaden the scope of surveillance and monitor the burden of disease and associated antibiotic drug susceptibility patterns nationwide, we began expanding our surveillance network in January 2023 to include clinics affiliated with Popular Diagnostic Centre Ltd (PDCL), a large, Bangladesh-based diagnostic services provider organization. As of May 2024, the network encompassed 20 clinics across 11 districts, including 10 in Dhaka (Figure 1, panel A). Leveraging this expanded passive surveillance for typhoid fever, we report data from January 2023–September 2024, describing the emergence, spread, and genomic epidemiology of a ceftriaxone-resistant clone of *Salmonella* Typhi in Bangladesh.

The Study

PDCL clinics are outpatient facilities that perform physician-prescribed blood cultures for patients. If a blood culture yields *Salmonella* Typhi, technicians transport the isolate to the Child Health Research Foundation (CHRF, https://chrfbd.org) laboratory for serovar confirmation and antibiotic drug susceptibility testing against ampicillin, cefixime, ceftazidime, ceftriaxone, meropenem, chloramphenicol, trimethoprim/sulfamethoxazole, ciprofloxacin, and azithromycin. Those processes follow established methodologies, including biochemical and slide-agglutination tests (*Salmonella*-agglutinating antiserum; Thermo Fisher Scientific, https://www.thermofisher.com) and Clinical and Laboratory Standards Institute–guided Kirby-Bauer disc diffusion methods (Oxoid; Thermo Fisher Scientific) (*8*).

We identified the first ceftriaxone-resistant *Salmonella* Typhi isolate on April 27, 2024, at the PDCL clinic

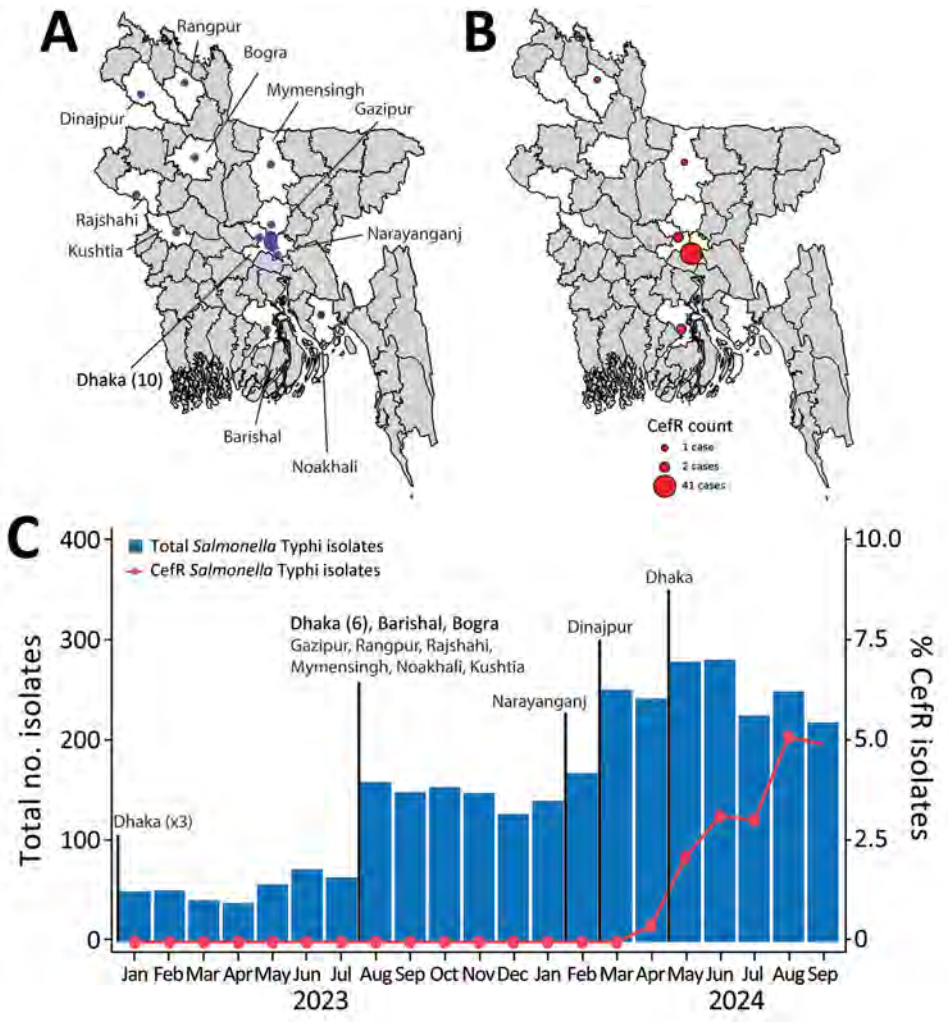

Figure 1. Overview of study of an outbreak of ceftriaxone-resistant *Salmonella enterica* serovar Typhi in Bangladesh, 2024. A) Locations of the 20 study clinics across 11 districts of Bangladesh (blue dots). White indicates districts where the study clinics are located are shown in white; gray indicates districts not included in this study. B) Geographic distribution of CefR *Salmonella* Typhi isolates across Bangladesh. The size of each red dot represents the number of isolates per district. C) Timeline of the surveillance network, showing the inclusion of clinics (text labels) and the total number of *Salmonella* Typhi isolates and CefR isolates detected. Our surveillance efforts began in January 2023 with 3 clinics in Dhaka; more clinics in various locations across Bangladesh were added through May 2024. CefR, ceftriaxone-resistant.

in Narayanganj, a city 30 km from Dhaka, which was added to our surveillance network in February 2024. Subsequent monthly detection of ceftriaxone-resistant strains continued through the study period, culminating in 47 cases by September 2024. Of those, 41 cases were from Narayanganj and 6 were from other districts (Figure 1, panel B). The isolation rate of ceftriaxone-resistant *Salmonella* Typhi increased from 0% to 5% of all isolates during March 2024–September 2024 (Figure 1, panel C). All 47 isolates were resistant to amoxicillin and ceftriaxone, nonsusceptible to fluoroquinolones, but sensitive to chloramphenicol, trimethoprim/sulfamethoxazole, azithromycin, and meropenem (Table).

To investigate the basis of ceftriaxone resistance, we performed whole-genome sequencing on 17 of the 47 resistant *Salmonella* Typhi isolates (Appendix, https://wwwnc.cdc.gov/EID/31/7/24-1987-App1.pdf). Those isolates included 14 from Narayanganj and 1 each from Barishal, Mymensingh, and Rangpur. We prepared genomic libraries using the New England Biolabs DNA library preparation kit (New England Biolabs, https://www.neb.com) and sequenced on a NextSeq2000 platform (2 × 150 bp). We performed genome assembly using Unicycler v0.5.1 (*9*) and analyzed raw fastq files with Mykrobe v0.13.0 (D.J. Ingle et al., unpub. data, https://www.biorxiv.org/content/10.1101/2024.09.30.613582v1).

We classified all 17 ceftriaxone-resistant genomes as genotype 4.3.1.2, noting that ceftriaxone resistance was conferred by the $bla_{\text{CTX-M-15}}$ gene, which showed 100% sequence identity with the gene found in extensively drug-resistant *Salmonella* Typhi strains from Pakistan (genotype 4.3.1.1.P1) (*3*). We performed phylogenetic analysis using Bowtie2, Samtools, Gubbins, and RAxML, following the pipeline described previously (*10*).

We identified an IncY plasmid in all 17 sequenced strains, which we further characterized using plasmidSPAdes v3.15.5 (*11*). We generated the longest

plasmid sequence of 103.9 kbp from isolate STY_0313. This IncY plasmid, referred to as pCROB1, carried the $bla_{CTX\text{-}M\text{-}15}$ gene and encoded a phage element (Figure 2). Public Health England previously identified a similar phage-plasmid associated with genotype 4.3.1.1 among travel-related typhoid cases from Iraq (*6*), suggesting a unique genotype-plasmid lineage underpinning the ongoing outbreak in Bangladesh.

Genotype 4.3.1.2 is rarely identified in Bangladesh and accounted for only 0.5% (7/1,356) of all *Salmonella* Typhi whole-genome sequences available for 1999–2018 (*13*). The genotype is more commonly found in India and Nepal (Figure 3). To investigate the phylogenetic context of genotype 4.3.1.2, we constructed a tree using global database sequences from genotype 4.3.1 and its subtypes, with a focus on 4.3.1.2 and its sublineages (Appendix). We found that the recent ceftriaxone-resistant isolates from Bangladesh are closely related to strains from India and Nepal, rather than to earlier 4.3.1.2 genotypes from Bangladesh (Figure 3). However, our research showed no strains from India or Nepal were reported to be ceftriaxone resistant or to carry the pCROB1 plasmid. We propose naming this distinct subclade lineage 4.3.1.2.B1. Although researchers have reported ceftriaxone resistance in genotype 4.3.1.2 strains from India (*5*), the molecular basis of resistance in lineage 4.3.1.2.B1 differs, suggesting an independent acquisition of the ceftriaxone-encoding phage-plasmid by this genotype.

Table. Clinical, demographic, and epidemiologic features of patients with ceftriaxone-resistant *Salmonella enterica* serovar Typhi 4.3.1.2.B1 infections based on data from an outbreak in Bangladesh, 2024

Characteristic	No. (%) patients, n = 21
Sex	
M	15 (72)
F	6 (28)
Age, y	
1–5	7 (33)
6–10	3 (14)
11–15	4 (19)
16–20	3 (14)
21–25	2 (10)
>25	2 (10)
Clinical characteristics	
Fever	21 (100)
Headache	11 (52)
Cough	10 (47)
Abdominal pain	11 (52)
Breathing difficulty	3 (14)
Vomiting	7 (33)
Diarrhea	6 (28)
Jaundice*	1 (5)
Nausea	2 (10)
Anorexia	2 (10)
Treatment outcome	
Recovered	21 (100)
Treatment location	
Outpatient department	14 (67)
Inpatient department	7 (33)
Initial antibiotic received	
Third-generation cephalosporin	12 (57)
Cefixime	7 (30)
Ceftriaxone	4 (19)
Ceftibuten	1 (5)
Second-generation cephalosporin: cefuroxime	1 (5)
Azithromycin	4 (19)
Ciprofloxacin	1 (5)
Ciprofloxacin + azithromycin	1 (5)
Tazobactam/piperacillin	1 (5)
Unknown	1 (5)
Second antibiotic received	
Third-generation cephalosporin: ceftriaxone	2 (10)
Meropenem	5 (24)
Azithromycin	1 (5)
Amoxicillin/clavulanic acid, amikacin	1 (5)
Ttrimethoprim/sulfamethoxazole	1 (5)
Unknown	1 (5)

*Participant had concomitant hepatitis A virus infection.

To better understand the progression of disease in patients with ceftriaxone-resistant typhoid, we selected 35 cases (identified through August 31, 2024) for telephone interviews, successfully completing 21 (60%). Most (65%, 13/21) patients initially received either second-generation (cefuroxime 5%, 1/21) or third-generation (57%, 12/21; including cefixime [30%, 7/21], ceftriaxone [19%, 4/21], and ceftibuten [5%, 1/21]) cephalosporins. Forty-six percent (6/13) of patients switched to meropenem (23%, 3/13), azithromycin (8%, 1/13), or trimethoprim/sulfamethoxazole (8%, 1/13). One patient could not recall the second antibiotic used. All patients recovered; average illness duration was 19 (range 12–28) days. No patients reported travel outside Bangladesh, suggesting local circulation of this strain. Three cases occurred outside Narayanganj, the initial outbreak site; 2 patients had no travel history to Narayanganj within 15 days of illness onset, indicating potential spread to other districts.

Conclusions

Our detection of a unique genotype-plasmid lineage—4.3.1.2.B1, carrying the $bla_{CTX\text{-}M\text{-}15}$ gene on the pCROB1 plasmid—associated with an outbreak of ceftriaxone-resistant *Salmonella* Typhi in Bangladesh represents a concerning development because of the strain's potential for regional and international spread (*2*). Given the observed local spread of this lineage, healthcare systems may need to prepare for a shift back to older antibiotics, such as trimethoprim/sulfamethoxazole and chloramphenicol. Of note, 4.3.1.2.B1 strains remain sensitive to those drugs, indicating that first-line antibiotic drugs may serve as viable alternatives to azithromycin and meropenem.

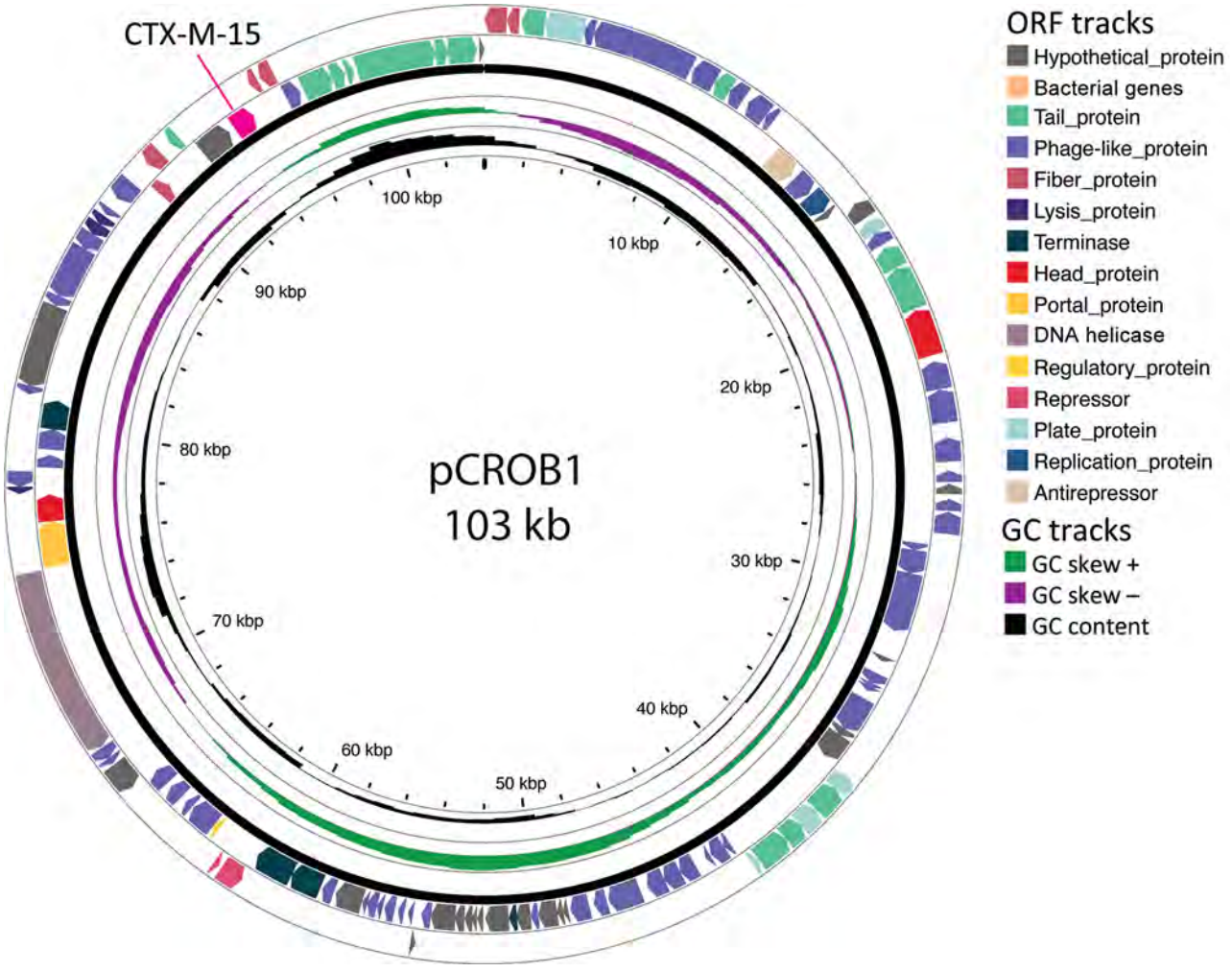

Figure 2. Annotated map of plasmid pCROB1 from study of an outbreak of ceftriaxone-resistant *Salmonella enterica* serovar Typhi, Bangladesh, 2024. pCROB1 harbors the $bla_{\text{CTX-M-15}}$ gene and includes an intact phage element, as annotated using PHASTEST (*12*). Tracks around the plasmid map highlight GC content and predicted ORFs. GC, guanine and cytosine nucleotides; OFR, open reading frame.

Seven patients in this study received third-generation cephalosporins and recovered from fever; however, we did not follow those cases to investigate relapse rates and other complications that could result from improper antibiotic use.

Our investigation of a unique strain of ceftriaxone-resistant *Salmonella* Typhi emerging in Bangladesh underscores the role of widespread ceftriaxone use in selecting for antimicrobial-resistant strains of typhoid fever. The outbreak was detected in April 2024, but the clone could have been circulating in Narayanganj before detection in our surveillance network. Because ceftriaxone remains a cornerstone of empirical treatment for typhoid, its declining efficacy is of great public health concern. Public health efforts should focus on bolstering antimicrobial stewardship and public education on appropriate antibiotic drug use, strengthening surveillance systems, and implementing and promoting immunization with typhoid conjugate vaccines to curb further spread of resistant strains.

This article was preprinted at https://www.medrxiv.org/content/10.1101/2024.12.24.24319600v1.

Acknowledgments

We are grateful to the CHRF team, especially Md. Shariful Islam, Md. Shakiul Kabir, Lima Akter, Md. Zillur Rahman, Md. Humayun Kabir, Khursheda Afrin Khushi, and Monalisa, for their efforts in coordinating the timely transfer of *Salmonella* Typhi isolates and data from PDCL to CHRF, data management, aiding in the lab, and

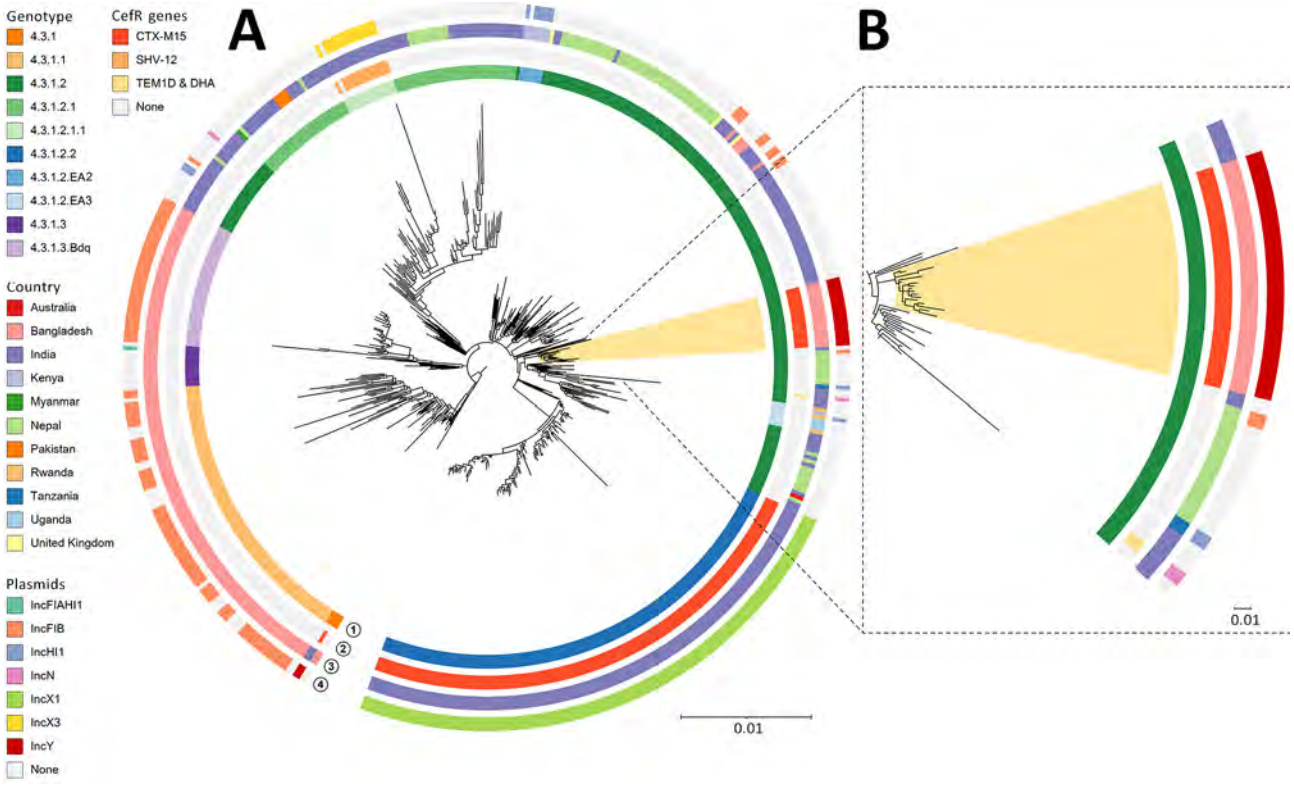

Figure 3. Phylogenetic tree of *Salmonella* Typhi genotype 4.3.1, including the 17 CefR 4.3.1.2.B1 strains detected in findings from a study of an outbreak of CefR *S. enterica* serovar Typhi, Bangladesh, 2024. A) Phylogenetic tree of 546 genomes belonging to genotype 4.3.1 and its subtypes. CefR strains sequenced in our study belong to genotype 4.3.1 and are highlighted in yellow. Tree was built following a pipeline described earlier (*10*) and displays different CefR genes, countries of isolation, and associated plasmid elements. For context, 529 genomes from genotype 4.3.1 and its subtypes were also included. Of those, 249 (10%) were randomly selected from 2,567 genomes (genotype 4.3.1.2 and subtypes) available on Pathogenwatch by genotype, year, and country (accessions available for 2,542; accessed on 14 July 2024), and 280 were from previous studies conducted in Bangladesh, India, and Pakistan (*14*). B) Zoomed-in view of the subclade containing the CefR strains from our study in Bangladesh. Scale bars indicate mean nucleotide substitutions per site. CefR, ceftriaxone-resistant.

conducting phone follow-ups. This study would not have been possible without the invaluable support of the PDCL staff in facilitating the careful storage and transfer of the isolates.

Ethical approval for this study was obtained from the Ethics Review Boards of Bangladesh Shishu Hospital and Institute (IRB no. Admin/BSHI/2022/2058) and the CHRF (IRB no. CHRFIRB/07-12-2023/02). Raw fastq files of sequences from this study have been submitted to the European Nucleotide Archive (accession no. ERP167392).

This work was supported by the Bill & Melinda Gates Foundation (grant nos. INV-051975 and INV-008335).

About the Author

Dr. Hooda is a senior scientist at the Child Health Research Foundation in Dhaka, Bangladesh, specializing in infectious diseases, antimicrobial resistance, and the development of innovative interventions like bacteriophages for public health challenges. His work focuses on advancing research capacity in low- and middle-income countries, including genomic analysis and pediatric infection monitoring, while fostering global collaborations to combat pressing health issues.

References

1. Stanaway JD, Reiner RC, Blacker BF, Goldberg EM, Khalil IA, Troeger CE, et al.; GBD 2017 Typhoid and Paratyphoid Collaborators. The global burden of typhoid and paratyphoid fevers: a systematic analysis for the Global Burden of Disease Study 2017. Lancet Infect Dis. 2019;19:369–81. https://doi.org/10.1016/S1473-3099(18)30685-6
2. Hooda Y, Tanmoy AM, Sajib MSI, Saha S. Mass azithromycin administration: considerations in an increasingly resistant world. BMJ Glob Health. 2020;5:e002446. https://doi.org/10.1136/bmjgh-2020-002446
3. Klemm EJ, Shakoor S, Page AJ, Qamar FN, Judge K, Saeed DK, et al. Emergence of an extensively drug-resistant *Salmonella enterica* serovar Typhi clone harboring a promiscuous plasmid encoding resistance to

fluoroquinolones and third-generation cephalosporins. MBio. 2018;9:e00105–18. https://doi.org/10.1128/mBio.00105-18
4. Djeghout B, Saha S, Sajib MSI, Tanmoy AM, Islam M, Kay GL, et al. Ceftriaxone-resistant *Salmonella* Typhi carries an IncI1-ST31 plasmid encoding CTX-M-15. J Med Microbiol. 2018;67:620–7. https://doi.org/10.1099/jmm.0.000727
5. Argimón S, Nagaraj G, Shamanna V, Sravani D, Vasanth AK, Prasanna A, et al. Circulation of third-generation cephalosporin resistant *Salmonella* Typhi in Mumbai, India. Clin Infect Dis. 2022;74:2234–7. https://doi.org/10.1093/cid/ciab897
6. Godbole G, McCann N, Jones SM, Dallman TJ, Brown M. Ceftriaxone-resistant *Salmonella* Typhi in a traveller returning from a mass gathering in Iraq. Lancet Infect Dis. 2019;19:467. https://doi.org/10.1016/S1473-3099(19)30176-8
7. Saha S, Islam M, Uddin MJ, Saha S, Das RC, Baqui AH, et al. Integration of enteric fever surveillance into the WHO-coordinated Invasive Bacterial-Vaccine Preventable Diseases (IB-VPD) platform: a low cost approach to track an increasingly important disease. PLoS Negl Trop Dis. 2017;11:e0005999. https://doi.org/10.1371/journal.pntd.0005999
8. Tanmoy AM, Hooda Y, Sajib MSI, Rahman H, Sarkar A, Das D, et al. Trends in antimicrobial resistance amongst *Salmonella* Typhi in Bangladesh: a 24-year retrospective observational study (1999–2022). PLoS Negl Trop Dis. 2024;18:e0012558. https://doi.org/10.1371/journal.pntd.0012558
9. Wick RR, Judd LM, Gorrie CL, Holt KE. Unicycler: resolving bacterial genome assemblies from short and long sequencing reads. PLOS Comput Biol. 2017;13:e1005595. https://doi.org/10.1371/journal.pcbi.1005595
10. Tanmoy AM, Hooda Y, Sajib MSI, da Silva KE, Iqbal J, Qamar FN, et al. Paratype: a genotyping tool for *Salmonella* Paratyphi A reveals its global genomic diversity. Nat Commun. 2022;13:7912. https://doi.org/10.1038/s41467-022-35587-6
11. Antipov D, Hartwick N, Shen M, Raiko M, Lapidus A, Pevzner PA. plasmidSPAdes: assembling plasmids from whole genome sequencing data. Bioinformatics. 2016;32:3380–7. https://doi.org/10.1093/bioinformatics/btw493
12. Wishart DS, Han S, Saha S, Oler E, Peters H, Grant JR, et al. PHASTEST: faster than PHASTER, better than PHAST. Nucleic Acids Res. 2023;51(W1):W443–50. https://doi.org/10.1093/nar/gkad382
13. Carey ME, Dyson ZA, Ingle DJ, Amir A, Aworh MK, Chattaway MA, et al.; Global Typhoid Genomics Consortium Group Authorship. Global diversity and antimicrobial resistance of typhoid fever pathogens: insights from a meta-analysis of 13,000 *Salmonella* Typhi genomes. eLife. 2023;12:e85867. https://doi.org/10.7554/eLife.85867
14. Argimón S, David S, Underwood A, Abrudan M, Wheeler NE, Kekre M, et al.; NIHR Global Health Research Unit on Genomic Surveillance of Antimicrobial Resistance. Rapid genomic characterization and global surveillance of *Klebsiella* using Pathogenwatch. Clin Infect Dis. 2021;73(Suppl_4):S325–35. https://doi.org/10.1093/cid/ciab784

Address for correspondence: Senjuti Saha, Child Health Research Foundation, SEL-Huq Skypark, 23/2 Khilji Rd, Block-B, Mohammadpur Dhaka, 1207, Bangladesh; email: senjutisaha@chrfbd.org

Genomic Deletion of PfHRP2 and PfHRP3 in *Plasmodium falciparum* Strains, Ethiopia, 2009

Tamirat Gebru Woldearegai, Tina Krüger, Sindew Mekasha Feleke, Hassen Mamo, Tesfaye Gelanew, Vanessa Krohmer, Sabine Belard, Peter G. Kremsner, Jana Held, Miriam Rodi, Andrea Kreidenweiss

Author affiliations: Institute of Tropical Medicine, University Hospital Tübingen, Tübingen, Germany (T.G. Woldearegai, T. Krüger, V. Krohmer, S. Belard, P.G. Kremsner, J. Held, M. Rodi, A. Kreidenweiss); German Center for Infection Research, partner site Tübingen, Tübingen (T.G. Woldearegai, S. Belard, P.G. Kremsner, J. Held, A. Kreidenweiss); La Trobe University, Melbourne, Victoria, Australia (S.M. Feleke); Ethiopian Public Health Institute, Addis Ababa, Ethiopia (S.M. Feleke); College of Natural and Computational Sciences, Addis Ababa University, Addis Ababa (S.M. Feleke, H. Mamo); Armauer Hansen Research Institute, Addis Ababa (T. Gelanew); Centre de Recherches Médicales de Lambaréné, Lambaréné, Gabon (P.G. Kremsner, J. Held, A. Kreidenweiss)

DOI: https://doi.org/10.3201/eid3107.241676

Plasmodium falciparum strains lacking *P. falciparum* histidine-rich protein 2 (PfHRP2) and PfHRP3 threaten malaria rapid test reliability. We show that *pfhrp2/pfhrp3*–deleted parasites circulated in Ethiopia as early as 2009, before widespread PfHRP2-based rapid test use, and had high *pfhrp3* deletion prevalence. Monitoring of *pfhrp2* and of *pfhrp3* deletions is needed.

Malaria caused by *Plasmodium falciparum* remains a major health problem. In 2023, an estimated 263 million cases and 597,000 deaths were seen worldwide; most were in Africa. Introduction of rapid diagnostic tests (RDTs) has substantially increased malaria diagnosis and malaria control. *P. falciparum* histidine-rich protein 2 (PfHRP2)–detecting RDTs rely on monoclonal antibodies raised against PfHRP2. Those monoclonal antibodies cross-detect PfHRP3 because of shared amino acid repeats.

The development of malaria RDTs began in the early 1990s; however, it was not until 2008 that quality-controlled and reliable RDTs became available. The World Health Organization policy shift in 2010 to a test-and-treat strategy boosted widespread use of RDTs, and RDT sales increased to >415 million in 2022 (*1*). In 2010 in the Amazon region of Peru, researchers identified the first *P. falciparum* strains that lacked the *pfhrp2* gene (and *pfhrp3* gene) and caused false-negative PfHRP2 RDT results (*2*). Subsequent studies identified *pfhrp2* gene–deleted and *pfhrp3* gene–deleted parasites in other malaria-endemic regions; the highest frequencies were reported in the Amazon region in South America and parts of East Africa, including Ethiopia (*3*). The high frequency of gene deletions in countries in East Africa has already led to a policy switch toward non-PfHRP2 RDTs in Eritrea, Djibouti, and, in 2022, Ethiopia (*4*), despite the lack of reliable alternative RDT types.

We suspected that treatment guided by PfHRP2-based RDTs selects for PfHRP2 test–negative parasites that can be further transmitted and spread (*3*). In the Amazon region of Peru, where the first *pfhrp2*-deleted and *pfhrp3*-deleted parasites were found, PfHRP2-based RDTs were not in common use (*2*).

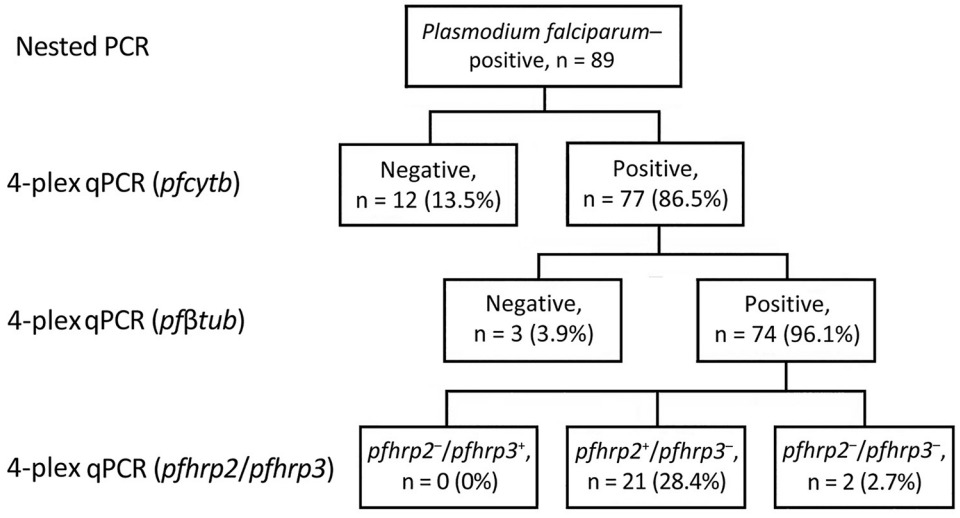

Figure. *pfhrp2* and *pfhrp3* deletion frequency in genomic deletion of PfHRP2 and PfHRP3 antigens in *Plasmodium falciparum* strains, Ethiopia, 2009. *P. falciparum*–positive samples from 89 persons, previously identified by species-specific PCR were analyzed by 4-plex qPCR for the presence of *P. falciparum* by *pfcytb* to confirm DNA quality and quantity by amplification of the single copy gene *pfβtub* and then for deletion of *pfhrp2* and *pfhrp3*. *pfcytb, P. falciparum* cytochrome b; *pfβtub, P. falciparum* β-tubulin; *pfhrp*, *P. falciparum* histidine-rich protein; qPCR, quantitative PCR.

Table. Study population and *pfhrp2* and *pfhrp3* deletion outcomes per study region in genomic deletion of PfHRP2 and PfHRP3 in *Plasmodium falciparum* strains, Ethiopia, 2009*

Study sites	No. samples analyzed	Patient median age, y (range)	Patient sex, % F	Patient sex, % M	*pfcytb*$^+$/*pfβtub*$^+$, no.	*pfhrp2*$^+$/*pfhrp3*$^-$, no. (%)†	*pfhrp2*$^-$/*pfhrp3*$^+$, no. (%)†	*pfhrp2*$^-$/*pfhrp3*$^-$, no. (%)†
Jimma	66	18 (1–73)	46	54	63	19 (30.2)	0 (0)	2 (3.2)
Harar	23	25 (6–60)	30	70	11	2 (18.2)	0 (0)	0 (0)
Total	89	21 (1–73)	38	62	74	21 (28.4)	0 (0)	2 (2.7)

pfβtub, P. falciparum β-tubulin; *pfcytb: P. falciparum* cytochrome b; PfHRP, *P. falciparum* histidine-rich protein.
†Percentages were calculated by using the total number of eligible samples (*pfcytb*$^+$/*pfbtub*$^+$) from each site as denominator.

To shed light on the multifactorial forces driving the spread of parasites with gene deletions, we retrospectively analyzed samples collected in Ethiopia in 2009, which was a time when PfHRP2-based RDTs were not yet used globally. We obtained the samples from eastern and southwestern regions of the country (Appendix Figure 1, https://wwwnc.cdc.gov/EID/article/31/7/24-1676-App1.pdf).

We used 4-plex quantitative PCR (qPCR) analysis on 89 samples that had already tested positive for *P. falciparum* monoinfection by using species-specific PCR as previously reported (*5*) and that were available in sufficient quantities for testing (*6*) (Appendix); 74 were quality confirmed. Of those 74 samples, 2 (2.7%) were negative for *pfhrp2* and *pfhrp3* (*pfhrp2*$^-$/*pfhrp3*$^-$) (Figure). We did not detect any *pfhrp2* single deletions (*pfhrp2*$^-$/*pfhrp3*$^+$), but 21 samples (28.4%) lacked *pfhrp3* (*pfhrp2*$^+$/*pfhrp3*$^-$). Because sample size was limited, we were unable to analyze regional differences. Most (63/74) samples were from the southwestern (Jimma) region, where >90% of the deletions were found (Table). PfHRP2 RDTs were not performed on the sample set.

To further profile the *pfhrp3* gene locus in the 23 samples lacking *pfhrp3* (targeting the 5′ end of *pfhrp3* exon 2), we reassessed the samples by using a modified 4-plex qPCR that targets the 3′ region of *pfhrp3* exon 2 (*7*) (Appendix Figure 2). Of 21 analyzed samples (2 samples had insufficient material), 7 samples were positive for *pfhrp3* (Appendix Table 1). We profiled 5 of those samples (2 samples lacked material) by PCR (primer pairs 3, 4, and 5) that spanned various regions within the *pfhrp3* locus. All 5 samples had a *pfhrp3* gene deletion (Appendix Table 2, Figure 2). We therefore recommend continued use of unmodified 4-plex qPCR (*6*).

Studies of *pfhrp2* and *pfhrp3* deletions in the *P. falciparum* population in Africa with a sufficiently large sample size are lacking (*8*). Before intensive use of PfHRP2-based RDTs, parasites with *pfhrp2* deletions were already present but at very low frequencies and only in association with *pfhrp3* deletions. In contrast, the percentage (28%) of *pfhrp3*-deleted parasites was surprisingly high and agrees with multiple studies from Ethiopia conducted since 2015 (Appendix Table 3).

Our data clarify the emergence and spread of PfHRP2 diagnostic–resistant parasites, supporting Feleke et al. (*3*). Frequently occurring *pfhrp3* deletions might favor selection and spread of occasionally occurring *pfhrp2* deletions under the selective pressure of intensive use of PfHRP2 RDTs followed by antimalarial treatment. Studies published in 2020 and 2021 identified a major role of PfHRP3 in the accuracy of PfHRP2 RDTs, particularly at low parasitemia, where cross-binding can mask *pfhrp2* deletions and result in a positive test (*9*,*10*). In contrast, absence of PfHRP3 in *pfhrp2*-deleted strains results in a false-negative RDT and ultimately leads to positive selection of *pfhrp2*-deleted *P. falciparum*. Those results are particularly relevant in areas of low transmission and with extensive use of PfHRP2 RDTs and antimalarial treatment (*3*; O.J. Watson et al., unpub. data, http://medrxiv.org/lookup/doi/10.1101/2023.10.21.23297352). The frequency of *pfhrp2* and *pfhrp3* deletions is much lower in West and Central Africa countries that have a high transmission rate (O.J. Watson et al., unpub. data).

Use of different molecular tests provided valuable insights into the challenges of deletion detection and nature of *pfhrp3* gene deletion. We confirmed 4-plex qPCR results by using 3 PCRs with commonly used primers and highlight that outcomes might vary depending on the assays applied. *pfhrp3* deletions might contribute to the spread of *pfhrp2*-deleted *P. falciparum* and should be routinely monitored along with *pfhrp2* in deletion surveillance studies.

About the Author

Dr. Woldearegai is a postdoctoral researcher at the Institute of Tropical Medicine, University Hospital Tübingen, Tübingen, Germany. His primary research interests include diagnostics, molecular epidemiology, and transmission of malaria and other tropical infectious diseases.

References

1. World Health Organization. T3: test, treat and track: scaling up diagnostic testing, treatment and surveillance for malaria. Geneva: The Organization; 2012.
2. Gamboa D, Ho MF, Bendezu J, Torres K, Chiodini PL, Barnwell JW, et al. A large proportion of *P. falciparum* isolates in the Amazon region of Peru lack *pfhrp2* and *pfhrp3*: implications for malaria rapid diagnostic tests. PLoS One. 2010;5:e8091. https://doi.org/10.1371/journal.pone.0008091

3. Feleke SM, Reichert EN, Mohammed H, Brhane BG, Mekete K, Mamo H, et al. *Plasmodium falciparum* is evolving to escape malaria rapid diagnostic tests in Ethiopia. Nat Microbiol. 2021;6:1289–99. https://doi.org/10.1038/s41564-021-00962-4
4. Federal Democratic Republic of Ethiopia, Ministry of Health. National malaria guidelines, 5th edition [cited 2025 Feb 24]. https://www.scribd.com/document/589612562/National-Malaria-Guideline-2022
5. Woldearegai TG, Kremsner PG, Kun JFJ, Mordmüller B. *Plasmodium vivax* malaria in Duffy-negative individuals from Ethiopia. Trans R Soc Trop Med Hyg. 2013;107:328–31. https://doi.org/10.1093/trstmh/trt016
6. Krueger T, Ikegbunam M, Lissom A, Sandri TL, Ntabi JDM, Djontu JC, et al. Low prevalence of *Plasmodium falciparum* histidine-rich protein 2 and 3 gene deletions—a multiregional study in Central and West Africa. Pathogens. 2023;12:455. https://doi.org/10.3390/pathogens12030455
7. Grignard L, Nolder D, Sepulveda N, Berhane A, Mihreteab S, Kaaya R, et al. Corrigendum to 'A novel multiplex qPCR assay for detection of *Plasmodium falciparum* with histidine-rich protein 2 and 3 (pfhrp2 and pfhrp3) deletions in polyclonal infections'. EBioMedicine. 2021;65:103261. https://doi.org/10.1016/j.ebiom.2021.103261
8. World Health Organization. Malaria threat map [cited 2024 May 7]. https://apps.who.int/malaria/maps/threats/#/maps?theme=diagnosis&mapType=diagnosis%3A0&bounds=%5B%5B-204.77944076891063%2C-57.16726526146551%5D%2C%5B204.77944076891237%2C77.99489257835737%5D%5D&insecticideClass=PYRETHROIDS&insecticideTypes=&assayTypes=&synergistTypes=&species=&vectorSpecies=&surveyTypes=&plasmodiumSpecies=&drugs=&mmType=1&excludeLowerPatients=false&excludeLowerSamples=false&endemicity=false&storyMode=false&storyModeStep=0&years=1996%2C2009&deletionType=HRP2_HRP3_PROPORTION_DELETION
9. Gatton ML, Chaudhry A, Glenn J, Wilson S, Ah Y, Kong A, et al. Impact of *Plasmodium falciparum* gene deletions on malaria rapid diagnostic test performance. Malar J. 2020;19:392. https://doi.org/10.1186/s12936-020-03460-w
10. Kong A, Wilson SA, Ah Y, Nace D, Rogier E, Aidoo M. HRP2 and HRP3 cross-reactivity and implications for HRP2-based RDT use in regions with *Plasmodium falciparum* hrp2 gene deletions. Malar J. 2021;20:207. https://doi.org/10.1186/s12936-021-03739-6

Address for correspondence: Andrea Kreidenweiss, Institute of Tropical Medicine, University Hospital Tübingen, Wilhelmstrasse 27, D-72074 Tübingen, Germany; email: andrea.kreidenweiss@uni-tuebingen.de

Promising Effects of Duck Vaccination against Highly Pathogenic Avian Influenza, France, 2023–2024

Claire Guinat, Lisa Fourtune, Sébastien Lambert, Eva Martin, Guillaume Gerbier, Andrea Jimenez Pellicer, Jean-Luc Guérin, Timothée Vergne

Author affiliations: Interactions Hôtes-Agents Pathogènes, Université de Toulouse, INRAE, ENVT, Toulouse, France (C. Guinat, L. Fourtune, S. Lambert, E. Martin, J.-L. Guérin, T. Vergne); Direction Générale de l'Alimentation, Ministère de l'Agriculture et de la Souveraineté Alimentaire, Paris, France (G. Gerbier, A. Jimenez Pellicer)

DOI: https://doi.org/10.3201/eid3107.241445

Highly pathogenic avian influenza causes substantial poultry losses and zoonotic concerns globally. Duck vaccination against highly pathogenic avian influenza began in France in October 2023. Our assessment predicted that 314–756 outbreaks were averted in 2023–2024, representing a 96%–99% reduction in epizootic size, likely attributable to vaccination.

Highly pathogenic avian influenza (HPAI) H5 viruses of clade 2.3.4.4b continue to affect diverse regions and species worldwide. Since 2020, this ongoing panzootic has reached unprecedented scale, causing the death or culling of >130 million poultry across 67 countries, substantially threatening food security (*1*). Mass mortality in wild birds and spillover to >48 mammal species across 26 countries have raised conservation and zoonotic concerns (*2*).

Although most countries rely on poultry depopulation and movement restrictions to control HPAI, France recently implemented preventive vaccination (*3*). Since October 2023, domestic ducks in the production stage are vaccinated with the Volvac B.E.S.T. AI+ND vaccine (Boehringer Ingelheim, https://www.boehringer-ingelheim.com), administered at 10 and 28 days, and, in high-risk zones and during winter, a third dose at 56 days (*4*). In May 2024, the campaign expanded to include the RESPONS AI H5 vaccine (Ceva Animal Health, https://www.ceva.us). Vaccinating breeder ducks remains optional. As of July 1, 2024, >35 million ducks had received 2 doses and 1.5 million had received 3 doses (*4*).

In 2023–2024, only 10 HPAI H5 poultry outbreaks were reported, substantially reduced from 1,374 in 2021–2022 and 396 in 2022–2023 (Figure, panels A, B).

Those 10 outbreaks (6 in turkeys, 3 in ducks, and 1 in chickens) were attributed to ≥4 primary introductions. The infected duck farms shared similar viruses, supporting lateral transmission: 2 occurred in vaccinated flocks with suboptimal immune protection or early virus exposure, and 1 occurred in an unvaccinated breeder flock (*5*). In contrast, outbreaks continued in nonvaccinating countries in Europe. Despite encouraging results, the extent to which vaccination contributed to this reduction remains unclear.

We compared the reduction in outbreaks to what would have been expected based on historical outbreak patterns and external infection pressure and considered potential explanations. We extracted HPAI H5 clade 2.3.4.4b detection data in Europe (2016–2024) from the EMPRES Global Animal Disease Information System (https://empres-i.apps.fao.org). For each epidemiologic year (September 1–August 31), we retrieved poultry outbreak numbers in France. We defined candidate predictors using poultry outbreak and wild bird case numbers from neighboring countries as proxies for external infection pressure, supported by phylogenetic links between circulating viruses in those regions (*6*,*7*). Predictors combined time windows (1–3 months before the first poultry outbreak in France) and regions (region 1 [Norway, Sweden, Finland]; region 2 [Germany, Denmark, The Netherlands, Belgium]; region 3 [United Kingdom, Ireland]; region 4 [Bulgaria, Romania, Hungary, Poland, Czech Republic]) (Appendix Table 1, Figure 1, https://wwwnc.cdc.gov/EID/article/31/7/24-1445-App1.pdf). We assumed consistent surveillance across years, likely valid for poultry because of standardized programs in Europe but less certain for wild birds given the opportunistic nature of passive surveillance. Using quasi-Poisson univariate regressions, we identified the predictor most statistically associated with yearly

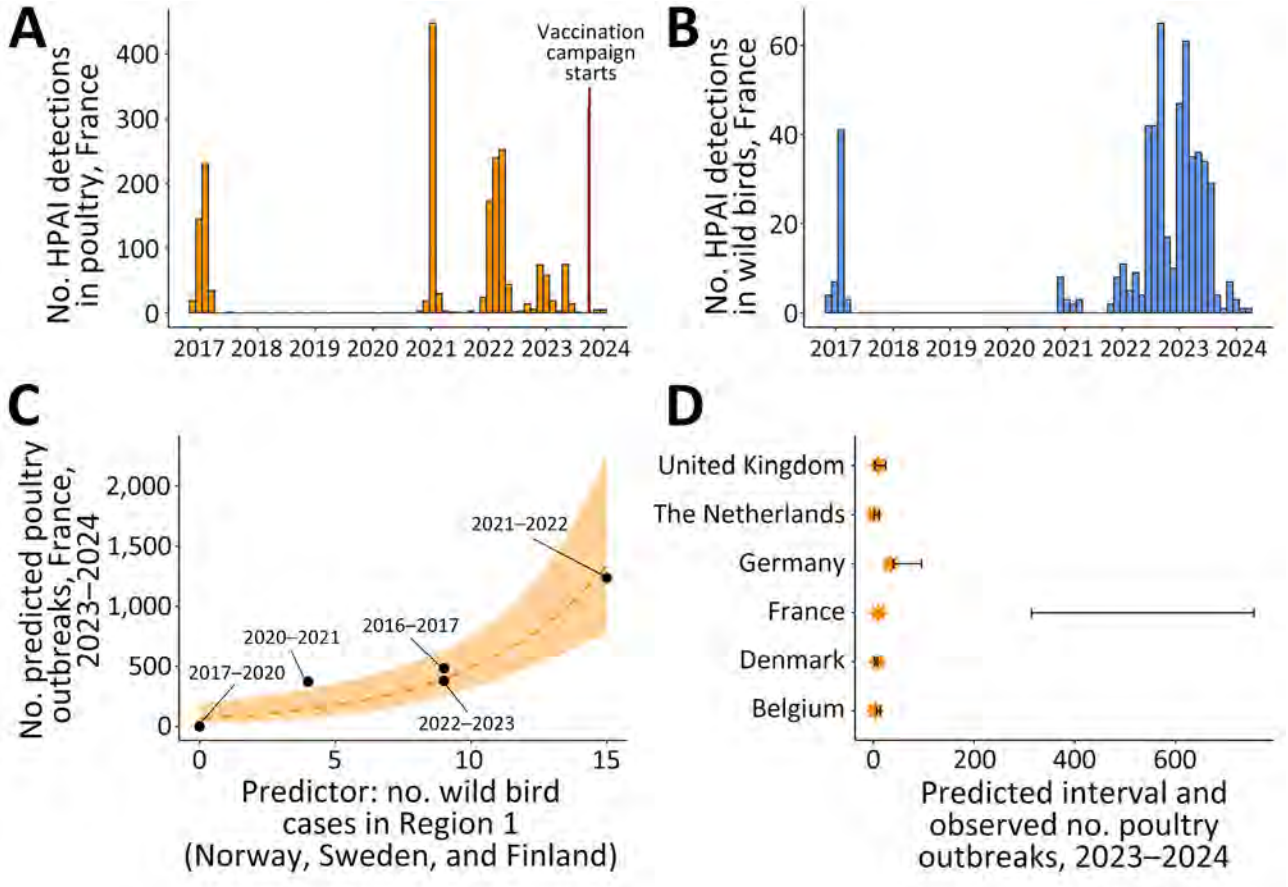

Figure. Distribution of and predicted numbers of HPAI H5 cases in study of promising effects of duck vaccination against HPAI, France, 2023–2024. A) Temporal distribution of HPAI H5 clade 2.3.4.4b poultry outbreaks in France. Red vertical line indicates start of duck vaccination campaign (October 1, 2023). B) Temporal distribution of HPAI H5 clade 2.3.4.4b wild bird cases in France. C) Predicted number of HPAI H5 poultry farm outbreaks in France as a function of the predictor variable: number of HPAI H5 wild bird cases in region 1 (Norway, Sweden, Finland). Black dots represent observed number of outbreaks in France in 2016–2023. D) Predicted and observed number of HPAI H5 poultry farm outbreaks in France and in heavily affected, nonvaccinating countries in Europe in 2023–2024. Orange stars represent observed numbers; error bars represent 95% prediction intervals. HPAI, highly pathogenic avian influenza.

outbreak numbers in France during the prevaccination period 2016–2023 ($p<0.05$, pseudo-$R^2>0.80$). We then used the 2023–2024 value of that predictor to predict the expected number of outbreaks in France, assuming no changes in mitigation strategies. To validate the method, we applied the same approach to heavily affected and nonvaccinating countries in Europe (Appendix Table 2, Figure 2).

The best predictor of the number of poultry outbreaks in France was the number of wild bird cases in region 1 a month before the first outbreak. That association does not imply direct causation but likely reflects infection pressure and spillover risk. Using this variable, the model predicted 487 (95% CI 314–756) outbreaks in France in 2023–2024 (Figure, panel C), greatly exceeding the 10 observed (96%–99% reduction). By contrast, predictions for other countries closely matched observed numbers, supporting model validity (Figure, panel D). Outbreak numbers in Germany were near the lower prediction bound, possibly reflecting improved biosecurity or changes in poultry population dynamics, which remain to be investigated.

Our findings suggest the reduction in France's outbreak numbers in 2023–2024 likely resulted from vaccination, an intervention absent in other countries in Europe. Although general declines in wild bird cases might have reduced environmental contamination (*1*), that alone cannot explain the discrepancy in France, because such a trend would be expected elsewhere in Europe (Appendix Figure 1). Moreover, the number of primary virus introductions in France in 2023–2024 (n = 4) remained within the same range as in previous waves (*8*,*9*). Although the duck population declined in 2020–2022 because of previous outbreaks, it increased in 2023 (*5*), ruling out reduced duck population as an explanation. Assuming farm biosecurity and other measures (e.g., movement restrictions and indoor confinement) remained unchanged, vaccination appears the most likely driver of the reduction. Whether duck vaccination might have indirectly protected unvaccinated poultry or other factors (e.g., changes in virus virulence) contributed remain to be investigated (*5*). Given differences in poultry sectors between countries, the vaccination strategy used in France, if applied elsewhere, might not yield similar outcomes. Further modeling of vaccination coverage is needed to better quantify its direct effects. However, the potential of vaccination to reduce HPAI incidence and protect both animal and public health warrants consideration.

This article was published as a preprint at https://www.biorxiv.org/content/10.1101/2024.08.28.609837v2.

Data used in this study are available from the Food and Agricultural Organization's global animal health database (https://empres-i.apps.fao.org).

This study was performed in the framework of the Chair for Avian Health and Biosecurity, hosted by the National Veterinary College of Toulouse and funded by the French Ministry of Agriculture and Food, General Directorate for Food.

C.G., L.F., S.L., and T.V. designed the study. L.F. provided data resources. C.G., L.F., and E.M. analyzed the data. S.L. and T.V. provided guidance around the analysis. C.G. prepared the manuscript. All authors reviewed and approved the final manuscript.

About the Author

Dr. Guinat is a research scientist at the Institut National de Recherche pour l'Agriculture, l'alimentation et l'Environnement (INRAE) in spatial and molecular epidemiology of animal infectious diseases. Her research focuses on investigating the transmission dynamics of zoonotic and animal infectious diseases to improve control.

References

1. Fusaro A, Gonzales JL, Kuiken T, Mirinavičiūtė G, Niqueux É, Ståhl K, et al.; European Food Safety Authority; European Centre for Disease Prevention and Control; European Union Reference Laboratory for Avian Influenza. Avian influenza overview December 2023–March 2024. EFSA J. 2024;22:e8754.
2. Plaza PI, Gamarra-Toledo V, Euguí JR, Lambertucci SA. Recent changes in patterns of mammal infection with highly pathogenic avian influenza A(H5N1) virus worldwide. Emerg Infect Dis. 2024;30:444–52. https://doi.org/10.3201/eid3003.231098
3. Nielsen SS, Alvarez J, Bicout DJ, Calistri P, Canali E, Drewe JA, et al.; EFSA Panel on Animal Health and Animal Welfare (AHAW), European Union Reference Laboratory for Avian Influenza. Vaccination of poultry against highly pathogenic avian influenza—part 1. Available vaccines and vaccination strategies. EFSA J. 2023;21:e08271.
4. Ministry of Agriculture and Food Sovereignty. Avian influenza: France's vaccination plan [in French] [cited 2024 Jul 1]. https://agriculture.gouv.fr/tout-ce-quil-faut-savoir-sur-le-plan-daction-vaccination-iahp-en-france
5. ANSES. Opinion on the reassessment of HPAI management measures in light of the current vaccination strategy [in French] [cited 2025 Feb 11]. https://www.anses.fr/fr/system/files/SABA2024SA0083.pdf
6. Guillemain M, Plaquin B, Caizergues A, Bacon L, De Wiele AV. Anatidae migration: general pattern, evolutions, and epidemiological consequences [in French]. Bull Epidemiological Animal Health Food. 2021;92:1–4.
7. Xu Y, Gong P, Wielstra B, Si Y. Southward autumn migration of waterfowl facilitates cross-continental

transmission of the highly pathogenic avian influenza H5N1 virus. Sci Rep. 2016;6:30262. https://doi.org/10.1038/srep30262
8. Briand F-X, Niqueux E, Schmitz A, Martenot C, Cherbonnel M, Massin P, et al. Highly pathogenic avian influenza A(H5N8) virus spread by short- and long-range transmission, France, 2016–17. Emerg Infect Dis. 2021;27:508–16. https://doi.org/10.3201/eid2702.202920
9. Briand FX, Niqueux E, Schmitz A, Martenot C, Cherbonnel M, Massin P, et al. Multiple independent introductions of highly pathogenic avian influenza H5 viruses during the 2020-2021 epizootic in France. Transbound Emerg Dis. 2022;69:4028–33. https://doi.org/10.1111/tbed.14711

Address for correspondence: Claire Guinat, UMR IHAP ENVT-INRAE, 23 chemin des capelles, 31300 Toulouse, France; email: claire.guinat@envt.fr

Increasing Predominance of Norovirus GII.17 over GII.4, United States, 2022–2025

Leslie Barclay, Jan Vinjé

Author affiliation: Centers for Disease Control and Prevention, Atlanta, Georgia, USA

DOI: https://doi.org/10.3201/eid3107.250524

Norovirus GII.17 outbreaks in the United States increased from <10% during the 2022–23 season to 75% during the 2024–25 season, surpassing the number of GII.4 outbreaks. The norovirus season also started earlier in 2024–25 than in previous seasons. Continued norovirus surveillance is needed to detect and monitor emerging strains.

Norovirus is the leading cause of acute gastroenteritis outbreaks in the United States (*1*). Genetically, noroviruses are classified into 10 genogroups (GI–GX) and further into 48 genotypes and 60 P-types (*2*). Most outbreaks are caused by genogroup GI and GII viruses. During 2011–2024, GII.4 viruses have caused >50% of US outbreaks each season (defined as September 1 of one year through August 31 of the next) (*3*).

Laboratory surveillance of norovirus in the United States is conducted through CaliciNet, a network of public health laboratories from local, state, and federal agencies (*4*). As previously reported (*5*), several countries, including the United States, observed an increase in GII.17 cases and outbreaks during the 2023–24 season. Initially, GII.17 outbreaks in the United States remained below GII.4 outbreak numbers. We present an updated analysis on the increase of GII.17 outbreaks since September 2022.

We analyzed the genotype distribution of outbreaks uploaded to CaliciNet during September 2022–April 2025. We grouped genotypes into 3 categories: GII.17, GII.4 (including GII.4 Sydney, GII.4 San Francisco, and GII.4 Wichita), and other genotypes (all other GI and GII genotypes). Complete GII.17 genome sequences for 2022–2024 have been reported previously (*5*), and strains representing the 2024–25 season are available from GenBank (accession nos. PV588655–8 and PV588796–7).

During the 2022–23 season, GII.17 accounted for 7.5% and GII.4 for 48.9% of all outbreaks (Figure 1). The next season (2023–24), the percentage of GII.17 outbreaks increased to 34.3%, whereas GII.4 outbreaks declined to 27.7% (Figure 1). By the 2024–25 season, GII.17 outbreaks had increased markedly to 75.4%, whereas GII.4 outbreaks further decreased to 10.7% (Figure 1). In addition, during 2022–23 and 2023–24, seasonality was primarily driven by GII.4 viruses, showing peak activity in February 2023 and March 2024, whereas during the 2024–25 season, norovirus peaked in January 2025 (Figure 2).

In April 2024, the percentage of GII.17 outbreaks increased to 47.4%, overtaking GII.4 outbreaks (23.7%), and from May 2024 through March 2025, GII.17 accounted for >50% of all outbreaks each month (Figure 2). During September–December of the 2024–25 season, GII.17 accounted for 46.3% of all outbreaks, compared with 13.4% in 2022–23 and 17.1% in 2023–24 during the same 4-month period. We observed no regional differences in distribution of GII.4 and GII.17 outbreaks.

Our data highlight a substantial shift in genotype distribution of norovirus outbreaks in the United States from 2022 to 2025, with GII.17 emerging as the predominant genotype. That shift coincides with a notable decline in GII.4, which has traditionally been the leading cause of US outbreaks. In 2014, several countries in Asia reported a GII.17 strain that completely replaced GII.4 Sydney (*6*). That strain was also detected in several countries in Europe and the United States (*6–8*), but in 2016, GII.4 viruses rebounded across the globe and became predominant again (*4*,*9*).

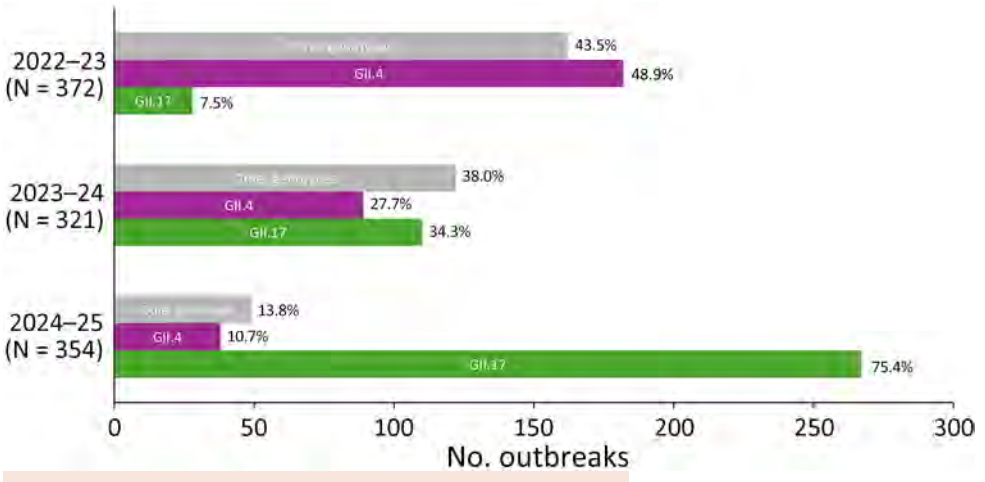

Figure 1. Increase in outbreaks of norovirus GII.17 over GII.4, United States, 2022–2025. Seasons are defined as September 1 of one year to August 31 of the next. The 2024–25 season is truncated to September 2024–April 2025. Other genotypes: GI.1, GI.2, GI.3, GI.4, GI.5, GI.6, GI.7, GII.1, GII.2, GII.3, GII.6, GII.7, GII.8, GII.10, GII.12, GII.13, GII.14, GII.21, GII.27, and GIX.1.

The likely ancestor of the current GII.17 virus is a strain that caused an outbreak in Romania in 2021 (*5*).

In the United States, the norovirus season typically starts in early December (*1*,*4*), but in 2024–25, the onset of the season was in early October 2024, an observation further supported by data from NoroSTAT (https://www.cdc.gov/norovirus/php/reporting/norostat-data.html). In 2023–24, we observed a prolonged outbreak season with cases continuing into the summer, likely the result of sustained circulation of GII.17. In contrast, the 2022–23 and 2024–25 seasons showed a more typical pattern, in which cases rapidly decline during the spring months. Cannon et al. (*4*) reported a decline after the winter peak in all 3 seasons they studied, and Wikswo et al. (*1*) reported a yearly decrease in the number of outbreaks each March over a 10-year study period. Those and other studies have also shown that GII.4 viruses are the main driver for norovirus seasonality (*1*,*4*,*7*). With the decrease of GII.4 outbreaks since 2024, it is too soon to determine whether GII.17 viruses will continue to cause an earlier onset of the norovirus season.

Our data highlight the value of CaliciNet, a national laboratory-based surveillance network that uses

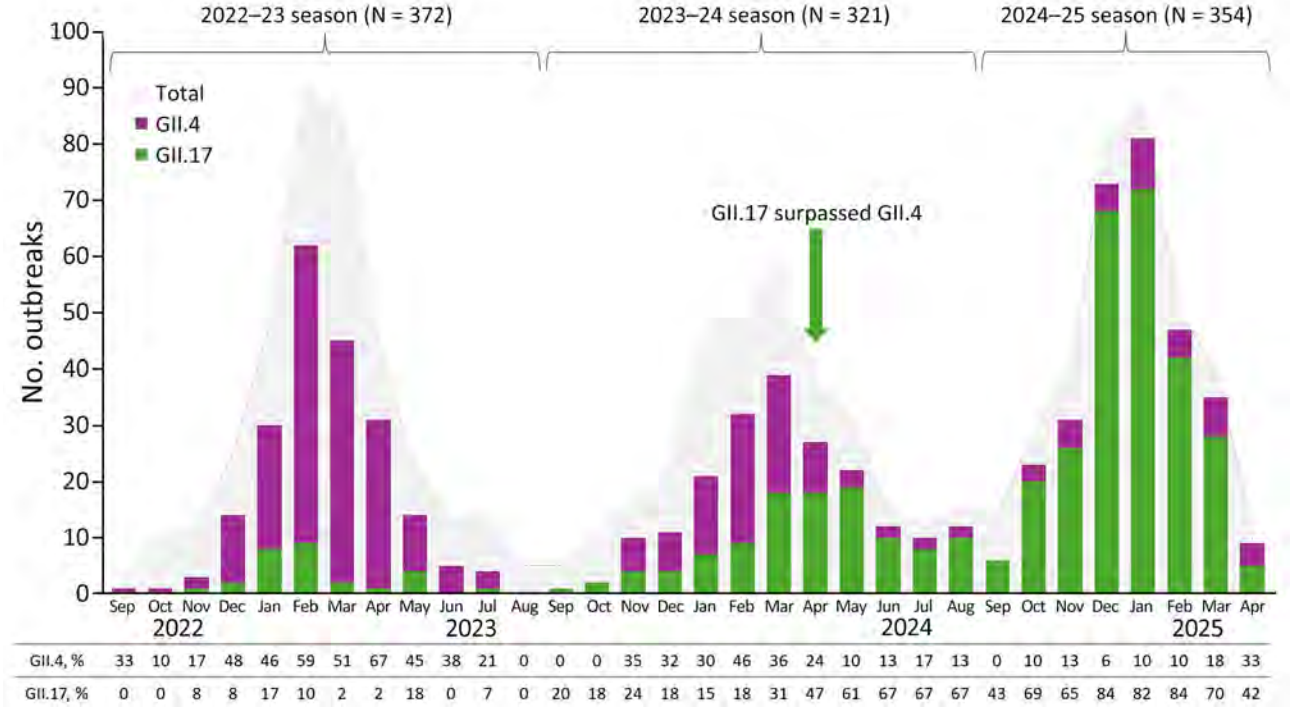

Figure 2. Numbers and percentages of norovirus GII.17 and GII.4 outbreaks compared with total number of outbreaks by month, United States, September 2022–April 2025. Seasons are defined as September 1 of one year to August 31 of the next. The 2024–25 season is truncated to September 2024–April 2025.

standardized norovirus typing methods, including whole-genome sequencing. Norovirus surveillance plays a crucial role in detecting and monitoring emerging strains, serving as an early warning system that enables rapid response to outbreak investigations and timely implementation of interventions and prevention strategies.

In conclusion, GII.17 has caused 75% of all norovirus outbreaks during the 2024–25 season so far, thereby replacing GII.4 as the predominant norovirus outbreak strain in the United States. Additional sequence analysis of complete GII.17 genomes and identification of cross-protective neutralizing antibodies of GII.17 compared with GII.4 viruses could help clarify whether GII.17 viruses will persist. Continued surveillance is needed to determine if this genotype remains the dominant genotype, as well as whether the norovirus season continues to start earlier than previous years.

Acknowledgments

We thank our CaliciNet laboratory network for their contribution in providing norovirus sequence data and Preeti Chhabra for critical reading of the manuscript and submission of the GII.17 sequences to GenBank.

About the Authors

Ms. Barclay is a microbiologist at the National Calicivirus Laboratory, Viral Gastroenteritis Branch, Division of Viral Diseases, National Center for Immunization and Respiratory Diseases, Centers for Disease Control and Prevention. Her research interest is surveillance of noroviruses and other viral gastroenteritis viruses.

Dr. Vinjé is a team lead at the National Calicivirus Laboratory, Centers for Disease Control and Prevention. His research interests include all aspects of viral gastrointestinal disease, including detection, characterization, and prevention and control of norovirus infections.

References

1. Wikswo ME, Roberts V, Marsh Z, Manikonda K, Gleason B, Kambhampati A, et al. Enteric illness outbreaks reported through the National Outbreak Reporting System—United States, 2009–2019. Clin Infect Dis. 2022;74:1906–13. https://doi.org/10.1093/cid/ciab771
2. Chhabra P, de Graaf M, Parra GI, Chan MC, Green K, Martella V, et al. Updated classification of norovirus genogroups and genotypes. J Gen Virol. 2019;100:1393–406. https://doi.org/10.1099/jgv.0.001318
3. Barclay L, Montmayeur AM, Cannon JL, Mallory ML, Reyes YI, Wall H, et al. Molecular evolution and epidemiology of norovirus GII.4 viruses in the United States. J Infect Dis. 2025 Feb 26 [Epub ahead of print]. https://doi.org/10.1093/infdis/jiaf100
4. Cannon JL, Barclay L, Collins NR, Wikswo ME, Castro CJ, Magaña LC, et al. Genetic and epidemiologic trends of norovirus outbreaks in the United States from 2013 to 2016 demonstrated emergence of novel GII.4 recombinant viruses. J Clin Microbiol. 2017;55:2208–21. https://doi.org/10.1128/JCM.00455-17
5. Chhabra P, Wong S, Niendorf S, Lederer I, Vennema H, Faber M, et al. Increased circulation of GII.17 noroviruses, six European countries and the United States, 2023 to 2024. Euro Surveill. 2024;29:2400625. https://doi.org/10.2807/1560-7917.ES.2024.29.39.2400625
6. Chan MCW, Hu Y, Chen H, Podkolzin AT, Zaytseva EV, Komano J, et al. Global spread of norovirus GII.17 Kawasaki 308, 2014–2016. Emerg Infect Dis. 2017;23:1359–1354. https://doi.org/10.3201/eid2308.161138
7. de Graaf M, van Beek J, Vennema H, Podkolzin AT, Hewitt J, Bucardo F, et al. Emergence of a novel GII.17 norovirus—end of the GII.4 era? Euro Surveill. 2015;20:21178. https://doi.org/10.2807/1560-7917.ES2015.20.26.21178
8. van Beek J, de Graaf M, Al-Hello H, Allen DJ, Ambert-Balay K, Botteldoorn N, et al.; NoroNet. Molecular surveillance of norovirus, 2005–16: an epidemiological analysis of data collected from the NoroNet network. Lancet Infect Dis. 2018;18:545–53. https://doi.org/10.1016/S1473-3099(18)30059-8
9. Zhu X, Zhang P, Yan W, Dong F, Xu D, Yuan R, et al. A new wave of resurgence for GII.4 Sydney in Huzhou, particularly GII.4 Sydney[P16], between 2019 and 2023. BMC Infect Dis. 2025;25:241. https://doi.org/10.1186/s12879-025-10648-5

Address for correspondence: Jan Vinjé, Centers for Disease Control and Prevention, 1600 Clifton Rd NE, Mailstop H18-7, Atlanta, GA 30329-4018, USA; email: ahx8@cdc.gov

Fatal Acute Hypoxemic Respiratory Failure Caused by *Burkholderia thailandensis*, China

Pei Zhang,[1] Dai Kuang,[1] Shaowen Chen, Wei Liu, Xuehan Duan, Yang Chen, Xuming Wang, Qianfeng Xia, Hua Wu

Author affiliations: Hainan General Hospital, Affiliated Hainan Hospital of Hainan Medical University, Haikou, China (P. Zhang, Y. Chen, X. Wang, H. Wu); NHC Key Laboratory of Tropical Disease Control, School of Tropical Medicine, Hainan Medical University, Haikou (D. Kuang, W. Liu, Q. Xia); Second Affiliated Hospital of Hainan Medical University, Haikou (S. Chen); Linyi Traditional Chinese Medical Hospital, Linyi, China (X. Duan)

DOI: https://doi.org/10.3201/eid3107.241920

We report on a patient in China with no underlying illnesses who died of *Burkholderia thailandensis* infection despite timely treatment. This case challenges the perception that *B. thailandensis* is nonlethal or has low virulence. Increased clinical awareness and prompt diagnosis are essential for managing *B. thailandensis* infections and preventing fatal outcomes.

Burkholderia thailandensis is commonly regarded as nonpathogenic, whereas *B. pseudomallei* is recognized as the most clinically relevant species known to cause melioidosis (*1*). We describe a rare case of fatal acute hypoxemic respiratory failure and septic shock caused by *B. thailandensis* in a previously healthy person from Hainan Province, China. The Institutional Review Board at Hainan General Hospital approved the study protocol.

A 58-year-old male rice farmer from the central region of Hainan Province was admitted to an emergency department on May 23, 2019. He exhibited an unexplained onset of cough, sputum production, chest tightness, and shortness of breath that had persisted for 8 days. He did not smoke, have a previous family history of those respiratory conditions, or have immune deficiencies. His vital signs and laboratory test results were recorded at admission (Appendix Table 1, https://wwwnc.cdc.gov/EID/article/31/7/24-1920-App1.pdf). His acute physiology and chronic health evaluation II score was 24 and sequential organ failure assessment score was 13 after 1 day of hospitalization. A chest computed tomography scan (Figure) revealed a large high-density shadow in the left lung field and a small effusion in the left pleural cavity, indicating a substantial infection in the left lung. Tigecycline was administered for infection control.

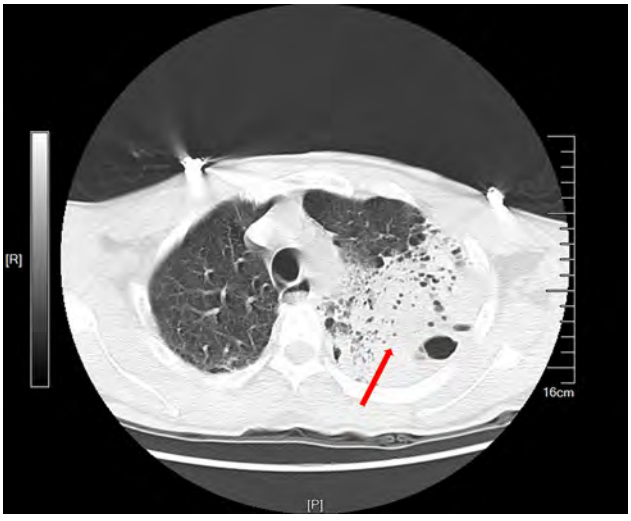

Figure. Chest computed tomography scan of patient who died of acute hypoxemic respiratory failure caused by *Burkholderia thailandensis*, China. Scan shows left lung consolidation and pleural effusion. Red arrow indicates a large high-density shadow in the left lung field. Scale indicates actual size of anatomical structures and lesions. P, posterior; R, right.

Bronchoalveolar lavage fluid was submitted for bacterial culture on May 24, 2019. After 48 hours of incubation, colonies consisted of short gram-negative bacilli (Appendix Figure 1). We performed matrix-assisted laser desorption/ionization time-of-flight mass spectrometry profiling (Appendix Figure 2), 16S rRNA-based phylogenetic tree analysis (Appendix Figure 3, panel A), and biochemical identification (Appendix Figure 4). We identified the isolate as *B. thailandensis* strain HNBT001.

Whole-genome sequencing using Illumina (https://www.illumina.com) and Pacific Biosciences (https://www.pacb.com) pipelines revealed the *B. thailandensis* strain consisted of 2 circular sequences: a 3,929,948-bp chromosome and a 2,858,975-bp chromosome (GenBank accession no. GCA_048688115.1), having an average G/C nucleotide content of 67.53%. We used values of digital DNA–DNA hybridization (dDDH) and average nucleotide identity (ANI) to compare the isolated strain with representative genomes of *Burkholderia* spp. in the National Center for Biotechnology Information RefSeq database (https://www.ncbi.nlm.nih.gov/refseq; accessed on June 6, 2024). Using the Type Genome Server (*2*), we found pairwise comparison with a *B. thailandensis* reference genome (assembly no. GCF_001718635.1) indicated the genomes of the strain in our study had a dDDH

[1]These authors contributed equally to this article.

formula d4 value of 89% and an ANI value of 98.9%; both values exceeded the thresholds for prokaryotic species delineation (70% for dDDH) (*3*) and bacterial species differentiation (96% for ANI) (Appendix Figure 5) (*4*). The HNBT001 strain was classified as sequence type 80, previously identified in both non–human-associated (E264) and human-associated (FDAARGOS 240 and 2022Dzh) strains (Appendix Figure 3, panel B).

On the basis of antimicrobial susceptibility test results (Appendix Table 2), we replaced tigecycline with imipenem for infection treatment. The patient's symptoms lessened after 2 days of imipenem therapy. However, despite a transient improvement in symptoms, his blood oxygenation gradually deteriorated while receiving invasive mechanical ventilation support, leading to multiorgan dysfunction, manifesting as scattered low-density lesions of the liver, splenomegaly, persistent thrombocytopenia, and acute renal failure characterized by substantially elevated serum creatinine levels. In addition, on day 6 of hospitalization, peripheral edema developed. After progressive clinical deterioration, the patient elected to withdraw from further treatment and was discharged after an 8-day hospital admission. During hospitalization, he was treated with imipenem for 5 days. The patient died 3 days after discharge.

B. thailandensis is generally considered nonpathogenic and is commonly found in tropical and subtropical environments, particularly in humid soil and water (*5*). In this case, the patient was a farmer who had early clinical manifestations of cough, phlegm, chest tightness, and shortness of breath and was likely exposed to *B. thailandensis* through contact with contaminated soil or water. However, unlike most reported cases, this patient had no previous underlying health conditions.

This case occurred in Hainan Province, located >1,400 km from regions where 2 other cases have been documented in China (*6*,*7*). However, medical experts with extensive experience believed insufficient evidence existed to identify *B. thailandensis* in the first case (*6*,*8*). Through 16S rRNA gene analysis (Appendix Figure 3) and taxonomic comparisons in GenBank (accession no. GCA_011578485.1), we classified the strain in this case as *B. thailandensis*. In the previous case involving wound infection (*7*), colonization by nonvirulent *B. thailandensis* could not be definitively excluded. In our case, despite the identification of multiple potential virulence genes in the HNBT001 strain (Appendix Table 3), exact pathogenic mechanisms remain to be elucidated through further research. Because of the high potential for *B. thailandensis* to be misidentified as *B. pseudomallei* (*9*), the prevalence and public health impact of *B. thailandensis* might be considerably underestimated.

In conclusion, contrary to the previously held opinion that *B. thailandensis* is nonpathogenic or of low virulence, we show it can cause severe infections even in immunocompetent patients and potentially fatal outcomes in otherwise healthy persons. We strongly advise medical personnel to place greater emphasis on strengthening biosafety precautions during both laboratory work and clinical treatment involving this underestimated pathogen.

The patient's family provided written informed consent encompassing the disclosure of clinical particulars, identifying images, and other relevant data.

This work was supported by the Hainan Province Science and Technology Special Fund (fund no. ZDYF2022SHFZ050), National Natural Science Foundation of China (grant nos. 82370018 and 82000011), National Natural Science Fund Cultivating 530 Project of Hainan General Hospital, and Hainan Clinical Research Center.

Contributions: D.K., H.W., and Q.X. conceived and designed the experiments. P.Z., S.C., X.D., X,W., and D.K. performed the experiments. D.K., W.L., and Y.C. analyzed and interpreted the data. H.W. and Q.X. provided reagents, materials, and analysis data. P.Z. and D.K. wrote the paper.

About the Author

Ms. Zhang is a research scientist in clinical microbiology at Hainan General Hospital, Haikou, China. Her research focuses on the study of pathogenic microorganisms within medical institutions to enhance knowledge of infectious diseases and their effects on public health.

References

1. Yu Y, Kim HS, Chua HH, Lin CH, Sim SH, Lin D, et al. Genomic patterns of pathogen evolution revealed by comparison of *Burkholderia pseudomallei*, the causative agent of melioidosis, to avirulent *Burkholderia thailandensis*. BMC Microbiol. 2006;6:46. https://doi.org/10.1186/1471-2180-6-46
2. Meier-Kolthoff JP, Göker M. TYGS is an automated high-throughput platform for state-of-the-art genome-based taxonomy. Nat Commun. 2019;10:2182. https://doi.org/10.1038/s41467-019-10210-3
3. Goris J, Konstantinidis KT, Klappenbach JA, Coenye T, Vandamme P, Tiedje JM. DNA-DNA hybridization values and their relationship to whole-genome sequence similarities. Int J Syst Evol Microbiol. 2007;57:81–91. https://doi.org/10.1099/ijs.0.64483-0
4. Richter M, Rosselló-Móra R. Shifting the genomic gold standard for the prokaryotic species definition. Proc Natl

Acad Sci USA. 2009;106:19126–31. https://doi.org/10.1073/pnas.0906412106
5. Hall CM, Stone NE, Martz M, Hutton SM, Santana-Propper E, Versluis L, et al. *Burkholderia thailandensis* isolated from the environment, United States. Emerg Infect Dis. 2023;29:618–21. https://doi.org/10.3201/eid2903.221245
6. Chang K, Luo J, Xu H, Li M, Zhang F, Li J, et al. Human infection with *Burkholderia thailandensis*, China, 2013. Emerg Infect Dis. 2017;23:1416–8. https://doi.org/10.3201/eid2308.170048
7. Li J, Tan J, Xiong X, Zhong Q, Lu W. *Burkholderia thailandensis* isolated from infected wound, southwest China, 2022. Emerg Infect Dis. 2024;30:1055–7. https://doi.org/10.3201/eid3005.230743
8. Dance DAB, Sarovich D, Price EP, Limmathurotsakul D, Currie BJ. Human infection with *Burkholderia thailandensis*, China, 2013. Emerg Infect Dis. 2018;24:953–4. https://doi.org/10.3201/eid2405.180238
9. Watthanaworawit W, Roberts T, Hopkins J, Gassiep I, Norton R, Robinson MT, et al. A multi-country study using MALDI-TOF mass spectrometry for rapid identification of *Burkholderia pseudomallei*. BMC Microbiol. 2021;21:213. https://doi.org/10.1186/s12866-021-02276-1

Addresses for correspondence: Hua Wu, Department of Laboratory Medicine, Hainan General Hospital, No.19, Xiuhua Road, Xiuying District, Haikou 570311, China; email: syjykwuhua@163.com; and Qianfeng Xia, NHC Key Laboratory of Tropical Disease Control, School of Tropical Medicine, Hainan Medical University, 3 Xueyuan Rd, Haikou 570102, China; email: xiaqianfeng@hainmc.edu.cn

Septic Arthritis and Osteomyelitis in Finger Caused by *Mycoplasma phocimorsus* from Brown Bear, Alaska, USA

Benjamin P. Westley, Alan Swenson, Shanna Berry-Vo, Stephanie Wettin, Daniel R. Brown

Author affiliations: Private practice, Anchorage, Alaska, USA (B.P. Westley, S. Berry-Vo); Orthopedics Physicians of Alaska, Anchorage (A. Swenson, S. Wettin); College of Veterinary Medicine, University of Florida, Gainesville, Florida, USA (D.R. Brown)

DOI: https://doi.org/10.3201/eid3107.250419

Mycoplasma phocimorsus is an identified zoonotic agent of musculoskeletal infections. Osteomyelitis developed in a patient after injury sustained while skinning a bear, and he experienced delayed diagnosis after ineffective treatments. Clinicians should use doxycycline or moxifloxacin therapy in treatment-refractory cases with exposure to seals, cats, or bears while awaiting molecular diagnostics results.

In September 2024, a 29-year-old hunter sought care 7 days after he lacerated his left fifth finger while skinning a brown bear (*Ursus arctos*) on the Alaska Peninsula near Ivanof Bay, Alaska, USA. The injury occurred when separating paw bones to free skin. His hand and knife contacted the bear's mouth before injury, but the intestinal tract was not penetrated. He reported 3 days of redness and painful swelling over the proximal interphalangeal (PIP) joint. He was placed on oral trimethoprim/sulfamethoxazole (160 mg/800 mg) and topical mupirocin (2% cream, 3×/d). On day 5 of illness, he developed fever and tachycardia and was admitted to a hospital. His temperature was 38.2°C and pulse 108 beats/min; blood pressure and respiratory rate were unremarkable. A laceration with scant drainage but substantial edema was present over the dorsal left fifth PIP joint (Figure 1). Peripheral leukocyte count was 8,300 cells/μL (reference range 4,500–11,0000 cells/μL), and C-reactive protein level was 11.6 mg/L (reference range 0.2–3.0 mg/L). Radiographs showed soft tissue swelling without bone or joint abnormality.

We administered 1 dose of ceftriaxone (2 g), followed by piperacillin/tazobactam (3 g/375 mg every 8 h) and vancomycin (1.25 g every 8 h) for 3 days. We performed surgery on day 6 of illness and noted left fifth finger PIP septic arthritis and necrotic extensor tendon disruption. Gram stains of debrided tissue revealed no organisms. We inoculated tissue on tryptic soy agar with 5% sheep blood, chocolate blood agar, and MacConkey agar plates and in chopped meat broth and prepared *Brucella* blood agar, phenylethyl alcohol blood, and *Bacteroides* bile esculin and laked *Brucella* blood agar with kanamycin and vancomycin plates. We saw no growth after 7-day incubation. Blood monitored for 5 days on a BACTEC-FX blood culture system (Becton Dickinson, https://www.bd.com) grew no organisms. Fever resolved on day 6 of illness, and on day 8 of illness, we discharged the patient with trimethoprim/sulfamethoxazole (160 mg/800 mg 2×/d for 21 d) and amoxicillin/clavulanate (875 mg/125 mg 2×/d for 21 d).

On day 46 of illness, the patient had repeat debridement of the finger because of persistent swelling and magnetic resonance imaging evidence of PIP joint osteomyelitis (Figure 2). Leukocyte count was 10,300 cells/μL, erythrocyte sedimentation rate was 5 mm/h (reference range <15 mm/h), and C-reactive protein level was 8.6 mg/L. Vancomycin and piperacillin/tazobactam treatment was repeated concurrently for 3 days. At surgery, we found substantial cartilage and bone erosive changes in the PIP joint. Gram stain of operative tissue revealed no organisms, and we detected no growth in conventional aerobic and anaerobic bacterial cultures after 7-day incubation. Fungal cultures inoculated on Sabouraud and brain-heart infusion agar showed no growth. On day 49 of illness, doxycycline (100 mg 2×/d) was started.

On day 53 of illness, tissue from surgery sent to the University of Washington Molecular Microbiology Laboratory for broad-range 16S rDNA PCR bacterial detection revealed *Mycoplasma phocimorsus* (GenBank accession no. PV641041) using methods described elsewhere (*1*). The amplified 315-nt sequence was 100% identical with the 16S rRNA gene sequence of *M. phocimorsus* type strain M5725.

In December 2024, the patient completed 42 days of doxycycline according to standard treatment guidelines for osteomyelitis. Although pain and swelling improved, decreased range of motion persisted at the end of therapy. One month later, he had no signs or symptoms of relapsing infection.

Seal finger was described in 1907 as a painful swollen finger that developed after an injury when butchering seals (*2*). In 2014, several authors treated a ringed seal (*Pusa hispida*) hunter in Alaska for seal finger and hip septic arthritis caused by a *Mycoplasma* species detected by 16s rRNA sequencing, but they could not propogate the organism in culture (*3*). Nine years later, researchers isolated 6 independent strains of a *Mycoplasma* species from patients from Scandinavia after contact with seals and proposed the name *M. phocimorsus* (*4*). Strains were susceptible to doxycycline and moxifloxacin and showed >99.5% rRNA similarity with the sequence identified in the seal hunter from Alaska, confirming *M. phocimorsus* is present in Alaska. Subsequently, *M. phocimorsus* was identified as the cause of tenosynovitis after a cat scratch (*5*). Our patient had no exposure to seals and minimal exposure to a dog and cat owned by his mother.

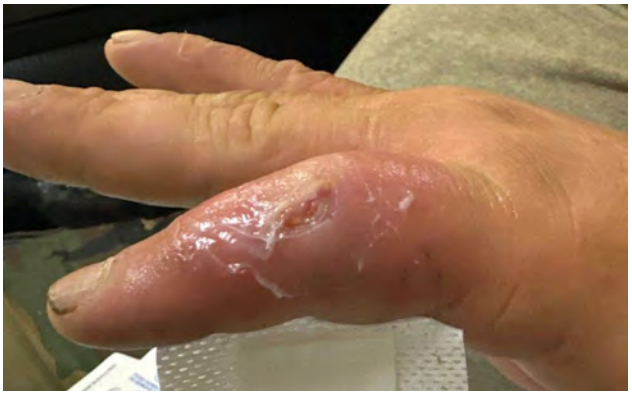

Figure 1. Finger laceration in case of septic arthritis and osteomyelitis in finger caused by *Mycoplasma phocimorsus* from brown bear (*Ursus arctos*), Alaska, 2024. Left fifth finger laceration occurred while skinning a brown bear. Laceration is shown overlying the proximal interphalyngeal joint with surrounding edema.

Harbor seals (*Phoca vitulina*), sea otters (*Enhydra lutris*), and Steller sea lions (*Eumetopias jubatus*) are encountered in that region of Alaska (D.D.W. Hauser, University of Alaska, pers. comm., email, 2024 Mar 14). Brown bears are voracious hunters and scavengers, so this case may reflect transient colonization after predation of an infected seal or other animal. However, *Mycoplasma* species occur

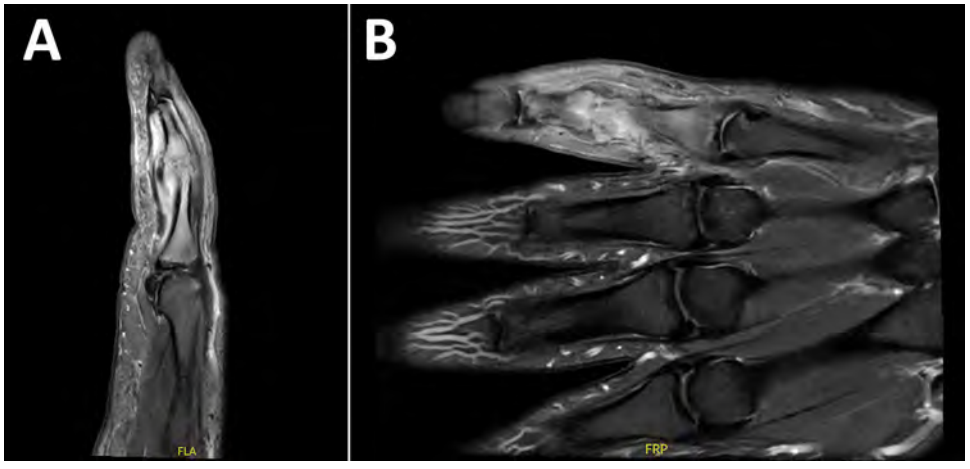

Figure 2. Magnetic resonance imaging in case of septic arthritis and osteomyelitis in finger caused by *Mycoplasma phocimorsus* from brown bear (*Ursus arctos*), Alaska, 2024. Left fifth finger sagittal (A) and coronal (B) images demonstrate edema of the proximal and middle phalanges on short tau inversion recovery sequences, suggestive of osteomyelitis.

in brown bear gut microbiomes (*6*), suggesting that brown bears may be frequent reservoirs of *M. phocimorsus*. As in previous cases, this patient experienced delayed diagnosis and ineffective treatments because of *Mycoplasma* species' resistance to most antibiotic drugs and inability to be grown in conventional cultures. Clinicians should remain alert to the possibility of *M. phocimorsus* infection after exposure to seals, cats, or bears and initiate doxycycline or moxifloxacin therapy while awaiting confirmatory molecular testing, particularly in treatment-refractory infections.

Acknowledgments

We thank our patient for his replies to our repeated queries regarding specifics of his hunt and his injuries and for his verbal and written permission to publish this report. We also thank the University of Washington Molecular Microbiology Laboratory for providing testing services and the *Mycoplasma phocimorsus* sequence.

About the Author

Dr. Westley is an infectious diseases clinician in Anchorage, Alaska. His research interests include zoonotic diseases, tuberculosis, and HIV.

References

1. Lee SA, Plett SK, Luetkemeyer AF, Borgo GM, Ohliger MA, Conrad MB, et al. *Bartonella quintana* aortitis in a man with AIDS, diagnosed by needle biopsy and 16S rRNA gene amplification. J Clin Microbiol. 2015;53:2773–6. https://doi.org/10.1128/JCM.02888-14
2. Bidenknap JH. Seal finger [in Dutch]. Norsh Mag Legevidenskaben. 1907;68:515–23.
3. Westley BP, Horazdovsky RD, Michaels DL, Brown DR. Identification of a novel *Mycoplasma* species in a patient with septic arthritis of the hip and seal finger. Clin Infect Dis. 2016;62:491–3. https://doi.org/10.1093/cid/civ875
4. Skafte-Holm A, Pedersen TR, Frølund M, Stegger M, Qvortrup K, Michaels DL, et al. *Mycoplasma phocimorsus* sp. nov., isolated from Scandinavian patients with seal finger or septic arthritis after contact with seals. Int J Syst Evol Microbiol. 2023;73:006163. https://doi.org/10.1099/ijsem.0.006163
5. Skafte-Holm A, Pedersen TR, Frølund M, Stegger M, Hallstrøm S, Rasmussen A, et al. Mycoplasma phocimorsus in woman with tendinous panaritium after cat scratch, Denmark. Emerg Infect Dis. 2025;31:380–2. https://doi.org/10.3201/eid3102.241219.
6. Trujillo SM, McKenney EA, Hilderbrand GV, Mangipane LS, Rogers MC, Joly K, et al. Correlating gut microbial membership to brown bear health metrics. Sci Rep. 2022;12:15415. https://doi.org/10.1038/s41598-022-19527-4

Address for correspondence: Benjamin P. Westley, 3500 LaTouche St, Ste 200, Anchorage, AK 99508, USA; email: westley.ben@gmail.com

Next-Generation Sequencing Techniques to Diagnose Culture-Negative Subacute Native Aortic Endocarditis

Delphine Vetterli,[1] Morgana Zennaro,[1] Virginie Tacchini, Joannes Alexander Lobrinus, Virginie Prendki, Vladimir Lazarevic, Jacques Schrenzel

Author affiliations: Geneva University Hospitals Department of Medicine, Geneva, Switzerland (D. Vetterli, M. Zennaro); Geneva University Hospitals Division of Cardiology, Geneva (V. Tacchini); Geneva University Hospitals Department of Pathology, Geneva (J.A. Lobrinus); Geneva University Hospitals Department of Rehabilitation and Geriatrics, Geneva (V. Prendki); Genomic Research Laboratory, Faculty of Medicine, Geneva University, Geneva (V. Lazarevic, J. Schrenzel); Geneva University Hospitals Division of Infectious Diseases, Geneva (V. Prendki, J. Schrenzel); Geneva University Hospitals Bacteriology Laboratory, Geneva (J. Schrenzel)

DOI: https://doi.org/10.3201/eid3107.241739

Next-generation sequencing might improve diagnosis of infective endocarditis. A case in Switzerland was initially attributed to *Solobacterium moorei* bacteria. Metagenomic analysis of the affected heart valve detected *Streptococcus gordonii*, but not *S. moorei*, illustrating that the results of molecular detection can vary depending on sampling time and anatomic site.

Plasma microbial cell-free DNA (mcfDNA) refers to extracellular microbial DNA in plasma, which has a half-life of a few minutes (*1*). Next-generation sequencing using mcfDNA is emerging as a diagnostic tool in infections with negative cultures, including endocarditis. Persistence of mcfDNA is associated with metastatic infection (*2*). We used next-generation mcfDNA sequencing to identify the causative agent in a fatal case of infective endocarditis.

An 89-year-old man with aortic stenosis and preserved heart function sought care for weakness in Geneva, Switzerland. He had recently sought care at University Hospital of the Canary Islands (Tenerife, Spain) after a fall; elevated troponin (2,172 ng/L) and procalcitonin (157 mg/L) were observed. He received empiric meropenem and linezolid before he returned to Switzerland against medical advice. In Geneva, he had no fever or peripheral signs of endocarditis. Investigations revealed mild inflammation (C-reactive

[1]These authors are co–first authors.

protein 17 mg/L), acute kidney injury (creatinine 387 μmol/L), stroke, and carotid stenosis. Transesophageal echocardiography showed an aortic valve perforation and a 4 mm para-aortic abscess at the root of the aorta, without suspected vegetation (Figure 1). Blood cultures remained negative after 5 days. We started conservative treatment with ceftriaxone (2 g every 12 h intravenously) and vancomycin (15 mg/kg every 12 h intravenously). mcfDNA next-generation sequencing (Noscendo, https://noscendo.com) identified *Solobacterium moorei* (13 reads). We adjusted the patient's treatment to ceftriaxone (2 g every 12 h intravenously) and metronidazole (500 mg every 6 h intravenously) for 6 weeks.

Despite initial improvement, the patient experienced heart failure and a second-degree AV block. His condition declined 12 weeks later, and he died. At autopsy, the heart showed a heavily calcified, perforated noncoronary leaflet of the aortic valve with a 15 × 10-mm blood-filled neocavity beneath it, extending to the valvular ring (Figure 2). Although we did not detect pus, our findings strongly suggested infective endocarditis because degenerative processes do not typically cause valve perforation or cavity formation. Those conditions are consistent with infective endocarditis (IE). A second mcfDNA test detected no bacteria.

We performed metagenomic next-generation sequencing (mNGS) of the valve tissue as previously described (*3*). We identified 1.28 million human reads and 36,629 reads from the spiked (8.5×10^4) control organism *Bacillus spizizenii*, along with 4,654 reads from *Streptococcus gordonii*, 146 reads from *S. sanguinis*, and 11 reads from *Cutibacterium acnes* (European Nucleotide Archive accession no. PRJEB81450). We used MetaPhlAn2 (https://huttenhower.sph.harvard.edu/metaphlan2) to confirm *S. gordonii*, which suggested it was the dominant pathogen in tissue (*4*). Reads identified as *S. sanguinis* were likely *S. gordonii* as well because of their high genomic similarity. We detected no *Solobacterium moorei* in the tissue. *S. moorei* is a gram-positive anaerobic rod from oral and intestinal microbiota. Although rarely detected, it has been implicated in human infections, especially in immunocompromised patients (*5*–*7*). Its identification is difficult because of its slow growth. It is generally susceptible to antimicrobial drugs for anaerobic infections, although resistance to rifampin and moxifloxacin has been reported (*8*).

This case demonstrates the utility of mcfDNA and metagenomic sequencing in culture-negative endocarditis. After negative routine work-up, we performed mcfDNA because the conservative management prevented valve resection. Although *S. moorei* was detected in plasma initially, a follow-up mcfDNA test 6 weeks after antimicrobial treatment was negative. That result likely indicates bacterial clearance, because it slightly exceeds the median 38-day positivity duration observed in infective endocarditis (*9*). *S. gordonii* was the only pathogen identified in valve tissue. The discrepancy between cfDNA and mNGS may reflect differing bacterial loads, sampling timing, or antimicrobial impact (*10*).

Our findings suggest an endocarditis caused by both *S. gordonii* and *S. moorei* organisms in which *S. moorei* mcfDNA predominated during the initial

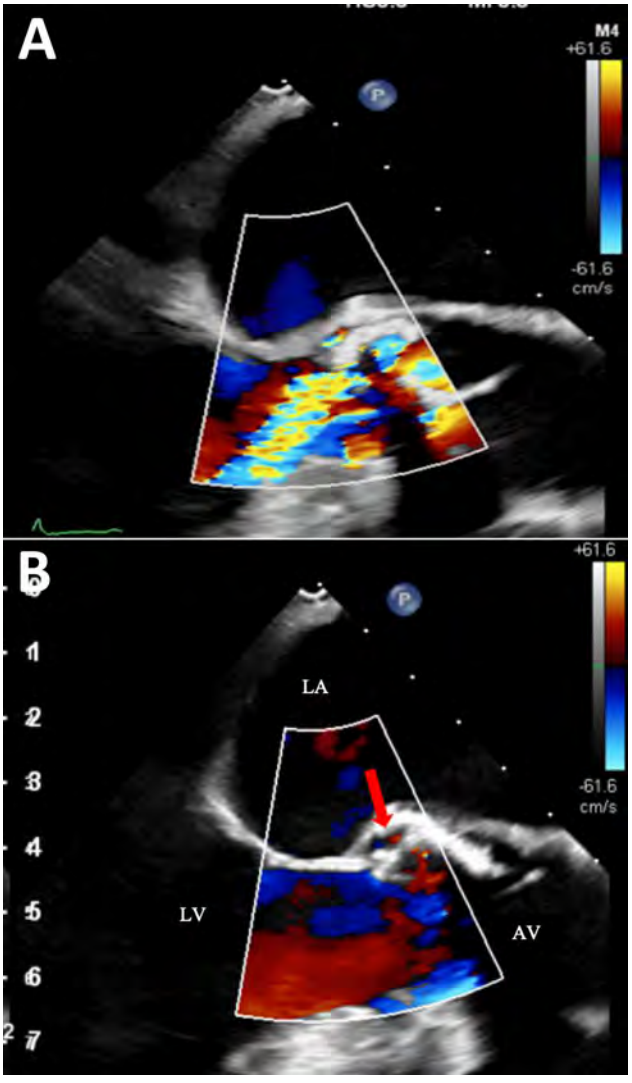

Figure 1. Color doppler echocardiography images from fatal case of subacute native aortic endocarditis, Geneva, Switzerland. A) Mid-esophageal long-axis view during diastole, showing moderate to severe aortic regurgitation. B) Mid-esophageal long-axis view with left ventricular chamber, aortic valve, and aortic root during systole. Red arrow indicates systolic flow with the pseudoaneurysm. AV, open aortic valve; LA, left atrial; LV, left ventricle.

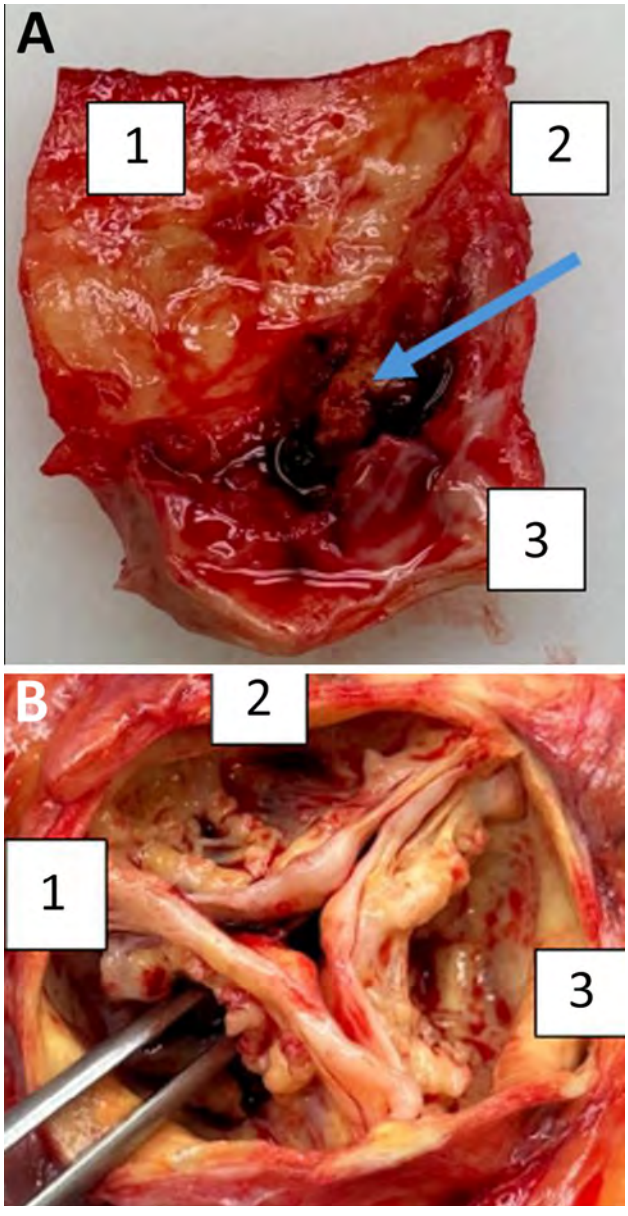

Figure 2. Autopsy results from fatal case of subacute native aortic endocarditis, Geneva, Switzerland. A) Autopsy material of the ascendant aorta (1) with the open blood-filled neocavity of 15 × 10 mm (blue arrow) just beneath the perforated noncoronary leaflet of the AV (2) and extending to the valvular ring (3). B) Autopsy material of the open aortic valve with perforated noncoronary leaflet (1), left coronary leaflet (2), and right coronary leaflet (3).

sampling but its culture likely failed because of antimicrobial exposure. In contrast, *S. gordonii* DNA seemed to persist longer in the valve tissue, suggesting greater stability in that environment. The absence of *S. moorei* in the valve tissue raises questions about its pathogenic role; its presence in mcfDNA could represent a transient bacteremia, another unrelated site of infection, or a contamination, but its relative abundance may have masked initial detection of *S. gordonii* bacteria. *S. gordonii* is a known endocarditis pathogen causing destructive IE, and its pathogenic role is therefore highly probable.

In case of a high suspicion of IE and when surgery is not feasible, we advise collecting additional blood or plasma samples at least 2 times within the first 24–48 hours. If blood cultures yield negative results, stored samples can undergo mcfDNA analysis. Testing multiple samples improves diagnostic reliability by minimizing the risk for unrelated transient bacteremia or contamination. If valve removal occurs, mNGS should be done as a final test for pathogen identification.

In summary, we report a case of destructive native aortic valve endocarditis without fever or marked inflammation. mcfDNA and mNGS were essential to identify the pathogen. Molecular diagnostics are valuable in culture-negative infections, particularly when conventional methods and tissue sampling are limited.

About the Author

Dr. Vetterli is a chief resident in the primary care medicine department at the University Hospitals of Geneva. She has a special interest in mentorship and teaching. Dr. Zennaro is a resident physician in the internal medicine department at the University Hospitals of Geneva.

References

1. Grumaz S, Stevens P, Grumaz C, Decker SO, Weigand MA, Hofer S, et al. Next-generation sequencing diagnostics of bacteremia in septic patients. Genome Med. 2016;8:73. https://doi.org/10.1186/s13073-016-0326-8
2. Eichenberger EM, de Vries CR, Ruffin F, Sharma-Kuinkel B, Park L, Hong D, et al. Microbial cell-free DNA identifies etiology of bloodstream infections, persists longer than conventional blood cultures, and its duration of detection is associated with metastatic infection in patients with *Staphylococcus aureus* and gram-negative bacteremia. Clin Infect Dis. 2022;74:2020–7. https://doi.org/10.1093/cid/ciab742
3. Ramakrishnan G, Kronig I, Gaïa N, Lazarevic V, Schrenzel J. *Mycoplasma genitalium* endocarditis in prosthetic aortic valve. Emerg Infect Dis. 2023;29:2164–6. https://doi.org/10.3201/eid2910.221639
4. Manghi P, Blanco-Míguez A, Manara S, NabiNejad A, Cumbo F, Beghini F, et al. MetaPhlAn 4 profiling of unknown species-level genome bins improves the characterization of diet-associated microbiome changes in mice. Cell Rep. 2023;42:112464. https://doi.org/10.1016/j.celrep.2023.112464
5. Liu WJ, Xiao M, Yi J, Li Y, Kudinha T, Xu YC. First case report of bacteremia caused by *Solobacterium moorei* in China, and literature review. BMC Infect Dis. 2019;19:730. https://doi.org/10.1186/s12879-019-4359-7
6. Alauzet C, Aujoulat F, Lozniewski A, Ben Brahim S, Domenjod C, Enault C, et al. A new look at the genus *Solobacterium*: a retrospective analysis of twenty-seven cases

of infection involving *S. moorei* and a review of sequence databases and the literature. Microorganisms. 2021;9:1229. https://doi.org/10.3390/microorganisms9061229
7. Detry G, Pierard D, Vandoorslaer K, Wauters G, Avesani V, Glupczynski Y. Septicemia due to *Solobacterium moorei* in a patient with multiple myeloma. Anaerobe. 2006;12:160–2. https://doi.org/10.1016/j.anaerobe.2006.04.002
8. Pedersen RM, Holt HM, Justesen US. *Solobacterium moorei* bacteremia: identification, antimicrobial susceptibility, and clinical characteristics. J Clin Microbiol. 2011;49:2766–8. https://doi.org/10.1128/JCM.02525-10
9. Lazarevic V, Gaïa N, Pham TT, de Lorenzi-Tognon M, Girard M, Mauffrey F, et al. Identification of causative agents of infective endocarditis by metagenomic next-generation sequencing of resected valves. Front Cell Infect Microbiol. 2025;15:1532257. https://doi.org/10.3389/fcimb.2025.1532257
10. Eichenberger EM, Degner N, Scott ER, Ruffin F, Franzone J, Sharma-Kuinkel B, et al. Microbial cell-free DNA identifies the causative pathogen in infective endocarditis and remains detectable longer than conventional blood culture in patients with prior antibiotic therapy. Clin Infect Dis. 2023;76:e1492–500. https://doi.org/10.1093/cid/ciac426

Address for correspondence: Jacques Schrenzel, Division of Infectious Diseases, Department of Medicine, Geneva University Hospitals and University of Geneva, Geneva, Switzerland; email: jacques.schrenzel@hug.ch

Syphilis as Rare Cause of Pyogenic Liver Abscess

Danielle Meyer, Michele Granada

Author affiliation: Abbott Northwestern Hospital, Minneapolis, Minnesota, USA

DOI: http://doi.org/10.3201/eid3107.250744

Syphilis has a wide range of possible symptoms, making it difficult to diagnose. We report a rare case of liver abscess secondary to *Treponema pallidum* in a man in Minnesota, USA, who had well-controlled HIV infection. This case emphasizes the importance of appropriate screening for syphilis, especially in high-risk populations.

Syphilis is a sexually transmitted infection caused by the spirochete bacterium *Treponema pallidum*. Its diverse manifestations can make syphilis difficult to diagnose. The disease progresses through 4 main stages. The early phase begins with a localized skin lesion at the site of inoculation. If left untreated, hematogenous dissemination can lead to secondary syphilis, characterized by a diffuse maculopapular rash and systemic symptoms. Tertiary syphilis represents a later stage that can affect multiple organ systems. Involvement of the liver is uncommon and can result in syphilitic hepatitis or hepatic gummas, granulomatous soft tissue lesions with central necrosis. We report an exceptionally rare case of syphilitic liver abscess confirmed with 16s rDNA PCR.

A 52-year-old man in Minnesota, USA, with a history of well-controlled HIV infection (CD4 count 767) on a regimen of dolutegravir/rilpivirine sought treatment for symptoms including 3 months of diarrhea and bilateral ankle edema. Two weeks before his initial visit and at the request of his healthcare provider, the man provided blood samples for laboratory assessment, which revealed elevated levels of alkaline phosphatase (ALP [557 IU/L; reference range 35–144 IU/L]), aspartate transaminase (AST [67 IU/L; reference range 10–35 IU/L]), and alanine aminotransferase (ALT [160 IU/L; reference range 9–46 IU/L]). Repeat laboratory results 1 week later showed persistently elevated ALP (484 IU/L), AST (58 IU/L), and ALT (88 IU/L). An abdomen ultrasound demonstrated hepatic steatosis.

Physical examination was notable for edema in bilateral lower extremities. Blood analysis revealed further elevation of ALP (586 IU/L), AST (68 IU/L), and ALT (102 IU/L). Abdomen and pelvis computed tomography with contrast (Figure, panel A) identified a 3.8 × 2.3 × 3.3-cm peripheral mass in the right lobe of the liver, and he was subsequently admitted to the hospital for further evaluation.

Viral hepatitis serology test results were negative. A stool multiplex PCR test was positive for *Shigella*. Abdominal magnetic resonance imaging (Figure, panel B) confirmed a 2.4-cm rim-enhancing lesion in the lateral aspect of segments 5 and 6 of the liver. Ultrasound-guided aspiration of the liver lesion yielded 1 mL of yellow, purulent fluid and provided 4 core biopsy samples. The patient elected to leave the hospital early and was discharged home with a 4-week course of oral ciprofloxacin (500 mg 2×/d) and metronidazole (500 mg 2×/d) for empiric coverage of possible hepatic abscess as well as coverage for shigellosis.

One week later, liver abscess cultures were negative. Pathology revealed a benign abscess, background intact liver parenchyma, and negative results for neoplasia. We requested 16s rDNA and 28s rDNA

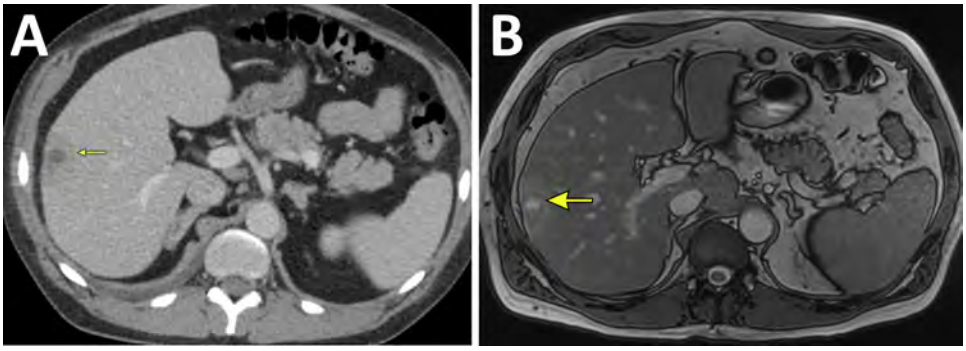

Figure. Imaging findings from a study of syphilis as a rare cause of pyogenic liver abscess in an HIV-positive man in Minnesota, USA. Computed tomography (A) and magnetic resonance imaging (B) of the abdomen and pelvis show rim-enhancing lesion (yellow arrows) in segments 5 and 6 of the liver.

PCR tests on liver tissue. The man visited his healthcare provider for routine follow-up. Screening for *T. pallidum* antibody demonstrated reactivity, and rapid plasma reagin (RPR) testing revealed elevated results (1:32). Previous RPR titers were negative. The man received 1 doseof intramuscular benzathine penicillin (2.4 million units). The following day, 16s rDNA PCR testing of a liver tissue sample was positive for *T. pallidum*. The man subsequently completed 2 additional weekly doses of benzathine penicillin. One week after completing treatment, his RPR test result was 1:64, and tests measuring his hepatic function and C-reactive protein were within reference ranges. Computed tomography of his abdomen and pelvis showed a reduction in the hepatic lesion to 1.1 × 0.9 cm, a marked improvement in size and appearance and consistent with healing.

Syphilis resulting in abscess is rare. Few cases have been reported, including abscess associated with the pituitary gland (*1*), lungs (*2*), scrotum (*3*,*4*), and lymph nodes (*5*). Three cases (*6*,*7*) in the 1920s described what were thought to be liver abscesses caused by syphilis. Researchers presumed their findings based on symptoms and examination findings suggestive of liver abscess in the setting of positive serologic results and symptomatic improvement with treatment. However, the suspected abscesses were neither drained nor confirmed with further testing.

In this patient, the clinical picture was complicated by shigellosis, which was the likely etiology of his diarrhea. He did not have additional symptoms suggestive of hepatic abscess. He did have persistently elevated liver enzymes, particularly ALP. Liver function tests are abnormal in up to 39% of patients diagnosed with early syphilis, most of whom are asymptomatic (*8*). Furthermore, an increase in RPR titers immediately after treatment is not uncommon in early stages of treatment and is not indicative of treatment failure. This patient had a marked decrease in abscess size and resolution of transaminitis. Our question initially was if this was syphilitic gumma of tertiary syphilis, but given the absence of granulomatous inflammation on pathology, this man's case more likely demonstrated secondary syphilis with syphilitic hepatitis.

In its early stage, syphilitic hepatitis can be asymptomatic with a disproportionally elevated ALP in the setting of secondary syphilis, resulting in rare occurrences of abscesses in the liver. It can also cause hepatic inflammatory masses in HIV-positive men who have sex with men (*9*). This case demonstrates a rare and diagnostically complex clinical manifestation of secondary syphilis, emphasizing the importance of appropriate screening for syphilis, especially in high-risk populations whose laboratory and imaging assessments reveal elevated liver enzymes and hepatic mass lesions.

Acknowledgments

We thank William C. McDonald for his work relevant to this case.

About the Author

Dr. Meyer is a resident physician in internal medicine at Abbott Northwestern Hospital, Minneapolis, Minnesota, whose areas of interest are infection prevention and control, as well as antimicrobial stewardship.

Dr. Granada is an infectious disease physician at Abbott Northwestern Hospital and Vice Chairman of the Allina Health Antimicrobial Stewardship Program Committee. Her areas of interest are infections in the immunocompromised host, infective endocarditis, staphylococcus aureus bacteremia, cardiac device infections, HIV/AIDS, sexually transmitted illnesses, and antimicrobial stewardship.

References

1. Colantonio MA, Shepherd K, Shannon B. Syphilis and HIV co-infection presenting with a pituitary abscess: a rare case presentation. Radiol Case Rep. 2025;20:3526–30. https://doi.org/10.1016/j.radcr.2025.04.026
2. Futami S, Takimoto T, Nakagami F, Satoh S, Hamaguchi M, Kuroyama M, et al. A lung abscess caused by secondary

syphilis—the utility of polymerase chain reaction techniques in transbronchial biopsy: a case report. BMC Infect Dis. 2019;19:598. https://doi.org/10.1186/s12879-019-4236-4
3. Agrawal V, Ranjan R. Scrotal abscess consequent on syphilitic epididymo-orchitis. Trop Doct. 2019;49:45–7. https://doi.org/10.1177/0049475518809240
4. White CG, Challacombe BJ, Dasgupta P. Syphilitic scrotal abscess: the great mimic returns. Int J Clin Pract Suppl. 2005;59:62–3. https://doi.org/10.1111/j.1742-1241.2005.00310.x
5. Duffield AS, Borowitz MJ. Syphilitic lymphadenitis with abscess formation involving cervical lymph nodes. Blood. 2018;131:707. https://doi.org/10.1182/blood-2017-11-817247
6. Mehta VN. A case of syphilis of the liver suggesting liver abscess. Ind Med Gaz. 1926;61:230.
7. Hunter WK. Two cases of syphilis of the liver with symptoms of abscess formation. Glasgow Med J. 1922;98:225–31.
8. Adachi E, Koibuchi T, Okame M, Sato H, Kikuchi T, Fujii T, et al. Liver dysfunction in patients with early syphilis: a retrospective study. J Infect Chemother. 2013;19:180–2. https://doi.org/10.1007/s10156-012-0440-5
9. Hagen CE, Kamionek M, McKinsey DS, Misdraji J. Syphilis presenting as inflammatory tumors of the liver in HIV-positive homosexual men. Am J Surg Pathol. 2014;38:1636–43. https://doi.org/10.1097/PAS.0000000000000264

Address for correspondence: Michele Granada, Allina Health Infectious Diseases–Abbott Northwestern Hospital, Infectious Diseases–ANGMA, 2800 Chicago Ave S, Ste 250, Minneapolis, MN 55407, USA; email: mdgranada@me.com

Genomic Characterization of *Leishmania tropica* in Cutaneous Leishmaniasis, Somali Region, Ethiopia, 2023

Adugna Abera,[1] Pieter Monsieurs,[1] Myrthe Pareyn, Dereje Beyene, Geremew Tasew, Allison Aroni-Soto, Mahlet Belachew, Desalegn Geleta, Bethlehem Adnew, Bokretsion Gidey, Henok Tadesse, Atsbeha Gebreegziabxier, Rajiha Abubeker, Abraham Ali, Ketema Tafess, Tobias F. Rinke de Wit, Johan van Griensven, Jean-Claude Dujardin, Dawit Wolday,[2] Malgorzata Anna Domagalska[2]

DOI: https://doi.org/10.3201/eid3107.241607

Author affiliations: College of Natural and Computational Sciences, Addis Ababa University, Addis Ababa, Ethiopia (A. Abera, D. Beyene); Ethiopian Public Health Institute, Addis Ababa (A. Abera, G. Tasew, M. Belachew, D. Geleta, B. Gidey, H. Tadesse, A. Gebreegziabxier, R. Abubeker, A. Ali, D. Wolday); Institute of Tropical Medicine, Antwerp, Belgium (P. Monsieurs, M. Pareyn, A. Aroni-Soto, J. van Griensven, J.-C. Dujardin, M.A. Domagalska); Armauer Hansen Research Institute, Addis Ababa (B. Adnew); Adama Science and Technology University, Adama, Ethiopia (K. Tafess); Amsterdam Institute for Global Health and Development, Amsterdam University Medical Centre, University of Amsterdam, Amsterdam, the Netherlands (T.F.R. de Wit); Michael G. DeGroote Institute for Infectious Disease Research, Hamilton, Ontario, Canada (D. Wolday); McMaster Immunology Research Center, Health Sciences, McMaster University, Hamilton (D. Wolday)

We sequenced *Leishmania tropica* genomes from 8 human skin samples collected in a newly emerging focus of cutaneous leishmaniasis in the Somali region of Ethiopia. We found a variant with unique genomic signatures of drug resistance. Public health officials should use genomic surveillance to slow expansion of *L. tropica*.

Since the successful Kala-Azar elimination program in the Indian subcontinent, the hotspot of worldwide leishmaniasis has moved to East Africa (*1*). Among the different affected countries, Ethiopia deserves particular attention, given the heterogeneous eco-epidemiology of leishmaniasis, its clinical polymorphism, and the complex taxonomy of *Leishmania tropica* parasites. The disease is endemic in different biotopes from lowlands to highlands, and transmission involves different hosts and vectors (*2*). The 4 major clinical forms of leishmaniasis are visceral leishmaniasis (VL), causing 2,500–4,000 reported cases, and 3 forms of cutaneous leishmaniasis (CL), localized, diffuse, and muco-cutaneous, causing ≈50,000 reported cases. *L. donovani* (VL and occasionally CL) and *L. aethiopica* (all 3 CL forms) are the most reported species, and *L. tropica* (CL) was isolated once from a human patient (*2*); several interspecies hybrids have been observed (*3*).

The epidemiology of the disease is affected by human migration and displacement because of famine and regular conflicts in the country and by environmental changes. We previously highlighted the need for genomic surveillance of leishmaniasis by using highly sensitive, resolutive, and untargeted whole-genome sequencing (WGS) methods (*4*) for the following reasons: since the discovery of

[1]These authors contributed equally to this article.

[2]These senior authors contributed equally to this article.

hybridization and genetic introgression (*5*), robust species identification should theoretically be on the basis of multigenic approaches covering several regions of the genome (and not only single gene approaches); WGS is needed to assess the genetic similarity among parasites sampled from different patients, thereby confirming the outbreak nature of a focus; and WGS can be used to find signatures of drug resistance and guide patient management.

In August 2023, an outbreak of CL was detected among immunologically naive militia recently deployed in the eastern Somali region of Ethiopia. That area did not have a previous history of CL, but sporadic cases of VL were reported. The clinical manifestations of the CL cases (multiple wet lesions) was not comparable to what is typically observed in Ethiopia and neighboring countries (single dry lesions). Hsp70 amplicon sequencing identified the CL pathogen as *L. tropica* (A. Abera et al., unpub. data, https://www.medrxiv.org/content/10.1101/2024.10.05.24314933v1).

We undertook a more in-depth molecular characterization of *L. tropica* samples collected in the focus in the Somali region (Figure 1). We used direct genome sequencing of *Leishmania* in host tissues (SureSelect sequencing;AgilentTechnologies,https://www.agilent.com) that did not require parasite isolation and cultivation (*6*). That method was previously validated for *L. donovani* in bone marrow (*6*) and blood samples (*7*), and we used it for the first time for skin samples from CL patients.

We submitted 8 of the CL samples from the Somali region for SureSelect sequencing by using a capture panel of probes designed for the *L. aethiopica* genome. SureSelect sequencing should work well with phylogenetically related species such as *L. tropica*. We used competitive mapping (Appendix Figure 1, https://wwwnc.cdc.gov/EID/article/31/7/24-1607-App1.pdf) and phylogenetic analysis (Appendix Figure 2) for the species identification of the 8 samples. Those samples (Appendix Figure 2, yellow arrow) clearly branch in the *L. tropica* cluster and are genetically very different from *L. aethiopica*, *L. major*, *L. donovani*, and interspecies hybrids.

In a second step, we only focused on *L. tropica* genomes (Figure 2). That focus provided 4 major insights. The 8 Somali region parasites constitute a *L. tropica* variant not previously reported in analyzed

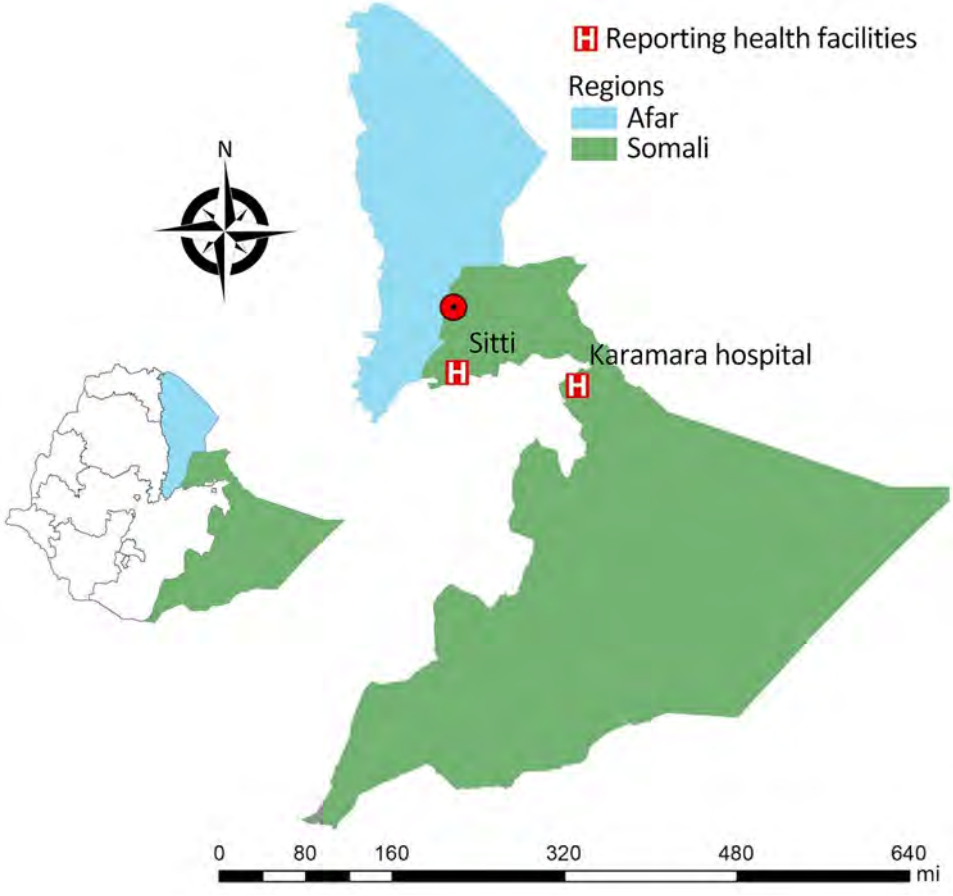

Figure 1. Locations of the healthcare facilities (HF) for the 8 study patients in genomic characterization of *Leishmania tropica* in cutaneous leishmaniasis, Somali region, Ethiopia, 2023. Map of Ethiopia shows the Afar region in blue and the Somali region in green. Two cases (S04 and S06) were diagnosed at Duunyar Health Center, located at the border of the Afar and Somali regions, where the outbreak occurred (red dot). One case (S12) was diagnosed at Sitti Primary Hospital, and 5 cases (WH08, WH09a, WH11, WH12, and WH15) were reported at Jigjiga University Sheik Hassen Yabare Comprehensive Specialized Hospital (CSH), each marked by a red H.

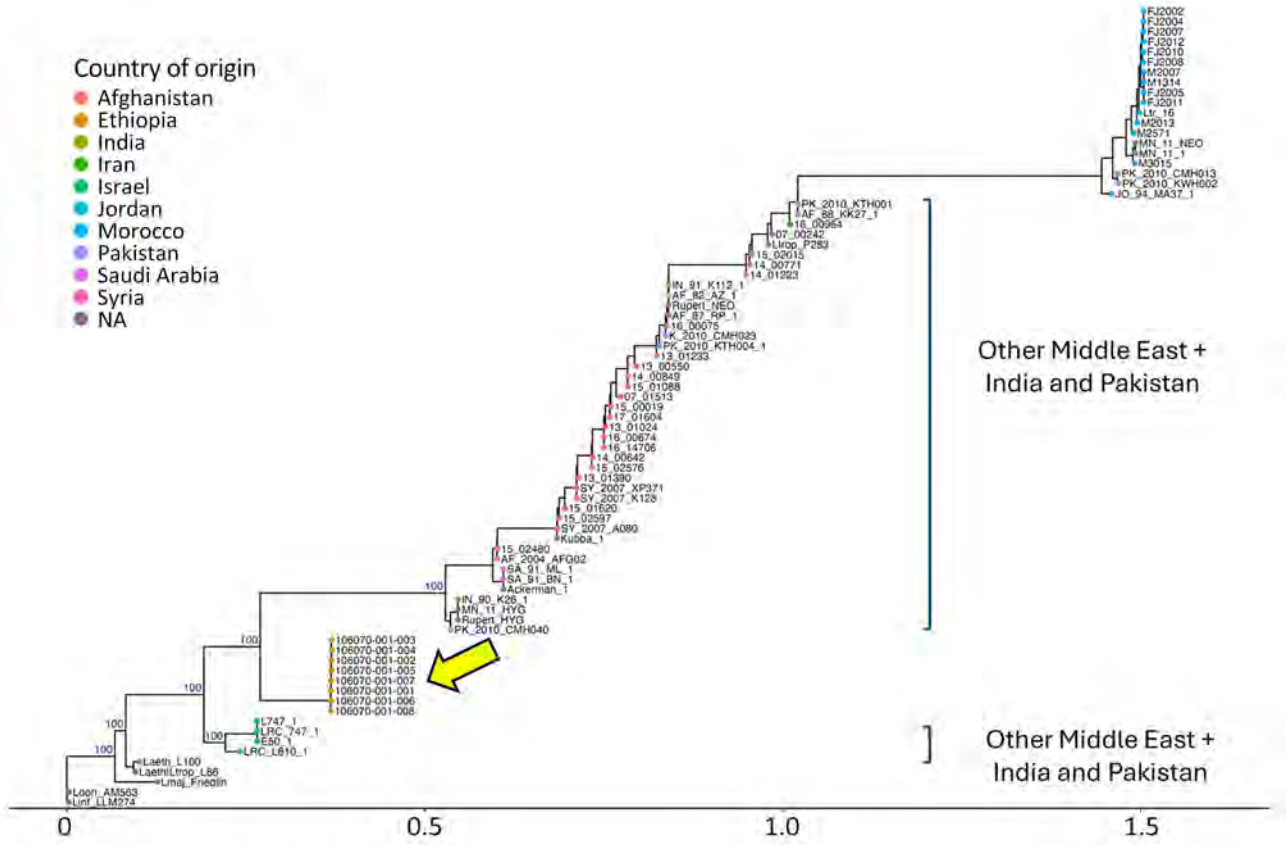

Figure 2. Rooted phylogenetic tree for genomic characterization of *Leishmania tropica* in cutaneous leishmaniasis, Somali region, Ethiopia, 2023. Phylogenetic tree of all publicly available *L. tropica* genomes (Appendix Table 3, https://wwwnc.cdc.gov/EID/article/31/7/24-1607-App1.pdf) was generated with RAxML (https://github.com/amkozlov/raxml-ng) with the general time reversible and gamma substitution model and showing close clustering of the 8 samples from Ethiopia (yellow arrow). Blue text indicates crucial bootstrap values. The *L. infantum* LLM274 genome was included as an outgroup. Scale bar indicates number of single-nucleotide polymorphism differences. NA, geographic origin of the *L. tropica* sample is unknown.

genomes. Those variants form a distinct cluster separate from genotypes reported thus far from Israel and Jordan and other Middle East variants. The *L. tropica* variants cluster together and are genetically homogeneous (on average, 122 single-nucleotide polymorphisms between samples), consistent with an outbreak-related scenario. We also found homozygous missense mutations or frameshifts in 14 genes reported to be involved in drug resistance, mostly antimony (Appendix Figure 3). That signature has not previously been reported in the *L. tropica* genome, which confirms the unique character of the samples from this region. Further work is required to understand the clinical effects of the discovery.

L. tropica is essentially endemic in Morocco, Turkey, Syria, Israel, Iraq, Azerbaijan, Iran, Uzbekistan, Afghanistan, Pakistan, and India (*8*). The broad distribution of *L. tropica* likely results from the anthroponotic nature of *L. tropica* transmission and the old communication axes in many of those countries, such as trade routes. In some regions, sporadic cases are reported, and the disease is thought to be zoonotic; possible animal reservoirs included hyraxes, bats, or wild rodents (*9*). The high genomic homogeneity in our sampled population shows the occurrence of an *L. tropica* outbreak in the Somali region of Ethiopia. We do not have the ability to trace whether the origin of the outbreak was a primary human case from which the parasite population spread or an animal reservoir. Nevertheless, this study highlights the risk for further expansion of the parasites from the human cases in the focus in the Somali region of Ethiopia. Public health officials should use genomic surveillance in humans, insect vectors, and animals in Ethiopia and neighboring countries, such as Kenya, where *L. tropica* was recently reported (*10*), to slow expansion of *L. tropica*.

This article was preprinted at https://doi.org/10.1101/2024.10.15.617758.

Genomic sequence reads of the parasites from the 8 samples have been submitted to the National Center for Biotechnology Information Sequence Read Archive (https://www.ncbi.nlm.nih.gov/sra; Bioproject no. PRJNA1172382).

This study was financially supported by the Belgian Directorate-General for Development Cooperation Framework Agreement 5 Ethiopia program (awarded to J.v.G. and G.T.), the Dioraphte Foundation (Spatial-CL, project no. CFP-RD2020 20020401), EpiGen-Ethiopia (project no. 101103188, funded through the Global Health EDCTP3 program–European Union), and the Flemish Ministry of Science and Innovation (to M.A.D.).

About the Author

Dr. Abera is a senior researcher at the Ethiopian Public Health Institute. His research focuses on molecular epidemiology, drug resistance, diagnostics, and metagenomics research applied to malaria, neglected tropical diseases, and arboviral diseases in Ethiopia.

References

1. Alvar J, Beca-Martínez MT, Argaw D, Jain S, Aagaard-Hansen J. Social determinants of visceral leishmaniasis elimination in Eastern Africa. BMJ Glob Health. 2023;8:e012638. https://doi:10.1136/bmjgh-2023-012638.
2. Hailu A, Di Muccio T, Abebe T, Hunegnaw M, Kager PA, Gramiccia M. Isolation of *Leishmania tropica* from an Ethiopian cutaneous leishmaniasis patient. Trans R Soc Trop Med Hyg. 2006;100:53–8. https://doi.org/10.1016/j.trstmh.2005.04.017
3. Hadermann A, Heeren S, Maes I, Dujardin JC, Domagalska MA, Van den Broeck F. Genome diversity of *Leishmania aethiopica*. Front Cell Infect Microbiol. 2023;13:1147998. https://doi.org/10.3389/fcimb.2023.1147998
4. Domagalska MA, Dujardin JC. Next-generation molecular surveillance of TriTryp diseases. Trends Parasitol. 2020;36:356–67. https://doi.org/10.1016/j.pt.2020.01.008
5. Lypaczewski P, Matlashewski G. *Leishmania donovani* hybridisation and introgression in nature: a comparative genomic investigation. Lancet Microbe. 2021;2:e250–8. https://doi.org/10.1016/S2666-5247(21)00028-8
6. Domagalska MA, Imamura H, Sanders M, Van den Broeck F, Bhattarai NR, Vanaerschot M, et al. Genomes of *Leishmania* parasites directly sequenced from patients with visceral leishmaniasis in the Indian subcontinent. PLoS Negl Trop Dis. 2019;13:e0007900. 10.1371/journal.pntd.0007900
7. Monsieurs P, Cloots K, Uranw S, Banjara MR, Ghimire P, Burza S, et al. Source tracing of *Leishmania donovani* in emerging foci of visceral leishmaniasis, Western Nepal. Emerg Infect Dis. 2024;30:611–3. https://doi.org/10.3201/eid3003.231160
8. World Health Organization. Control of the leishmaniases: WHO TRS N°949 [cited 2024 Sep 11]. https://www.who.int/publications/i/item/WHO-TRS-949
9. Kassahun A, Sadlova J, Benda P, Kostalova T, Warburg A, Hailu A, et al. Natural infection of bats with *Leishmania* in Ethiopia. Acta Trop. 2015;150:166–70. https://doi.org/10.1016/j.actatropica.2015.07.024
10. Owino BO, Matoke-Muhia D, Alraey Y, Mwangi JM, Ingonga JM, Ngumbi PM, et al. Association of *Phlebotomus guggisbergi* with *Leishmania major* and *Leishmania tropica* in a complex transmission setting for cutaneous l eishmaniasis in Gilgil, Nakuru county, Kenya. PLoS Negl Trop Dis. 2019;13:e0007712. https://doi.org/10.1371/journal.pntd.0007712

Address for correspondence: Adugna Abera, Ethiopian Public Health Institute, Arbagnoch St, PO Box 1242, Addis Ababa, Ethiopia; email: adugnabe@yahoo.com

Syphilitic Aortitis with Concomitant Neurosyphilis in Asymptomatic Patient

Evan Czulada, Quinn Seau, Tyler Geshay, Danny Rayes, Trevor Wyand, Ethan Fraser, Ronald Beaulieu, Justin Beckett

Author affiliations: Emory University Hospital, Atlanta, Georgia, USA (E. Czulada); Georgetown University School of Medicine, Washington, DC, USA (E. Czulada, Q. Seau); Georgetown University Hospital, Washington (T. Geshay, D. Rayes, T. Wyand, R. Beaulieu, J. Beckett); National Institutes of Health, Bethesda, Maryland, USA (E. Fraser).

DOI: https://doi.org/10.3201/eid3107.250646

We report a rare case of syphilitic aortitis with possible neurosyphilis in an asymptomatic 89-year-old man in Washington, DC, USA. This case highlights the need to consider emerging infectious causes of aortitis, even in patients without classic risk factors, by using multimodality imaging with confirmatory serologic and cerebrospinal fluid testing.

Syphilitic aortitis is exceptionally rare. However, syphilis, caused by the bacterium *Treponema pallidum*, has reemerged as a global public health concern, and the Centers for Disease Control and Prevention has reported >200,000 cases in the United States in 2022 (*1*). After 10–30 years, ≈10% of untreated persons

will develop syphilitic aortitis. Early recognition and treatment are imperative to avoid high rates of death (2), although the broad differential of aortitis can complicate diagnosis. In this article, we describe a rare case of syphilitic aortitis in an asymptomatic, elderly patient in which using imaging, serology, and epidemiologic context helped guide diagnosis.

An 89-year-old man with a history of chronic lymphedema, deep vein thrombosis, and peripheral artery disease sought care at Georgetown University Hospital in Washington, DC, USA, having experienced 1 week of right leg erythema and swelling. At admission, his laboratory results revealed leukocytosis and elevated inflammatory markers. Computed tomography (CT) of the patient's right leg revealed soft tissue changes consistent with cellulitis unresponsive to antimicrobial drugs. Because of the concern for sepsis, we broadened the patient's antimicrobial regimen, and an infectious disease consultation prompted further evaluation for alternative sources.

Contrast-enhanced CT of the chest showed circumferential soft tissue enhancement of the ascending aorta, aortic arch, and branching vessels, suggestive of aortitis versus intramural hematoma (Appendix Figure, https://wwwnc.cdc.gov/EID/article/31/7/25-0646-App1.pdf). Follow-up magnetic resonance angiography confirmed a diagnosis of aortitis (Figure). We consulted rheumatology because of the patient's elevated inflammatory markers but had low suspicion for autoimmune disease after more specific antibody testing results were negative.

Because of our concern for an infectious etiology, we pursued serologic testing. Initial chemoluminescence immunoassay testing was reactive for syphilis, and subsequent rapid plasma reagin testing was positive with a 1:4 titer result. Despite no neurologic symptoms, we conducted cerebrospinal fluid (CSF) analysis that was negative by Venereal Disease Research Laboratory (VDRL) testing but positive for fluorescent treponemal antibody absorption. Full CSF results revealed a slightly elevated red blood cell count, slightly low monocytes, and unremarkable leukocyte and protein counts. Findings were inconsistent across all samples.

Ultimately, we attributed the patient's underlying aortic pathology to syphilitic aortitis with concomitant neurosyphilis. The patient was treated with

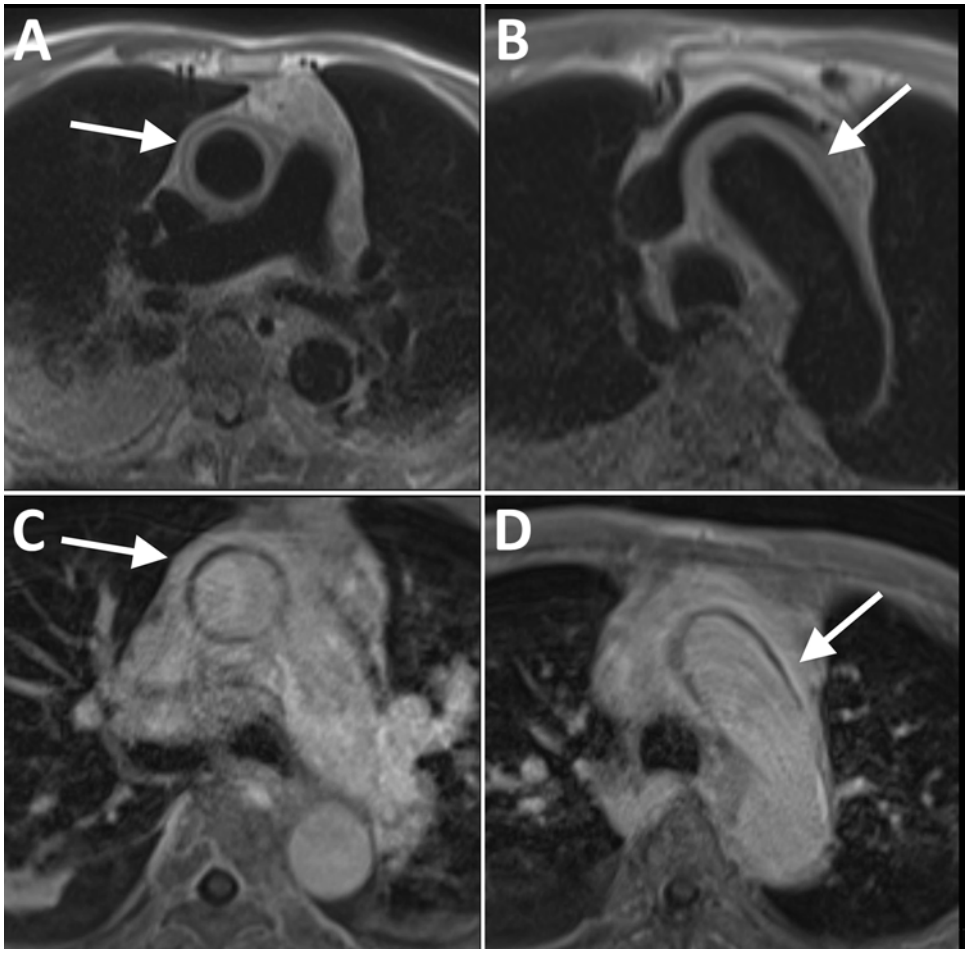

Figure. Electrocardiogram-gated magnetic resonance imaging of the ascending aorta in an 89-year-old patient with syphilitic aortitis and concomitant neurosyphilis, Washington, DC, USA. A, B) A circumferential periaortic T2 hyperintense signal was depicted at the main pulmonary artery (A) and aortic arch (B) on black blood prepared half-Fourier acquisition single-shot turbo spin-echo sequence images (white arrows). C, D) Contrast-enhanced T1-weighted magnetic resonance images at the main pulmonary artery (C) and aortic arch (D) show wall thickening and enhancement (white arrows) compatible with aortitis.

a 7-day course of intravenous penicillin G (3 million units every 4 h), and was prescribed the same treatment for an additional 7 days at discharge. The patient was discharged with reduced leg swelling, unremarkable vital signs, and resolved leukocytosis, but he was lost to follow-up.

This article describes the diagnosis of syphilitic aortitis with suspected neurosyphilis in an asymptomatic, elderly man with no classic symptoms or risk factors after using multimodality imaging and confirmatory testing. At 89 years of age, this patient is unusual and has a rare manifestation of syphilis, which is again rising in prevalence.

Our patient reported no cardiovascular symptoms, no prior syphilis diagnosis or treatment, no recollection of genital lesions, and no history of high-risk sexual behavior. Of note, he resided in Washington, DC, where syphilis rates are among the highest in the United States and have increased each year (*3*). Those data underscore the importance of considering *T. pallidum* infection in patients from high-risk areas, even in the absence of symptoms or traditional risk factors. Prompt treatment is critical, because some cases of syphilitic aneurysmal formation confer a 2-year mortality rate >80% (*4*). However, recognizing syphilitic aortitis can be challenging because of longstanding limitations in diagnostic strategies.

For source identification and subsequent control, whole-body imaging is typically indicated. Although CT imaging is sufficient for most aortopathies (*2*), it cannot reliably differentiate between hematoma and aortitis because of tissue density matching. Accordingly, a magnetic resonance aortogram provided further delineation of the abnormality, which was more indicative of aortitis than a hematoma because a hematoma is usually irregularly shaped and primarily diagnosed by using density-based imaging such as CT. Although not used in this case, fluorodeoxyglucose positron emission tomography/CT can be useful to evaluate differential causes of unexplained fever associated with vasculitis and ascertain treatment efficacy in cases of tertiary syphilis (*5*–*7*).

After ruling out more common autoimmune diseases, we chose treponemal-specific chemoluminescence immunoassay testing for suspicion of syphilitic aortitis. We selected this reverse sequence strategy because of institutional preference and high pretest probability (*8*), and a positive rapid plasma reagin titer of 1:4 confirmed active syphilis. Furthermore, diffuse syphilitic disease of the aorta necessitated CSF testing (*9*), showing negative VDRL and positive fluorescent treponemal antibody absorption. VDRL testing has poor sensitivity, and fluorescent treponemal antibody absorption has poor specificity. Fluorescent treponemal antibody absorption might be influenced by trace red blood cell contamination from the CSF (*10*). Nonetheless, intravenous penicillin G was initiated because of patient preference and the risk of not treating our elderly patient.

Syphilitic aortitis remains a rare but challenging diagnosis, especially in patients without typical symptoms or risk factors. This report highlights the importance of stepwise imaging and serologic testing in identifying syphilitic aortitis. CT scan is a reasonable first radiographic study, but magnetic resonance imaging can better define the underlying etiology. As syphilis cases continue to rise, clinicians should use local epidemiologic trends to ensure early disease detection.

Acknowledgments

We thank the patient for his consent to publish this case study.

About the Author

Dr. Czulada graduated from Georgetown University School of Medicine in 2025 and is currently an internal medicine resident at Emory University Hospital in Atlanta, GA. His research interests include cardiac electrophysiology and the intersection of cardiology and infectious disease, with a special focus on Chagas cardiomyopathy.

References

1. Centers for Disease Control and Prevention. Sexually transmitted infections surveillance, 2023 [cited 2024 Jul 5]. https://www.cdc.gov/sti-statistics/media/pdfs/2024/11/2022-STI-Surveillance-Report-PDF.pdf
2. Bley TA, Francois CJ. Inflammatory and infectious vascular disorders. In: Abbara S, Kalva SP, editors. Problem solving in cardiovascular imaging. Philadelphia: Elsevier; 2013. p. 412–22.
3. Health DC. 2023 Annual Epidemiology & Surveillance Report. 2023 [cited 2025 Apr 21]. https://dchealth.dc.gov/sites/default/files/dc/sites/doh/publication/attachments/2023-Annual-Surveillance-Report-v13.pdf
4. Girardi LN. Syphilitic aortitis: the bigger picture. J Thorac Cardiovasc Surg. 2017;154:e27–8. https://doi.org/10.1016/j.jtcvs.2017.04.052
5. Kim J, Song HC. Role of PET/CT in the evaluation of aortic disease. Chonnam Med J. 2018;54:143–52. https://doi.org/10.4068/cmj.2018.54.3.143
6. Kalbi D, Li A, Hari A, Chun K. The utility of 18F-FDG PET/CT in active aortitis: a case study and literature review. J Nucl Med. 2023;64(S1):p1230.
7. Hayashida T, Sueyoshi E, Sakamoto I, Uetani M, Chiba K. PET features of aortic diseases. AJR Am J Roentgenol. 2010;195:229–33. https://doi.org/10.2214/AJR.09.3952

8. Ortiz DA, Shukla MR, Loeffelholz MJ. The traditional or reverse algorithm for diagnosis of syphilis: pros and cons. Clin Infect Dis. 2020;71(Suppl 1):S43–51. https://doi.org/10.1093/cid/ciaa307
9. Workowski KA, Bolan GA; Centers for Disease Control and Prevention. Sexually transmitted diseases treatment guidelines, 2015. MMWR Recomm Rep. 2015;64(RR-03):1–137.
10. Hamill MM, Ghanem KG, Tuddenham S. State-of-the-art review: neurosyphilis. Clin Infect Dis. 2024;78:e57–68. https://doi.org/10.1093/cid/ciad437

Address for correspondence: Evan Czulada, Emory University Hospital, 1364 Clifton Rd NE, Atlanta, GA 30322, USA; email: eczulad@emory.edu

Plasmodium knowlesi Malaria in Persons Returning to Israel from Thailand, 2023

Yael Paran, Ami Neuberger, Muna Massarwa, Maisam Amar, Julia Vainer, Moran Szwarcwort Cohen, Ohad Shalom, Shirly Elbaz, Maya Davidovich, Oscar David Kirstein, Tamar Grossman

Author affiliations: Tel Aviv Sourasky Medical Center, Tel Aviv, Israel (Y. Paran); Division of Internal Medicine, Rambam Health Care Campus, Haifa, Israel (A. Neuberger, M. Massarwa); Technion Faculty of Medicine, Haifa (A. Neuberger, M. Amar); Infectious Disease Unit, Lady Davis Carmel Medical Center, Haifa (M. Amar); Public Health Laboratories–Jerusalem, Public Health Services, Ministry of Health, Jerusalem, Israel (J. Vainer, S. Elbaz, M. Davidovich, O.D. Kirstein, T. Grossman); Microbiology Laboratory, Rambam Health Care Campus, Haifa (M.S. Cohen); Microbiology Laboratory, Tel Aviv Sourasky Medical Center, Tel Aviv (O. Shalom)

DOI: https://doi.org/10.3201/eid3107.250444

We describe 2 cases of *Plasmodium knowlesi* malaria in persons from Israel who traveled to Thailand in 2023. One patient, likely infected in northwestern Thailand, might signal geographic expansion into areas not previously associated with human infection. The infection's rarity in travelers, diagnostic challenges, and potential severity underscore the importance of clinical awareness.

Plasmodium knowlesi, known as the fifth human malaria parasite, is a zoonotic malaria species maintained in a sylvatic cycle involving long-tailed (*Macaca fascicularis*) and pig-tailed (*Macaca nemestrina*) macaques and *Anopheles* (*Cellia*) *leucosphyrus* mosquitoes (*1*). In Thailand, anthroponotic malaria cases have decreased because of intervention programs, whereas *P. knowlesi* infections have increased, raising public health concerns (*2*,*3*). We report 2 cases of *P. knowlesi* malaria in persons from Israel who traveled to Thailand in 2023. Patient 1 likely acquired malaria in northwestern Thailand and might represent a sentinel case for geographic expansion. Patient 2 was infected in a recognized endemic focus.

In July 2023, a 25-year-old man (patient 1) sought care for fever, chills, nausea, and retro-orbital pain 1 day after returning from a 7-month trip across Southeast Asia. He spent his final month in northern Thailand, beginning in Chiang Mai and ending with 12 days in Pai, Mae Hong Son Province (Figure 1). He reported jungle trekking, monkey sightings, and no use of malaria prophylaxis. An initial rapid diagnostic test for detecting histidine-rich protein 2 and aldolase was negative, and another for detecting histidine-rich protein 2 and lactate dehydrogenase was weakly positive. A thick smear was initially negative, but a repeat smear 3 hours later revealed nonspeciated *Plasmodium*. Laboratory findings included leukopenia, thrombocytopenia, increased bilirubin and transaminase levels, and increased C-reactive protein level. TaqMan real-time PCR targeting the 18S rDNA gene performed at the Parasitology Reference Laboratory (https://www.gov.il/he/departments/units/parasite-reference-lab) confirmed *P. knowlesi* (*4*,*5*). PCR and 18S rDNA sequencing yielded a 939-bp fragment with 99.36% identity to *P. knowlesi* strain H in PlasmoDB (https://plasmodb.org/plasmo/app/record/gene/PKNH_0320900). We treated the patient with artemether/lumefantrine (80 mg/480 mg at 0 and 8 hours and then every 12 hours for a total of 6 doses), and he fully recovered without recrudescence.

In March 2023, we evaluated a 34-year-old man (patient 2), who had spent 6 months in Southeast Asia, for *P. knowlesi* by using the same molecular diagnostics. He spent his last 2 weeks on Koh Phayam Island in Ranong Province, a recognized endemic area (Figure 1) (*2*). He reported jungle hiking and macaque contact and did not use prophylaxis. We also treated patient 2 with standard oral artemether/lumefantrine, and he fully recovered.

We sequenced the polymorphic C-terminal region of the *Pkmsp1* gene to explore genetic diversity. The sequence from patient 1 (northern Thailand)

showed 1 synonymous mutation, differentiating it from the *P. knowlesi* H strain in PlasmoDB (https://plasmodb.org/plasmo/app/record/gene/PKNH_0728900). The closest sequences were from Malaysia, consistent with shared ancestry (*6*). The translated amino acid sequence matched haplotype H3, which was similar to an amino acid sequence predicted from isolate JF837348 from southern Thailand. The isolate from patient 2 (southern Thailand) was identical to isolate JF837351 from southern Thailand and matched haplotype H2 that is common in the region (*6*,*7*) (Figure 2).

The Institutional Review Board (Helsinki Committee, https://www.tasmc.org.il/rd/en/next-unit/helsinki-committee) of Tel Aviv Sourasky Medical Center waived ethical approval. We deposited sequences in GenBank (patient 1: 18S rDNA, accession no. PV123279, and *Pkmsp1*, accession no. PV132709; patient 2: 18S rDNA, accession no. PV123278, and *Pkmsp1*, accession no. PV132708).

Figure 1. Travel locations of persons with *Plasmodium knowlesi* malaria returning to Israel from Thailand, 2023. Patient 1 might represent a sentinel case of human *P. knowlesi* infection acquired in northern Thailand. Patient 2 visited Koh Phayam Island in Ranong Province in southern Thailand, a recognized endemic area near the Malaysia border. Map created with ArcGIS Pro software version 3.3.2 (ESRI, https://www.esri.com).

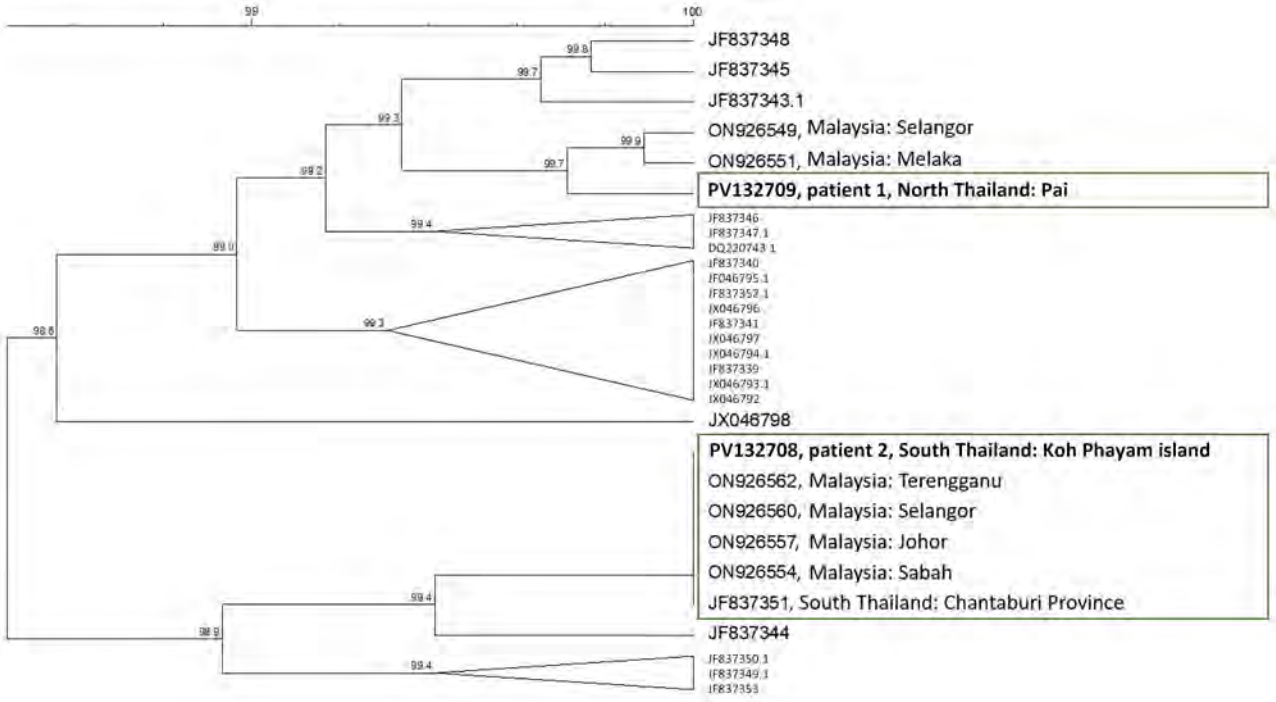

Figure 2. Phylogenetic analysis of *Pkmsp1* sequences for *Plasmodium knowlesi* malaria in persons returning to Israel from Thailand, 2023. Dendogram was based on an 850-bp fragment of the C-terminal region of *Pkmsp1*, including all published sequences from Thailand, the isolates from patients 1 and 2 in this study (bold text), and the most closely related sequences identified through BLAST (https://blast.ncbi.nlm.nih.gov) analysis. No exact matches were identified for patient 1 (northern Thailand); the geographic origin of 2 closely related sequences is indicated. For patient 2 (southern Thailand), several identical sequences were found in GenBank (green box). Accession numbers are given. Clustering analysis was performed by using the unweighted pair group with arithmetic mean method with open gap penalty set to 100% and unit gap penalty set to 0%, without correction. Scale bar indicates percentage similarity between sequences.

The likely exposure of patient 1 in Pai or Chiang Mai represents the northernmost documented location of *P. knowlesi* human infection in Thailand. Previously, the northernmost reported endemic cases were in Tak Province, bordering Myanmar and Uttaradit province, near the Laos border (*8*). The genetic divergence of the isolate from patient 1 might reflect local parasite diversity or the limited sequence data from northern Thailand and neighboring regions. The Pkmsp1 protein is subject to purifying selection by the host immune system, with surviving variants potentially representing fitter strains. Ongoing genomic surveillance is needed to determine whether patient 1 reflects true local transmission or indicates a broader haplotype range in the region.

Although >280,000 Israelis visited Thailand in 2023, no other confirmed malaria cases were reported among returning travelers, and no other *P. knowlesi* cases have been reported in Israel in >20 years. In addition to its rarity in travelers, *P. knowlesi* malaria poses diagnostic challenges because of rapid diagnostic test insensitivity and morphologic similarity to other *Plasmodium* species, increasing the likelihood of underdiagnosis. Parasitemia levels might be low early in infection, but clinicians should remain alert to the potential for rapid progression to hyperparasitemia, which is a key risk factor for severe malaria attributed to the ability of *P. knowlesi* to infect all erythrocyte stages and its short asexual replication cycle (*9*,*10*). In Malaysia, severe malaria occurred in 6%–9% of cases in district hospitals and up to 29% in tertiary care (*9*).

Both patients reported here met Centers for Disease Control and Prevention criteria for chemoprophylaxis, having stayed in forested regions near international borders (https://wwwnc.cdc.gov/travel/yellowbook/2024/preparing/yellow-fever-vaccine-malaria-prevention-by-country#6419). The patients' extended travel and jungle exposure highlight the importance of itinerary-specific pretravel counseling.

In conclusion, *P. knowlesi* malaria in patient 1 might represent early evidence of zoonotic spillover of *P. knowlesi* in a new area (northern Thailand). Traveler-based surveillance and molecular tools can provide early warning of geographic shifts in malaria transmission. Heightened clinical awareness and improved diagnostics are essential for timely detection and control.

Acknowledgments

We thank Rona Grossman and David Maimoun for assistance with protein sequence analysis and insightful discussions and Belina Neuberger for valuable language editing services.

About the Author

Dr. Paran is an infectious disease specialist at the Tel Aviv Sourasky Medical Center in Tel Aviv, Israel. Her research interests focus on emerging infectious diseases and geographical medicine.

References

1. Singh B, Kim Sung L, Matusop A, Radhakrishnan A, Shamsul SS, Cox-Singh J, et al. A large focus of naturally acquired *Plasmodium knowlesi* infections in human beings. Lancet. 2004;363:1017–24. https://doi.org/10.1016/S0140-6736(04)15836-4
2. US President's Malaria Initiative. Thailand malaria profile: FY 2024. Washington (DC): US Agency for International Development; 2024.
3. World Health Organization. World Malaria Report 2024: addressing inequity in the global malaria response. Geneva: The Organization; 2024.
4. Divis PC, Shokoples SE, Singh B, Yanow SK. A TaqMan real-time PCR assay for the detection and quantitation of *Plasmodium knowlesi*. Malar J. 2010;9:344. https://doi.org/10.1186/1475-2875-9-344
5. Shokoples SE, Ndao M, Kowalewska-Grochowska K, Yanow SK. Multiplexed real-time PCR assay for discrimination of *Plasmodium* species with improved sensitivity for mixed infections. J Clin Microbiol. 2009;47:975–80. https://doi.org/10.1128/JCM.01858-08
6. Tapaopong P, Chainarin S, Mala A, Rannarong A, Kangkasikorn N, Kusolsuk T, et al. Declining genetic polymorphism of the C-terminus Merozoite Surface Protein-1 amidst increased Plasmodium knowlesi transmission in Thailand. Malar J. 2024;23:342. https://doi.org/10.1186/s12936-024-05162-z
7. Jongwutiwes S, Buppan P, Kosuvin R, Seethamchai S, Pattanawong U, Sirichaisinthop J, et al. Plasmodium knowlesi Malaria in humans and macaques, Thailand. Emerg Infect Dis. 2011;17:1799–806. https://doi.org/10.3201/eid1710.110349
8. Narapakdeesakul D, Pengsakul T, Kaewparuehaschai M, Thongsahuan S, Moonmake S, Lekcharoen P, et al. Zoonotic simian malaria parasites in free-ranging Macaca fascicularis macaques and human malaria patients in Thailand, with a note on genetic characterization of recent isolates. Acta Trop. 2023;248:107030. https://doi.org/10.1016/j.actatropica.2023.107030
9. Barber BE, Grigg MJ, Cooper DJ, van Schalkwyk DA, William T, Rajahram GS, et al. Clinical management of *Plasmodium knowlesi* malaria. Adv Parasitol. 2021;113:45–76. https://doi.org/10.1016/bs.apar.2021.08.004
10. Lee WC, Cheong FW, Amir A, Lai MY, Tan JH, Phang WK, et al. *Plasmodium knowlesi*: the game changer for malaria eradication. Malar J. 2022;21:140. https://doi.org/10.1186/s12936-022-04131-8

Address for correspondence: Tamar Grossman, Reference Parasitology Laboratory, Public Health Laboratories–Jerusalem, Israeli Ministry of Health, Yaakov Eliav 9, Jerusalem 9134302, Israel; email: tamar.grossman@moh.gov.il

Corrections

Vol. 30, No. 6

The first author's name has changed in Evaluating Humoral Immunity Elicited by XBB.1.5 Monovalent COVID-19 Vaccine (X.H. Wrynla et al.). The article has been corrected online (https://wwwnc.cdc.gov/eid/article/30/6/24-0051_article).

Vol. 30, No. 8

Figure 3 had several errors in Detection of Nucleocapsid Antibodies Associated with Primary SARS-CoV-2 Infection in Unvaccinated and Vaccinated Blood Donors (E. Grebe et al.). The article has been corrected online (https://wwwnc.cdc.gov/eid/article/30/8/24-0659_article).

Emerging Infections Network Survey of Screening for Cryptococcal Antigenemia, United States, 2024

Kaitlin Benedict, Alexander Jordan, Jeremy A.W. Gold, Dallas J. Smith, Tom Chiller, Ian Hennessee, Philip M. Polgreen, Susan E. Beekmann

Author affiliations: Centers for Disease Control and Prevention, Atlanta, Georgia, USA (K. Benedict, A. Jordan, J.A.W. Gold, D.J. Smith, T. Chiller, I. Hennessee); University of Iowa Carver College of Medicine, Iowa City, Iowa, USA (P.M. Polgreen, S.E. Beekmann)

DOI: https://doi.org/10.3201/eid3107.250295

We polled infectious disease specialists about cryptococcal antigen screening for patients initiating HIV antiretroviral therapy. Of 215 respondents, 33% reported typically obtaining screening for patients with CD4 counts <200 cells/mm^3 and 63% for counts <100 CD4 cells/mm^3. Uncertainty about cryptococcal antigen screening benefits and recommendations suggests opportunities for education and increased screening.

Cryptococcosis is a severe disease caused by the environmental fungus *Cryptococcus*. In the United States, an estimated 3.4–6.5 cases/100,000 population and nearly 5,000 cryptococcosis-associated hospitalizations occur each year; most cases are associated with immunosuppression (*1*,*2*). Approximately one third of patients with cryptococcosis have HIV (*1*,*2*).

Cryptococcal antigen (CrAg) testing is a simple, rapid, inexpensive, and highly accurate diagnostic method. It can detect early asymptomatic cryptococcal infection in blood weeks to months before symptom onset, enabling early treatment and resulting in less illness and death. US federal guidelines recommend routine CrAg screening for persons with HIV and CD4 counts ≤200 cells/mm^3 (*3*). However, few data exist about CrAg screening practices in the United States. To gain preliminary insights about CrAg screening use and identify potential barriers, we polled members of the Emerging Infections Network (EIN), a provider-based network supported by the Centers for Disease Control and Prevention and the Infectious Disease Society of America (*4*).

EIN emailed a link to an online poll (https://ein.idsociety.org/surveys/survey/181/) 3 times during October 30–November 15, 2024, to its >3,100 network members. We analyzed percentages of responses to questions about CrAg screening utility for patients other than those with advanced HIV; CrAg blood test use for adult and adolescent patients with advanced HIV in 4 clinical scenarios (newly initiating antiretroviral therapy [ART], reinitiating ART, experiencing ART failure, or seriously ill regardless of ART status); barriers to obtaining CrAg testing; and management of patients with a positive CrAg screening test.

In total, 215 EIN members responded. Most were infectious disease physicians who primarily care for adult patients (91%) and practice at university or teaching hospitals (57%) (Table 1). When asked whether patient groups other than those with advanced HIV should routinely receive CrAg screening, 40% of respondents said no, 33% said yes (solid organ or stem cell transplant patients were often mentioned in free-text responses), and 27% were unsure.

Of the 215 EIN members who responded, 181 (84%) reported caring for adult or adolescent patients with HIV in the past year. Those respondents participated in the remaining survey questions. The percentages of respondents who reported always or often obtaining CrAg screening for patients with HIV, by CD4 cell count, were as follows: newly initiating ART, <100 cells/mm^3, 63%; <200 cells/mm^3, 33%; reinitiating ART, <100 cells/mm^3, 35%; <200 cells/mm^3, 17%; experiencing ART failure, <100 cells/mm^3, 20%; <200 cells/mm^3, 8%; and seriously ill regardless of ART status, <100 cells/mm^3, 77%; <200 cells/mm^3, 68% (Table 2).

The primary reported barriers (respondents could choose >1 barrier) to obtaining CrAg screening among patients with HIV and CD4 <200 cells/mm^3 were uncertainty about the benefit (42%) and uncertainty around CrAg screening recommendations (32%). Ten percent expressed concern about delaying ART, 2% reported CrAg test unavailability, and 42% reported none of the specified barriers. When asked about managing a patient with a positive CrAg screening test result (respondents could choose >1 answer), respondents noted they would perform lumbar puncture and order cerebrospinal fluid testing (79%), evaluate for meningitis symptoms (77%), obtain a CrAg titer (69%), and treat with fluconazole while awaiting cerebrospinal fluid test results (36%).

The poll of EIN members showed moderate (33%–63%, depending on CD4 count) adherence to National Institutes of Health, World Health

Organization, and European Confederation of Medical Mycology and International Society for Human & Animal Mycology recommendations for obtaining CrAg screening for patients with advanced HIV who are initiating ART (*3*,*5*,*6*). A modest percentage of respondents (42%) was unsure of the benefit of CrAg screening. In general, limited data exist regarding US CrAg screening implementation (*7*). In addition, approximately 1 in 3 respondents expressed uncertainty about CrAg screening recommendations, and 1 in 10 expressed concerned about delaying ART, which might relate to general awareness of multiple guidelines but unfamiliarity with differences among them. For example, only the World Health Organization (*5*) and the European Confederation of Medical Mycology and International Society for Human & Animal Mycology (*6*) explicitly recommend CrAg screening for patients with HIV who are reinitiating ART, which was not commonly reported (17%–35%) in the poll.

Most respondents (almost 80%) reported that they typically obtain lumbar punctures and evaluate for meningitis symptoms among patients with positive CrAg screening tests, consistent with guidelines. CrAg screening utility for patients without HIV (e.g., transplant recipients) is unclear and has not been well studied (*8*,*9*); 60% of respondents indicated that the practice might be useful or that they were unsure. More research is needed regarding CrAg screening utility among patients without HIV.

A limitation of the survey is that poll respondents might not be generalizable to all US infectious disease physicians. Furthermore, results might overestimate CrAg screening use because of self-selection bias among respondents who chose to participate in the survey based on perceived importance of CrAg

Table 1. Practice characteristics and testing practices reported by 215 US infectious disease providers in Emerging Infections Network survey of screening for cryptococcal antigenemia, United States, 2024*

Characteristic	Responses, no. (%)†
Primary practice setting	n = 214
Community hospital	48 (22)
Nonuniversity teaching hospital	39 (18)
University hospital	84 (39)
Veterans Affairs or Department of Defense hospital	13 (6)
City, county, or public hospital	10 (5)
Children's hospital	10 (5)
Cancer facility	2 (1)
Outpatient only	3 (1)
Other	5 (2)
Respondent type	n = 212
Infectious disease physician (primarily for adults)	192 (91)
Infectious disease physician (primarily for children)	14 (7)
Other	3 (1)
Besides adult and adolescent patients with advanced HIV, do you think that other patient groups should be routinely screened for cryptococcal antigenemia?	n = 209
Yes	69 (33)
No	84 (40)
Not sure	56 (27)
Which barriers, if any, concern you or prevent you from obtaining CrAg testing for patients with HIV who are initiating or reinitiating ART and have a CD4 cell count <200 cells/mm^3?‡	n = 178
Unsure of benefit of CrAg screening	74 (42)
Uncertainty around CrAg screening recommendations	57 (32)
Concern about delaying ART initiation or reinitiation	18 (10)
Long turnaround time for send-out CrAg testing	13 (7)
Difficulty of interpreting CrAg test results	10 (6)
CrAg testing not available at my facility/institution	4 (2)
Challenges with insurance coverage	4 (2)
Other	2 (1)
None of the choices	74 (42)
Which of the following would you consider doing for a patient with a positive CrAg screening test result?‡	n = 181
Not applicable/I do not order CrAg testing	7 (4)
Perform lumbar puncture and order cerebrospinal fluid testing for *Cryptococcus* or CrAg	143 (79)
Evaluate for symptoms of meningitis	140 (77)
Obtain CrAg titer	124 (69)
Treatment with fluconazole while awaiting CSF results	65 (36)
Other	7 (4)
None of these	1 (0.6)

*ART, antiretroviral therapy; CrAg, cryptococcal antigen; CSF, cerebrospinal fluid; N, total number of responses.
†Among respondents who answered each question.
‡Respondents could select all that apply.

Table 2. Cryptococcal antigen blood test use for patients with advanced HIV, reported by 215 US infectious disease providers in Emerging Infections Network survey of screening for cryptococcal antigenemia, United States, 2024*

Characteristic	CD4 count, no. (%)†	
	<100 cells/mm^3	<200 cells/mm^3
Newly initiating ART	n = 171	n = 166
Never	23 (13)	34 (20)
Rarely	22 (13)	43 (26)
Sometimes	19 (11)	34 (20)
Often	27 (16)	19 (11)
Always	80 (47)	36 (22)
Reinitiating ART	n = 168	n = 160
Never	35 (21)	48 (30)
Rarely	28 (17)	44 (28)
Sometimes	47 (28)	41 (26)
Often	20 (12)	13 (8)
Always	38 (23)	14 (9)
Experiencing ART failure	n = 166	n = 161
Never	44 (27)	57 (35)
Rarely	37 (22)	47 (29)
Sometimes	51 (31)	44 (27)
Often	20 (12)	8 (5)
Always	14 (8)	5 (3)
Seriously ill‡	n = 176	n = 168
Never	8 (5)	11 (7)
Rarely	5 (3)	16 (10)
Sometimes	27 (15)	27 (16)
Often	43 (24)	38 (23)
Always	93 (53)	76 (45)

*ART, antiretroviral therapy.
†Among respondents who answered each question.
‡Regardless of ART status.

screening. Future surveys of CrAg screening practices among other specialist populations might be useful because of increased integration of HIV care into primary care. Our results reveal potential opportunities for improvement in advancing understanding of and adherence to CrAg screening guidelines among a sample of EIN members.

Emerging Infections Network queries are designated as non–human subjects research by the institutional review board of the University of Iowa. This activity was reviewed by the Centers for Disease Control and Prevention and was conducted consistent with applicable federal law and CDC policy (e.g., 45 C.F.R. part 46.102(l)(2), 21 C.F.R. part 56; 42 U.S.C. §241(d); 5 U.S.C. §552a; 44 U.S.C. §3501 et seq.).

This work was funded by the Centers for Disease Control and Prevention (cooperative agreement no. 5 and grant no. NU50CK000574).

About the Author

Ms. Benedict is an epidemiologist in the Mycotic Diseases Branch, Division of Foodborne, Waterborne, and Environmental Diseases, National Center for Emerging and Zoonotic Infectious Diseases, Centers for Disease Control and Prevention, Atlanta, Georgia, USA. Her research interests include the epidemiology and prevention of fungal infections.

References

1. Rayens E, Rayens MK, Norris KA. Demographic and socioeconomic factors associated with fungal infection risk, United States, 2019. Emerg Infect Dis. 2022;28:1955–69. https://doi.org/10.3201/eid2810.220391
2. Benedict K, Smith DJ, Gold JAW. Epidemiology of cryptococcosis among patients with commercial health insurance and patients with Medicaid, United States, 2016–2022. Open Forum Infect Dis. 2024;11:ofae260. https://doi.org/10.1093/ofid/ofae260
3. National Institutes of Health. Guidelines for the prevention and treatment of opportunistic infections in adults and adolescents with HIV cryptococcosis [cited 2024 Nov 23]. https://clinicalinfo.hiv.gov/en/guidelines/hiv-clinical-guidelines-adult-and-adolescent-opportunistic-infections/cryptococcosis
4. Pillai SK, Beekmann SE, Santibanez S, Polgreen PM. The Infectious Diseases Society of America Emerging Infections Network: bridging the gap between clinical infectious diseases and public health. Clin Infect Dis. 2014;58:991–6. https://doi.org/10.1093/cid/cit932
5. World Health Organization. Guidelines for diagnosing, preventing and managing cryptococcal disease among adults, adolescents and children living with HIV [cited 2024 Nov 25]. https://www.who.int/publications/i/item/9789240052178
6. Chang CC, Harrison TS, Bicanic TA, Chayakulkeeree M, Sorrell TC, Warris A, et al. Global guideline for the diagnosis and management of cryptococcosis: an initiati ve of the ECMM and ISHAM in cooperation with the ASM. Lancet Infect Dis. 2024;24:e495–512. https://doi.org/10.1016/S1473-3099(23)00731-4
7. Temfack E, Bigna JJ, Luma HN, Spijker R, Meintjes G, Jarvis JN, et al. Impact of routine cryptococcal antigen screening and targeted preemptive fluconazole therapy in antiretroviral-naive human immunodeficiency virus–infected adults with CD4 cell counts <100/μL: a systematic review and meta-analysis. Clin Infect Dis. 2019;68:688–98. https://doi.org/10.1093/cid/ciy567
8. Miwa T, Okamoto K, Ikeuchi K, Yamamoto S, Okugawa S, Ichida A, et al. The role of frequent screening or diagnostic testing of serum cryptococcal antigen in liver transplant recipients: a descriptive epidemiology. Open Forum Infect Dis. 2024;11:ofae255. https://doi.org/10.1093/ofid/ofae255
9. George I, Rajasingham R, Powderly W, Boulware D. Routine cryptococcal antigen screening in solid organ transplant recipients: is it time to save lives and money? Open Forum Infect Dis. 2017;4(Suppl 1):S55. https://doi.org/10.1093/ofid/ofx162.128

Address for correspondence: Kaitlin Benedict, Centers for Disease Control and Prevention, 1600 Clifton Rd NE, Mailstop H24-9, Atlanta, GA 30329-4018, USA; email: jsy8@cdc.gov

Albrecht Dürer (1471–1528), *The Syphilitic*, 1496 (detail). Broadsheet: text and woodcut. 15.7 in × 11.4 in/40 cm × 29 cm. Source: Wellcome Collection, London, UK (https://wellcomecollection.org/works/pt87tf6m).

The Syphilitic—Dürer's Woodcut, a Pandemic Unveiled

Alexis Demas

In 1496, Albrecht Dürer, at the age of just 25, created a haunting woodcut to accompany a poem authored by German physician Theodoric Ulsenius. Entitled *The Syphilitic*, the image portrays a grotesque figure with bloated limbs, ulcerated skin, and a contorted face—an image both spiritual and pathological. Born in Nuremberg in 1471, Dürer would become one of the most influential figures of the Northern Renaissance, renowned for his technical mastery in engraving, his profound interest in humanist thought, and his innovative fusion of scientific observation and artistic expression. Although this woodcut dates to 1496, the prominent inscription of 1484 above the afflicted figure refers to a planetary conjunction that was, at the time, widely seen as an ominous sign. Dürer thus connects the astronomical event of 1484 with the outbreak of the

Author affiliation: Le Havre Hospital, Le Havre, France

DOI: https://doi.org/10.3201/eid3107.AC3107

disease he depicted 12 years later, framing it within a cosmological and prophetic context.

This woodcut is one of the earliest known artistic representations of syphilis, capturing a moment when Europe was gripped by a new and devastating disease. Far beyond an artistic curiosity, this woodcut serves as a visual document—a Renaissance-era screenshot—preserving the medical, cultural, and existential shock of an emerging infectious disease. The accompanying Latin text was composed by Theodoricus Ulsenius, a German physician and humanist active in the late 15th Century. Although little is known about Ulsenius's life, he is remembered for his medical writings and his interest in astrological explanations for disease, reflecting the intellectual currents of his era.

Syphilis, or the French disease as it was known in early texts, made its first explosive appearance in Europe in 1495, during the siege of Naples. The timing was no coincidence. Historical and microbiological evidence suggests that returning members of Christopher Columbus's crew introduced a New World subspecies of *Treponema* (likely the agent of yaws), which rapidly evolved into the sexually transmitted *Treponema pallidum* in the environmental and social conditions of Europe. In a tragic irony of microbial globalization, this pathogen traveled eastward across the Atlantic while, simultaneously, European settlers from Europe carried diseases such as measles and smallpox westward, decimating the immunologically naive Native Americans. What emerged was an unintentional epidemic spread, waged not with intent, but with oblivious contact.

The image created by Dürer is imbued with dense and deliberate symbolism. The afflicted man stands prominently in the foreground, raising his hands toward the heavens in a gesture of despair and supplication, as if pleading for a divine explanation for his suffering. He is clothed in a loose, tattered robe, designed to conceal his skin and the visible lesions that emerge on the exposed areas: his face, legs, and hands. The garment, rendered in vivid red tones, accentuates his vulnerability and social isolation, the striking color drawing immediate attention. His emaciated features and hunched posture vividly evoke the physical devastation wrought by the disease. Behind him, an elaborate coat of arms displays a grotesque face, possibly symbolizing the French Disease. The accompanying Latin text by Ulsenius attributes the cause of the epidemic to a celestial phenomenon: the conjunction of Jupiter and Saturn in the sign of Scorpio. In an age when science, astrology, and theology were inseparably intertwined, such a cosmological explanation sought to make sense of a disease perceived as either divine punishment or an apocalyptic omen. Thus, Dürer's composition serves not merely as a depiction of physical suffering but as a complex meditation on fate, human frailty, and the blurred boundaries between medical and metaphysical knowledge.

From a modern diagnostic perspective, the image invites an exercise in iconodiagnosis (the retrospective medical diagnosis carried out on a work of art depicting a human person). The skin lesions and facial features evoke differential considerations including leprosy, psoriasis, or even advanced scabies. But the timing of the image, just 1 year after the Europe outbreak, strongly favors a florid case of secondary or early tertiary syphilis. Dürer's woodcut captures the grotesque morphology and rapid dissemination of a novel pathogen whose biologic behavior defied both

Figure. Full broadsheet of Albrecht Dürer's The Syphilitic, showing text of poem authored by German physician Theodoric Ulsenius. Source: Wellcome Collection, London, UK (https://wellcomecollection.org/works/pt87tf6m).

Galenic medicine and moral explanation (the interpretation of disease as both a natural imbalance of the bodily humors, according to Galenic medical theory, and as a consequence of moral or sinful behavior).

Artists, often more sensitive to the undercurrents of their time than chroniclers or physicians, became inadvertent epidemiologists. Their works encode patterns of disease and perception. Just as Pieter Bruegel's *The Triumph of Death* reflected the cultural impact of plague, Dürer's syphilitic figure chronicles a microbial invasion frozen in time. Rather than depicting a microbial event in real time, Dürer's woodcut offers a visual chronicle of a society grappling with a new and terrifying disease, blending observable symptoms with astrological and moral interpretations of human suffering. These images allow today's physicians, historians, and scientists to revisit the past with clinical insight and to better understand how societies respond to emerging diseases.

Despite centuries of medical progress, syphilis remains with us. Recent epidemiologic reports from the World Health Organization show a rising global incidence of syphilis and other sexually transmitted infections, particularly among young adults and marginalized populations. This resurgence, despite the availability of effective antibiotics and preventive tools, prompts a reevaluation of our current strategies for public health education, access to care, and behavioral interventions.

The pandemic of the 1490s may seem distant, but it holds direct lessons for today. In both instances, newly mobile populations, evolving pathogens, and delayed institutional responses allowed infections to flourish. The human body, caught between biology and belief, becomes the ultimate witness to history.

Dürer's syphilitic figure, though carved in wood more than 5 centuries ago, reminds us that microbes are protagonists in the story of civilization. Microbiological incursions are often sudden, the consequences lasting, and their documentation—through science and art—are essential to our understanding. In today's era of emerging pathogens and renewed global vulnerability, this Renaissance woodcut stands not only as an artistic relic but as a timeless warning.

Bibliography

1. Charlier P, Perciaccante A, Kluger N, Nerlich AG, Appenzeller O, Donell ST, et al. Iconodiagnosis: guidelines and recommendations. Ethics Med Public Health. 2023;31:100951. https://doi.org/10.1016/j.jemep.2023.100951
2. Demas A. Another one bites the dust: contribution of neurologists to STI prevention strategies. Ethics Med Public Health. 2025;33:101048. https://doi.org/10.1016/j.jemep.2025.101048
3. Franzen C. Syphilis in composers and musicians—Mozart, Beethoven, Paganini, Schubert, Schumann, Smetana. Eur J Clin Microbiol Infect Dis. 2008;27:1151–7. https://doi.org/10.1007/s10096-008-0571-x
4. Frith J. Syphilis—its early history and treatment until penicillin and the debate on its origins. J Mil Veterans Health. 2012;20:49–58.
5. Harper KN, Ocampo PS, Steiner BM, George RW, Silverman MS, Bolotin S, et al. On the origin of the treponematoses: a phylogenetic approach. PLoS Negl Trop Dis. 2008;2:e148. https://doi.org/10.1371/journal.pntd.0000148
6. Kluger N, Perciaccante A, Charlier P. Iconodiagnosis: a review of common pitfalls before publishing a case. J Eur Acad Dermatol Venereol. 2022;36:e285–6. https://doi.org/10.1111/jdv.17796
7. Knell RJ. Syphilis in renaissance Europe: rapid evolution of an introduced sexually transmitted disease? Proc Biol Sci. 2004;271:S174–6.
8. Pontius AA. Icono-diagnosis, a medical-humanistic approach, detecting Crouzon's malformation in Cook Islands' prehistoric art. Perspect Biol Med. 1983;27:107–20. https://doi.org/10.1353/pbm.1983.0030
9. Quétel C. History of syphilis. Baltimore (MD): The Johns Hopkins University Press; 1990.
10. Tognotti E. The rise and fall of syphilis in Renaissance Europe. J Med Humanit. 2009;30:99–113.

Address for correspondence: Alexis Demas, Department of Neurology, Le Havre Hospital, 29 avenue Pierre Mendès, Le Havre CEDEX 76290, France; email: dr.alexisdemas@gmail.com

EMERGING INFECTIOUS DISEASES®

Upcoming Issue

- Emergence of Clade Ib Monkeypox Virus—Current State of Evidence
- Enhancing Surveillance of Viral Respiratory Infections—Lessons Learned from a SARS-CoV-2 Outbreak in a Maximum-Security Prison, Australia
- Rapid Emergence and Evolution of SARS-CoV-2 Intrahost Variants among COVID-19 Patients with Prolonged Infections, Singapore
- *Scheffersomyces spartinae* Fungemia among Pediatric Patients, Pakistan, 2020–2024
- The Burden and Molecular Epidemiology of Group A *Streptococcus* among American Indian Individuals in the White Mountain Apache Tribal Lands, 2016–2019
- Multidisciplinary Tracking of Highly Pathogenic Avian Influenza A(H5N1) Outbreak in Griffon Vultures, Southern Europe, 2022
- Estimated COVID-19 Periodicity and Correlation with SARS-CoV-2 Spike S1 Antigenic Diversity, United States
- Gastric Submucosal Tumor in Patient Infected with *Dioctophyme renale*, South Korea
- Case Report of Clade Ib Monkeypox Virus Infection Linked to Travel to Democratic Republic of the Congo, Thailand, 2024
- Microsporidial Keratoconjunctivitis Caused by *Vittaforma corneae*, Sea of Galilee, Israel, 2022-2024
- Progression from *Candida auris* Colonization Screening to Clinical Case Status, United States, 2016–2023
- ACE2 Receptor Usage across Animal Species by SARS-CoV-2 Variants
- Genomic Surveillance Detection of SARS-CoV-1–Like Virus Taxa in *Rhinolophidae* Bats, Bandarban Region, Bangladesh
- Complete Genome Analysis of African Swine Fever Virus Isolated from Wild Boar, India, 2021
- Nipah Virus Antibodies in Bats, Philippines, 2013–2022
- Crimean-Congo Hemorrhagic Fever Virus Africa 1 Lineage in *Hyalomma dromedarii* Ticks, Algeria, 2023
- Henipavirus in Northern Short-Tailed Shrew, Alabama, USA

Complete list of articles in the August issue at https://wwwnc.cdc.gov/eid/#issue-324

Earning CME Credit

To obtain credit, you should first read the journal article. After reading the article, you should be able to answer the following, related, multiple-choice questions. To complete the questions (with a minimum 75% passing score) and earn continuing medical education (CME) credit, please go to http://www.medscape.org/journal/eid. Credit cannot be obtained for tests completed on paper, although you may use the worksheet below to keep a record of your answers.

You must be a registered user on http://www.medscape.org. If you are not registered on http://www.medscape.org, please click on the "Register" link on the right hand side of the website.

Only one answer is correct for each question. Once you successfully answer all post-test questions, you will be able to view and/or print your certificate. For questions regarding this activity, contact the accredited provider, CME@medscape.net. For technical assistance, contact CME@medscape.net. American Medical Association's Physician's Recognition Award (AMA PRA) credits are accepted in the US as evidence of participation in CME activities. For further information on this award, please go to https://www.ama-assn.org. The AMA has determined that physicians not licensed in the US who participate in this CME activity are eligible for AMA PRA Category 1 Credits™. Through agreements that the AMA has made with agencies in some countries, AMA PRA credit may be acceptable as evidence of participation in CME activities. If you are not licensed in the US, please complete the questions online, print the AMA PRA CME credit certificate, and present it to your national medical association for review.

Article Title

Multicenter Case–Control Study of Behavioral, Environmental, and Geographic Risk Factors for Talaromycosis, Vietnam

CME Questions

1. Which of the following statements regarding talaromycosis is most accurate?

A. Talaromycosis was rare until the HIV epidemic in the 1980s
B. Talaromycosis is most commonly encountered in sub-Saharan Africa
C. Mortality due to talaromycosis decreases to < 3% of patients if treated with antifungal therapy
D. The primary reservoir of *Talaromyces marneffei* is ticks from the genus Haemaphysalis

2. Which of the following demographic and disease variables was most associated with cases of talaromycosis vs controls in the current study?

A. Being a woman
B. Lower absolute lymphocyte count
C. Lower cluster of differentiation (CD)4 count
D. Older age

3. Which of the following variables was the most significant risk factor for talaromycosis in the current study?

A. Lack of fluconazole prophylaxis
B. Lack of antiretroviral therapy
C. Farming animal exposure
D. Raw animal product consumption

4. Which geographic area had the highest ratio of cases of talaromycosis to controls in the current study?

A. Lowlands; river delta
B. Highlands
C. Urban center
D. Coastal setting